

2010 Atomic, Molecular, Optical Sciences Research Meeting



**Airlie Conference Center
Warrenton, Virginia
September 26-29, 2010**



U.S. DEPARTMENT OF
ENERGY

Office of
Science

Office of Basic Energy Sciences
Chemical Sciences, Geosciences &
Biosciences Division

Foreword

This volume summarizes the 2010 Research Meeting of the Atomic, Molecular and Optical Sciences (AMOS) Program sponsored by the U. S. Department of Energy (DOE), Office of Basic Energy Sciences (BES), and comprises descriptions of the current research sponsored by the AMOS program. The research meeting is held annually for the DOE laboratory and university principal investigators (PIs) within the BES AMOS Program to facilitate scientific interchange among the PIs and to promote a sense of program identity.

The BES/AMOS program is vigorous and innovative, and enjoys strong support within the Department of Energy. This is due entirely to our scientists, the outstanding research they perform, and its relevance to DOE missions. FY2010 has been an exciting year for BES and the research community. New initiatives included the Early Career Research Program, the Graduate Fellowship Program, and the Energy Innovation Hubs. Experiments at the Linac Coherent Light Source (LCLS) began last fall, and involved participation as well as leadership by many in the AMOS program. As illustrated in this volume, the AMOS community continues to explore new scientific frontiers relevant to the DOE mission and the strategic challenges facing our nation and the world.

We are deeply indebted to the members of the scientific community who have contributed valuable time toward the review of proposals and programs, either by mail review of grant applications, panel reviews, or on-site reviews of our multi-PI programs. These thorough and thoughtful reviews are central to the continued vitality of the AMOS program.

We are privileged to serve in the management of this research program. In performing these tasks, we learn from the achievements of, and share the excitement of, the research of the scientists and students whose work is summarized in the abstracts published on the following pages.

Many thanks to the staff of the Oak Ridge Institute for Science and Education, in particular Loretta Friend and Connie Lansdon, and to the Airlie Conference Center for assisting with the meeting. We also thank Diane Marceau, Robin Felder, and Michaelena Kyler-King in the Chemical Sciences, Biosciences, and Geosciences Division for their indispensable behind-the-scenes efforts in support of the BES/AMOS program. We also appreciate Mark Pederson's coordination of computational resources and interactions with related DOE program offices. Finally, thanks to Larry Rahn for his expert help in assembling this volume.

Jeffrey L. Krause
Michael P. Casassa
Chemical Sciences, Geosciences and Biosciences Division
Office of Basic Energy Sciences
Department of Energy

**Cover Art Courtesy of Diane Marceau
Chemical Sciences, Geosciences and Biosciences
Division, Basic Energy Sciences, DOE**

**This document was produced under contract number DE-AC05-06OR23100
between the U.S. Department of Energy and Oak Ridge Associated Universities.**

**The research grants and contracts described in this document are supported by the
U.S. DOE Office of Science, Office of Basic Energy Sciences, Chemical Sciences,
Geosciences and Biosciences Division.**

Agenda

2010 Meeting of the Atomic, Molecular and Optical Sciences Program
Office of Basic Energy Sciences
U. S. Department of Energy

Airlie Center, Warrenton, Virginia, September 26-29, 2010

Sunday, September 26

3:00-6:00 pm **** Registration ****
6:00 pm **** Reception (No Host) ****
7:00 pm **** Dinner ****

Monday, September 27

7:30 am **** Breakfast ****

8:45 am *Welcome and Introductory Remarks*
Jeff Krause, BES/DOE

Session I Chair: **Andreas Becker**

9:00 am *Probing Complexity Using the ALS and the LCLS*
Nora Berrah, Western Michigan University

9:30 am *Exploring Atoms with Intense X-Rays at the LCLS*
Steve Southworth, Argonne National Laboratory

10:00 am *New Directions in Intense-Laser Alignment*
Tamar Seideman, Northwestern University

10:30 am **** Break ****

11:00 am *Attosecond and Ultra-Fast X-Ray Science*
Pierre Agostini, Ohio State University

11:30 am *Strong Field Rescattering Physics*
Chii-Dong Lin, Kansas State University

12:00 noon *Isolated Attosecond Pulse Dynamics*
Dan Neumark, Lawrence Berkeley National Laboratory

12:30 pm **** Lunch ****

Session II Chair: **Marcos Dantus**

- 4:00 pm *Structural Dynamics in Chemical Systems*
Kelly Gaffney, SLAC National Accelerator Laboratory
- 4:30 pm *Interatomic Coulombic Decay (ICD) in Xenon Difluoride*
Bob Dunford, Argonne National Laboratory
- 5:00 pm *Molecular Dynamics with Ion and Laser Beams*
Itzik Ben-Itzhak, Kansas State University
- 5:30 pm *Introduction to Attosecond Gathering*
- 6:00 pm ***** Reception (No Host) *****
- 6:30 pm ***** Dinner *****

Session III Chair: **Margaret Murnane**

- 7:30 pm *Attosecond Gathering*

Tuesday, September 28

- 7:30 am ***** Breakfast *****

Session IV Chair: **Jerry Seidler**

- 8:30 am *Ultrafast X-Ray Coherent Control*
David Reis, SLAC National Accelerator Laboratory
- 9:00 am *Laser-Produced Coherent X-Ray Sources*
Don Umstadter, University of Nebraska
- 9:30 am *Laser Control of Molecular Dynamics*
Tom Weinacht, Stony Brook University
- 10:00 am *Optical Two-Dimensional Spectroscopy of Disordered Semiconductor Quantum Wells and Quantum Dots*
Steve Cundiff, JILA/University of Colorado
- 10:30 am ***** Break *****
- 11:00 am *Electron/Photon Interactions with Atoms/Ions*
Alfred Msezane, Clark Atlanta University
- 11:30 am *Single Exciton Optical Gain in Semiconductor Nanocrystals Using Engineered Exciton/Exciton Interactions*
Victor Klimov, Los Alamos National Laboratory
- 12:00 noon *Studies of Autoionizing States Relevant to Dielectronic Recombination*
Tom Gallagher, University of Virginia
- 12:30 pm ***** Lunch *****

Session V

Chair: **Martin Centurion**

- 4:00 pm *Low-Energy Electron Interactions with Interfaces and Biological Targets*
Thom Orlando, Georgia Tech
- 4:30 pm *Electron-Driven Excitation and Dissociation of Molecules*
Ann Orel, University of California, Davis
- 5:00 pm *Breakup of Atoms and Molecules by Multiple Photoionization or Electron Attachment*
Bill McCurdy, LBNL/University of California, Davis
- 5:30 pm *Electron-Driven Processes in Polyatomic Molecules*
Vince McKoy, California Institute of Technology
- 6:00 pm ***** Reception (No Host) *****
- 6:30 pm ***** Dinner *****

Wednesday, September 29

- 7:30 am ***** Breakfast *****

Session VI

Chair: **Abbas Ourmazd**

- 8:30 am *Ultracold Molecules: Physics in the Quantum Regime*
John Doyle, Harvard University
- 9:00 am *Theoretical Investigations of Atomic Collision Physics*
Alex Dalgarno, Harvard University
- 9:30 am *Interactions of Ultracold Molecules: Collisions, Reactions, and Dipolar Effects*
Dave DeMille, Yale University
- 10:00 am ***** Break *****
- 10:30 am *Photoabsorption by Free and Confined Atoms and Ions*
Steve Manson, Georgia State University
- 11:00 am *Recent Work Using the LTDSE Method for Atomic Collisions*
Dave Schultz, Oak Ridge National Laboratory
- 11:30 am *Closing Remarks*
Jeff Krause, BES/DOE
- 11:45 am ***** Lunch *****
- 1:00 pm Discussion
- 3:00 pm Adjourn

Table of Contents

Laboratory Research Summaries (by institution)

AMO Physics at Argonne National Laboratory	1
<i>Femtosecond Electronic Response of Atoms to Ultra-Intense X-Rays</i>	
Linda Young.....	2
<i>Resonant Nonlinear X-Ray Processes at High X-Ray Intensity</i>	
Elliot Kanter	3
<i>Non-linearity in the X-Ray Regime at LCLS</i>	
Gilles Doumy	4
<i>Femtosecond X-Ray Two-Photon Photoelectron Spectroscopy of Organic Molecules</i>	
Steve Southworth	5
<i>Optical Control of Excitation and Decay of Core-Excited States</i>	
Steve Southworth	6
<i>Ion Hole Dynamics in Strong-Field Ionization</i>	
Robin Santra.....	7
<i>X-Ray Scattering from 3-D Aligned Asymmetric Molecules—Theory</i>	
Robin Santra.....	7
<i>X-Ray Scattering from Laser-aligned Molecules—Experiment</i>	
Gilles Doumy	8
<i>High-Repetition-Rate Laser and X-Ray Experiments</i>	
Steve Southworth	9
<i>X-Ray Imaging of Trapped Nanoparticles</i>	
Norbert Scherer	10
<i>Interatomic Coulombic Decay (ICD) in Xenon Difluoride</i>	
Bob Dunford	11
<i>Short Pulse X-Rays at the Advanced Photon Source</i>	
Linda Young.....	11
J.R. Macdonald Laboratory - Overview 2010.....	17
<i>Structure and Dynamics of Atoms, Ions, Molecules, and Surfaces: Molecular Dynamics with Ion and Laser Beams</i>	
Itzik Ben-Itzhak	19

<i>Probing Autoionization using Attosecond Pulses Generated with Generalized Double Optical Gating</i> Zenghu Chang	23
<i>Structure and Dynamics of Atoms, Ions, Molecules and Surfaces: Atomic Physics with Intense Short Laser Pulses and Synchrotron Radiation</i> Lew Cocke	27
<i>Interaction of Atomic Ladder Systems with Trains of UltraFast Pulses</i> Brett DePaola	31
<i>Atoms and Molecules in Intense Laser Pulses</i> Brett Esry	35
<i>Controlling Molecular Rotations of Asymmetric Top Molecules: Methods and Applications</i> Vinod Kumarappan	39
<i>Strong Field Rescattering Physics – Self-Imaging of a Molecule by its Own Electrons</i> Chii-Dong Lin	43
<i>Structure and Dynamics of Atoms, Ions, Molecules and Surfaces: Atomic Physics with Ion Beams, Lasers and Synchrotron Radiation</i> Uwe Thumm	47
<i>Strong-Field Time-Dependent Spectroscopy</i> Carlos Trallero	51
Atomic, Molecular and Optical Sciences at Los Alamos National Laboratory	55
<i>Engineered Electronic and Magnetic Interactions in Nanocrystal Quantum Dots</i> Victor Klimov	55
Atomic, Molecular and Optical Sciences at LBNL	59
<i>Inner-Shell Photoionization and Dissociative Electron Attachment of Small Molecules</i> Ali Belkacem and Thorsten Weber	60
<i>Electron-Atom and Electron-Molecule Collision Processes</i> Tom Rescigno and Bill McCurdy	64

Ultrafast X-Ray Science Laboratory at LBNL.....	69
<i>Soft X-Ray High Harmonic Generation and Applications in Chemical Physics</i>	
Oliver Gessner	69
<i>Applications of the Femtosecond Undulator Beamline at the Advanced Light Source to Solution-Phase Molecular Dynamics</i>	
Robert Schoenlein	70
<i>Time-Resolved Studies and Non-linear Interaction of Femtosecond X-Rays with Atoms and Molecules</i>	
Thorsten Weber and Ali Belkacem	71
<i>Theory and Computation</i>	
Bill McCurdy and Martin Head-Gordon	72
<i>Attosecond Atomic and Molecular Science</i>	
Steve Leone and Dan Neumark	73
Atomic and Molecular Physics Research at Oak Ridge National Laboratory.....	77
<i>Erosion of a-C:H and a-C:D Thin Films by Low-Energy Atomic and Molecular H and D Ion Beam Irradiation</i>	
Fred Meyer	77
<i>Low-Energy Atomic and Molecular Ion Collisions using Merged-Beams</i>	
Charlie Havener	79
<i>Electron-Molecular Ion Interactions</i>	
Mark Bannister	80
<i>Molecular Ion Interactions (The MIRF ICCE Trap)</i>	
Randy Vane	82
<i>Manipulation and Decoherence of Rydberg Wavepackets</i>	
Carlos Reinhold.....	85
<i>Molecular Dynamics Simulations of Chemical Sputtering</i>	
Carlos Reinhold.....	86
<i>Development of Theoretical Methods for Atomic and Molecular Collisions</i>	
Dave Schultz	87

PULSE: The PULSE Institute for Ultrafast Energy Science at SLAC.....	95
<i>High Harmonic Generation and Electronic Structure</i>	
Markus Gühr.....	98
<i>Strong Field Control of Coherence in Molecules and Solids</i>	
Phil Bucksbaum	102
<i>Solution Phase Chemical Dynamics</i>	
Kelly Gaffney.....	106
<i>Non-periodic Imaging at the Stanford PULSE Institute</i>	
Mike Bogan	109

University Research Summaries (by PI)

<i>Coherent Control of Electron Dynamics</i> Andreas Becker	113
<i>Probing Complexity Using the ALS and the LCLS</i> Nora Berrah	117
<i>Strongly Anisotropic Bose and Fermi Gases</i> John Bohn	121
<i>Ultrafast Electron Diffraction from Aligned Molecules</i> Martin Centurion	125
<i>Atomic and Molecular Physics in Strong Fields</i> Shih-I Chu	129
<i>Formation of Ultracold Molecules</i> Robin Côté	133
<i>Optical Two-Dimensional Spectroscopy of Disordered Semiconductor Quantum Wells and Quantum Dots</i> Steve Cundiff	137
<i>Theoretical Investigations of Atomic Collision Physics</i> Alex Dalgarno	141
<i>Understanding and Controlling Strong-Field Laser Interactions with Polyatomic Molecules</i> Marcos Dantus	145
<i>Production and Trapping of Ultracold Polar Molecules</i> Dave DeMille	147
<i>Attosecond and Ultra-Fast X-Ray Science</i> Lou DiMauro and Pierre Agostini	151
<i>Imaging of Electronic Wave Functions during Chemical Reactions</i> Lou DiMauro, Pierre Agostini and Terry Miller	155
<i>High Intensity Femtosecond XUV Pulse Interactions with Atomic Clusters</i> Todd Ditmire	159
<i>Ultracold Molecules: Physics in the Quantum Regime</i> John Doyle	163

<i>Atomic Electrons in Strong Radiation Fields</i>	
Joe Eberly	167
<i>Reaction Imaging and the Molecular Coulomb Continuum</i>	
Jim Feagin	171
<i>Studies of Autoionizing States Relevant to Dielectronic Recombination</i>	
Tom Gallagher	175
<i>Experiments in Ultracold Collisions and Ultracold Molecules</i>	
Phil Gould	179
<i>Physics of Correlated Systems</i>	
Chris Greene	183
<i>Using Strong Optical Fields to Manipulate and Probe Coherent Molecular Dynamics</i>	
Bob Jones	187
<i>Molecular Dynamics Probed by Coherent Electrons and X-Rays</i>	
Henry Kapteyn and Margaret Murnane	191
<i>Detailed Investigations of Interactions between Ionizing Radiation and Neutral Gases</i>	
Allen Landers	197
<i>Properties of Actinide Ions from Measurements of Rydberg Ion Fine Structure</i>	
Steve Lundeen	201
<i>Theory of Threshold Effects in Low-Energy Atomic Collisions</i>	
Joe Macek	205
<i>Ionization of Free and Confined Atoms and Ions</i>	
Steve Manson	209
<i>Electron-Driven Processes in Polyatomic Molecules</i>	
Vince McKoy	213
<i>Electron/Photon Interactions with Atoms/Ions</i>	
Alfred Msezane	217
<i>Theory and Simulations of Nonlinear X-Ray Spectroscopy of Molecules</i>	
Shaul Mukamel	221
<i>Nonlinear Photoacoustic Spectroscopies Probed by Ultrafast EUV Light</i>	
Keith Nelson	225
<i>Free-Space Excitation of Propagating Surface Plasmon Polaritons</i>	
Lukas Novotny	229

<i>Electron-Driven Excitation and Dissociation of Molecules</i> Ann Orel	233
<i>Low-Energy Electron Interactions with Liquid Interfaces and Biological Targets</i> Thom Orlando	237
<i>Structure from Fleeting Illumination of Faint Spinning Objects in Flight</i> Abbas Ourmazd and Peter Schwander	241
<i>Energetic Photon and Electron Interactions with Positive Ions</i> Ron Phaneuf	245
<i>Resonant and Nonresonant Photoelectron-Vibrational Coupling</i> Erwin Poliakoff and Robert Lucchese	249
<i>Control of Molecular Dynamics: Algorithms for Design and Implementation</i> Hersch Rabitz and Tak-San Ho	253
<i>Ultracold Sodium and Rubidium Mixtures: Collisions, Interactions and Heteronuclear Molecule Formation</i> Chandra Raman	257
<i>Coherent and Incoherent Transitions</i> Francis Robicheaux	259
<i>Table-Top Sources of Coherent Soft X-Ray and X-Ray Light</i> Jorge Rocca and Henry Kapteyn	263
<i>Ultrafast Holographic X-Ray Imaging and its Application to Picosecond Ultrasonic Wave Dynamics in Bulk Materials</i> Christoph Rose-Petruck	267
<i>New Directions in Intense-Laser Alignment</i> Tamar Seideman	271
<i>New Scientific Opportunities through Inelastic X-Ray Scattering at 3rd- and 4th-Generation Light Sources</i> Jerry Seidler	275
<i>Dynamics of Few-Body Atomic Processes</i> Tony Starace	279
<i>Femtosecond and Attosecond Laser-Pulse Energy Transformation and Concentration in Nanostructured Systems</i> Mark Stockman	283

<i>Laser-Produced Coherent X-Ray Sources</i> Don Umstadter	287
<i>Combining High Level Ab Initio Calculations with Laser Control of Molecular Dynamics</i> Tom Weinacht and Spiridoula Matsika	291
<i>Cold and Ultracold Polar Molecules</i> Jun Ye	295
Author Index	297
Participants	302

Laboratory Research Summaries
(by institution)

AMO Physics at Argonne National Laboratory

G. Doumy, R. W. Dunford, E. P. Kanter, B. Krässig, S. H. Southworth, and L. Young
Argonne National Laboratory, Argonne, IL 60439

gdoumy@aps.anl.gov, dunford@anl.gov, kanter@anl.gov, kraessig@anl.gov, southworth@anl.gov, young@anl.gov

Overview

The Argonne AMO physics program aims at a quantitative understanding of x-ray interactions with atoms and molecules from the weak-field limit explored at the Advanced Photon Source (APS) to the strong-field regime accessible at the Linac Coherent Light Source (LCLS). Single photon x-ray processes can be dramatically altered in the presence of strong optical fields, and we exploit ultrafast x-ray sources to study these effects. Conversely, the atomic or molecular response to strong optical fields is itself of great interest due to the discovery of phenomena such as high-order harmonic generation and attosecond pulse generation. The use of tunable, polarized APS x-rays to probe such processes *in situ* can lead to new physical insights and quantitative structural information not accessible by other techniques. We are exploring three thrust areas. First, APS x rays probe laser-controlled motions, for example, x-ray spectroscopy and x-ray diffraction by laser-aligned molecules. Second, x-ray processes such as photoabsorption and inner-shell vacancy decay can be controlled by an intense optical laser field. Third, we are exploring the intense x-ray regime at the LCLS and observing phenomena that were previously inaccessible such as x-ray two-photon photoelectron spectroscopy of molecules. Theory is a key component of our program by predicting phenomena that motivate experiments and by simulating and interpreting measured results. We also anticipate the development of 1-ps tunable x rays for spectroscopic and structural investigations of laser controlled motions as part of the APS upgrade project.

Notable progress in the previous year includes results from the first LCLS experiments in the 800-2000 eV range using the AMO end station. The Argonne AMO group led two experiments on intense x-ray interactions with atomic neon. The first experiment used ion charge-state yields and photoelectron and Auger-electron spectroscopy to explore sequential multi-photon absorption leading to high charge states, including fully-stripped Ne^{10+} . In the second experiment, electron spectroscopy was used to observe a two-photon inner-shell resonant process. Members of the Argonne AMO group also participated in LCLS experiments led by other groups. Developments at the Advanced Photon Source include installation of a 10-W, variable repetition-rate, 1064-nm laser at the 7ID x-ray beamline. This laser was used for laser-pump/x-ray probe experiments on molecular alignment at 54 kHz and photoexcitation of solvated nickel porphyrin at 135 kHz. A new instrument designed for x-ray scattering by laser-aligned molecules was commissioned on the high-flux 14ID beamline. Theory and calculations were applied to understanding intense x-ray interactions in LCLS experiments, and the time-dependent configuration interaction singles (TDCIS) method was developed to treat electronic channel-coupling effects in strong-field processes. Theory and calculations were also applied to x-ray scattering from 3-D aligned asymmetric molecules and x-ray diffraction from silver nanowires in anticipation of experiments. Finally, the Advanced Photon Source Upgrade (APS-U) was granted Critical Decision 0. The APS-U includes the Short Pulse X-ray (SPX) facility that will use RF-deflection cavities to produce picosecond, tunable x rays for time-resolved scattering and spectroscopy.

High-intensity x-ray science at LCLS

Femtosecond electronic response of atoms to ultra-intense X-rays (L. Young, G. Doumy, E. P. Kanter, B. Krässig, Y. Li¹, A. M. March, S. T. Pratt², R. Santra³, S. H. Southworth, N. Rohringer⁴, L. F. DiMauro⁵, C. A. Roedig⁵, N. Berrah⁶, L. Fang⁶, M. Hoener^{6,7}, P. H. Bucksbaum⁸, J. P. Cryan⁸, S. Ghimire⁸, J. M. Glowina⁸, D. A. Reis⁸, J. D. Bozek⁹, C. Bostedt⁹, M. Messerschmidt⁹)

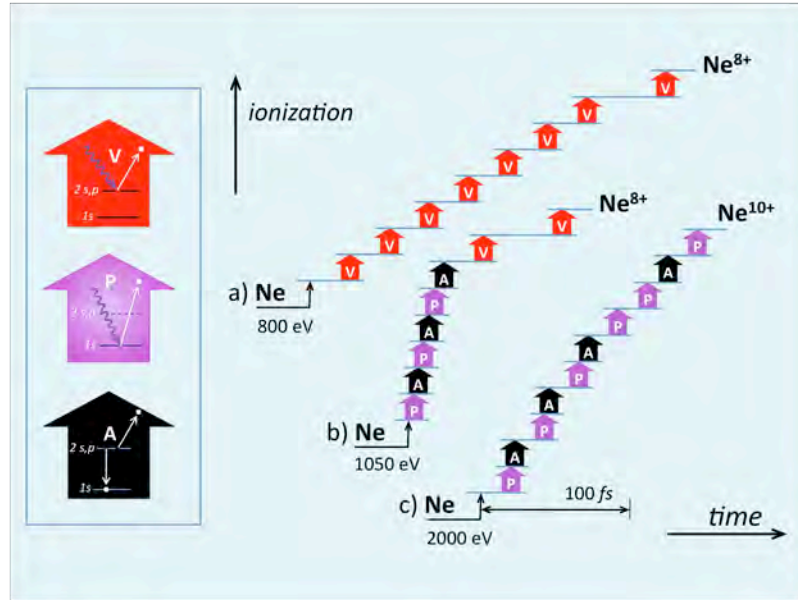


Fig.1 Diagram of the multiphoton absorption mechanisms in neon induced by ultra-intense X-ray pulses. X-rays with energies below 870 eV ionize 2s,p-shell valence electrons (V, red arrow). Higher energy X-rays give rise to photoemission from the 1s shell (P, purple arrow), and in the consequent Auger decay the 1s-shell vacancy is filled by a 2s,p-shell electron and another 2s,p electron is emitted (A, black arrow). These V, P and A processes are shown in more detail in the inset; they all increase the charge of the residual ion by one. Main panel, three representative schemes of multiphoton absorption stripping the neon atom. The horizontal direction indicates the time for which atoms are exposed to the high-intensity X-ray radiation field, and vertical steps indicate an increase in ionic charge due to an ionization step, V, P or A. Horizontal steps are approximately to scale with a flux density of 150 X-ray photons per \AA^2 per fs, and indicate the mean time between photoionization events or Auger decay.

The Linac Coherent Light Source (LCLS) at SLAC, the world's first x-ray free electron laser with peak brilliance 8 orders of magnitude higher than conventional synchrotron sources, began user operations on October 1, 2009. This first user experiment at the LCLS sought to explore the response of prototypical neon atoms when they are exposed to unprecedented levels of fluence ($\sim 10^5$ x-ray photons per \AA^2) and intensity ($\sim 10^{18}$ W/cm²) of ultrafast (~ 100 fs) radiation pulses from the LCLS concentrated inside a micron-sized focus. At this fluence each neon atom sequentially absorbs several photons during a single pulse. The atom is multiply ionized either from the outside in, or from the inside out, depending on whether K-shell

ionization is possible and the atom is additionally ionized by Auger decay. This situation is illustrated for different x-ray energies in Figure 1, a) for 800 eV x-ray energy, which is below the *K*-shell binding energy, b) 1050 eV, where initial *K* shell ionization is possible but the energy is not high enough to ionize the *K*-shell of more highly charged species, c) 2000 eV, above all ionization thresholds. The rates for multiple x-ray absorption in these sequences depend on the ionization cross-section, the x-ray fluence, and on whether or not atomic electrons are available for removal. In this context the rates for Auger decay are dependent only on the electronic configuration and decrease with increasing charge states. As a result the production of hollow neon ions with two *K*-shell vacancies increases with increasing intensity, but the rate of x-ray absorption decreases for a hollow ion until the *K*-shell is repopulated by Auger decay. Even for x-ray energies above all thresholds, at high intensities a bare Ne^{10+} ion can only be achieved if the pulse length is long enough to accommodate all necessary Auger decay times. We found that the main features of our observations could be quantitatively modeled with a standard, perturbative description of photoabsorption and Auger decay as ingredients to a set of rate equations for the different absorption sequences. The modeling also revealed that two independent observations in our experiment, namely the ratio of neon ion charge state distributions and the ratio of double-to-single *K*-shell ionization for long and short x-ray pulses, norminally 230 fs and 80 fs, match significantly shorter x-ray pulse durations. This work was published in the July 1, 2010 issue of Nature Vol. 466, p. 56-61 (Ref. [7]) and was also the subject of Nature's 'News and Views' column in the same issue.

Resonant nonlinear x-ray processes at high x-ray intensity (E.P. Kanter, G. Doumy, B. Krässig, S.T. Pratt², R. Santra³, S.H. Southworth, L. Young, Y. Li¹, A. M. March, N. Rohringer⁴, J. Bozek⁹, C. Bostedt⁹, M. Messerschmidt⁹, L. DiMauro⁵, C. Roedig⁵, N. Berrah⁶, M. Hoener^{6,7}, L. Fang⁶, P. Bucksbaum⁸, D. Reis⁸)

In this experiment, we investigated resonant nonlinear x-ray processes in atomic Ne at high x-ray intensity. Atomic neon is a simple target with dipole resonant features, at well-defined energies, within the photon energy range spanned by the LCLS at inception, ~800-2000 eV. Thus, it is a natural choice with which to test theoretical understanding of resonant nonlinear x-ray processes. At high photon energies resonant absorption by inner-shell electrons will dominate all x-ray photoprocesses, with cross sections ~100× greater than those for non-resonant valence ionization. On an inner-shell resonance, absorption/stimulated emission cycles (Rabi flopping) will be the dominant photoinduced process. With this in mind, Rohringer and Santra have calculated modifications to the resonant Auger effect induced by high intensity x-rays [30].

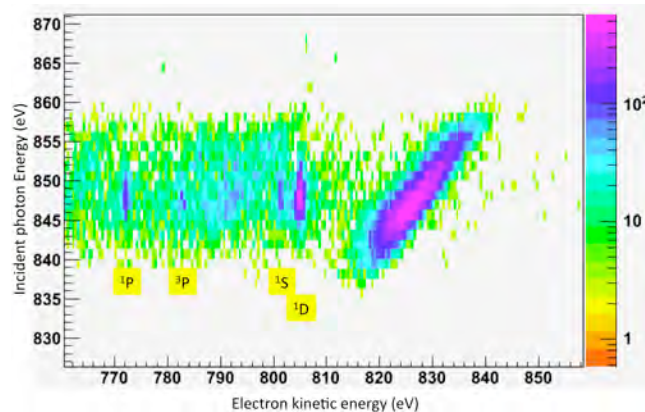


Fig. 2. Electron spectra as a function of photon energy. A 2p vacancy is created by photoionization (shown by diagonal island at right). Subsequent 1s-2p resonance is evidenced by the vertical Auger lines.

Calculations using the LCLS design parameters (10^{13} photons/pulse, 230 fs pulse duration, 1 μm focal diameter) showed that the x-ray peak intensity ($\sim 10^{18}$ W/cm²) is sufficient to induce Rabi oscillations in the 1s-3p transition at 867.1 eV within the 2.4 fs lifetime of 1s vacancy states. Oscillations were predicted to appear in single-shot resonant-Auger-electron line profiles, and averaging over an ensemble of shots produces a distinct broadening of the line profile.

Resonances can be used to enhance x-ray multiphoton processes. At photon energies less than the binding energy of the 1s electron, *resonant* (sequential) two-photon absorption has a significantly larger cross section than *non-resonant* (non-sequential) two-photon absorption; though both generate the same final state of the system - an atom with a 1s hole plus an *s*- or *d*-wave photoelectron. Capitalizing on this resonance phenomenon, we have studied two-photon absorption in neon at 848.6 eV, where, as we have demonstrated, the first photon ionizes the Ne 2p electron and the second photon excites the Ne⁺ 1s-2p resonance. Ne⁺ 1s⁻¹ *K-LL* Auger electrons are the signature of this resonant two-photon creation of a 1s hole (see Fig. 2). This generation of a 2p hole orbital is advantageous for observing/studying the Rabi-cycling phenomenon, because the Ne⁺ 1s-2p dipole matrix element is 5.6 \times larger than that for the 1s-3p transition in Ne.

We have followed the response of the neon atom on the two-photon 1s-2p resonance at 848.6 eV as a function of x-ray FEL pulse width and pulse energy. For narrow x-ray pulses, the signature of 1s hole creation is weak. As the pulse width is increased, the Auger line appears and, at high intensity, is broadened as Rabi-oscillations become important in comparison to the normal diagram line (¹D) measured far above the continuum threshold.

Non-linearity in the x-ray regime at LCLS (G. Doumy, L. Young, E. P. Kanter, B. Krässig, R. Santra³, N. Rohringer⁴, L. F. DiMauro⁵, C. A. Roedig⁵, C. I. Blaga⁵, A. DiChiara⁵, N. Berrah⁶, L. Fang⁶, M. Hoener^{6,7}, P. H. Bucksbaum⁸, J. P. Cryan⁸, S. Ghimire⁸, J. M. Glowia⁸, D. A. Reis⁸, J. D. Bozek⁹, C. Bostedt⁹, M. Messerschmidt⁹)

The very first experiment using the newly available intense femtosecond x-ray pulses at LCLS have made clear that the interaction with atoms is dominated by sequential single photon ionization in competition with Auger and radiative decays. The very high brightness of the x-ray source could also be expressed as an electric field peak intensity reaching values above 10^{17} W/cm², which in the optical domain corresponds to a strong field interaction where the electric field is commensurate with the electronic binding energy. While the situation in the x-ray regime was expected to be very different (for example, there should be no ponderomotive effect in those conditions), LCLS provided nonetheless the first testing ground to try and observe non-linear transitions such as non-sequential two-photon ionization.

Similarly to the previous experiment, our target was neon atoms. The first attempt consisted in looking for ionization of a 1s electron using x-ray pulses with a photon energy far below the *K*-edge (870 eV) and pre-edge resonances. In practice, we used 100 fs pulses at 780 eV, with an intensity estimated around 5×10^{16} W/cm². Two-photon ionization of the *K*-shell electron was to be detected by the Auger electrons emitted during relaxation. Unfortunately, we only observed a small Auger signal explainable by the presence of a very small amount of second harmonic radiation (<0.05%), which is not eliminated by the transport and focusing optics at this wavelength. While it suggests that the intensity was not sufficiently high, arguably the most intense part of the pulse does not interact with neutral atoms, since sequential ionization of the valence electrons is active during the leading edge of the pulse.

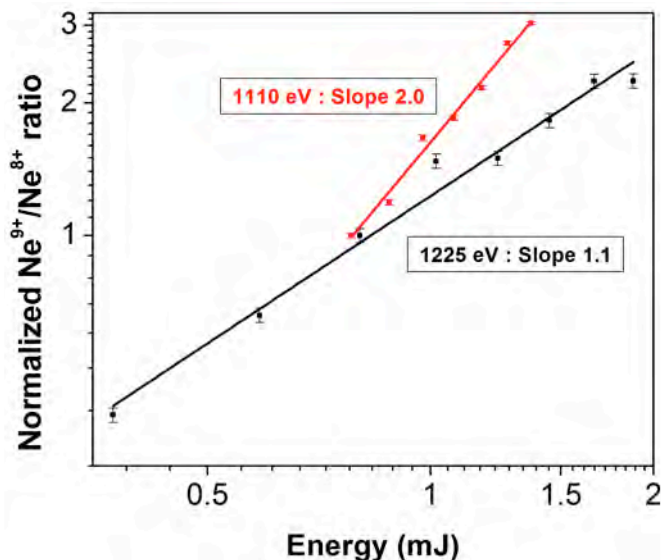


Fig. 3. Ratio of the yields of Ne^{9+} and Ne^{8+} as a function of pulse energy using 1110 eV and 1225 eV x-ray energies.

The fact that atoms could in a single pulse be completely stripped of all energetically accessible electrons provided us with an alternative target: Helium-Like Neon (Ne^{8+}). Its ionization potential (1196 eV) allowed us to tune the photon energy above and below the threshold, while eliminating risks of second harmonic contamination. Studying the evolution of the ratio between Ne^{8+} and Ne^{9+} ions as a function of pulse energy can indicate whether the formation of Ne^{9+} results from a non-linear process or not. The results in Fig. 3 clearly indicate that indeed below the energy threshold, we observe a quadratic behavior. However, calculations with a relatively simple model using rate equations actually show that even below Ne^{8+} ionization threshold, it is possible to produce Ne^{9+} through a sequence of one-photon ionizations involving excited states of Ne^{7+} and Ne^{8+} that has to beat the Auger relaxation, and that it also results in a quadratic behavior for the calculated ratio. In the absence of tested values for the two-photon ionization cross section, it is difficult to establish from our work which mechanism (two-photon or sequence of one-photon) dominates, but nonetheless we can safely conclude that at the intensities currently attained in LCLS experiments, non-linear phenomena are negligible in matters of damage for example.

During the first experimental runs at LCLS, the first attempt at a cross-correlation measurement of x-rays and NIR laser light was made by observing the production of sidebands around the Auger electron spectrum due to the dressing of neon atoms by a strong laser field. In the coming experimental run, we are going to extend this by trying both to characterize the shortest LCLS pulses that LCLS can produce (by extending the sub-optical cycle streak camera method developed in the XUV for attosecond physics) and attempting ultrafast measurements with sub-femtosecond resolution by looking concurrently at the photoline from K -shell ionization and Auger electrons. The hope is that photoionization, happening only during the ultrashort x-ray pulse, can act as a starting clock. Then, temporal information about subsequent processes, in our case Auger decay, would be ‘encoded’ in the energy shift of the electrons. We plan to use light coming from an OPA in the mid-infrared to obtain better time resolution as well as somewhat relaxed constraints on the x-ray pulse duration.

Femtosecond x-ray two-photon photoelectron spectroscopy of organic molecules (S. H. Southworth, E. P. Kanter, B. Krässig, G. Doumy, A. M. March, D. Ray, L. Young, Y. Li¹, S. T.

Pratt², J. Bozek⁹, N. Berrah⁶, P. Bucksbaum⁸, L. DiMauro⁵, R. Santra³, N. V. Kryzhevoi¹⁰, L. S. Cederbaum¹⁰)

Calculational studies have shown that a novel photoelectron spectroscopic technique can be developed using intense, femtosecond x-ray pulses from a free-electron laser in which two photons eject two *K*-shell electrons from one or two atomic sites of a polyatomic molecule [2,14]. In the case of organic molecules such as aminophenol, the LCLS x-ray pulse duration can be short compared with the 5-7 fs lifetimes of *K*-vacancies in the constituent atoms C, N, and O. The second photon can therefore be absorbed prior to Auger decay of the first vacancy and fragmentation of the molecular ion. The second *K*-shell photoelectron provides unique information on the chemical environment and electron-correlation effects that are inaccessible in traditional x-ray photoelectron spectroscopy. After introducing in Ref. [14] the concept of x-ray two-photon photoelectron spectroscopy for probing the inner-shell two-particle Green's function of molecules, detailed *ab initio* calculations were performed on the inner-shell double ionization spectra of ortho-, meta-, and para-aminophenol [2]. An experiment will be conducted at the LCLS to record single-core-hole (one photon) and double-core-hole (two photon) photoelectron and Auger-electron spectra of the aminophenols. Comparisons will be made with the *ab initio* calculations to test and further develop the calculational methods.

Control of x-ray interactions with strong laser fields

Optical control of excitation and decay of core-excited states (S. H. Southworth, G. Doumy, E. P. Kanter, B. Krässig, Y. Li¹, A. M. March, S. T. Pratt², D. Ray, L. Young, R. Santra³, C. Bostedt⁹, J. Bozek⁹, R. Coffee⁹)

Optical control of resonant x-ray absorption was demonstrated theoretically [20,34] and experimentally [11] in the case of Ne $1s^{-1}nl$ ($l = 0, 1, 2, \dots$) core-excited states with 2.4-fs lifetimes. An 800-nm, 10^{13} W/cm² laser couples the Ne $1s^{-1}3p$ and $1s^{-1}3s$ states and gives rise to x-ray transparency at the $1s \rightarrow 3p$ resonance while the laser field is present. Direct excitation of the $1s^{-1}3s$ state by x-ray absorption is dipole forbidden, but the laser field couples it to the $1s^{-1}3p$ state. The $1s \rightarrow 3p$ absorption line splits and a minimum appears in the cross section, thus producing optically controlled x-ray transparency. More generally, the laser dressing field redistributes oscillator strength among the $1s^{-1}nl$ ($l = 0, 1, 2, \dots$) series of states. X-ray transparency was demonstrated at the ALS femtosecond spectroscopy beamline using x-ray absorption through a gas cell of neon [11]. To investigate optical control of core-excited states in greater detail, we have proposed to use LCLS x rays and high-resolution, angle-resolved Auger-electron spectroscopy. The proposed measurements will determine the final states produced by optical coupling of the Ne $1s^{-1}nl$ ($l = 0, 1, 2, \dots$) states. With the x-ray energy tuned near the 867.1-eV nominal energy of the $1s \rightarrow 3p$ resonance, an 800-nm coupling laser will produce a coherent superposition of the $1s^{-1}3p$ and $1s^{-1}3s$ states that are split by 1.88 eV. The populations of the coupled states will be projected onto the final states recorded in the Auger-electron spectra. Auger spectra will be recorded as a function of laser intensity to correlate the laser-mixed and field-free states. The x-ray intensity can be controlled in LCLS experiments by control of the pulse energy, duration, and focal spot size. At x-ray intensities $\sim 10^{18}$ W/cm², Rabi oscillations induced between the Ne ground state and $1s^{-1}3p$ resonance will modify resonant Auger lines [30]. Auger spectra can be recorded from the weak-field regime, where an atom absorbs a single photon, to the strong-field regime where core-state populations are modified by

the intense x-ray field. The goal is to determine how intense optical and x-ray fields, separately and in combination, can control excitation and decay of core-excited states.

Ion hole dynamics in strong-field ionization (L. Greenman¹¹, P. J. Ho, S. Pabst³, E. Kamarchik¹¹, D. Mazziotti¹¹ and R. Santra³)

Atomic and molecular ions generated in a strong optical field generally are not in the electronic ground state. The ion hole dynamics for such ions is characterized by the electronic quantum-state populations and by the coherences among the electronic quantum states. Our previous work [16,35-38] focused on the ion hole dynamics associated with the most outer-valence single-hole states with a total angular momentum of $j = 1/2$ or $j = 3/2$. In Ref. [1], we implement the time-dependent configuration interaction singles (TDCIS) method to include the ionization channels beyond the most outer-valence shells. This method also allows one to take into account of multielectron effects in strong-field ionization. For instance, through the Coulomb interaction, the ionized electron driven strongly by the laser field can affect the ion hole dynamics. In our TDCIS implementation, we add to the exact nonrelativistic many-electron Hamiltonian a radial complex absorbing potential (CAP) to absorb the photoelectron wave packet when it reaches the end of the spatial grid. The orbitals for TDCIS calculation is determined by diagonalizing the sum of the Fock operator and the CAP using a flexible pseudo-spectral grid for the radial degree of freedom and spherical harmonics for the angular degrees of freedom. The CAP is chosen such that the occupied orbitals in the Hartree-Fock ground state remain unaffected. Within TDCIS, the many-electron wave packet is expanded in terms of the Hartree-Fock ground state and its single excitations. The virtual orbitals satisfy non-standard orthogonality relations, which must be taken into consideration in the calculation of the dipole and Coulomb matrix elements required for the TDCIS equations of motion. We employ a stable propagation scheme derived by second-order finite differencing of the TDCIS equations of motion in the interaction picture and subsequent transformation to the Schrödinger picture. Using the TDCIS wave packet, we calculate the expectation value of the dipole acceleration and the reduced density matrix of the residual ion. These calculated quantities thus allow one to study electronic channel-coupling effects in strong-field processes.

Ultrafast x-ray probes of photoinduced dynamics

X-ray scattering from 3-D aligned asymmetric molecules—theory (S. Pabst³, P. J. Ho, R. Santra³)

In previous theoretical [21,29,33] and experimental [32] studies of laser alignment, we used linearly polarized laser pulses to prepare small, spatially aligned molecules for x-ray studies. With linearly polarized laser pulses, the molecules can be aligned along their most polarizable axis, but one has no control over the rotational motion along this axis. The ability to overcome this limitation will open the door for three-dimensional structural studies of asymmetric molecules. It has been shown that an elliptically polarized pulse or two linearly polarized pulses can be used to create an ensemble of three-dimensionally aligned molecules [39]. In Ref. [10], we theoretically and numerically analyze x-ray scattering from asymmetric-top molecules three-dimensionally aligned using elliptically polarized laser light. A rigid-rotor model is assumed. The principal axes of the polarizability tensor are assumed to coincide with the principal axes of the moment of inertia tensor. Several symmetries in the Hamiltonian are identified and exploited to enhance the efficiency of solving the time-dependent Schrödinger

equation for each rotational state initially populated in a thermal ensemble. Using a phase-retrieval algorithm, the feasibility of structure reconstruction from a quasi-adiabatically aligned sample is illustrated for the organic molecule naphthalene. The spatial resolution achievable strongly depends on the laser parameters, the initial rotational temperature, and the x-ray pulse duration. We demonstrate that for a laser peak intensity of 5 TW/cm^2 , a laser pulse duration of 100 ps, a rotational temperature of 10 mK, and an x-ray pulse duration of 1 ps, the molecular structure may be probed at a resolution of 1 Angstrom (see Fig. 4).

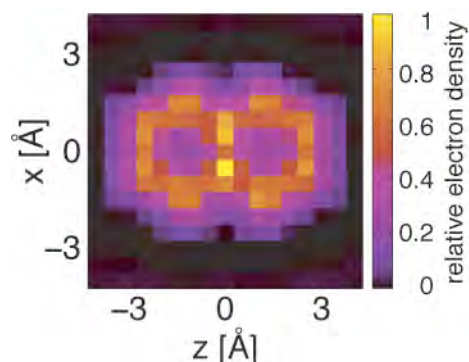


Fig. 4. Structure of naphthalene reconstructed from the diffraction signals obtained from 10-mK molecules exposed to 1-ps x-ray pulse and 100-ps laser pulse.

X-ray scattering from laser-aligned molecules—experiment (G. Doumy, P. J. Ho, E. P. Kanter, B. Krässig, A. M. March, D. Ray, R. Santra³, S. H. Southworth, L. Young, T. J. Graber¹², R. W. Henning¹²)

This work builds upon our previous demonstration of an x-ray microprobe of laser-aligned bromotrifluoromethane (CF_3Br) molecules [32]. As in the previous work, the duration of the x-ray probe pulse is ~ 100 ps, which is of similar magnitude as molecular rotational periods, and TW laser pulses with ~ 100 ps duration at 1 kHz are used to produce quasi-adiabatic molecular alignment in a gaseous sample cooled by supersonic expansion. Whereas in our previous work the x-ray probe was based on resonant x-ray absorption and fluorescence detection, the goal of this work is to collect diffraction patterns of coherently scattered x-rays from laser aligned ensembles of molecules, guided by theoretical predictions made in our group [10,13,21].

The cross section for coherent x-ray scattering is orders of magnitude lower than that of resonant absorption and a demonstration of coherent scattering from a molecular beam requires significantly higher x-ray flux and sample density than in the work of Ref. [32]. We have therefore built a new target chamber for use at the high flux beamline APS Sector 14-ID-B (two in-line undulators and pink beam operation, $\Delta E/E \sim 2\%$, 10^{10} photons per pulse). The chamber design incorporates a skimmed molecular beam target with a pulsed nozzle and a 60° viewing angle for forward scattered x-rays. Scattered x-rays are collected by the Sector 14 Mar 165 high-resolution CCD detector. The chamber is mounted on a specially designed table with 5 motorized degrees of freedom that can be wheeled into the tight space of the 14-ID-B hutch to straddle the existing table with minimal disturbance to the equipment for macromolecular crystallography located at this beamline. The setup incorporates a set of two 100-mm length Kirkpatrick-Baez mirrors to refocus the x-ray beam to about $20 \times 40 \mu\text{m}^2$ at the intersection of the x-ray beam and the molecular beam. The existing Spitfire Ti:Sapphire laser system was modified

such that the uncompressed output could be directly transported to our new experimental setup, providing a beam of 800-nm, 4.5-mJ laser pulses of ~ 150 ps duration at 1 kHz. A first experimental run with this setup, using a cw gas nozzle and without the aligning laser, provided x-ray scattering images for CF_3Br , but also revealed the need to reduce scattered x-rays from slits and windows in the beam path. Preparations for our next beam time include improvements in beam collimation, laser beam controls, setting up diagnostics for beam overlap, and characterizing the pulsed molecular beam source.

High-repetition-rate laser and x-ray experiments (A. M. March, A. Stickrath², S. H. Southworth, E. P. Kanter, B. Krässig, G. Doumy, D. Ray, L. X. Chen^{2,13}, L. Young, T. C. Briles¹⁴, D. Yost¹⁴, T. Schibli¹⁴, J. Ye¹⁴)

Tunable, polarized, x-ray pulses from synchrotron-based sources provide a route to observing molecular motion on picosecond timescales and Angstrom length scales. Due to the high stability, brightness (10^{13} photons/s/0.01% bandwidth) and MHz repetition rates, synchrotron sources enable the acquisition of data with good statistics. However, due to the mismatch in the repetition rates of intense laser pulses (~ 1 -5 kHz) and synchrotron x-ray pulses (6.5 MHz at APS), it has been difficult to achieve high statistics for laser-pump/x-ray probe experiments that track transient states of matter following a controlled excitation from equilibrium. To remedy this, we have implemented a high repetition rate (variable between 50 kHz and 6.5 MHz), 10-W laser system at the 7ID beamline of the Advanced Photon Source. Laser pulses at 1.06 μm wavelength and either 10 ps or 130 ps duration are synchronized to the storage ring RF signal with a precision of 250 fs. Nonlinear optical techniques provide laser radiation of other colors. Early applications are to study and control gas-phase atoms and molecules in strong optical fields and to study photoinduced structural dynamics of solvated molecules.

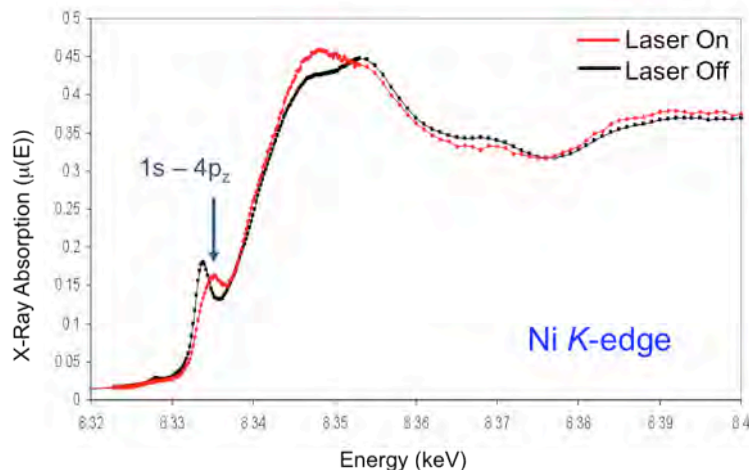


Fig. 5. Transient x-ray absorption spectrum of photo-excited nickel porphyrin

In our first experiment, a liquid jet of a 2-mM solution of nickeltetramesitylporphyrin (NiTMP) in toluene was photoexcited with 532-nm, 10-ps, 6- μJ pulses at 135 kHz and the transient x-ray absorption spectrum was recorded across the Ni *K*-edge (see Fig. 5). The transient absorption spectrum was measured by recording Ni *K-L* x-ray fluorescence pulses gated on one of the 24 electron bunches in the storage ring. X-ray pulses from the single bunch passed through the liquid jet at 271 kHz, and every other pulse was gated "laser-on" in synchronization

with the 135 kHz laser pulses. A laser/x-ray time-delay scan of the laser-on/laser-off ratio at the $1s \rightarrow 4p_z$ feature indicated in Fig. 5 is consistent with the 200-ps lifetime of the laser-induced T_1 triplet state [40]. X-ray absorption fine structure (EXAFS) of photo-excited NiTMP was recorded in addition to the near-edge structure shown in Fig. 5.

A long-term goal of this research project is to utilize passive enhancement cavities as demonstrated by the JILA group [41-43] to increase intra-cavity pulse energies by a factor of ~ 100 . Increased pulse energies will enable laser-pump/x-ray probe experiments at the full 6.5-MHz repetition rate of the APS. High repetition-rate techniques will also make optimum use of the ~ 1 -ps pulses that will be produced at the Short Pulse X-ray (SPX) facility planned for the APS Upgrade and described below.

X-ray imaging of trapped nanoparticles (M. Pelton¹⁵, N. Scherer¹¹, J. Sweet¹⁵, P. Ho, T. Graber¹², G. Doumy, D. Ray, L. Young, AMO Group)

Beyond x-ray diffraction imaging of ensembles of laser-aligned molecules in the gas phase we propose to use an x-ray microprobe to image a single trapped and aligned nanoparticle in solution. Atomic level imaging of a nanoparticle in its native environment, in the presence of water background, with laser trapping to confine the particle such that dynamics on a nanometer scale could be monitored: all of these would represent major steps forward from the present status of x-ray imaging of single nanoparticles fixed to a solid support. Pelton and Scherer have developed a new approach to manipulate single and few nanoparticles that has the potential to arrange particles into designed assemblies [44]. Anisotropic metal nanoparticles, such as those shown in Fig. 6, can be held stably in an optical trap for several minutes, and have their long axis aligned with the linear polarization of the trapping laser. Using x-ray diffraction to determine the structure of a trapped metal nanoparticle will demonstrate the necessary principles required for x-ray structure determination of single trapped macromolecules. Initially, single silver nanowires on a thin membrane will be studied as a proof of principle on Sector 14, where a high single pulse photon flux and a co-located picosecond laser system is available for studies of laser-induced nanoparticle melting.

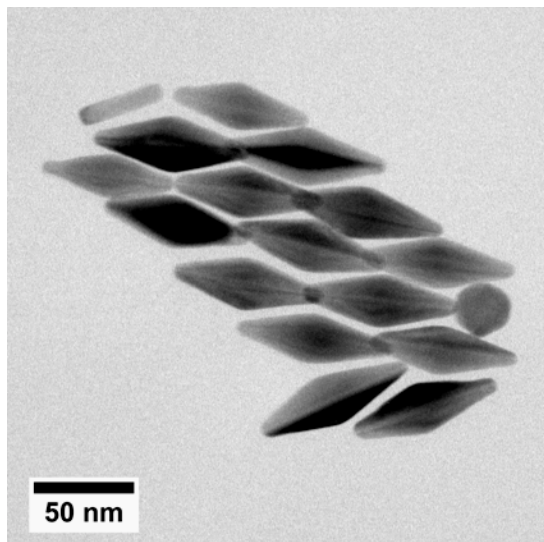


Fig. 6. A transmission-electron microscope (TEM) image of a small array of Au bipyramid nanoparticles. This arrangement formed spontaneously upon drying a solution of particles on the carbon-grid substrate.

Interatomic Coulombic Decay (ICD) in xenon difluoride (R. W. Dunford, E. P. Kanter, B. Krässig, R. Santra³, S.H. Southworth, L. Young)

Absorption of an x-ray gives rise to excitation or ionization of an inner-shell electron. The resulting vacancy is quickly filled and generally results in a cascade of x-ray and Auger transitions. The different possible decay paths lead to a range of possible final charge states. If this occurs in an atom that is part of a molecule or cluster, it can cause loss of valence electrons not localized on the central atom and produce two or more charge centers. This is then followed by a Coulomb explosion of the system. The process, termed Interatomic Coulombic Decay (ICD), was observed by Morishita, *et al.* [45] in experiments on argon dimers. Our work was motivated by a theoretical study of ICD in XeF_n molecules by Buth, Santra and Cederbaum [46]. The main point is that ICD leads to the production of more positive charges per absorbed x-ray photon and boosts damage in materials when they are exposed to x rays. To explore this process, we compared the charge states produced following inner-shell photoionization of isolated Xe atoms and the Xe atoms in xenon difluoride XeF_2 . The goal of the experiment was to gain an understanding of ICD and explore potential practical implications relating to material damage.

In the experiment, a beam of either Xe or XeF_2 was directed across a 35 keV x-ray beam from the Advanced Photon Source (APS). The x-rays had sufficient energy to photoionize the K-shell of Xe. Fluorescence from the resulting inner-shell vacancy decays was observed by a Ge x-ray spectrometer. These photons also provided the start signal for determining the ion time-of-flight TOF. Using a trick, we were able to get time resolution much better than that normally expected from a Ge detector. The idea is based on the fact that the bunches from the APS have excellent timing characteristics. We simply identify the particular bunch associated with the event, and correct the start time to correspond to the arrival of that bunch. This allows us to obtain sharp TOF peaks. A multi-hit position sensitive detector was used to detect the ions. The mass and charge states of the ions are determined by measuring the ion TOF. Using the x-ray energy measured by the Ge detector to tag the initial state, we determine the changes in the ion charge state distributions as a function of the initial hole state.

The data analysis for this experiment is still in progress but initial work shows an interesting result for a subset of events which are triple coincidences involving a F^{2+} ion, a F^{3+} ion, and a Xe^{q+} ion of charge q . The center of the distribution of the total charge of these three fragments is higher than the center of the charge state distribution of the atomic Xe target by more than two charge states. Theoretical modeling will be required to determine if this shift is due to ICD. Other subsets of data show similar results. In the future, we can extend this study to more complicated systems such as XeF_4 which will provide further insight into the ICD process.

Short pulse x rays at the Advanced Photon Source (L. Young, P. G. Evans¹⁶, L. X. Chen^{2,13}, R. Clarke¹⁷, M. Beno¹, E. M. Dufresne¹, D. Keavney¹, Y. Li¹, D. R. Reis⁸, S. H. Southworth, D. Tiede², D. Walko¹, AMO Group, XSD staff)

The Short Pulse X-ray (SPX) facility will extend time-resolved x-ray scattering and spectroscopy to the picosecond timescale while retaining the powerful characteristics of synchrotron radiation, i.e. user-controlled continuous tunability of energy, polarization and bandwidth combined with exquisite x-ray energy and pulse length stability over a wide energy range. Experiments at the SPX will produce one picosecond stroboscopic snapshots of molecular rotations, molecular excited state transition structures, stress/strain wave propagation, magnetic domain wall dynamics, phase transitions and the coupling between electronic, vibrational and magnetic degrees of freedom in condensed matter systems. Transformational

developments are now taking place in high-average-power pulsed laser technology, with substantially increased repetition rates that promise to make highly efficient use of the MHz x-ray repetition rates of the SPX. The SPX is an important component of the APS Upgrade, which was granted Critical Decision 0 on April 22, 2010.

High-repetition-rate, synchrotron-based, short x-ray pulses are produced at the SPX using the innovative method of rf-deflection of the stored electron bunches to allow efficient temporal slicing of the relatively long (~100 ps) x-ray pulses at the full repetition rate of the storage ring. This method was originally proposed by Zholents *et al.* [47] and simulated for the Advanced Photon Source (APS) storage ring lattice by Borland [48]. Two rf-deflection cavities are used: first to induce a correlation between the longitudinal position of an electron within the bunch and its vertical momentum, i.e. a chirp, and second to undo the chirp, such that the electron trajectory around the remainder of the storage ring is unaffected. Between the two cavities, variable duration x-ray pulses can be selected by slitting the x-ray beam and/or adjusting the rf-deflection voltage. The SPX rf-cavities will be placed in the downstream end of Sector 6 and the upstream end of Sector 8, respectively. Since both Sectors 6 and 8 are slated for 8-m long straight sections, they can accommodate standard undulators of 2.4-m length in addition to the rf-deflection cavities. The straight section and bending magnet of Sector 7 will have the chirped electron beam and produce short-duration x-ray pulses.

The planned SPX experimental facilities consist of 4 independently operating end stations providing time-resolved diffraction, microscopy, spectroscopy with hard and soft x-rays, and a novel time-dispersed diffraction capability. The facilities will consist of 3 beamlines. Two of the SPX beamlines will use radiation from canted undulators in a standard 4.8 m straight section. A third will use a bending magnet source. An energy range of 4 to 35 keV on the hard x-ray insertion device beamlines will be available to address a variety of chemical, molecular and materials science experiments. An energy range of 200-2000 eV will be available at the soft x-ray beamline. Figure 7 shows the beamline layout and experimental control rooms associated with the SPX experimental facilities.

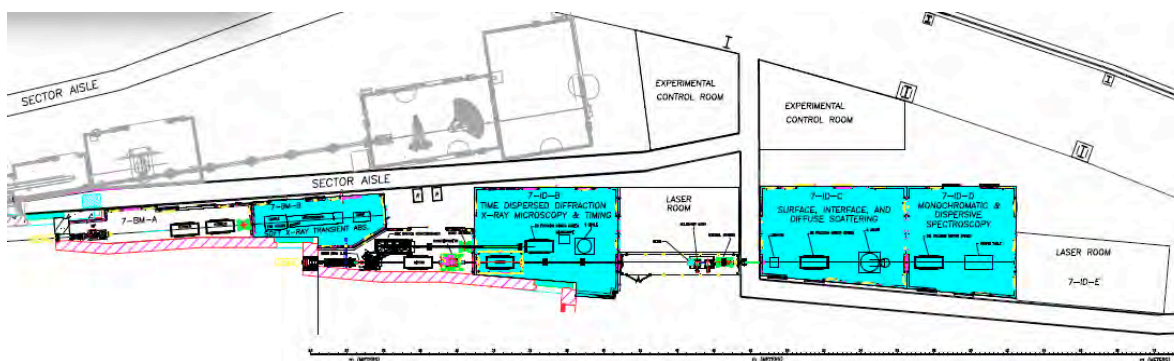


Fig 7. Proposed layout for the Short-Pulse X-ray Facility. Four independent end stations for short-pulse x-ray studies are planned. Canted undulators in the Sector 7 straight section provide independent sources for the 7-ID-C/D and 7-ID-B insertion device beamlines. The Sector 7 bending magnet will deliver soft x-rays. Experiments with 100-ps pulses will continue on adjacent sectors.

Affiliations of collaborators

- ¹X-Ray Science Division, Argonne National Laboratory
²Chemical Sciences and Engineering Division, Argonne National Laboratory
³Present address: CFEL at DESY, Hamburg, Germany
⁴Lawrence Livermore National Laboratory, Livermore, CA
⁵Ohio State University, Columbus, OH
⁶Western Michigan University, Kalamazoo, MI
⁷Lawrence Berkeley National Laboratory, Berkeley, CA
⁸PULSE Center, SLAC, Stanford, CA
⁹Linac Coherent Light Source, SLAC, Stanford, CA
¹⁰University of Heidelberg, Heidelberg, Germany
¹¹University of Chicago, Chicago, IL
¹²BioCARS, University of Chicago, IL
¹³Northwestern University, Evanston, IL
¹⁴JILA, University of Colorado, Boulder, CO
¹⁵Center for Nanoscale Materials, Argonne National Laboratory
¹⁶University of Wisconsin, Madison, WI
¹⁷University of Michigan, Ann Arbor, MI

Publications (2008 - 2010)

- [1] L. Greenman, P. J. Ho, S. Pabst, E. Kamarchik, D. A. Mazziotti, and R. Santra, "Implementation of the time-dependent configuration interaction singles method for atomic strong-field processes," *Phys. Rev. A*, accepted (2010).
- [2] N. V. Kryzhevoi, R. Santra, and L. S. Cederbaum, "Inner-shell single and double ionization potentials of aminophenol isomers," *J. Chem. Phys.*, submitted (2010).
- [3] E. Goulielmakis, Z.-H. Loh, A. Wirth, R. Santra, N. Rohringer, V. S. Yakovlev, S. Zherebtsov, T. Pfeifer, A. M. Azzeer, M. F. Kling, S. R. Leone, and F. Krausz, "Real-time observation of valence electron motion," *Nature*, accepted (2010).
- [4] L. Fang, M. Hoener, O. Gessner, F. Tarantelli, S. T. Pratt, O. Kornilov, C. Buth, M. Gühr, E. P. Kanter, C. Bostedt, J. D. Bozek, P. H. Bucksbaum, M. Chen, R. Coffee, J. Cryan, M. Glownia, E. Kuk, S. R. Leone, and N. Berrah, "Double core hole production in N₂: beating the Auger clock," *Phys. Rev. Lett.*, in press (2010).
- [5] J. P. Cryan, J. M. Glownia, J. Andreasson, A. Belkacem, N. Berrah, C. I. Blaga, C. Bostedt, J. Bozek, C. Buth, L. F. DiMauro, L. Fang, O. Gessner, M. Guehr, J. Hajdu, M. P. Hertlein, M. Hoener, O. Kornilov, J. P. Marangos, A. M. March, B. K. McFarland, H. Merdji, V. Petrovic, C. Raman, D. Ray, D. Reis, F. Tarantelli, M. Trigo, J. White, W. White, L. Young, P. H. Bucksbaum, and R. N. Coffee, "Auger electron angular distribution of double core hole states in the molecular reference frame," *Phys. Rev. Lett.*, in press (2010).
- [6] J. M. Glownia, J. Cryan, J. Andreasson, A. Belkacem, N. Berrah, C. I. Blaga, C. Bostedt, J. Bozek, L. F. DiMauro, L. Fang, J. Frisch, O. Gessner, M. Gühr, J. Hajdu, M. P. Hertlein, M. Hoener, G. Huang, O. Kornilov, J. P. Marangos, A. M. March, B. K. McFarland, H. Merdji, V. S. Petrovic, C. Raman, D. Ray, D. A. Reis, M. Trigo, J. L. White, W. White, R. Wilcox, L. Young, R. N. Coffee, and P. H. Bucksbaum, "Time-resolved pump-probe experiments at the LCLS," *Optics Express*, submitted (2010).
- [7] L. Young, E. P. Kanter, B. Krässig, Y. Li, A. M. March, S. T. Pratt, R. Santra, S. H. Southworth, N. Rohringer, L. F. DiMauro, G. Doumy, C. A. Roedig, N. Berrah, L. Fang, M. Hoener, P. H. Bucksbaum, J. P. Cryan, S. Ghimire,

J. M. Glowia, D. A. Reis, J. D. Bozek, C. Bostedt, and M. Messerschmidt, "Femtosecond electronic response of atoms to ultra-intense x-rays," *Nature* **466**, 56 (2010).

[8] M. Hoener, L. Fang, O. Kornilov, O. Gessner, S. T. Pratt, M. Gühr, E. P. Kanter, C. Blaga, C. Bostedt, J. D. Bozek, P. H. Bucksbaum, C. Buth, M. Chen, R. Coffee, J. Cryan, L. DiMauro, M. Glowia, E. Hosler, E. Kukk, S. R. Leone, B. McFarland, M. Messerschmidt, B. Murphy, V. Petrovic, D. Rolles, and N. Berrah, "Ultra-intense x-ray induced ionization, dissociation, and frustrated absorption in molecular nitrogen," *Phys. Rev. Lett.* **104**, 253002 (2010).

[9] S. Pabst and R. Santra, "Alignment of asymmetric-top molecules using multiple-pulse trains," *Phys. Rev. A* **81**, 065401 (2010).

[10] S. Pabst, P. J. Ho, and R. Santra, "Computational studies of x-ray scattering from three-dimensionally-aligned asymmetric-top molecules," *Phys. Rev. A* **81**, 043425 (2010).

[11] T.E. Glover, M.P. Hertlein, S.H. Southworth, T.K. Allison, J. van Tilborg, E.P. Kanter, B. Krässig, H. R. Varma, B. Rude, R. Santra, A. Belkacem, and L. Young. "Controlling x-rays with light", *Nature Phys.* **6**, 69 (2010).

[12] H. R. Varma, M. F. Ciappina, N. Rohringer, and R. Santra, "Above-threshold ionization in the x-ray regime," *Phys. Rev. A* **80**, 053424 (2009).

[13] P. J. Ho, D. Starodub, D. K. Saldin, V. L. Shneerson, A. Ourmazd, and R. Santra, "Molecular structure determination from x-ray scattering patterns of laser-aligned symmetric-top molecules," *J. Chem. Phys.* **131**, 131101 (2009).

[14] R. Santra, N. V. Kryzhevoi, and L. S. Cederbaum, "X-ray two-photon photoelectron spectroscopy: A theoretical study of inner-shell spectra of the organic para-aminophenol molecule," *Phys. Rev. Lett.* **103**, 013002 (2009).

[15] B. Krässig, R.W. Dunford, E. P. Kanter, E. C. Landahl, S.H. Southworth, and L. Young, "A simple cross-correlation technique between infrared and hard x-ray pulses," *Applied Physics Letters* **94**, 171113 (2009).

[16] N. Rohringer and R. Santra, "Multichannel coherence in strong-field ionization," *Phys. Rev. A* **79**, 053402 (2009).

[17] P. J. Ho, M. R. Miller, and R. Santra, "Field-free molecular alignment for studies using x-ray pulses from a synchrotron radiation source," *J. Chem. Phys.* **130**, 154310 (2009).

[18] L. Young, R. W. Dunford, E. P. Kanter, B. Krässig, R. Santra, S. H. Southworth, "Strong-field control of x-ray processes," In *Pushing the Frontiers of Atomic Physics: Proceedings of the XXI International Conference on Atomic Physics*, R. Côté, P.L. Gould, M. Rozman and W.W. Smith, Eds., World Scientific Publishing Co., NJ, Singapore (2009), p. 344-353.

[19] R. Santra, "Concepts in x-ray physics," *J. Phys. B* **42**, 023001 (2009).

[20] H. R. Varma, L. Pan, D. Beck, and R. Santra, "X-ray absorption near-edge structure of laser-dressed neon," *Phys. Rev. A* **78**, 065401 (2008).

[21] P. J. Ho and R. Santra, "Theory of x-ray diffraction from laser-aligned symmetric-top molecules," *Phys. Rev. A* **78**, 053409 (2008).

[22] A. S. Sandhu, E. Gagnon, R. Santra, V. Sharma, W. Li, P. Ho, P. Ranitovic, C. L. Cocke, M. M. Murnane, and H. C. Kapteyn, "Observing the creation of electronic Feshbach resonances in soft x-ray-induced O₂ dissociation," *Science* **322**, 1081 (2008).

[23] I. A. Sulai, Q. Wu, M. Bishof, G. W. F. Drake, Z.-T. Lu, P. Mueller, and R. Santra, "Hyperfine suppression of $2^3S_1 - 3^3P_J$ transitions in ^3He ," *Phys. Rev. Lett.* **101**, 173001 (2008).

[24] L. Young, C. Buth, R.W. Dunford, P. Ho, E.P. Kanter, B. Krässig, E.R. Peterson, N. Rohringer, R. Santra, and S.H. Southworth. "Using strong electromagnetic fields to control x-ray processes" Proceedings of the Pan-American Advanced Studies Institute, Buzios, Brazil 2008, in press *Revista Mexicana de Fisica*.

[25] C. Buth, R. Santra, and L. Young. "Refraction and absorption of x-rays by laser-dressed atoms," Proceedings of the Pan-American Advanced Studies Institute, Buzios, Brazil, 2008, in press *Revista Mexicana de Fisica*.

[26] P. Ho and R. Santra, "Theory of x-ray diffraction by laser-aligned molecules," Proceedings of the Pan-American Advanced Studies Institute, Buzios, Brazil, 2008, in press *Revista Mexicana de Fisica*.

[27] C. Buth and R. Santra, "X-ray refractive index of laser-dressed atoms," *Phys. Rev. A* **78**, 043409 (2008).

[28] E. P. Kanter, R. Santra, C. Hoehr, E. R. Peterson, J. Rudati, D. A. Arms, E. M. Dufresne, R. W. Dunford, D. L. Ederer, B. Kraessig, E. C. Landahl, S. H. Southworth, and L. Young, "Characterization of the spatiotemporal evolution of laser-generated plasmas," *J. Appl. Phys.* **104**, 073307 (2008).

[29] C. Buth and R. Santra, "Rotational molecular dynamics of laser-manipulated bromotrifluoromethane studied by x-ray absorption," *J. Chem. Phys.* **129**, 134312 (2008).

[30] N. Rohringer and R. Santra, "Resonant Auger effect at high x-ray intensity," *Phys. Rev. A* **77**, 053404 (2008).

[31] R. Santra, R. W. Dunford, E. P. Kanter, B. Kraessig, S. H. Southworth, and L. Young, "Strong-field control of x-ray processes," *Advances in Atomic, Molecular, and Optical Physics* **56**, 219 (2008).

[32] E. R. Peterson, C. Buth, D. A. Arms, R. W. Dunford, E. P. Kanter, B. Kraessig, E. C. Landahl, S. T. Pratt, R. Santra, S. H. Southworth, and L. Young, "An x-ray probe of laser-aligned molecules," *Appl. Phys. Lett.* **92**, 094106 (2008).

[33] C. Buth and R. Santra, "Theory of x-ray absorption by laser-aligned symmetric-top molecules," *Phys. Rev. A* **77**, 013413 (2008).

Other cited references

[34] C. Buth, R. Santra, and L. Young, "Electromagnetically induced transparency for x rays," *Phys. Rev. Lett.* **98**, 253001 (2007).

[35] L. Young, D. A. Arms, E. M. Dufresne, R. W. Dunford, D. L. Ederer, C. Höhr, E. P. Kanter, B. Krässig, E. C. Landahl, E. R. Peterson, J. Rudati, R. Santra, and S. H. Southworth, "X-Ray Microprobe of Orbital Alignment in Strong-Field Ionized Atoms," *Phys. Rev. Lett.* **97**, 083601 (2006).

[36] C. Höhr, E. R. Peterson, N. Rohringer, J. Rudati, D. A. Arms, E. M. Dufresne, R. W. Dunford, D. L. Ederer, E. P. Kanter, B. Kraessig, E. C. Landahl, R. Santra, S. H. Southworth, and L. Young, "Alignment dynamics in a laser-produced plasma," *Phys. Rev. A* **75**, 011403(R) (2007).

[37] Z.-H. Loh, M. Khalil, R. E. Correa, R. Santra, C. Buth, and S. R. Leone, "Quantum state-resolved probing of strong-field-ionized xenon atoms using femtosecond high-order harmonic transient absorption spectroscopy," *Phys. Rev. Lett.* **98**, 143601 (2007).

[38] S. H. Southworth, D. A. Arms, E. M. Dufresne, R. W. Dunford, D. L. Ederer, C. Höhr, E. P. Kanter, B. Kraessig, E. C. Landahl, E. R. Peterson, J. Rudati, R. Santra, D. A. Walko, and L. Young, "K-edge x-ray absorption spectroscopy of laser-generated Kr^+ and Kr^{2+} ," *Phys. Rev. A* **76**, 043421 (2007).

- [39] J. J. Larsen, *et al.*, Phys. Rev. Lett. 85, 2470 (2000); J. G. Underwood, *et al.*, Phys. Rev. Lett. 94, 143002 (2005); K. F. Lee, *et al.*, Phys. Rev. Lett. 97, 173001 (2006).
- [40] L. X. Chen, X. Zhang, E. C. Wasinger, K. Attenkofer, G. Jennings, A. Z. Muresan, and J. S. Lindsey, "Tracking electrons and atoms in a photoexcited metalloporphyrin by x-ray transient absorption spectroscopy," J. Am. Chem. Soc. **129**, 9616 (2007).
- [41] R. J. Jones and J. Ye, "Femtosecond pulse amplification by coherent addition in a passive optical cavity," Opt. Lett. **27**, 1848 (2002).
- [42] E. O. Potmas, C. Evans, X. S. Xie, R. J. Jones, and J. Ye, "Picosecond-pulse amplification with an external passive optical cavity," Opt. Lett. **28**, 1835 (2003).
- [43] R. J. Jones, K. D. Moll, M. J. Thorpe, and J. Ye, "Phase-coherent frequency combs in the vacuum ultraviolet via high-harmonic generation inside a femtosecond enhancement cavity," Phys. Rev. Lett. **94**, 193201 (2005).
- [44] M. Pelton, M. Liu, H. Y. Kim, G. Smith, P. Guyot-Sionnest, and N. F. Scherer, "Optical trapping and alignment of single gold nanorods by using plasmon resonances," Opt. Lett. **31**, 2075 (2006).
- [45] Y. Morishita *et al.*, "Experimental evidence of interatomic Coulombic decay from the Auger final states in argon dimers," Phys. Rev. Lett. **96**, 243402 (2006).
- [46] C. Buth, R. Santra, and L. S. Cederbaum, "Impact of interatomic electronic decay processes on Xe 4d hole decay in the xenon fluorides," J. Chem. Phys. **119**, 10575 (2003).
- [47] A. Zholents, P. Heimann, M. Zolotarev, and J. Byrd, "Generation of subpicosecond x-ray pulses using RF orbit deflection," Nucl. Instrum. Methods Phys. Res. A **425**, 385 (1999).
- [48] M. Borland, "Simulation and analysis of using deflecting cavities to produce short x-ray pulses with the Advanced Photon Source," Phys. Rev. ST Accel. Beams **8**, 074001 (2005).

J.R. MACDONALD LABORATORY - OVERVIEW 2010

The J.R. Macdonald Laboratory focuses on the interaction of intense laser pulses with matter — specifically, observing and controlling single atoms and molecules on short time scales. The eventual goal is to make this time scale the natural one on which the electrons move in matter. Doing so will add to our existing capability to trace nuclear motion in molecules using femtosecond laser pulses. All of these activities build towards the ultimate goal of understanding the dynamical processes of reactions well enough to control them. To this end, we are advancing theoretical modeling and computational approaches as well as experimental techniques and taking advantage of our expertise in particle imaging techniques (such as COLTRIMS, VMI, MDI, etc.). Most of our research projects¹ are associated with one of the two themes: “Attosecond Physics” and “Control”. The boundary between these themes, however, is sometimes not well defined. A few examples are briefly mentioned below.

1) **Attosecond physics:** The goal of the efforts under this theme is to follow, in real time, electronic motion in atoms and molecules. However, attosecond pulses can also serve as very precise triggers or probes of the femtosecond-scale nuclear motion in molecules. We have characterized the temporal shape of single, 140 attosecond pulses generated by the generalized double optical gating method and demonstrated attosecond pulse generation with arbitrary carrier-envelope phase driving pulses. We have employed these pulses in time-resolved studies of autoionization of Ar atoms. Using an attosecond pulse train in an EUV/infrared pump-probe scheme, we have explored He and D₂ ionization. The quantitative re-scattering theory simplifies the interpretation of spectra from experiments combining attosecond pulse trains with infrared pulses, such as in the He experiment mentioned above. It has also been applied successfully to many other scenarios involving high harmonic generation and the related phenomenon of electron rescattering. Further, we have followed theoretically the dissociative ionization of H₂ in an attosecond pulse train and delayed infrared laser pulse.

2) **Control:** Methods for controlling the motion of heavy particles in small molecules continue to be developed. Theoretically, the ability to control the dissociation of molecules (e.g., H₂⁺) into different final channels has been investigated using pulse pairs or the carrier-envelope phase. Experimentally, we have used a $\omega+2\omega$ field to localize the electron on a specific nucleus of a dissociating D₂⁺ in experiments on D₂ and D₂⁺ beams. We have also controlled the final product in the dissociation of an HD⁺ beam and oriented CO molecules, using the phase between the two colors as a control knob. Theory support was essential for the interpretation of these phenomena. We have improved our ability to align asymmetric top molecules and measure their degree of alignment using optical methods as well as single-shot VMI. We have studied an atomic ladder system with a finite pulse train and explored it with a free-running oscillator.

In addition to the laser related research, we have conducted some collision studies using our high- and low-energy accelerators. Some of this work is conducted in collaboration with visiting scientists (for example, S. Lundeen, J. Shinpaugh & L. Toburen, E. Wells).

Like the visitors benefiting from the use of our facilities, we pursue several outside collaborations at other facilities and with other groups (e.g., ALS, Århus, Auburn University, University of Colorado, FLASH, LCLS, Max-Planck Institutes for Quantum Optics and Kernphysik, Sao Carlos, Tokyo, Weizmann Institute of Science, and others).

¹Details of the projects are provided in the individual contributions of the PIs: *I. Ben-Itzhak, Z. Chang, C.L. Cocke, B.D. DePaola, B.D. Esry, V. Kumarappan, C.D. Lin, and U. Thumm.*

Finally, it is hard to summarize this year without mentioning the removal of the LINAC — after about 20 years of service — to make room for expanding our laser facility. The laser facilities are being reorganized to make room for a new 10 kHz laser system and to optimize the space for the new experimental faculty in the lab, including the recent hire of Carlos Trallero as an assistant professor in our department. The Lab is in a transition period now, and we are confident that our recent hires and plans for our facility and group will maintain the strong tradition of the Macdonald Lab.

Structure and Dynamics of Atoms, Ions, Molecules, and Surfaces: Molecular Dynamics with Ion and Laser Beams

Itzik Ben-Itzhak, J. R. Macdonald Laboratory, Kansas State University
Manhattan, KS 66506; ibi@phys.ksu.edu

The goal of this part of the JRML program is to study the different mechanisms for molecular fragmentation initiated by ultrashort intense laser pulses or following fast or slow collisions. To this end we typically use molecular ion beams as the subject of our studies and have a close collaboration between theory and experiment. Examples of our recent work are given below.

Controlled dissociation of a molecular ion beam using intense two-color laser fields

We have achieved control of the dissociation of the benchmark H_2^+ molecule using a two-color field. Of particular interest is the first observation of channel asymmetry upon dissociation of HD^+ by such a field. On the technical side this experiment is the first of its kind demonstrating that “pump-probe” experiments may be feasible in spite of the very low density of ion beam targets. In another experiment we provide clear evidence for the elusive “zero-photon dissociation” of H_2^+ – a process driven by “two colors” within the laser bandwidth.

Two-color (ω - 2ω) control, J. McKenna, D. Ursrey, D. Ray, B. Gaire, M. Zohrabi, J. Hernandez, F. Anis, K.D. Carnes, C.L. Cocke, B.D. Esry, and I. Ben-Itzhak – Electron localization on a specific nucleus during strong-field dissociation of a molecular ion is controlled by the relative phase between the 790 and 395 nm components of a linearly-polarized ultrashort laser pulse. We have observed both *spatial* and *channel* asymmetries experimentally for an HD^+ beam target. The spatial asymmetry, which has been observed before (e.g., [1-2]), has been understood as being due to the breaking of the spatial symmetry of the driving field. This symmetry can also be broken by the carrier-envelope phase (CEP) of a few-cycle pulse [3]. In contrast, the channel asymmetry, namely the controlled dissociation into either $H^+ + D(1s)$ or $H(1s) + D^+$, is independent of the spatial asymmetry and is not as easily understood in the language of driving field asymmetry. The fact that previous measurements have shown no channel asymmetry [1] was explained theoretically [4] by the need for a longer wavelength than the typically used ~ 800 nm.

We achieved control over the dissociation of molecular ions using the phase delay of an intense two-color (790 and 395 nm) laser field. Specifically, an *up-down* asymmetry was produced in the dissociation of D_2^+ and HD^+ . More importantly, we observed a *channel* asymmetry between the HD^+ reaction products, $H^+ + D$ and $H + D^+$. The results, shown in Fig. 1(right), are interpreted in terms of interference between vibrationally-resolved dissociation pathways and are qualitatively reproduced by our 3D time-dependent Schrödinger equation (TDSE) calculations, also shown in the figure. Explicitly, the asymmetry is observed where the contributions from the $1s\sigma \rightarrow 2p\sigma - 1\omega$ (bond softening at 790 nm) and the $1s\sigma \rightarrow 2p\sigma - 2\omega \rightarrow 2p\sigma - 1\omega$ (395 nm absorption followed by 790 nm emission) are comparable. Note that, this experiment is the first “pump-probe” experiment of its kind on a molecular ion beam – a very thin target ($\sim 10^{-13}$ – 10^{-12} Torr). We believe that before too long it will be feasible to carry out time-resolved dynamic imaging and control experiments on ion beams, though further development of the experimental systems is still needed, which we plan to pursue.

Zero-photon dissociation (ZPD), B. Gaire, J. McKenna, A.M. Sayler, F. Anis, M. Zohrabi, Nora G. Johnson, J.J. Hua, K.D. Carnes, B.D. Esry, and I. Ben-Itzhak – To explain a very low KER feature in their data, Posthumus *et al.* [5] suggested an intriguing mechanism, which they named “zero-photon dissociation”, as it involves no net photon absorption by the dissociating H_2^+ . Recently, the same group repeated their measurements of dissociative ionization of H_2 by

263 nm pulses, about 150 fs long, but this time they presented an alternative interpretation involving resonance-enhanced multiphoton ionization (REMPI) [6].

In order to eliminate the competing REMPI process we have studied the dissociation of an H_2^+ beam in 10 fs, 790 nm laser pulses. We have measured very low kinetic energy release (KER) near 0 eV from the dissociation of H_2^+ using a crossed-beams coincidence three-dimensional momentum imaging setup [7] – after an upgrade allowing KER measurements down to zero. The results, shown in Fig. 1(Left), exhibit a clear KER peak near zero for intensities above 10^{13} W/cm² – the proposed signature of ZPD. This assessment is strongly supported by our theoretical work, as shown in the figure. Finally, instead of involving vibrational trapping as the key ingredient of the ZPD mechanism, we suggest that ZPD is driven by the absorption of a somewhat more energetic photon followed by the stimulated emission of a less energetic photon, both within the laser bandwidth. This would explain why short pulses are needed (broad band) and suggest that it is the highly excited vibrational states who contribute to this process. We plan to study the effect of the pulse chirp on ZPD and explore isotopic effects in HD^+ .

These projects were presented as invited talks at SILAP 2009, and Atomic Physics 2009.

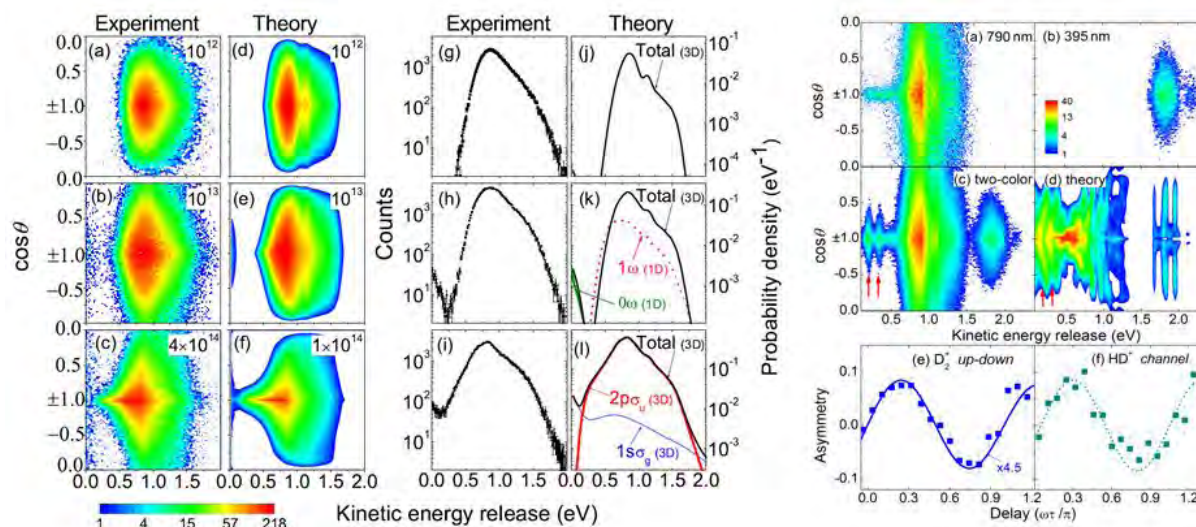


Figure 1. Left: (a-f) KER-cos θ plots for the dissociation of H_2^+ in 10 fs, 790 nm pulses at intensities indicated (in W/cm²): (a-c) experiment, and (d-f) 3D TDSE theory. (g-l) same as (a-f) but for KER distributions integrated over all angles. The additional lines in (k) are from our 1D Floquet-like theory method ($\times 0.25$). In (l) the total dissociation probability density is overlaid with the individual $1\sigma_g$ and $2p\sigma_u$ contributions. The dynamic range of the false color in (a-f) is the same for all density plots. **Right:** *Experiment:* KER-cos θ distributions for dissociation of D_2^+ for (a) 790 nm, 6×10^{14} W/cm², (b) 395 nm, 4×10^{12} W/cm², and (c) a mixed two-color field for the pulses used in (a) and (b). *Theory:* Probability density in (d) corresponds to the experiment in (c), but for 790nm at 10^{13} W/cm² and 395 nm at 10^{12} W/cm². Pulse durations for both wavelengths are 40 fs in experiment and theory. Data points in (e) show the measured up-down asymmetry parameter for D_2^+ , and in (b) the channel-asymmetry parameter for HD^+ as a function of two-color phase integrated over $0.14 < \text{KER} < 0.5$ eV. The solid curve in (e) is a full TDSE calculation and the dashed curve in (f) is a sinusoidal fit with π periodicity. All error bars denote statistical uncertainty.

Intense short pulse laser-induced ionization and dissociation of molecular-ion beams

The goal for these projects was to extend our knowledge of H_2^+ and apply it to more complex molecules in intense ultrafast laser pulses.

Studies of the benchmark H_2^+ and H_2 molecules provide the foundation for our understanding of the behavior of diatomic and somewhat more complex molecules in intense ultrashort laser pulses. To extend this knowledge base, we explored vibrational suppression in H_2^+ dissociation (Pub. #16) in addition to the projects described above. Taking advantage of our improved energy

resolution we have studied the KER shift as a function of the sign of the pulse chirp (Pub. #20) as well as higher order effects (in collaboration with the Weizmann Institute of Science). In addition, we continued our studies of the benchmark polyatomic molecule, H_3^+ , in which we focused on the dissociation channel and the study of a high KER feature in the single ionization channel. All these projects benefited from the strong collaboration with the theory group of Esry.

Armed with better understanding of the benchmark systems above, we explored more complex molecules. For example, we studied the dissociation of electronic and vibrationally cold CO^{2+} – an effectively two-level system undergoing perpendicular transitions (Pub. #21). In another example, we identified dissociation pathways in O_2^+ using vibrationally-resolved KER spectra. In collaboration with Eric Wells (Augustana College) we are making progress in controlling molecular processes by pulse shaping using a genetic algorithm (GA) (Pub. #18-19). Recently, Matthias Kling joined our efforts to incorporate a velocity map imaging (VMI) setup into the feedback loop of the GA. This should allow us to control more unique targets.

In addition to our laser studies, we conducted a few collision experiments between keV molecular ion beams and atomic targets. For example, at present we are investigating collision induced dissociation accompanied by target ionization.

Future plans: We will continue interrogating H_2^+ beams with laser pulses, in particular exploring how to extend our recent two-color studies to the even more challenging pump-probe experiments. We will also continue our studies of more complex molecules such as H_3^+ isotopologues, CO^+ , NO^{2+} etc. Finally, we will continue to improve our collision setup to enable high resolution Q-value measurements, which will then be implemented to probe molecular ion beams produced by intense ultrashort laser pulses.

References:

1. B. Sheehy, B. walker, and L. F. DiMauro, Phys. Rev. Lett. **74**, 4799 (1995).
2. D. Ray *et al.*, Phys. Rev. Lett. **103**, 223201 (2009).
3. M. F. Kling *et al.*, Science **312**, 246 (2006).
4. E. Charron, A. Giusti-Suzor, and F. H. Mies, Phys. Rev. Lett. **75**, 2815 (1995).
5. J.H. Posthumus *et al.*, J. Phys. B **33**, L563 (2000).
6. J.H. Posthumus *et al.*, Phys. Rev. Lett. **101**, 233004 (2008).
7. I. Ben-Itzhak *et al.* Phys. Rev. Lett. **95**, 073002 (2005)

Publications of DOE sponsored research in the last 3 years:

23. “Dynamic control of the fragmentation of CO^{q+} excited states generated using high-order harmonics”, W. Cao, S. De, K.P. Singh, S. Chen, M. Schöffler, A. Alnaser, I. Bocharova, G. Laurent, D. Ray, M.F. Kling, I. Ben-Itzhak, I. Litvinyuk, A. Belkacem, T. Osipov, T. Rescigno, and C.L. Cocke, Phys. Rev. A (2010) – [accepted](#).
22. “Resonances in electron-capture total cross sections for C^{4+} and B^{5+} collisions with $\text{H}(1s)$ ”, P. Barragán, L.F. Errea, F. Guzmán, L. Mández, I. Rabadán, and I. Ben-Itzhak, Phys. Rev. A **81**, 062712 (2010).
21. “Vibrationally-cold CO^{2+} in intense ultrashort laser pulses”, J. McKenna, A.M. Saylor, F. Anis, Nora G. Johnson, B. Gaire, Uri Lev, M.A. Zohrabi, K.D. Carnes, B.D. Esry, and I. Ben-Itzhak, Phys. Rev. A **81**, 061401(R) (2010).
20. “Tracing the photodissociation probability of H_2^+ in intense fields using chirped laser pulses”, Vaibhav S. Prabhudesai, Uri Lev, Adi Natan, Barry D. Bruner, Adi Diner, O. Heber, D. Strasser, D. Schwalm, I. Ben-Itzhak, J.J. Hua, B.D. Esry, Y. Silberberg, and D. Zajfman, Phys. Rev. A **81**, 023401 (2010).
19. “Closed-loop control of vibrational population in CO^{2+} ”, E. Wells, J. McKenna, A.M. Saylor, Bethany Jochim, Neal Gregerson, R. Averin, M. Zohrabi, K.D. Carnes, and I. Ben-Itzhak, J. Phys. B **43**, 015101 (2009).
18. “Examining the feedback signals used in closed-loop control of intense laser fragmentation of CO^+ ”, E. Wells, Michael Todt, Bethany Jochim, Neal Gregerson, R. Averin, Nathan G. Wells, N.L. Smolnisky, Nathan Jastram, J. McKenna, A.M. Saylor, Nora G. Johnson, M. Zohrabi, B. Gaire, K.D. Carnes, and I. Ben-Itzhak, Phys. Rev. A **80**, 063402 (2009).

17. “Controlling two-electron dynamics in double photoionization of lithium by initial state preparation”, G. Zhu, M. Schuricke, J. Steinmann, J. Albrecht, J. Ullrich, I. Ben-Itzhak, T.J.M Zourus, J. Colgan, M. Pindzola, and A. Dorn, *Phys. Rev. Lett.* **103**, 103008 (2009).
16. “Suppressed dissociation of H_2^+ vibrational states by reduced dipole coupling”, J. McKenna, F. Anis, B. Gaire, Nora G. Johnson, M. Zohrabi, K.D. Carnes, B.D. Esry, and I. Ben-Itzhak, *Phys. Rev. Lett.* **103**, 103006 (2009).
15. “Benchmark measurements of H_3^+ nonlinear dynamics in intense ultrashort laser pulses”, J. McKenna, A.M. Saylor, B. Gaire, Nora G. Johnson, K.D. Carnes, B.D. Esry, and I. Ben-Itzhak, *Phys. Rev. Lett.* **103**, 103004 (2009).
14. “Dissociation and ionization of an HD^+ beam induced by intense 395-nm ultrashort laser pulses”, J. McKenna, A.M. Saylor, B. Gaire, Nora G. Johnson, E. Parke, K.D. Carnes, B.D. Esry, and I. Ben-Itzhak, *Phys. Rev. A* **80**, 023421 (2009).
13. “Laser-induced multiple ionization of molecular ion beams: N_2^+ , CO^+ , NO^+ , and O_2^+ ”, B. Gaire, J. McKenna, Nora G. Johnson, A.M. Saylor, E. Parke, K.D. Carnes, and I. Ben-Itzhak, *Phys. Rev. A* **79**, 063414 (2009).
12. “Permanent dipole transitions remain elusive in HD^+ strong-field dissociation”, J. McKenna, A.M. Saylor, B. Gaire, Nora G. Johnson, M. Zohrabi, K.D. Carnes, B.D. Esry and I. Ben-Itzhak, *J. Phys. B* **42**, 121003 (2009) – Fast Track Communication.
11. “Rapid Formation of H_3^+ from ammonia and methane following 4 MeV proton impact”, Bethany Jochim, Amy Lueking, Laura Doshier, Sharayah Carey, E. Wells, Eli Parke, M. Leonard, K.D. Carnes, and I. Ben-Itzhak, *J. Phys. B* **42**, 091002 (2009) – Fast Track Communication.
10. “Bond rearrangement following collisions between fast ions and ammonia or methane”, E. Wells, E. Parke, Laura Doshier, Amy Lueking, Bethany Jochim, Sharayah Carey, Mat Leonard, K.D. Carnes, and I. Ben-Itzhak, *Application of Accelerators in Research and Industry*, edited by B.L. Doyle and F.D. McDaniel (AIP press, New York 2009), vol. **1099**, p. 133.
9. “Interrogating molecular-ion beams by ultra-short laser pulses”, I. Ben-Itzhak, J. McKenna, A.M. Saylor, B. Gaire, Nora G. Johnson, E. Parke, and K.D. Carnes, *Application of Accelerators in Research and Industry*, edited by B.L. Doyle and F.D. McDaniel (AIP press, New York 2009), vol. **1099**, p. 146.
8. “Molecular ion beams interrogated with ultrashort intense laser pulses”, Itzik Ben-Itzhak, *Progress in Ultrafast Intense Laser Science IV*, Series: Springer Series in Chemical Physics, Vol. **91**, edited by K. Yamanouchi, A. Becker, R. Li, and S.L. Chin (Springer, New York 2009) p. 67 – invited.
7. “Elusive enhanced-ionization structure for H_2^+ in intense ultrashort laser pulses”, I. Ben-Itzhak, P.Q. Wang, A.M. Saylor, K.D. Carnes, M. Leonard, B.D. Esry, A.S. Alnaser, B. Ulrich, X.M. Tong, I.V. Litvinyuk, C.M. Maharjan, P. Ranitovic, T. Osipov, S. Ghimire, Z. Chang, and C.L. Cocke, “Elusive enhanced-ionization structure for H_2^+ in intense ultrashort laser pulses”, *Phys. Rev. A* **78**, 063419 (2008).
6. “High kinetic energy release upon dissociation and ionization of N_2^+ beams by intense few-cycle laser pulses”, B. Gaire, J. McKenna, A.M. Saylor, Nora G. Johnson, E. Parke, K.D. Carnes, B.D. Esry, and I. Ben-Itzhak, *Phys. Rev. A* **78**, 033430 (2008).
5. “Enhancing high-order above-threshold dissociation of H_2^+ beams with few-cycle laser pulses”, J. McKenna, A.M. Saylor, F. Anis, B. Gaire, Nora G. Johnson, E. Parke, J.J. Hua, H. Mashiko, C.M. Nakamura, E. Moon, Z. Chang, K.D. Carnes, B.D. Esry, and I. Ben-Itzhak, *Phys. Rev. Lett.* **100**, 133001 (2008).
4. “Measuring the dissociation branching ratio of heteronuclear ND^+ ”, J. McKenna, A.M. Saylor, B. Gaire, Nora G. Johnson, E. Parke, K.D. Carnes, B.D. Esry, and I. Ben-Itzhak, *Phys. Rev. A* **77**, 063422 (2008).
3. “Soft fragmentation of carbon monoxide by slow highly charged ions”, E. Wells, T. Nishide, H. Tawara, K.D. Carnes, and I. Ben-Itzhak, *Phys. Rev. A* **77**, 064701 (2008).
2. “Ionization and dissociation of molecular ion beams caused by ultrashort intense laser pulses”, I. Ben-Itzhak, A.M. Saylor, P.Q. Wang, J. McKenna, B. Gaire, Nora G. Johnson, M. Leonard, E. Parke, K.D. Carnes, F. Anis, and B.D. Esry, *Journal of Physics: Conference Series* **88**, 012046 (2007).
1. “Determining intensity dependence of ultrashort laser processes through focus z -scanning intensity-difference spectra: application to laser-induced dissociation of H_2^+ ”, A.M. Saylor, P.Q. Wang, K.D. Carnes, and I. Ben-Itzhak, *J. Phys. B* **40**, 4367 (2007).

In addition to the close collaboration with the theory group of *Brett Esry*, some of our studies are done in collaboration with *Z. Chang’s* group, *Lew Cocke’s* group, *C.W. Fehrenbach*, and others.

Probing autoionization using attosecond pulses generated with generalized double optical gating

Zenghu Chang

J. R. Macdonald Laboratory, Department of Physics,
Kansas State University, Manhattan, KS 66506, chang@phys.ksu.edu

The goals of this aspect of the JRML program are (1) to generate single isolated attosecond pulses using 25 fs lasers without the need of locking the carrier-envelope phase for scaling XUV photon flux. (2) to find methods that can temporally characterize ultrabroad bandwidth attosecond pulses, (2) to use the isolated attosecond pulses for studying correlated electron dynamics in the autoionization of atoms.

1. Isolated attosecond pulse generation without the need of stabilizing the carrier-envelope phase of driving lasers. *Steve Gilbertson, Sabih D. Khan, Yi Wu, Michael Chini, and Zenghu Chang.*

The main difficulties in the generation of single isolated attosecond pulses have been the requirements on the pulse duration and the stability of the carrier-envelope (CE) phase of the driving laser. The attosecond pulse generation methods of amplitude gating and polarization gating both require CE phase locked few cycle laser pulses ideally <5 fs in duration. These two requirements are beyond the capabilities of many labs. Furthermore, to scale up the photon flux of the isolated attosecond pulses that have limited the applications to linear processes so far, one wishes to use pettawatt class lasers. However, due to large power fluctuations and low repetition rate, locking the CE phase of such ultra-high power lasers has not been demonstrated.

All of the current single isolated attosecond pulse generation schemes rely on gating a single XUV pulse from a pulse train by effectively reducing the generation laser to pulse durations on the order of the attosecond pulse train period. Since CE phase fluctuations play a large role in the attosecond pulse number per shot, locking the CE phase is critical to the quality of pulses produced. In previous experiments, the “gate width”, or region of the generating laser that produces the attosecond burst of photons, was set to be equal to the attosecond pulse train period. For amplitude gating and polarization gating (PG), this is half of an optical cycle of the fundamental laser period and for the Double Optical Gating (DOG) and the Generalized DOG this is one optical cycle. Once the gate width is set, the CE phase is locked so that the most efficient pulse with the smoothest spectrum is generated. For other phase values, two attosecond pulses per shot can be generated.

By setting the gate width sufficiently narrow with the Generalized Double Optical Gating, we demonstrated that single isolated attosecond pulses can be generated with any arbitrary carrier-envelope phase value of the driving laser. The carrier-envelope phase only affects the photon flux, not the pulse duration or contrast. Our results show that isolated attosecond pulses can be generated using carrier-envelope phase un-stabilized 23 fs pulses directly from chirped pulse amplifiers. The ability to generate isolated attosecond pulses without the need to lock the CE phase opens the door for the generation of high flux attosecond pulses with pettawatt class lasers that do not have the ability to stabilize the CE phase, which is crucial for investigating attosecond nonlinear processes.

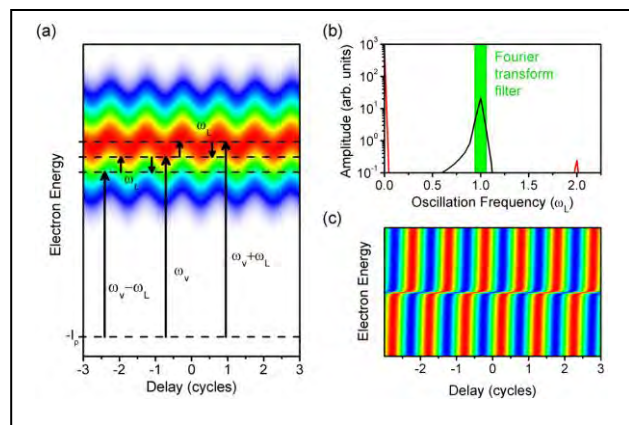
Interestingly, applying the same idea to gating schemes that use the fundamental laser field only will not work well. In that case, the attosecond pulse spacing is half of a laser cycle. Even when the gate width is half of a laser cycle, two attosecond pulses can still be generated if the CE phase is not set appropriately. One may think of reducing the gate width to a quarter of the laser cycle to accomplish the same as what the GDOG does, however, that is too short because it takes one half laser cycle for the electron to return to the parent ion.

2. PROOF, a new method for characterizing broadband isolated attosecond pulses. *Michael Chini, Steve Gilbertson, Sabih D. Khan, and Zenghu Chang.*

The measurement of isolated attosecond pulses has so far been performed with the attosecond streak camera or attosecond transient recorder technique, whereby the attosecond XUV pulse is converted into its electron replica through photoemission in atoms. The electrons are then momentum-shifted in a near infrared (NIR) laser field. The electron spectrum is measured as a function of the delay between the XUV and NIR pulses, and the time information of the attosecond pulse is encoded in the streaked photoelectron spectrum using the classical time-to-momentum conversion relationship. The streaked photoelectron spectrogram can then be used to retrieve the attosecond pulse, a technique known as FROG-CRAB (Frequency-Resolved Optical Gating for Complete Reconstruction of Attosecond Bursts). The attosecond pulse is retrieved by matching the measured spectrogram to a FROG-CRAB trace reconstructed from a guessed pulse amplitude and phase. The FROG-CRAB technique has a major limitation. It assumes that the bandwidth of the attosecond pulse is much smaller than the central energy of the photoelectrons. This central momentum approximation is needed to apply the FROG phase retrieval techniques developed for measurement of femtosecond lasers, and it poses a limitation on the shortest attosecond pulses that can be characterized at a given center photon energy. Even in the current state-of-the-art experiments, the central momentum approximation is only barely met, and measurement of even shorter pulses would almost certainly violate the approximation.

We developed a new technique for characterizing attosecond pulses, whereby the spectral phase of the attosecond pulse is extracted from the oscillation component with the dressing laser frequency in the photoelectron spectrogram. This technique, termed PROOF (Phase Retrieval by Omega Oscillation Filtering), can be applied to characterizing attosecond pulses with ultrabroad bandwidths. The spectral phase encoding in PROOF can be described by quantum interference of the continuum states caused by the dressing laser. The interference of those states coupled by the dressing laser causes the electron signal at a constant energy to oscillate with the delay, as illustrated in Fig.(a).

The sinusoidal oscillation of the energy is governed by the amplitude and phase of each of the interfering XUV spectral components. When the component of the oscillation with the dressing laser central frequency ω_L is extracted, as shown in Fig. (b) and (c), the interference is related to the spectral phases $\phi(\omega_v - \omega_L)$, $\phi(\omega_v)$, and $\phi(\omega_v + \omega_L)$ of the three XUV frequency components separated by the laser photon energy. The spectral phase can therefore be decoded from the ω_L oscillation of the signal at each energy, measured as a function of delay between the XUV pulse and the NIR field.



In PROOF, the ω_L component shown in Fig. (c) is obtained by a filter illustrated in Fig. (b). To decode the spectral phase difference, one needs to find the spectral phase that reproduces the trace in (c). Retrieving the spectral phase from these oscillations reduces to a minimization problem. Unlike FROG-CRAB, this method does not use FROG phase retrieval algorithms, and the central momentum approximation is not needed. PROOF has many advantages over other techniques, in that it is not limited to narrow bandwidth pulses and it can be performed with low dressing laser intensities. It can therefore be used to characterize the phase of recently generated gated high harmonic spectra supporting atomic unit pulse durations, or even zeptosecond pulses.

3. Time-resolved autoionization experiments with attosecond transient absorption. *He Wang, Michael Chini, Shouyuan Chen, Chang-Hua Zhang, Feng He, Yan Cheng, Yi Wu, Uwe Thumm, and Zenghu Chang.*

Electron correlation plays important roles in determining the properties of atoms, molecules and condensed matter such as high- T_c superconductors. However, directly observation of correlated electron motion in condensed phase is still a challenge. On the contrary, atoms are simpler, which can serve as the springboard between atomic physics and the complex systems. An attosecond transient absorption setup was established in our lab to study time-resolved autoionization in atoms, which is governed by electron-electron correlation. The Fano profile, which is the signature of the autoionization process, has widespread significance in many scientific disciplines. For decades, spectral-domain measurements with synchrotron radiation have served as a window into the rich dynamics of autoionization. However, the synchrotron pulse duration is too long (100 fs to 100 ps) to probe Fano resonances in the time domain since the autoionization lifetimes of noble gases can be as short as a few femtoseconds. We demonstrated the first transient absorption experiment using isolated attosecond pulses to probe the $3s3p^6np$ 1P autoionizing states in argon and show that the autoionization process is strongly modified by an intense few-cycle near infrared laser field.

To control and measure the autoionizing states of argon atoms, a pump-probe scheme with a Mach-Zehnder configuration was used in the experiment. The carrier-envelope phase stabilized 1 mJ, 5 to 8 fs NIR pulses centered at 750 nm were split into two parts. Half of the beam generated the isolated attosecond pulse using the generalized double optical gating (GDOG) from argon gas, and the corresponding XUV supercontinuum spectrum covered the energy range between 20 eV and 40 eV. Measurements with an attosecond streak camera and reconstruction by the FROG-CRAB method confirmed the pulse duration to be ~ 140 as. The attosecond XUV pulse passed through a 300 nm Al foil and was focused to a second glass gas cell filled with 25 torr of argon gas where more than 80% of the XUV was absorbed. Meanwhile, the other half of the NIR beam was recombined collinearly with the attosecond pulse at the second gas cell by a hole-drilled mirror which reflected a portion of the NIR and allowed the XUV to pass. A lens was used to focus the NIR to the second gas cell. The delay between the NIR and XUV pulses was introduced by a piezo-electric transducer. A CW green laser was co-propagated in both arms of the interferometer to stabilize and control the delay between the NIR and XUV pulses. The transmitted XUV pulse through the second cell was dispersed by a transmission grating on the MCP/phosphor and CCD image recorder. The spectrometer resolution was estimated to be 50 meV.

The capability of synchronizing an intense 8 fs NIR pulse and a 140 as XUV pulse on an argon gas target allows us to control the autoionization process with a lifetime of less than 10 fs. In the experiment, the autoionization process was initiated by an isolated attosecond pulse and modified by a NIR laser. The $3s3p^65p$ and $3s3p^66p$ states primarily exhibit an energy shift as well as broadening and weakening of the resonances. Most interestingly, $3s3p^64p$ exhibits a dramatic splitting which is asymmetric with respect to zero delay. Numerical simulations revealed that the splitting of the $3s3p^64p$ 1P line is caused by the coupling between two short-lived highly excited states in the strong laser field. Coupling between such short-lived highly-excited states has never before been studied, as it requires laser pulses much shorter than the autoionization lifetime. By changing the delay between the two pulses, we have demonstrated control over the resonance energy, line width and the q parameter which characterize the autoionization process. Therefore, control of the autoionization process in argon clearly demonstrated that isolated attosecond pulses are crucial tools for studying electron correlation dynamics

We have participated in studying dynamics in molecules (lead by Dörner at the University of Frankfurt), and x-ray lasers (lead by Rocca at Colorado State University). We also worked on micro-machining using the ultrafast lasers lead by Lei at KSU.

PUBLICATIONS (2009-2010). Complete Publications since 2008 can be found at <http://www.phys.ksu.edu/personal/chang/publications.htm>.

1. Y. Wang, M. Berrill, F. Pedaci, M.M. Shakya, S. Gilbertson, Z. Chang, E. Granados, B. M. Luther, M. A. Larotonda, J.J. Rocca, "Measurement of 1 picosecond soft x-ray laser pulses from an injection-seeded plasma amplifier," *Phys. Rev. A* **79**, 023810 (2009).
2. S. Lei, S. Devarajan, and Z. Chang, "A comparative study on the machining performance of textured cutting tools with lubrication," *Int. J. Mechatronics and Manufacturing Systems* **2**, 401 (2009).
3. Michael Chini, He Wang, Sabih D. Khan, Shouyuan Chen, and Zenghu Chang, "Retrieval of Satellite Pulses of Single Isolated Attosecond Pulses," *Appl. Phys. Lett.* **94**, 161112 (2009).
4. Chengquan Li, Eric Moon, Hiroki Mashiko, He Wang, Christopher M. Nakamura, Jason Tackett, and Zenghu Chang, "Mechanism of Phase-Energy Coupling in *f*-to-2*f* Interferometry," *Applied Optics* **48**, 1303 (2009).
5. Shuting Lei, Sasikumar Devarajan, and Zenghu Chang, "A Study of Micropool Lubricated Cutting Tool in Machining of Mild Steel," *Journal of Materials Processing Technology* **209**, 1612 (2009).
6. (Book chapter, Invited) Zenghu Chang, "Chapter 20: Attosecond Optics," *Handbook of Optics* Vol. II, sponsored by Optical Society of America, Edition 3, 2009, McGraw Hill. ISBN: 9780071498906.
7. Michael Chini, Hiroki Mashiko, He Wang, Shouyuan Chen, Chenxia Yun, Shane Scott, Steve Gilbertson, and Zenghu Chang, "Delay control in attosecond pump-probe experiments," *Opt. Express* **17**, 21459 (2009).
8. Ximao Feng, Steve Gilbertson, Hiroki Mashiko, He Wang, Sabih D. Khan, Michael Chini, Yi Wu, Kun Zhao, and Zenghu Chang, "Generation of isolated attosecond pulses with 20 to 28 femtosecond lasers," *Phys. Rev. Lett.* **103**, 183901 (2009).
9. Shouyuan Chen, Michael Chini, He Wang, Chenxia Yun, Hiroki Mashiko, Yi Wu and Zenghu Chang, "Carrier-envelope phase stabilization and control of 1KHz, 6 mJ, 30 fs laser pulses from a Ti:sapphire regenerative amplifier," *Appl. Opt.* **48**, 5692 (2009).
10. Hiroki Mashiko, Steve Gilbertson, Ximao Feng, Chenxia Yun, Sabih D. Khan, He Wang, Michael Chini, Chen Shouyuan, and Zenghu Chang, "XUV supercontinua supporting pulse durations of less than one atomic unit of time," *Optics Letters* **34**, 3337 (2009).
11. Chenxia Yun, Shouyuan Chen, He Wang, Michael Chini and Zenghu Chang "Temperature feedback control for long-term carrier-envelope phase locking," *Applied Optics* **48**, 5127 (2009).
12. Steve Gilbertson, Ximao Feng, Sabih Khan, Michael Chini, He Wang, Hiroki Mashiko, and Zenghu Chang, "Direct measurement of an electric field in femtosecond Bessel-Gaussian beams," *Optics Letters* **34**, 2390 (2009).
13. He Wang, Eric Moon, Michael Chini, Hiroki Mashiko, Chengquan Li, and Zenghu Chang, "Coupling between energy and carrier-envelope phase in hollow-core fiber based *f*-to-2*f* interferometers," *Optics Express* **17**, 12082 (2009).
14. Eric Moon, He Wang, Steve Gilbertson, Hiroki Mashiko and Zenghu Chang, "Advances in Carrier-Envelope Phase Stabilization of Grating-Based Chirped-Pulse Lasers," *Laser and Photonics Reviews* **4**, 160 (2009).
15. He Wang, Michael Chini, Sabih D. Khan, Shouyuan Chen, Steve Gilbertson, Ximao Feng, Hiroki Mashiko and Zenghu Chang, "Practical issues of retrieving isolated attosecond pulses," *J. Phys.* **B42**, 134007 (2009).
16. Michael Chini, Steve Gilbertson, Sabih D. Khan, and Zenghu Chang, "Characterizing ultrabroadband attosecond lasers," *Opt. Express* **18**, 13006 (2010).
17. Steve Gilbertson, Yi Wu, Sabih D. Khan, Michael Chini, Kun Zhao, Ximao Feng, and Zenghu Chang, "Isolated attosecond pulse generation using multicycle pulses directly from a laser amplifier," *Phys. Rev. A* **81**, 043810 (2010).
18. He Wang, Michael Chini, Yi Wu, Eric Moon, Hiroki Mashiko and Zenghu Chang, "Carrier-envelope phase stabilization of 5 fs, 0.5 mJ, pulses from adaptive phase modulators," *Applied Physics B* **98**, 291 (2010).
19. Ximao Feng, Steve Gilbertson, Sabih D. Khan, Michael Chini, Yi Wu, Kevin Carnes, and Zenghu Chang, "Calibration of electron spectrometer resolution in attosecond streak camera," *Optics Express* **18**, 1316 (2010).
20. B. Ulrich, A. Vredenburg, A. Malakzadeh, M. Meckel, K. Cole, M. Smolarski, Z. Chang, T. Jahnke, and R. Dörner, "Double ionization mechanisms of the argon dimer in intense laser fields," *Phys. Rev. A* **82**, 013412 (2010).
21. Steve Gilbertson, Sabih D. Khan, Yi Wu, Michael Chini, and Zenghu Chang, "Isolated attosecond pulse generation without the need to stabilize the carrier-envelope phase of driving lasers," *Phys. Rev. Lett.* (Accepted, 2010).
22. Qi Zhang, Kun Zhao, and Zenghu Chang, "Determining time resolution of microchannel plate detectors for electron time-of-flight spectrometer," *Rev. Sci. Instrum.* **81**, 073112 (2010).
23. Zenghu Chang and P. Corkum, "Attosecond optics, the first decade and beyond," *JOSA B*, (in printing, 2010).

Structure and Dynamics of Atoms, Ions, Molecules and Surfaces: Atomic Physics with Intense Short Laser Pulses and Synchrotron Radiation

C.L.Cocke, Physics Department, J.R. Macdonald Laboratory, Kansas State University,
Manhattan, KS 66506, cocke@phys.ksu.edu

During the past year we have used IR/EUV pump/probe experiments to study the influence of resonances on the interaction of He with attosecond pulses; we have used velocity-map-imaging(VMI) to study rescattered electrons generated by short one- (800 nm) and two-color (400/800nm) strong field pulses from rare gases; we have used pump/probe VMI measurements to study in real time vibrational wave packets in molecular oxygen; we have used two-color IR pump/IR probe to demonstrate orientation of CO molecules; we have used full cycle attosecond EUV/IR probe to manipulate the asymmetric dissociation of D₂ molecules; and we have used two-color IR pump/probe pulses to manipulate asymmetric dissociation in D₂.

Progress:

1) **Attosecond pulse trains interacting with He in the presence of an IR field.** *P. Ranitovic , X. M. Tong, B. Gramkow , S. De , B. DePaola , K. P. Singh , W. Cao , M. Magrakvelidze , D. Ray, I. Bocharova , H. Mashiko , A. Sandhu , E. Gagnon , M. M. Murnane , H.C. Kapteyn , I. Litvinyuk and C. L. Cocke.* We have concluded a series of measurements on the yield of photoelectrons and He⁺ ions from the interaction of an attosecond pulse train (APT) of EUV (11th-17th harmonics of 800 nm) on He in the presence of an IR field. The yield both in the overlap region and when the IR comes after the APT are very sensitive to the wavelengths of the harmonics, an effect we attribute to the role of resonant population of excited states of the He neutral. This work has now been published [*10].

2) **Momentum images of backscattered electrons released from rare-gas targets by intense laser pulses:** *D.Ray, I.Bocharova,, P.Ranitovic, S.De, I.V.Litvinyuk, A.T.Le, C.D.Lin, G.G.Paulus and C.L.Cocke.* It is now well established that rescattering electrons, or high energy ATI electrons (HATI) , generated by short intense laser pulses can be quantitatively described by factoring the amplitude for the process into a product of a “wave packet” and the differential cross section for free electrons scattering from the ionic target (QRS,[1,2]). In order to provide quantitative benchmark data to test the limits of validity of this approach we have used velocity-map-imaging (VMI) to measure momentum spectra for HATI electrons from Ar and Xe over a wide range of laser intensities. We have extracted differential cross sections for electron-ion scattering from the data and have compared these to theoretical cross sections calculated in the single active electron/effective potential model. For a given scattering energy, cross sections extracted for different intensities are found to be in good agreement with each other, as is predicted by QRS. The theoretical cross sections are in good, but not perfect, agreement with the extracted cross sections.

We have also used two-color (800/400 nm) fields to generate HATI electrons from Xe and have measured the dependence of the spectra on the relative phase ϕ of the two colors. The shape of the corresponding wave form is very similar to that of a short carrier-envelope-phase controlled IR pulse, and elicits a response from an atomic and molecular target very similar to the CEP stabilized pulse. We find that the HATI electron energy and yield are left-right asymmetric, due to the asymmetric wave form, and very dependent on the phase. The results are in good

agreement with both a solution to the time-dependent Schrödinger equation and a QRS calculation. By matching the measured results in phase with theoretical ones the experimental establishment of the absolute value of ϕ is straightforward and precise.

3) Tracking nuclear wave-packet dynamics in molecular oxygen ions with few-cycle infrared laser pulses, *S. De, I. A. Bocharova, M. Magrakvelidze, D. Ray, W. Cao, B. Bergues, U. Thumm, M. F. Kling, I. V. Litvinyuk, and C. L. Cocks*. We have used IR/IR (800 nm) pump/probe spectroscopy to study in real time the wave packet dynamics in the dication of molecular oxygen. The first IR pulse (8 fs in length) launches (coherent) wave packets onto several excited states of the dication (the intermediate molecule). These wave packets, after a delay of up to 1700 fs, are then probed by a second pulse which ionizes the molecular ion further. VMI is used to measure the resulting momenta of the molecular fragments O^{q+} and the kinetic energy release (KER) corresponding to each intermediate molecule is measured. Two types of wave packet motion are observed, one corresponding to dissociative states and one to (quasi)-bound states of the intermediate molecule. By plotting the kinetic energy release (KER) of the bound states as a function of delay we observe two types of vibrational motion. First, the oscillation of the packets in the well (very similar for several identified states) gives rise to a modulation of the yield with a period near 33 fs. This motion washes out after several periods. Second, at times of 955 and 1490 fs this vibrational structure is found to “revive”. The revival times can be used to identify, with the use of theoretical calculations [3], the states responsible. The revival times are evaluated with greater precision than previous spectroscopic calculations allowed. A sample spectrum showing both the vibrational wave-packet motion and the revivals is shown in fig. 1. This work has been published in [*1].

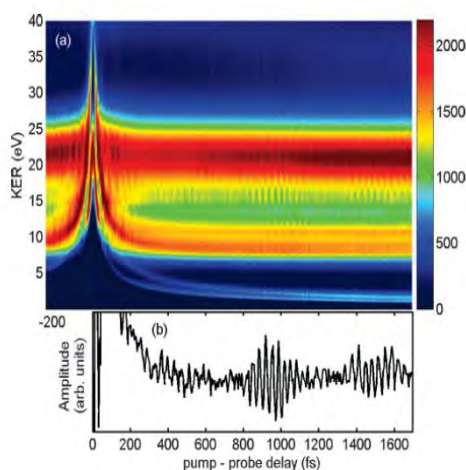


Fig. 1. KER versus pump-probe delay for O^{2+} ions observed with a VMI arrangement. The band near 22 eV results from the population of the dication of O_2 by the pump pulse followed by the ionization to the O^{2+}/O^+ channel after some delay. Vibrational wave packets give rise to oscillatory behavior with a period of 33 fs, which is strong initially, then washes out, then “revives” for times near 950 and 1490 fs.

4) Field-Free Orientation of CO Molecules by Femtosecond Two-Color Laser Fields, *S. De, I. Znakovskaya, D. Ray, F. Anis, Nora G. Johnson, I. A. Bocharova, M. Magrakvelidze, B. D. Esry, C. L. Cocks, I. V. Litvinyuk, and M. F. Kling*. A well known approach for aligning molecules is to subject them to a short laser pulse of duration much less than the rotational times of the molecule, thereby launching the molecule into a rotational wave packet. This wave packet revives at integral fractions of the rotational period of the molecule, at which times the wave packet corresponds to substantial alignment of the molecule. If a single color IR pulse is used, no orientation (as opposed to alignment) of the wave packet is possible even for a heterogeneous molecule, due to the symmetry of the IR field. If a two-color (400/800 nm) field is used,

however, the pump field can have a preferred direction and can orient, not just align, the molecule. We have used VMI measurements together with two-color pump/one color probe to demonstrate that the pump indeed orients the molecule. The data are compared to a theoretical calculation by B. Esry and F. Anis, and good agreement is found. This work is published [*7].

5) Control of Electron Localization in Deuterium Molecular Ions using an Attosecond Pulse Train and a Many-Cycle Infrared Pulse, *K. P. Singh, F. He, P. Ranitovic, W. Cao, S. De, D. Ray, S. Chen, U. Thumm, A. Becker, M. M. Murnane, H. C. Kapteyn, I. V. Litvinyuk, and C. L. Cocke*. When D_2 is illuminated by EUV with a photon energy above the first ionization potential, a vibrational wave packet can be created in the ground state 1σ potential curve of D_2^+ . In a strict Franck-Condon transition, a small portion of this wave packet will find itself in the continuum (“ground state dissociation”) but most of the packet will remain bound. If an IR field is sufficient strength (few $\times 10^{13}$ W/cm²) is present however, the bound state wave packet can be induced to dissociate through “bond softening” when the wave packet reaches near the outer turning point. The dissociation leads to a deuteron and a neutral ground state deuterium atom. In the present case the initial wave packet is launched by an APT. Such a wave packet commonly recurs every half cycle of the IR, in which case there can be no asymmetry of emission of the subsequent dissociation regardless of the relative phase ϕ of the IR and APT. In this case, however, we use a two-color (400/800 nm) to generate the APT, which results on only a single recurrence of the APT per IT cycle. Under these conditions, we have the possibility to direct in which direction the deuteron will be emitted. A small, but significant, asymmetry, is observed, oscillating with ϕ . The results are in agreement with a coupled-channels model calculation. This is a very simple case of using a weak non-ionizing IR field to control the direction of emission of the reaction products in a EUV-generated fragmentation process. This work has appeared in [*4].

6) Ion-Energy Dependence of Asymmetric Dissociation of D_2 by a Two-Color Laser Field, *D. Ray, F. He, S. De, W. Cao, H. Mashiko, P. Ranitovic, K. P. Singh, I. Znakovskaya, U. Thumm, G. G. Paulus, M. F. Kling, I. V. Litvinyuk, and C. L. Cocke*. Similar to the situation described in item (5), a single two-color IR field can lead to the asymmetric dissociation of D_2^+ . The process is now initiated by the strong-field removal of one electron to launch a wave packet on the 1σ potential curve of D_2^+ . The subsequent action of the IR field mixes the 1σ and $2p\sigma$ potentials and can lead to a linear combination of these orbitals which represents a preferred emission of the deuteron to the left or right. Such an asymmetry was previously observed in refs. {4,5}. We have measured this emission as a function of the kinetic energy release of the deuteron, using VMI, and have found that the observed asymmetry is very dependent on the KER. It approximately reverses in going from one-photon (~bond-softening) to two-photon (~above threshold dissociation) regions of KER, and reverses again when one enters the rescattering region of KER, where the dissociation step is caused by the return of the electron to recollide with the D_2^+ ion. The results are in good agreement with a theoretical coupled-channel calculation carried out in the $1\sigma-2p\sigma$ basis. This work has been published in [*6].

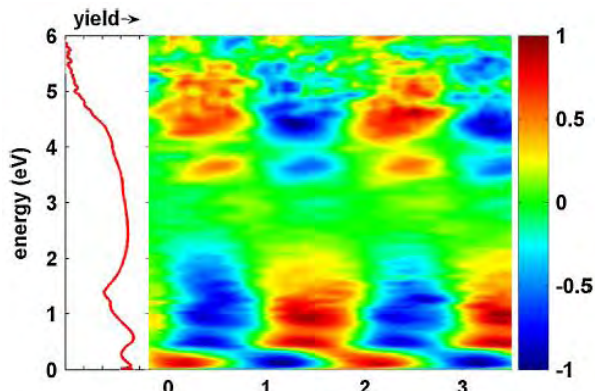


Fig. 2. Left-right asymmetry of the emission of d^+ ions from a two-color 45 fs pulse on D_2 as a function of the relative phase of the two colors (400 nm and 800 nm) and the kinetic energy release of the fragments. Three major regions of asymmetry are seen for one-photon, two-photon and rescattering energies. From [*6].

Future plans:

We will continue EUV attosecond pump/IR probe experiments, further VMI IRpump/IRprobe experiments on light molecules over longer time periods and further impulsive orientation experiments on light molecules. We will participate in the ALS collaboration [*2,3,4,8,9].

Publications 2009-10 not previously listed, identified in text at [*#]:

- 1) Tracking nuclear wave-packet dynamics in molecular oxygen ions with few-cycle infrared laser pulses, De, I. A. Bocharova, M. Magrakvelidze, D. Ray, W. Cao, B. Bergues, U. Thumm, M. F. Kling, I. V. Litvinyuk, and C. L. Cocke, *Phys. Rev. A* 82, 013408 (2010).
- 2) Carbon K-shell photoionization of fixed-in-space C₂H₄, T. Osipov, M. Stener, A. Belkacem, M. Schöffler, Th. Weber, L. Schmidt, A. Landers, M. H. Prior, R. Dörner, and C. L. Cocke, *Phys. Rev. A* 81, 033429 (2010).
- 3) Carbon K-shell photoionization of fixed-in-space C₂H₄, T. Osipov, M. Stener, A. Belkacem, M. Schöffler, Th. Weber, L. Schmidt, A. Landers, M. H. Prior, R. Dörner, and C. L. Cocke, *Phys. Rev. A* 81, 033429 (2010).
- 4) Control of Electron Localization in Deuterium Molecular Ions using an Attosecond Pulse Train and a Many-Cycle Infrared Pulse, K. P. Singh, F. He, P. Ranitovic, W. Cao, S. De, D. Ray, S. Chen, U. Thumm, A. Becker, M. M. Murnane, H. C. Kapteyn, I. V. Litvinyuk, and C. L. Cocke, *Phys. Rev. Lett.* 104, 023001 (2010).
- 5) Separation of Auger transitions into different repulsive states after K-shell photoionization of N₂ molecules, N. A. Cherepkov, S. K. Semenov, M. S. Schöffler, J. Titze, N. Petridis, T. Jahnke, K. Cole, L. Ph. H. Schmidt, A. Czasch, D. Akoury, O. Jagutzki, J. B. Williams, C. L. Cocke, T. Osipov, S. Lee, M. H. Prior, A. Belkacem, A. L. Landers, H. Schmidt-Böcking, Th. Weber, and R. Dörner, *Phys. Rev. A* 80, 051404 (2009).
- 6) Ion-Energy Dependence of Asymmetric Dissociation of D₂ by a Two-Color Laser Field, D. Ray, F. He, S. De, W. Cao, H. Mashiko, P. Ranitovic, K. P. Singh, I. Znakovskaya, U. Thumm, G. G. Paulus, M. F. Kling, I. V. Litvinyuk, and C. L. Cocke, *Phys. Rev. Lett.* 103, 223201 (2009).
- 7) Field-Free Orientation of CO Molecules by Femtosecond Two-Color Laser Fields, S. De, I. Znakovskaya, D. Ray, F. Anis, Nora G. Johnson, I. A. Bocharova, M. Magrakvelidze, B. D. Esry, C. L. Cocke, I. V. Litvinyuk, and M. F. Kling, *Phys. Rev. Lett.* 103, 153002 (2009).
- 8) Photoelectron and Auger-electron angular distributions of fixed-in-space CO₂, F. P. Sturm, M. Schöffler, S. Lee, T. Osipov, N. Neumann, H.-K. Kim, S. Kirschner, B. Rudek, J. B. Williams, J. D. Daughhete, C. L. Cocke, K. Ueda, A. L. Landers, Th. Weber, M. H. Prior, A. Belkacem, and R. Dörner, *Phys. Rev. A* 80, 032506 (2009).
- 9) Angular Correlation between Photoelectrons and Auger Electrons from K-Shell Ionization of Neon, A. L. Landers, F. Robicheaux, T. Jahnke, M. Schöffler, T. Osipov, J. Titze, S. Y. Lee, H. Adaniya, M. Hertlein, P. Ranitovic, I. Bocharova, D. Akoury, A. Bhandary, Th. Weber, M. H. Prior, C. L. Cocke, R. Dörner, and A. Belkacem, *Phys. Rev. Lett.* 102, 223001 (2009).
- 10) IR-assisted ionization of helium by attosecond extreme ultraviolet radiation, P. Ranitovic, X. M. Tong, B. Gramkow, S. De, B. DePaola, K. P. Singh, W. Cao, M. Magrakvelidze, D. Ray, I. Bocharova, H. Mashiko, A. Sandhu, E. Gagnon, M. M. Murnane, H.C. Kapteyn, I. Litvinyuk and C. L. Cocke, *New J. Phys.* 12, 013008 (2010).
- 11) Dynamic field-free orientation of polar molecules by intense two-color femtosecond laser pulses, I.V. Litvinyuk, S. De, D. Ray, N.G. Johnson, I. Bocharova, M. Magrakvelidze, F. Anis, B.D. Esry, C.L.Cocke, I. Znakovskaya and M. F. Kling, *J. Phys.: Conf. Ser.* 194, 032013 (2010).

References:

- [1] T. Morishita et al., *Phys. Rev. Lett.* **100**, 013903 (2008).
- [2] Z. Chen et al., *Phys. Rev. A* 79, 033409 (2009); C. D. Lin et al. *J. Phys. B* 43, 122001 (2010).
- [3] M. Lundqvist et al., *J. Phys. B* **29**, 499 (1996).
- [4] B. Sheehy et al., *Phys. Rev. Lett.* **74**, 4799 (1995).
- [5] M. R. Thompson, et al., *J. Phys. B: At. Mol. Opt. Phys.* **30**, 5755 (1997).

Interaction of Atomic Ladder Systems with Trains of UltraFast Pulses

B. D. DePaola, Physics Department, J.R. Macdonald Laboratory, Kansas State University,
Manhattan, KS 66506, depaola@phys.ksu.edu

During the past year we have used a pulse shaper to convert single pulses from the KLS into short trains of pulses. We have also directly used the output of the free-running oscillator as “infinite” trains of ultrafast pulses. We measured resonant excitation and ionization of a ladder system in atomic Rb by both kinds of ultrafast pulse trains.

Introduction

The interaction of atoms and molecules with trains of ultrafast pulses has been of great interest in the past decade. One-color pump-probe spectroscopy [1], an example of the simplest (or at least, shortest) pulse train, has been used to measure both atomic and molecular structure, and to measure how the structure can evolve in time [2]. At the other extreme, direct frequency comb spectroscopy (DFCS), pioneered by J. Ye, S. Cundiff and others [3], is usually discussed in the frequency domain. However, it can be thought of [4] as the interaction of an atomic or molecular system with a (nearly) infinite train of ultrafast optical pulses. In the past year, we have explored a domain that lies between these two extremes: the interaction of an atomic system with a finite, but greater than 2, train of ultrafast pulses. Progress in these experiments is discussed in section 1. More recently, we have been investigating the interaction of an atomic ladder system with the pulse train coming from a *free running* oscillator. It would seem that DFCS cannot be done with such a free running pulse train because its Fourier transform does not give rise to the regular, sharp, and well-defined “teeth” of a frequency comb. However, by running the experiment in reverse, that is, by detecting an excitation event and only then measuring the temporal and phase properties of the train, we show that a free-running oscillator *can* be used for extremely high resolution spectroscopy. Progress in these experiments is discussed in section 2.

Our target of choice for all of our experiments is Rb. The reasons for this are several. First, the structure of Rb is very precisely known. Thus, the transition frequencies we measure can be compared with known values. Second, Rb is a ladder system that has convenient transition energies. In particular, the transitions in the $5s-5p_{3/2}-5d_{3/2,5/2}$ ladder system are all within the bandwidth of Ti:Sapphire lasers. Third, Rb can readily be cooled to a couple of hundred microKelvin. *This is important because it allows us to completely neglect Doppler effects in our analysis.* This includes not only Doppler broadening and its deleterious effects on ultrahigh resolution spectroscopy, but also spurious phase effects [5] that could complicate the interpretation of finite pulse train interaction with ladder systems. Fourth, atomic Rb can be photoassociated into molecular Rb_2 . The structure of large internuclear separation Rb_2 is not well known, and will provide an interesting subject for study with the tools described in both sections 1 and 2.

Progress:

1) Interaction of a finite pulse train with an atomic ladder system. *H. U. Jang, B. Lomsadze, C. W. Fehrenbach, and B. D. DePaola*

One of the purposes of this series of experiments is to bridge the physics between the single-color pump/probe spectroscopy techniques and direct frequency comb spectroscopy (DFCS). In the former, typical pump-probe delay times are from tens of attoseconds to some picoseconds. In the latter, typical pulse separations are some nanoseconds – which are of the same timescale as the radiative or other relaxation lifetimes of many systems of interest. On the other hand, the frequency comb combines the broad bandwidth of the pump/probe system, with incredibly sharp frequency resolving capability. Conceptually, the physics of the interaction of a train of pulses with a 2-level system is simple: the first

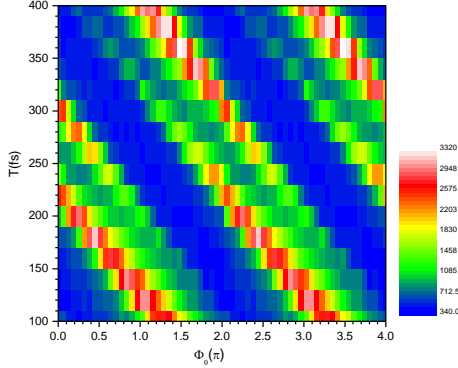


Figure 1: Landscape plot of Rb^+ counts versus T and φ_0 . In these data the train consisted of 11 pulses.

Furthermore, adding more slits increases the number of interference terms and gives rise to greater contrast in the interference pattern. In the case of optical pulses, a greater number of pulses should give rise to greater contrast, and added sharpness, in the excitation process. The same general model can be applied to a 3-level ladder system, though clearly interferences should exist between the two “back to back” 2-level systems. In our experiments the 3-level ladder consists of the $5s$ - $5p_{3/2}$ - $5d$ states of atomic Rb. We detect Rb($5d$) production through its photoionization by the same pulse train that does the excitation.

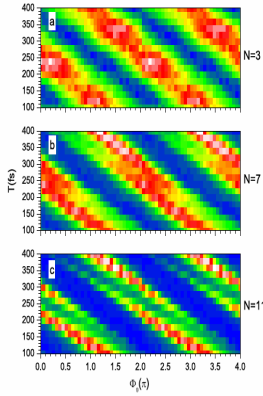
In these experiments we use a pulse shaper placed between the oscillator and amplifier in the KLS system. In principle, we could program the pulse shaper to generate an arbitrary number of identical pulses, each having an identical phase jump from the pulse preceding it. However, in order to do this, we would need to shape both the spectral phase and amplitude of the input pulse. Unfortunately, the non-linear gain of the amplifier would distort the spectral amplitude of the shaped pulse, making this approach problematic. Fortunately, we achieve nearly the same goal of a train of uniformly separated pulses, each having an identical (and controllable) phase jump, by programming in a particular class of spectral phase, the sinusoidal spectral phase $\varphi(\omega) = A \sin(\omega T + \varphi_0)$, where A , T , and φ_0 are input parameters to our pulse shaper. In the time domain, this creates an infinite train of pulses:

$$E_{out}(t) = \sum_{n=-\infty}^{+\infty} J_n(A) E_{in}(t - nT) e^{-in\varphi_0} \quad (1)$$

Here, $E_{in/out}$ are the input and output electric fields, respectively, and J_n is the ordinary Bessel function. We can see from Eq. 1 that the pulse shaping parameter T is just the time between pulses, φ_0 is the pulse to pulse phase jump, and A in some way controls the pulse amplitudes. In fact, the Bessel function does not allow total control of the pulse amplitudes, but does allow us to control the number of pulses having amplitudes sufficiently large to cause significant excitation. The measured Rb^+ signal for a train of 11 pulses interacting with the Rb ladder system is shown in Fig. 1. Here we plot Rb^+ production as a function of T , and φ_0 . The broad diagonal structure is due to the above-mentioned interference in the $5s$ - $5p$ 2-level system, while the slashes across the broad structures are due to the interferences in the $5p$ - $5d$ 2-level system.

In Fig. 2 we show the results for trains of 3, 7, and 11 pulses. As expected, the structure is seen with greater sharpness and contrast as the number of pulses in the train is increased. While they are in general agreement with the simple interference model, some aspects of these data are not yet understood. For example, why is the $5s$ - $5p$ structure so much stronger than that for the $5p$ - $5d$? Why do the 2 sets of

pulse excites some fraction of the population to the upper state, at which point, the phase of the excited state wave function begins to evolve as $\exp(i\omega t)$. At some time τ later, the next pulse can excite more of the population. If the total phase difference between the two excitation paths, including the phase shift of the second pulse with respect to the first, is an even multiple of π , we have constructive interference and an enhancement of the excitation process. If the total phase difference is an odd multiple of π , we have destructive interference and a reduction in excitation. By changing either the time between pulses, or the phase shift between pulses, one can smoothly move from constructive to destructive interference and back again. The physics is akin to 2-slit interference: in both cases, the phase difference between different paths gives rise to the interference.



structures interfere with each other destructively, instead of constructively as one might naively expect? These questions will be addressed in future experiments and rigorous calculations.

Finally, we point out that the physics we learn from these measurements is very general. The time scale of the entire train is a few picoseconds, making stochastic processes completely negligible. Thus, what we learn about this process can also be applied to, for example, trains of attosecond pulses interacting with atomic or molecular systems [6].

Figure 2: Same as Fig. 1, but with 3, 7, and 11 pulses in the train.

2) Interaction of a free-running oscillator with an atomic ladder system: “Backwards” Direct Frequency Comb Spectroscopy. *B. Lomsadze, H. U. Jang, C.W. Fehrenbach, and B. D. DePaola*

The development of frequency combs has revolutionized the field of metrology. Using the comb as a source of reference lines enables one to do incredibly accurate spectroscopy that is absolutely referenced to accurate radio frequency signals. A more recent advance in comb technology was the revelation [7] that, rather than only being used as a set of reference lines, the comb could be directly used for spectroscopy; this technique is referred to as direct frequency comb spectroscopy (DFCS). In DFCS, one scans the frequency of the comb teeth until one of them is in resonance with a transition, at which point excitation occurs and one observes fluorescence, ionization, etc. The frequencies of the teeth in the comb are scanned either through adjustment of the laser cavity length, which changes the repetition rate, f_{rep} , the frequency by which teeth in a comb are separated, or through adjustment of the laser pump power or an inter-cavity dispersive element either of which changes the offset frequency, f_0 . The frequency of the n^{th} tooth is given by $f_n = nf_{\text{rep}} + f_0$. Unlike a frequency comb, for which f_0 and f_{rep} are tightly controlled, in a free-running oscillator the repetition rate, and carrier envelope phase, φ_{CE} (related to f_0 by $\varphi_{\text{CE}} = 2\pi \frac{f_0}{f_{\text{rep}}}$) are generally free to drift. In the experiments described in this section, we nevertheless are able to do spectroscopy on the sub-MHz level using a free-running oscillator.

The motivation is that a great deal of effort goes into controlling f_0 and f_{rep} ; if we can achieve nearly the same results without exercising that control, the technique of DFCS will have been opened up to far more users. In our preliminary experiments, we concentrated on a semi-free-running laser. That is, we lock f_0 and allow f_{rep} to freely drift. We lock f_0 by first measuring it in a standard f-2f interferometer [3] and compare it with an arbitrary reference frequency. The difference is fed to a loop that servos the oscillator’s pump laser power. The oscillator interacts with the same Rb system described in Section 1. With f_0 locked and f_{rep} freely running, we then wait for an ion signal to be produced through resonant multi-photon excitation/ionization. Upon detection of an ion, we immediately measure f_{rep} . We then plot the measured ion yield as a function of f_{rep} , just as one would do in conventional DFCS. The major difference is that in DFCS one would only scan f_{rep} back and forth through one cycle of resonances, while in backwards DFCS (BDFCS) one can generally expect a much greater range of f_{rep} . This is not a problem since the spectrum is (nearly) periodic, at least to the accuracy of the measurement. Thus consecutive cycles of the spectrum can be added together to improve statistics. A portion of a sample measurement is shown in Fig. 3. Each of the sharp spikes in the data represents a resonance in the 3-level system. Note that because we are measuring ionization, rather than fluorescence originating from a 5d state, we also observe resonances in the 5s-5p manifold of states. The estimated resolution roughly MHz – considerably worse than has been achieved before using a true frequency comb. We believe that this is not due to a weakness in the method, but rather from Zeeman and ac Stark shifts which have not yet been

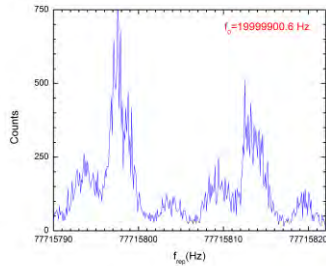


Figure 3: Spectrum of Rb taken with a free-running laser oscillator. Each sharp line indicates a resonant transition.

dealt with. In this figure, adjacent cycles have *not* been added. This portion of the spectrum represents about 10 minutes of data taking. The extremely sharp structure in the data are quite reproducible in f_{rep} over the nearly 100 cycles of data acquisition (only 2 of which are shown here), and correspond quite closely with the measurements of Ye *et al.* [7] in their pioneering experiments on the same system. Note, however, that the resonances do not reproduce in amplitude. More study is required, however we believe this is simply counting statistics. We have already begun measurements in which a completely free-running oscillator interacts with the same atomic ladder system; the results are promising.

References

1. V. Blanchet, *et al.*, Chem. Phys. Lett. **233**, 491 (1995).
2. M. Mudrich *et al.* Phys. Rev. Lett. **100**, 023401 (2008).
3. S. T. Cundiff and J. Ye, Rev. Mod. Phys. **75**, 325 (2003).
4. D. Felinto, Phys. Rev. A **80**, 013419 (2009).
5. M. A. Bouchene, Phys. Rev. A **66**, 065801 (2002).
6. K. J. Schafer *et al.*, Phys. Rev. Lett., **92**, 023003 (2004).
7. A. Marian *et al.*, Sci. **306**, 2023 (2004).

Selected Papers published in the past 3 years

- “Interaction of a finite train of short pulses with an atomic ladder system”, H. U. Jang, B. Lomsadze, M. L. Trachy, G. Veshapidze, C. W. Fehrenbach, and B. D. DePaola, Phys. Rev. A (submitted).
- “Coherent population trapping with controlled interparticle interactions”, H. Schempp, G. Günter, C. S. Hofmann, C. Giese, S. D. Saliba, B. D. DePaola, T. Amthor, and M. Weidemüller, Phys. Rev. Lett. **104**, 173602 (2010).
- “IR-assisted ionization of helium by attosecond extreme ultraviolet radiation”, P. Ranitovic *et al.*, New J. Phys., **12**, 013008 (2010).
- “MOTRIMS: Magneto-Optical Trap Recoil Ion Momentum Spectroscopy”, B. D. DePaola, R. Morgenstern, and N. Andersen, Adv. At. Mol. Opt. Phys. **55**, 139-189 (2008).
- “Measurement of population dynamics in stimulated Raman adiabatic passage”, M. A. Gearba *et al.*, Phys. Rev. A **76**, 013406 (2007).
- “Pathway for two-color photoassociative ionization with ultrafast optical pulses in a Rb magneto-optical trap”, G. Veshapidze, M. L. Trachy, H. U. Jang, C. W. Fehrenbach, and B. D. DePaola, Phys. Rev. A **76**, 051401(R) (2007).
- “Photoassociation in cold atoms via ladder excitation”, M. L. Trachy, G. Veshapidze, M. H. Shah, H. U. Jang, and B. D. DePaola, Phys. Rev. Lett. **99**, 043003 (2007).

Atoms and molecules in intense laser pulses

B.D. Esry

J. R. Macdonald Laboratory, Kansas State University, Manhattan, KS 66506

esry@phys.ksu.edu

<http://www.phys.ksu.edu/personal/esry>

Program Scope

The primary goal of my program is to quantitatively understand the behavior of simple benchmark systems in ultrashort, intense laser pulses. As we gain this understanding, we will work to transfer it to other more complicated systems. In this effort, my group works closely with the experimental groups in the J.R. Macdonald Laboratory, including, in particular, the group of I. Ben-Itzhak.

A second component of my program is to develop novel analytical and numerical tools to (i) more efficiently and more generally treat these systems and (ii) provide rigorous, self-consistent pictures within which their non-perturbative dynamics can be understood. The ultimate goal is to uncover the simplest picture that can explain the most.

1. The single active electron approximation revisited

Recent progress For multielectron atoms, the single active electron approximation (SAE) provides essentially the only means of calculating their response to intense laser pulses. Generally, the SAE assumes that the core electrons are frozen and do not respond to the laser field. A simple model potential can then be constructed for the one electron to be treated dynamically. While this potential can be calculated from the many-electron wave function, it is more often obtained by fitting the spectrum of a parametrized potential to the experimental spectrum of the atom in question.

One problem with such model potentials is that they support not only the allowed states of the valence electron, but also the Pauli-forbidden states of the core. The valence electron should not be allowed to occupy any of these core states at any point during the dynamics. Satisfying the exclusion principle thus requires that extra steps be taken.

Several methods of excluding the occupied states have been used in the literature, including not excluding them. The accuracy of these methods can be tested by comparing them with the essentially exact approach of expanding the wave function on the field-free eigenstates — minus the occupied orbitals — of the model potential. This close-coupling (CC) approach is not often used as it is much less efficient computationally. Instead, grid-based methods with the model potential modified to eliminate occupied orbitals are favored. Two of the more common modifications are: (i) adding a “soft wall” at short distances [1] and (ii) constructing a pseudopotential whose ground state is the valence orbital with its nodes removed [2,3].

Figure 1 shows the photoelectron momentum spectrum, plotted as a function of energy E and cosine of the angle from the laser polarization $\cos\theta$. In each case, the approximate calculation is plotted alongside the exact CC calculation. Since the laser pulse used was only two cycles long, the spectra show considerable asymmetry. The important point, however, is that in each case the spectra also show differences from the CC spectrum. The differences are not qualitative, nor would one expect them to be — but they are quantitative and systematic. The energy spectra displayed in the topmost panel show some of the differences more clearly.

Future plans Given the trend towards using theory to extract laser pulse parameters, it is important to be able to provide error bars for the approximations made in the theory. Our study of the SAE approximation is one step in this direction, and we will pursue others as well. We will also try to find computational approaches that let us remove the occupied orbitals from the SAE model potential without the substantial performance penalty of close-coupling.

2. Quantitative theory vs experiment comparison for H_2^+ dissociation

Recent Progress We have been working closely with I. Ben-Itzhak’s group to test our ability to calculate the momentum distribution of p +H fragments following dissociation of H_2^+ by an intense 10 fs laser pulse. Their dissociation measurements provide a stringent test for theory as they are complete, having the full momentum distribution of the fragments as well as being cleanly separated from other possible channels by coincidence requirements [4].

We purposefully kept the peak laser intensity rather low to minimize ionization as it cannot currently be included in our calculation. All other physical degrees of freedom, however, are included in our solution of

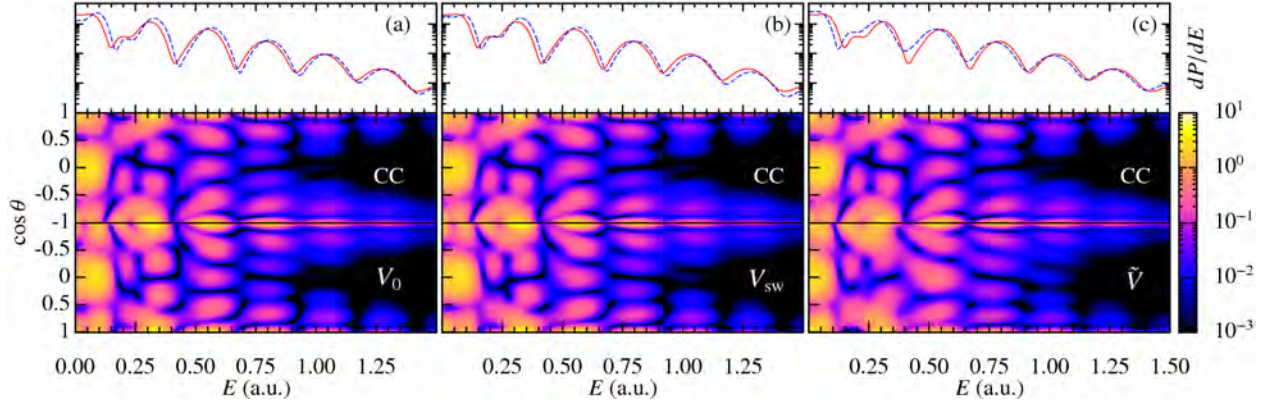


Figure 1: The photoelectron spectra for Ar in a 180 nm, 1.8 cycle, 8.75×10^{14} W/cm² laser pulse calculated in different approximations: CC, close-coupling (exact); V_0 , unmodified potential including occupied orbitals; V_{sw} , soft-wall potential [1]; \tilde{V} , pseudopotential [2,3]. Note that the momentum distributions E - $\cos \theta$ are mirrored about $\cos 180^\circ = -1$ in each case. The top panel shows the CC energy spectrum (red solid line) and the comparison spectrum (blue dashed line).

the time-dependent Schrödinger equation [P3,P10]. More specifically, we account for nuclear vibration and rotation as well as electronic excitation up to the p -H(3ℓ) manifold.

Since our calculations are nearly exact in this intensity regime, at least to a given numerical precision, the goal of the comparison is primarily to test what averaging steps are most important in achieving agreement with experiment. Some averages are easy to identify: vibrational, thermal, focal volume, and experimental resolution. For H_2^+ , which has 20 vibrational states, these averages already imply propagating roughly 45,000 different cases in time. We have done these calculations and performed the four averages above.

Unfortunately, while our calculations agree reasonably well with the experiment, we have so far failed to achieve total agreement. Since our averaging assumed a perfectly stable and characterized Gaussian laser pulse throughout the duration of the experiment — which was almost certainly not true — the first candidates to resolve the remaining experimental/theoretical discrepancy are the laser pulse parameters. We have tested for errors in the magnitude of these parameters, but they are not sufficient to explain the discrepancies. Calculations with the actual pulse shape retrieved during the experiment were also insufficient, even though the pulse was not perfectly Gaussian.

Future Plans The most likely explanation for the remaining disagreement is that the laser pulse parameters actually fluctuated during the experiment, implying further averaging of the calculations is necessary. The laser parameters, however, were not well enough characterized to allow such an average to be carried out.

This experience suggests two improvements on the experimental side that will facilitate future comparisons of theory with experiment. The first improvement is to regularly measure the laser pulse parameters during the experiment. The second improvement is to increase the stability of the laser pulse parameters, minimizing the pulse-to-pulse fluctuations. Even better would be to stabilize the pulse around a simple standard form — like a Gaussian. The latter would have the added benefits of increasing the ability of theory to quantitatively predict an experimental outcome and increasing the reproducibility of the experiment.

Since part of the difficulty in identifying the causes of the remaining disagreement is the fact that the spectra for 10 fs pulses are relatively featureless, we also intend to repeat the experiment and calculations with a longer pulse. Our goal is a 40–50 fs transform-limited pulse as it is then possible to measure vibrational structure in the spectra. Such structured spectra pose a bigger challenge to theory, and the longer pulses pose a bigger challenge computationally.

3. Carrier-envelope phase effects at long wavelengths

Recent Progress We extended our studies of carrier-envelope phase effects — begun in Ref. [5] and continued during the past three years in Pubs. [P1,P9,P16,P20] — to the dissociation of H_2^+ in few-cycle long wavelength laser pulses. Sources for such pulses are becoming increasingly available and are especially well suited to the study of vibrational motion in molecules. The carrier-envelope phase (CEP), φ , is defined from the laser’s electric field as $\mathcal{E}(t) = \mathcal{E}_0(t) \cos(\omega t + \varphi)$ for some pulse envelope $\mathcal{E}_0(t)$ and carrier frequency ω .

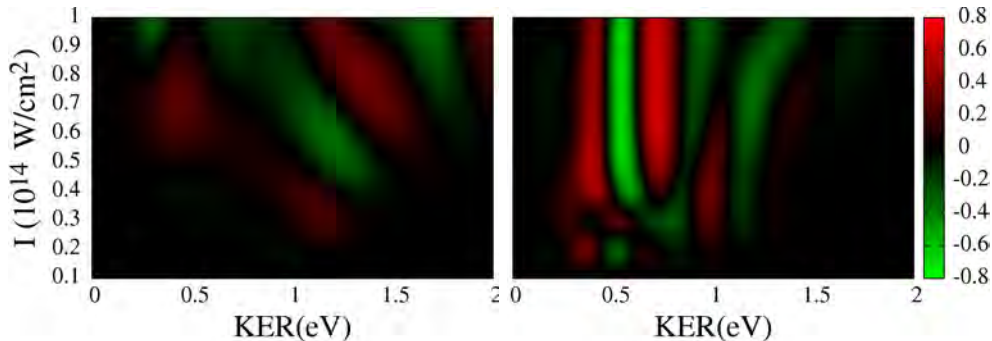


Figure 2: The intensity dependence of the normalized asymmetry A for dissociation of the $v=6$ state of H_2^+ in a three-cycle Gaussian laser pulse for 800 nm (left panel) and 1200 nm (right panel).

Figure 2 shows the normalized dissociation asymmetry,

$$A = \frac{P_{\text{up}} - P_{\text{down}}}{P_{\text{up}} + P_{\text{down}}},$$

calculated from the time-dependent Schrödinger equation including nuclear rotation. The probabilities P_{up} (P_{down}) were extracted from the full momentum distribution of the $p+\text{H}$ fragments by integrating over the entire upper (lower) hemisphere. The left panel shows the usual 800 nm case; and the right, 1200 nm. Each shows the result for a single initial state, $v=6$, and neither has been averaged in any way. The 800 nm asymmetry is clearly smaller and, due to its tilted structure with intensity, will get even smaller after averaging over the intensity distribution in the laser’s focal volume. The 1200 nm asymmetry is considerably larger, and its KER structure is nearly intensity-independent. The asymmetry thus survives intensity averaging nearly intact. While only $v=6$ is shown, these results are typical for the other vibrational states as well.

Future Plans We will investigate the CEP dependence of dissociation more systematically for wavelengths between 800 nm and roughly 1600 nm, looking for the conditions that optimize the asymmetry of the measurable signal — that is, including all of the averaging over vibrational, rotational, and intensity distributions. We will also try to understand the wavelength dependence of the asymmetry in the framework of our general theory presented in Pubs. [P1,P9]. Since our theory shows that CEP effects can be understood as coherent control via the interference of at least two pathways whose relative phases are determined by φ , then understanding CEP in H_2^+ can pave the way for understanding and predicting CEP effects in larger molecules.

References

1. H.G. Muller, Phys. Rev. A **60**, 1341 (1999).
2. W.J. Stevens, M. Krauss, H. Basch, and P.G. Jasien, Can. J. Chem. **70**, 612 (1992).
3. M.B. Gaarde, K.J. Schafer, K.C. Kulander, B. Sheehy, D. Kim, and L.F. DiMauro, Phys. Rev. Lett. **84**, 2822 (2000).
4. P.Q. Wang, A.M. Sayler, K.D. Carnes, J.F. Xia, M.A. Smith, B.D. Esry, and I. Ben-Itzhak, Phys. Rev. A **74**, 043411 (2006).
5. V. Roudnev, B.D. Esry, and I. Ben-Itzhak, Phys. Rev. Lett. **93**, 163601 (2004).

Publications of DOE-sponsored research in the last 3 years

- P20. “Comparison of theoretical analyses of intense-laser-induced molecular dissociation,” B. Abeln, J.V. Hernández, F. Anis, and B.D. Esry, J. Phys. B **43**, 155005 (2010).
- P19. “Vibrationally-cold CO^{2+} in intense ultrashort laser pulses,” J. McKenna, A.M. Sayler, F. Anis, N.G. Johnson, B. Gaire, U. Lev, M.A. Zohrabi, K.D. Carnes, B.D. Esry, and I. Ben-Itzhak, Phys. Rev. A **81**, 061401(R) (2010).
- P18. “Tracing the photodissociation probability of H_2^+ in intense fields using chirped laser pulses,” V.S. Prabhudesai, U. Lev, A. Natan, B.D. Bruner, A. Diner, O. Heber, D. Strasser, D. Schwalm, I. Ben-Itzhak, J.J. Hua, B.D. Esry, Y. Silberberg, and D. Zajfman, Phys. Rev. A **81**, 023401 (2010).

- P17. “Field-free orientation of CO molecules by femtosecond two-color laser fields,” S. De, I. Znakovskaya, D. Ray, F. Anis, N.G. Johnson, I.A. Bocharova, M. Magrakvelidze, B.D. Esry, C.L. Cocke, I.V. Litvinyuk, and M.F. Kling, *Phys. Rev. Lett.* **103**, 153002 (2009).
- P16. “Enhancement of carrier-envelope phase effects in photoexcitation of alkali atoms,” F. Anis and B.D. Esry, *J. Phys. B* **42**, 191001(FTC) (2009).
- P15. “Suppressed dissociation of H_2^+ vibrational states by reduced dipole coupling,” J. McKenna, F. Anis, B. Gaire, N.G. Johnson, M. Zohrabi, K.D. Carnes, B.D. Esry, and I. Ben-Itzhak, *Phys. Rev. Lett.* **103**, 103006 (2009).
- P14. “Benchmark measurements of H_3^+ nonlinear dynamics in intense ultrashort laser pulses,” J. McKenna, A.M. Sayler, B. Gaire, N.G. Johnson, K.D. Carnes, B.D. Esry, and I. Ben-Itzhak, *Phys. Rev. Lett.* **103**, 103004 (2009).
- P13. “Intense 395 nm ultrashort laser-induced dissociation and ionization of an HD^+ beam,” J. McKenna, A.M. Sayler, B. Gaire, N.G. Johnson, E. Parke, K.D. Carnes, B.D. Esry, and I. Ben-Itzhak, *Phys. Rev. A* **80**, 023421 (2009).
- P12. “Laser-induced multiphoton dissociation branching ratios for H_2^+ and D_2^+ ,” J.J. Hua and B.D. Esry, *Phys. Rev. A* **80**, 013413 (2009).
- P11. “Permanent dipole transitions remain elusive in HD^+ strong-field dissociation,” J. McKenna, A.M. Sayler, B. Gaire, N.G. Johnson, M. Zohrabi, K.D. Carnes, B.D. Esry and I. Ben-Itzhak, *J. Phys. B* **42**, 121003(FTC)(2009).
- P10. “Rotational dynamics of dissociating H_2^+ in a short intense laser pulse,” F. Anis, T. Cackowski, and B.D. Esry, *J. Phys. B* **42**, 091001(FTC) (2009).
- P9. “The role of mass in the carrier-envelope phase effect for H_2^+ dissociation,” J.J. Hua and B.D. Esry, *J. Phys. B* **42**, 085601 (2009).
- P8. “Elusive enhanced ionization structure for H_2^+ in intense ultrashort laser pulses,” I. Ben-Itzhak, P.Q. Wang, A.M. Sayler, K.D. Carnes, M. Leonard, B.D. Esry, A.S. Alnaser, B. Ulrich, X.M. Tong, I.V. Litvinyuk, C.M. Maharjan, P. Ranitovic, T. Osipov, S. Ghimire, Z. Chang, and C.L. Cocke, *Phys. Rev. A* **78**, 063419 (2008).
- P7. “Isotopic pulse-length scaling of molecular dissociation in an intense laser field,” J.J. Hua and B.D. Esry, *Phys. Rev. A* **78**, 055403 (2008).
- P6. “High kinetic energy release upon dissociation and ionization of N_2^+ beams by intense few-cycle laser pulses,” B. Gaire, J. McKenna, A.M. Sayler, N.G. Johnson, E. Parke, K.D. Carnes, B.D. Esry, and I. Ben-Itzhak, *Phys. Rev. A* **78**, 033430 (2008).
- P5. “Intensity dependence in the dissociation branching ratio of ND^+ using intense femtosecond laser pulses,” J. McKenna, A.M. Sayler, B. Gaire, N.G. Johnson, E. Parke, K.D. Carnes, B.D. Esry, and I. Ben-Itzhak, *Phys. Rev. A* **77**, 063422 (2008).
- P4. “Enhancing high-order above-threshold dissociation of H_2^+ beams with few-cycle laser pulses,” J. McKenna, A.M. Sayler, F. Anis, B. Gaire, N.G. Johnson, E. Parke, J.J. Hua, H. Mashiko, C.M. Nakamura, E. Moon, Z. Chang, K.D. Carnes, B.D. Esry, and I. Ben-Itzhak, *Phys. Rev. Lett.* **100**, 133001 (2008).
- P3. “Role of nuclear rotation in dissociation of H_2^+ in a short laser pulse,” F. Anis and B.D. Esry, *Phys. Rev. A* **77**, 033416 (2008).
- P2. “Ionization and dissociation of molecular ion beams caused by ultrashort intense laser pulses,” I. Ben-Itzhak, A.M. Sayler, P.Q. Wang, J. McKenna, B. Gaire, N.G. Johnson, M. Leonard, E. Parke, K.D. Carnes, F. Anis, and B.D. Esry, *J. Phys.: Conf. Ser.* **88**, 012046 (2007).
- P1. “General theory of carrier-envelope phase effects,” V. Roudnev and B.D. Esry, *Phys. Rev. Lett.* **99**, 220406 (2007).

Controlling molecular rotations of asymmetric top molecules: methods and applications

V. Kumarappan

James R. Macdonald Laboratory, Department of Physics
Kansas State University, Manhattan, KS 66506
vinod@phys.ksu.edu

1 Program Scope

The goal of this part of the James R. Macdonald Laboratory's research program is to develop better methods of aligning and orienting polyatomic molecules for ultrafast AMO experiments, including high-harmonic generation and photoelectron spectroscopy. So far, almost all experiments that use aligned molecules have been carried out on linear molecules. The development of more effective alignment/orientation methods for asymmetric top molecules will allow these experiments to be extended to a much larger class of molecules. We use non-adiabatic alignment with non-resonant femtosecond laser pulses to align/orient molecules and velocity map imaging and non-linear optical methods to quantify the degree of alignment. At this point, we are still at a developmental stage. We have built a kHz single-shot velocity map imaging (VMI) spectrometer, developed a tomographic method for measuring 3D momentum distributions using a VMI spectrometer, and developed a new optical scheme for characterizing alignment.

2 Recent progress

2.1 Optical measurements:

(Xiaoming Ren, Varun Makhija, Vinod Kumarappan)

During the last year, my group has concentrated on measuring alignment optically. The goals of developing such methods are: (a) to be able to measure alignment — including 3D alignment — rapidly so that a feedback algorithm can be efficiently used to optimize the degree of alignment, (b) to facilitate direct characterization of the alignment in a dense sample suitable for high harmonic generation, and (c) to be able to measure alignment of any molecules that can be aligned/oriented. Fragment ion detection techniques such as VMI fall short on all three requirements. Fragment ion imaging is slow compared to optical measurements, requires low target density to avoid space charge and detector saturation effects, and is suitable only for molecular fragments for which the axial recoil approximation holds true.

Femtosecond degenerate four wave mixing (fs-DFWM) was chosen as the non-linear optical probe of alignment. By measuring the time evolution of the lab-frame χ_3 — which is a convolution of the molecular frame χ_3 and the angular distribution of the molecules in the target — the degree of alignment can be determined. A folded BOXCARS scheme [1] was adopted so that a background-free measurement can be made. The three probe beams are generated by sending a single enlarged pulse through an aluminium plate with three holes drilled at three corners of a square. The pump beam is recombined with the probe beam before the aluminum plate using a two-inch mirror with

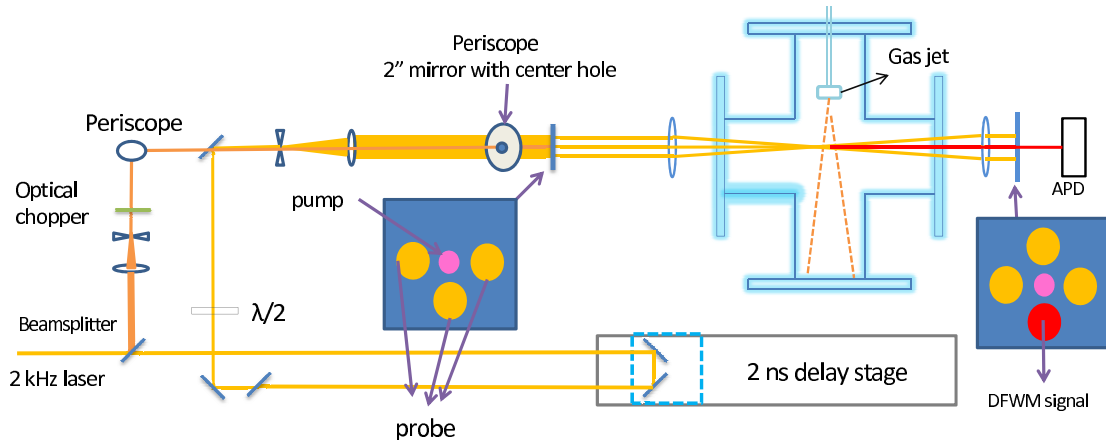


Figure 1: Schematic diagram of the fs-DFWM setup. Pump and probe beams are overlapped on the two inch mirror, which has a 6 mm hole, and the single probe beam is split into three beams using an aluminium plate with suitable holes, and DFWM signal is spatially filtered using a pinhole (not shown) in front of the avalanche photodiode (APD).

a hole drilled in the center so that the pump occupies the center of the square defined by the probe beams. The beams are focused using a single lens, ensuring automatic spatial and temporal overlap with minimum jitter. Figure 1 shows the optical setup. The measurement scheme is thus a two-beam experiment masquerading as a four-beam experiment, providing the benefits of the latter while maintaining the stability of the former.

This scheme has an additional advantage over previous DFWM measurements of strong-field alignment. Previous measurements have used two strong beams to set up a transient grating, and then probed the time-evolution of this grating by diffracting a third beam off it. The use of two strong pulses sets up a spatial profile of alignment that has anharmonic contributions from the highly non-linear nature of the alignment process, and an electron density grating due to ionization that also contributes to the signal [2, 3]. This complicates the interpretation of the measurements, requiring a simplified treatment of measurement which is applicable only for weak alignment. Our scheme, on the other hand, uses three weak beams as the probe in a pure χ_3 process, allowing a simple interpretation of the results even in the case of strong alignment of the sample.

A supersonic pulsed valve operating at 1 kHz produces a cold gas target. Rotational temperatures of ~ 1 K have been measured after the adiabatic expansion has become collision-free [4], but the temperature near the nozzle has yet to be characterized. The valve can be operated with up to 100 bar backing pressure, generating a dense target suitable for high harmonic generation (HHG) experiments. The short duration of the gas pulse, $\sim 10 \mu\text{s}$, allows the chamber to be maintained at less than 2×10^{-5} Torr, minimizing absorption by the background gas. By using molecules seeded in helium gas, we also expect to be able to align and generate harmonics from larger molecular targets such as substituted benzenes.

The laser operates at 2 kHz, and the pump beam is mechanically chopped at 500 Hz. This dual-chopping scheme allows large gains in signal-to-noise ratio. Figure 2 shows the measured signal from alignment of nitrogen gas at 60 bar backing pressure. No collisional dephasing is evident up to 100 ps, an excellent indication of the low collision rate in the target. Since the signal from a BOXCARs measurement is essentially background free, we expect to be able to do this measurement down to a target pressure of about 1 Torr. This ability to operate with lower target density is essential for one of our primary goals, which is to align asymmetric tops well. By seeding such molecules in a

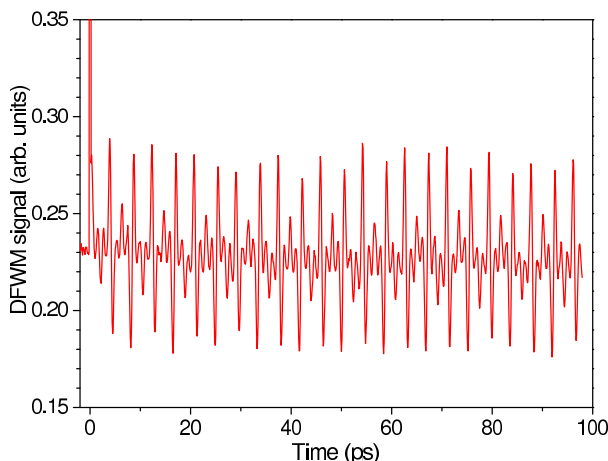


Figure 2: DFWM measurement of alignment of nitrogen. The supersonic jet was operated with 60 bar backing pressure. Pump and probe pulses were ~ 50 fs.

high pressure He jet, we can obtain a rotationally cold target. A low temperature has been shown to substantially improve the degree of alignment [7]. The valve body can be heated to 250°C to allow control over target density and to avoid clustering.

2.2 Calculations:

(*Xiaoming Ren, Varun Makhija, Vinod Kumarappan*)

In order to understand the rotational dynamics of asymmetric tops in one- and two-color fields (which are required for orienting molecules), we have developed code to calculate the evolution of alignment and orientation. Two separate codes have been written. The first calculates the alignment and orientation dynamics of linear molecules via the polarizability and the hyper-polarizability interactions. The second code simulates 1D alignment of asymmetric top molecules such as sulphur dioxide (SO_2) and iodobenzene ($\text{C}_6\text{H}_5\text{I}$). We make use of the symmetries pointed out in [8] to reduce the computational time required to run this calculation. The next step will be to include (a) the hyper-polarizability interaction to calculate orientation in two color fields and (b) arbitrary polarizations to calculate 3D alignment. These calculations will help us in designing better alignment techniques and in interpreting experimental data.

3 Work in progress and outlook

Until recently, these experiments suffered from a lack of adequate beam pointing stability, primarily due to a poor beam line and large distance from the laser. Overlap between pump and probe beams had to be re-optimized every few minutes, making it difficult to carry out any systematic measurements. A new beam transport line has substantially improved stability and improved the quality of data in both the VMI and the optical measurements. The DFWM measurement has produced reliable data only with the new beam transport system. Manuscripts on both the kHz VMI apparatus and the DFWM measurement are being prepared for publication.

The James R. Macdonald Laboratory is in the process of a major reorganization of lab space, with the goal of completing the process in 2012. These experiments will move into the same room as the laser, and the acquisition of the recently-funded PULSAR laser will substantially increase available beam time.

An experiment is in progress (in collaboration with Matthias Kling and Lew Cocke) to try to orient an asymmetric top molecule (iodobenzene) using an ω - 2ω scheme. The VMI spectrometer is being used in this experiment to characterize the alignment and orientation of the molecules. Non-resonant laser-induced alignment proceeds through the interaction of the polarizability tensor of the molecule with the laser electric field. Since this tensor is always symmetric, it is impossible to induce orientation using this interaction. But the first hyper-polarizability interaction is not constrained in this manner, and has been shown to be capable of producing oriented ensembles with two-color pumps both in the non-adiabatic [5] and the adiabatic limits [6]. Utilizing the hyper-polarizability thus opens the way to studying orientation dependent molecular processes such as strong-field ionization with a carrier-envelope-phase controlled few-cycle pulse. We have already devoted some beam time to this experiment, and expect to conclude the measurements in the next month or two.

A phase/amplitude/polarization pulse shaper is being built, and should be operational within the next 2-3 months. With the ability to measure alignment rapidly (≤ 1 s per measurement) either optically or with the kHz VMI system, and a genetic algorithm to control the pulse shaper, we expect to be able to optimize the degree of alignment of cold asymmetric top molecules. The DFWM scheme we use for measurement places no restrictions on the polarization of the pump beam, and we expect to be able to characterize 3D alignment by measuring different components of χ_3 in the lab frame. The full 3D distribution of molecules can then be measured using a tomographic VMI technique that we developed recently. These experiments will be our main priority over the next year.

An XUV spectrometer is also being designed and built. Once this spectrometer is online, we expect to be able to measure high harmonics from aligned/oriented molecules. The goal is to be able to follow electron dynamics in molecules via the HHG process. These experiments will be carried out in collaboration with Carlos Trallero.

References

- [1] J. A. Shirley, R. J. Hall, and A. C. Eckbreth, *Optics Letters* **5**, 380 (1980). The folded BOX-CARS geometry is a phase-matching scheme for four-wave mixing in which three non-collinear beams interact in a medium to produce a signal beam that propagates in a fourth direction. The name originates from the wave-vector addition diagram for Coherent Anti-Stokes Raman Scattering (CARS) in this geometry, which is a folded rectangle or box. Due to the spatial separation of the signal beam from the input beams, this geometry produces a background-free signal.
- [2] A. Rouzée, V. Renard, S. Guérin *et al.*, *Physical Review A* **75**, 7 (2007).
- [3] A. Rouzée, V. Renard, S. Guérin *et al.*, *Journal of Raman Spectroscopy* **38**, 969 (2007).
- [4] U. Even, J. Jortner, D. Noy *et al.*, *Journal of Chemical Physics* **112**, 8068 (2000).
- [5] S. De, I. Znakovskaya, D. Ray *et al.*, *Physical Review Letters* **103**, 153002 (2009).
- [6] K. Oda, M. Hita, S. Minemoto *et al.*, *Physical Review Letters* **104**, 213901 (2010).
- [7] V. Kumarappan, C. Z. Bisgaard, S. S. Viftrup *et al.*, *Journal of Chemical Physics* **125**, 7 (2006).
- [8] S. Pabst, P. J. Ho, and R. Santra, *Physical Review A* **81**, 043425 (2010).

Strong field rescattering physics – self-imaging of a molecule by its own electrons

C. D. Lin

J. R. Macdonald Laboratory, Kansas State University
Manhattan, KS 66506
e-mail: cdlin@phys.ksu.edu

Program Scope:

We investigate the interaction of intense laser pulses with atoms and molecules by focusing on rescattering phenomena. Based on the quantitative rescattering theory (QRS) we established recently, we have: (1) examined high-order harmonic generation (HHG) from molecules and compared to experiments; (2) investigated electron diffraction by the rescattering electrons and its implications for dynamic chemical imaging; (3) studied the momentum correlation of the two electrons in nonsequential double ionization. We have also studied the macroscopic propagation effect of HHG in the medium and formulated the two-path interference model for probing attosecond electron wave packets.

Introduction

When an atom or molecule is exposed to an intense infrared laser pulse, an electron which was released earlier may be driven back by the laser field to recollide with the parent ion. The collisions of electrons with the ion may result in high-order harmonic generation (HHG), the emission of high-energy above-threshold-ionization (HATI) electrons and non-sequential double ionization (NSDI). Based on the quantitative rescattering theory (QRS) established in 2009 we are now capable of studying HHG, HATI and NSDI processes at the quantitative level such that they can be compared directly with experimental data.

1. QRS for HATI electrons and dynamic chemical imaging with infrared lasers

Recent progress

Our earlier work established that it is possible to extract **field-free** elastic differential cross sections (DCS) of the target atomic or molecular ions from the HATI spectra. These DCS's are the same electron diffraction images obtained by standard gas-phase electron diffraction (GED) except in GED the incident electrons have energies of the order of tens to hundreds of keV's. In GED, the molecular structure can be easily retrieved since the diffraction images can be calculated using the Independent Atom Model (IAM). For HATI, the returning electrons have energies from 15-50 eV for Ti-Sa lasers at their typical intensity of 10^{14} W/cm². Thus even if the DCS can be extracted from the HATI spectra, there is no simple procedure to extract molecular structure.

Recently we have shown that the DCS at large scattering angles in electron-molecule collisions can be described by the IAM model if the collision energies are higher than 50 or 100 eV. These energies can be easily reached by MIR lasers, making it possible to probe the structure of a molecule using the HATI spectra. Since MIR lasers of durations of a few femtoseconds are already available, this implies that it is possible to use MIR lasers for dynamic imaging of a transient molecule. A report of this investigation is given in B1 and in A3.

Ongoing projects and future plan

We are working with experimental groups in order to be able to analyze HATI electron spectra from simple molecules generated by MIR lasers. We need to generalize the IAM model for singly charged molecular ions. In the near future, experimentally it is desirable to obtain HATI spectra from oriented/aligned molecules. This would allow us to use diffraction images from oriented/aligned molecules to extract the bond lengths and/or angles of a molecule. This

advantage is not available to conventional GED where diffraction images are only taken with isotropic distributed molecules. We retrieve molecular structure parameters using genetic algorithm.

2. QRS Theory for HHG

Recent progress

In the last year we have applied QRS to obtain HHG spectra from aligned N_2 and CO_2 molecules, to explain experiments carried out at JILA, Stanford, Ottawa, and Saclay. These studies include the magnitude and phase of the harmonics, the polarization and ellipticity, as well as the alignment and intensity dependence. The results are reported in A9, A10, A11 and B2. The QRS theory relies on accurate photoionization transition dipole matrix elements of molecules. We obtained these in collaboration with Professor Robert Lucchese. Combining with the QRS, we can obtain HHG spectra from single molecules without much computational effort, and the results have been shown to agree quite well with experiments.

Ongoing projects and future plan

The HHG spectra measured in experiments include the propagation of the dipole field in the medium. To compare theoretical calculations with experiments, macroscopic propagation should be included. We have recently developed our own propagation codes. Using single-atom dipoles obtained from QRS, we solved the Maxwell equations that govern the propagation of the fundamental and the harmonics in the medium. We are now able to obtain HHG spectra that can be compared directly with experimental measurements. For HHG from Ar by 1200 nm and 1300 nm lasers, we have been able to reproduce the experimental spectra over the 30-90 eV region from Ottawa. We adjusted laser intensity and gas pressure till we achieved best fits. Our next goal is to include propagation effects on HHG generated from molecules. This will allow us to compare our understanding of molecular HHG at the quantitative level, and hopefully resolve the differences often seen in HHG from different laboratories.

We are now moving into HHG from nonlinear molecules. The MO-ADK tunneling ionization rates and HHG within the strong field approximation, the effect of macroscopic propagation within the SFA for nonlinear molecules have been checked. Once we obtain the transition dipole matrix elements from the code of Robert Lucchese, we will be ready to study HHG from the more interesting nonlinear molecules.

3. QRS theory for NSDI

Recent progress

We have extended the QRS to study nonsequential double ionization (NSDI) of He by lasers in the last year at the level of obtaining the correlation spectra of the two ejected electrons. This is an interesting problem since in NSDI both the electron-electron interaction and electron-laser interaction cannot be treated perturbatively. According to the rescattering model, NSDI can be due to direct (e,2e)-type collision, but can also be due to electron impact excitation followed by tunneling ionization in the laser field. Using the standard electron collision theories in the framework of QRS, we have been able to show that the correlated two-electron spectra reported by Staudte et al (PRL99, 263002, 2007) can be explained. For the (e,2e) part we have shown in A2 that the finger-like structure in the observed spectra clearly is due to electron-electron repulsion.

On-going projects and future plan

In the process of trying to understand the spectra due to excitation-tunneling mechanism, we concluded that experimental data show contributions from a new mechanism of NSDI—the sequential tunneling ionization of two electrons from doubly excited states that are formed through resonant capture via recollisions. This mechanism has never been addressed but is

expected to be the dominant mechanism for complex atoms (molecules). In the coming year we will continue to study NSDI for rare gas atoms where many experimental data exist, thus allowing the study of target dependence in NSDI.

4. Attosecond Physics and others

Recent progress and on-going projects

We studied electron spectra of He in the combined fields of APT (attosecond pulse train) and infrared (IR). The APT is used to excite the 3p state and the continuum states. After a time delay, an IR is applied. The continuum electron generated by APT and the one by IR from the 3p can interfere. We developed an analytical theory (see A1) to describe the two-path interference. Such a theory makes it simple to analyze the interference spectra in APT+ IR experiments.

We have been examining the time evolution of a Fano resonance. Fano resonance has been observed and formulated in the energy domain. In a real time-dependent setting, an initial pulse generates a bound state and a continuum. As the time evolves, the interaction of the bound state with the continuum results in the decay of the bound state, and eventually reveals itself as a Fano resonance. Before this asymptotic limit is reached, can one observe its wave packet, either in the energy domain or in the time domain? We have formulated such a problem and are in the process of identifying methods where such time evolution can be probed experimentally. The next step is to generalize the method to include all the states that can be reached in a single attosecond pulse, a situation that has been made possible with the emergence of single attosecond pulses.

There are other works published in the last year (see the A-list below) that are not mentioned here. A Topical Review of the QRS from the works of 2008-10 has been published in June 2010, see A3.

Publications (Papers published before 2009 are not listed here)

Published papers

A1. N. N. Choi, T. F. Jiang, T. Morishita, M-H. Lee and C. D. Lin, "Theory of probing attosecond electron wave packets via two-path interference of angle-resolved photoelectrons", Phys. Rev. A82, 013409 (2010)

A2. Zhangjin Chen, Yaqui Liang and C. D. Lin, "Quantum Theory of Recollisional (e, 2e) Process in Strong Field Nonsequential Double Ionization of Helium", Phys. Rev. Lett. 104, 253201 (2010)

A3. C. D. Lin, A. T. Le, Z. J. Chen, T. Morishita and R. Lucchese, "Strong field rescattering physics—self-imaging of a molecule by its own electrons", **Topical Review**, J. Phys. B43, 122001 (2010).

A4. Cheng Jin, Anh-Thu Le, Song-Feng Zhao, Robert Lucchese and C. D. Lin, "Determination of structure parameters in strong-field tunneling ionization theory of molecules" Phys. Rev. A81, 033421 (2010).

A5. Song-Feng Zhao, Cheng Jin, Anh-Thu Le, T. F. Jiang and C. D. Lin, "Determination of structure parameters in strong-field tunneling ionization theory of molecules", Phys. Rev. A81, 033423 (2010).

A6. Toru Morishita, Toshihito Umegaki, Shinichi Watanabe and C D Lin "High-resolution spatial and temporal microscopy with intense-laser-induced rescattering electrons" J. Phys.: Conf. Ser. 194 012011 (2010)

A7. Zhangjin Chen, T. Wittmann, B. Horvath and C. D. Lin, "Complete real-time temporal waveform characterization of single-shot few-cycle laser pulses" Phys. Rev. A80, 061402 (R) (2009).

- A8. Song-Feng Zhao, Cheng Jin, Anh-Thu Le, T. F. Jiang, and C. D. Lin, “Analysis of angular dependence of strong field tunneling ionization for CO₂”, *Phys. Rev. A* **80**, 051402(R) (2009).
- A9. Anh-Thu Le, R. R. Lucchese and C. D. Lin, “Uncovering multiple orbitals influence in high-harmonic generation from aligned N₂”, *J. Phys. B* **42**, 211001 (2009)
- A10. Anh-Thu Le, R.R. Lucchese, S. Tonzani, T. Morishita, C.D. Lin, “ Quantitative rescattering theory for high-order harmonic generation from molecules”, *Phys. Rev. A* **80**, 013401 (2009).
- A11. A. T. Le, R. R. Lucchese, M. T. lee and C. D. Lin, “Probing molecular frame photoionization via laser generated high-order harmonics from aligned molecules”, *Phys. Rev. Lett.* **102**, 203001 (2009).
- A12. Zhangjin Chen, A. T. Le, T. Morishita and C. D. Lin,” Quantitative rescattering theory for laser-induced high-energy plateau photoelectron spectra”, *Phys. Rev. A.* **79**, 033409 (2009).
- A13. Z. J. Chen, A. T. Le, Toru Morishita, and C. D. Lin, “Origin of species dependence of high-energy plateau photoelectron spectra”, *J. Phys B (fast track)*, *J. Phys. B* **42**, 061001 (2009).
- A14. T. Morishita, M. Okunishi, K. Shimada, G. Prumper, Z. J. Chen, S. Watanabe, K. Ueda, and C. D. Lin, “ Retrieval of experimental differential electron-ion elastic scattering cross sections from high-energy ATI spectra of rare gas atoms by infrared lasers”, *J. Phys. B.* **42**, 105205 (2009).
- A15. S. Micheau, Z. J. Chen, A. T. Le, J. Rauschenberger, M. F. Kling and C. D. Lin, “Accurate retrieval of target structure and laser parameters of few-cycle pulses from photoelectron momentum spectra”, *Phys. Rev. Lett.* **102**, 073001 (2009).
- A16. Samuel Micheau, Zhangjin Chen , Toru Morishita, Anh-Thu Le and C. D. Lin, “Robust carrier-envelope phase retrieval of few-cycle laser pulses from high-energy photoelectron spectra in the above-threshold ionization of atoms”, *J. Phys. B* **42**, 065402 (2009).
- A17. Samuel Micheau, Zhangjin Chen, Toru Morishita, Anh-Thu Le and C. D. Lin, “Quantitative rescattering theory for non-sequential double ionization of atoms by intense laser pulses”, *Phys. Rev. A* **79**, 013417 (2009)
- A18. Cheng Jin, A. T. Le and C. D. Lin, “Retrieval of target photo-recombination cross sections from high-order harmonics generated in a macroscopic medium”, *Phys. Rev. A* **79**, 053413 (2009).
- A19. Junliang Xu, Hsiao-Ling Zhou, Zhangjin Chen and C. D. Lin, “Genetic-algorithm implementation of atomic potential reconstruction from differential electron scattering cross sections”, *Phys. Rev. A* **79**, 052508 (2009).

Papers submitted for publication

- B1. Junliang Xu, Z. J. chen, A. T. Le and C. D. Lin, “Self-imaging of molecules from diffraction spectra by laser-induced rescattering electrons”, submitted to *Phys. Rev. A.* (June 8, 2010)
- B2. Anh-Thu Le, R. R. Lucchese and C. D. Lin, “Polarization and ellipticity of high-order harmonics from aligned molecules generated by linearly polarized intense laser pulses”, accepted (PRA).
- B3. C. D. Lin, Anh-Thu Le and Zhangjin Chen, “Theory of Dynamic Imaging of Molecules with intense infrared laser pulses”, Springer book- submitted July 6, 2010.

Structure and Dynamics of Atoms, Ions, Molecules and Surfaces: Atomic Physics with Ion Beams, Lasers and Synchrotron Radiation

Uwe Thumm, J.R. Macdonald Laboratory, Kansas State University
Manhattan, KS 66506 thumm@phys.ksu.edu

1. Laser-molecule interactions

Project scope: We develop numerical and analytical tools to i) efficiently predict the effects of strong laser fields on the bound and free electronic and nuclear dynamics in small molecules and ii) to fully image the laser-controlled nuclear and electronic dynamics.

Recent progress: We investigated the dissociation and ionization of $H_2^{(+)}$, $D_2^{(+)}$, $N_2^{(q+)}$, and $O_2^{(q+)}$ [1] in short intense laser pulses. We explored the possibility of controlling the electronic motion in dissociating H_2^+ [2] and D_2^+ [3,4] and studied the controlled manipulation of bound vibrational wave packets with carrier-envelope phase (CEP) stabilized laser pulses [2], two-color laser fields [4], and attosecond pulse trains [5]. We applied quantum-beat imaging techniques in order to discuss and quantify ro-vibrational couplings in D_2^+ under the influence of pulsed and continuum wave laser light [6,7,8].

Example 1: Dissociative ionization of H_2 in an attosecond pulse train and delayed laser pulse (with Feng He).

The ionization of H_2 in a single attosecond XUV pulse (SAP) generates a nuclear wave packet in H_2^+ which is entangled with the emitted photoelectron wave packet. The nuclear wave packet dynamics can be observed by dissociating H_2^+ in a delayed IR laser pulse. If H_2^+ is ionized by a sequence of XUV pulses of an attosecond pulse train (APT) (Fig. 1), whether or not the corresponding sequence of nuclear wave packets in H_2^+ is detected as a coherent or incoherent superposition depends on whether and how the photoelectrons are observed. We simulated the nuclear dynamics in this XUV pump - IR probe scenario and analyzed our numerical results for both, single attosecond pump pulses and pump-pulse trains of different lengths and temporal spacings between individual XUV pulses. By superimposing nuclear wave packets in H_2^+ generated by individual pulses in the pump-pulse train *incoherently*, we calculated proton kinetic energy release (KER) spectra [5] in good qualitative agreement with the experiment of [R1].

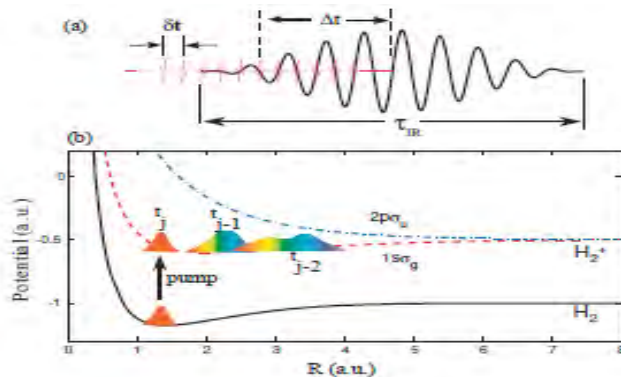


Fig. 1. (a) Schematic of the APT and IR laser field. The time delay Δt is the offset between the centers of the APT and IR pulses. The pulse duration of the IR pulse is τ_{IR} , and the separation between subsequent attosecond pulses is Δt . (b) The relevant Born-Oppenheimer potential curves of H_2 and H_2^+ . A sequence of nuclear vibrational wave packets is generated on the $1s\sigma_g$ electronic ground state potential curve of H_2^+ by repeated ionization of H_2 in subsequent XUV pulses of the APT.

Since photoelectrons carry phase information, the degree of coherence in the observed KER in an APT - delayed IR pulse experiment will change if photoelectrons are detected in coincidence with molecular fragments. Without the observation of coincident photoelectrons, we anticipate the KER to be devoid of coherence effects between subsequently launched nuclear wave packets, whereas coherence effects are expected to be most prominent if photoelectrons are detected in extremely narrow momentum bins and coincident with molecular fragments [5].

Future plans: We anticipate refined experiments in which protons and XUV-pulse emitted electrons are detected in coincidence. Assuming that such experiments can be carried out with sufficiently large count rates, we predict an interesting transition from an incoherent to a coherent superposition of nuclear wave packets as

photoelectrons are recorded in increasingly narrower momentum bins. For the coherent proton KER spectra, we find an extremely sensitive dependence on the IR wavelength, that might be exploited to characterize the IR laser pulse in terms of interference effects (in both delay and proton energy) in fragment KER spectra (Fig. 2). With regard to future numerical simulations, even for the simplest molecule, H_2 , more work is needed in order to establish a firm *lower* limit for the effect of nuclear wave packet interferences on KER spectra [5].

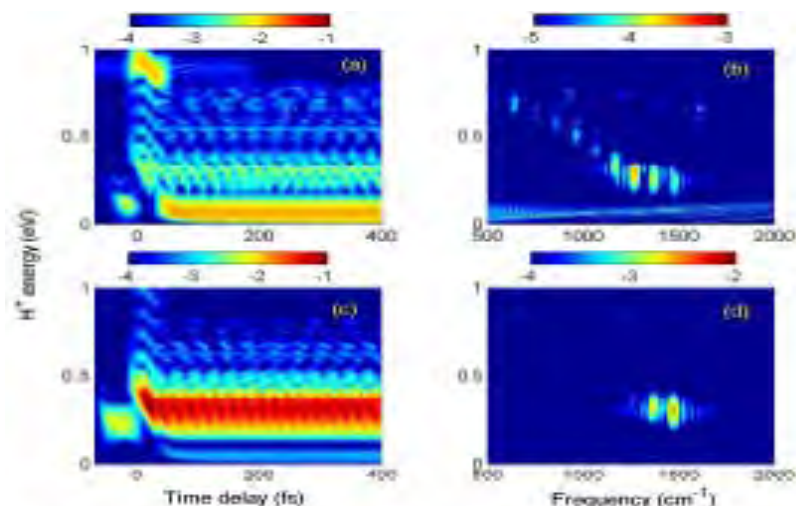


Fig. 2. Time-dependent proton energy distributions (left column) and corresponding power spectra (right column) for H_2 exposed to an APT and a delayed 30-cycle IR laser pulse with a peak intensity of 10^{13} W/cm². The APT consists of 14 alternating attosecond XUV pulses. Maximal coherence is assumed for the superposition individual H_2^+ nuclear wave packets.

(a) and (b): Results for an IR carrier wavelength of $\lambda_{IR}=800$ nm.

(c) and (d): Results for $\lambda_{IR}=727$ nm.

Example 2 : Electron localization in molecular fragmentation of H_2 with CEP stabilized laser pulses (in collaboration with the J. Ullrich group /Heidelberg). Fully differential data for H_2 dissociation in ultrashort (6fs, 760nm), linearly polarized, intense (0.44 P W/cm²) laser pulses with a stabilized CEP were recorded with a reaction microscope. Depending on the CEP, the molecular orientation, and the KER, a symmetric proton emission at low KERs (0–3 eV) was measured to be much stronger than reported by previously [R2]. Our wave packet propagation calculations [2] reproduce the salient features and discard, together with the observed KER-independent electron asymmetry, the first ionization step as the reason for the asymmetric proton emission (Fig. 3).

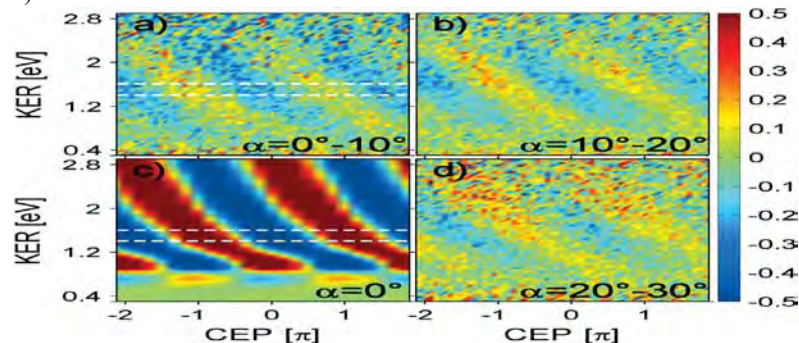


Fig. 3 . Dissociation asymmetry in dependence of the KER and the CEP for proton emission angles between (a) 0–10, (b) 10–20, and (d) 20–30 degrees with respect to the laser polarization axis. (c) Results of our time-dependent Schrödinger equation (TDSE) calculations. A solely relative CEPs were measured, the axes of the experimental data were shifted to fit the calculation.

Future plans: Even though the asymmetry in our experiment shows a similar CEP and KER-dependence as in [R3], the physical situation considered there, an incoherent sum of vibrational states, is different. Instead, a wave packet is produced in the first step [6], pointing to the possible control of chemical reactions through attosecond steering of electrons in a new type of “pump-control” experiments. Switching on the control laser at the time when the wave packet approaches the coupling regions should strongly enhance population transfer and asymmetry contrast. Control then can be achieved by changing the pump-probe-delay. One might envision that nuclear wave packets are efficiently guided through coupling regions via CEP stabilized pump-control schemes, steering the electronic motion on a sub-femtosecond time scale.

Example 3 : Quantum-beat (QB) analysis of the rotational-vibrational dynamics in D_2^+ (with Maia Magrakvelidze, Martin Winter, and Rüdiger Schmidt). The rapid ionization of D_2 in a short and intense laser pulse generates a rotational-vibrational (RV) nuclear wave packet in D_2^+ [7,9]. By solving the TDSE in full dimensionality, we simulated the coherent evolution of such wave packets and discussed their ro-vibrational

dynamics [8]. Within a harmonic time-series analysis of the evolving nuclear probability density, we characterized the RV dynamics in D_2^+ in an external intense linearly polarized infrared laser field in terms of QB spectra in which both, the internuclear distance R and molecular orientation are resolved (Fig. 4) [6,8].

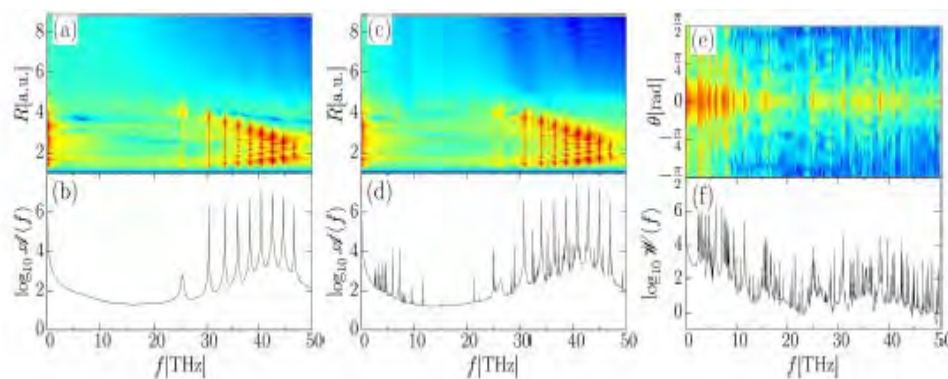


Fig. 4. (a,c) Angle-integrated $A(R,f)$. (e) Internuclear-distance integrated power spectra, $W(\theta, f)$. (b,d,f) Corresponding spectral line intensities for the evolution of aligned (a,b) and rotating (c-f) D_2^+ molecular ions in a 10^{13} W/cm² cw laser field.

Based on numerical examples for the nuclear dynamics without and under the influence of pulsed and continuous-wave (cw) laser light, we discussed and quantified the signature of RV couplings in QB spectra and to what extent the quantum-beat analysis of measured time-dependent fragment kinetic energy release spectra is expected to image the laser-dressed RV structure of D_2^+ [8].

Future plans: Extending this technique to more complicated polyatomic molecular systems and reaction complexes may enable the investigation of molecular dynamics across the (field-modified) potential barrier along a particular reaction coordinate, and, thus, provide a basis for novel multidimensional optical-control schemes for chemical reactions. We also envision to apply this method to quantify the progression of decoherence in the nuclear motion based on a time series of KER spectra.

2. Laser-assisted photoemission from adsorbate-covered metal surfaces: Time-resolved core-hole relaxation dynamics from sideband profiles (with Chang-hua Zhang)

Project scope: We attempt to model the time-resolved photo-electron emission and Auger decay in pump-probe and streaking experiments with complex targets, such as clusters, carbon nanotubes, and surfaces.

Recent progress: Illumination of an adsorbate-covered metal surface with an XUV and a delayed IR laser pulse can result in sidebands in the photoelectron (PE) spectra [R4]. We developed a theoretical model for the delay-dependent PE spectra and showed how the relaxation dynamics of XUV-induced core-level holes in adsorbate atoms can be deduced from the temporal shift between sideband peaks in the spectra of secondary adsorbate (Auger) electrons and conduction band (CB) PEs from the substrate (Fig. 5) [10,11,12].

In comparison with gaseous targets, we found a characteristic sideband-intensity enhancement in the laser-assisted photoemission from the substrate core-levels [11,12]. This effect can be tested in experiments with tunable XUV wavelength. Our calculated PE spectra support first time-resolved experiments for Xe-covered Pt(111) surfaces, promoting the direct analysis in the time domain of surface dynamical processes. This intensity redistribution between the main and sideband peaks in core level PE spectra from metals surfaces is related to the transport of photoreleased electrons in the substrate [10,12].

Future plans: (1) Since the transport (in our model the electron mean-free path λ) depends on the PE kinetic energy, and thus the XUV frequency ω_x , we anticipate future tests of this predicted sideband enhancement effect in experiments with tunable ω_x . (2) While we believe fully localized states are a good approximation for the 4f state in tungsten [10,11], the fully delocalized plane wave (jellium) approximation [13] does not take into account that 5d6s CB states in tungsten have some localized character. For a fixed value of $\lambda=5$, allowing for partial localization of the CB states decreases the temporal shift between core and CB levels. This decrease

would be compensated by increasing λ to a value closer to accepted values [11,12]. We plan to improve our modeling of (i) the metal CB and (ii) the propagation of photoelectrons inside the solid.

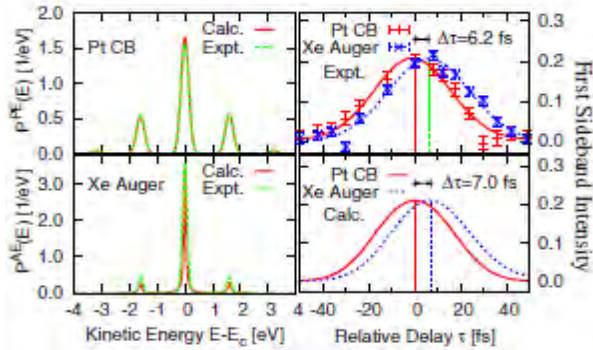


Fig. 5. Theoretical and experimental [R4] PE spectra for laser-assisted photoemission from a Xe/Pt(111) surface. **Left:** Sideband intensities for no delay ($\tau=0$) between XUV and IR pulses for XUV-emitted Pt CB electrons from the Fermi level (top) and Xe AEs (bottom). **Right:** Experimental (top) and calculated (bottom) first sideband intensities for Pt CB electrons and Xe AEs, revealing a temporal shift $\Delta\tau$. Sideband intensities in the AE spectra are multiplied by a factor of 2.16.

Publications (2009-2010):

- [1] *Tracking dynamic wave packets in the O_2 dication using a pump/probe approach*, S. De, I. Bocharova, M. Magrakvelidze, D. Ray, W. Cao, B. Bergues, U. Thumm, M. F. Kling, I. V. Litvinyuk, and C. L. Cocke, *Phys. Rev. A* **82**, 013408 (2010).
- [2] *Electron Localization in Molecular Fragmentation of H_2 with CEP stabilized Laser Pulses*, M. Kremer, B. Fischer, B. Feuerstein, V. L. B. De Jesus, V. Sharma, C. Hofrichter, A. Rudenko, U. Thumm, C. D. Schröter, R. Moshhammer, and J. Ullrich, *Phys. Rev. Lett.* **103**, 213003 (2009).
- [3] *Control of electron localization in molecules using XUV and IR pulses*, K. P. Singh, W. Cao, P. Ranitovic, S. De, F. He, D. Ray, S. Chen, U. Thumm, A. Becker, M. M. Murnane, H. C. Kapteyn, I. Litvinyuk, and C. L. Cocke, *Phys. Rev. Lett.* **104**, 023001 (2010).
- [4] *Ion-energy dependence of asymmetric dissociation of D_2 by a two-color laser field*, D. Ray, F. He, S. De, W. Cao, H. Mashiko, P. Ranitovic, K. P. Singh, I. Znakovskaya, U. Thumm, G. G. Paulus, M. F. Kling, I. Litvinyuk, and C. L. Cocke, *Phys. Rev. Lett.* **103**, 223201 (2009).
- [5] *Dissociative ionization of H_2 in an XUV pulse train and delayed IR laser pulse*, F. He and U. Thumm, *Phys. Rev. A* **81**, 053413 (2010).
- [6] *Multidimensional quantum-beat spectroscopy: Towards the complete temporal and spatial resolution of the nuclear dynamics in small molecules*, M. Winter, R. Schmidt, and U. Thumm, *Phys. Rev. A* **80**, 031401(R) (2009).
- [7] *Quantum-beat imaging of the nuclear dynamics in D_2^+ : Dependence of bond softening and bond hardening on laser intensity, wavelength, and pulse duration*, M. Magrakvelidze, F. He, T. Niederhausen, I. V. Litvinyuk, and U. Thumm, *Phys. Rev. A* **79**, 033410 (2009).
- [8] *Angular dependence of the strong-field ionization of randomly oriented hydrogen molecules*, M. Magrakvelidze, F. He, S. De, I. Bocharova, D. Ray, I. Litvinyuk, and U. Thumm, *Phys. Rev. A* **79**, 033408 (2009).
- [9] *Quantum-beat analyses of the rotational-vibrational dynamics in D_2^+* , M. Winter, R. Schmidt, and U. Thumm, *New Journal of Physics*, *New J. of Phys.* **12**, 023023 (2010).
- [10] *Attosecond photoelectron spectroscopy of metal surfaces*, C.-H. Zhang and U. Thumm, *Phys. Rev. Lett.* **102**, 123601 (2009).
- [11] *Time-resolved IR laser-assisted XUV photoelectron spectroscopy of metal surfaces*, C.-H. Zhang and U. Thumm, invited paper, XXVI ICPEAC, Kalamazoo, *Journal of Physics: Conf. Series* **194**, 012055 (2009).
- [12] *Time-resolved core-hole decay in laser-assisted photoemission from adsorbate-covered metal surfaces*, C.-H. Zhang and U. Thumm, *Phys. Rev. A* **80**, 032902 (2009).
- [13] *Band-gap-confinement and image-state-recapture effects in the survival of anions scattered from metal surfaces*, A. Schmitz, J. Shaw, H. S. Chakraborty, and U. Thumm, *Phys. Rev. A* **81**, 042901 (2010).

References: [R1] Kelkensberg *et al.*, *Phys. Rev. Lett.* **103**, 123005 (2009) [R2] M. F. Kling *et al.*, *Science* **312**, 246 (2006). [R3] J. J. Hua and B. D. Esry, *J. Phys. B* **42**, 085601 (2009). [R4] L. Miaja *et al.*, *Phys. Rev. Lett.* **101**, 046101 (2008).

Strong-Field Time-Dependent Spectroscopy

Carlos A. Trallero

Physics Department, J.R. Macdonald Laboratory,
Kansas State University, Manhattan, KS 66506, carlos@phys.ksu.edu

1 Scope

My main goal is to develop new spectroscopic methods using strong, ultrashort pulses. This new spectroscopy means learning about the quantum nature of molecules and atoms by studying their interaction with intense pulsed fields. Topics in which I am interested include: attosecond spectroscopy and coherent control of molecules and atoms with shaped femtosecond pulses. Combining pulse shaping, field-free alignment, and high harmonic generation (HHG), it will be possible in the future to create a movie of the electron's probability density in a specific excited quantum state. The research outline to follow below contains the initial steps I propose to follow in order to achieve this milestone goal.

2 Introduction

As a new faculty member, my first priority is to setup an ultrafast laboratory to accomplish the research plans outlined below. My plans for the lab include an XUV spectrometer for attosecond experiments, an optical parametric amplifier (OPA) for generating femtosecond pulses at different wavelengths, and an ultra broadband pulse shaper using an acousto optical modulator (AOM) in the Fourier plane as the spatial light modulator (SLM). In addition to this equipment I plan to make use of the current expertise developed in the group in momentum imaging. In particular, velocity mapping imaging (VMI) chambers for ions and electrons. Future additions will be a high energy OPA and a pulse shaper for mid-irfrared wavelengths.

3 Attosecond science with HHG

I propose to use long wavelength few-cycle pulses to drive the harmonic generation process, to obtain a continuum and featureless harmonic spectrum that can resolve sub eV features in the molecular quantum structure. So far, most research groups use long wavelength for driving HHG mainly to extend the harmonic cutoff (increase the XUV photon energy). However, in recent experiments we have discovered that, for most molecules, the most interesting region lies in the low energy part of the spectrum below 40eV. At these low energies, the emitted photon is close to the ionization potential, thus carrying with it valuable information about the molecular states. Some of the features we expect to see are auto-ionizing states, shape resonances, and intermediate states en route to ionization. With HHG we can now resolve the quantum structure of molecules and atoms as a function of energy, time, and molecular angle, which represents a big step forward compared to traditional spectroscopic methods.

Another advantage of using long wavelengths is that the returning electron wavepacket is featureless for most of the energy spectrum. This fact is important since it allows for easier comparison between the observed HHG spectra and the tabulated photoionization cross sections [1]. During my postdoc, we developed a new source of $1.8\mu\text{m}$, two cycle pulses [2]. By using these pulses we extend the range of molecules that can be studied using HHG since the ionization rate is much smaller which means that for molecules with low ionization potential the emission of harmonics can happen at a larger range of intensities. Using harmonic generation as a sub eV resolution spectroscopic tool is a novel idea that I propose to carry on at JRML. There will be a strong collaboration with C.D. Lin's group in the theoretical aspects and with V. Kumarappan for the alignment and orientation of molecules.

There is also some evidence that by using these pulses to generate harmonics it is possible to produce isolated attosecond pulses. The signature of single attosecond pulses appears in the HHG spectrum as a totally continuum spectrum at certain intensities, indicating that the mechanism is that of ionization gating. By using COLTRIMS or an electron VMI it will be possible to experimentally confirm the presence of isolated XUV bursts. The main advantage to this approach of producing attosecond pulses is that producing few cycle pulses at long wavelengths is almost trivial and does not require the high complexity of producing a single cycle pulse at 800nm or complicated gate mechanisms.

Since HHG is a coherent macroscopic process, having a detailed description of what happens in the generating medium is of great importance. This is a field where both theory and experiment are lacking in depth. What I propose, is to make correlated measurements of harmonic spectra and ions. This can yield more information about the relation between HHG, ionization, and density of emitters. By measuring the ions and XUV spectra as a function of the molecular jet and laser focus positions, laser intensity, pressure, and alignment angle, a very exhaustive compilation of all macroscopic parameters involved in the HHG can be done. An ultimate goal of mine is to obtain a universal quantity that can describe the efficiency of harmonic generation and apply this knowledge towards the design of more efficient XUV sources and attosecond lasers. As a starting point I will use the recently developed formalism by C.D. Lin of fully characterized propagation simulations [3] to fit some recently acquired HHG spectra as a function of intensity.

All the experiments I have proposed so far use linearly polarized light to produce harmonics. However, when elliptically polarized light is used, sub-cycle temporal information can be extracted from evolving molecules. While a molecular bond is breaking, in the single-active-electron picture, the valence electron's wavefunction is stretched between the two fragments of the molecule. At the breaking, the wavefunction becomes localized and the electron belongs to only one of the remaining fragments of the molecule. When the latter happens, HHG won't occur as there will be no interference between the continuum and bound parts of the electron's wave function. I propose to study how this process happens using elliptically polarized light. In this case, when the electron leaves it can probe the other fragment until the breaking point. Since the returning time of the electron is very fast, it will be possible to probe extremely fast chemical reactions such as those involving hydrogen bonds.

One proposed chemical reaction is the ring opening of cyclohexadiene. This particular molecule, when excited, goes through two conical intersections before opening. While this reaction has been studied before using other methods, no one has been able to resolve the fast oscillations that the molecule undergoes before breaking. I believe that a scheme like the one proposed here should be able to resolve such fast structural changes. For this topic I will join forces with Itzik and Esry as they are also studying conical intersections.

4 Strong field coherent control in molecular systems

The following part my research will be focused on the quantum control of molecules and atoms in the strong field limit where the field distorts the quantum states of the atom or molecule and perturbation theory breaks down.

For these control experiments, I propose to use a white light, or super continuum pulse shaper. By having access to such a large bandwidth, a greater degree of control can be achieved. One main issue that most coherent control experiments encounter is that the probe pulse often distorts the molecule itself, making clean measurements of how much population has been transferred between quantum states impossible. To avoid this, I propose to use an XUV pulse as a probe that can extract the electron from the molecule without going through all the intermediate states. By performing measurements with and without the control pulse, it will be possible to determine how much population was transferred between states. The goal is to show a *full population transfer in evolving molecules in the presence of dynamic Stark shifts*

Once proven that multiphoton population inversion is possible in molecular systems, I will carry out a systematic study of different molecules as a function of parameterized pulse shapes. Previous results, including work in my Ph.D. thesis [4], showed that unique features appear when using pulse shapes such as spectral steps and chirps to drive multiphoton transitions in strong fields. For strong fields, not only the resonant frequency is important, but also the dynamic Stark shift and, in the case of molecules, nuclear dynamics. All these factors create a unique signature for each molecule, thus becoming a *strong field spectroscopy with shaped femtosecond pulses*. For all the topics mentioned in this section a strong collaboration

with U. Thumm is underway.

By means of a pulse shaper, it is also possible to perform pump-probe experiments where nearly all parameters are changed systematically and faster than using mechanical equivalents. It is possible to change the delay, intensity, pulse duration, center wavelength of each pulse and the relative carrier envelope phase (CEP) between pump and probe. The CEP phase in a typical pump-probe experiment changes as a function of delay and can not be controlled. Using a pulse shaper this CEP phase between pump and probe can be locked or changed arbitrarily within attosecond resolution. My goal in these sets of experiments is to first demonstrate what is the maximum resolution in the relative phase (between the pump and probe pulses) and then to study how sensitive different experiments, such as multiphoton transitions in atoms, are to this new parameter. This technique can become a new method of performing *attosecond coherent control with femtosecond pulse shaping*

5 High harmonic generation of systematically excited molecules

Finally, I want to merge the two fields of coherent control and attosecond physics. I propose to use a scheme such as a diffraction grating of excited molecules to probe the angle dependent orbitals of excited molecules. For this experiment, I plan to use the same ultra-broadband pulse shaper in a non-collinear geometry together with a few cycle pulse in the far infrared that generates harmonics. The shaped pulses will target an specific excited state that will then be probed using HHG. This can provide a systematic way of probing excited states in aligned molecules. By changing the pulse shape we can excite different states without the need of using different wavelengths.

This method can develop not only as an enhancement for studying quantum systems with harmonic generation, but also as a tool for coherent control experiments as it allows for nearly background-free measurements.

References

- [1] J. W. Gallagher et al. Absolute cross sections for molecular photoabsorption, partial absolute cross sections for molecular photoabsorption, partial photoionization, and ionic photofragmentation processes. *Journal of Physical and Chemical Reference Data*, 17:9, 1988.
- [2] Bruno E. Schmidt et al. Compression of 1.8 μm laser pulses to sub two optical cycles with bulk material. *Applied Physics Letters*, 96(12):121109, 2010.
- [3] Cheng Jin et al. Retrieval of target photo-recombination cross sections from high-order harmonics generated in a macroscopic medium. *Physical Review A*, 79:053413, 2009.
- [4] Carlos Trallero-Herrero and Thomas C. Weinacht. Transition from weak to strong field coherent control. *Phys. Rev. A*, 75, 2007.

Engineered Electronic and Magnetic Interactions in Nanocrystal Quantum Dots

Victor I. Klimov

*Chemistry Division, C-PCS, MS-J567, Los Alamos National Laboratory
Los Alamos, New Mexico 87545, klimov@lanl.gov, <http://quantumdot.lanl.gov>*

1. Program Scope

Using semiconductor nanocrystals (NCs) one can produce extremely strong spatial confinement of electronic excitations not accessible with other types of nanostructures. Because of spatial constraints imposed on electron and hole wavefunctions, electronic energies in NCs are directly dependent upon their dimensions, which is known as the quantum-size effect. This effect has been a powerful tool for controlling spectral responses of NCs and enabling potential applications such as multicolor labeling, optical amplification, and low-cost lighting. In addition to spectral tunability, strong spatial confinement results in a significant enhancement of carrier-carrier interactions that lead to a number of novel physical phenomena including large splitting of electronic states induced by electron-hole (e-h) exchange coupling, ultrafast multiexciton decay via Auger recombination, high-efficiency intraband relaxation via e-h energy transfer, and direct generation of multiple excitons by single absorbed photons via carrier multiplication. Understanding the fundamental physics of electronic and magnetic interactions under conditions of extreme quantum confinement and the development of methods for controlling these interactions represent the major thrusts of this project. Research topics studied here include single-exciton optical gain using engineered exciton-exciton interactions, tunable magnetic exchange with paramagnetic ions in core/shell heterostructures, and Auger recombination in NCs of direct- and indirect-gap materials. In addition to their fundamental significance, these studies are relevant to a number of emerging applications of NCs in areas such as low-threshold lasing, solid-state lighting, spintronics and magneto-optical imaging.

2. Recent Progress

During the past year, our work in this project has focused on studies of the electronic structure of band-edge states in PbSe NCs using time-resolved photoluminescence (PL) spectroscopy in high magnetic fields, single-NC spectroscopy of novel thick-shell CdSe/CdS core/shell nanostructures ("giant" NCs or g-NCs), effects of photoionization in PbSe NCs, and magnetic interactions in Mn-doped NCs. During 2008 - 2010, our work resulted in 20 peer-reviewed publications including: a report in *Nature Materials*; a feature article in *Acc. Chem. Res.*; 5 *Phys. Rev. Letters*; 3 *J. Am. Chem. Soc.* papers; and 4 *Nano Letters*. The studies conducted in this project were presented in 41 invited conference talks and numerous university seminars. The results of this project were also highlighted in the plenary address at the recent *Quantum Dot 2010* Conference in Nottingham, UK. Below, we provide a description of two pieces of our work in which we study a fine structure splitting of exciton states in PbS NCs [1] and spectral signatures of multiexcitons in CdSe/CdS g-NCs [2].

2.1 Peculiarities of exciton fine-structure in PbSe NCs. Electron-hole exchange interactions, crystal structure, band symmetry, spin-orbit coupling, and shape anisotropy all influence the underlying level ordering and oscillator strengths of band-edge excitons in colloidal NCs. Understanding this "exciton fine structure" is especially important in NCs because it governs both absorptive and emissive optical properties. For example, in the common case of CdSe NCs these properties combine to split the band-edge exciton into the now well-established fine structure of five distinct levels, wherein the lowest excited state is an optically-forbidden "dark" exciton that lies as much as 2-15 meV below the nearest optically-allowed "bright" exciton.

In contrast with wide-gap semiconductors like CdSe (which have wurtzite/zincblende structure and direct bandgaps at the Brillouin-zone center) lead-salt semiconductors such as PbSe are narrow-gap materials having rock-salt crystal structure and direct gaps at the four-fold degenerate L-point at the Brillouin zone edge. In further distinction, electrons and holes in PbSe exhibit very similar masses and giant g-factors ($g \sim 30$) due to strong spin-orbit coupling. As such, the exciton fine structure in lead-salt NCs is expected to be rather different, and several theoretical studies have been reported for PbSe NCs. Four-band envelope wavefunction methods first suggested 1 - 5 meV exchange energies and predicted an optically-allowed exciton ground state, whereas tight-binding calculations anticipated that the nominally degenerate L-points are split in NCs by tens of meV due to intervalley

coupling. More recently, empirical pseudopotential approaches suggested that PbSe NCs possess a single optically-forbidden exciton ground state that lies 2 - 17 meV below a 3-fold degenerate manifold of optically-allowed exciton levels.

To experimentally study the fine structure of exciton states in PbSe NCs, we have measured the PL spectrum and PL decay time (τ) of PbSe NCs at temperatures down to 270 mK and in high magnetic fields up to 15 T. We find that τ increases sharply below 10 K, but saturates near 500 mK. In marked contrast to the “conventional” exciton fine structure found in CdSe and other wide-gap NCs (i.e., clear dark and bright exciton levels with orders-of-magnitude different oscillator strengths, well-separated in energy by 2 -15 meV), the dynamics in PbSe NCs fit remarkably well to a different exciton structure containing two weakly-emitting states with comparable oscillator strength, that are split by a surprisingly small energy of only 290-870 μ eV for NC radii from 2.3 to 1.3 nm. Importantly, magnetic fields reduce τ only below 10 K, consistent with field-induced mixing between these two states. Further, magnetic circular dichroism studies establish the magnetic Zeeman energy of the 1S absorbing exciton states in PbSe NCs for the first time (g_{ex} ranges from 2-5), and magneto-PL from the emitting excitons reveals >10% circular polarization, also implicating contributions from Zeeman-split excitons. Thus, these studies provide compelling experimental evidence for a new type of exciton fine structure in rocksalt PbSe NCs that is qualitatively different from that found in NCs of more common wide-bandgap semiconductors such as CdSe.

2.2 Highly emissive multiexcitons in the steady-state PL of “giant” CdSe/CdS NCs. Previous studies of carrier recombination dynamics in semiconductor NCs under intense pulsed excitation have shown that Auger decay is a general phenomenon that dominates multiexciton dynamics in these nanostructures, irrespective of composition, core/shell geometry, or shape. This process is especially detrimental in lasing applications of NCs,

as it leads to very short (picoseconds) optical gain lifetimes. It also limits the performance of NC-based light emitting diodes and photovoltaic cells because it introduces an additional recombination channel in charged nanoparticles. Thus, the development of Auger-recombination-free NCs would greatly benefit a large number of emerging NC-based technologies.

Recently, we reported a new class of NCs (termed g-NCs) that comprise a small CdSe core (3 - 4 nm diameter) encapsulated in a thick shell (10 - 19 monolayers) of wider band gap CdS. Our initial spectroscopic studies of these structures indicated a significant improvement in photostability of g-NCs compared to standard particles, as well as a much higher tolerance to harsh chemical and heat treatments, and a significant suppression of PL intermittency (“blinking”) observed in single-dot measurements. Additionally, we observed a significant suppression of Auger decay in ensemble studies of g-NCs where we directly monitored dynamics of single and biexciton emission [9]. Based on these measurements, we inferred that the lower bound of the biexciton Auger decay time was 15 ns, which was ca. 75 times longer than in standard CdSe/ZnS nanocrystals possessing a similar emission wavelength.

Our recent work in the present

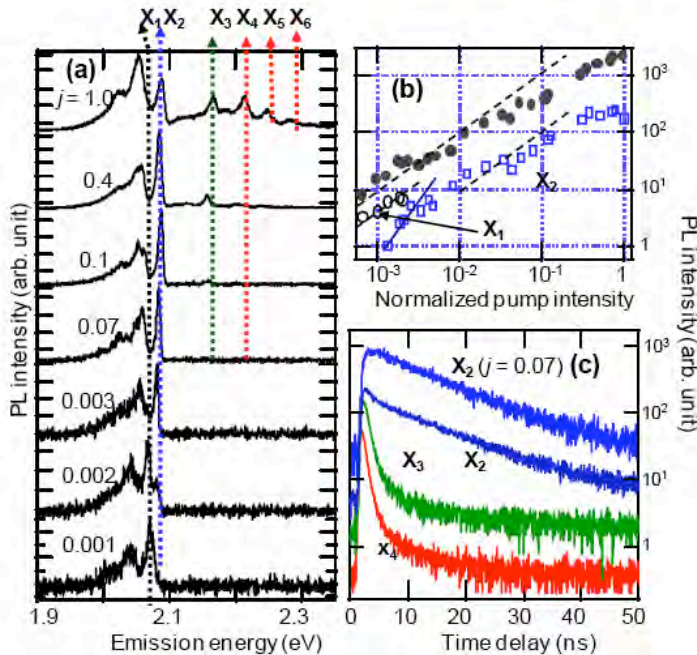


Figure 1. (a) cw-PL spectra of the individual g-NC measured for different per-pulse fluences (indicated in normalized units in the figure). In addition to the single-exciton (X_1), the spectra reveal the biexciton (X_2) bands as well as four more higher-energy peaks (labeled X_3 – X_6) that are due to emission of triexcitons and other multiexcitons of higher order. (b) Pump-intensity dependence of the X_1 (black open circles) and the X_2 (blue open squares) features along with the spectrally integrated PL intensity (gray solid circles); dashed and solid lines correspond to linear and quadratic dependences, as expected for excitons and biexcitons, respectively. (c) PL dynamics measured at the positions of the X_2 , X_3 , and X_4 features for $j = 1$. The X_2 trace indicates that the biexciton decay is characterized by ~ 10 ns time constant, which is significantly longer than in standard NCs emitting at the same wavelength.

project has produced new evidence of significantly suppressed Auger decay in g-NCs, based on a large body of spectroscopic data obtained from single-dot measurements under both continuous-wave (*cw*) and pulsed excitation and for two different pump photon energies (532 and 405 nm). Specifically, in contrast to single-dot PL spectra of standard NCs, which show emission solely due to single excitons under *cw* excitation independent of pump level, high-pump-intensity g-NC emission spectra are dominated by features due to biexcitons. Based on the spectral position of emission peaks, we conclude that the 532 nm pump (direct excitation of the CdSe core) results solely in neutral species, while the 405 nm pump (excitation of the CdS shell) can produce either neutral or charged excitations. We observe that both charged and neutral biexcitons, as well as charged excitons (trions), are highly emissive, and the corresponding emission peaks do not saturate at high pump levels. This is in contrast to the PL signal of standard NCs, which saturates as a result of the fast Auger decay that leads to suppression of emission from biexciton and charged states. Using intense pulsed excitation, we are even able to observe efficient emission from multiexcitons of higher order – 3 and above (Figure 1). Together, these results confirm a significant enhancement in multiexciton emission yields in g-NCs compared to standard NCs, which directly points toward greatly suppressed Auger recombination and an opportunity to utilize these newly opened photon-conversion pathways for a range of applications from efficient light emission to energy harvesting.

3. Future Plans

3.1 Fundamental reasons underlying suppression of Auger recombination in g-NCs. In our future work, we will study a series of CdSe/CdS samples with progressively increasing shell thickness (H). For these samples, we will record single exciton and biexciton decay as a function of H , which will allow us to determine the critical shell thickness for which the Auger-recombination-free behavior develops. In parallel, we will monitor the changes in the internal structure of the NCs using analytical techniques such as Raman scattering. These studies will help us to understand, for example, whether the growth of the CdS shell is accompanied by the formation of the interfacial graded layer with alloyed composition. As indicated by recent theoretical studies (Cragg & Efros, *Nano Lett.* **10**, 2010), formation of such a layer may represent one of the reasons for suppressed Auger recombination in these nanostructures.

3.2 Tunable magnetic interactions in Mn-doped core-shell NCs. We will continue our studies of magneto-optical properties of colloidal ZnSe/CdSe core/shell nanocrystals doped with different concentrations of Mn. We first introduced these structures in ref. [7], where we demonstrated that by changing the thickness of the outer shell we could tune both the magnitude and the sign of the exciton-Mn exchange interaction. These previous studies were conducted exclusively using magnetic-circular dichroism spectroscopy. In our future work, we will extend these measurements to studies of magneto-PL spectra and dynamics. Further, we will perform a side-by-side comparison with similar measurements of non-magnetic NCs as well as bulk ZnMnSe films. The effect of Mn concentration and CdSe shell thickness on the Zeeman splitting and the strength of Mn-Mn coupling will be studied. One specific focus of this work will be the effect of magnetic field on emission due to internal Mn transitions at ~ 2.15 eV. In bulk semiconductors, Mn emission is not polarized. However, our preliminary studies indicate the development of a significant degree of polarization of Mn PL in doped NCs under applied magnetic field. In this project, we will attempt to elucidate the reasons for this unusual behavior.

3.3. Effects of quantum confinement on emission spectra and dynamics of Ge NCs. Recently, we developed a new synthetic route for the fabrication of high quality colloidal Ge NCs [11]. In addition to relatively small size dispersity ($<10\%$) and good environmental stability, these NCs show high emission yields approaching 10% at room temperature. Previously, we used these NC to elucidate the effect of quantum confinement on Auger recombination [6]. These studies produced very interesting results that indicated an orders of magnitude enhancement in Auger decay in these NCs compared to bulk Ge. We explained this observation as the effect of mixing of the direct and indirect-gap band minima induced by spatial confinement. We expect that this mixing will have a profound effect on exciton emission, and especially radiative decay dynamics. Ge is an indirect gap material, in which emission is phonon-assisted process. Since it is the second-order effect, the probability of radiative recombination in bulk Ge is very low. As indicated by high emission efficiencies measured for Ge nanoparticles, the rate of radiative decay is greatly enhanced by effects of spatial confinement. In this project, we will investigate the competition between radiative and nonradiative recombination in Ge NCs as a function of particle size. We will further study the temperature and magnetic-field dependent decay dynamics which will help us to elucidate the structure of the low-energy emitting states in these novel NCs.

4. Publications (2008 - 2010)

1. R. D. Schaller, S. A. Crooker, D. A. Bussian, J. M. Pietryga, J. Joo, V. I. Klimov, Revealing the exciton fine structure in PbSe nanocrystal quantum dots, *Phys. Rev. Lett.* (August, 2010).
2. H. Htoon, A. V. Malko, D. Bussian, J. Vela-Becerra, Y. Chen, J. A. Hollingsworth, V. I. Klimov, Highly Emissive Multiexcitons in Steady-State Photoluminescence of Individual “Giant” CdSe/CdS Core/Shell Nanocrystals, *Nano Lett.* **10**, 2401 (2010).
3. D. C. Lee, I. Robel, J. M. Pietryga, V. I. Klimov, Infrared-active heterostructured nanocrystals with ultralong carrier lifetimes.” *J. Am. Chem. Soc.* **132**, 9960 (2010).
4. M. Sykora, A. Y. Kuposov, J. A. McGuire, R. K. Schulze, O. Tretiak, J. M. Pietryga, V. I. Klimov, Effect of air exposure on surface properties, electronic structure and carrier relaxation in PbSe nanocrystals.” *ACS Nano* **4**, 2021 (2010).
5. J. A. McGuire, M. Sykora, J. Joo, J. M. Pietryga, V. I. Klimov, Apparent versus true carrier multiplication yields in semiconductor nanocrystals.” *Nano Lett.* **10**, 2049 (2010).
6. I. Robel, R. Gresback, U. Kortshagen, R. D. Schaller, V. I. Klimov, Universal size-dependent trends in Auger recombination in direct- and indirect-gap semiconductor nanocrystals, *Phys. Rev. Lett.* **102**, 177404 (2009).
7. D. Bussian, M. Ying, S. A. Crooker, M. Brynda, A. L. Efros, V. I. Klimov, Tunable magnetic interactions in manganese-doped inverted core/shell ZnSe/CdSe nanocrystals, *Nature Mater.* **8**, 35 (2009).
8. H. Htoon, S. A. Crooker, M. Furis, S. Jeong, Al. L. Efros, V. I. Klimov Anomalous circular polarization of photoluminescence spectra of individual CdSe nanocrystals in an applied magnetic field, *Phys. Rev. Lett.* **102**, 017402 (2009).
9. F. Garca-Santamara, Y. Chen, J. Vela, R. D. Schaller, J. A. Hollingsworth and V. I. Klimov, Suppressed Auger recombination in “giant” nanocrystals boosts optical gain performance, *Nano Lett.* **10**, 3482 (2009).
10. J. Joo, J. M. Pietryga, J. A. McGuire, S.-H. Jeon, D. J. Williams, H.-L. Wang and V. I. Klimov, A reduction pathway in the synthesis of PbSe nanocrystal quantum dots, *J. Am. Chem. Soc.* **131**, 10620 (2009).
11. D. C. Lee, J. M. Pietryga, I. Robel, D. J. Werder, R. D. Schaller, V. I. Klimov, Colloidal Synthesis of infrared-emitting germanium nanocrystals *J. Am. Chem. Soc. (Communication)* **131**, 3436 (2009).
12. D. Bussian, A. Malko, H. Htoon, Y. Chen, J. A. Hollingsworth, V. I. Klimov, Quantum optics with nanocrystal quantum dots in solution: Quantitative study of clustering, *J. Phys. Chem.* **113**, no. 6, 2241 (2009).
13. J. A. McGuire, J. Joo, J. M. Pietryga, R. D. Schaller, and V. I. Klimov, New aspects of carrier multiplication in semiconductor nanocrystals, *Acc. Chem. Res.* **41**, 1810 (2008).
14. J. Vela, B. S. Prall, P. Rastogi, D. J. Werder, J. L. Casson, D. J. Williams, V. I. Kimov, J. A. Hollingsworth, Sensitization and protection of lanthanide ion emission in In₂O₃:Eu nanocrystal quantum dots, *J. Phys. Chem. C* **112**, 20246 (2008).
15. B.Q. Sun, A.T. Findikoglu, M. Sykora, D.J. Werder, and V.I. Klimov, Hybrid photovoltaics based on semiconductor nanocrystals and amorphous silicon, *Nano Lett.* **9**, 1235 (2009).
16. M. Durach, A. Rusian, V. I. Klimov, M. I. Stockman, Nanoplasmonic renormalization and enhancement of Coulomb interactions, *New J. Phys.* **10**, 105011 (2008).
17. J. M. Pietryga, K. K. Zhuravlev, M. Whitehead, V. I. Klimov, R. D. Schaller, Evidence for barrierless Auger recombination in PbSe nanocrystals: A pressure-dependent study of transient optical absorption, *Phys. Rev. Lett.* **101**, 217401 (2008).
18. M. Sykora, L. Mangolini, R. D. Schaller, U. Kortshagen, D. Jurbergs, and V. I. Klimov, Size-dependent intrinsic radiative decay rates of silicon nanocrystals at large confinement energies, *Phys. Rev. Lett.* **100**, 067401 (2008).
19. V. I. Klimov, J. A. McGuire, R. Schaller, and V. I. Rupasov, Scaling of multiexciton lifetimes in semiconductor nanocrystals, *Phys. Rev. B* **77**, 195324 (2008).
20. H. Htoon, M. Furis, S. A. Crooker, S. Jeong, V. I. Klimov, Linearly-polarized ‘fine structure’ of the bright exciton state in individual CdSe nanocrystal quantum dots, *Phys. Rev. B* **77**, 035328 (2008).

Atomic, Molecular and Optical Sciences at LBNL

A. Belkacem, C.W. McCurdy, T. Rescigno and T. Weber

Chemical Sciences Division, Lawrence Berkeley National Laboratory, Berkeley, CA 94720

Email: abelkacem@lbl.gov, cwmccurdy@lbl.gov, tnrescigno@lbl.gov, tweber@lbl.gov

Objective and Scope

The AMOS program at LBNL is aimed at understanding the structure and dynamics of atoms and molecules using photons and electrons as probes. The experimental and theoretical efforts are strongly linked and are designed to work together to break new ground and provide basic knowledge that is central to the programmatic goals of the Department of Energy. The current emphasis of the program is in three major areas with important connections and overlap: inner-shell photo-ionization and multiple-ionization of atoms and small molecules; low-energy electron impact and dissociative electron attachment of molecules; and time-resolved studies of atomic processes using a combination of femtosecond X-rays and femtosecond laser pulses. This latter part of the program is folded in the overall research program in the Ultrafast X-ray Science Laboratory (UXSL).

The experimental component at the Advanced Light Source makes use of the Cold Target Recoil Ion Momentum Spectrometer (COLTRIMS) to advance the description of the final states and mechanisms of the production of these final states in collisions among photons, electrons and molecules. Parallel to this experimental effort, the theory component of the program focuses on the development of new methods for solving multiple photo-ionization of atoms and molecules. This dual approach is key to break new ground and solve the problem of photo double-ionization of small molecules and unravel unambiguously electron correlation effects.

Inner-Shell Photoionization and Dissociative Electron Attachment of Small Molecules

Ali Belkacem and Thorsten Weber

Chemical Sciences Division, Lawrence Berkeley National Laboratory, Berkeley, CA 94720

Email: abelkacem@lbl.gov, tweber@lbl.gov

Objective and Scope

This program is focused on studying photon and electron impact ionization, excitation and dissociation of small molecules and atoms. The first part of this project deals with the interaction of X-rays with atoms and simple molecules by seeking new insight into atomic and molecular dynamics and electron correlation effects. These studies are designed to test advanced theoretical treatments by achieving a new level of completeness in the distribution of the momenta and/or internal states of the products and their correlations. The second part of this project deals with the interaction of low-energy electrons with small molecules with particular emphasis on Dissociative Electron Attachment (DEA). Both studies are strongly linked to our AMO theoretical studies led by C. W. McCurdy and T. Rescigno and are designed to break new ground and provide basic knowledge that is central to the programmatic goals of BES in electron-driven chemistry. Both experimental studies (photon and electron impact) make use of the powerful COLd Target Ion Momentum Spectroscopy (COLTRIMS) method to achieve a high level of completeness in the measurements.

Carbon K-shell photoionization of fixed-in-space C₂H₄.

Using the COLTRIMS technique we performed kinematically complete experiments measuring the photoionization of the carbon K-edge of fixed in space ethylene molecules for different photon energies (293, 302, 306, 318eV - linear polarized), while focusing on the symmetric break-up channel (CH₂⁺ + CH₂⁺). In this case the core electron was ionized and the core hole underwent a fast decay by emission of a secondary Auger electron and the resulting dication promptly broke up through a Coulomb explosion. The coincident measurement of the reaction products along with the data collection and analysis on the event-by-event basis allowed us to obtain the multi differential angular distribution of photoelectrons in the body-fixed frame of ethylene molecules. With the knowledge of the total cross section and the photo electron angular distributions in the molecular frame the s and p contributions as a function of photon energy could be derived. We also found a molecular geometry effect at higher photon energies which manifests itself in a preferred emission of the photo electrons along the polarization vector for the s and p transition. Moreover we completed a very comprehensive theoretical study of the reaction. A set of dipole transition matrix elements was calculated and extracted (7 amplitudes and 5 relative phases) from the experimental results. These matrix elements along with the complete angular distributions showed a very good qualitative agreement between the experiment and the theoretical model used. From the $l = 3, m = 0$ partial wave contribution to the electron angular distribution we concluded the presence of an f-wave shape resonance found

around 10eV above the carbon K-edge in the ethylene molecule. This was predicted for many years and could now be directly visualized for the first time in the Molecular Frame Angular Photoelectron Distributions (MFPADs).

Kinematically complete experimental study of the dissociation pathways of the singly ionized CO molecule.

We studied the dissociation of the singly ionized carbon monoxide molecule, followed by subsequent autoionization of O^+ , by detecting for the first time all four final fragments ($C^+ + O^+ + 2e$) in coincidence. In this experiment the supersonic jet of carbon monoxide was illuminated by the 43 eV x-ray beam at the Advanced Light Source. Although some direct double ionization of CO molecule was observed, the energetics dictated that most of the registered events must be attributed to single ionization followed by an autoionization in the atomic state of the oxygen. The energy of the slow electron is constant and independent of the first electron energy or of the nuclear kinetic energy release (KER) which is a clear signature of autoionization. The molecular dissociation of CO^+ ion followed by autoionization of the oxygen has been observed before. In this study we performed the most kinematically complete experiment where by simultaneously measuring the vector momenta of all particles we were able to extract the KER of the reaction together with the energies and complete angular distributions of photo-electron and autoionization electron in the body-fixed molecular frame. The study of these detailed angular distributions as a function of polarization and KER reveal a surprising dissociation dynamics. Comparison with theoretical calculations by colleagues Rescigno and Orel shine light on the molecular states involved in the initial process of photo-ionization. We observe a strong correlation between the angle of emission of the photo-electron and the angle of emission of the autoionization electron despite the fact that autoionization takes place in the atomic oxygen when the molecule has already fully dissociated. Further studies both experimental and theoretical are on-going to understand the origin of this unique photo and autoionization electron correlation.

Dissociative electron attachment to water molecules: imaging of the dissociation dynamics of the water anion.

A Coltrims spectrometer has been modified for measuring the angular dependence and kinetic energy release of negative ion fragments arising from dissociative electron attachment to water and heavy water molecules. The resonant attachment of a low energy electron to a water molecule occurs via three metastable electronic states of the H_2O anion, whose vertical transition energies determine the incident electron energy at which attachment occurs. Following the electron attachment a competition between autodetachment of the electron and very fast molecular dynamics that keeps the electron attached to the nuclei takes place. This fast dynamics is key in converting electronic energy to nuclear motion. The dissociation of the three resonance states of the anion (2B_1 , 2A_1 and 2B_2) involves complicated polyatomic dynamics involving conical intersection and, perhaps Renner-Teller effects, and occurs in several interesting ways. The angular dependence of dissociative attachment depends both on the entrance amplitude and the more complicated nuclear dynamics of the anion transient state. We find that the attachment of the electron to the molecule is exquisitely sensitive to the orientation of the molecule with respect to the incoming electron. The measured angular distributions of the anion fragments (O^- or H^-) confirm quite well the concept of entrance amplitude and the unique angular selectivity of electron attachment for each resonance.

We extended the dissociative electron attachment measurements to methanol and ethanol where we replaced the OH with a deuterated OD to study the similarities and differences associated with the hydroxyl functional group in each case. Similar to the water case, the resonance are located in the 6-12 eV electron energy range. In both cases we find the attachment to occur preferably when the electron impinges along the OD bond and the location of the bond that is broken by dissociative attachment (OD bond, CO bond or CH bond) is exquisitely sensitive to the electron electron energy.

Future Plans

We plan to continue application of the COLTRIMS approach to achieve complete descriptions of the single photon double ionization of CO and its analogs. Of particular interest is an in-depth study of the “photo-autoionization” electron correlation and entanglement. We will focus on the double Auger decay of small CO molecules after photo excitation and photo ionization of inner shell electrons. The main scientific goals are to investigate the dissociation pathways and ionization mechanism during the double Auger decay. We plan to continue using our new “electron impact Coltrims” to study dissociation electron attachment to some biologically relevant molecules.

Recent Publications

1) M.S. Schoeffler, J. Titze, N. Petridis, T. Jahnke, K. Cole, L.Ph.H. Schmidt, A. Czasch, D. Akoury, O. Jagutzki, J.B. Williams, N.A. Cherepkov, S.K. Semenov, C.W. McCurdy, T.N. Rescigno, C.L. Cocke, T. Osipov, S. Lee, M.H. Prior, A. Belkacem, A.L. Landers, H. Schmidt-Boecking, Th. Weber, R. Dorner, “*Ultrafast probing of core hole localization in N₂*”, Science 320, 920 (2008).

2) K. Kreidi, D. Akoury, T. Jahnke, Th. Weber, A. Staudte, M. Schoffler, N. Neumann, J. Titze, L. Ph. H. Schmidt, A. Czasch, O. Jagutzki, R.A. Costa Fraga, R.E. Grisenti, M. Smolarski, P. Ranitovic, C.L. Cocke, T. Osipov, H. Adaniya, J.C. Thompson, M.H. Prior, A. Belkacem, A. Landers, H. Schmidt-Bocking, R. Dorner, “*Interference in the collective electron momentum in double photoionization of H₂*”, Phys. Rev. Lett. 100, 133005 (2008)

3) T. Osipov, T.N. Rescigno, Th. Weber, S. Miyabe, T. Jahnke, A.S. Alnaser, M.P. Hertlein, O. Jagutzki, L. Ph. Schmidt, M. Schoffler, L. Foucar, S. Schossler, T. Havermeier, M. Odenweller, S. Voss, B. Feinberg, A.L. Landers, M.H. Prior, R. Dorner, C.L. Cocke, A. Belkacem, “*Fragmentation pathways for selected electronic states of the acetylene dication*”, J. Phys. B: At. Mol. Opt. Phys. 41, 091001 (2008)

4) M. Schoffler, K. Kreidi, D. Akoury, T. Jahnke, Th. Weber, A. Staudte, N. Neumann, J. Titze, L. Ph. H. Schmidt, A. Czasch, O. Jagutzki, R.A. Costa Fraga, R.E. Grisenti, R. Diez Muino, N.A. Cherepkov, S.K. Semenov, P. Ranitovic, C.L. Cocke, T. Osipov, H. Adaniya, J.C. Thompson, M.H. Prior, A. Belkacem, A. L. Landers, H. Schmidt-Bocking, R. Dorner, “*Photo double ionization of H₂: Two-center interference and its dependence on the internuclear distance*”, Phys. Rev. A 78, 013414 (2008)

5) A.L. Landers, F. Robicheaux, T. Jahnke, M. Schoffler, T. Osipov, J. Titze, S.Y. Lee, H. Adaniya, M. Hertlein, P. Ranitovic, I. Bocharova, D. Akoury, A. Bhandary, Th. Weber, M.H. Prior, C.L. Cocke, R. Dorner and A. Belkacem, “*Angular correlation between photoelectrons and Auger electrons from K-shell ionization of neon*”, Phys. Rev. Lett. 102, 223001 (2009).

- 6) F. Sturm, M. Schoeffler, S. Lee, T. Osipov, S. Kirschner, N. Neumann, H.-K. Kim, B. Rudek, J. Williams, J. Daughhete, C.L. Cocke, K. Ueda, A. Landers, Th. Weber, M.H. Prior, A. Belkacem, and R. Doerner. "Photo and Auger electron angular distributions of fixed-in-space CO_2 ", Phys. Rev. A **80**, 032506 (2009).
- 7) S.K. Semenov, M.S. Schoeffler, J. Titze, N. Petridis, T. Jahnke, K. Cole, L.P.H. Schmidt, A. Czasch, D. Akoury, O. Jagutzki, J.B. Williams, T. Osipov, S. Lee, M.H. Prior, A. Belkacem, A.L. Landers, H. Schmidt-Bocking, Th. Weber, N.A. Cherepkov, R. Doerner, "Auger decay $1s_g$ and $1s_u$ hole states of the N_2 molecule: Disentangling decay routes from coincidence measurements", Phys. Rev. A **81**, 043426 (2010).
- 8) T. Osipov, M. Stener, A. Belkacem, M. Schoeffler, Th. Weber, L. Schmidt, A. Landers, M.H. Prior, R. Doerner and C.L.Cocke, "Carbon K-shell photoionization of fixed-in-space C_2H_4 ", Phys. Rev. A **81**, 033429 (2010).
- 9) T. Osipov, Th. Weber, T.N. Rescigno, S.Y. Lee, A.E. Orel, M. Schoeffler, F.P. Sturm, S. Schoessler, U. Lenz, T. Havermeier, M. Kuhnelt, T. Jahnke, J.B. Williams, D. Ray, A. Landers, R. Doerner and A. Belkacem, "Formation of inner-shell autoionizing CO^+ states below the co^{2+} threshold", Phys. Rev. A **81**, 011402 (2010).
- 10) H. Adaniya, B. Rudek, T. Osipov and A. Belkacem, "Experimental study for dissociative attachment to water molecule in the $2B1$ resonance", Journal of physics, conference series, volume 194, pages 194-200 (2009)
- 11) N.A. Cherepkov, S.K. Semenov, M.S. Schoeffler, J. Titze, N. Petridis, T. Jahnke, K. Cole, L. Ph. Schmidt, A. Czasch, D. Akoury, O. Jagutzki, J.B. Williams, C.L. Cocke, T. Osipov, S. Lee, M.H. Prior, A. Belkacem, A.L. Landers, H. Schmidt-Bocking, Th. Weber and R. Doerner, "Separation of Auger transitions into different repulsive states after K-shell photoionization of N_2 molecules" Phys. Rev. A **80**, 051404 (2009)
- 12) H. Adaniya, B. Rudek, T. Osipov, D.J. Haxton, T. Weber, T.N. Rescigno, C.W. McCurdy and A. Belkacem, "Imaging the molecular dynamics of dissociative electron attachment to water", Phys. Rev. Lett. **103**, 233201 (2009)

Electron-Atom and Electron-Molecule Collision Processes

T. N. Rescigno and C. W. McCurdy

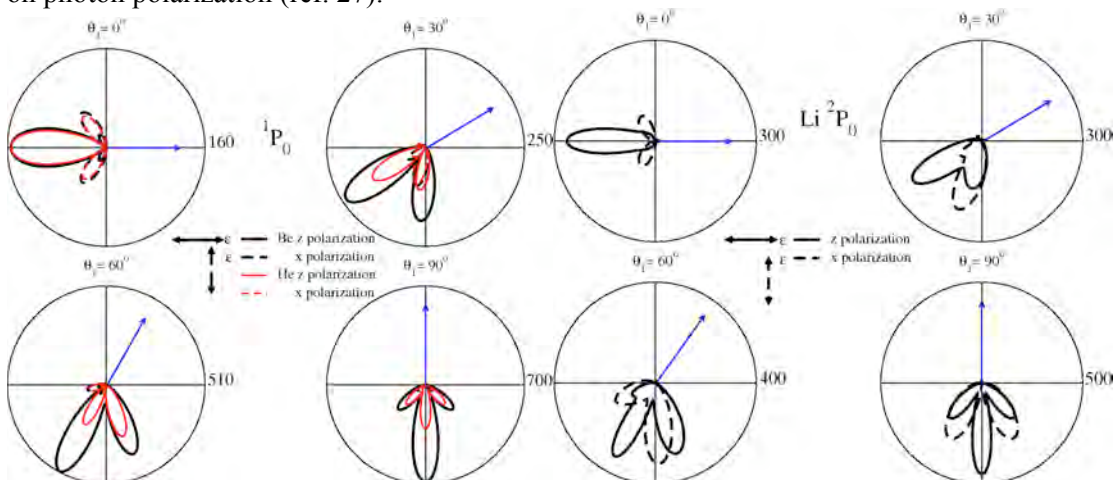
Chemical Sciences, Lawrence Berkeley National Laboratory, Berkeley, CA 94720

tnrescigno@lbl.gov, cwmccurdy@lbl.gov

Program Scope: This project seeks to develop theoretical and computational methods for treating electron and photon processes that are important in electron-driven chemistry and physics and that are currently beyond the grasp of first principles methods, either because of the complexity of the targets or the intrinsic complexity of the processes themselves. A major focus is the development of new methods for solving multiple photoionization and electron-impact ionization of atoms and molecules. New methods are also being developed and applied for treating low-energy electron collisions with polyatomic molecules and clusters. A state-of-the-art approach is used to treat multidimensional nuclear dynamics in polyatomic systems during resonant electron collisions and predict channeling of electronic energy into vibrational excitation and dissociation.

Recent Progress and Future Plans:

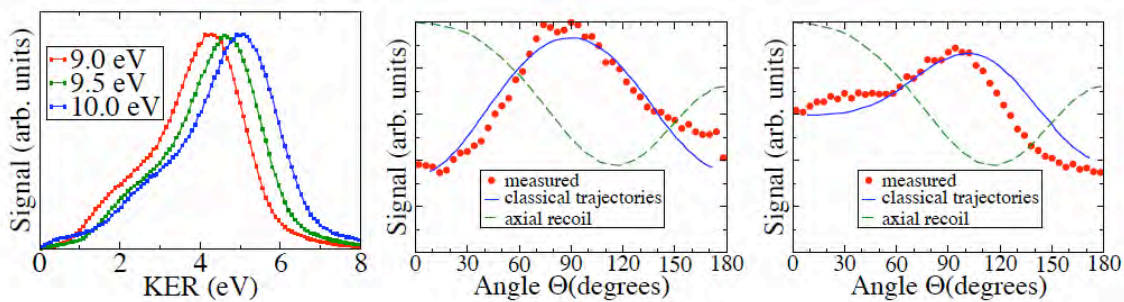
We have continued our studies of strongly correlated processes that involve several electrons in the continuum. The computational framework for this work is provided by the exterior complex scaling (ECS) formalism, implemented with finite elements and the discrete variable representation (FEM/DVR). To extend this approach to be able to treat multi-electron targets with two active electrons, we have developed a hybrid approach for atomic systems in which the inner-shell electrons are described by atomic orbitals while the outer active electrons are described in the full primitive basis of FEM/DVR functions. We exploit the finite element aspect of the representation by using only DVR functions in the first few elements to expand the inner atomic orbitals, while the outer elements are spanned by the remaining DVR functions. Because the DVR functions have compact support, the entire hybrid basis of orbitals plus primitive DVR functions is orthonormal. Furthermore, we are able to retain much of the simplicity of the original FEM/DVR approach in the computation of two-electron matrix elements with this method. We used this method to study photo-double ionization of ground-state Be (ref. 25) as well as fully differential double ionization cross sections excited and aligned Li and Be and their dependence on photon polarization (ref. 27).



Triple differential cross sections for double photoionization of excited and aligned 1P_0 Be, 1P_0 He and 2P_0 Li at 20 eV total photoelectron energy and equal energy sharing, showing dependence of cross sections on direction of photon polarization. Blue arrows indicate direction of fixed electron.

The treatment of molecular ionization dynamics beyond the Born-Oppenheimer approximation, which will be a key issue in the study of ultrafast processes with X-ray pulses, requires fast and accurate theoretical methods. To this end, we initiated an ECS-based, FEM/DVR method in prolate spheroidal coordinates, which are the natural choice of coordinates for diatomic targets. In our first two studies (refs. 13 and 17) we formulated the method and demonstrated its viability with calculations on the bound and continuum states of H_2^+ . We have since followed up with an extension to two-electron targets. By suitably modifying the approach we had developed for the spherical case, we were able to retain key simplifications in the computation of two-electron matrix elements of $1/r_{12}$ by formulating their evaluation as the solution of two-center Poisson equation. Comparison of single and triple differential photo-double ionization cross sections computed using single-center expansions and the prolate spheroidal FEM/DVR showed, not surprisingly, much more rapid convergence with the new method. We also discovered that, while the shapes of the fully differential double ionization cross sections were completely consistent with our earlier calculations, the magnitude of the DPI cross sections shows a surprising sensitivity to small changes in the target wave functions. This is a simple reflection of the fact that double ionization is a pure correlation effect and is thus sensitive to minor components of the initial-state wave function, which are difficult to obtain accurately with single-center expansion. Our results have been submitted to Physical Review A (ref. 29). Extension of this approach to study ionization dynamics of more complicated diatomic targets is planned and will follow a parallel path to the hybrid orbital, FEM/DVR approach that we successfully employed in our extension to atomic targets with more than two electrons. We should also mention that this methodology is playing a key role in our studies of ultrafast molecular dynamics beyond the Born-Oppenheimer approximation.

Our benchmark studies of dissociative electron attachment (DEA) to water have been extended with a collaborative experimental/theoretical effort aimed at imaging and interpreting the dynamics of the dissociation process. Our earlier prediction that O^- production via the $8.5 \text{ eV } ^2\text{A}_1$ resonance proceeds mainly through 3-body breakup was confirmed by momentum imaging experiments in our AMO program. Those experiments also provided striking images of the angular patterns of H^- and O^- production from the 8.5 eV resonance that could not be explained using the axial recoil approximation. We were able to successfully explain the observed angular distributions by combining body-frame entrance amplitudes from ab initio calculations with classical trajectories on the anion potential surface that detail precisely how the water anion dissociates. This joint experimental/theoretical study was highlighted in a Physical Review Letter. We are currently working on a similar study of H^- and O^- production from the higher $^2\text{B}_2$ resonance which will focus on how the conical intersection between the $^2\text{B}_2$ and $^2\text{A}_1$ resonances controls the dissociation dynamics.



H^- production from DEA to water via the $^2\text{A}_1$ resonance. Angular distributions show breakdown of axial recoil approximation and change with kinetic energy release. Center panel: 2 eV KER. Right panel: 4 eV KER.

Publications (2008-2010):

1. D. A. Horner, W. Vanroose, T. N. Rescigno, F. Martin and C. W. McCurdy, Role of Nuclear
2. K. Houfek, T. N. Rescigno and C. W. McCurdy, Probing the Nonlocal Approximation to Resonant Collisions of Electrons with Diatomic Molecules, *Phys. Rev. A* **77**, 012710 (2008).
3. M. S. Schoeffler, J. Titze, N. Petridis, T. Jahnke, D. Akoury, K. Cole, L. Ph. H. Schmidt, A. Czasch, O. Jagutzki, N. A. Cherepkov, S. K. Semenov, C. W. McCurdy, T. N. Rescigno, C. L. Cocke, T. Osipov, S. Lee, M. H. Prior, A. Belkacem, A. Lander, H. Schmidt-Boecking, Th. Weber, and R. Doerner, Ultrafast probing of core hole localization in N₂, *Science* **320**, 920 (2008)
4. T. Osipov, T. N. Rescigno, T. Weber, S. Miyabe, T. Jahnke, A. Alnaser, M. Hertlein, O. Jagutzki, L. Schmidt, M. Schoeffler, L. Foucar, S. Schoessler, T. Havermeier, M. Odenweller, S. Voss, B. Feinberg, A. Landers, M. Prior, R. Doerner, C. L. Cocke and A. Belkacem, Fragmentation Pathways for Selected Electronic States of the Acetylene Dication, *J. Phys. B* **41**, 091001 (2008)
5. P. L. Bartlett, A. T. Stelbovics, T. N. Rescigno and C. W. McCurdy, "Application of Exterior Complex Scaling to Positron-Hydrogen Collisions Including Rearrangement", *Phys. Rev. A* **77**, 032710 (2008).
6. D. A. Horner, T. N. Rescigno and C. W. McCurdy, Decoding sequential vs non-sequential two-photon double ionization of helium using nuclear recoil, *Phys. Rev. A* **77**, 030703(R) (2008).
7. L. Campbell, M. Brunger and T. N. Rescigno, "Carbon dioxide electron cooling rates in the atmospheres of Mars and Venus", *J. Geophys. Res.-Planets* **113**, 2008JE003099 (2008).
8. F. L. Yip, C. W. McCurdy and T. N. Rescigno, "A hybrid Gaussian-discrete variable representation approach to molecular continuum processes II: application to photoionization of diatomic Li₂⁺", *Phys. Rev. A* **78**, 023405 (2008).
9. D. A. Horner, T. N. Rescigno and C. W. McCurdy, "Triple Differential Cross sections and Nuclear Recoil in Two-Photon Double Ionization of Helium", *Phys. Rev. A* **78**, 043416 (2008).
10. D. A. Horner, S. Miyabe, T. N. Rescigno, C. W. McCurdy, F. Morales and F. Martin, "Classical Two-Slit Interference Effects in Photo-double Ionization of Molecular Hydrogen at High Energies", *Phys. Rev. Lett.* **101**, 183002 (2008).
11. D. J. Haxton, T. N. Rescigno and C. W. McCurdy, "Three-body breakup in dissociative electron attachment to the water molecule", *Phys. Rev. A* **78**, 040702(R) (2008).
12. J. Fernández, F. L. Yip, T. N. Rescigno, C. W. McCurdy and F. Martín, "Two-center effects in one-photon single ionization of H₂⁺, H₂ and Li₂⁺ with circularly polarized light", *Phys. Rev. A* **79**, 043409 (2009).
13. L. Tao, C. W. McCurdy and T. N. Rescigno, "Grid-based methods for diatomic quantum scattering problems: a finite-element, discrete variable representation in prolate spheroidal coordinates", *Phys. Rev. A* **79**, 012719 (2009).
14. F. Morales, F. Martín, D. A. Horner, T. N. Rescigno and C. W. McCurdy, "Two-photon double ionization of H₂ at 30 eV using Exterior Complex Scaling", *J. Phys. B* **42**, 134013 (2009).
15. S. Miyabe, C. W. McCurdy, A. E. Orel and T. N. Rescigno, "Theoretical study of asymmetric molecular-frame photoelectron angular distributions for C 1s photoejection from CO₂", *Phys. Rev. A* **79**, 053401 (2009).
16. L. Tao, C. W. McCurdy and T. N. Rescigno, "Grid-based methods for diatomic quantum scattering problems II: Time-dependent treatment of single- and two-photon ionization of H₂⁺", *Phys. Rev. A* **80**, 013401 (2009).
17. H. Adaniya, B. Rudek, T. Osipov, D. J. Haxton, T. Weber, T. N. Rescigno, C. W. McCurdy and A. Belkacem, "Imaging the dynamics of dissociative electron attachment to water", *Phys. Rev. Lett.* **103**, 233201 (2009).
18. T. N. Rescigno, C. S. Trevisan and A. E. Orel, Comment on "Electron-induced bond-breaking at low energies in HCOOH and Glycine: The role of very short-lived s* anion states", *Phys. Rev. A* **80**, 046701 (2009).
19. T. Osipov, Th. Weber, T. N. Rescigno, S. Y. Lee, A. E. Orel, M. Schöffler, F. P. Sturm, S. Schössler, U. Lenz, T. Havermeier, M. Kuehnel, T. Jahnke, J. B. Williams, D. Ray, A. Landers, R.

- Dörner and A. Belkacem, "Formation of inner-shell autoionizing CO^+ states below the CO^{++} threshold" *Phys. Rev. A* **81**, 011402(R) (2010).
20. D. A. Horner, T. N. Rescigno and C. W. McCurdy, "Nuclear Recoil Cross Sections from Time-dependent Studies of Two-Photon Double Ionization of Helium (with)" *Phys. Rev. A* **81**, 023410 (2010).
 21. A. Palacios, D. A. Horner, T. N. Rescigno and C. W. McCurdy, "Two-photon double ionization of the helium atom by ultrashort pulses", *J. Phys. B* (accepted).
 22. F. L. Yip, C. W. McCurdy and T. N. Rescigno, "Hybrid Orbital and Numerical Grid Representation for Electronic Continuum Processes: Double Photoionization of Atomic Beryllium", *Phys. Rev. A* **81**, 053407 (2010).
 23. F. L. Yip, C. W. McCurdy and T. N. Rescigno, "Double Photoionization of excited Lithium and Beryllium", *Phys. Rev. A* **81**, 063419, (2010).
 24. A. Palacios, D. A. Horner, T. N. Rescigno and C. W. McCurdy, "Two-photon double ionization of the helium", *J. Phys. B* (accepted).
 25. L. Tao, C. W. McCurdy and T. N. Rescigno, "Grid-based methods for diatomic quantum scattering problems III: Double photoionization of molecular hydrogen in prolate spheroidal coordinates", *Phys. Rev. A* (submitted).
 26. W. Cao, S. De, K. P. Singh, S. Chen, M. S. Schöffler, A. Alnaser, I. A. Bocharova, G. Laurent, D. Ray, M. F. Kling, S. Zherebtsov, I. Ben-Itzhak, I. V. Litvinyuk, A. Belkacem, T. Osipov, T. N. Rescigno and C. L. Cocke, "Dynamic control of the fragmentation of CO^{9+} excited states generated with high-order harmonics", *Phys. Rev. A* (submitted).

Ultrafast X-ray Science Laboratory

C. William McCurdy (Director), Ali Belkacem, Oliver Gessner, Martin Head-Gordon, Stephen Leone, Daniel Neumark, Robert W. Schoenlein, Thorsten Weber

Chemical Sciences, Lawrence Berkeley National Laboratory, Berkeley, CA 94720

CWMcCurdy@lbl.gov, ABelkacem@lbl.gov, OGessner@lbl.gov, MHead-Gordon@lbl.gov,
SRLeone@lbl.gov, DMNeumark@lbl.gov, RWSchoenlein@lbl.gov, TWeber@lbl.gov

Program Scope: This program seeks to bridge the gap between the development of ultrafast X-ray sources and their application to understand processes in chemistry and atomic and molecular physics that occur on both the femtosecond and attosecond time scales. There five subtasks in the UXSL effort, outlined below.

Recent Progress and Future Plans:

1. Soft X-ray high harmonic generation and applications in chemical physics

This part of the laboratory is focused on the study of ultrafast chemical dynamics enabled by novel femtosecond VUV and soft x-ray light sources. Laboratory based setups centered around several high-order harmonic generation light sources operate at up to 3 kHz repetition rate. The light sources are complemented by state-of-the-art photoelectron and ion imaging techniques and a newly installed VUV spectrometer for transient absorption measurements.

The first real-time observation of dynamics in electronically excited helium nanodroplets has revealed a neutral interband relaxation mechanism that is significantly more efficient than the previously observed indirect ionization mechanism (Fig. 1). Photoelectron and ion imaging experiments have tracked the emergence of atomic Rydberg atoms from VUV excited droplets with femtosecond time resolution. Transient photoelectron angular distributions strongly indicate that Rydberg atoms with different principle quantum numbers are emitted in different orbital angular momentum states. A newly implemented 3D momentum-resolved ion imaging capability has revealed rich

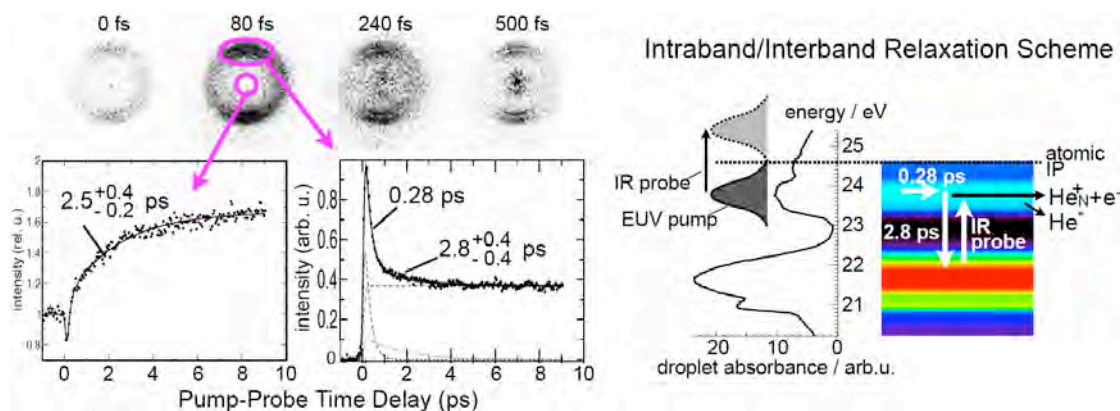


Figure 1: VUV-pump/IR-probe study of helium nanodroplets. Transient photoelectron images (left) reveal an efficient interband relaxation mechanism in VUV excited droplets (right).

dynamics for all ionic fragments. The dominant monomer and dimer ions exhibit time-dependent kinetic energy distributions. In particular the kinetic energies of the dimer ions are surprisingly high, indicating the existence of an extremely efficient energy conversion mechanism inside the excited droplets.

The construction of a high-resolution VUV transient absorption setup is almost completed. An existing Hettrick spectrometer has been interfaced with a capillary-based high-order harmonics light source in an effort to push the realm of femtosecond transient absorption measurements into the water window. The first recordings of static absorption spectra of Xe atoms around 70 eV photon energy have just demonstrated the functionality of the setup.

Some of the first experiments at the Linac Coherent Light Source (LCLS) have been performed within the framework of collaborative projects lead by Nora Berrah (Western Michigan University) and Ryan Coffee (SLAC National Accelerator Laboratory). UXSL lead in particular the analysis and modeling of frustrated absorption in N₂ molecules exposed to ultrashort intense x-ray pulses (Berrah). Other significant efforts by UXSL researchers contributed to the first LCLS pump-probe experiments on transiently aligned N₂ molecules (Coffee) and the determination of molecular double core hole generation efficiencies (Berrah).

2. Applications of the femtosecond undulator beamline at the Advanced Light Source to solution-phase molecular dynamics

The objective of this research program is to advance our understanding of solution-phase molecular dynamics using ultrafast x-rays as time-resolved probes of the evolving electronic and atomic structure of solvated molecules. Two beamlines have been developed at the Advanced Light Source, with the capability for generating ~200 fs x-ray pulses from 200 eV to 10 keV. We have also developed a new capability for transmission XAS studies of thin liquid samples in the soft x-ray range, based on a novel Si₃N₄ cell design with controllable thickness <1 μm.

Present research is focused on charge-transfer processes in solvated transition-metal complexes, which are of fundamental interest due to the strong interaction between electronic and molecular structure. In particular, Fe^{II} complexes exhibit strong coupling between structural dynamics, charge-transfer, and spin-state interconversions. This year we have focused on understanding the evolution of the valence electronic structure, and the influence of the ligand field dynamics on the Fe 3*d* electrons, using time-resolved XANES measurements at the Fe L-edge. Picosecond and femtosecond studies show a clear 1.7 eV dynamic shift in the Fe-L₃ absorption edge with the ultrafast formation of the high-spin state on a 200 fs time scale. This reflects the evolution of the ligand-field splitting, and is the first time-resolved solution-phase transmission spectra ever recorded in the soft x-ray region. Comparison with charge-transfer multiplet calculations reveals a reduction in ligand field splitting of ~1 eV in the high-spin state. A significant reduction in orbital overlap between the central Fe-3*d* and the ligand N-2*p* orbitals is directly observed, consistent with the expected 0.2 Å increase in Fe-N bond length upon formation of the high-spin state. The overall occupancy of the Fe-3*d* orbitals remains constant upon spin crossover, suggesting that the reduction in σ-donation is compensated by significant attenuation of π-back-bonding in the metal-ligand interactions.

A second area of focus is on the structural dynamics of liquid water following

coherent vibrational excitation of the O-H stretch (in collaboration with A. Lindenberg et al. at Stanford). Time-resolved results at the O K-edge show distinct changes in the near-edge spectral region that are indicative of a transient temperature rise of 10K following laser excitation and rapid thermalization of vibrational energy. The rapid heating at constant volume creates an increase in internal pressure, ~ 8 MPa, which is manifest by spectral changes that are distinct from those induced by temperature alone. Femtosecond studies of hydrogen bond dynamics reveal the dynamic conversion of strongly hydrogen-bonded water structures to more disordered structures with weaker hydrogen-bonding on a 700 fs time scale.

An important goal is to apply time-resolved X-ray techniques to understand the structural dynamics of more complicated reactions in a solvent environment. Future research will focus on charge-transfer, and ligand dynamics in bi-transition-metal complexes and porphyrins, as well as reaction dynamics of solvated halide molecules. Solvated metal carbonyls represent a model system where photo-induced ligand dissociation is strongly solvent dependent. In these complexes, the molecular intermediates and solvent exchange mechanisms are poorly understood. Time-resolved XAS will provide important new insight to the molecular dynamics.

3. Time-resolved studies and non-linear interaction of femtosecond x-rays with atoms and molecules:

An extension of non-linear processes and two-color pump-probe to the extreme ultraviolet (XUV) spectral region was until recently considered unfeasible due to a lack of sufficiently intense short-wavelength radiation sources. In recent years, higher-order harmonic generation has reached intensities high enough as to induce two or three photon ionization processes. The



Figure 2: Photograph of the MISTERS apparatus currently under construction. The supersonic gas jet comes from the top and is skimmed in a two stage jet dump in the bottom (not visible here). The two stage differential pumping stage is mounted to the left. The tip-tilt xyz split mirror back focusing unit (not shown) will be attached to the right.

The design and construction of our intense XUV source is based on scaling-up in energy of the loose focusing high harmonic generation scheme. Pump/probe delay is achieved with a newly constructed split mirror interferometer (SMI). VUV and XUV wavelength selection in each arm of the SMI is achieved through a combination of transmission filters and coatings on the two D-shaped mirrors. We applied our two-color VUV/XUV pump-probe system to the study non-Born-Oppenheimer dynamics in excited-state ethylene. To follow the dynamics onto the ground state potential energy surface, we conducted experiments using 7.7 eV photons as a pump and in one case the 19th harmonic (29.45 eV) of the fundamental as a probe and in another case a band of EUV harmonics (17-23 eV) as a probe. These XUV probe photons allow us to break the C-C bond and observe transient structures such as ethylidene. In both experiments, the pump and the probe act on the molecule perturbatively through single photon excitation. We

observe a transient increase in the CH_3^+ fragment production using ion time-of flight spectroscopy providing evidence for hydrogen migration in ethylene following $\pi\pi^*$ excitation. For this coming fiscal year we are planning an upgrade of our HHG system from 10 Hz to higher repetition rate to enable the application of our successful COLTRIMS technique to time-resolved studies. The construction of the new Momentum Imaging Spectroscopy for Time Resolved Studies (MISTERS) apparatus shown in Fig. 2 began in the second half of 2008. The main chamber and the two stage super sonic gas jet are assembled and combined to one setup. A two-stage differential pumping stage and most parts of the tip-tilt xyz split mirror back focusing unit are mounted.

A dedicated reaction microscope is in the design phase. The intricate simulations of the electromagnetic fields must consider the high rate from the background single ionization events and an electro-optical lens system, which is needed to increase the resolution on the recoil-ion side. In an initial phase the setup will be optimized for a two-color two-photon single ionization of rare gas atoms like He, Ne and Ar.

4. Theory and computation

We have developed computational methods that allow the accurate treatment of multiple ionization of atoms and molecules by short pulses in the VUV and soft X-ray regimes. We have extended our numerical methods based on the finite-element discrete variable representation to the essentially exact time-dependent treatment of two electron atoms in a radiation field, including the rigorous extraction of the amplitudes for ionization from these wave packets and separation of single and double ionization probabilities. These developments have been applied to short pulse single and double ionization of helium and have showed new effects that appear only for subfemtosecond pulses.

Most recently we have found an intrinsically two-electron interference phenomenon, shown in Fig. 3, in which subfemtosecond UV pulses can be used to probe spin entanglement directly. Applications to pump/probe investigations of correlation in the doubly excited states of helium are in progress using a new time propagation scheme that involves simultaneous explicit and implicit steps. Calculations on many-electron atoms and molecules are underway with a new Multiconfiguration Time-dependent Hartree Fock method using prolate spheroidal coordinates for the treatment of general diatomics including nuclear motion without the Born-Oppenheimer approximation.

We are also developing tractable theories for molecular excited states, including bright and dark states and their intersections. A new quasidegenerate perturbation theory building upon single excitation CI (CIS) has been formulated, implemented and tested. It is self-interaction-free, and efficient enough to apply to systems in the 50-100 atom regime. The analytical gradient of this model has been formulated and implemented which opens the way for exploring potential energy surfaces. We have formulated new spin-flip models that can properly treat low-lying dark excited states that have large

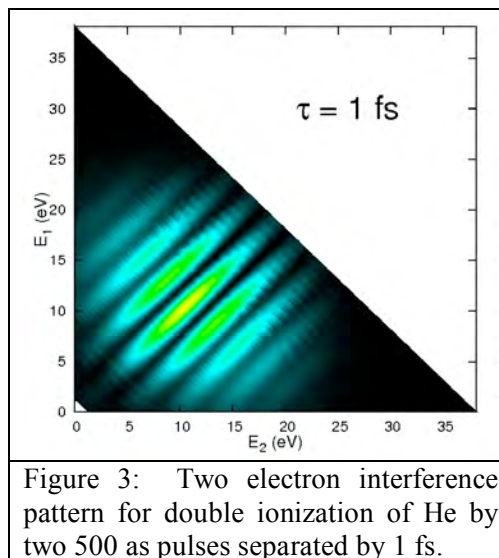


Figure 3: Two electron interference pattern for double ionization of He by two 500 as pulses separated by 1 fs.

double excitation contributions . The most general version of this work successfully resolved delicate energy differences on the order of cal/mol between singlet, triplet and quintet states of tetraradicaloid non-Kekule hydrocarbons.

We have just finished an initial study of the excited states of small helium clusters to complement experimental efforts. This work characterizes the nature of the excitations in clusters including He7 and He25, using CIS. Very encouraging agreement was obtained with experimental measurements of the excitation spectrum in larger clusters (~300 atoms) (figure on next page). Finally, we have also explored improvements to real-time time-dependent DFT by imposing exact conditions.

5. Attosecond atomic and molecular science

During the last year, we have adopted a new method of generating isolated attosecond pulses based on the "Double-Optical Gating" (DOG) method developed by Chang and co-workers for harmonic generation in a rare gas medium. This method involved a considerable re-design of our apparatus, but the result has been (a) considerably more reliable isolated attosecond pulse generation, (b) shorter attosecond pulses, and (c) perhaps most importantly, attosecond pulses at much lower photon energies than the 80-100 eV energy range characteristic of our earlier efforts.

The principle and implementation of double-optical gating is illustrated in Fig. 4. A 5-7 fs, carrier-envelope-phase stabilized 800 nm pulse passes through two quartz plates and a BBO crystal in order to generate three optical fields: a driving field (red) at 800 nm, a gating field (green) also at 800 nm, and a 400 nm field polarized in the same plane as the driving field. The gating field is perpendicular to the driving field and is phase-shifted by 90°, so that when the two fields are of similar amplitude, no high harmonic generation (HHG) results from the net circularly polarized field; HHG occurs only when

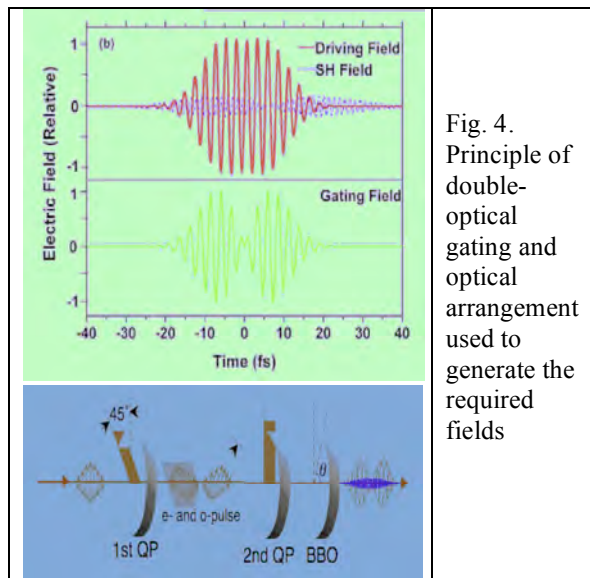


Fig. 4. Principle of double-optical gating and optical arrangement used to generate the required fields

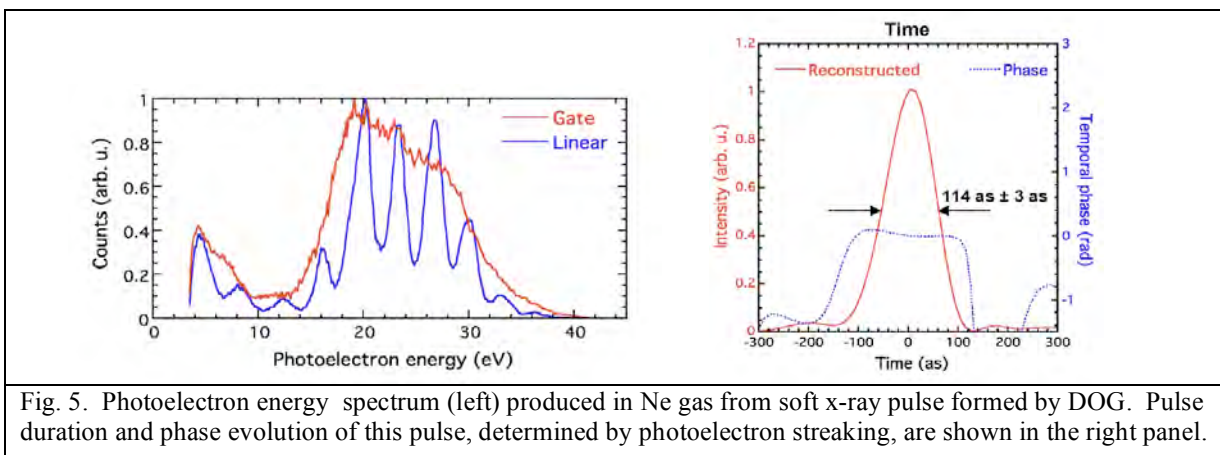


Fig. 5. Photoelectron energy spectrum (left) produced in Ne gas from soft x-ray pulse formed by DOG. Pulse duration and phase evolution of this pulse, determined by photoelectron streaking, are shown in the right panel.

the gating field is off. As shown by Chang, the presence of the 400 nm relaxes the conditions under which isolated attosecond pulses can be generated with this overall configuration.

Fig. 5 shows the energy spectrum and pulse width obtained in our laboratory by carrying out DOG in Ar gas, and then measuring the resulting photoelectron spectrum of Ne. The photoelectron spectrum is unstructured, as expected for an isolated attosecond pulse, and is most intense from 20-30 eV, corresponding to photon energies of 40-50 eV (the ionization potential of Ne is 21.6 eV). To obtain the phase and temporal profile of the pulse, we have carried out photoelectron streaking measurements using the soft x-ray pulse and co-propagating 800 nm pulse incident on a Ne target. The results, also shown in Fig. 5, indicate a pulse with a flat phase and pulse duration of 114 ± 3 as. Experiments are currently underway in which the time-resolved ionization and fragmentation dynamics of SF₆ and other small molecules excited by the attosecond pulse will be investigated with a combination of photoelectron streaking and time-resolved mass spectrometry.

Publications, by Subtask (2008-2010)

1. Christer Z. Bisgaard, Owen J. Clarkin, Guorong Wu, Anthony M. D. Lee, Oliver Geßner, Carl C. Hayden, Albert Stolow, "Time-Resolved Molecular Frame Dynamics of Fixed-in-Space CS₂ Molecules", *Science* **323**, 1464 (2009).
2. N. Huse, H. Wen, D. Nordlund, E. Szilagy, D. Daranciang, T.A. Miller, A. Nilsson, R.W. Schoenlein, and A.M. Lindenberg, "Probing the hydrogen-bond network of water via time-resolved soft x ray spectroscopy," *Phys. Chem. Chem. Phys.*, **11**, 3951–3957 (2009) – cover article.
3. N. Huse, M. Khalil, T.-K. Kim, A.L. Smeigh, L. Jamula, J.K. McCusker, and R.W. Schoenlein, "Probing reaction dynamics of transition-metal complexes in solution via time-resolved x-ray spectroscopy," *J. Phys. Conf.*, **148**, 012043 (2009).
4. N. Huse, T.-K. Kim, M. Khalil, L. Jamula, J.K. McCusker, and R.W. Schoenlein, "Probing reaction dynamics of transition-metal complexes in solution via time-resolved soft x-ray spectroscopy," in **Ultrafast Phenomena XVI**, Springer Series in Chemical Physics, **92**, P. Corkum, S. De Silvestri, K.A. Nelson, E. Riedle, R.W. Schoenlein, Eds., Springer-Verlag, (2009).
5. H. Wen, N. Huse, R.W. Schoenlein, and A.M. Lindenberg, "Ultrafast conversions between hydrogen bond structures in liquid water observed by femtosecond x-ray spectroscopy," *J. Chem. Phys.*, **131**, 234505 (2009).
6. N. Huse, T.-K. Kim, L. Jamula, J.K. McCusker, F.M.F. de Groot, and R.W. Schoenlein, "Photo-Induced Spin-State Conversion in Solvated Transition Metal Complexes Probed via Time-Resolved Soft X-ray Spectroscopy," *J. Am. Chem. Soc.*, **132**, 6809-6816 (2010).
7. C. C. Wang, O. Kornilov, O. Gessner, J. H. Kim, D. S. Peterka, and D. M. Neumark, "Photoelectron Imaging of Helium Droplets Doped with Xe and Kr Atoms", *J. Phys. Chem. A*, **112**, 9356 (2008).
8. Oleg Kornilov, Chia C. Wang, Oliver Bünermann, Andrew T. Healy, Mathew Leonard, Chunte Peng, Stephen R. Leone, Daniel M. Neumark, and Oliver Gessner, "Ultrafast Dynamics in Helium Nanodroplets Probed by Femtosecond Time-Resolved EUV Photoelectron Imaging", *J. Phys. Chem. A* **114**, 1437 (2010).
9. Oleg Kornilov, Russell Wilcox, and Oliver Gessner, "Nanograting-based compact VUV spectrometer and beam profiler for in-situ characterization of high-order harmonic generation light sources", *Rev. Sci. Instrum.* **81**, 063109 (2010).
10. M. Hoener, L. Fang, O. Kornilov, O. Gessner, S. T. Pratt, M. Gühr, E. P. Kanter, C. Blaga, C. Bostedt, J. D. Bozek, P. H. Bucksbaum, C. Buth, M. Chen, R. Coffee, J. Cryan, L. DiMauro, M. Glowia, E.

- Hosler, E. Kukk, S. R. Leone, B. McFarland, M. Messerschmidt, B. Murphy, V. Petrovic, D. Rolles, and N. Berrah, “Ultra-intense X-ray Induced Ionization, Dissociation, and Frustrated Absorption in Molecular Nitrogen”, *Phys. Rev. Lett.* **104**, 253002 (2010).
11. James M. Glowonia, J. Cryan, J. Andreasson, A. Belkacem, N. Berrah, C. I. Blaga, C. Bostedt, J. Bozek, L. F. DiMauro, L. Fang, J. Frisch, O. Gessner, M. Gühr, J. Hajdu, M. P. Hertlein, M. Hoener, G. Huang, O. Kornilov, J. P. Marangos, A. M. March, B. K. McFarland, H. Merdji, V. S. Petrovic, C. Raman, D. Ray, D. A. Reis, M. Trigo, J. L. White, W. White, R. Wilcox, L. Young, R. N. Coffee, and P. H. Bucksbaum, “Time-resolved pump-probe experiments at the LCLS”, *Opt. Express*, accepted (2010).
 12. L. Fang, M. Hoener, O. Gessner, F. Tarantelli, S. T. Pratt, O. Kornilov, C. Buth, M. Gühr, E. P. Kanter, C. Bostedt, J. D. Bozek, P. H. Bucksbaum, M. Chen, R. Coffee, J. Cryan, M. Glowonia, E. Kukk, S. R. Leone, and N. Berrah, “Double core hole production in N₂: Beating the Auger clock”, *Phys. Rev. Lett.*, accepted (2010).
 13. James P. Cryan, J. M. Glowonia, J. Andreasson, A. Belkacem, N. Berrah, C. I. Blaga, C. Bostedt, J. Bozek, C. Buth, L. F. DiMauro, L. Fang, O. Gessner, M. Guehr, J. Hajdu, M. P. Hertlein, M. Hoener, O. Kornilov, J. P. Marangos, A. M. March, B. K. McFarland, H. Merdji, V. Petrovic, C. Raman, D. Ray, D. Reis, F. Tarantelli, M. Trigo, J. White, W. White, L. Young, P. H. Bucksbaum, and R. N. Coffee, “Auger electron angular distribution of double core hole states in the molecular reference frame”, *Phys. Rev. Lett.*, accepted (2010).
 14. O. Gessner, O. Kornilov, M. Hoener, L. Fang, and N. Berrah, “Intense Femtosecond X-ray Photoionization Studies of Nitrogen - How Molecules interact with Light from the LCLS” in *Ultrafast Phenomena XVII*, submitted (2010).
 15. J. van Tilborg, T.K. Allison, T.W. Wright, M.P. Hertlein, R.W. Falcone, Y. Liu, H. Merdji and A. Belkacem, “Femtosecond isomerization dynamics in the ethylene cation measured in an EUV-pump NIR probe configuration”, *J. Phys. B: At. Mol. Opt. Phys.* **42** (2009) 081002.
 16. T.K. Allison, J. van Tilborg, T.W. Wright, M.P. Hertlein, R.W. Falcone, and A. Belkacem, “Separation of high order harmonics with fluoride windows”, *Optics Express* **17**, (2009) 8941.
 17. K. Motomura, H. Fukuzawa, L. Foucar, X-J Liu, G. Prumper, K. Ueda, N. Saito, H. Iwayama, K. Nagaya, H. Murakami, M. Yao, A. Belkacem, M. Nagasono, A. Higashiya, M. Yabashi, T. Ishikawa, H. Ohashi, and H. Kimura, “Multiple ionization of atomic argon irradiated by EUV free-electron laser pulses at 62 nm: evidence of sequential electron strip” *J. Phys. B: At. Mol. Opt. Phys.* **42**, Fast Track Communication, (2009) 221003
 18. J. van Tilborg, T. Allison, T.K. Wright, M.P. Hertlein, Y. Liu, H. Merdji, R. Falcone, and A. Belkacem, “EUV-driven femtosecond dynamics in ethylene”, *Journal of Physics, Conference Series* **194**, 012015 (2009).
 19. T.E. Glover, M.P. Hertlein, S.H. Southworth, T.K. Allison, J. van Tilborg, E.P. Kanter, B. Krassig, H.R. Varma, B. Rude, R. Santra, A. Belkacem and L. Young, “Controlling X-rays with light”, *Nature Physics* **6**, 69 (2010)
 20. Y.H. Jiang, A. Rudenko, J.F. Perez-Torres, O. Herrwerth, L. Foucar, M. Kurka, K. U. Kuhnel, M. Toppin, E. Plesiat, F. Morales, F. Martin, M. Lezius, M.F. Kling, T. Jahnke, R. Doerner, J.L. Sanz-Vicario, J. van Tilborg, A. Belkacem, M. Schultz, K. Ueda, T.J.M. Zouros, S. Dusterer, R. Treusch, C.D. Schroter, R. Moshhammer, and J. Ullrich, “Investigating two-photon double ionization of D₂ by XUV-pump-XUV-probe experiments”, *Phys. Rev. A* **81**, 05140(R) (2010).
 21. Y.H. Jiang, A. Rudenko, E. Plesiat, L. Foucar, M. Kurka, K. U. Kuhnel, Th. Ergler, J.F. Perz-Torres, F. Martin, O. Herrwerth, M. lezius, M.F. Kling, J. Titze, T. jahnke, R. Doerner, J.L. Sanz-Vicario, M. Schoffler, J. van Tilborg, A. Belkacem, K. Ueda, T.J.M. Zouros, S. Dusterer, R. Treusch, C.D. Schroter, R. Moshhammer, and J. Ullrich, “Tracing direct and sequential two-photon double ionization of D₂ in femtosecond extreme-ultraviolet laser pulses”, *Phys. Rev. A* **81**, 021401 (R) (2010).
 22. A. Palacios, T. N. Rescigno and C. W. McCurdy, Cross Sections for Short-Pulse Single and Double Ionization of Helium, *Phys. Rev. A* **77**, 032716 (2008).

23. A. Palacios, T. N. Rescigno and C. W. McCurdy, "Time-dependent treatment of two-photon resonant single and double ionization of helium by ultrashort laser pulses", *Phys. Rev. A* **79**, 033402 (2009).
24. Liang Tao, W. Vanroose, B. Reps, T. N. Rescigno, and C. W. McCurdy, "Long-time solution of the time-dependent Schrödinger equation for an atom in an electromagnetic field using complex coordinate contours" *Phys. Rev. A* **80**, 063419 (2009).
25. A. Palacios, T. N. Rescigno and C. W. McCurdy, "Two-electron time-delay interference in atomic double ionization by attosecond pulses," *Phys. Rev. Lett.* **103**, 253001 (2009).
26. M Kurka , J Feist , D A Horner , A Rudenko , Y H Jiang , K U Kühnel , L Foucar , T N Rescigno, C W McCurdy , R Pazourek , S Nagele , M Schulz , O Herrwerth , M Lezius , M F Kling , M Schöffler , A Belkacem , S Dusterer , R Treusch , B I Schneider , L A Collins , J Burgdörfer , C D Schröter , R Moshhammer and J Ullrich, "Differential cross sections for non-sequential double ionization of He by 52 eV photons from the Free Electron Laser in Hamburg, FLASH" *New J. Phys.* **12**, 073035 (2010).
27. D. Casanova, Y.M. Rhee and M. Head-Gordon, "Quasidegenerate scaled opposite spin second order perturbation corrections to single excitation configuration interaction", *J. Chem. Phys.* **128**, 164106 (2008)
28. Y.M. Rhee and M. Head-Gordon, "Quartic-scaling analytical gradient of quasidegenerate scaled opposite spin second order perturbation corrections to single excitation configuration interaction", *J. Chem. Theor. Comput.* **5**, 1224 (2009).
29. Y.M. Rhee, D. Casanova, and M. Head-Gordon, "Performance of quasi-degenerate scaled opposite spin perturbation corrections to single excitation configuration interaction for excited state structures and excitation energies with application to the stokes shift of 9-methyl-9,10-dihydro-9-silaphenanthrene", *J. Phys. Chem. A* **113**, 10564 (2009).
30. D. Casanova and M. Head-Gordon, "The spin-flip extended single excitation configuration interaction method", *J. Chem. Phys.* **129**, 064104 (2008).
31. D. Casanova, L.V. Slipchenko, A.I. Krylov, and M. Head-Gordon, "Double spin-flip approach within equation-of-motion coupled cluster and configuration interaction formalisms: Theory, implementation and examples" *J. Chem. Phys.* **130**, 044103 (2009).
32. D. Casanova, and M. Head-Gordon, "Restricted active space spin-flip configuration interaction approach: Theory, implementation and examples", *Phys. Chem. Chem. Phys.* **11**, 9779 (2009).
33. K.D. Closser and M. Head-Gordon, "Ab initio calculations on the electronically excited states of small helium clusters", *J. Phys. Chem. A* (in press, DOI: 10.1021/jp103532q)
34. Y. Kurzweil, and M. Head-Gordon, "Improving approximate-optimized effective potentials by imposing exact conditions: Theory and applications to electronic statics and dynamics", *Phys. Rev. A* **80**, 012509 (2009).
35. A. Jullien, T. Pfeifer, M. J. Abel, P. M. Nagel, J. Bell, D. M. Neumark, and S. R. Leone, "Ionization phase-match gating for wavelength-tunable isolated attosecond pulse generation," *Appl. Phys. B* **93**, 433 (2008).
36. T. Pfeifer, M. J. Abel, P. M. Nagel, A. Jullien, Z.-H. Loh, M. J. Bell, D. M. Neumark, and S. R. Leone, "Time-resolved spectroscopy of attosecond quantum dynamics," *Chem. Phys. Lett.* **463**, 11 (2008).
37. M. J. Abel, T. Pfeifer, A. Jullien, P. M. Nagel, M. J. Bell, D. M. Neumark, and S. R. Leone, "Carrier-envelope phase-dependent quantum interferences in multiphoton ionization," *J. Phys. B: At. Mol. Opt. Phys.* **42**, 075601 (2009).
38. T. Pfeifer, M. J. Abel, P. M. Nagel, W. Boutu, M. J. Bell, Y. Liu, D. M. Neumark, and S. R. Leone, "Measurement and optimization of isolated attosecond pulse contrast," *Opt. Lett.* (in press) (2009).
39. M. J. Abel, T. Pfeifer, P. M. Nagel, W. Boutu, M. J. Bell, C. P. Steiner, D. M. Neumark, and S. R. Leone, "Isolated attosecond pulses from ionization gating of high harmonic emission," *Chem. Phys.* (submitted).

**ATOMIC AND MOLECULAR PHYSICS RESEARCH
AT
OAK RIDGE NATIONAL LABORATORY**

David R. Schultz, Group Leader, Atomic Physics
[schultzd@ornl.gov]
ORNL, Physics Division, P.O. Box 2008
Oak Ridge, TN 37831-6372

Principal Investigators

M.E. Bannister, S. Deng,* I.N. Draganic,* P.R. Harris,* C.C. Havener, J.H. Macek,
F.W. Meyer, C.O. Reinhold, D.R. Schultz, and C.R. Vane

*Postdoctoral Fellow

The OBES atomic physics program at ORNL has as its overarching goal the understanding of states and interactions of atomic-scale matter. These atomic-scale systems are composed of singly and multiply charged atomic ions, charged and neutral molecules, atoms, electrons, solids, and surfaces. Particular species and interactions are chosen for study based on their relevance to gaseous or plasma environments of basic energy science interest such as those in fusion energy, gas phase chemistry, and plasma processing. Toward this end, the program has developed and operates the Multicharged Ion Research Facility (MIRF) that has recently undergone a broad, multi-year upgrade. Work is also performed as needed at other facilities such as ORNL's Holifield Radioactive Ion Beam Facility (HRIBF) and the heavy-ion storage ring facilities at Stockholm University (CRYRING and soon DESIREE). Closely coordinated theoretical activities support this work as well as provide leadership in complementary or synergistic research.

Erosion of a-C:H and a-C:D Thin Films by Low-Energy Atomic and Molecular H and D Ion Beam Irradiation – *F.W. Meyer, P.R. Harris, W. Jacob, T. Schwarz-Selinger, and U. von Toussaint*

Ion-surface interactions play an essential role in many applications ranging from semiconductor device technology to magnetic fusion. The plasma-material interface is a critical bottleneck in fusion power conversion. A recent panel report to the Fusion Energy Sciences Advisory Committee (FESAC) found that four of the top five critical knowledge gaps for fusion involve the Plasma-Materials Interface (PMI). Just completed fusion community Research Needs Workshops (RENEW) have recommended new PMI research programs and facilities to *advance the science and technology of plasma-surface interactions*.

In line with these recommendations, we have continued this past year our studies of the interactions of slow H or D ions with carbon based surfaces. Our measurements focus on the energy region below the physical sputtering threshold (<50 eV) where chemical sputtering is the main mechanism for material erosion. This energy region is also the anticipated particle energy regime of the ITER divertor.

Most recently, we have been focusing on a comparison of chemical sputtering yields for atomic and molecular species of the same velocity, as a test of the commonly made assumption of identical sputtering yields when normalized to the number of D atoms in the incident projectiles. In our earlier measurements of CD₄ production by atomic vs. molecular projectiles using a quadrupole mass spectrometer (QMS) [1], we found projectile dependent methane yields below

~60 eV/D, where the D^+ projectiles had the smallest yields and D_3^+ projectiles had the largest yields. The effect increased with decreasing energy and amounted to about a factor of two at 10 eV/D. At higher energies, where immediate dissociation of incident molecular projectiles is highly probable, the observed yields for equivelocity incident atomic and molecular ions are the same, as has been noted in previous work. The molecular size effect is also evident in recently completed total erosion measurements of plasma-deposited, amorphously hydrogenated and deuterated carbon thin films (a-C:H and a-C:D) with a hydrogen or deuterium content of 30 % that were prepared and analyzed at IPP-Garching. For these measurements, the thin films were exposed to equal velocity atomic and molecular hydrogen or deuterium beams to fluences of $1-2 \times 10^{18}$ H or D/cm².

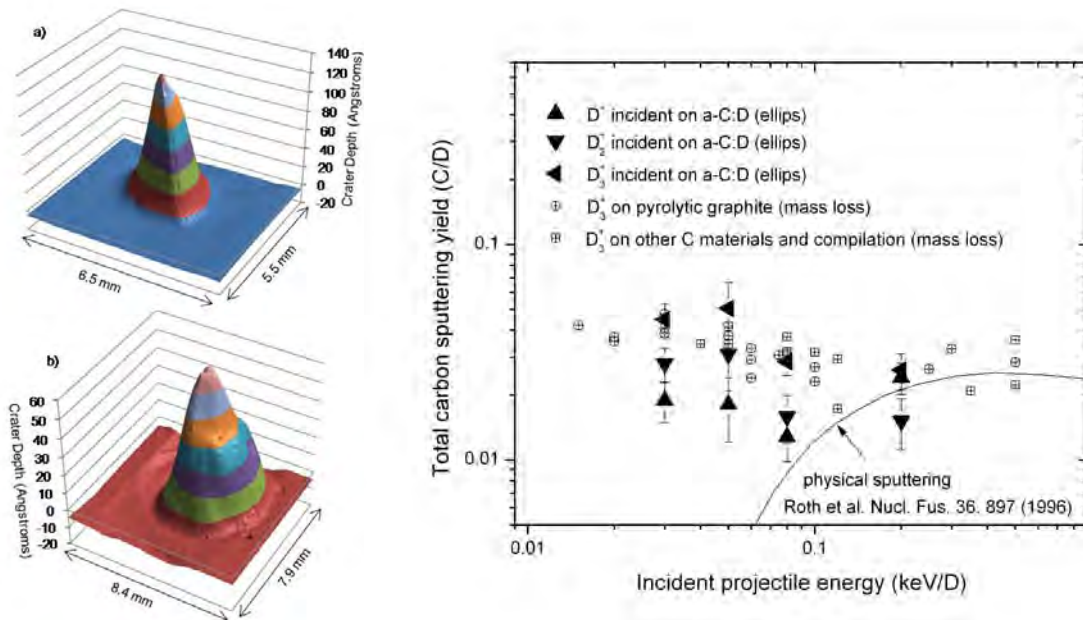


Figure 1. (left) 2-D ellipsometry post- and pre-exposure scan differences for (a) 80 eV/D D^+ exposure and (b) 80 eV/D D_2^+ showing typical crater depth distributions; (right) ellipsometry-based sputtering yield results for D^+ , D_2^+ , and D_3^+ ions incident on a-C:D, and comparison to mass loss results [2].

Beam energies were in the range 30 – 200 eV/H or D. From 2-D ellipsometry scans such as shown in Figure 1 (left), and the known thin film density, the total C removal could be determined. Normalization to the integrated number of incident H or D projectiles, obtained from simple beam current integration multiplied by the number of H or D atoms per incident projectile (e.g., 1, 2, or 3 for D^+ , D_2^+ , or D_3^+ , respectively) gives the total C yield per H or D. While there is no significant difference between the different projectiles at the highest energy of 200 eV/H or D, dramatic differences between $H^+(D^+)$ and $H(D_3^+)$ projectiles, ranging from a factor of 2 to almost 5, are observed at all lower investigated energies, with the observed differences between $H^+(D^+)$ and $H_2^+(D_2^+)$ being in the range 1.3 to 1.7. Our yield results for triatomic H and D ions incident on the respective hydrogenated and deuterated thin films obtained by ellipsometry are in excellent agreement with earlier mass loss results of Balden and Roth [2]. Considering the smaller yields per H or D we find for the atomic incident ions, it is evident that for incident molecular ions, particularly the triatomic species, synergistic effects in energy deposition density due to the close proximity of the constituents at critical times of the surface interactions lead to significant enhancement of chemical sputtering yields. For this reason, low energy yields

measured using molecular projectiles but claimed to represent those relevant for incident atomic projectiles should be treated with caution.

-
- [1] L.I. Vergara, F.W. Meyer, H.F. Krause, P. Träskelin, K. Nordlund, E. Salonen, *J. Nucl. Mater.* **357**, 9 (2006).
[2] M. Balden and J. Roth, *J. Nucl. Mater.* **280**, 39 (2000).

Low-Energy Atomic and Molecular Ion Collisions Using Merged Beams – C.C. Havener

Charge transfer (CT) in molecular ion-neutral interactions can proceed through dynamically coupled electronic, vibrational, and rotational degrees of freedom. Using the upgraded ORNL ion-atom merged-beams apparatus absolute direct charge transfer is explored from keV/u collision energies where the collision is considered “ro-vibrationally frozen” to sub-eV/u collision energies where collision times are long enough to sample vibrational and rotational modes. Our first molecular ion measurement [1] was performed for $D_2^+ + H$ and benchmarks high-energy theory and for the first time vibrationally specific adiabatic theory for the $(H_2-H)^+$ complex, the most fundamental ion-molecule two-electron system. CT molecular ion studies have been expanded to measurements for $D_3^+ + H$ from 2 eV/u to 2 keV/u. A threshold is observed around 4 eV with a change of slope in the measured cross section at 100 eV/u possibly due to the opening up of an additional dissociation channel after CT.

An 808-nm 2-kW diode laser has been purchased and will be installed on the merged-beams negative beamline in a neutralization configuration similar to that developed for the self-merged beams collaboration [2] at Columbia. With the new laser, neutral C beams will be available to explore both multi-electron capture and the synthesis of hydrocarbons via atom pickup reactions. Care must be taken to minimize any excited C states produced during photodetachment of the loosely bound (2D) C- excited states [3].

With the intense beams available from the 14.5 GHz all-permanent magnet ECR ion source on the HV platform, we are able to expand our previous CT studies of bare- and H-like ions with the merged-beams technique. With the expected delivery of an X-ray quantum calorimeter [4] to ORNL in 2011, we plan to record the CT produced X-ray spectra in the range 0.3 keV/u - 2 keV/u with high spectral resolution (up to 6-eV FWHM) for bare and H-like ions on H. Relative line intensities will be used to estimate the state selective CT cross sections, which will provide a detailed comparison with theory. In preparation for these relative measurements, absolute total cross sections for single electron capture by H-like ions of C, N, O, and fully-stripped O ions from atomic hydrogen have been measured this last year in an expanded range of relative collision energies (0.01 keV/u - 20 keV/u). In general, the new merged-beams results are in good agreement with previous ORNL H-oven measurements. However, at lower energies the new measurements consistently show a decreasing CT cross section for the H-like ions. This unexpected result is being explored with atomic-orbital and molecular-orbital close coupling calculations. Our measurements for $O_8^+ + H$ shown in Figure 1 below indicate the need for state-selective studies.

Good agreement is observed at 200 eV/u and above with our previous hydrogen-oven measurements that are significantly below the more recent CT theory. The larger theoretical total cross section is attributed to the predicted increase in capture to the $n=6$ shell of O^{7+} . Below 200 eV/u our new measurements do suggest a somewhat increasing trend which may be attributed to the importance of the $n=6$ shell, but at a much lower energy than predicted. The disagreement with theory for such a fundamental system will easily be explored in greater detail with the X-ray emission measurements planned for next year.

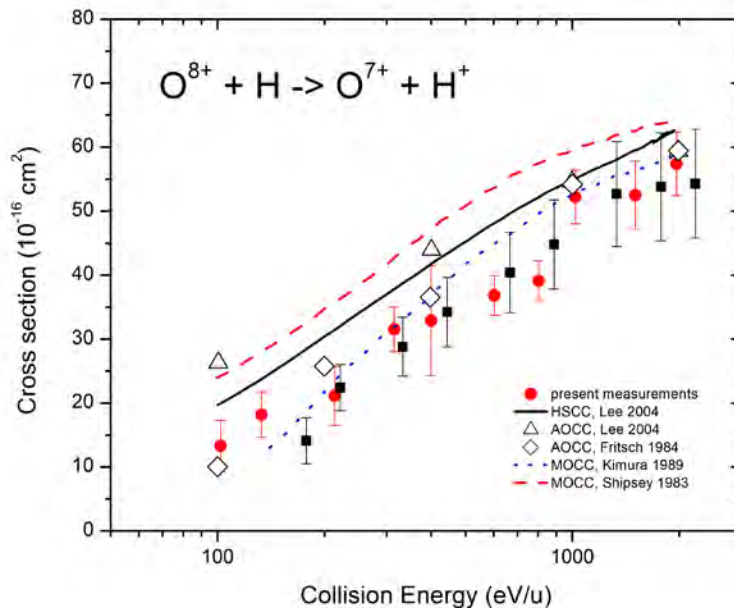


Figure 1. The ORNL merged-beams charge-exchange cross section measurements for fully stripped oxygen ion on atomic hydrogen, $\text{O}^{8+} + \text{H} \rightarrow \text{O}^{7+} + \text{H}^+$, are presented with previous theoretical and experimental data.

- [1] V. Andrianarijaona, J.J. Rada, R. Rejoub, and C.C. Havener, *J. Phys.: Conf. Ser.* **194**, 082018, 2009.
- [2] H. Bruhns, H. Kreckel, K. Miller, M. Lestinsky, B. Seredyuk, W. Mitthumsiri, B.L. Schmitt, M. Schnell, X. Urbain, M.L. Rappaport, C.C. Havener, and D.W. Savin, *Rev. Sci. Instrum.* **81**, 013112 (2010).
- [3] A.O. Lindahl, D. Hanstorp, O. Forstner, N.D. Gibson, T. Gottwald, K. Wendt, C.C. Havener, and Y. Liu, *J. Phys. B: At. Mol. Opt. Phys.* **43**, 115008 (2010).
- [4] J. McCammon, *Low Temp Phys.* **151**, 715 (2008).
- [5] T.-G. Lee, M. Heese, A.-T. Le, and C.D. Lin, *Phys. Rev. A* **70**, 012702 (2004).

Electron-Molecular Ion Interactions – M.E. Bannister, C.R. Vane, and S. Deng

Electron-driven fragmentation of molecular ions provides a testable platform for investigating and fully developing our understanding of the mechanisms involved in electronic charge and energy redistribution in many-body quantum mechanical systems, and is important from a fundamental point of view, i.e., to control material processes at the level of electrons, a Grand Challenge in Basic Energy Sciences. These dissociative processes are also practically important in that electron-ion collisions are generally ubiquitous in plasmas, and molecular ions can constitute significant populations in low- to moderate-temperature plasmas. Neutral and charged radicals formed in dissociation of molecules in these plasmas represent some of the most highly reactive components in initiating and driving further chemical reaction pathways in a wide variety of environments, such as the divertor and edge regions in fusion reactors, plasma enhanced chemical vapor deposition reactors, and environments where chemistries are driven by secondary electron cascades, for example in the upper atmosphere of the earth, and cooler regions of the solar or other stellar atmospheres. It is absolutely critical to have available accurate rates,

branching fractions, and other kinematical parameters of the various possible relevant collision processes in order to correctly model these environments.

Dissociative Excitation and Ionization: Measurements of cross sections for electron-impact dissociative excitation (DE) and dissociative ionization (DI) of molecular ions have continued using the MIRF crossed-beams apparatus [1]. In coordination with our dissociative recombination (DR) investigations of ozone ions [2], we have investigated the DE and DI channels for these ions. Our measurements demonstrate that, unlike the DR process which is dominated by the production of three oxygen atoms, the DE process leading to the formation of O^+ ions favors the $O^+ + O_2$ two-body channel over the $O^+ + O + O$ three-body channel. However, over the entire energy range of the measurements (3 - 100 eV), the DE/DI channels producing O_2^+ are dominant. This is not surprising when one considers the energy thresholds for DE of ground-state O_3^+ ions: 0.64 eV for the $O_2^+ + O$ channel and 2.19 eV for the $O^+ + O_2$ channel.

Measurements of absolute cross sections have also been made for the dissociation of $C_2D_5^+$ producing the CD_3^+ fragment ion. The experimental results indicate a DE threshold consistent with the value of 6.0 eV for the $CD_3^+ + CD_2$ channel. A clear onset of DI contributions is observed above the predicted threshold of 16.4 eV. Future investigations will measure DE/DI cross sections for the production of other fragment ions, especially CD_2^+ and $C_2D_2^+$. Another interesting experiment that will be carried out concerns whether the C_2^+ dicarbon cation can be formed directly by electron-impact dissociation of $C_2H_x^+$ ions.

Other measurements were performed for the electron-impact dissociation of OD^+ producing O^+ ions and HeH^+ yielding He^+ fragments. The latter system is a sensitive probe of the internal states of the target ions – our measurements with “hot” HeH^+ ions produced in an ECR source showed a DE threshold several eV lower than that for “cold” ions measured at the CRYRING ion storage ring [3].

The dissociation experiments discussed above used molecular ions produced by the ORNL MIRF Caprice ECR ion source [4], but other cooler sources will also be used in order to understand the role of electronic and ro-vibrational excited states. A second ion source, a hot-filament Colutron ion source, is presently online and is expected to produce fewer excited molecular ions.

An even colder pulsed supersonic gas expansion ion source, very similar to the one used for measurements [5] on the dissociative recombination of rotationally cold H_3^+ ions at CRYRING, is under development for use at the ORNL MIRF. Additionally, work continues on a similar supersonic source that uses a piezoelectric mechanism for more reliable pulsed valve operation. With this range of ion sources, one can study dissociation with both well-characterized cold sources and with intrinsically hotter sources producing ions that better approximate the excited state populations in plasma environments found in applications such as fusion, plasma processing, and astronomy. Another source being implemented at the MIRF for the study of electron-molecular ion interactions is an electrospray ionization source that will produce ions from large, fragile biomolecules such as nucleotides and peptides, allowing us to probe the fundamental mechanisms of fragmentation in very complex molecular systems, and especially effects in processes important in mass spectrographic techniques used for analyzing heavy molecular ions.

Dissociative Recombination: Recent measurements [6] performed at the CRYRING heavy ion storage ring on the dissociative recombination of the water cluster ion $D_5O_2^+$ yielded some interesting results. DR of this ion produces $D + 2 D_2O$ almost exclusively with a kinetic energy release of up to 5.1 eV. Through imaging of the DR fragments at an interaction of zero eV, it was determined that as much as 4 eV of this excess energy can be stored internally in the D_2O molecular fragments, with a propensity for populating highly excited states.

Further studies of molecular ion neutralization processes in our ongoing collaboration with the group of Mats Larsson and Richard Thomas at Stockholm University are in the midst of transition

because of the impending move of CRYRING from the Manne Siegbahn Laboratory to GSI in Germany and the opening of the Double ElectroStatic Ion Ring ExpERiment (DESIREE) in the Department of Physics at Stockholm University. The DESIREE ion storage ring facility (currently undergoing assembly and testing at the Stockholm University AlbaNova Center for Physics, Astronomy, and Biotechnology) is centered around two intersecting, all electrostatic rings, operating in a single < 10 K, ultra-high vacuum environment. DESIREE will provide a unique opportunity to study fundamental mutual neutralization processes for near-zero energy collisions of positive and negative atomic ions, as well as afford an expansion of capabilities for studies of more complex (heavier) molecular ion systems involved in a variety of charge transfer dissociation processes involving merged positive and negative ions stored and state-prepared in a cryogenic environment. The first experiments at DESIREE will involve measurements of mutual neutralization between H^+ and H^- (and isotopes) at low relative collision energies, with first injection of positive ions expected by the end of 2010.

-
- [1] M.E. Bannister, H.F. Krause, C.R. Vane *et al.*, Phys. Rev. A **68**, 042714 (2003).
 [2] V. Zhaunerchyk, W.D. Geppert, M. Larsson, R.D. Thomas, E. Bahati, M.E. Bannister, M.R. Fogle, C.R. Vane, and F. Österdahl, Phys. Rev. Lett. **98**, 223201 (2007).
 [3] C. Strömholm, J. Semaniak, S. Rosén, H. Danared, S. Datz, W. van der Zande, and M. Larsson, Phys. Rev. A **54**, 3086 (1996).
 [4] F.W. Meyer, in *Trapping Highly Charged Ions: Fundamentals and Applications*, edited by J. Gillaspay (Nova Science, Huntington, NY, 1997), p. 117.
 [5] B.J. McCall *et al.*, Nature **422**, 500 (2003).
 [6] R.D. Thomas, V. Zhaunerchyk, F. Hellberg, A. Ehlerding, W.D. Geppert, E. Bahati, M.E. Bannister, M.R. Fogle, C.R. Vane, A. Pettrignani, P.U. Andersson, J. Öjekull, J.B.C. Pettersson, W.J. van der Zande, and M. Larsson, J. Phys. Chem. **114**, 4843 (2010).

Molecular Ion Interactions (The MIRF ICCE Trap) – C.R. Vane, M.E. Bannister, S. Deng, and C.C. Havener

A rather unique experimental capability is under development at the ORNL MIRF for detailed, state-specific measurements of dissociation processes occurring for interactions of molecular ions with free electrons and atomic targets. An Ion Cooling and Characterization Endstation (ICCE Trap) has recently been developed and commissioned at the ORNL MIRF. It has been designed to provide a variety of enhanced experimental capabilities for studies of the interactions of complex atomic and molecular ions with electrons, as well as with atomic and molecular targets, that lead to fragmentation. Development of the ICCE trap apparatus is in direct support of our mission goal of establishing experimental capabilities necessary for selectively producing and manipulating atomic and molecular ions for studies of a broad range of plasma relevant ion-ion interactions in as a near state-controlled a manner as possible. Interpretation of measurements of multi-fragment dissociation of complex molecular and cluster ion systems requires increased levels of control over the internal state populations of the reacting partners, as well as highly detailed and complete information from analysis and detection systems. To provide these capabilities, we have designed, constructed, and instrumented an electrostatic reflecting ion beam linear trap of the *Zajfman* design [1,2] as an experimental endstation on the MIRF high-energy beamline that will enable stored cooling and state characterization of molecular ions of essentially any mass. Basic components of the ICCE TRAP are indicated schematically in Figure 1.

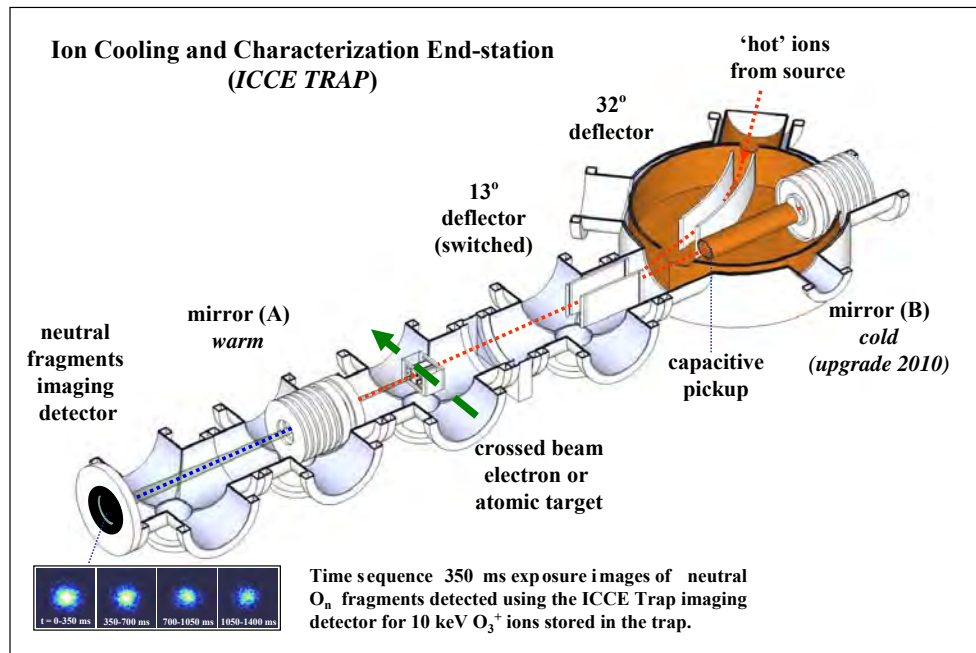


Figure 1. Schematic of the MIRROR Ion Cooling and Characterization Endstation, showing side injection of ions into the linear, double electrostatic mirror trap, instrumented with crossed electron and atomic target beams (with recoil ion detection) and a dissociation neutral fragment imaging detector.

Pulses of ions are injected from the side through a pulsed parallel plate 13° deflector into a 1.5-meter-long electrostatic-mirror trap. The side-injection design, a first for linear electrostatic traps, was chosen to avoid the necessity of fast ($<1 \mu\text{s}$) switching of the high-voltage mirror electrodes, and to enable storage of high-energy ion beams. This permits taking advantage of the kinematic emission of high-energy dissociation fragments to make their detection as highly efficient as possible. This ultrahigh vacuum, all-electrostatic device permits effective long-term (seconds) storage of high-energy ion beams where excited internal states decay by radiative cooling and dissociation processes can be explored as a function of storage time.

Stored ion beams are produced in several ion sources, including a permanent-magnet ECR ion source mounted on the MIRROR high-voltage platform for ‘hot’ atomic and molecular ions, and a pulsed, supersonic expansion discharge source for internally ‘cold’ molecular ions (CMIS), mounted on a stand-alone 10-kV isolated cabinet. As noted previously, the CMIS is similar in design to one used previously at CRYRING [3] for cold H_3^+ dissociative recombination measurements, and is capable of providing a nearly completely vibrational ground-state population of light molecular ions. For more fragile, very heavy molecular ions, an electrospray ion source (ESI) developed at the ORNL Chemical Sciences Division for production of biomolecular ions has also been mounted on the 10-kV platform. Intense species directly obtained from the ESI as heavy as Tetramethyl ammonium bromide cations have been injected into the trap. Techniques being developed by our colleagues at Stockholm University (for the DESIREE program) for prior accumulation of more sparsely ESI generated biomolecular ion species are also planned for future implementation at the MIRROR ICCE for pulsed injection into the trap.

The complete ion cooling and characterization endstation consists of an ultra-high vacuum transport beamline and chambers with computer controlled, fast-reaction electrostatic deflection and focusing elements, a fully electrostatic 38-mm diameter aperture mirror trapping system, and either a crossed beam, low-energy (5–100 eV), high-current electron target [4], or an atomic

beam target with recoil ion detection located between the trap mirrors. The apparatus is instrumented with a number of beam diagnostic and product characterization components, including two imaging detectors for velocity analysis of neutral fragments arising from fragmentation of the trapped molecular ions, either by collisions with gas atoms (collisional dissociation (CD) and dissociative electron capture (DEC)), or with the electrons (dissociative excitation or ionization (DE, DI), and less likely, dissociative recombination (DR)). The ion trap presently operates at room temperature with vacuum at $\sim 1 \times 10^{-10}$ Torr and ion internal state cooling proceeding through radiative decay is thermodynamically limited to 300°K . Improvements in the next year will include installation of an overall copper liner over one mirror section cooled to $< 70^\circ \text{K}$ using commercial stirling cryocoolers, with later planned connection of one of the mirrors (B) and its shroud to a $\sim 4^\circ \text{K}$ helium cryocooler.

Initial work is concentrated on trapping and cooling of a number of relatively simple ions including O^+ , O_2^+ , and O_3^+ ions, and on measurements of DEC from H_2 , Ne, and Ar and electron impact dissociation (DE, DI, and DR) as functions of electron energy for various trapping/cooling times. The ozone ion results are being compared with our prior DR measurements for vibrationally cold O_3^+ at CRYRING at zero electron energy [5], which indicated almost complete three-body dissociation, forming predominantly electronically excited $\text{O} (^3\text{P}$ and $^1\text{D})$ atoms. Fragment imaging measurements of the three-body channel resulting from DEC of O_3^+ on the residual H_2 gas have been completed as a function of storage/cooling time in the ICCE trap. The distributions of total displacement (TD) between the three O atoms measured on the imaging detector are directly related to the total kinetic energy of release (KER) due to the dissociation process. The TD distribution measured during the first 2 ms of trapping, when the ozone ions are still “hot” indicates that DEC is more likely during that time period than for a storage time of more than 100 ms when the O_3^+ ions have radiated away much of their internal energy.

Preliminary studies of the dissociative excitation of O_3^+ and OH^+ by 5-25 eV electrons from the crossed electron beam target have been performed as a function of ion storage time. Background counts on the detector resulting from stray, low-energy electrons from the electron target being accelerated by the positive high voltages of the electrostatic mirrors have been suppressed. However, for the 1.5-m long trap region at 10^{-10} Torr, dissociation was dominated by DEC and CD with the background gas, making the study of DE very difficult. Reduction of these background processes by the improved vacuum conditions associated with future cryo-cooling of the ICCE trap as noted above are needed in order to complete quantitative measurements of DE.

Long term ion storage over the ~ 3 -m length of the trapping orbit places severe limits on tolerable strengths of stray fields. Reduction of magnetic fields along the trap axis with a modified Helmholtz coil arrangement has yielded an increased lifetime of ions stored in the trap. For example, measured $1/e$ lifetimes for 10-keV K^+ ions have exceeded two seconds with this improvement as indicated in Figure 2. In addition, by modifying the electric potential configuration in the electrostatic mirrors, we have extended the energy range of singly charged ions stored in the trap to 15 keV, with achievable mirror potentials high enough to trap ions greater than 16 keV. The higher ion beam energies enable full collection of fragments from dissociation channels with higher KERs for a given imaging detector size and position. Different electric potential configurations on the mirrors have been investigated, resulting in confirmation of various operational modes of trapping as originally noted by Zajfman et al. [6]. For example, with the trap operating in a “bunching” mode, the initial pulse of ions side-injected into the trap (usually on the order of ten microseconds long) remains automatically bunched temporally and spatially for storage times greater than 100 ms, corresponding to typically many thousands of reflections between the mirrors depending on the trapped ion velocity, without imposing any additional RF bunching fields.

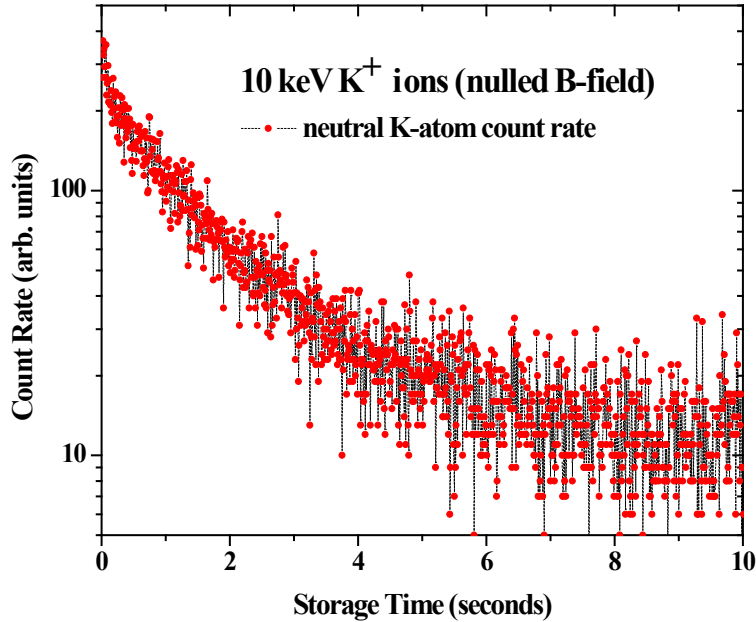


Figure 2. Storage lifetime plot for 10-keV K^+ ions in the ICCE Trap with external B-fields nulled along trapped ion orbit.

- [1] O. Heber *et al.*, Rev. Sci. Instrum. **76**, 013104 (2005).
- [2] H.F. Krause *et al.*, AIP Conf. Proc. **576**, 126-129 (1994).
- [3] B.J. McCall *et al.*, J. Phys.: Conf. Ser. **4**, 92 (2005); Nature **422**, 500 (2003).
- [4] P.D. Witte, PhD Thesis, University of Heidelberg (2002).
- [5] V. Zhaunerchyk *et al.*, Phys. Rev. A **77**, 022704 (2008).
- [6] D. Zajfman *et al.*, J. Opt. Soc. Am. **20**, 1028 (2003).

Manipulation and Decoherence of Rydberg Wavepackets – *C.O. Reinhold*

Current experimental techniques allow production of Rydberg atoms in well-defined quantum states with very large principal quantum numbers for which the Kepler period $T_n = 2\pi n^3$ (atomic units) becomes quite long (~ 4 ns at $n \sim 300$). It is thus straightforward using commercial pulse generators to apply carefully tailored electric field pulses whose characteristic times (durations, and/or rise/fall times) are much less than T_n . These can be used to engineer (and probe) electronic wavepackets and to examine dephasing and decoherence [1]. Even though high- n Rydberg atoms are extremely fragile, large angular momentum wavepackets are quite robust and their coherence can be maintained for microseconds or hundreds of Kepler periods (see Figure 1) [2]. The main challenge to theory is the development of control protocols for steering mesoscopic Rydberg wavepackets, which may show quantum behavior but are not manageable by fully quantum simulations due to the vast number of quantum states involved. We employ a hybrid quantized-classical trajectory method (QCTMC) that is capable of capturing the essential wavepacket dynamics. Our protocol for producing circular wavepackets leads to temporal interferences of spatially separated Schrödinger cat-like wavepackets. We are currently working on protocols for measuring [3] and controlling the phase of the cat states. We are also studying the decoherence of the wavepackets by adding a controlled amount of noise in the electromagnetic pulses. Noise might also be introduced experimentally by adding a dilute gas of particles. In the long term we would like to extend the present techniques to engineer two-electron wavepackets involving distant electrons in two interacting Rydberg atoms. This work is

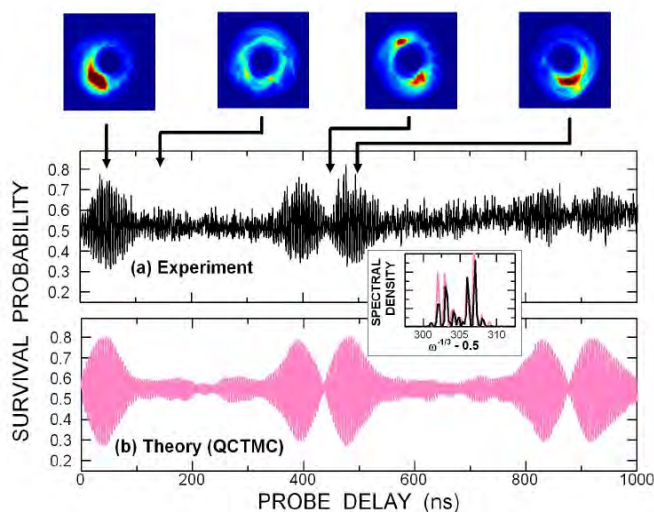


Figure 1. (a) Survival probabilities measured for parent $n_i = 305$ K atoms subject to a pump field $F_y^{pump} = -5$ mV cm^{-1} of 86 ns duration as a function of time after turn-off of the pump field using a 6 ns 100 mV cm^{-1} probe pulse. (b) Results of QCTMC simulations. Quantum revivals are evident around 440 ns and 880 ns. The middle inset shows the frequency spectrum calculated from the Fourier transform of the experimental and theoretical results as a function of $n = \omega^{-1/3} - 0.5$.

performed in collaboration with F.B. Dunning (Rice Univ.) and S. Yoshida and J. Burgdörfer (Vienna Univ. of Technology).

- [1] F.B. Dunning, J.J. Mestayer, C.O. Reinhold, S. Yoshida, and J. Burgdörfer, Topical Review, *J. Phys. B* **42**, 022001 (2009).
- [2] C.O. Reinhold, S. Yoshida, J. Burgdörfer, B. Wyker, J.J. Mestayer, and F.B. Dunning, Fast Track Communication, *J. Phys B* **42**, 091003 (2009).
- [3] S. Yoshida, C.O. Reinhold, J. Burgdörfer, B. Wyker, and F.B. Dunning, *Phys. Rev. A* **81**, 063428 (2010).

Molecular Dynamics Simulations of Chemical Sputtering – C.O. Reinhold and P.S. Krstic

Advances in fusion energy research are dependent on understanding the interaction of the plasma with the bounding surfaces. Physical and chemical processes resulting from this interaction lead to surface erosion and particle deposition, which degrades fusion performance. Little is known for low impact energies (below ~ 50 eV H, D, and T impact) where chemical processes dominate, since experiments are very difficult to perform. In an attempt to bridge the gap of data, we have undertaken a series of molecular dynamics simulations using the available experimental data above 15 eV for validation. This work is done in parallel to experiments at ORNL by F.W. Meyer and co-workers. We have performed molecular dynamics (MD) simulations using many-body Reactive Empirical Bond Order (REBO) potentials for atoms and molecules impacting on a large simulation cell consisting of a mixture of a few thousand carbon and hydrogen atoms representing the surface. We study surface erosion due to cumulative bombardment. The latter sequentially breaks and passivates bonds and leads to the formation of stable hydrocarbon terminal moieties that are ultimately detached in a collision. We have found that chemical sputtering yields increase with projectile mass but not as dramatically as expected. Only a weak dependence on the mass was found in the number of hydrocarbon moieties of supersaturated surfaces created by cumulative bombardment and, thus, the root of the mass dependence was found to be directly related to the probability for breaking the C–C bonds that attach such moieties [1]. We have analyzed the threshold energies of chemical sputtering reaction channels and showed that they are nearly mass independent, as expected from elementary bond-breaking chemical reactions involving hydrocarbons. Calculated sputtering yields agree with experimental data for the total yield of hydrocarbons containing a single carbon atom. However simulations overestimate the yield of molecules containing three or more carbon atoms. Since the quality of

the simulations critically depends on the quality of the potentials, we are currently working on the development of better many-body potentials. In the longer term we plan to extend our simulations to study materials different from pure carbon such as mixed materials including C, W, Li, H.

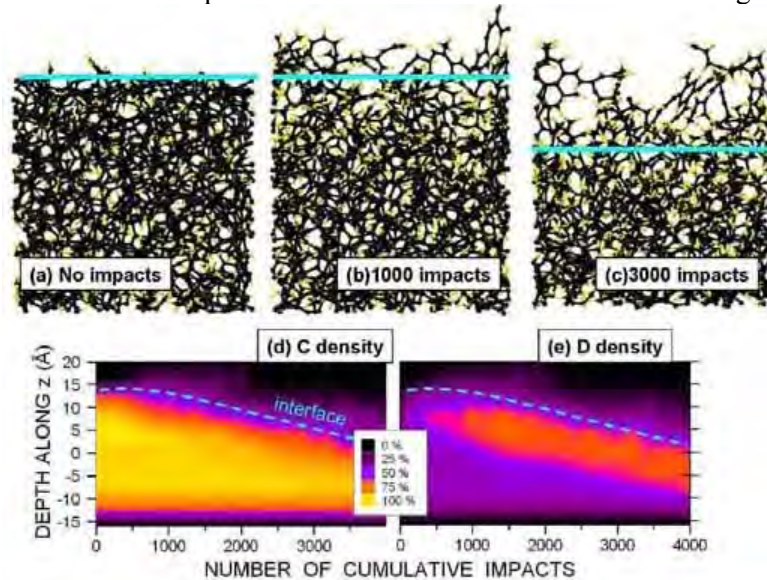


Figure 1. (a)-(c) Evolution of the simulation cell during cumulative bombardment by 20 eV D atoms. The yellow (black) spheres denote deuterium (carbon) atoms. (d) and (e) Development of the densities of carbon and deuterium atoms in the simulation cell as a function of the number of cumulative D impacts. The light blue lines denote the position of the interface. The depth $z=0$ represents the midpoint of the initial cell. The color-coding shows the ratio of the density to the bulk carbon density (see scale in the inset).

[1] C.O. Reinhold, P.S. Krstic, S.J. Stuart, H. Zhang, P.R. Harris, and F.W. Meyer, *J. Nucl. Mater.* **401**, 1 (2010).

Development of Theoretical Methods for Atomic and Molecular Collisions – *D.R. Schultz, S.Y. Ovchinnikov, J.B. Sternberg, and J.H. Macek*

The goal of understanding, and ultimately controlling, atomic-scale dynamics and ultrafast phenomena provides a strong motivation to study atomic and molecular interactions as a fundamental test bed to probe, for example, the transfer of energy and charge. In addition, plasma science applications, such as fusion energy, material processing, and the chemistry of the upper atmosphere, continue to drive such study because of the need for greater predictive understanding of the underlying atomic and molecular processes. These basic and applied research needs therefore require the development of theoretical methods to either reach new levels of accuracy for fundamental systems or novel completeness for complex systems. Over the past year, projects have therefore been undertaken along these lines using both the lattice, time-dependent Schrödinger equation (LTDSE) approach (e.g., [1]) and its recent extension to reach asymptotic final continuum states, the regularized LTDSE (RLTDSE) [2] method.

In particular, following our previous description of unexpected vortices in the electronic probability density in ion-atom collisions [3], which both influence angular momentum transfer and persist to asymptotic distances where they should be observable, we have found similar and contrasting formation of vortices that are also unanticipated during interaction of short electric field pulses with atoms [4]. In the ion-atom collision, we found that a number of “smoke ring” vortices formed at critical points in the transfer of angular momentum associated with transitions

between quasimolecular states, but that the dominant vortex was of the “tornado” morphology associated with the dynamic form of the potential (i.e., double-Coulomb well) experienced by the electron. This spurred us to consider the interaction of an electric field pulse with an atom because the dynamic potential, in contrast, is the sum of both an attractive (from the nuclear Coulomb charge) and a repulsive (from the electric pulse) force on the electron, and because of previous intriguing experimental and theoretical work in a similar regime by the Bucksbaum (e.g., [5]) and Dunning (e.g., [6]) groups (ultrashort, half-cycle pulses on Rydberg atoms).

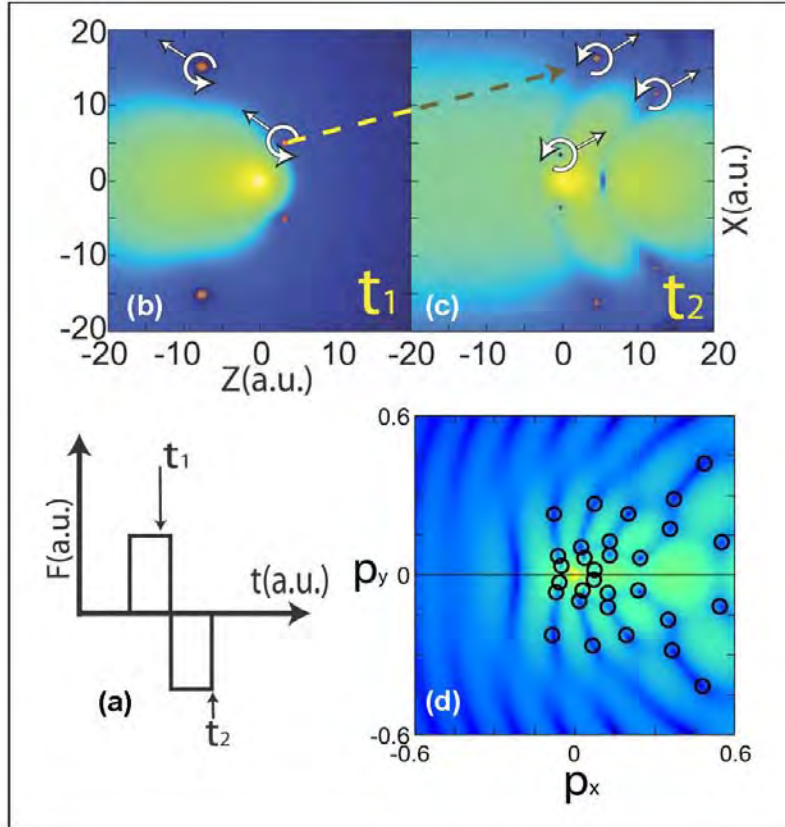


Figure 1. An atomic hydrogen atom subject to two successive short electric field pulses (a) of opposite sign, each of 16 a.u. duration. Ring vortices are formed on the righthand side of the atom, expand around the atom, and move off downstream shown (b) at $t=t_1=12$ a.u. As the field direction is reversed, the next vortices to form do so on the lefthand side of the atom, expand around the atom, and move off to the right. Note that the field turns the previously formed vortices around and drives them to the right as well. The vortex positions and direction of motion at the end of the second pulse, $t=t_2=32$ a.u. are shown in (c). The dashed arrow identifies the position and direction of the second vortex formed during the first pulse at the end of the second pulse. The spectrum of ejected electrons resulting from the two electric field pulses at asymptotic distances is shown in (d) showing the positions of vortices, primarily those formed latest in time and being associated with the lowest electronic momentum.

For short electric field pulses, we have found that smoke ring vortices form associated with transitions between states (including the continuum), move as quasiparticles, and persist to asymptotic distances (as illustrated in Figure 1), while tornado vortices are absent. We have found

that the vortices form at times and in regions dictated by a hydrodynamic picture of the electronic evolution as a specific instance of the Navier-Stokes equations. Moreover, the creation and dynamics of these vortices can be manipulated by tailoring series of electric field steps and should be observable in the resulting spectrum of ejected electrons. In the coming year we will further explore the consequences of varying the interaction potential on the formation and evolution of vortices, and in particular the effects the variations have on the transfer of angular momentum, by comparing proton- and antiproton-impact of atoms. Such comparisons, pursued by us and by other research groups particularly when antiprotons first became readily available for atomic collision experiments (see, e.g., the review of Ref. [7] and our more recent LTDSE studies [8,9]), allow a single characteristic of the collision, in this case the projectile charge, to be varied, in contrast to comparison of proton- and electron-impact collisions where both the charge and mass are simultaneously varied.

-
- [1] D.R. Schultz, M.R. Strayer, and J.C. Wells, *Phys. Rev. Lett.* **82**, 3976 (1999).
 [2] T.-G. Lee, S.Y. Ovchinnikov, J.B. Sternberg, V. Chupryna, D.R. Schultz, and J.H. Macek, *Phys. Rev. A* **76**, 050710(R) (2007).
 [3] J.H. Macek, J.B. Sternberg, S.Y. Ovchinnikov, T.-G. Lee, and D.R. Schultz, *Phys. Rev. Lett.* **102**, 134201 (2009).
 [4] S.Y. Ovchinnikov, J.B. Sternberg, J.H. Macek, T.-G. Lee, and D.R. Schultz, *Phys. Rev. Lett.* (2010) submitted.
 [5] J. Ahn, D.N. Hutchinson, C. Raman, and P.H. Bucksbaum, *Phys. Rev. Lett.* **86**, 1179 (2001).
 [6] F.B. Dunning, J.J. Mestayer, C.O. Reinhold, S. Yoshida, and J. Burgdörfer, *J. Phys. B* **42**, 022001 (2009).
 [7] D.R. Schultz, R.E. Olson, and C.O. Reinhold, *J. Phys. B* **24**, 521 (1991).
 [8] D.R. Schultz, P.S. Krstic, C.O. Reinhold, and J.C. Wells, *Phys. Rev. Lett.* **76**, 2882 (1996).
 [9] D.R. Schultz and P.S. Krstic, *Phys. Rev. A* **67**, 022712 (2003).

References to Publications of DOE Sponsored Research from 2008-2010 (descending order)

Year 2010 Publications

“Encoding and Decoding Phase Information in High-n Circular Wave Packets,” S. Yoshida, C.O. Reinhold, J. Burgdörfer, B. Wyker, and F.B. Dunning, *Phys. Rev. A* **81**, 063428 (2010).

“Isotope Dependence of Chemical Erosion of Carbon,” C.O. Reinhold, P.S. Krstic, S.J. Stuart, H. Zhang, P.R. Harris, and F.W. Meyer, *J. Nucl. Mater.* **401**, 1 (2010).

“Steering Quantum States Towards Classical Bohr-Like Orbits,” F.B. Dunning, C.O. Reinhold, S. Yoshida, and J. Burgdörfer, *Am. J. Phys.* **78**, 796 (2010).

“Nearly Complete Ion-Solar Suppression by Photo-detachment,” P. Andersson, A. Lindahl, D. Hanstorp, C.C. Havener, Y. Liu, and Y. Liu, *J. Appl. Phys.* **107**, 026102 (2010).

“A Novel Merged Beams Apparatus to Study Anion-Neutral Reactions,” H. Bruhns, H. Kreckel, K. Miller, M. Lestinsky, B. Sedyuk, W. Mitthumsiri, B.L. Schmitt, M. Schnell, D.W. Savin, X. Urbain, M.L. Rappaport, and C.C. Havener, *Rev. Sci. Instrum.* **81**, 13112 (2010).

“Hot Water from Cold. The Dissociative Recombination of Water Cluster Ions,” R.D. Thomas, V. Zhaunerchyk, F. Hellberg, A. Ehlerding, W.D. Geppert, E. Bahati, M.E. Bannister, M.R. Fogle, C.R. Vane, A. Pettrignani, P. Andersson, J. Ojekull, J.B. Pettersson, W.J. van der Zande, and M. Larsson, *J. Phys. Chem. A* **114**, 4843 (2010).

“Plasma Potential and Energy Spread Determination using Ion Beams Extracted from an Electron Cyclotron Resonance (ECR) Source,” P.R. Harris and F.W. Meyer, *Rev. Sci. Instrum.* **81**, 02A310 (2010).

“Origin, Evolution, and Imaging of Vortices in Proton-Hydrogen Collisions,” D. R. Schultz, J. H. Macek, J. B. Sternberg, S. Yu, Ovchinnikov, and T.-G. Lee, *J. Phys.: Conf. Series* **194**, 012041 (2010).

Year 2009 Publications

“Chemical Sputtering, Surface Damage and Modification of Graphite by Low Energy Impact of Atomic and Molecular Deuterium Projectiles,” F.W. Meyer, H. Zhang, P.R. Harris, H.M. Meyer, III, and M.J. Lance, *Proc. 31st Symposium on Applied Surface Analysis, Santa Cruz, CA, Apr. 22-24, 2009.*

“Steady-State and Transient Hydrocarbon Production in Graphite by Low Energy Impact of Atomic and Molecular Deuterium Projectiles,” H. Zhang and F.W. Meyer, *J. Nucl. Mater.* **390–391**, 127 (2009).

“Resonant Ionization Laser Ion Source for Radioactive Ion Beams,” Y. Liu, J.R. Beene, T. Gottwald, C.C. Havener, C. Mattolat, J. Lassen, K. Wendt, and C.R. Vane, *Am. Inst. Phys. Conf. Proc.* **1099**, 141 (2009).

“Investigation of Charge Transfer in Low Energy $D_2^+ + H$ Collisions using Merged Beams,” V.M. Andrianarijaona, J.J. Rada, R.A. Rejoub, and C.C. Havener, *J. Phys.: Conf. Ser.* **194**, 012043 (2009).

“Evolution of Carbon Surfaces under Simulated Bombardment by Deuterium,” S.J. Stuart, M.L. Fallet, P.S. Krstic, and C.O. Reinhold, *J. Phys.: Conf. Ser.* **194**, 012059 (2009).

“Electron-Impact Dissociation of CD_3^+ and CH_3^+ Ions Producing CD_2^+ , CH^+ , and C^+ Fragment Ions,” E.M. Bahati, M. Fogle, C.R. Vane, M.E. Bannister, R.D. Thomas, and V. Zhaunerchyk, *Phys. Rev. A* **79**, 052703 (2009).

“Isotope Effects in Low Energy Ion-Atom Collision,” C.C. Havener, D.G. Seely, J.D. Thomas, and T.J. Kvale, *Am. Inst. Phys. Conf. Proc.* **1099**, 150 (2009).

“Comment on Nondispersing Bohr Wave Packets,” S. Yoshida, C.O. Reinhold, J. Burgdörfer, and F.B. Dunning, *Phys. Rev. Lett.* **103**, 149301 (2009).

“Burning Plasma - Wall Interactions,” P.S. Krstic and C.O. Reinhold, *Am. Inst. Phys. Conf. Proc.* **1161**, 75 (2009).

“An Ion Cooling and State Characterization Apparatus for Studies of Molecular Ion Dissociative Interactions,” S. Deng, C.R. Vane, M.E. Bannister, C.C. Havener, F.W. Meyer, H.F. Krause, R.L. Hettich, D. Goeringer, and G.J. Van Berkel, *J. Phys.: Conf. Ser.* **194**, 142010 (2009).

“Production, Characterization, and Measurement of H(D) Beams on the ORNL Merged-Beams Experiment,” J.D. Thomas, T.J. Kvale, S.M.Z. Strasser, D.G. Seely, and C.C. Havener, *Am. Inst. Phys. Conf. Proc.* **1099**, 154 (2009).

“Production of Long-Lived H_2^- , HD^- , and D_2^- during Grazing Scattering Collisions of H_2^+ , H_3^+ , D_2^+ , D_3^+ , and D_2H^+ Ions with KBr, KCl, and LiF Surfaces,” D.G. Seely, F.W. Meyer, H. Zhang, and C.C. Havener, Am. Inst. Phys. Conf. Proc. **1099**, 159 (2009).

“Evolution of Quantum Systems from Microscopic to Macroscopic Scales,” S.Yu. Ovchinnikov, J.H. Macek, J.S. Sternberg, T.-G. Lee, and D.R. Schultz, Am. Inst. Phys. Conf. Proc. **1099**, 164 (2009).

“Low-Energy Grazing Ion-Scattering from Alkali-Halide Surfaces: A Novel Approach to C-14 Detection,” F.W. Meyer, E. Galutschek, and M. Hotchkis, Am. Inst. Phys. Conf. Proc. **1099**, 308 (2009).

“High-Energy Laser-Accelerated Electron Beams for Long-Range Interrogation,” N.J. Cunningham, S. Banerjee, V. Ramanathan, N. Powers, N. Chandler-Smith, R. Vane, D. Schultz, S. Pozzi, S. Clarke, J. Beene, and D. Umstadter, Am. Inst. Phys. Conf. Proc. **1099**, 638 (2009).

“Efficient Isobar Suppression by Photodetachment in the RF Quadrupole Ion Cooler,” Y. Liu, C.C. Havener, T.L. Lewis, A. Galindo-Uribarri, and J.R. Beene, Am. Inst. Phys. Conf. Proc. **1099**, 737 (2009).

“Large Scale Quantum Coherence of Nearly Circular Wavepackets,” C.O. Reinhold, S. Yoshida, J. Burgdörfer, B. Wyker, J.J. Mestayer, and F.B. Dunning, *Fast Track Communication*, J. Phys B **42**, 091003 (2009).

“Transfer of Rovibrational Energies in Hydrogen Plasma-Carbon Surface Interactions,” P.S. Krstic, E.M. Hollmann, C.O. Reinhold, S.J. Stuart, R.P. Doerner, D. Nishijima, and A.Yu. Pigarov, J. Nucl. Materials **390-391**, 88 (2009).

“Creation of Non-Dispersive Bohr-Like Wavepackets,” J.J. Mestayer, B. Wyker, F.B. Dunning, S. Yoshida, C.O. Reinhold, and J. Burgdörfer, Phys. Rev. A **79**, 033417 (2009).

“Hydrogen Reflection in Low-Energy Collisions with Amorphous Carbon,” C.O. Reinhold, P.S. Krstic, and S. J. Stuart, Nucl. Instrum. Meth. Phys. Res. B **267**, 691 (2009).

“Plasma-Surface Interactions of Hydrogenated Carbon,” P. S. Krstic, C.O. Reinhold, and S.J. Stuart, Nucl. Instrum. Meth. Phys. Res. B **267**, 704 (2009).

“Engineering Atomic Rydberg States with Pulsed Electric Fields,” F.B. Dunning, J.J. Mestayer, C.O. Reinhold, S. Yoshida, and J. Burgdörfer, Topical Review, J. Phys. B **42**, 022001 (2009).

“Origin Evolution and Imaging of Vortices in Atomic Processes,” J.H. Macek, J.B. Sternberg, S.Yu. Ovchinnikov, T.-G. Lee, and D.R. Schultz, Phys. Rev. Lett. **102**, 134201 (2009).

Year 2008 publications

“Attosecond Time Delays in Heavy-Ion Induced Fission Measured by Crystal Blocking,” J.U. Anderson, J. Chevallier, J.S. Foster, S.A. Karamian, C.R. Vane, J.R. Beene, A. Galindo-Uribarri, J. Gomez de la Campa, C.J. Gross, H.F. Krause, E. Padilla-Rodal, D.C. Radford, D. Shapira, C. Broude, F. Malaguti, and A. Uguzzoni, Phys. Rev. C **78**, 064609 (2008).

- “Rotating Dual-Wire Beam Profile Monitor Optimized for Use in Merged-Beams Experiments,” D.G. Seely, H. Bruhns, D.W. Savin, T.J. Kvale, E. Galutschek, H. Aliabadi, and C.C. Havener, *Nucl. Instrum. Methods Phys. Res.* **585**, 69 (2008).
- “Chemical Sputtering and Surface Damage by Low-Energy Atomic and Molecular Hydrogen and Deuterium Projectiles,” F.W. Meyer, H. Zhang, M.J. Lance, and H.F. Krause, *Vacuum* **82**, 880 (2008).
- “Surface Modification and Chemical Sputtering of Graphite Induced by Low-Energy Atomic and Molecular Deuterium Ions,” H. Zhang, F.W. Meyer, H.M. Meyer III, M.J. Lance, *Vacuum* **82**, 1285 (2008).
- “Electron-Impact Ionization of Be-like C III, N IV, and O V,” M.R. Fogle, E. Bahati Musafiri, M.E. Bannister, C.R. Vane, S.D. Loch, M.S. Pindzola, C.P. Ballance, R.D. Thomas, V. Zhaunerchyk, P. Bryans, W. Mitthumsiri, and D.W. Savin, *Astrophys. J. Suppl. Ser.* **175**, 543 (2008).
- “Dissociative Recombination of BH_2^+ : The Dominance of Two-Body Breakup and an Understanding of the Fragmentation,” V. Zhaunerchyk, E. Vigen, W. Geppert, M. Hamberg, M. Danielsson, M. Kaminska, M. Larsson, R.D. Thomas, E. Bahati Musafiri, and C.R. Vane, *Phys. Rev. A* **78**, 024701 (2008).
- “Dissociative Recombination Dynamics of the Ozone Cation,” V. Zhaunerchyk, W. Geppert, F. Österdahl, M. Larsson, R.D. Thomas, E. Bahati Musafiri, M.E. Bannister, M.R. Fogle, and C.R. Vane, *Phys. Rev. A* **77**, 022704 (2008).
- “Tailoring Very-High- n Circular Wavepackets,” C.O. Reinhold, S. Yoshida, J. Burgdörfer, J.J. Mestayer, B. Wyker, J.C. Lancaster, and F.B. Dunning, *Phys. Rev. A* **78**, 063413 (2008).
- “Energy and Angle Spectra of Sputtered Particles for Low-Energy Deuterium Impact of Carbon,” P.S. Krstic, C.O. Reinhold, and S.J. Stuart, *J. Appl. Phys.* **104**, 103308 (2008).
- “Measurement and Modeling of Hydrogen Molecule Rotational Accommodation on Graphite,” E.M. Hollmann, P.S. Krstic, R.P. Doerner, D. Nishijima, A. Yu. Pigarov, C.O. Reinhold, and S.J. Stuart, *Plasma Phys. Control. Fusion* **50**, 102001 (2008).
- “Extracting Irreversible Dephasing Rates from Electric Dipole Echoes in Rydberg Stark Wavepackets,” S. Yoshida, C.O. Reinhold, J. Burgdörfer, W. Zhao, J.J. Mestayer, J.C. Lancaster, and F.B. Dunning, *Phys. Rev. A* **78**, 063414 (2008).
- “Realization of Localized Bohr-like Wavepackets,” J.J. Mestayer, B. Wyker, J.C. Lancaster, F.B. Dunning, C.O. Reinhold, S. Yoshida, and J. Burgdörfer, *Phys. Rev. Lett.* **100**, 243004 (2008).
- “Occupation of Fine-Structure States in Electron Capture and Transport,” M. Seliger, C.O. Reinhold, T. Minami, D.R. Schultz, S. Yoshida, J. Burgdörfer, E. Lamour, J.-P. Rozet, and D. Vernhet, *Phys. Rev. A* **77**, 042713 (2008).
- “Total and State-Selective Charge Transfer in $He^{2+} + H$ Collisions,” T. Minami, T.-G. Lee, M.S. Pindzola, and D.R. Schultz, *J. Phys. B* **41**, 134201 (2008).

“Time-Dependent Lattice Methods for Ion-Atom Collisions in Cartesian and Cylindrical Coordinate Systems,” M.S. Pindzola and D.R. Schultz, Phys. Rev. A **77**, 014701 (2008).

“Transferring Rydberg Wavepackets between Islands across the Chaotic Sea,” S. Yoshida, C.O. Reinhold, J. Burgdörfer, J.J. Mestayer, J.C. Lancaster, and F.B. Dunning, Phys. Rev. A **77**, 013411 (2008).

“Low-Energy Charge Transfer for Collisions of Si^{3+} with Atomic Hydrogen,” H. Bruhns, H. Kreckel, D.W. Savin, D.G. Seely, and C.C. Havener, Phys. Rev. A **77**, 064702 (2008).

The PULSE Institute for Ultrafast Energy Science at SLAC

M. Bogan, P.H. Bucksbaum (Director), H. Dürr, K. Gaffney, M. Gühr, A. Lindenberg, T. Martinez, D. Reis (Deputy Director), J. Stohr, SLAC National Accelerator Laboratory, phb@slac.stanford.edu

PULSE Vision Statement, 2010 : The ultrafast laser science initiative underway now at the SLAC National Accelerator Laboratory, has as its centerpiece the Linac Coherent Light Source. LCLS, has been conducting user operations now for nearly a year. It routinely exceeds its original design goals, and reaches new milestones regularly in both tuning capability and instrumentation. Its x-rays are a billion times more brilliant than any other laboratory source. This new class of x-ray sources is revolutionizing many areas of science by making it possible for the first time to see atomic scale structures and simultaneously track atomic motions of the underlying nanoscale processes of energy conversion and transport.

The PULSE mission is to advance the frontiers of ultrafast science at SLAC with particular emphasis on discovery and Grand Challenge energy-related research enabled by LCLS. The PULSE Institute initiates and leads multidisciplinary collaborative research programs in studies of atoms, molecules, and nanometer-scale systems, where motion and energy transfer occurs on picosecond, femtosecond, and attosecond time scales. Ultrafast energy research at PULSE combines the disciplines of atomic and molecular physics, ultrafast chemistry and biochemistry, ultrafast condensed matter and materials science, ultrafast x-ray science, nanoscale x-ray imaging science, and the enabling science for next-generation ultrafast light and electron sources. Our metrics of success are the level of the ultrafast science challenges we address, and our progress toward and impact on their solution.

SLAC Photon Science Directorate Reorganization: PULSE has completed a transition mandated by SLAC's reorganization of the Photon Science Directorate. The Institute is no longer a research division at SLAC, but it still has the status as a Stanford University Independent Laboratory, organized under the office of the Stanford Associate Provost and Dean of Research. The DOE component of PULSE research is now organized by SLAC through two of its newly chartered research divisions. Approximately 40% of the PULSE DOE research portfolio is now managed by the newly-created SLAC Materials Science Division, while the remaining 60% is managed by a new SLAC Chemical Science Division. This annual summary concerns the Chemical Science component. We anticipate that this organizational change will allow PULSE to pursue broader collaborative activities in ultrafast science.

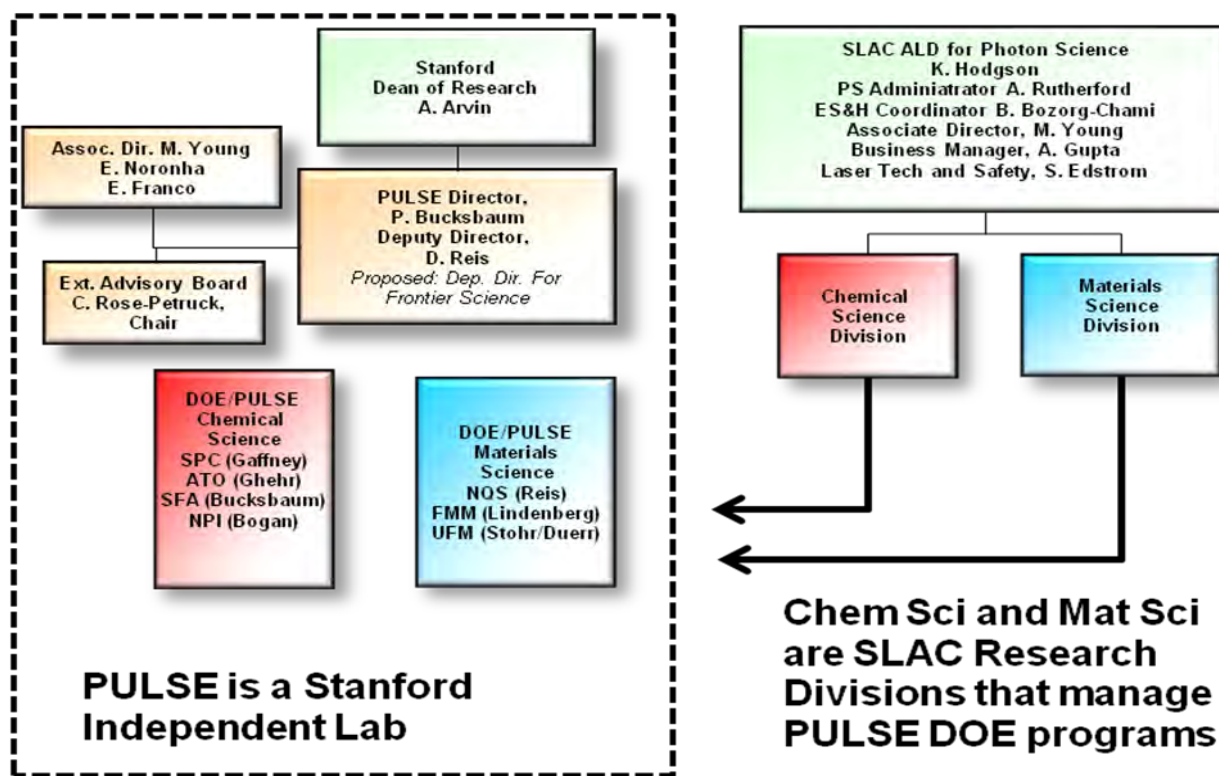
The PULSE Institute Laboratory Building at SLAC: PULSE now occupies a newly renovated 18,000 sf laboratory and office building, formerly known as the SLAC Central Lab. This is SLAC's first venue for laboratory-scale research, and is a model for future program expansion at SLAC. The renovated space provides 18000sf of laboratory and office areas, to enable us to develop close collaborations in important ultrafast areas such as time-resolved photoemission, time-resolved x-ray scattering, support for ultrafast biological imaging, and multidimensional spectroscopy.

PULSE also takes advantage of our proximity to SSRL and to LCLS to build strong SLAC core facilities in laser science and accelerator science. PULSE research utilizes the capabilities of LCLS, but also goes beyond this. For example, PULSE has a vigorous program on high harmonics generation and associated measurement techniques for atoms and molecules on the sub-femtosecond timescale. PULSE research extends to the research floor of the SPEAR3 synchrotron at SLAC, where ultrafast lasers can create transient conditions that are probed by synchrotron radiation. Finally, PULSE develops frontier research that makes use of technologies such as ultrafast imaging of biological and nanoscale materials, and ultrafast x-ray studies of matter in extreme environments. Our aim is to establish the leadership of SLAC research in these areas to solve fundamental challenges in basic energy science.

Education and Outreach: The major educational, physical research, engineering research, and medical research activities at Stanford provide strong support for all of our activities in PULSE. In addition, PULSE has run a successful international ultrafast X-ray Summer School. **The Ultrafast X-ray Summer School** is a five day residential program hosted annually by PULSE. The goal is to disseminate information and train students and post-docs on new opportunities in ultrafast science, particularly using X-ray Free Electron Lasers. Lectures are presented by expert scientists in this exciting new field. The attendees are expected to

participate in the discussions and to prepare a mock beamtime proposal poster with input from the instrument scientists for the Linac Coherent Light Source. This year's Ultrafast X-ray Summer School was co-directed by Aaron Lindenberg and Ken Schafer. Next year we will begin an arrangement with CFEL at DESY to alternate responsibility for the summer school. The school will be directed by CFEL scientist Robin Santra, with PULSE scientist Hermann Duerr as co-chair.

PULSE maintains a **visitors program** to enable researchers from around the world to work in our center. These visitors are extremely valuable to the PULSE primary research program. Visitors are given an office, access to PULSE laboratories and institute services, and some expense reimbursement, according to SLAC rules. PULSE extends to them the Stanford designation of Visiting Scientist or Visiting Professor (in line with their rank at their home institution), which entitles them to access to the Stanford Housing Office and the use of the Stanford Library. The budget for this program is relatively modest, particularly when one considers that a senior investigator with major talents and established abilities can be associated as a sabbatical visitor for a year, for less than the cost of a Postdoc. In 2009-2010 the sabbatical visitors were Steve Durbine (Purdue), Ken Schaffer and Mette Gaarde (LSU) and Jon Marangos (Imperial).



Organization Chart for the PULSE Institute

Tasks supported by the Chemical Sciences FWP: These tasks are aimed at the control and imaging of chemical dynamics, from electrons in small molecules to atoms in clusters. The emphasis is on grand challenges for energy science. The proposed research utilizes our core strengths in molecular theory (Martinez), ultrafast spectroscopy (Gaffney), quantum control (Bucksbaum) and strong field AMO physics (Gühr and Bucksbaum). The imaging expertise in PULSE includes biological imaging (Bogan) with laser manipulation of targets for imaging (Bucksbaum) and our special abilities to capture and image ultrafast processes as they happen. Tasks in this area utilize the PULSE Institute building as well as SPEAR3 and the LCLS AMO, CXI, and XPP end stations. Subtasks:

- **Attosecond Coherent Electron Dynamics (ATO)** Task Leader Markus Gühr. (co-leader P. Bucksbaum) This task studies the fastest timescales in chemical physics involved with electron correlation, and nonradiative chemical processes, connecting LCLS research to the new field of attophysics.
- **Strong Fields in Molecules (SFA)** Task Leader Phil Bucksbaum. This task incorporates and extends strong-field quantum control to LCLS experiments in molecular dynamics and molecular imaging. Strong field effects in atoms and molecules can be studied using ultrafast x rays, or employed to create targets for x-ray imaging. In addition, LCLS is itself the world's first source of coherent volt/Ångstrom fields of x-ray radiation. A separate component of this program in ultrafast x-ray scattering is in the Nonequilibrium Dynamics in Solids task.
- **Solution-Phase Chemical Dynamics (SPC)** Task Leader Kelly Gaffney. This task explores ultrafast chemical processes in solutions, utilizing LCLS, synchrotrons, and the PULSE labs. Emphasis is on the ultrafast dynamics of energy conversion in chemistry.
- **Nonperiodic Imaging (NPI)** Task Leader Michael Bogan. This task studies nonperiodic nanoscale imaging, one of the greatest new opportunities for LCLS. The frontier science questions under study range from nanobiology to aerosol chemistry to combustion.

Find out more: <http://pulse.slac.stanford.edu>

High harmonic generation and electronic structure

Markus Gühr, Todd Martinez and Philip H. Bucksbaum

Stanford PULSE Institute, Stanford Linear Accelerator Center, Menlo Park, CA 94025

and

Physics Department, Stanford University, Stanford, CA 94305

Scope: The goal of this task is to investigate non-adiabatic molecular processes and electronic dynamics using high harmonic spectroscopy (HHS) as a probe. Over the past year, we have been implementing a transient Bragg grating scheme for high harmonic generation (HHG) that allows increased sensitivity of HHS on optically excited states and disperses the harmonics in space, thereby making a spectrometer obsolete. In addition, we have been investigating the influence of phase matching on HHS. To prepare for future attosecond spectroscopy at free electron laser sources, we have been participating in experiments at the linac coherent light source (LCLS) that uncover double-core-hole decays in molecules.

Recent Progress

J. P. Farrell, L. Spector, B. K. McFarland, M. Chalfin, P. H. Bucksbaum and M. Gühr

a) Bragg Gratings for High Harmonic Generation. We have worked on using HHG to visualize electronic dynamics and we were exploring molecular degrees of freedom to shape the HHG spectrum. HHG is decomposed into three steps including 1) ionization from *several* molecular orbitals [10], 2) acceleration of the ionized electron in the laser field and 3) recombination of that electron with the ionized orbitals transferring the electron kinetic energy into photons. In the final step of HHG, an interference pattern between the recombining electron wave and the ionized orbital develops. The combination of short electron de Broglie wavelengths ($\sim 1 \text{ \AA}$) with the sub-laser-cycle recombination time allows us to deduce orbital structures from the harmonic amplitude and phase. We are currently working on implementing this high harmonic spectroscopy (HHS) technique to study transient processes on photoexcited electronic states that play a crucial role in photochemistry. However, such processes are weak-field phenomena, which limits the overall excited state population and the HHS sensitivity to the excitation.

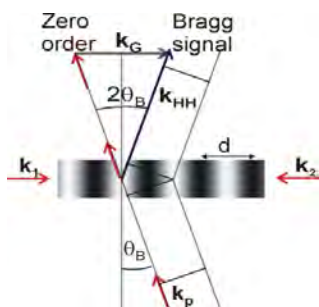


Fig. 1: Bragg grating scheme: Two counterpropagating grating beams k_1 and k_2 , where $k_{1,2} = 2\pi/\lambda$ that create a standing wave with a period $d = \lambda/2$ and reciprocal lattice vector $k_G = 2\pi/d$. A probe pulse with wavelength λ_p and wave vector k_p is focused in the grating and harmonics of order n with wavelength $\lambda_{HH} = \lambda_p/n$ are produced. Since we are operating in the thick grating or Bragg regime, a strong diffraction of the harmonics is only observed at their Bragg angle.

Transient gratings are generally applied in the IR to UV range to overcome the reduced sensitivity problem. Two excitation pulses, intersecting under a small angle α , create an excitation grating in the sample while a third (probe) pulse is diffracted from the grating. The diffracted signal has high sensitivity to excited state dynamics. We implemented the grating scheme for HHG where the harmonics are dispersed in angle within a diffraction order to enable HHS analysis [5] (see Fig. 1). This is achieved by enlarging the angle α to 180 deg., resulting in a shorter grating period d , which disperses the harmonics to distinguishable angles without an additional grating element. Thereby we construct a Bragg grating that is highly selective in its wavelength acceptance resulting in dispersed and distinguishable harmonics.

A maximum diffraction efficiency above 10% is measured by comparing the intensities of the zero order and the Bragg diffracted signal. Figure 2A shows the scattered Bragg peaks as a function of angle with respect to the grating normal. Seven harmonics, corresponding to a 45% bandwidth are distinguishable. Towards higher harmonics the modulation contrast vanishes. Superimposed on the peaks are the calculated Bragg angles. This indicates that the peaks can be interpreted as dispersed harmonics.

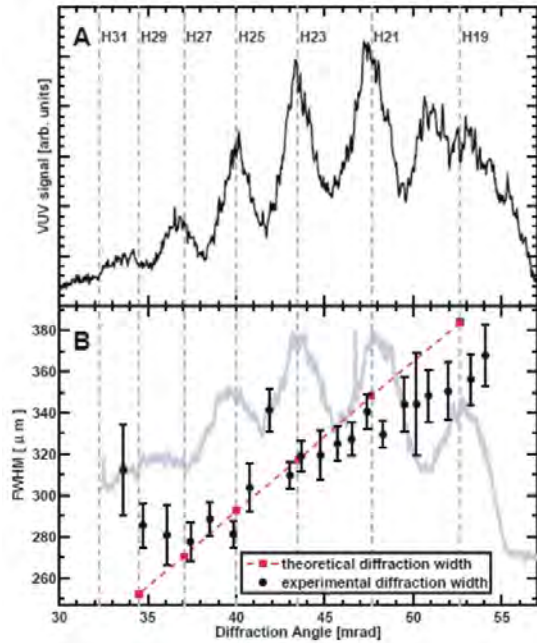


Fig. 2: **A)** Bragg diffracted harmonics with the expected Bragg angle for the respective harmonics overlapped as dashed lines. **B)** Width of the experimental diffraction pattern as a function of diffraction angle (solid black circles) overlapped with the theoretical expectation based on the wavelength of the diffracted harmonics.

To prove that the distinct peaks correspond to dispersed harmonics of different wavelength, we performed a coherent diffraction experiment by translating a $50\mu\text{m}$ slit through the angular peaks in Fig. 2B and collecting the diffraction image on the same CCD camera. The widths of the central diffraction peaks, given as the circles in Fig. 4B, decreases as we move the slit to smaller angles, which demonstrates how the wavelength of the peaks becomes shorter for the harmonics diffracted at smaller angles. A comparison of the measured diffraction width with the predicted Fraunhofer width of the harmonics (solid squares in Fig. 2B) shows a good agreement, which confirms our interpretation that the peaks are different dispersed harmonics. Our results indicate that we have a temporal and spectral resolution from the Bragg grating. Apart from the use in HHS, the high efficiency will also allow the scheme to be useful for switching the angle of a HHG output within a short time interval.

b) Phase matching effects in HHS. Using the example of atomic Ar, we show that high harmonic generation (HHG) amplitude and phase are subject to Cooper minima seen in photoionization. The vacuum ultraviolet (VUV) photoionization of Ar causes population transfer from the 3P electronic ground state of Ar to the *d* or *s* continuum states which is described by the photoionization dipole matrix element. In the recombination step of HHG an electronic dipole transition between the continuum states and the electronic ground state results in the emission of VUV radiation. Recombination is described by the complex conjugate of the photoionization dipole element. Thus any information obtained from photoionization or absorption spectroscopy can in principle be applied to the HHG spectrum. We investigate the Cooper minimum of argon as a test case for this hypothesis. The Cooper minimum results from the nodal structure of an electronic ground state and is reflected in a sign change of the energy dependent dipole matrix element. Due to this sign change the excitation or recombination probability must go to zero at a particular energy. We have observed a minimum in the HHG spectrum of Ar and confirmed its interpretation as a Cooper minimum by measuring π phase shift of the Ar harmonics around the HHG minimum [7].

Figure 3 shows a HHG spectrum of Ar taken with a special grating that focuses only in the spectral dimension but preserves the harmonic beam divergence orthogonal to the spectral axis. Harmonic radiation emerging from so called short trajectories is preferentially phase matched on axis whereas the long trajectories emit radiation off-axis. On axis, a Cooper minimum can be clearly identified around harmonic 33. Off axis, the minimum vanishes and we attribute this to a changed phase matching of the harmonics.

We have started a collaboration with Mette Gaarde and Ken Schafer (both LSU) to explain the details in the shifts of the Cooper minimum. Current experimental results combined with theory predict that the

phase jump of the 3P-d matrix element does not shift as a function of electric field or intensity. However, the subtleties of phase matching combined with the relative phase between the different recombination channels clearly indicate that phase matching conditions have to be explored before interpreting harmonic amplitude as a sign of electronic structure.

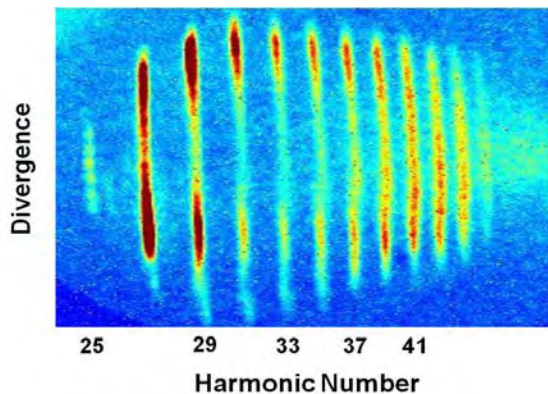


Fig. 3: Harmonic spectrum of argon, showing the divergence of the harmonic beam as a function of harmonic number. The center of the divergence axis corresponds to the propagation axis of the harmonic generation laser. The „hole“ in the center around harmonic 33 corresponds to the Cooper minimum of Ar. For larger divergences, this minimum vanishes due to phase matching effects.

c) Molecular double core hole decay. We have been part of experimental teams at LCLS devoted to the investigation of double core holes and their decay. The high x-ray flux of new free electron lasers allows to create atoms or molecules with doubly ionized core shells. We have been concentrating in particular on molecules, where the double core hole can be located on one nucleus or distributed over two nuclei. We have observed the Auger decay [2] and photoelectrons [1] emerging from these highly excited molecules and found reduced absorption for x-ray excitation pulses that are shorter than the Auger decay lifetime [4].

d) Simulation of HHG and Photoionization processes. We have implemented an optimal spawning algorithm [13-15] which can accommodate basis set expansion due to tunnelling phenomena in the *ab initio* multiple spawning method. This has been tested on low-dimensional model systems and shown to accelerate the convergence of the method. As described below, we will also incorporate new equations of motion for the basis function centers as we build up the AIMS methodology to treat both electronic and nuclear wavepackets. We have also incorporated a more accurate treatment of the photoionization process for time-resolved photoelectron spectroscopy (photoionization is the inverse of the final recombination step in HHG). We have extended our Franck-Condon approach to include the dipole matrix elements involving the bound and free electron wavefunctions. First results on uracil and thymine suggest that this extension does not affect the predicted TRPES spectrum dramatically, and treatment of the vibrational factors may be important. We have collaborated with Belkacem and Allison at LBNL in order to model the ion yield in time-resolved VUV/VUV and VUV/XUV photoionization experiments on ethylene.

Future Plans

M. Gühr and P. H. Bucksbaum

a) Non-adiabatic dynamics. We have first experimental results on HHG on the triatomic SO_2 . We plan to perform HHS on photoexcited SO_2 , which undergoes non-adiabatic dynamics occurring in so-called conical intersections (CI). The conical intersections are crucial for biological processes such as light harvesting, primary visual processes and UV stabilization of DNA. In this context, we have submitted an LCLS proposal to measure non-adiabatic dynamics of photoexcited thymine. We are a part of LCLS experimental teams, which is documented in the attached publication list.

b) Electron correlation. The electron-electron correlation effects, which are neglected in the Hartree-Fock (HF) approximation, are expected to be highlighted at the attosecond time scale. Around each individual electron, the density of other electrons is reduced by both exchange and Coulomb interactions (correlation hole). The “instant” removal of an electron will lead to charge migration dynamics aimed at filling this hole. In other words, the charge hole created on the neutral molecular ground state is not an eigenstate of the ionic system, leading to a coherent superposition of cationic states. The attosecond time

scale of the electron dynamics is determined by the energy differences among the excited cationic states. We plan to directly monitor the charge migration in the time domain, giving us insight into electron correlation. This involves spectroscopy with VUV laser sources and LCLS laser pulses.

c) Simulation of HHG and TRPES. In the next funding period, we will be investigating the replacement of the classical equations of motion for the basis function centers in AIMS with ring-polymer molecular dynamics equations. This has the advantage of ensuring that there is no zero-point energy leakage and is expected to be critical as the wavepackets described by AIMS are extended to include both electronic and nuclear parts. We will also include vibrational effects in photoelectron spectra by propagating wavepackets on the cation state and Fourier transforming the resulting correlation function to obtain the spectrum. This may resolve the outstanding disagreement between theory and experiment for the excited state lifetime of ethylene (ion yield photoionization experiments give a range of 20-30fs, while the best theory predicts 90-100fs).

Publications over the past 3 years

- 1) L. Fang, M. Hoener, O. Gessner, F. Tarantelli, S.T. Pratt, O. Kornilov, C. Buth, M. Gühr, E.P. Kanter, C. Bostedt, J.D. Bozek, P.H. Bucksbaum, M. Chen, R. Coffee, J. Cryan, M. Glowonia, E. Kukk, S.R. Leone, and N. Berrah, Double core hole production in N₂: Beating the Auger clock, *Phys. Rev. Lett.*, accepted (2010)
- 2) J. P. Cryan, J. M. Glowonia, J. Andreasson, A. Belkacem, N. Berrah, C. I. Blaga, C. Bostedt, J. Bozek, C. Buth, L. F. DiMauro, L. Fang, O. Gessner, M. Guehr, J. Hajdu, M. P. Hertlein, M. Hoener, O. Kornilov, J. P. Marangos, A. M. March, B. K. McFarland, H. Merdji, V. Petrovic, C. Raman, D. Ray, D. Reis, F. Tarantelli, M. Trigo, J. White, W. White, L. Young, P. H. Bucksbaum, R. N. Coffee, Auger electron angular distribution of double core hole states in the molecular reference frame, *Phys. Rev. Lett.*, accepted (2010)
- 3) J. M. Glowonia, J. Cryan, J. Andreasson, A. Belkacem, N. Berrah, C. I. Blaga, C. Bostedt, J. Bozek, L. F. DiMauro, L. Fang, J. Frisch, O. Gessner, M. Gühr, J. Hajdu, M. P. Hertlein, M. Hoener, G. Huang, O. Kornilov, J. P. Marangos, A. M. March, B. K. McFarland, H. Merdji, V. S. Petrovic, C. Raman, D. Ray, D. A. Reis, M. Trigo, J. L. White, W. White, R. Wilcox, L. Young, R. N. Coffee, P. H. Bucksbaum, Time resolved pump-probe experiments at the LCLS, *Optics Express*, **18**, 17620 (2010)
- 4) M. Hoener, L. Fang, O. Kornilov, O. Gessner, S. T. Pratt, M. Gühr, E. P. Kanter, C. Blaga, C. Bostedt, J. D. Bozek, P. H. Bucksbaum, C. Buth, M. Chen, R. Coffee, J. Cryan, L. DiMauro, M. Glowonia, E. Hosler, E. Kukk, S. R. Leone, B. McFarland, M. Messerschmidt, B. Murphy, V. Petrovic, D. Rolles, and N. Berrah, Ultraintense X-Ray Induced Ionization, Dissociation, and Frustrated Absorption in Molecular Nitrogen, *Phys. Rev. Lett.*, **104**, 253002 (2010)
- 5) J. P. Farrell, L. S. Spector, M. B. Gaarde, B. K. McFarland, P. H. Bucksbaum and M. Gühr, Strongly Dispersive Transient Bragg Grating for High Harmonics, *Optics Letters*, **35**, 2028 (2010)
- 6) J. P. Farrell, B. K. McFarland, P. H. Bucksbaum, and M. Gühr, Calibration of a high harmonic spectrometer by laser induced plasma emission, *Optics Express* **17**, 15134-15144 (2009)
- 7) B. K. McFarland, J.P. Farrell, P. H. Bucksbaum and M. Gühr, High harmonic phase of nitrogen, *Phys. Rev. A*, **80**, 033412 (2009)
- 8) J.P. Farrell, B. K. McFarland, M. Gühr, and P. H. Bucksbaum, Relation of high harmonic spectra to electronic structure in N₂, *Chem. Phys.*, **366**, 15-21 (2009)
- 9) M. Gühr, B. K. McFarland, J.P. Farrell and P. H. Bucksbaum, High harmonic generation from multiple molecular orbitals of N₂, *Ultrafast Phenomena XVI*, Springer (2008)
- 10) B. K. McFarland, J.P. Farrell, P. H. Bucksbaum and Markus Gühr, High Harmonic Generation from multiple orbitals N₂, *Science* **322**, 1232 (2008)
- 11) M. Gühr, B. K. McFarland, J. P. Farrell and P. H. Bucksbaum, High harmonic generation on N₂ and CO₂ beyond the two point model, *J. Phys. B: At. Mol. Opt. Phys.*, **40**, 3745-3755 (2007)
- 12) P. Bucksbaum, The future of attosecond spectroscopy, *Science* **317**, 766 (2007)
- 13) S. Yang, J. D. Coe, B. Kaduk, and T. J. Martínez, An "Optimal" Spawning Algorithm for Adaptive Basis Set Expansion in Nonadiabatic Dynamics, *J. Chem. Phys.* **130** 134113 (2009).
- 14) S. Yang and T. J. Martínez, Nonclassical Phase Space Jumps and Optimal Spawning, in *Advances in the Theory of Atomic and Molecular Systems*, E ds. P. P iecuch, J. M aruani, G . D elgado-Barrio and S. W ilson (New York, Springer, 2009).
- 15) S . Y ang and T . J . M artínez, A b I nitio M ultiple S pawning: F irst P rinciples D ynamics Around C onical Intersections, in *Conical Intersections: Theory, Computation, and Experiment*, E ds. W . D omcke and H . K oppel (World Scientific, Singapore, in press).

Strong Field Control of Coherence in Molecules and Solids

Philip H. Bucksbaum and David Reis, Stanford PULSE Institute for Ultrafast Energy Science, SLAC National Accelerator Laboratory, Menlo Park, CA 94025, phb@slac.stanford.edu

This subtask concerns strong field control of molecules (SFA). Our efforts are directed towards investigations of strong-field induced coherent processes in atoms and molecules that are of value as either LCLS experiments or ultrafast x-ray diagnostics. This includes ultrafast and high-field studies of laser-matter interactions in solids, directed by David Reis. Progress this year involved several LCLS experiments. progress in several other areas: formation of coherent transient alignment in molecules; studies of short wavelength electronic coherences; and a proposal approved for our first studies of strong field processes using LCLS. A substantial portion of the condensed matter portion of this program, as related to nonequilibrium phonon dynamics has been moved to the DMSE FWP in FY10-12.

Recent Progress:

Much of the recent progress this year concerned our LCLS experiments. Here's a very brief synopsis, based on six publications from this work, which have come out within the past few months:

This first paper describes the commissioning of the LCLS and the AMO instrument, in which PULSE participated.

First lasing and operation of an ångstrom-wavelength free-electron laser P. Emma, et al., SLAC collaboration, with coauthors from PULSE P.H. Bucksbaum and R. Coffee. Nat Photon advance online publication. <http://dx.doi.org/10.1038/nphoton.2010.176> Summary: The recently commissioned Linac Coherent Light Source is an X-ray free-electron laser at the SLAC National Accelerator Laboratory. It produces coherent soft and hard X-rays with peak brightness nearly ten orders of magnitude beyond conventional synchrotron sources and a range of pulse durations from 500 to <10 fs (10–15 s). With these beam characteristics this light source is capable of imaging the structure and dynamics of matter at atomic size and timescales. The facility is now operating at X-ray wavelengths from 22 to 1.2 Å and is presently delivering this high-brilliance beam to a growing array of scientific researchers. We describe the operation and performance of this new 'fourth-generation light source'.

The next paper was the first experiment performed at LCLS. The Young group at ANL took the lead here, with participation from PULSE: The summary describes how the intense focused x-ray laser was capable of fully stripping Ne atoms through rapid sequential inner shell ionization and Auger relaxation; and how very short pulses were unable to fully strip the atoms because the pulse duration was shorter than the spontaneous relaxation process:

Young, L., E. P. Kanter, et al. with PULSE participants P.H. Bucksbaum, J. Cryan, J.M. Glowonia, D.A. Reis, "Femtosecond electronic response of atoms to ultra-intense X-rays." Nature 466(7302): 56-61. <http://dx.doi.org/10.1038/nature09177> Here we reveal the nature of the electronic response in a free atom to unprecedented high-intensity, short-wavelength, high-fluence radiation (respectively $10^{18} \text{ W cm}^{-2}$, 1.5–0.6 nm, $\sim 10^5$ X-ray photons per Å²). At this fluence, the neon target inevitably changes during the course of a single femtosecond-duration X-ray pulse—by sequentially ejecting electrons—to produce fully-stripped neon through absorption of six photons. Rapid photoejection of inner-shell electrons produces 'hollow' atoms and an intensity-induced X-ray transparency. Such transparency, due to the presence of inner-shell vacancies, can be induced in all atomic, molecular and condensed matter systems at high intensity. Quantitative comparison with theory allows us to extract LCLS fluence and pulse duration. Our successful modelling of X-ray/atom interactions using a straightforward rate equation approach augurs favourably for extension to complex systems.

The third paper studies the process of frustrated absorption due to ultrashort and ultraintense x-ray pulses, using N₂ as a target gas. This data for this work actually was done over two successive LCLS runs in Fall

2009: The first run was led by the group of Nora Berrah from Western Michigan University, and the second run, using shorter LCLS pulses, was led by the Bucksbaum group at PULSE, with Ryan Coffee as spokesperson. The lead for the paper was the Berrah group.

Hoener, M., L. Fang, et al, Western Michigan; PULSE participants R. Coffee, J. Cryan, J.M. Glowia, M. Guehr, R. McFarland. "Ultraintense X-Ray Induced Ionization, Dissociation, and Frustrated Absorption in Molecular Nitrogen." Phys. Rev. Lett. 104(25): 253002. <http://dx.doi.org/10.1103/PhysRevLett.104.253002>. Summary: Sequential multiple photoionization of the prototypical molecule N₂ is studied with femtosecond time resolution using the Linac Coherent Light Source (LCLS). A detailed picture of intense x-ray induced ionization and dissociation dynamics is revealed, including a molecular mechanism of frustrated absorption that suppresses the formation of high charge states at short pulse durations. The inverse scaling of the average target charge state with x-ray peak brightness has possible implications for single-pulse imaging applications.

The next paper is the first attempt to study the ions using Auger electron spectroscopy. Emphasis was on spectroscopy of multiple core holes created in a single molecule.

L. Fang, M. Hoener, et al., Western Michigan Collaboration; PULSE participation by J. Cryan, J.M. Glowia, P.H. Bucksbaum, "Double core hole production in N₂: Beating the Auger clock," Phys. Rev. Letters, in press 2010, We investigate the creation of double K-shell holes in N₂ molecules via sequential absorption of two photons on a timescale shorter than the core hole lifetime by using intense x-ray pulses from the Linac Coherent Light Source free electron laser. The production and decay of these states is characterized by photoelectron spectroscopy and Auger electron spectroscopy. In molecules, two types of double core holes are expected, the first with two core holes on the same N atom, and the second with one core hole on each N atom. We report the first direct observations of the former type of core hole in a molecule, in good agreement with theory, and provide an experimental upper bound for the relative contribution of the latter type.

Following the initial work on double core holes, we continued looking at the details Auger electrons from double-core holes that provide information about correlated molecular electrons. We added the ability to align the molecules using the impulsive alignment methods we have developed at PULSE. This work was led by the PULSE Bucksbaum group with Ryan Coffee as spokesperson. Two papers have now been accepted for publication about this work. The first concerns the development of pump-probe capabilities at LCLS. We were the first user group to carry out such experiments, and had to commission the first timing experiments:

James M. Glowia, J. Cryan, M. Gühr, B. K. McFarland, H. Merdji, V. S. Petrovic, D. A. Reis, M. Trigo, J. L. White, R. N. Coffee, and P. H. Bucksbaum from PULSE, plus collaborators from ANL, Imperial College, Western Michigan University, Georgia Tech, SLAC, Ohio State, LBNL, "Time-resolved pump-probe experiments at the LCLS," Opt. Express 18, 17620-17630 (2010) <http://www.opticsinfobase.org/oe/abstract.cfm?URI=oe-18-17-17620>. The first time-resolved x-ray/optical pump-probe experiments at the SLAC Linac Coherent Light Source (LCLS) used a combination of feedback methods and post-analysis binning techniques to synchronize an ultrafast optical laser to the linac-based x-ray laser. Transient molecular nitrogen alignment revival features were resolved in time-dependent x-ray-induced fragmentation spectra. These alignment features were used to find the temporal overlap of the pump and probe pulses. The strong-field dissociation of x-ray generated quasi-bound molecular dications was used to establish the residual timing jitter. This analysis shows that the relative arrival time of the Ti:Sapphire laser and the x-ray pulses had a distribution with a standard deviation of approximately 120 fs. The largest contribution to the jitter noise spectrum was the locking of the laser oscillator to the reference RF of the accelerator, which suggests that simple technical improvements could reduce the jitter to better than 50 fs.

With the pump-probe timing protocol established for LCLS, we then proceeded to repeat the nitrogen double-core hole Auger spectroscopy, but with angular resolution. This gave us the first look at correlation

effects in this exotic system, which may be an important mode for transient chemical analysis at intense fourth generation x-ray sources. The paper reporting this work was just accepted by Physical Review Letters, and is our sixth paper this year from LCLS.

James P. Cryan, J. M. Glowacki, M. Guehr, B. McFarland, V. Petrovic, D. Reis, J.L. White, P. H. Bucksbaum, R. N. Coffee, PULSE Institute; plus collaborators from SLAC, Uppsala, LBNL, Western Michigan, Ohio State, LSU, Imperial College, ANL, Saclay, Georgia Tech, Kansas State, Prugia, "Auger electron angular distribution of double core hole states in the molecular reference frame," accepted by Physical Review Letters, 2010. Summary: Using 1.1 keV photons for sequential x-ray ionization of impulsively aligned molecular nitrogen, we observed a rich single-site double core vacancy Auger electron spectrum near 413 eV, in good agreement with ab initio calculations, and we measured the corresponding Auger electron angle dependence in the molecular frame. The sequential creation of core-level double vacancies was not possible until the unprecedented x-ray peak intensities of an x-ray free electron laser (xFEL).

Core-level double vacancies have been observed in atomic systems via a single photon double ionization process. However, the sequential formation of double core vacancies relies on the extremely high peak intensity of the the Linac Coherent Light Source (LCLS) xFEL to induce photoionization rates that exceed Auger relaxation rates. Sequentially produced double core vacancies represent a novel process that has been proposed as a new tool for femtosecond-scale chemical analysis of molecular dynamics, because of an enhanced sensitivity to the valence environment.

We have also observed what we believe to be the first nonperturbative high harmonics generated in bulk periodic solids. This work, done in collaboration with the DiMauro group at OSU observed harmonics up to 19th order and extending well above the band-gap of the ZnO sample. Depending on crystal orientation, we can generate odd or odd and even harmonics, and these harmonics are relatively insensitive to ellipticity of the driving field. We submitted the results to Nature Physics (Ghimire et al., 2010) and are currently responding to the referee reports.

Finally, we have made substantial progress in using time-resolved x-ray diffuse scattering to study non-equilibrium phonon dynamics throughout the Brillouin zone in photoexcited semiconductors. We have shown surprisingly long-lived non-equilibrium effects including emission of high wavevector phonons extending over several nanosecond after excitation (Trigo et al. submitted 2010). These results performed at the APS demonstrate that we will be able to use the LCLS to study ultrafast electron-phonon and phonon-phonon interactions with atomic scale resolution in time and space.

Future work:

Our latest approved experiment for LCLS is a study of the ring-opening reaction in cyclohexadiene, which is important for understanding light induced biochemistry such as vitamin D production in living systems. This experiment will be carried out in the summer of 2010. In order to do this we will have to commission two major additions to the AMO capabilities at LCLS: Hard uv (266nm) excitation pulses; and velocity map imaging (VMI) of ion fragments produced by the x-rays. We are also collaborators on several other LCLS projects this year, involving attosecond streak experiments (Lou DiMauro, Ohio State lead) and organic molecule spectroscopy (Steve Southworth, ANL lead) as well as optical x-ray nonlinear mixing (Ernie Glover, LBNL lead), phonon dynamics in photoexcited bismuth (David Fritz, SLAC lead) as well as several other condensed matter experiments.

We have submitted several new proposals to LCLS to look at various aspects of high field x-ray physics. These include studies of bond formation in organic molecules, nonlinear x-ray optics, and x-ray probes of light-induced coherent structure. We are also working with LCLS instrument scientists to commission new capabilities, including single-shot timing of the x-ray timing and pulse shape.

1. Broege, D., R.N. Coffee, and P.H. Bucksbaum, 2008a, "Strong-field impulsive alignment in the presence of high temperatures and large centrifugal distortion," Phys. Rev. A, 78, 035401.

2. Broege, D. W., Coffee, R., Bucksbaum, P.H. (2009). "Impulsive longitudinal molecular alignment." Bull. Am. Phys. Soc. 54:7: B6.04.
3. Broege, D. W., R. N. Coffee, et al. (2008). "Strong-field impulsive alignment in the presence of high temperatures and large centrifugal distortion." Physical Review A (Atomic, Molecular, and Optical Physics) 78(3): 035401-3. <http://link.aps.org/abstract/PRA/v78/e035401>
4. Bucksbaum, P. H. (2007). "The Future of Attosecond Spectroscopy." Science 317(5839): 766-769. <http://www.sciencemag.org/cgi/content/abstract/317/5839/766>
5. Bucksbaum, P. H. (2009). AMO Research at the LCLS X-Ray Laser. Conference on Lasers and Electro-Optics/International Quantum Electronics Conference, Optical Society of America.
6. Coffee, R. N., Cryan, J., Bucksbaum, P.H. (2009). "Rotational decoherence in a dense gas of multiply kicked N₂." Bull. Am. Phys. Soc. 54:7: B6.2.
7. Coffee, R. N., P. H. Bucksbaum, et al. (2007). "Direct Dissociation and Laser Modulated Predissociation of N₂⁺." Conference on Lasers and Electro-Optics/Quantum Electronics and Laser Science Conference and Photonic Applications Systems Technologies: JThD26. <http://www.opticsinfobase.org/abstract.cfm?URI=QELS-2007-JThD26>
8. Coffee, R. N., J. P. Cryan, et al. (2009). "Impulsive Alignment of N₂ with a Train of 8 Pulses." Conference on Lasers and Electro-Optics/International Quantum Electronics Conference: IWB1. <http://www.opticsinfobase.org/abstract.cfm?URI=IQEC-2009-IWB1>
9. Cryan, J. P., Coffee, R., Bucksbaum, P.H. (2009). "High Degrees of Impulsive Alignment in Repetitively Excited N₂ at STP." Bull. Am. Phys. Soc. 54:7: Q5.09.
10. Cryan, J. P., P. H. Bucksbaum, et al. (2009). "Field-free alignment in repetitively kicked nitrogen gas." Physical Review A (Atomic, Molecular, and Optical Physics) 80(6): 063412-5. <http://link.aps.org/abstract/PRA/v80/e063412>
11. Ding, Y., Z. Huang, et al. (2009). "Generation of attosecond x-ray pulses with a multicycle two-color enhanced self-amplified spontaneous emission scheme." Physical Review Special Topics - Accelerators and Beams 12(6): 060703. <http://link.aps.org/abstract/PRSTAB/v12/e060703>
12. EmmaP, AkreR, et al. (2010). "First lasing and operation of an angstrom-wavelength free-electron laser." Nat Photon advance online publication. <http://dx.doi.org/10.1038/nphoton.2010.176>
13. Fritz, D. M., D. A. Reis, et al. (2007). "Ultrafast Bond Softening in Bismuth: Mapping a Solid's Interatomic Potential with X-rays." Science 315(5812): 633-636. <http://www.sciencemag.org/cgi/content/abstract/315/5812/633>
14. Gabrysch, M., E. Marklund, et al. (2008). "Formation of secondary electron cascades in single-crystalline plasma-deposited diamond upon exposure to femtosecond x-ray pulses." Journal of Applied Physics 103(6): 064909. <http://link.aip.org/link/?JAP/103/064909/1>
15. Glowonia, J. M., J. Cryan, et al. (2010). "Time-resolved pump-probe experiments at the LCLS." Opt. Express 18(17): 17620-17630. <http://www.opticsexpress.org/abstract.cfm?URI=oe-18-17-17620>
16. Hillyard, P. B., K. J. Gaffney, et al. (2007). "Carrier-Density-Dependent Lattice Stability in InSb." Physical Review Letters 98(12): 125501. <http://link.aps.org/abstract/PRL/v98/e125501>
17. Hoener, M., L. Fang, et al. (2010). "Ultraintense X-Ray Induced Ionization, Dissociation, and Frustrated Absorption in Molecular Nitrogen." Phys. Rev. Lett. 104(25): 253002. 10.1103/PhysRevLett.104.253002
18. Lindenberg, A. M., S. Engemann, et al. (2008). "X-Ray Diffuse Scattering Measurements of Nucleation Dynamics at Femtosecond Resolution." Physical Review Letters 100(13): 135502. <http://link.aps.org/abstract/PRL/v100/e135502>
19. Young, L., E. P. Kanter, et al. (2010). "Femtosecond electronic response of atoms to ultra-intense X-rays." Nature 466(7302): 56-61. <http://dx.doi.org/10.1038/nature09177>
20. M. Trigo, J. Chen, S. Ghimire, Y. M. Sheu, V. Vishwanath, T. Graber, R. Henning, and D. A. Reis. Imaging nonequilibrium phonons. Submitted, 2010.
21. S. Ghimire, A. D. DiChiara, E. Sistrunk, P. Agostini, L. F. DiMauro, and D. A. Reis. Observation of high-order harmonic generation in a bulk crystal. Nature Physics, Responding to Referee Report, 2010.
22. M. Trigo and D. Reis. Time-resolved x-ray scattering from coherent excitations in solids. MRS Bulletin, 35:514–519, 2010.
23. Alexei Grigoriev; Paul G. Evans; Mariano Trigo; David Reis; Linda Young; Robert W. Dunford; Elliot P. Kanter; Bertold Krässig; Robin Santra; Stephen H. Southworth; Lin X. Chen; David M. Tiede; Klaus Attenkofer; Guy Jennings; Xiaoyi Zhang; Timothy Graber; Keith Moffat, Picosecond Structural Dynamics at the Advanced Photon Source Synchrotron Radiation News, 1931-7344, Volume 23, Issue 2, 2010, Pages 18 – 25
24. D. A. Reis. Squeezing more out of ultrafast x-ray measurements. Physics, 2:33, Apr 2009.

Solution Phase Chemical Dynamics
Principal Investigator: Kelly J. Gaffney
PULSE Institute, Photon Science, SLAC,
Stanford University, Menlo Park, CA 94025
Telephone: (650) 926-2382
Fax: (650) 926-4100
Email: kgaffney@slac.stanford.edu

I. Program Scope: The initial stages of efficient photochemical reactions invariably occur on the femtosecond (fs) to picosecond (ps) time scale. Identifying the mechanisms for directed and efficient channeling of solar energy to chemical energy will be a principle objective of this research sub-task. The effective conversion of light to chemical energy necessitates directing the energy flow, which requires the suppression of the thermodynamic driving force to convert the light energy to heat and re-establish equilibrium. The effectiveness of molecular photo-catalysts depends critically on the excited state electronic structure and dynamics. Preserving the harvested energy within the electronic degrees of freedom represents a critical step to efficient light harvesting and depends intimately on the complex interplay between electronic and nuclear motion. While the investigation of non-adiabatic dynamics has been widely pursued with time resolved optical spectroscopy, the complexity of the phenomena and dual influence of nuclear and electronic arrangement on these optical signals has made unambiguous interpretation of experimental data unusual. We propose to disentangle this coupled evolution of the electrons and nuclei by probing the molecular structure with ultrafast x-ray scattering and the electronic structure with ultrafast x-ray spectroscopy.

We will also investigate equilibrium chemical dynamics. The assembly and conformation of soft-matter depends critically on non-covalent interactions. These interactions, such as ion pairing, hydrogen bonding, and van der Waals attractions contribute to the assembly of nanostructures in a broad range of chemical and materials science applications as well. While the formation and folding of nanometer complexes generally involves the formation of numerous non-covalent interactions, the intrinsic interactions are generally well defined local interactions: hydrogen bond formation, ion pairing, and higher-order electrostatic interactions. We propose to study the thermal dynamics of H-bonding and ion pairing dynamics with the objective of generating a molecular-scale, mechanistic understanding conformational dynamics in solution. We will investigate these conformational dynamics with time resolved vibrational spectroscopy, x-ray photon correlation spectroscopy, and molecular dynamics simulations.

II. Scientific Progress:

Mechanistic studies of hydrogen bond exchange in aqueous ionic solution: Hydrogen bonds (H-bonds) provide the intermolecular adhesion that dictates the unique properties of liquid water and aqueous solutions. Though H-bonds constrain the local ordering and orientation of molecules in solution, these local H-bond networks disband and reform on the picosecond time scale. This structural lability critically influences chemical and biological transformations. Our understanding of the dynamics of hydrogen bond dissociation and reformation has been transformed by the union of ultrafast vibrational spectroscopy and molecular dynamics simulations, but the detailed mechanism for H-bond switching in aqueous solution remains uncertain. Recent simulation studies of water and aqueous ionic solutions have proposed that H-bond exchange involves large angular jumps of 60 to 70°. However, the substantial complexities inherent in simulating the structural and dynamical properties of water highlight the importance of validating this proposal experimentally.

We have used multidimensional vibrational correlation spectroscopy (2DIR) to confirm the large angle jump hypothesis in a solution of 6M sodium perchlorate dissolved in water. The dissolution

of NaClO₄ in isotopically mixed water generates two deuterated hydroxyl stretch (OD) frequencies: OD groups donating a H-bond to another water molecule (OD_w) absorb at 2534 cm⁻¹, whereas OD groups donating a H-bond to a perchlorate anion (OD_p) absorb at 2633 cm⁻¹. This spectroscopic distinction between the OD_w and OD_p provides the opportunity to track H-bond exchange by monitoring the growth in the cross-peak intensity in the time-dependent 2D spectra. By using polarization resolved 2DIR we have been able to determine the magnitude of the orientational change associated with H-bond switching between the OD_w and OD_p configurations. Our results show that a water molecule shifts its donated H-bonds between water and perchlorate acceptors by means of large, prompt angular rotation. Using a jump-exchange kinetic model, we extract an average jump angle of 49±4°, in qualitative agreement with the jump angle observed in molecular dynamics simulations of the same aqueous NaClO₄ solution.

Ligand exchange dynamics in aqueous ionic solution: Ligand exchange in solution represents a fundamental solvent controlled reaction. While the separation between ligand and metal ion provides the intuitive reaction coordinate, fluctuations in the solvent structure surrounding the ligand - metal ion pair explicitly influence the solution phase reaction mechanism. Molecular dynamics (MD) simulations provide the most direct route to mechanistic understanding of thermal reaction dynamics in ionic solutions, but the 20 to 30 ps durations of *ab initio* molecular dynamics simulations¹¹⁻¹⁶ limit the accessible conformational dynamics and classical simulations depend upon the empirical force fields utilized to perform the MD simulations. Given these limitations, benchmark dynamical measurements provide a critical complement to the MD simulation studies.

We have used 2DIR spectroscopy to investigate Mg²⁺ and SCN⁻ association and dissociation dynamics in a solution of 3.4 M Mg(ClO₄)₂ and 1.2 M NaSCN dissolved in D₂O. We have successfully resolved the inter-conversion between the MgNCS⁺ contact ion pair and free SCN⁻ anion configurations. We observe the contact ion pair dissociation time constant to be 52 ± 10 ps. In solutions where we replace the Mg(ClO₄)₂ with MgCl₂, we do not see evidence for MgNCS⁺ contact ion pair dissociation. Given the stronger ionic interaction between Mg²⁺ and Cl⁻ than Mg²⁺ and ClO₄⁻, we attribute the observed dynamics to anion ligand exchange between thiocyanate and perchlorate.

Characterization of charge transfer excitations in coordination compounds with hard x-ray resonant inelastic x-ray scattering: The photo-catalytic activity of coordination compounds derives in large part from their ability to donate photo-excited electrons to a substrate or accept substrate electrons into the photo-generated hole. Understanding the character of the molecular orbitals involved in these charge transfer processes represents an important step to interpreting their role in photo-catalyzing chemical reactivity. Optical electronic spectroscopy extending from the mid-infrared to the ultraviolet has been used extensively to study electronic transitions in many coordination systems. While a powerful probe of the electronic structure, these optical techniques struggle to decompose the electronic states into their ligand and metal components. X-ray absorption and emission spectroscopies (XAS and XES, respectively) make this decomposition possible, particularly with the assistance of quantum chemical calculations. Core level absorption and emission spectroscopies project unoccupied and occupied electronic states onto localized parent atoms, making them an excellent tool for characterizing the metal and ligand contributions to the valence electronic structure of coordination compounds.

By specifically focusing on emission energies resonant with the occupied valence orbitals of coordination compounds, we observe the molecular orbitals involved in electronic charge-transfer states with a technique applicable to all transition metal complexes. Unlike optical spectroscopy, RIXS can easily distinguish between ligand-to-metal and metal-to-ligand charge transfer (LMCT and MLCT) excitations and provide information about the covalency of the molecular orbitals involved in the excitations. We have demonstrated the capacity of the measurement by studying a

series of different transition metal hexacyanide complexes. While we have yet to determine the viability of the method, the goal is to correlate the electronic structure properties characterized with RIXS with the electronic relaxation dynamics observed with ultrafast optical methods.

Characterizing the electronic relaxation pathway in a model coordination compound:

Coordination compounds possess many of the requisite attributes to function as successful photocatalysts, including strong substrate binding, strong visible absorption, and facile charge transfer between the photo-excited catalyst and the substrate. Despite these appealing properties, ultrafast electronic excited state relaxation undermines the efficiency of many potential photocatalysts. For organic photo-physics and photo-chemistry, conical intersections play a central role in determining the rate of energy flow between different electronics states, but the relative importance of non-adiabatic dynamics in coordination complexes has yet to be determined.

We have chosen to focus on the excited state dynamics of ferric hexacyanide because of the molecule's high symmetry and compatibility with x-ray spectroscopic measurements. We have used polarization resolved vibrational spectroscopy to study the ultrafast electronic relaxation dynamics in ferric hexacyanide following ligand-to-metal charge transfer (LMCT) excitation in the UV. We are able to confirm the importance and nature of the ligand excited states that govern the relaxation pathway. The relaxation from the LMCT to a ligand field excited state leads to the splitting of the CN stretch mode from the triply degenerate T_{1u} , to two stretching frequencies. This splitting reflects the reduction in molecular symmetry for octahedral to square planar, a reduction in symmetry that is expected for the only energetically accessible ligand field excited states.

Publications:

1. Ultrafast Bond Softening in Bismuth: Mapping a Solid's Interatomic Potential with X-rays: D.M. Fritz, *et al. Science* **315**, 633 (2007).
2. Carrier Density Dependent Lattice Stability in InSb: P.B. Hillyard, *et al. Phys. Rev. Lett.* **98**, 125501 (2007).
3. Imaging Atomic Structure and Dynamics with Ultrafast X-ray Scattering: K.J. Gaffney, H.N. Chapman, *Science* **316**, 1444 (2007).
4. X-ray Diffuse Scattering Measurements of Nucleation Dynamics at Femtosecond Resolution: A.M. Lindenberg, *et al. Phys. Rev. Lett.* **100**, 135502 (2008).
5. Ultrafast Carrier Induced Disorder in InSb Studied with Density Functional Perturbation Theory: P.H. Hillyard, D.A. Reis, K.J. Gaffney, *Phys. Rev. B* **77**, 195213 (2008).
6. Efficient Multiple Exciton Generation Observed in Colloidal PbSe Quantum Dots with Temporally and Spectrally Resolved Intraband Excitation: M. Ji, S. Park, S.T. Connor, T. Mokari, Y. Cui, K.J. Gaffney, *Nano. Lett.* **9**, 1217 (2009).
7. Ultrafast Dynamics of Hydrogen Bond Exchange in Aqueous Ionic Solutions: S. Park, M. Odelius, K.J. Gaffney, *J. Phys. Chem. B* **113**, 7825 (2009).
8. Characterization of Charge Transfer Excitations in hexacyanomanganate(III) with Mn K-Edge Resonant Inelastic X-ray Scattering, D.A. Meyer, U. Bergmann, X. Zhang, K.J. Gaffney, *J. Chem. Phys.* **132**, 134502 (2010).
9. Ligand Exchange Dynamics in Aqueous Solution Studied with 2DIR Spectroscopy: S. Park, M. Ji, K.J. Gaffney, *J. Phys. Chem. B* **114**, 6693 (2010).
10. Large Angular Jump Mechanism Observed for Hydrogen Bond Exchange in Aqueous Perchlorate Solution: M. Ji, M. Odelius, K.J. Gaffney, *Science* **328**, 1003 (2010).
11. Dynamics of Ion Assembly in Solution: 2DIR Spectroscopy Study of LiNCS in Benzonitrile: M. Ji, S. Park, K.J. Gaffney, *J. Phys. Chem. Lett.* **1**, 1771 (2010).

Non-Periodic Imaging at the Stanford PULSE Institute

Michael J. Bogan

Stanford PULSE Institute for Ultrafast Energy Science
SLAC National Accelerator Laboratory, Menlo Park, CA 94025

Email: mbogan@slac.stanford.edu

PROGRAM SCOPE From complex biological systems to ubiquitous airborne particulate matter regulating our climate and interacting with our lungs, nanoscale non-periodic structures dominate our natural world. Over the past six years, we have helped pioneer a revolutionary single particle coherent x-ray diffractive imaging (CXDI) approach to view this nanoscale world using ultrafast x-ray free-electron-lasers (FELs). CXDI utilizes the ultrafast and ultrabright x-ray pulses to overcome resolution limitations in x-ray microscopy imposed by x-ray induced damage to the sample by “diffracting before destroying” the sample on sub-picosecond timescales. Early experiments were performed on the FLASH soft x-ray free electron laser (FEL) where we experimentally verified “diffract and destroy” science (Chapman2009) and pioneered the experimental methods in FLASH diffractive imaging (Barty2008; Bogan2008; Boutet2008; Marchesini2008). The main goal of this program is to extend these experiments to the hard x-rays of LCLS to fulfill the promises of revolutionizing structural biology, aerosol science, and characterization of essentially all nanomaterials by allowing a diffraction pattern to be recorded from non-periodically structured materials, potentially as small as a single molecule.

CXDI is elegant in its experimental simplicity: a coherent x-ray beam illuminates the sample and the far-field diffraction pattern of the object is recorded on an area detector. These measured diffraction intensities are proportional to the modulus squared of the Fourier transform of the wave exiting the object. An inversion of the diffraction pattern to an image in real space requires the retrieval of the phases of the diffraction pattern. Our shrinkwrap algorithm is now particularly robust and practical. The algorithm reconstructs images ab initio which overcomes the difficulty of requiring knowledge of the high-resolution shape of the diffracting object. CXDI overcomes the restrictions of limited-resolution x-ray lenses, offering a means to produce images of general non-crystalline objects at a resolution only limited in principle by the x-ray wavelength and by radiation-induced changes of the sample during exposure. While we are primarily motivated to image biological macromolecules, the general imaging techniques, diagnostics and optics, sample manipulation, and understanding of materials in intense x-ray fields, are of fundamental importance to ultrafast x-ray science and cut across all areas of research of PULSE.

Our program at the PULSE Institute for Ultrafast Energy Science is part of an international collaboration whose goal is to perform coherent x-ray imaging of non-periodic structures using x-ray FELs, such as the Linac Coherent Light Source (LCLS). Within this context our research is focused on single particle CXDI. For many lensless imaging algorithms used for CXDI it is convenient when the data satisfies an oversampling constraint that requires the sample to be an isolated object, i.e. an individual “free standing” portion of disordered matter delivered to the center of the x-ray focus. By definition, this type of matter is an aerosol. PULSE houses unique lab space and expertise for the generation and manipulation of aerosols for single particle CXDI. This expertise has been leveraged for the development of the Coherent x-ray Imaging (CXI) endstation at LCLS and has resulted in a broad array of collaborators for PULSE interested in collecting single particle diffraction from specific systems at LCLS. Besides contributions to biologically oriented experiments within the international CXI collaboration, PULSE leads efforts to pioneer CXDI of airborne particulate matter such as fractal aggregates and interrogation electrohydrodynamically atomization processes. The experimental opportunities of non-periodic imaging (NPI) with LCLS are enormous and we are just at the beginning of a new era of the study of disordered matter with ultrafast x-rays.

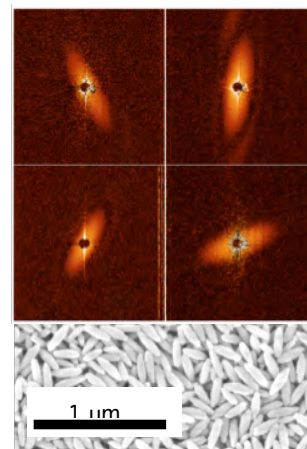
RECENT PROGRESS In FY2010, significant effort was directed toward moving into and equipping our new lab space at SLAC. This lab space was occupied in June 2009 and, besides our day-to-day research,

was used as the primary research space for our collaborators during our four LCLS beamtimes, starting in December 2009. We have recruited outstanding talent necessary to support the rapidly growing CXDI program at PULSE. Our team now consists of a Research Associate (Dmitri Starodub), a postdoc (Christina Hampton) and a grad student (Raymond Sierra).

Single-shot diffraction of particles in unknown random orientations: We have performed FLASH single particle CXDI on a wide array of aerosols including nanoparticle clusters formed from nebulized droplets, concentrically atomized ellipsoidal nanoparticles, dry powder-dispersed carbon nanofibers, flame-generated nanoparticles and intact marine microorganisms (Chapman2009). We captured the highest resolution images of airborne aerosols ever recorded. Single particle morphology was resolved to 35 nm. The critical importance of this work to aerosol science and nanotechnology was highlighted by its acceptance as the first ever Aerosol Research Letters manuscript published by the Aerosol Science and Technology journal of the American Association of Aerosol Research (Bogan2010).

A key milestone on the path toward single molecule imaging with x-ray FELs was reached when we collected the first data set of identical particles in random orientations was recorded at FLASH (Fig 1). 2D reconstructions of these particles revealed the nanostructure of individual particles (Bogan2010). This data was distributed to many research groups to expedite classification and 3D reconstruction algorithm developments and spawning recent results with our collaborator's new cryptotomography approach for single-shot CXDI (Loh2010).

Fig 1: Diffraction patterns of single ellipsoidal nanoparticles in unknown random orientations collected at FLASH, 7 nm wavelength, 10 fs, 10^{12} ph/pulse. Scanning electron micrograph of particles (bottom).



Single particle CXDI of fractal aggregates: With single particle CXDI at FLASH now firmly established, we are focusing on applying its unique capabilities to the challenges of energy science. PULSE has developed a full experimental model to simulate imaging combustion-generated particles, lead by Research Associate Dmitri Starodub. First we built a physical model of our target sample, soot. The process of soot particle formation is described by slow diffusion of primary monomers and clusters, which stick together with high probability upon contact. This mechanism, a diffusion-limited cluster aggregation (DLCA), results in the growth of mass fractals. Their morphology is characterized by the scaling law, $N = k_0(R_g/a)^D$, where N is the number of primary particles in a fractal, D is the Hausdorff dimension, a is the monomer radius, R_g is the radius of gyration, and k_0 is the coefficient, which can be interpreted as a density of monomers. Examples of simulated agglomerates are presented Fig. 2, corresponding to the sizes of (a) 100, (b) 300, and (c) 900 primary particles of radius 15 nm. Next we derived a quantitative expression to estimate the scattered signal from a fractal aggregate described in further detail in (Bogan2010). As an example, diffraction patterns were calculated for a single x-ray

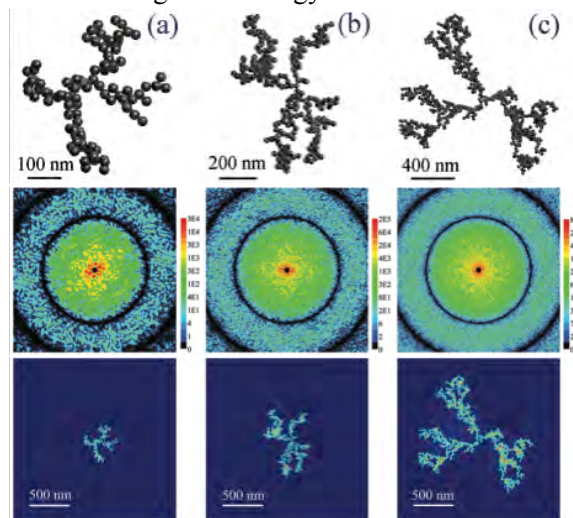


Fig 2. Simulated soot particles of different sizes (1st row), corresponding diffraction patterns (2nd row) and reconstructed images (3rd row). The aggregates are composed of (A) 100, (B) 300, and (C) 900 spherical monomers. X-ray parameters: 10^{12} photons per pulse at the energy of 177 eV (7 nm wavelength) focused to a 10 μm spot.

pulse exposure to the fractal particles, with a carbon monomer with radius 15 nm. We anticipate that single particle CXDI, such as the soot experiment simulated here, will be used in conjunction with conventional *in situ* particle sizing methods like differential mobility analysis or engine exhaust particle sizing to open new perspectives on aerosol particle morphology related to combustion processes and *in situ* aerosol synthesis. A key advantage of CXDI measurements relative to electron microscopy is that the high velocity particle beam rapidly replenishes samples, making the method high throughput. For example, the hundreds of images of single particles captured on substrates typically used in studies of soot aggregates can be captured in less than a few minutes using an x-ray FEL.

Sacrificial Tamperers for CXDI: Intense and ultrashort x-ray pulses from free-electron lasers open up the possibility for near-atomic resolution imaging without the need for crystallization. Such experiments require high photon fluences and pulses shorter than the time to destroy the sample. We recently described results with a new femtosecond pump-probe diffraction technique employing coherent 0.1 keV x rays from the FLASH soft x-ray free-electron laser. We showed that the lifetime of a nanostructured sample can be extended to several picoseconds by a tamper layer to dampen and quench the sample explosion, making <1 nm resolution imaging feasible (Hau-Riege2010).

X-ray investigations of electrohydrodynamic atomization: Understanding the impact of sample delivery on sample structure, development of new highly efficient sample delivery methodologies, and improving particle inlet efficiencies is critical for single particle and single molecule imaging at LCLS. We recently performed the first experiments of x-ray scattering from electrosprayed nanomaterials. The small-angle x-ray scattering of biological materials and nanoparticles in electrosprays helps us characterize the morphological changes of several classes of particles (ranging from single proteins to larger macromolecular aggregates) upon electrospray injection into air and vacuum. We observed unexpected instabilities of the liquid jet upon x-ray exposure that limited the collection of scattering derived from particles contained in the solution. This ‘capillary-free’ small-angle x-ray scattering approach potentially provides advantages over conventional BioSAXS solution scattering approaches. These insights have provided new perspectives on x-ray liquid jet interactions that are being integrated into our new liquid jet systems being developed for femtosecond crystallography and nanomaterial imaging at the Coherent X-ray Imaging endstation for LCLS.

Innovations in image reconstruction algorithms Diffraction from the individual molecules of a molecular beam, aligned parallel to a single axis by a strong electric field or other means, has been proposed as a means of structure determination of individual molecules. As in fiber diffraction, all the information extractable is contained in a diffraction pattern from incidence of the diffracting beam normal to the molecular alignment axis. We demonstrated new methods of structure solution for this case (Saldin2010; Starodub2010). One is based on the iterative projection algorithms for phase retrieval applied to the coefficients of the cylindrical harmonic expansion of the molecular electron density. We also demonstrated the ability to recover the angular correlation functions of a single particle from measured diffraction patterns. Another is the holographic approach utilizing presence of the strongly scattering reference atom for a specific molecule.

First LCLS CXDI Results: We recently performed the first CXDI experiments at LCLS during four beamtimes in December 2009 and June 2010. Data from these experiments is currently under internal embargo until the first publications are accepted (Chapman2010; Kirian2010; Seibert2010). This systematic series of diffraction experiments grew in complexity and included studies of well-characterized single particles delivered as aerosols through an aerodynamic lens stack as well as biological/nanomaterials delivered in a liquid jet. As we develop the fundamental science behind NPI with hard x-rays, we will establish LCLS as one of the most powerful tools in aerosol science and nanotechnology, provide critical early insights into single particle diffraction, and help unravel the mystery of the structure of water.

FUTURE PLANS *Expected Progress in FY2011:* We will continue our experimental campaign at LCLS, performing the first CXDI experiments with hard x-rays at the XPP endstation. We will work in

conjunction with LCLS staff to field the LCLS CXI instrument. We will continue to develop the particle beam generation and diagnostics instrumentation necessary to perform any experiments utilizing laser interactions with single particles. Significant effort will be directed toward moving into and equipping our new lab space at SLAC, beneficially occupied in July 2010, that will continue to be used as the primary research space for our collaborators during our LCLS beamtimes. We will also house specialized equipment such as the CAMP chamber and the CXI particle injector in our laboratories. The theory and data analysis effort at PULSE will expand in FY11 with the addition of a new postdoc, Duane Loh.

Expected Progress in FY2012: The focus of our work in FY12 will be single molecule diffraction at the CXI endstation and continued development of high efficiency single particle CXDI methodologies.

COLLABORATIONS: This work is done with colleagues from SLAC, Stanford, LLNL, Uppsala, LBNL, Arizona State University, TU Berlin, Max Planck Biomedical Heidelberg, and CFEL@DESY.

SELECTED PUBLICATIONS FROM DOE SPONSORED RESEARCH IN 2008-2010

- Barty, A., S. Boutet, et al. (2008). "Ultrafast single-shot diffraction imaging of nanoscale dynamics." Nature Photonics **2**: 415-419.
- Bajt, S., H. N. Chapman, et al. (2008). "A camera for coherent diffractive imaging and holography with a soft-X-ray free electron laser." Applied Optics **47**: 1673-1683.
- Benner, W. H., M. J. Bogan, et al. (2008). "Non-destructive characterization and alignment of aerodynamically focused particle beams using single particle charge detection." Journal of Aerosol Science **39**: 917-928.
- Bogan, M. J., W. H. Benner, et al. (2008). "Single particle X-ray diffractive imaging." Nano Letters **8**(1): 310-316.
- Bogan, M. J., S. Boutet, et al. (2010). "Aerosol imaging with a soft x-ray free electron laser." Aerosol Science and Technology **44**(3): i-vi.
- Bogan, M. J., S. Boutet, et al. (2010). "Single-shot femtosecond X-ray diffraction from ellipsoidal nanoparticles in random orientations." Physical Review Special Topics - Accelerators and Beams in revision.
- Bogan, M. J., D. Starodub, C. Y. Hampton, R. G. Sierra (2010). "Single particle coherent diffractive imaging with a soft X-ray free electron laser: Towards soot aerosol morphology " Journal of Physics B: Atomic, Molecular and Optical Physics: in review.
- Boutet, S., M. J. Bogan, et al. (2008). "Ultrafast soft X-ray scattering and reference-enhanced imaging of weakly scattering nanoparticles." Journal of Electron Spectroscopy and Related Phenomena **166-167**: 65-73.
- Chapman, H., P. Fromme, et al. (2010). Nature in review.
- Chapman, H. N. (2009). "X-ray imaging beyond the limits." Nature Materials **8**(4): 299-301.
- Chapman, H. N., S. Bajt, et al. (2009). "Coherent Imaging at FLASH." Journal of Physics: Conf. Ser. **186**: 012051.
- Hau-Riege, S. P., S. Boutet, et al. (2010). "Sacrificial tamper slows down sample explosion in ultrafast x-ray diffraction experiments." Physical Review Letters **104**: 064801.
- Kirian, R., H. N. Chapman, et al. (2010). Journal of Structural Biology in preparation.
- Loh, N. T. D., M. J. Bogan, et al. (2010). "Cryptotomography: the synthesis of 3D intensities from randomly oriented single-shot diffraction patterns." Physical Review Letters **104**: 225501.
- Marchesini, S., S. Boutet, et al. (2008). "Massively parallel X-ray holography." Nature Photonics **2**(9): 560-563.
- Saldin, D. K., V. L. Shneerson, et al. (2010). "Structure of a single particle from scattering by many particles randomly oriented about an axis: a new route to structure determination?" New Journal of Physics **12**: 035014.
- Seibert, M. M., T. Ekeberg, et al. (2010). Nature in review.
- Starodub, D., J. C. H. Spence, et al. (2010). "Reconstruction of the electron density of molecules with single axis alignment." SPIE Proceedings in press.

University Research Summaries
(by PI)

DOE-SISGR: Coherent Control of Electron Dynamics

Principal Investigator: Andreas Becker

Jing Su, Daniel Weflen, Shaohao Chen, Antonio Picoń, Agnieszka Jaroń-Becker

JILA and Department of Physics, University of Colorado at Boulder,
440 UCB, Boulder, CO 80309-0440

andreas.becker@colorado.edu

Introduction

Advances in laser technology and computing power, that have been made recently, enable us to enter a fundamentally new regime, where the complex, correlated interaction of electrons can be observed and controlled in real time. For the first time, we will be able to tackle some fundamental questions such as on which time scale electrons influence each other or how light can be used to observe ultrafast changes of molecular structure or as a catalyst to control chemical reactions at the level of electrons. In this project we theoretically analyze how electron dynamics in a molecule can be controlled using these new laser technologies. This includes the application and extension of control schemes, well-known in the field of femtochemistry, to the sub-femtosecond time scale of the correlated electron-nuclear dynamics in a molecule.

Recent Progress and Future Goals

Our activities in the first year of funding of the project can be summarized in the following three sub-projects.

A. Time-dependent analysis of few-photon coherent control schemes

Significant progress has been made recently in the understanding of few-photon coherent control schemes in the perturbative intensity regime. Such control schemes are often analyzed in the frequency domain, which provides the opportunity to understand the control over the transition probability in terms of interference effects between different pathways. For example, two-photon absorption probabilities can be tuned to zero or maximum by modifying the spectral phase of the pulse [1]. The corresponding pulses are called dark and bright pulses, respectively.

Since we are interested to apply these control schemes to the coupled electron-nuclear dynamics driven by an ultrashort laser pulse it is illustrative to examine the time evolution of these schemes as well. Such an analysis can provide complementary information about the control mechanisms from a direct comparison of the time evolution of the laser field with the instantaneous response of the quantum system. To this end, we have considered as a first conceptual study the hydrogen atom interacting with an ultraviolet laser pulse. The corresponding numerical solution of the Schrödinger equation can be performed within dipole approximation without further restrictions.

Results are obtained for two-photon excitation from the ground state of the hydrogen atom to the 2s state and the (2+1) photon ionization, in which the intermediate 2s state is reached by a resonant two-photon excitation process [2]. We have considered symmetric and antisymmetric phase distributions leading to dark and

bright pulses. For these pulses the temporal field distributions consist of many sub-pulses. For different phase distributions the results for the excitation probabilities are found to agree well with previously published experimental data (taken in Cs [1]). It is found that the maxima (minima) in the final excitation probabilities are due to constructive (destructive) interferences between the amplitudes induced by different sub-pulses. However, at intermediate time the population in the excited state may exceed the final transition probability and is, in particular, non-zero for dark pulses. Our results for the ionization probabilities are found to depend on the degree of excitation in the 2s state and the field strengths. This indicates that at the present field parameters the ionization proceeds via the resonant 2s state rather than as a non-resonant process.

Next, we have applied the same control schemes to the hydrogen molecular ion for a transition between the ground and the first excited (dissociative) state. It is found that the same pulse forms, used for dark pulses in the atomic case, do not lead to a cancelation of the transition probability in the molecular case. This can be well understood from the time-dependent perspective developed by us. Any dark pulse, suggested so far, consists of a sequence of sub-pulses. Since each of the wave packets pumped to the excited dissociative state starts to immediately evolve to larger internuclear distances, wave packets pumped at different times cannot destructively interfere with each other.

Future goals: We will apply these few-photon schemes to transitions between two bound states in the hydrogen molecular ion (or in a model for another diatomic molecule). Based on our conclusions from the time-dependent perspective so far, we expect that the well-known dark pulse forms again will not lead to a cancellation of the transition probability due to a likely population of a coherent superposition of vibrational states. However, if the time delay between the different sub-pulses coincides with the revival time of the vibrational wave packet induced by the coherent superposition, we may be able to generate a dark pulse for a two-photon transition between two bound states in a molecule.

B. Coherent control of electron localization

Recently, the control of the localization of the electron on one of the protons in a dissociating hydrogen molecular ion using intense ultrashort laser pulses has become a topic of active research [3-5]. We have started to analyze the control mechanisms behind this process more systematically. To this end, we consider the preparation of the molecular ion in a coherent superposition of vibrational states and the dependence of the degree of control on the wavelength of the pulse. An interesting preliminary result is that the control of the dissociation dynamics appears to be rather independent of the initial vibrational state distribution.

Another goal of the present project is to investigate coherent control of the electron dynamics in molecules larger than hydrogen molecular ion. Current state-of-the-art theoretical models of the interaction of the hydrogen molecular ion with intense laser pulses consider two dimensions for the electron dynamics and one dimension for the nuclear dynamics. While such models may be still useful for the analysis of electron dynamics in a chain of atoms, application of coherent control schemes to other molecules require higher-dimensional models. In a first step, we develop a computer

code for planar model molecules (2D electron and 2D nuclear dynamics) interacting with intense laser light of linear and circular polarization. We considered different propagation schemes and coordinate systems. In particular, the electron dynamics has been described by 2D Cartesian as well as by polar coordinates. First results show that the latter may be advantageous as long as one is solely interested in the electron dynamics in the bound states of the molecule, while it appears to be less attractive for the ionization process.

Future goals: We plan to extend our studies for the hydrogen molecular ion by varying the parameters of the driving pulse, in particular to mid-infrared laser wavelengths which do now become available in the laser labs. We will also analyze if for a given initial vibrational state distribution a pulse form can be generated such that the molecule does *not* dissociate. We plan to apply our models for planar molecules to H_3^{2+} and study if a current can be driven through the molecule and the localization of the electron at one of the three protons can be controlled. In the course of these studies we will also replace one of the protons by a heavier nucleus.

C. Multiphoton coherent control of vibrational excitation in non-polar molecules

Achieving full control over vibrational (and rotational) degrees of freedom of a molecule is a long-standing goal of coherent control. Many control schemes rely on optical dipole transitions, which are however forbidden for transitions between vibrational states in non-polar molecular ions such as the hydrogen molecular ion. We study alternative control schemes, in which the control is achieved via the first electronically excited state. Preliminary results of numerical simulations for the hydrogen molecular ion driven at mid-infrared laser wavelengths show that a transition between two vibrational states in the molecular ion can selectively be driven with high efficiency by a net two-photon transition, which corresponds to a multiphoton pump-dump transition via the first excited electronic state. Full control of the transition can be achieved using a chirped pulse or via the coherent accumulation of population in a series of pulses.

Future goals: We plan to extend our studies to other non-polar molecular ions and to study selective excitation into a superposition of vibrational states and the cooling of a given vibrational state distribution (e.g. a distribution induced by a Franck-Condon transition) to the ground vibrational state.

References

- [1] D. Meshulach and Y. Silberberg, *Nature* **396**, 239 (1998).
- [2] S. Chen, A. Jaroń-Becker, and A. Becker, *Phys. Rev. A* **82**, 013414 (2010).
- [3] V. Roudnev, B. D. Esry, and I. Ben-Itzhak, *Phys. Rev. Lett.* **93**, 163601 (2004).
- [4] M. F. Kling *et al.*, *Science* **312**, 246 (2006).
- [5] F. He, C. Ruiz, and A. Becker, *Phys. Rev. Lett.* **99**, 083002 (2007).

Publications of DOE sponsored research

Shaohao Chen, Agnieszka Jaroń-Becker, and Andreas Becker, *Time-dependent analysis of few-photon coherent control schemes*, *Physical Review A* **82**, 013414 (2010).

Probing Complexity using the ALS and the LCLS

Nora Berrah

Physics Department, Western Michigan University, Kalamazoo, MI 49008
e-mail:nora.berrah@wmich.edu

Program Scope

The objective of our research program is to explore complexity through *fundamental interactions between photons and gas-phase systems* to advance our understanding of correlated and many body phenomena. Our research investigations probe multi-electron interactions, the dynamics of interacting few body quantum systems and energy transfer processes from electromagnetic radiation. Most of our work is carried out in a strong partnership with theorists.

Our current interests include: 1) The study of non linear and strong field phenomena in the x-ray regime using the linac coherent light source (LCLS), the first x-ray ultra-fast free electron laser (FEL) facility at the SLAC National Laboratory. Our investigations focus on the interaction of intense and short LCLS pulses with atoms, molecules and clusters. 2) The study of correlated processes in select molecules, clusters and their anions using advanced techniques with vuv-soft x-rays from the Advanced Light Source (ALS) at Lawrence Berkeley Laboratory. We present here results completed and in progress this past year and plans for the immediate future.

Recent Progress

1) X-Ray Non-Linear Physics Studies of Molecules with Intense Ultrafast LCLS Pulses



The response of matter to ultrashort, intense x-ray pulses is virtually unknown, however, the fall of 2009 started an exciting new era of ultrafast hard x-ray-based imaging and spectroscopy experiments using the Linac Coherent Light Source (LCLS)[1-4]. In particular, we studied sequential multiple photoionization of molecule with femtosecond time resolution. Absorption of five or more photons resulted in the production of fully stripped N^{7+} ions. Furthermore, a detailed picture of intense x-ray induced ionization and dissociation dynamics was revealed, including a molecular mechanism of frustrated absorption that *suppresses the formation of high charge states at short pulse durations*. [1]

Fig. 1. LCLS undulator beamline along with a 3D plot of ion time of flight data as a function of pulse duration and intensity [1]

One intriguing possibility enabled by intense x-ray sources is the ability to produce atoms and molecules with multiple electron vacancies in core orbitals through the sequential absorption of multiple photons on a timescale *faster than Auger decay*. This process is important to investigate because it has been suggested that double core holes (DCH) could provide the basis for richer, more sensitive, spectroscopies than conventional inner-shell photoelectron spectroscopy. The different atomic sites in molecules introduce multiple possibilities for the DCH configurations, e.g., DCHs with both vacancies on a single site (DCHSS) and DCHs with single vacancies on two different sites (DCHTS). We reported the first experimental attempt to characterize the DCH states of a molecule, N_2 , by sequential two-photon absorption from the LCLS. The production and decay of these states was characterized by photoelectron spectroscopy, Auger electron spectroscopy, and mass spectrometry. [3]

Our findings break new ground in ultrafast x-ray science with direct relevance for future femtosecond x-ray induced chemical dynamics studies [2,3]. This includes implications for single-pulse imaging experiments since our work [1,4] demonstrates unambiguously that when intense energy is deposited in very short pulses (few fs), high charge states are suppressed. This effect could be used to reduce Coulomb-induced distortion of molecules during illumination by an imaging pulse.

2) Site-Selective Ionization and Relaxation Dynamics in Heterogeneous Nanosystems

We investigated energy and charge transfer mechanisms as well as fragmentation dynamics in site-selectively ionized heterogeneous core-shell clusters using a high-resolution photoelectron-ion coincidence technique. We showed that after inner-shell photoionization, energy or charge is transferred to neighboring atoms and that the subsequent charge localization depends on the site of ionization. Cluster bulk ionization leads to more distinct fragmentation channels than surface ionization. We attribute this to different electronic decay, charge localization, and fragmentation times and conclude that charge transfer and fragmentation dynamics are strongly influenced by the environment of the initially ionized atom [5].

3) Promoting a Core Electron to Fill a d-Shell: Threshold Law and Shape and Feshbach Resonances

Negative ions are important in many physical processes, e.g., stellar atmospheres, molecular clouds, atomic mass spectrometry, and plasma physics. They have also attracted much interest due to the qualitatively different features deriving from the short-ranged potential that binds them.

We have conducted the first measurements of the absolute cross sections for the formation of Pt^+ , Pt^{2+} , and Pt^{3+} following $4f$ and $5p$ inner-shell photoexcitation and detachment of $Pt\ 4f^{14}5d^96s^2\ 2D$. The Pt^{3+} production channel is dominated by $4f$ detachment and allows for the first observation of a d -wave Wigner threshold law following single-photon absorption. Our measurements show that promoting a $5p$ electron into the $5d$ orbital produces a shape resonance, while promoting a $4f$ electron produces Feshbach resonances, demonstrating the importance of core-valence interactions. Our work shows that the inner-shell photodetachment spectrum of transition-metal anions displays a rich structure due to the presence of the $5p$ and $4f$ electrons and the mostly filled d orbital. Finally, high-precision measurements of two Feshbach resonances from $4f \rightarrow 5d$ excitations are observed in Pt^+ and Pt^{2+} channels but are nearly completely absent in Pt^{3+} . These

observations coupled with previous studies show that orbital stabilization is generally, but not always, observed when a single vacancy orbital is filled [6].

Future Plans.

The principal areas of investigation planned for the coming year are:

1) We plan to carry out collaborative LCLS-based experiments and analyze the resulting data. **2)** We plan to carry out baseline experiments for the LCLS program and continue the data analysis of the Coulomb explosion investigations of large molecules and clusters using the ALS. **3)** We plan to continue the photodetachment experiments in the carbon anions cluster chain at the ALS and continue the analysis of the experiments conducted on the valence and K-shell photodetachment of C_{60}^- conducted in collaboration with the UNR, DU, ALS and Giessen groups.

Publications from DOE Sponsored Research

1. M. Hoener, L. Fang, O. Kornilov, O. Gessner, S.T. Pratt, M. Guehr, E.P. Kanter, C. Blaga, C. Bostedt, J.D. Bozek, P.H. Bucksbaum, C. Buth, M. Chen, R. Coffee, J. Cryan, L. DiMauro, M. Glowina, E. Hosler, E. Kukk, S.R. Leone, B. McFarland, M. Messerschmidt, B. Murphy, V. Petrovic, D. Rolles, and N. Berrah, "Ultra-intense X-ray Induced Ionization, Dissociation and Frustrated Absorption in Molecular Nitrogen" *Phys. Rev. Lett.* **104**, 253002 (Published June 23, 2010). First published work from LCLS.
2. N. Berrah, J. Bozek, J. T. Costello, S. Düstererd, L. Fanga, J. Feldhausd, H. Fukuzawae, M. Hoenera, Y. H. Jiang; P. Johnsson, E. T. Kennedy, M. Meyer,; R. Moshammer, P. Radcliffed, M. Richter, A. Rouzée; A. Rudenko, . A. Sorokind, K. Tiedtke, K. Ueda, . Ullrich, M. J. J. Vrakking "Non-linear processes in the interaction of atoms and molecules with intense EUV and X-ray fields from SA SE free electron lasers (FELs)" *Journal of Modern Optics, Topical Review*, **57**,xx (In press; Published online June 25, 2010).
3. L. Fang, M. Hoener, O. Gessner, F. Tarantelli, S.T. Pratt, O. Kornilov, C. Buth, M. Guehr, E.P. Kanter, C. Bostedt, J.D. Bozek, P.H. Bucksbaum, M. Chen, R. Coffee, J. Cryan, M. Glowina, E. Kukk, S.R. Leone, and N. Berrah, "Double core hole production in N_2 : Beating the Auger clock", *Phys. Rev. Lett* (in press)
4. L. Young, E. P. Kanter, B. Krässig, Y. Li, A. M. March, S. T. Pratt, R. Santra, S. H. Southworth, N. Rohringer, L. F. DiMauro, G. Doumy, C. A. Roedig, N. Berrah, L. Fang, M. Hoener, P. H. Bucksbaum, J. P. Cryan, S. Ghimire, J. M. Glowina, D. A. Reis, J. D. Bozek, C. Bostedt, M. Messerschmidt, "Femtosecond electronic response of atoms to ultraintense x-rays" *Nature* **466**, 56-61 (2010).
5. M. Hoener, D. Rolles, A. Aguilar, R. C. Bilodeau, D. Esteves, P. Olalde Velasco, Z. D. Pesic, E. Red, and N. Berrah, "Site-selective ionization and relaxation dynamics in heterogeneous nanosystems", *Phys. Rev. A*, **81**, 021201(R) (2010).
6. R. C. Bilodeau, I. Dumitriu, N. D. Gibson, C. W. Walter and N. Berrah, "Promoting a core electron to fill a d-shell: Threshold law and shape and Feshbach resonances" *Phys. Rev. A*, **80**, 031403R (2009)
7. Berrah, D. Rolles, Z. D. Pesic, M. Hoener, H. Zhang, A. Aguilar, R. C. Bilodeau, E. Red, J. D. Bozek, E. Kukk, R. Dies Muino and G. Ed Abajo, *Proceedings of Advances in X-ray and Inner-Shell Processes, Euro. Phys. J. Special Topics (EPJ) ST*, **169**, 59 (2009).

8. N. Berrah, R.C. Bilodeau, I. Dumitriu, D. Toffoli, and R. R. Lucchese, "Shape and Feshbach Resonances in Inner-Shell Photodetachment of Negative Ions, *J. Elect. Spectr. and Relat. Phen.* (in press)
9. D Rolles, G Prumper, H Fukuzawa, X-J Liu, J Harries, K. Ueda, Z D Pešić, I Dumitriu and N Berrah, "Molecular-frame angular distribution of normal and resonant Auger electrons" *J. Phys Conf Series* (in press) .
10. I. Dumitriu, R. Bilodeau, D. Gibson, W. Walter, A. Aguilar E. Reed and N. Berrah "Photoionization of Fe⁺", *Phys. Rev. A*, **81**, 053404 (2010).
11. Z. D. Pešić, D. Rolles, I. Dumitriu, and N. Berrah "Fragmentation Dynamics of Gas-Phase Furan Following K-shell Ionization" *Phys. Rev. A* **82**, 013401 (2010).
12. D. Rolles, H. Zhang, Z. D. Pešić, J. D. Bozek, and N. Berrah "Emergence of Band Structure in Valence Photoemission from Rare Gas Clusters" *Chem. Phys. Lett.* **468**, 148 (2009).
13. N. Berrah, D. Rolles, Z. D. Pešić, M. Hoener, H. Zhang, A. Aguilar, R. C. Bilodeau, E. Red, J. D. Bozek, E. Kukk, R. Dies Muino and G. Abajo, "Probing free Xe clusters from within" *Euro.Phys. J. Special Topics (EPJ) ST*, **169**, 59 (2009).
14. H. Zhang, D. Rolles, J.D. Bozek R. Bilodeau and N. Berrah, "Photoionization of argon clusters in the Ar 3s→np Rydberg resonance region", *J. Phys. B: At. Mol. Opt. Phys.*, **42**, 105103, (2009).
15. D. Rolles, G. Prumper, H. Fukuzawa, X.-J. Liu, Z. D. Pešić, R. F. Fink, A. N. Grum-Grzhimailo, I. Dumitriu, N. Berrah, and K. Ueda, "Molecular-Frame Angular Distributions of Resonant CO:C(1s) Auger Electrons", *Phys. Rev. Lett.* **101**, 263002 (2008).
16. G. Prumper, H. Fukuzawa, D. Rolles, K. Sakai, K. Prince, J. Harries, Y. Tamenori, N. Berrah, and K. Ueda, "Is CO C 1s Auger Electron Emission Affected by the Photoelectron?" *Phys. Rev. Lett.* **101**, 233202 (2008)
17. G Prümper, D Rolles, H Fukuzawa, X J Liu, Z Pešić, I Dumitriu, R R Lucchese, K Ueda and N. Berrah, "Measurements of molecular-frame Auger electron angular distributions at the CO C 1s⁻¹ 2π* resonance with high energy resolution", *J. Phys. B: At. Mol. Opt. Phys.* **41**, 215101 (2008).
18. Z. Pešić, D. Rolles, R.C. Bilodeau, I. Dumitriu and N. Berrah, "Three-Body Fragmentation of CO₂²⁺ upon K-shell Photoionization", *Phys Rev A*. *Phys. Rev. A* **78**, 051401 (2008) (rapid C.)
19. H. Zhang, D. Rolles, J.D. Bozek, B. Rude, R. C. Bilodeau and N. Berrah "Angular distributions of inner shell photoelectrons from rare-gas clusters", *Phys. Rev. A* **78**, 063201 (2008).
20. M. Wiedenhoef, A. A. Wills, X. Feng, S. Canton, J. Viehhaus, T. Gorczyca, U. Becker, and N. Berrah "Exchange and PCI effects on Angular Distribution in Xe 4d_{5/2}" *J. Phys. B.* **41** 095202, (2008).

Strongly Anisotropic Bose and Fermi Gases

Principal Investigator

John Bohn
JILA, UCB 440
University of Colorado
Boulder, CO 80309
Phone (303) 492-5426
Email bohn@murphy.colorado.edu

Program Scope

Thus far, this program has focused on the fundamental properties of dilute quantum degenerate gases whose constituent particles possess dipole moments. It is concerned with the implications of the dipole-dipole interactions on the structure, dynamics, and control of these gases, as well as their ability to provide prototypes for novel condensed matter systems and potentially useful materials. The properties of the gas are tunable to a high degree, by varying such quantities as the density of the gas, the orientation of the dipoles, the scattering length of the constituents, and the anisotropy of the trap in which they are held.

Recent Progress

We continue our investigations into the structure and stability of dipolar Bose-Einstein condensates. These matters get to the heart of the novelty of dipolar particles, namely, their anisotropic interparticle interactions, which are either repulsive or attractive depending on the relative orientation of the particles. An unusual consequence of this anisotropy, known for some time now, is the existence of excitations analogous to the roton mode in superfluid helium. In helium, this excitation determines many properties of the gas, including the velocity below which the fluid flows without resistance, as well as the features of correlated motion of the atoms in the fluid. We are developing the theory of how these excitations play out in realistic experimental circumstances for dipoles.

In dipolar BEC, the roton-like excitations offer far more variety than in liquid helium, inasmuch as their properties can be tuned via both the strength of the dipole moment and the anisotropy of the trap. Moreover, an idea going back to Landau suggests that the details of the roton spectrum are essential for determining the superfluid critical velocity in helium. We have recently explored this connection in detail in the dipolar BEC analog. We numerically simulate an experiment that was first attempted at MIT in sodium BEC, where a laser stirs the condensate with a speed either below or above the critical velocity for superfluidity. Such an experiment would be a direct probe of superfluidity. These simulations can clearly distinguish the breakdown of superfluidity as the speed of the probe is increased (see figure), as energy lost to excitations of collective modes introduce a drag force. In this work, we acknowledge useful discussions with Chandra Raman at the DOE Airlie meetings.

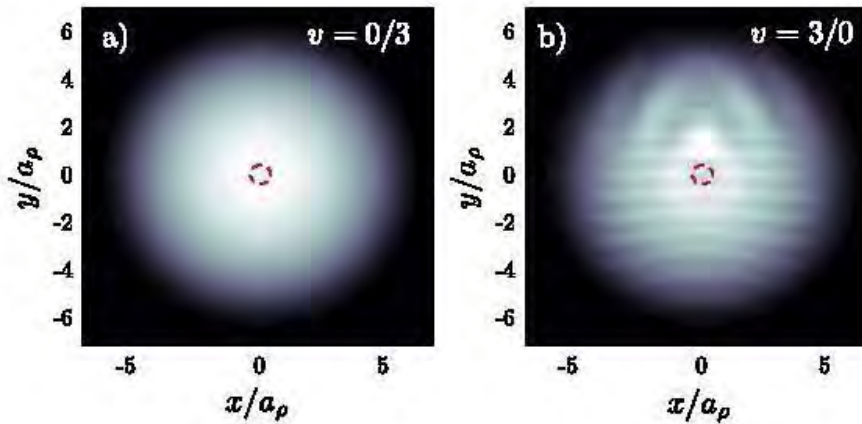


Figure. Density profiles for dipolar BEC's that have been “stirred” by a Gaussian probe whose width is given by the red circle, as viewed looking down on the BEC from the polarization axis. In the left-hand panel the probe is dragged below the superfluid critical velocity and remains undisturbed. In the right-hand panel, the probe's speed exceeds the critical velocity, and collective excitations occur.

Superfluidity is in turn expected to be intimately tied to the spectrum of elementary excitations of the fluid, via the traditional Landau criterion. We have verified that this is so for the dipolar BEC, where the experimental range of all parameters is substantially greater than in liquid helium. In particular, we have studied the critical velocity as a function of the density of the dipolar BEC. We find that the critical velocity rises at first as the density grows (due to dominance of repulsive interactions), while eventually it falls with increasing density, as the attractive part of the dipolar interaction, along with roton excitations, take over.

Future Plans

Further goals of this project include investigating dipolar BEC's in arrays of traps, where different BEC's can act on one another; incorporating the polarizability of the molecular dipoles, which explicitly relates the internal molecular degrees of freedom to the collective behavior of the condensate; and the intriguing possibility of roton-roton interactions, which could have profound further implications for superfluidity, and bring us closer to understanding the strongly-interacting Bose gas. These projects are currently underway, and will produce results published under the DOE auspices.

However, in the renewal grant, our focus will shift significantly, more in the direction of ultracold collisions of molecules, for which much theoretical work will be warranted in the near future to support experiments. Molecule collisions are better oriented toward novel chemistry than toward many-body physics, and will hopefully be more in accord with DOE needs and interests.

DOE-supported publication in the past three years

Manifestations of the Roton Mode in Dipolar Bose-Einstein Condensates

R. M. Wilson, S. Ronen, J. L. Bohn, and H. Pu, Phys. Rev. Lett. **100**, 245302 (2008).

Generalized Mean-Field Approach to a Resonant Bose-Fermi Mixture

D. C. E. Bortolotti, A. V. Avdeenkov, and J. L. Bohn, Phys. Rev. A **78**, 063612 (2008).

Stability and Excitations of a Dipolar Bose-Einstein Condensate with a Vortex

R. M. Wilson, S. Ronen, and J. L. Bohn, Phys. Rev. A **79**, 013621 (2008).

How Does a Dipolar Bose-Einstein Condensate Collapse?

J. L. Bohn, R. M. Wilson, and S. Ronen, Proceedings of the 17th International Laser Physics Conference, published in Laser Physics **19**, 547 (2009).

Angular Collapse of Dipolar Bose-Einstein Condensates

R. M. Wilson, S. Ronen, and J. L. Bohn, Phys. Rev. A **80**, 023614 (2009).
Featured in the *Virtual Journal of Atomic Quantum Fluids*, Sept. 2009.

Critical Superfluid Velocity in a Trapped Dipolar Gas

R. M. Wilson, S. Ronen, and J. L. Bohn, Phys. Rev. Lett. **104**, 094501 (2010).

Ultrafast Electron Diffraction from Aligned Molecules

Martin Centurion

Department of Physics and Astronomy, University of Nebraska, Lincoln, NE 68588-0299
mcenturion2@unl.edu

Program Scope or Definition

The aim of this project is to record time-resolved electron diffraction patterns of aligned molecules and to reconstruct the 3D molecular structure. The molecules will be aligned non-adiabatically using a femtosecond laser pulse. A femtosecond electron pulse will then be used to record a diffraction pattern while the molecules are aligned. The experiment consists of a laser system, a pulsed electron gun, a gas jet that contains the target molecules and a detector to capture the diffraction patterns. The diffraction patterns will then be processed to obtain the molecular structure.

Introduction

The experiment will consist of three main components: the electron gun, the laser system and the experimental chamber. First, a seeded supersonic gas jet is used to introduce the target molecules into the experiment and to cool the rotational temperature. A sample of molecules with a low rotational temperature will lead to a higher degree and duration of the alignment. Then, a femtosecond laser pulse intersects the molecules and aligns them along the direction of the laser polarization. The alignment survives only for a short time after the laser traverses the gas jet. A short electron pulse is then used to probe the molecules. The electron pulse is generated using an electron gun that is synchronized with the laser pulses. A small fraction of the laser energy is used to trigger electron emission from a photocathode, and the electrons are accelerated in a static field and collimated before reaching the target. The diffraction pattern from the aligned molecules is captured in a custom-made detector, and the image is stored on the computer for analysis.

A key to the success of the experiment is to capture the diffraction pattern during the short time in which the molecules are aligned. Previous experiments have shown that it is possible to observe conformational changes in isolated molecules with picosecond resolution using gas electron diffraction [1,2]. Recent experiments have shown that a temporal resolution of 3 ps is sufficient to detect the alignment following a dissociation reaction [3]. However, in order to extract 3D structural information from the diffraction patterns it is necessary to reach a higher degree of alignment. This can be achieved by using non-adiabatic alignment and improving the temporal resolution. A resolution of < 1 ps will allow us to capture the diffraction pattern while the distribution of molecules still shows a high degree of alignment. The current setup will also feature a detector with single-electron sensitivity. The detector consists of a phosphor screen, image intensifier and CCD which are all fiber coupled to maximize the transmission through each element. The phosphor screen converts each incident electron into photons which are

transmitted to the image intensifier and multiplied before reaching the CCD. Each incident electron will generate sufficient counts on the CCD to be detected. In addition, the current experiment will be performed at a repetition rate of 10 kHz, compared to 1 kHz of previous experiments, which will result in a significant improvement in the signal to noise ratio of the diffraction patterns.

Recent Progress (April/2010 to August/2010)

The design of all the major components of the experiment has been completed. These consist of two main vacuum chambers that will be differentially pumped: the electron gun and the main experimental chamber. Figure 1 shows the design of the two chambers. The electron gun will be pumped by a small turbo pump, while a diffusion pump will be used for the experimental chamber in order to more efficiently remove the gas load (the diffusion pump is not shown in the figure). Both pumps are already in place in the laboratory.

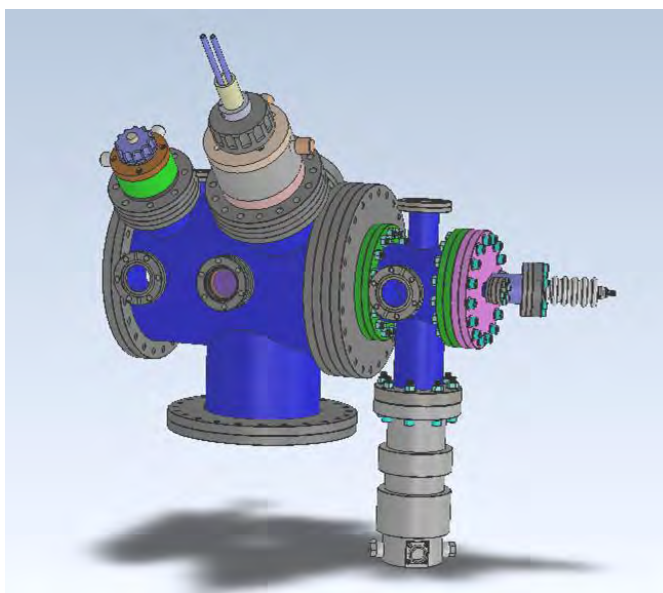


Figure 1. Experimental apparatus. The electron gun (right side) and experimental chamber are differentially pumped by a turbopump and a diffusion pump (not shown). A laser window on the right end allows the laser to enter the electron gun to trigger the photocathode.

A new laser system that will be used for this project has been installed and is now operational. The laser is a system from Coherent that produces 50 fs pulses with 1 mJ energy at a repetition rate of 10 kHz. The high repetition rate will be crucial for increasing the signal to noise ratio of the diffraction patterns and for reducing the integration time. The laser system provides more than sufficient pulse energy to trigger the photocathode and align the molecules.

The experimental chamber has been completed and delivered, while all the other components are currently being fabricated. We expect to receive and test the magnetic lens, beam block and electron gun in the next few weeks. The detector is expected to arrive at the end of the summer. The design of the nozzles has been finished and we expect to start with the fabrication soon. For the experiments, each laser pulse is split into two components. A small fraction of the energy is used in the electron gun, while most of the energy is used to align the molecules. The electron gun holds a gold-coated fused silica plate, which acts as the photocathode. The laser is incident from the back, with the gold surface in front held at a voltage of -30 kV. The laser pulse is converted to its third harmonic, such that the photon energy is slightly above the work function of the gold film. The main experimental chamber holds a magnetic lens to collimate the electron beam, a Laval nozzle for introducing a gas jet (the target molecules), a beam block and a custom detector that will capture and digitize the diffraction patterns with sufficient sensitivity to detect single electron hits.

Future Plans

Once all of the components of the experiment are in place, we will perform some preliminary experiments before moving on to time-resolved diffraction. First we will record static diffraction pattern to characterize the system and to measure the signal to noise level as a function of electron current. This will give us a good measurement of the integration time required to achieve a given resolution as the current is reduced to improve the temporal resolution, and will serve to develop the computational tools to analyze the diffraction patterns. The second experiment will be to determine the temporal overlap of the laser and electron pulses. This can most easily be done by using the laser to induce photoemission from a metal in the path of the electron or by ionizing the gas molecules. In both cases, the laser initiated changes result in a distortion of the electron beam due to local fields. While these effects evolve on time scales of tens of picoseconds, it has been shown that by identifying the instant where the changes are first observed it is possible to determine the temporal overlap to better than 1 ps. [4]

After these preliminary experiments we expect to take our first time-resolved diffraction patterns. We will use the laser to create a sample of non-adiabatically aligned molecules, and take diffraction patterns as a function of the delay between laser and electrons. There are several candidate molecules for first experiments, linear molecules such as carbon dioxide or carbon disulfide would be interesting because they would clearly show the effect of the laser, and the diffraction patterns will be relatively simple to analyze. A more complex molecule such as CF_3I would also be a good candidate because it will provide an example of a non-planar molecule.

If the electron pulse arrives shortly after the laser pulse the molecules will be aligned but in a field-free environment. When the molecules are at the highest degree of alignment we expect to see a large anisotropy in the diffraction pattern. In parallel to these experiments, we will work to develop the tools to analyze and recover structural information from the diffraction patterns. The reconstruction of structure from anisotropic diffraction patterns is currently an active area of research [5], and we expect to build on the existing work. Future experiments will also include

extending the alignment method to 3D alignment by using a pair of alignment pulses (or elliptically polarized pulses), diffracting from larger molecules and studying ultrafast conformational changes in molecules.

References

- [1] H. Ihee, V. A. Lobastov, U. M. Gomez et al., “Direct imaging of transient molecular structures with ultrafast diffraction”, *Science* 291, 458 (2001)
- [2] S. T. Park, A. Gahlmann A, Y. G. He et al., “Ultrafast Electron Diffraction Reveals Dark Structures of the Biological Chromophore Indole”, *Angew. Chem. Int. Ed* 47, 9496 (2008)
- [3] P. R. Reckenthaeler, M. Centurion, W. Fuss et al., “Time-resolved electron diffraction from selectively aligned molecules” *Phys. Rev. Lett.* 102, 213001 (2009)
- [4] H. Park, Z. Hao, X Wang et al., “Synchronization of femtosecond laser and electron pulses with subpicosecond precision”, *Rev. Sci. Inst.* 76, 083905 (2005)
- [5] D. K. Saldin, V. L. Shneerson, D. Starodub D et al., “Reconstruction from a single diffraction pattern of azimuthally projected electron density of molecules aligned parallel to a single axis”, *ACTA CRYSTALLOGR A* 66, 32 (2010).

References to publications of DOE sponsored research that have appeared in the past 3 years or that have been accepted for publication.

None.

Atomic and Molecular Physics in Strong Fields

Shih-I Chu

Department of Chemistry, University of Kansas

Lawrence, Kansas 66045

E-mail: sichu@ku.edu

Program Scope

In this research program, we address the fundamental physics of the interaction of atoms and molecules with intense ultrashort laser fields. The main objectives are to develop new theoretical formalisms and accurate computational methods for *ab initio* nonperturbative investigations of multiphoton quantum dynamics and very high-order nonlinear optical processes of one-, two-, and many-electron quantum systems in intense laser fields, taking into account detailed electronic structure information and many-body electron-correlated effects. Particular attention will be paid to the exploration of the effects of electron correlation on high-harmonic generation (HHG) and multiphoton ionization (MPI) processes, multi-electron response and underlying mechanisms responsible for the strong-field ionization of diatomic and small polyatomic molecules, time-frequency spectrum, coherent control of HHG processes for the development of tabletop x-ray laser light sources, and for the exploration of attosecond AMO processes, etc.

Recent Progress

1. *Ab initio* time-dependent density-functional-theory study of the frequency comb structure, coherence, and dephasing of many-electron atoms in the VUV-XUV regimes via high-order harmonic generation

In the past few years, femtosecond laser-based optical frequency combs have led to remarkable advancements in ultrafast science [1], high-precision optical frequency measurement and synthesis [2], and enabled optical atomic clocks [3]. As a universal optical frequency comb synthesizer, this method provides a direct link between optical and microwave frequencies. More recently, there is substantial experimental interest in the exploration of the feasibility of generating frequency comb in the extreme ultraviolet (xuv) and vacuum ultraviolet (vuv) regimes at a repetition frequency of more than 100 MHz via high-order harmonic generation (HHG) [4,5]. However, there are currently experimental difficulties in the realization of the frequency comb structure within each high harmonic, with the exception of the third-order harmonic case [5].

To advance this field, we have recently presented the first fully *ab initio* quantum investigation of the frequency comb structure and coherence within each order of the high-order harmonic generation spectrum of H atoms in the high-frequency vuv-xuv regime [6]. More recently, we have further extended the study to the rare gas systems [7] by means of the time-dependent density-functional theory (TDDFT) with optimized effective potential (OEP) and self-interaction correction (SIC) [8]. The TDDFT/OEP-SIC equations are solved accurately and efficiently by means of the time-dependent generalized pseudospectral [TDGPS] [9] technique. We found that a nested comb structure appears within each order of the harmonics, ranging from the first harmonic all the way to the cutoff region. We explore in detail the temporal coherence and robustness of the comb structure by varying the laser-pulse separation τ , the number of pulses N , the phase difference between pulses $\Delta\Phi$, and the laser intensity. The frequency comb structure and coherence are preserved in each harmonic regardless of the values of τ and N used for the case of weak and medium strong incident laser-pulse trains. The time-frequency characteristics of the HHG coherence structure are analyzed in details by means of the wavelet transform of the time-dependent induced dipoles. The interference modulation can be attributed to the constant phase relationship of harmonics among successive pulses. However, under superstrong fields, non-uniform and substantial ionization takes place during each pulse, jeopardizing the temporal coherence of the emitted frequency

comb modes. Finally, we found that the dynamical electron correlation, which is included in the present TDDFT/OEP-SIC treatment but not in the single-active electron model, is significant for the quantitative exploration of the frequency comb structure and coherence of higher harmonics [7].

2. Coherent Control of Multiphoton Resonance Dynamics in Intense Frequency-Comb Laser Fields: Generalized Floquet Theoretical Approach

We generalize the many-mode Floquet theorem (MMFT) [10,11] for the nonperturbative investigation of multiphoton resonance dynamics driven by intense frequency-comb laser fields [12]. The frequency comb structure generated by a train of short laser pulses can be exactly represented by a combination of the main frequency and the repetition frequency. MMFT allows non-perturbative and exact treatment of the interaction of a quantum system with the frequency-comb laser fields. We explore multiphoton resonance processes between a two-level system and frequency-comb laser. It is shown that there are simultaneous multiphoton resonance processes between the system and comb laser, and that they can be optimally controlled by tuning the pulse-to-pulse carrier-envelope phase (CEP) shift. HHG driven by intense frequency-comb laser has the comb structure with the same repetition frequency and different offset for each harmonic. Moreover, HHG can be (many-orders-of magnitude) dramatically enhanced by tuning the CEP shift due to simultaneous multiphoton resonance among all the comb frequencies [12].

3. Extension of High-order Harmonic Generation Cutoff via Coherent Control of Intense Few-Cycle Chirped Laser Pulses

We present an *ab initio* quantum investigation of the high-order harmonic generation (HHG) cutoff extension using intense few-cycle chirped laser pulses [13]. For a few-cycle chirped driving laser pulse, it is shown that significant cutoff extension can be achieved through the optimization of the chirping rate parameters. The HHG power spectrum is calculated by solving accurately and efficiently the time-dependent Schrödinger equation (TDSE) by means of the TDGPS method. In addition, we perform classical trajectory simulation of the strong-field electron dynamics and electron return map. It is found that the quantum and classical results provide complementary and consistent information regarding the underlying mechanisms responsible for the substantial extension of the cutoff region.

4. High Precision Study of the Orientation Effects in MPI/HHG of H_2^+ in Intense Laser Fields

Recently we have developed a TDGPS method for accurate and efficient treatment of the time-dependent Schrödinger equation (TDSE) of two-center diatomic molecules systems in prolate spheroidal coordinates [14,15]. This method naturally accounts for the symmetry of diatomic molecules and provides accurate description of Coulomb singularities due to non-uniform distribution of the grid points. The GPS method delivers high accuracy while using only moderate computer resources; it is easy to implement since no calculation of potential matrix elements is required, and kinetic energy matrices have simple analytical expressions. The method is applied to a fully *ab initio* 3D study of the orientation effects in MPI and HHG of H_2^+ subject to intense laser pulses. We discuss the multiphoton resonance and two-center interference effects in the HHG spectra which can lead both to enhancement and suppression of the harmonic generation [14].

5. Accurate Treatment of Above-Threshold-Ionization Spectra from Core Region of Time-Dependent Wave Packet: A New *ab initio* Time-Dependent Approach

The phenomenon of multiphoton above-threshold ionization (ATI) and the investigation of the resulting electron angular distributions has attracted much recent interest. This is related to advances in laser technology which made possible generation of ultrashort and intense laser pulses. For such pulses, the absolute or carrier-envelope phase (CEP) plays an important role and properties of the ejected electrons momentum (or energy-angular) distributions differ significantly from those for long pulses. Recent experiments were able to measure high-resolution fully differential data on ATI of noble gases. Thus accurate theoretical description of the electron distributions becomes an important and timely task.

In a recent work, we develop a new method for the accurate treatment of TDSE and electron energy and angular distributions after above-threshold multiphoton ionization [16]. The procedure does not require propagation of the wave packet at large distances, making use of the wave function in the core region. It is based on the extension of the Kramers–Henneberger picture of the ionization process while the final expressions involve the wave function in the laboratory frame only. The approach is illustrated by a case study of above-threshold ionization of the hydrogen atom subject to intense laser pulses. The ejected electron energy and angle distributions have been calculated and analyzed. We explore the electron spectrum dependence on the duration of the laser pulse and carrier-envelope phase [16].

6. Exploration of the Role of the Electronic Structure and Multi-electron Response in the MPI and HHG Processes of Diatomic Molecules in Intense Laser Fields

There have been much recent experimental and theoretical interests in the study of strong-field molecular ionization and HHG. Most theoretical studies in the recent past are based on approximate models such as the ADK model, strong-field approximation, etc. The effects of detailed electronic structure and multi-electron responses are often ignored. Although these models have some partial success in weaker field processes, they cannot provide an overall consistent picture of the ionization and HHG behavior of different molecules.

We have recently extended the *self-interaction-free* TDDFT [8] for nonperturbative investigation of the ionization mechanisms and the HHG power spectra of homonuclear (N_2 , O_2 , and F_2) and heteronuclear (CO) diatomic molecules in intense ultrashort lasers [17] for the case that the laser polarization axis parallels the molecular axis. Our studies reveal several intriguing behaviors of the nonlinear responses of molecules to intense laser fields: (a) It is found that detailed electron structure and correlated multielectron responses are important factors for the determination of the strong-field ionization behavior. Further, it is not adequate to use only the highest occupied MO (HOMO) for the description of the ionization behavior since the inner valence electrons can also make significant or even dominant contributions. (b) We predict substantially different nonlinear optical response behaviors for homonuclear (N_2) and heteronuclear (CO) diatomic molecules. In particular, we found that the MPI rate for CO is higher than that of N_2 . Furthermore, while laser excitation of the N_2 molecule can generate only odd harmonics, both even and odd harmonics can be produced from the CO molecule [17].

More recently, we have further extended the *all-electron* TDDFT approach [15] to the study of the effect of correlated multielectron responses on MPI [18] HHG [19] of diatomic molecules N_2 , O_2 , and F_2 in intense short laser pulses with arbitrary molecular orientation. We show that the contributions of inner molecular orbitals to the total MPI and HHG rates can be significant or even dominant over the HOMO, depending upon detailed electronic structure and symmetry, laser field intensity, and orientation angle.

7. Theoretical study of Orientation-dependent MPI of Small Polyatomic Molecules in Intense Ultrashort Laser Fields: A New Time-Dependent Voronoi-Cell Finite Difference Method

We develop a new grid-based time-dependent method for accurate investigation of multiphoton ionization (MPI) of small polyatomic molecules in intense ultrashort laser fields [20,21]. The electronic structure of polyatomic molecules is treated by the density-functional theory (DFT) with proper long-range potential and the Kohn–Sham equation is accurately solved by means of the Voronoi-cell finite difference (VFD) method on non-uniform and highly adaptive molecular grids utilizing geometrical flexibility of the Voronoi diagram. This method is generalized to the time-dependent problems with the split-operator time-propagation technique in the energy representation, allowing accurate and efficient non-perturbative treatment of attosecond electronic dynamics in strong fields [20]. The new procedure is applied to the study of MPI of N_2 and H_2O molecules in intense linearly-polarized and ultrashort laser fields with arbitrary field–molecule orientation [20]. Our results demonstrate that the orientation dependence of MPI is determined not just by the HOMO but also by the symmetries and dynamics of other contributing MOs. In particular, the inner MOs can show dominant contributions to the ionization

processes when the molecule is aligned in some specific directions w.r.t. the field polarization. This feature suggests a new way to selectively probe individual orbitals in strong-field electronic dynamics.

More recently, we have extended the TDVFD method to the study of multi-electron effects on the orientation dependence and photoelectron angular distribution (PAD) of multiphoton ionization of CO₂ in strong laser fields [21]. We performed TDDFT calculations for CO₂ by means of the TDVFD method with highly adaptive molecular grids. Calculated orientation-dependent plot of CO₂ MPI shows the center-fat propeller shape with 40° maximum, which is mainly contributed by two perturbed HOMOs. Our prediction agrees well with the recent experiments [22,23]. The PAD with various orientations illustrates characteristics of the HOMO symmetry including the nodal shapes and the peak spot at the field direction, explaining suppression and enhancement of MPI at corresponding orientation. It supports the relation between the orientation dependence of MPI and the orbital symmetry.

Future Research Plans

In addition to continuing the ongoing researches discussed above, we plan to initiate the following several new project directions: (a) Exploration of 3D orientation dependent MPI/HHG and ATI processes of diatomic molecules in intense laser pulses. (b) Further development of TDVFD method to the study of HHG in triatomic molecular systems. (c) Development of time-dependent *localized* Hartree-Fock (LHF)-DFT method for the study of singly, doubly, and triply excited states of Rydberg atoms and ions, inner shell excitations [24], as well as photoionization of atomic excited states [25]. (d) Coherent control of rescattering and attosecond phenomena in strong ultrashort fields.

References Cited (* Publications supported by the DOE program in the period of 2007-2010.)

- [1] M. Hentschel *et al.*, Nature (London) **414**, 509 (2001); M. Drescher *et al.*, Science **291**, 1923 (2001).
- [2] M. Fischer *et al.*, Phys. Rev. Lett. **92**, 230802 (2004); H. S. Margolis *et al.*, Science **306**, 1355 (2004).
- [3] M. Takamoto *et al.*, Nature (London) **435**, 321 (2005); S. A. Diddams *et al.*, Science **293**, 825 (2001).
- [4] C. Gohle, *et al.*, Nature (London) **436**, 234 (2005).
- [5] R. J. Jones, *et al.*, Rev. Lett. **94**, 193201 (2005).
- *[6] J. J. Carrera, S. K. Son, and S. I. Chu, Phys. Rev. A **77**, 031401(R) (2008).
- *[7] J. J. Carrera and S. I. Chu, Phys. Rev. A **79**, 063410 (2009).
- [8] S. I. Chu, J. Chem. Phys. **123**, 062207 (2005). (Invited review article)
- [9] X. M. Tong and S. I. Chu, Chem. Phys. **217**, 119 (1997).
- [10] T. S. Ho, S. I. Chu, and J. V. Tietz, Chem. Phys. Lett. **96**, 464 (1983); T. S. Ho and S. I. Chu, Phys. Rev. A **31**, 659 (1985).
- [11] S. I. Chu and D. A. Telnov, Phys. Rep. **390**, 1-131 (2004).
- *[12] S.-K. Son and S. I. Chu, Phys. Rev. A **77**, 063406 (2008).
- *[13] J. Carrera and S. I. Chu, Phys. Rev. A **75**, 033807 (2007).
- *[14] D. A. Telnov and S. I. Chu, Phys. Rev. A **76**, 043412 (2007).
- *[15] D. A. Telnov and S. I. Chu, Computer Phy. Comm. (in press, 2010).
- *[16] D. Telnov and S. I. Chu, Phys. Rev. A **79**, 043421 (2009).
- *[17] J. Heslar, J. Carrera, D. Telnov, and S. I. Chu, Int. J. Quantum Chem. **107**, 3159 (2007).
- *[18] D. A. Telnov and S. I. Chu, Phys. Rev. A **79**, 041401(R) (2009).
- *[19] D. A. Telnov and S. I. Chu, Phys. Rev. A **80**, 043412 (2009).
- *[20] S. K. Son and S. I. Chu, Chem. Phys. **366**, 91 (2009).
- *[21] S. K. Son and S. I. Chu, Phys. Rev. A **80**, 011403(R) (2009).
- [22] I. Thomann *et al.*, J. Phys. Chem. A **112**, 9382 (2008).
- [23] D. Pavičić, K. F. Lee, D. M. Rayner, P. B. Corkum, and D. M. Villeneuve, Phys. Rev. Lett. **98**, 243001 (2007).
- *[24] Z.Y. Zhou and S. I. Chu, Phys. Rev. A **75**, 014501 (2007).
- *[25] Z. Y. Zhou and S. I. Chu, Phys. Rev. A **79**, 053412 (2009).

Formation of Ultracold Molecules

Robin Côté

Department of Physics, U-3046
University of Connecticut
2152 Hillside Road
Storrs, Connecticut 06269

Phone: (860) 486-4912
Fax: (860) 486-3346
e-mail: rcote@phys.uconn.edu
URL: <http://www.physics.uconn.edu/~rcote>

Program Scope

Current experimental efforts to obtain ultracold molecules (*e.g.*, photoassociation (PA), buffer gas cooling, or Stark deceleration) raise a number of important issues that require theoretical investigations and explicit calculations.

This Research Program covers interconnected topics related to the formation of ultracold molecules. We propose to investigate schemes to form ultracold molecules, such as homonuclear dimers (alkali or alkaline earth) using stimulated and spontaneous processes. We will also study heteronuclear molecules, in particular those with large dipole moments like alkali hydrides or some bi-alkali dimers (*e.g.* LiCs or LiRb). In addition, we will investigate the enhancement of the formation rate via Feshbach resonances, paying special attention to quantum degenerate atomic gases. Finally, we will explore the possible formation of a new and exotic type of molecules, namely ultralong-range Rydberg molecules.

Recent Progress

Since the start of this Program (August 1st 2005), we have worked on several projects. We limit ourselves to work published over the last three years (since 2007).

• Formation of polar molecules

In two previous papers sponsored by DOE [E. Juarros, P. Pellegrini, K. Kirby, and R. Côté, *One-photon-assisted formation of ultracold polar molecules*. Phys. Rev. A **73**, 041403(R) (2006), and E. Juarros, K. Kirby, and R. Côté, *Laser-assisted Ultracold Lithium-hydride Molecule Formation: Stimulated vs. Spontaneous Emission*. J. Phys. B **39**, S965 (2006)], we explored the formation of LiH and NaH in their $X^1\Sigma^+$ ground electronic state from one- and two-photon photoassociative processes. Recently, we extended this work to the formation of LiH molecules in the $a^2\Sigma^+$ electronic state [1]. It is predicted to support one ro-vibrational level, leading to a sample in a pure single ro-vibrational state. We found that very large rate coefficients can be obtained by using the $b^3\Pi$ excited state, which supports only five or six bound levels. Because of the extreme spatial extension of their last “lobe”, the wave functions of the two uppermost bound levels have large overlap with the ($v = 0, J = 0$) bound level of $a^3\sigma^+$, leading to branching ratios ranging from 1% to 90%. This property implies that large amounts of LiH molecules could be produced in a single quantum state, a prerequisite to study degenerate molecular gases [1]. In this work, we also discuss the implication of the statistics of the components of LiH (fermions or bosons) on the chemical reaction rates when colliding with H, Li, or LiH.

• Homonuclear molecules

We analyzed results from two-photon photoassociative spectroscopy of the least-bound vibrational level ($v = 62$) of the $X^1\Sigma_g^+$ state of the $^{88}\text{Sr}_2$ dimer [2]. By combining measurements of the binding energy with an accurate short range potential and calculated van der Waals coefficients, we were able to determine the s -wave scattering length $a_{88} = -1.46a_0$. We also modeled the observed Autler-Townes resonance splittings. Through mass scaling, we determined the scattering lengths for all other isotopic combinations. These measurements provide confirmation of atomic

structure calculations for alkaline-earth atoms and provide valuable input for future experiments with ultracold strontium.

We suggested and analyzed a technique for efficient and robust creation of dense ultracold molecular ensembles in their ground rovibrational state [3]. In this approach, a molecule is brought to the ground state through a series of intermediate vibrational states via a multistate chainwise stimulated Raman adiabatic passage technique. We studied the influence of the intermediate states decay on the transfer process and suggested an approach that minimizes the population of these states, resulting in a maximal transfer efficiency. As an example, we analyzed the formation of $^{87}\text{Rb}_2$ starting from an initial Feshbach molecular state and taking into account major decay mechanisms due to inelastic atom-molecule and molecule-molecule collisions. Numerical analysis suggests a transfer efficiency $> 90\%$, even in the presence of strong collisional relaxation as are present in a high density atomic gas.

• Rydberg-Rydberg interactions

We began working on the Rydberg-Rydberg interactions to explain some spectral features observed in ^{85}Rb experiments. We calculated the long-range molecular potentials between two atoms in $70p$ in Hund's case (c), by diagonalization of an interaction matrix. We included the effect of fine structure, and showed how the strong ℓ -mixing due to long-range Rydberg-Rydberg interactions can lead to resonances in excitation spectra. Such resonances were first reported in S.M. Farooqi *et al.*, Phys. Rev. Lett. **91** 183002, where single UV photon excitations from the $5s$ ground state occurred at energies corresponding to normally forbidden transitions or very far detuned from the atomic energies. We modeled resonances observed near the $69d + 70s$ asymptote [4], and found that our theoretical results are in good agreement with the observations of our colleagues at UConn.

In a more recent work [5], we investigate the interaction between two rubidium atoms in highly excited Rydberg states, and show the existence of potential wells for 0_g^+ symmetry of doubly-excited atoms due to ℓ -mixing. These wells are shown to be robust against small electric fields, and to support many bound states. We calculated their predissociation and show that their lifetimes are limited by the lifetime of the Rydberg atoms themselves. We also study how these vibrational levels could be populated via photoassociation, and how the signature of the ad-mixing of various ℓ -character producing the potential wells becomes apparent in photoassociation spectra.

• Influence of Feshbach resonances on formation rates

We have started to investigate the formation of molecules using photoassociation of atoms in the vicinity of Feshbach resonances. In our initial work [6], we calculated the rate coefficients to form singlet molecules of LiNa using this Feshbach Optimized Photoassociation (FOPA) mechanism, and found that they increase by 10^{3-4} when compared to the off-resonance rate coefficients. We also gave a simple analytical expression relating the rate coefficient to the off-resonance rate coefficient and parameters of the resonance (such as its position and width).

We expanded this work to take into account the effect of saturation on the rate coefficient [7]. We computed rate coefficients and showed that new double-minima features would appear at large laser intensity near the resonance. We compared our theoretical results with recent experimental measurements, and found an extremely good agreement without any adjustable parameters.

We combined this idea of FOPA with our previous work using STIRAP [8]. We showed that it is possible to enhance the Rabi frequency between the continuum and an intermediate state so that the efficient transfer of a pair of atoms directly from the continuum into the ro-vibrational ground state becomes achievable with moderate laser intensities and pulse durations. This approach opens interesting perspectives, since it does not require degenerate gases to work efficiently.

Finally, we also explored the role of Feshbach resonance and spin-orbit coupling in the formation of ultracold LiCs molecules [9]. We analyzed the experimental data of our co-workers, and found that even in the case of unpolarized atomic spin states (*i.e.* a mixture of all m_f states), hyperfine coupling can modify the formation rate measurably.

• Energy surfaces and reactions

A recent effort in my group towards reactive scattering involving cold molecules and molecular ions has started with the calculation of energy energy surfaces for trimers, such as for Li₃ [10], where we study an energy surface necessary in the photoassociation of Li₂ with Li to form the Li₃ trimer.

Together with my collaborators, we have studied the collisions of trapped molecules with slow beams, particularly of OH($J = 3/2, MJ = 3/2, f$) molecules with ⁴He atoms [11]. We found that the calculated cross sections are consistent with recent experimental observations at low beam energies, and demonstrated the importance of including the effects of non-uniform trapping fields in theoretical simulations of cold collision experiments with trapped molecules and slow atomic beams.

We also calculated the structure and thermochemistry relevant to KRb+KRb collisions and reactions [12]. We found that the K₂Rb and KRb₂ trimers have global minima at higher energies than KRb+KRb, preventing the formation of those trimers by collisions. We also calculated the energy minima for the tetramer K₂Rb₂ and found it to have two stable planar structures. We have calculated the minimum energy reaction path for the reaction KRb+KRb to K₂+Rb₂ and found it to be barrierless.

Finally, we have started a new effort on molecular ions. In order to study their formation, we carefully calculate their energy surface and transition dipole moments. We started with alkaline-earth elements, since they can be cool to very low temperatures. In [13], we report *ab initio* calculations of the $X^2\Sigma_u^+$ and $B^2\Sigma_g^+$ states of the Be₂⁺ dimer. We found two local minima, separated by a large barrier, for the $B^2\Sigma_g^+$: we computed the spectroscopic constants and found good agreement with the recent measurements. We also calculated bound vibrational levels, transition moments and lifetimes in this state.

Future Plans

In the coming year, we plan to continue the alkali hydride work. We also will extend this work to other polar molecules relevant to the experimental community, such as LiCs, LiRb, LiK, etc. We also plan to continue our work on FOPA, by expanding our treatment to the time domain.

We expect to carry more calculations on Rydberg-Rydberg interactions and explore the possibility of forming metastable long-range doubly-excited Rydberg molecules as well as the experimental signature to be expected.

Finally, we will extend our work on surfaces of atom-diatom and diatom-diatom systems, as well as for molecular ions. Such systems are studied intensively in experiments, and theoretical guidance will become ever more important.

Publications sponsored by DOE

1. E. Juarros, K. Kirby, and R. Côté, *Formation of ultracold molecules in a single pure state: LiH in $a^3\Sigma^+$* . Phys. Rev. A **81**, 060704 (2010).
2. Y.N. Martinez de Escobar, P.G. Mickelson, P. Pellegrini, S.B. Nagel, A. Traverso, M. Yan, R. Côté, and T.C. Killian, *Two-photon photoassociative spectroscopy of ultracold ^{88}Sr* . Phys. Rev. A **78**, 062708 (2008).
3. E. Kuznetsova, P. Pellegrini, R. Côté, M.D. Lukin, and S.F. Yelin, *Formation of deeply bound molecules via adiabatic passage*. Phys. Rev. A **78**, 021402(R) (2008).
4. J. Stanojevic, R. Côté, D. Tong, S.M. Farooqi, E.E. Eyler, and P.L. Gould, *Long-range potentials and $(n+1)d + ns$ molecular resonances in an ultracold Rydberg gas*. Phys. Rev. A **78**, 052709 (2008).
5. N. Samboy, J. Stanojevic, and R. Côté, *Formation of Rydberg macrodimers and their properties*. In preparation: to be submitted to PRA Rapid. Comm.
6. P. Pellegrini, M. Gacesa, and R. Côté, *Giant formation rates of ultracold molecules via Feshbach Optimized Photoassociation*. Phys. Rev. Lett. **101**, 053201 (2008).
7. P. Pellegrini, and R. Côté, *Probing the unitarity limit at low laser intensities*. New J. Phys. **11**, 055047 (2009).
8. E. Kuznetsova, M. Gacesa, P. Pellegrini, S.F. Yelin, and R. Côté, *Efficient formation of ground state ultracold molecules via STIRAP from the continuum at a Feshbach resonance*. New J. Phys. **11**, 055028 (2009).
9. J. Deiglmayr, A. Grochola, M. Repp, R. Wester, M. Weidemüller, O. Dulieu, P. Pellegrini, and R. Côté, *Influence of a Feshbach resonance on the photoassociation of LiCs*. New J. Phys. **11**, 055034 (2009).
10. J.N. Byrd, J.A. Montgomery (Jr.), H.H. Michels, and R. Côté, *Electronic Structure of the $\text{Li}_2 [X^1\Sigma_g^+] + \text{Li}^*[P_2]$ Excited A'' Surface*, Int. J. of Quantum Chem **109**, 3626 (2009).
11. T. V. Tscherbul, Z. Pavlovic, H. R. Sadeghpour, R. Côté, and A. Dalgarno, *Collisions of trapped molecules with slow beams*. Accepted for publication in Phys. Rev. A.
12. J.N. Byrd, J.A. Montgomery (Jr.), and R. Côté, *Structure and thermochemistry of K_2Rb , KRb_2 and K_2Rb_2* , Accepted for publication in Phys. Rev. A., Rapid Comm.
13. S. Banerjee, J. N. Byrd, R. Côté, H. H. Michels, J. A. Montgomery, Jr. *Ab initio potential curves for the $X^2\Sigma_u^+$ and $B^2\Sigma_g^+$ states of the Be_2^+ : Existence of a double minimum*. Accepted for publication in Chem. Phys. Lett.

Optical Two-Dimensional Spectroscopy of Disordered Semiconductor Quantum Wells and Quantum Dots

Steven T. Cundiff

JILA, University of Colorado and NIST, Boulder, CO 80309-0440
cundiff@jila.colorado.edu

August 3, 2010

Program Scope: The goal of this program is to implement optical 2-dimensional Fourier transform spectroscopy and apply it to electronic excitations, including excitons, in semiconductors. Specifically of interest are quantum wells that exhibit disorder due to well width fluctuation and quantum dots. In both cases, 2-D spectroscopy will provide information regarding coupling among excitonic localization sites.

Progress: Over the last year we have made substantial progress in obtaining 2 dimensional Fourier transform (2DFT) spectra of “natural” quantum dots (QDs) that form in narrow quantum wells [1, 2, 3, 4]. We analyzed these spectra to measure the homogeneous linewidth within the inhomogeneously broadened ensemble, which corresponds to measuring the homogeneous linewidth as a function of dot size. By measuring the homogeneous linewidth as a function of temperature and excitation density, we are able to determine how the optically created excitons interact with phonons and other excitons. Motivated by these data, we also undertook a careful analysis of 2DFT lineshapes in the regime of moderate inhomogeneous broadening. This analysis was critical for obtaining quality fit to the experimental data.

We study an epitaxially grown single GaAs quantum well (QW) 15 monolayers thick, corresponding to ≈ 4.2 nm, with 35 nm $\text{Al}_{0.3}\text{Ga}_{0.7}\text{As}$ barriers. Epitaxial-growth interruption wait times on the order of tens of seconds at the top GaAs/ $\text{Al}_{0.3}\text{Ga}_{0.7}\text{As}$ interface result in monolayer width fluctuation in the QW thickness. These width fluctuation form island-like features known as interfacial or “natural” QDs, shown as a schematic in Fig. 1(a). The QD ensemble is inhomogeneously broadened because the sample has a distribution of QD sizes in the single GaAs layer. Excitons delocalized in the QW are also inhomogeneously broadened due to averaging of the wavefunction over high-frequency fluctuation at the $\text{Al}_{0.3}\text{Ga}_{0.7}\text{As}/\text{GaAs}$ interface, which are inherent to the epitaxial-growth process. These samples are provided by Drs. D. Gammon and A. Bracker of the Naval Research Laboratory.

While one-dimensional transient four-wave-mixing techniques can measure the homogeneous linewidth in the presence of inhomogeneous broadening in the photon echo geometry, prior knowledge of the nature of the broadening is required in order to correctly extract the homogeneous linewidth [5]. In contrast, 2DFTS has the advantage of being able to unfold a complicated TFWM spectrum onto two dimensions and allows for the measurement of the homogeneous and inhomogeneous linewidths simultaneously.

The signal radiated from a single layer of GaAs QDs is extremely weak and is often masked by pump scatter, which appears along the diagonal of the spectra because the pump is only self-coherent. To increase the signal-to-noise ratio, we use a 4-position phase cycling scheme, where we toggle the phases of the excitation pulses by π at each delay step τ_i and add or subtract the subsequent spectra [J]. Using this technique, pump light scattered in the phase-matched direction will cancel and only the desired TFWM signal and reference remain.

The inhomogeneous and homogeneous linewidths, are obtained by fitting a cross-sectional slice along the diagonal and cross diagonal (perpendicular to the diagonal), respectively. Calculations based on the two-level optical Bloch equations with strong inhomogeneous broadening show that $|S_I(\omega_\tau, T, \omega_t)|$, where τ is the delay between the first two pulses and T is the waiting time between the second and third pulses, is a Gaussian along the diagonal and a $\sqrt{\text{Lorentzian}}$ along the cross diagonal [L].

The homogeneous linewidth increases linearly with increasing energy (decreasing QD size) across the inhomogeneous distribution for all temperatures when using an average excitation power of 1.0 mW. At each temperature a

linear fit is performed and the values used are taken from these fits. Thermal broadening of the homogeneous linewidth for excitons in QDs has been modeled by considering the probability of phonon absorption and subsequent excitation of the exciton to higher-lying states [6]. Although this model fits the data well and the extracted activation energy is consistent with the one-phonon population activation mechanism, we rule out this possibility because we do not observe an activation peak in the 2D spectra for long T . For short T , population activation would increase the homogeneous linewidth but would not appear as an additional peak in the 2D spectra because the phase evolves during τ . By recording 2D spectra for long T , we can observe incoherent population dynamics because the phase does not evolve during T . If activation was the cause of the thermal broadening, it would appear as a blueshifted peak from line center along the emission axis.

The absence of an activation peak signifies that the thermal broadening is due to exciton population decay and pure dephasing processes. Theoretical and experimental studies have shown that, at elevated temperatures, exciton population decay contributes only weakly to the increase in the dephasing rate and that elastic exciton-phonon coupling dominates the excitonic dephasing [7, 8]. Calculations based on the Huang-Rhys theory predict a temperature dependence of the excitonic dephasing rate that is dependent on the phonon energy and QD size. The dephasing rate increases linearly with temperature when the energy of the acoustic phonons is much less than the energy separation between the ground and first excited states in the QD. At higher temperatures, when the thermal energy approaches the QD energy level separation, virtual ground state \rightarrow excited state \rightarrow ground state transitions may dephase the exciton polarization without affecting the population [8].

We measured the homogeneous linewidth temperature dependence as a function of energy offset from line center (QD size) and fit the thermal broadening. Both the activation energy and the phonon-exciton coupling strength increase with increasing exciton energy (decreasing QD size) across the inhomogeneous distribution. An increase in the activation energy is a direct result of the ground-to-excited state energy separation increasing with decreasing QD size. A larger activation energy for smaller QDs would indicate weaker thermal broadening; however we observe an increase of the slope of the linear fit to the homogeneous linewidth with temperature. Consequently, greater thermal broadening for smaller QDs is a result of a larger exciton-phonon coupling. The effect of the exciton-phonon coupling dominates the effect of the activation energy and is consistent with theory [8] which predicts greater exciton-phonon coupling for smaller QDs, and therefore a stronger temperature dependence.

The homogeneous linewidth depends on the excitation power due to excitation induced dephasing. As the average excitation power decreases, the linewidth decreases linearly to an extrapolated value of $30.6 \mu\text{eV}$ at zero excitation intensity. This zero excitation-density value is consistent with previous studies on single QDs [3, 6, 7] and confirms that the measured homogeneous linewidth of a QD ensemble using 2DFTS is similar to single QD values. At low temperature and extrapolating to zero excitation density, dephasing from phonon scattering and many-body interactions is negligible. Furthermore the low-strain growth process minimizes non-radiative recombination defect sites. Under these assumptions, the extrapolated homogeneous linewidth is radiative lifetime broadened with a lifetime 68 ps.

This analysis has been based on the ability of 2DFT spectroscopy to separate homogeneous and inhomogeneous broadening. A glance at a 2DFT spectrum gives a qualitative sense of the inhomogeneity: for a given resonance, the linewidth in the cross-diagonal direction is associated with homogeneous broadening, while the diagonal linewidth is related to inhomogeneous broadening. However, acquiring quantitative information about the homogeneous and inhomogeneous broadenings is more difficult because they are coupled along the diagonal and cross-diagonal directions

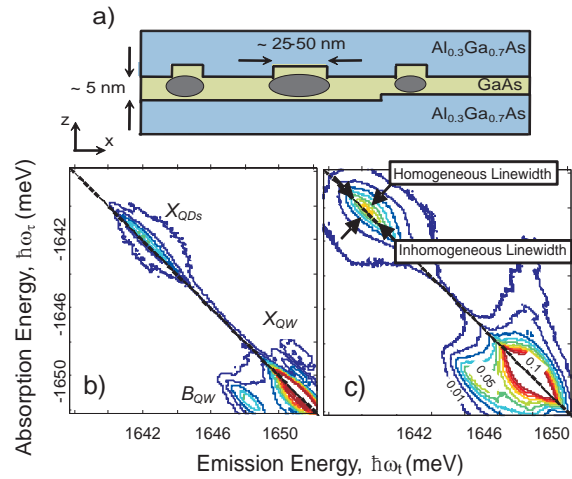


Figure 1: (Color) (a) Schematic diagram of the GaAs QD sample structure. Amplitude 2DFT spectrum (normalized to the QW peak and truncated to emphasize the QD signal) of QW and QD ensemble for TL = 6 K (a) and 50 K (b). The QW and QD homogeneous linewidths increase and the spectral features redshift with temperature.

of the spectrum. Consider the 2DFT spectrum of a purely homogeneously broadened resonance, which has the classic star shape familiar from NMR. In this case, the diagonal and cross-diagonal slices of an absolute value spectrum are Lorentzians with identical widths, and although there is no inhomogeneous broadening here, the diagonal width is not zero. If inhomogeneous broadening is added, the diagonal will broaden as expected, but the cross-diagonal will also widen slightly and change shape. Clearly there is coupling between the diagonal and cross-diagonal widths, and additional insight is needed in order to obtain quantitative information about the broadening in a 2DFT spectrum.

Past work on 2D lineshapes focused on managing the coupling between inhomogeneous and homogeneous broadening rather than understanding and isolating the individual contributions. The coupling degraded frequency resolution in NMR experiments; windowing functions improved the resolution of resonance peaks, but provided no insight into the connection between the lineshapes and dephasing. A different approach for molecular systems considered both rephasing and nonrephasing signals together, which reduced the coupling [9]. In theoretical work, Tokmakoff derived envelope lineshapes in the homogeneous and inhomogeneous limits from the Fourier transform of an absolute-value 2D time-domain solution of the optical Bloch equations [10].

We derived an analytical form for complex resonance lineshapes in 2DFTS signals for arbitrary homogeneous and inhomogeneous linewidths [L]. We began in the 2D time domain with the solution of the optical Bloch equations for a two-level system. Instead of Fourier transforming this 2D time signal to get the full 2DFT spectrum, we applied the projection-slice theorem of 2DFTs. This approach allowed us to determine an analytical form of diagonal and cross-diagonal slices in the 2D frequency data. This result provides a method of extracting the absolute homogeneous and inhomogeneous linewidths from a 2D Fourier-transform spectrum with arbitrary amounts of homogeneous and inhomogeneous broadening.

Future Plans: We plan concentrate on the natural quantum dots in the near future. We have taken preliminary data showing that the capture of carriers into the QD from the two-dimensional quantum well states can be observed in 2DFT spectroscopy as a cross-peak that grows as function of the waiting time, T . By studying the temperature dependence of the growth rate, insight into the physical mechanism will be gained. Most likely capture involves emission/scattering of multiple acoustic phonons.

We have also seen evidence that spectral diffusion due to excitons migrating among QDs of different sizes is also apparent in 2DFT spectra taken for different T . This process shows up as an off-diagonal feature below the diagonal. The specific details will give insight into the underlying physics. For example, the diffusion rate may be enhanced if there is a resonance due to an excited state in the larger dot.

We also plan to move to looking at self-organized InGaAs quantum dots. These samples present a challenge due to the longer wavelength, which can fall outside of the tuning range of the Ti:Sapphire laser used for these experiments.

Currently, we are working on a technical improvement to the way we do phase cycling. The current approach relies on moving the translation stages, which is slow and can only be done in fixed increments that may not be exactly the needed phase shift. We are exploring the use of liquid crystal phase modulators that will allow it to be done more rapidly and precisely. Recently, we successfully acquired three dimensional spectra, where both time delays between the incident pulses are scanned. We are exploring ways that a 3D spectrum provides new information.

Publication during the last 3 years from this project:

- A. T. Zhang, I. Kuznetsova, T. Meier, X. Li, R.P. Mirin, P. Thomas and S.T. Cundiff, "Polarization-dependent optical 2D Fourier transform spectroscopy of semiconductors," *Proc. Nat. Acad. Sci.* **104**, 14227 (2007).
- B. I. Kuznetsova, T. Meier, S.T. Cundiff, and P. Thomas, "Determination of homogeneous and inhomogeneous broadening in semiconductor nanostructures by two-dimensional Fourier-transform optical spectroscopy," *Phys. Rev. B* **76**, 153301 (2007).
- C. A. G. V. Spivey, C. N. Borca and S. T. Cundiff, "Correlation coefficient for dephasing of light-hole excitons and heavy-hole excitons in GaAs quantum wells," *Solid State Commun.* **145**, 303 (2008).
- D. L. Yang, T. Zhang, A.D. Bristow, S.T. Cundiff and S. Mukamel, "Isolating excitonic Raman coherence in semiconductors using two-dimensional correlation spectroscopy," *J. Chem. Phys.* **129**, 234711 (2008).
- E. A.D. Bristow, D. Karaiskaj, X. Dai and S.T. Cundiff, "All-optical retrieval of the global phase for two-dimensional Fourier-transform spectroscopy," *Opt. Express* **16**, 18017 (2008).

- F. X. Li, T. Zhang, S. Mukamel, R.P. Mirin and S.T. Cundiff, "Investigation of Electronic Coupling in Semiconductor Double Quantum Wells using Optical Two-dimensional Fourier Transform Spectroscopy," *Sol. State Commun.* **149**, 361-366 (2008).
- G. I. Kuznetsova, P. Thomas, T. Meier, T. Zhang, and S. T. Cundiff, "Determination of homogeneous and inhomogeneous broadenings of quantum-well excitons by 2DFTS: An experiment-theory comparison," to appear in *Physica Status Solidi (c)* **6**, 445 (2009).
- H. A.D. Bristow, D. Karaiskaj, X. Dai, R.P. Mirin and S.T. Cundiff, "Polarization dependence of semiconductor exciton and biexciton contributions to phase-resolved optical two-dimensional Fourier-transform spectra," *Phys. Rev. B* **79**, 161305(R) (2009).
- I. S.T. Cundiff, T. Zhang, A.D. Bristow, Denis Karaiskaj and X.Dai, "Optical Two-Dimensional Fourier Transform Spectroscopy of Semiconductor Quantum Wells, *Acct. Chem. Res.* **42**, 1423 (2009).
- J. A.D. Bristow, D. Karaiskaj, X. Dai, T. Zhang, C Carlsson, K.R. Hagen, R. Jimenez and S.T. Cundiff, "A Versatile Ultra-Stable Platform for Optical Multidimensional Fourier-Transform Spectroscopy," *Rev. Sci. Instr.* **80**, 073108 (2009).
- K. D. Karaiskaj, A.D. Bristow, L. Yang, X. Dai, R.P. Mirin, S. Mukamel and S.T. Cundiff, "Two-Quantum Many-Body Coherences in Two-Dimensional Fourier-Transform Spectra of Exciton Resonances in Semiconductor Quantum Wells," *Phys. Rev. Lett.* **104**, 117401 (2010).
- L. M.E. Siemens, G. Moody, H. Li, A.D. Bristow and S.T. Cundiff, "Resonance lineshapes in two-dimensional Fourier transform spectroscopy," *Opt. Express* **18**, 17699 (2010).

References

- [1] A. Zrenner, L. V. Butov, M. Hagn, G. Abstreiter, G. Böhm, and G. Weimann, "Quantum dots formed by interface fluctuation in AlAs/GaAs coupled quantum well structures," *Phys. Rev. Lett.* **72**(21), 3382–3385 (1994).
- [2] K. Brunner, G. Abstreiter, G. Böhm, G. Tröngle, and G. Weimann, "Sharp-line Photoluminescence and 2-photon Absorption of Zero-dimensional Biexcitons In A GaAs/AlGaAs Structure," *Appl. Phys. Lett.* **64**, 3320 (1994).
- [3] H. Hess, E. Betzig, T. Harris, L. Pfeiffer, and K. West, "Near-field Spectroscopy Of The Quantum Constituents Of A Luminescent System," *Science* **264**(5166), 1740–1745 (1994).
- [4] D. Gammon, E. Snow, and D. Katzer, "Excited-state Spectroscopy of Excitons in Single Quantum Dots," *Appl. Phys. Lett.* **67**(16), 2391–2393 (1995).
- [5] S. T. Cundiff, "Coherent Spectroscopy of Semiconductors," *Opt. Express* **16**, 4639–4664 (2008).
- [6] D. Gammon, E. Snow, B. Shanabrook, D. Katzer, and D. Park, "Homogeneous linewidths in the optical spectrum of a single gallium arsenide quantum dot," *Science* **273**, 87–90 (1996).
- [7] X. Fan, T. Takagahara, J. Cunningham, and H. Wang, "Pure dephasing induced by exciton-phonon interactions in narrow GaAs quantum wells," *Sol. State Commun.* **108**(11), 857–861 (1998).
- [8] T. Takagahara, "Theory of exciton dephasing in semiconductor quantum dots," *Phys. Rev. B* **60**(4), 2638–2652 (1999).
- [9] S. Faeder and D. Jonas, "Phase-resolved time-domain nonlinear optical signals," *Phys. Rev. A* **62**(3), art. no.–033,820 (2000).
- [10] A. Tokmakoff, "Two-dimensional line shapes derived from coherent third-order nonlinear spectroscopy," *J. Phys. Chem. A* **104**(18), 4247–4255 (2000).

Theoretical Investigations of Atomic Collision Physics

A. Dalgarno

Harvard-Smithsonian Center for Astrophysics, Cambridge, MA 02138

adalgarno@cfa.harvard.edu

We have been exploring a range of atomic and molecular processes with an emphasis on collisions in ultracold gases. We have continued studies of the thermalization of an initially energetic parcel of gas traversing a uniform bath gas. We begin the analysis with an accurate calculation of the interaction potential between the projectile and bath atoms or molecules. We ensure that the calculated interaction potential behaves correctly at large internuclear distances R as $-C/R^6$ where C is the van der Waals coefficient. It is a crucial parameter because we have shown that energy loss is determined by a sequence of collisions at small scattering angles, which is controlled by the long-range interaction. After completing calculations of the thermalization of nitrogen atoms in helium gas and argon gas, we examine the case of the heating of an initially cold parcel of hydrogen atoms in neon gas, which is of experimental interest. We were attempting to simulate an experiment proposed by Claudio Cesar and Paola Cirivelli. There are unexpected features of the experiment that we continue to investigate. We are investigating the thermalization of sulfur atoms and helium gas for which we have available a reliable interaction potential and for which measurements have been made.

Ultracold collisions of positive ions and neutral atoms are of increasing interest. The case of Yb^+ in Yb has been the subject of experiments by Grier et al. who measured the cross sections for charge exchange for pairs of different isotopes



where A and B label the isotopes. Grier et al. found that in the range of kinetic energy E from 3.4×10^{-6} to 4×10^{-3} eV, ratio of 1000 the rate coefficients for the isotope pairs with mass numbers 171, 172 and 174 are the same to a factor of a few and the rate coefficients of the forward and backward factors are equal to each other. We conclude ΔE may be put equal to zero for E much above 3×10^{-6} eV in which case the process simplifies to resonance charge exchange.

Resonance charge exchange is controlled by the lowest ${}^2\Sigma_g^+$ and ${}^2\Sigma_u^+$ states of Yb_2^+ . We have carried out refined calculations of the interaction potentials, again taking care to ensure that they behave correctly as $-1/2\alpha R^{-4}$ at large R where α is the electric dipole polarizability of Yb. They were calculated with the multi-reference average quadratic coupled-cluster method combined with the relativistic pseudo-potential. The derived polarizability is 144 a.u., in agreement with our earlier determination by a direct evaluation.

In resonance scattering of identical isotopes, $\Delta E = 0$ and elastic scattering cannot be distinguished from particles undergoing charge exchange. However, we have shown that with increasing energy, two distinct peaks develop in the angular distribution, one at forward scattering angles and the other at backward angles. Empirically forward scattering is attributed to elastic collisions and backward to charge exchange. At near zero energy the cross sections are sensitive to the isotope masses. The table presents the scattering lengths.

Table 1

	Isotope Mass Number						
	168	170	171	172	173	174	176
a_g	474	21477	2077	-2761	-43253	4453	-9715
a_u	-719	923	1866	3048	4608	7105	30815

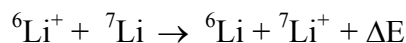
At energies above 10^{-4} eV, the extreme sensitivity no longer occurs and the Langevin formula in which the rate coefficients varies as the reduced mass $\mu^{-1/2}$ is remarkably successful, as also demonstrated by the experiments.

We have also determined the elastic and charge exchange cross sections for lithium for which we do know the isotope shift between ${}^6\text{Li}$ and ${}^7\text{Li}$. It is very small at 7.5×10^{-5} eV. The scattering lengths corresponding to the ${}^2\Sigma_g^+$ and ${}^2\Sigma_u^+$ interaction potentials for elastic scattering of ${}^6\text{Li}^+$ by ${}^6\text{Li}$ and ${}^7\text{Li}^+$ by ${}^7\text{Li}$ are given in table 2. As expected, they are very sensitive to the masses. Indeed, they have different signs.

Table 2

		α		β
${}^6\text{Li}+{}^7\text{Li}^+ \rightarrow {}^6\text{Li}^+ + {}^7\text{Li}$		286		145
	a_g		a_u	
${}^6\text{Li}^+ + {}^6\text{Li}^+$	-918		-1425	
${}^7\text{Li}^+ + {}^7\text{Li}^+$	14337		1262	

We have also calculated the charge exchange and elastic cross sections for the near resonant collisions of ions with atoms of a different isotopic mass



The Born-Oppenheimer approximation must be corrected and the theory we have constructed leads to a pair of coupled equations. The coupling operators connect nuclear and electronic motion and are proportional to the difference in mass of the isotopes. The potential energy curves are modified in such a way that they separate at large distance to the correct energetic limits, $\pm \Delta E/2$.

For the two channel problem, the zero energy elastic and inelastic collisions can be characterized by a complex scattering length $\alpha - i\beta$. For the ${}^6\text{Li}$ and ${}^7\text{Li}$ system, the scattering length is 286-145i. The imaginary part corresponds to a zero temperature rate coefficient of $2.1 \times 10^{-9} \text{ cm s}^{-1}$.

The Langevin rate coefficient, assuming reaction occurs with a probability of one half once the centrifugal barrier is overcome, is 1.6×10^{-9} in good agreement, perhaps by chance. The velocity dependence of the Langevin rate coefficient is the same as that holding in the Wigner regime though the physical principles appear to be different and exceptions do occur. In the Wigner regime the cross sections for the endothermic channel vary inversely as the velocity.

Splitting of the ${}^2\Sigma_g$ and ${}^2\Sigma_u$ potentials is critical in controlling the scattering of an ion and its parent atom. For ultra cold collisions, the interaction at large internuclear distances is needed. For Li_2^+ , conventional variational calculations of the kind we have carried out can achieve the required accuracy, but for more complex systems they become very challenging. $\Sigma_u - \Sigma_g$ splitting decreases exponentially and it is difficult to obtain comparable accuracy for the two states.

We have explored a method based on the Holstein-Herring formula which expresses the $\Sigma_u - \Sigma_g$ difference directly in terms of polarized wave functions. The formula yields the energy difference as an integral over the median plane, corrected for normalization. We tested the procedure for the

case of Li_2^+ for which we have elaborate variational calculations, and for H_2^+ for which exact numerical data are available. Table 3 lists results for Li_2^+ . H – H is Holstein-Herring

Table 3

R	8	9	10	12	15	20
Variational	0.0647	0.0489	0.03454	0.01538	0.00391	0.00032
H-H	0.0648	0.0473	0.3365	0.01566	0.00414	0.00034

There have been many studies of the use of magnetic fields to shift the energy levels of atomic and molecular systems into resonance with a transient collision complex, driving large changes in the parameters that control the collision. Extending an analysis by A.J. Moerdijk, B.J. Verhaar and T.M. Nagtegaal, we combine a coupled channel expansion with a field-dressed formalism to describe the collision complex in an external field. The scattering length is a function of the amplitude and frequency of the applied radio frequency field. We show that rf fields can induce Feshbach resonances whose positions and widths can be tuned by changing the parameters of the rf field.

Collisions of molecules are complicated events. An interesting example is provided by the hydroxyl radical OH which has $^2\Pi$ symmetry and is important in aeronomy and astronomy. Several studies have been reported on collisions of OH with the inert gases. Of particular interest are collisions of magnetically trapped OH molecules with He and with D_2 for which cross sections have been measured as a function of collision energy. We have extended collision theory to collisions of OH and CH molecules in the presence of electric fields and computed cross sections over a temperature range from 1K to 200 K. The electric field introduces structures which dominate the inelastic scattering by coupling states of opposite parity. Our total cross-sections are quite different from the measured cross sections.

The measurements refer to trap loss in the presence of a magnetic field which may modify the dynamics of the molecular collisions. We have analyzed the measured trap loss using a rigorous quantum mechanical theory of the scattering of $^2\Pi$ molecules in external fields, taking into account the effects of non-uniform magnetic and optical trapping fields in which it is assumed that trap loss occurs when the kinetic energy of the gas molecule exceeds the trap depth. The cross section for trap loss is always smaller than the total cross-section. The calculations yield a trap loss cross section consistent with the experimental data.

Responding to a query from Y. Takahashi and John Doyle, we initiated calculations on the properties of the molecule LiYb. We used a sophisticated multi-reference configuration interaction and coupled cluster method to determine the potential energy curves of the ground and low-lying excited states of LiYb.

We then included scalar relativistic effects by means of the Douglas-Kroll Hamiltonian and effective core potential and the spin-orbit complex was calculated by the full microscopic Breit-Pauli operator. The static dipole polarizability and Frank-Condon factors were obtained. The non-adiabatic interaction between the $2^2\Sigma$ and $3^2\Sigma$ states was calculated.

The ground state of LiYb has $^2\Sigma$ symmetry and it separates to $\text{Li}^2\text{S}+\text{Yb}^1\text{S}$. The second and third asymptotes are $\text{Li}^2\text{P}+\text{Yb}^1\text{S}$ and $\text{Li}^2\text{S}+\text{Yb}^3\text{P}$, which gives rise to molecular states $1^2\Pi$ and $2^2\Sigma$ and $3^2\Sigma$ and $2^2\Pi$. $\text{Li}^2\text{S}+\text{Yb}^3\text{P}$ also interact in the $^4\Sigma$ and $^4\Pi$ molecular states. Higher-lying states correlate to excited atoms, resulting from the configuration $4f5d$. They lie 0.5 eV higher and we do not consider them further. The spin unrestricted coupled cluster method taking account of the 1s 2s electrons of Li and 5s5p4f6s of Yb was used to obtain the potential energy curves of the $1^2\Sigma$ ground state and the excited $^4\Sigma$ and $^4\Pi$ states. For the excited doublet states a state-averaged multichannel self-consistent field including all spin-free doublets is applied.

The interaction potentials all behave asymptotically as $-C/R^6$. We have carried out independent calculations of the values of C_6 which also provide a test of the accuracy of the potential energy curves. The values of C_6 for the $1^2\Sigma$, $2^2\Sigma$ and $1^2\Pi$ states are 1606, 5994 and 2062 a.u. respectively. Electric dipole moments were obtained by expanding the energy change caused by weak electric fields, a procedure that also yields the dipole polarizability. Atomic data on spin-orbit splitting were used as tests of our procedure for evaluating the spin interactions and constructing the resulting potential energy curves. We find that the quartet states are weakly bound. The $1^4\Sigma$ has a dissociation energy of 4466 cm^{-1} and the $1^4\Pi$ has a dissociation energy of 781 cm^{-1} . There are crossings of the doublet and quartet states.

The electric dipole moment of the ground $^2\Sigma$ state is small, of the order of -0.06 Debye. That of the excited $^4\Sigma$ state may be larger. Elaborate calculations are in progress.

Publications 2008-2010

- P. Zhang, V. Kharchenko, A. Dalgarno, Y. Matsumi, T. Nakayama and K. Takahashi, Approach to Thermal Equilibrium in Atomic Collisions, *Phys. Rev. Lett.* 100, 103001, 2008.
- E. Bodo, P. Zhang and A. Dalgarno, Ultracold Ion-Atom Collisions: near Resonant Charge Exchange, *New J. Phys.* 10, 033024, 2008.
- P. Zhang and A. Dalgarno, Long-Range Interactions of Ytterbium Atoms, *Molec. Phys.*, 106, 1525, 2008.
- D. Vrinceanu and A. Dalgarno, Long-range Interaction between Ground and Excited State Hydrogen Atoms, *J. Phys. B At. Mol. Opt. Phys.* 41, 215202, 2008.
- T. V. Tscherbul, P. Zhang, H. R. Sadeghpour, N. Brahms, Y. S. Au, J. M. Doyle and A. Dalgarno, Collision-induced Spin Depolarization of Alkali-Metal Atoms in Cold ^3He Gas, *Phys. Rev. A* 78, 060703R 2008.
- T. V. Tscherbul, G. C. Groenenboom, R. V. Krems and A. Dalgarno, Dynamics of $\text{OH}(^2\Pi)$ -He Collisions In Combined Electric and Magnetic Fields, *Faraday Discuss.* 142, 127, 2009.
- M. J. Jamieson, A. Dalgarno, M. Aymar and J. Tharmel, A Study of Exchange Interactions in Alkali and Molecular Ion Dimers with Application to Charge Transfer in Cold Cs, *J. Phys. B: At. Mol. Phys. J. B* 42, 095203, 2009.
- S. Bovino, P. Zhang, V. Kharchenko and A. Dalgarno, Trapping Hydrogen Atoms from a Neon-Gas Matrix: A Theoretical Simulation, *J. Chem. Phys.* 131, 054302, 2009.
- Z. Pavlovich, T. V. Tscherbul, H. R. Sadeghpour, G. C. Groenenboom and A. Dalgarno, Cold Collisions of $\text{OH}(^2\Pi)$ Molecules with He Atoms in External Fields, *J. Phys. Chem. A* 113, 14670, 2009.
- P. Zhang, E. Bodo and A. Dalgarno, Near Resonance Charge Exchange in Ion-Atom Collisions of Lithium Isotopes, *J. Phys. Chem. A* 113, 15085, 2009.
- J. L. Nolte, B. H. Yang, P. C. Stancil, Teck-Ghee Lee, N. Balakrishnan, R. C. Forrey and A. Dalgarno, Isotope effects in complex scattering lengths for He collisions with molecular hydrogen, *Phys. Rev. A* 81, 014701, 2010.
- B.L. Burroughs, A. Dalgarno and M. Cohen, Calculation of exchange energies using algebraic perturbation theory, *Phys. Rev. A* 80, 1042508, 2010.
- T. V. Tscherbul, T. Calarco, I. Lesanovsky, R. V. Krems, A. Dalgarno and J. Schmiedmayer, rf-field-induced Feshbach resonances, *Phys. Rev. A* 81, 050701, 2010.
- N. Brahms, T. V. Tscherbul, P. Zhang, J. Klos, H. R. Sadeghpour, A. Dalgarno, J. M. Doyle, and T. G. Walker, Formation of van der Waals Molecules in Buffer Gas Cooled Magnetic Traps, *Phys. Rev. Lett.* 105, 033001, 2010.

SISGR: Understanding and Controlling Strong-Field Laser Interactions with Polyatomic Molecules

DOE Grant No. DE-SC0002325

Marcos Dantus, dantus@msu.edu

Department of Chemistry and Department of Physics, Michigan State University, East Lansing MI 48824

1. Program Scope

When intense laser fields interact with polyatomic molecules different types of processes lead to fragmentation, ionization and electromagnetic emission that can span essentially the entire energy spectrum. The objective of this project is to determine to what extent these processes can be controlled by modifying the phase and amplitude characteristics of the laser field according to the timescales for electronic, vibrational, and rotational energy transfer. Controlling the processes will lead to order-of-magnitude changes in the different outcomes from laser-matter interactions.

The proposed work involves experiments in which intense shaped laser pulses as short as 5fs in duration interact with a series of polyatomic molecules. Products of these interactions such as electrons, ions and photons, will be detected in order to provide valuable detailed information relevant to the electronic (<50 fs), and vibrational (10-1000 fs) and rotational (1-100 ps) coherence time scales, as well as the time for intramolecular vibrational randomization process (1-100 ps). The proposed work is unique because it seeks to combine knowledge from the field of atomic-molecular-optical physics with knowledge from the field of analytical chemistry, in particular ion chemistry. This multidisciplinary approach is required to understand to what extent the outcome from laser-molecule interactions depends on the field, and to what extent it is the result of ion stability. The information resulting from the systematic studies will be used to construct a theoretical model that tracks the energy flow in polyatomic molecules following interaction with an ultrafast pulse.

2. Recent Progress

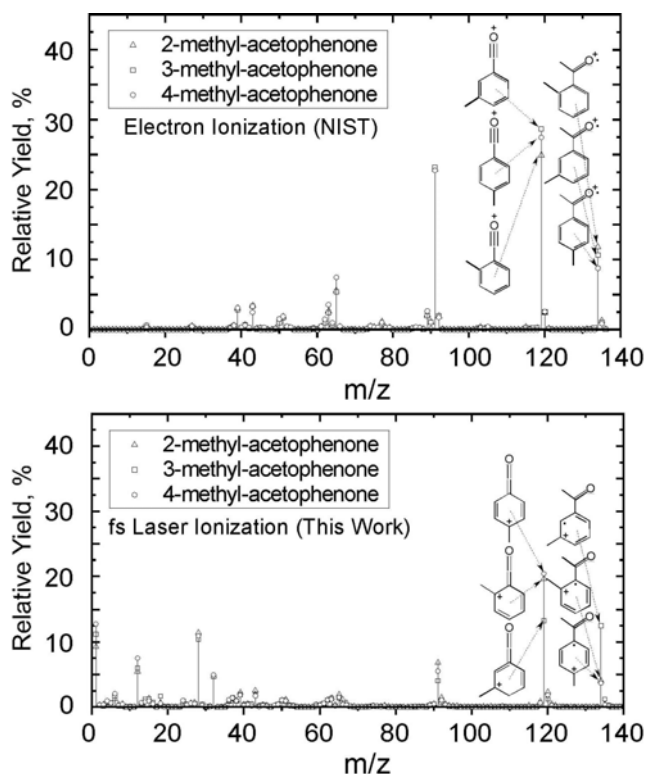


Fig. 1. Electron impact (obtained from NIST) and femtosecond laser induced dissociation mass spectra for three methyl substituted acetophenone compounds.

Our first project focused on the fragmentation of acetophenone and other acetophenone derivatives. This molecule has been the subject of a number of studies aimed at controlling its fragmentation with shaped ultrafast pulses. Previous work from our group focused on the identity of the fragments and inconsistencies with published data. Here we focused on ultrafast dynamics that determine the formation of the major fragments.

First we compared the electron impact (70eV) and femtosecond induced fragmentation of methylated acetophenone molecules. We find that electron impact causes few differences in fragmentation, however, femtosecond pulse ionization causes a large difference for 3-methyl acetophenone which has the methyl group in the meta (intermediate) position with respect to the carbonyl group. 3-methyl-acetophenone is found to fragment significantly less than the other two methylated isomers. In particular, the amplitude of the peak at 134 m/z for ortho and para substituted isomers is one third the amplitude of the meta substituted isomer. The decreased likelihood to fragment can be explained in terms of resonance structures of the long-lived radical ion species.

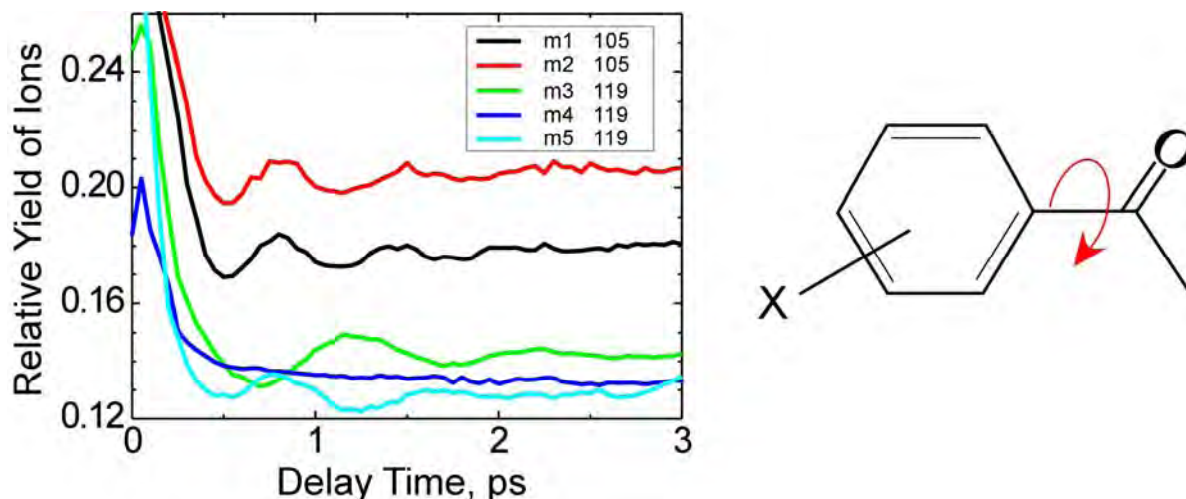


Fig. 2. Yields of benzoyl ion from acetophenone, d3-acetophenone, and three methyl acetophenone isomers plotted with respect to the delay between TL pump pulse and Chirped probe pulse. Molecules are m1: acetophenone; m2: d3-acetophenone; m3: 2-methyl-acetophenone; m4: 3-methyl-acetophenone; m5: 4-methyl-acetophenone. A schematic of the torsional vibration of the phenyl ring is shown on the right.

From the change in ion abundances with respect to the time delay between two pulses, we are able to elucidate a number of ladder climbing and ladder switching pathways and their time constants.¹ The yield of benzoyl ions, with 105 m/z , was found to oscillate in time. By examining deuterated acetophenone and methyl-substituted acetophenone isomers, we confirmed the oscillations were caused by the torsional motion of the carbonyl group. Substitutions that change the moment of inertia of the phenyl group (ortho substitution) lengthen the oscillation period. This observation indicates that appropriately timed pulses would be allowed to allow conformational control of chemical reactions. Our findings have been submitted for publication in the Journal of Physical Chemistry.

3. Future Plans

One of the remaining questions in our research on acetophenone is what causes the torsional motion of the carbonyl group. We assumed that there is a geometry change of the molecule as it is excited from the ground state to the excited state. Results from our ab initio calculations showed that the ion state is planar. We are presently performing four-wave mixing experiments to determine if stimulated Raman scattering by the femtosecond laser is the process that initiates the torsional motion. If this is the case we will have elucidated a means to introduce molecular motion prior to dissociation. We can then employ this approach for controlling other molecular systems.

One of the important goals of our proposed work was to upgrade our molecular beam in order to be able to carry out experiments in which photoelectron and photoions are detected in coincidence (PEPICO). Unfortunately, the vacuum requirements for such measurements (oil free 10^{-10} Torr) exceed the capabilities of our present system (diffusion pump, 10^{-7} Torr). We have requested supplemental funds to upgrade the pumping system so that we can carry out the PEPICO imaging experiments. The advantage of PEPICO will be that we will be able to determine how much energy was deposited in the molecule by the laser field to produce each of the different fragment ions. We will also be able to determine where the electron came out of in the molecule.

4. Publications Resulting from this Grant 2009-2010:

¹Xin Zhu, Vadim V. Lozovoy and Marcos Dantus, Photodissociation dynamics of polyatomic molecules from 10^{-14} to 10^{-10} sec studied by mass spectrometry," J. Phys. Chem. A. (submitted 2010).

Production and trapping of ultracold polar molecules

D. DeMille

Physics Department, Yale University, P.O. Box 208120, New Haven, CT 06520

e-mail: david.demille@yale.edu

Program scope: The goal of our project is to produce and trap polar molecules in the ultracold regime. Once achieved, a variety of novel physical effects associated with the low temperatures and/or the polar nature of the molecules should be observable. We will build on recent results from our group, in which we form and trap ultracold RbCs. We plan to transfer the vibrationally excited molecules currently trapped into their absolute internal ground state and then study the resulting sample of polar molecules. We will investigate a variety of techniques for creating, manipulating and probing this sample, including methods for “distilling” a pure ground-state sample, imaging detection, continuous accumulation of ground state-molecules, etc. Once in place, we will study chemical reactions at ultracold temperatures.

Our group has pioneered techniques to produce and state-selectively detect ultracold heteronuclear molecules. These methods yielded RbCs molecules at translational temperatures $T < 100 \mu\text{K}$, in any of several desired rovibronic states—including the absolute ground state, where RbCs has a substantial electric dipole moment. Our method for producing ultracold, ground state RbCs consists of several steps. In the first step, laser-cooled and trapped Rb and Cs atoms are bound together into an electronically excited state, via the process known as photoassociation (PA).¹ These states decay rapidly into a few, weakly bound vibrational levels in the ground electronic state manifold.² By proper choice of the PA resonance, we form metastable molecules exclusively in the $a^3\Sigma^+$ level. We also demonstrated the ability to transfer population from these high vibrational levels, into the lowest vibronic states $X^1\Sigma^+(v=0,1)$ of RbCs³ using a laser “pump-dump” scheme. Two sequential laser pulses drove population first “upward” into an electronically excited level, then “downward” into the vibronic ground state. In these initial experiments, the vibronic ground-state molecules were spread over a small number (2-4) of the lowest rotational levels, determined by the finite spectral resolution of the pump/dump lasers. We state-selectively detect ground-state molecules with a two-step, resonantly-enhanced multiphoton ionization process (1+1 REMPI) followed by time-of-flight mass spectroscopy.⁴

In more recent work, we have incorporated a CO₂-laser based 1D optical lattice into our experiments. This makes it possible to trap and accumulate vibrationally-excited RbCs molecules as they are formed. (Previously, the molecules were not subject to the magneto-optic trapping forces that held the atoms.) In this optical trap, we have demonstrated the ability to hold the precursor Rb and Cs atoms with long lifetimes ($\gtrsim 5$ s). We also have the ability to selectively remove either atomic species by resonant push-beams. We measure molecule number in individual states, using the same methods as earlier. We used these capabilities to measure inelastic (trap loss) cross-sections for individual RbCs vibrational levels on both Rb and Cs atoms in the ultracold regime.⁵ We also developed a simple theoretical model for these collisions which matches our data reasonably well. We hope to observe molecule-molecule collisions in the near future, once molecular densities are fully optimized.

We are now preparing to transfer this sample of trapped molecules to their absolute internal ground state. In this $X(v=0, J=0)$ state the molecules should be immune to all (two-body)

inelastic collisional loss processes, and should also possess a sizeable dipole moment ($\sim 1.3 D$). To accomplish this, we plan to use an improved version of the method we demonstrated earlier for producing (untrapped) ground-state molecules. A pair of lasers, tuned to the same transitions as used before, will again be used for the transfer. However, here we plan to use a coherent (STIRAP, Stimulated Raman Adiabatic Passage) process rather than the incoherent, stepwise method as before. Use of STIRAP is made possible by the small size of our sample and the resulting high Rabi frequencies attainable by tight focusing of single-mode diode lasers. We estimate transfer efficiencies of $\sim 80\%$ should be possible.

We have carefully considered limitations on STIRAP due to details of the molecular levels due to e.g. hyperfine and rotational structure. We find that high efficiency of ground-state molecule production almost certainly requires full control of all degrees of freedom, including nuclear spins. This analysis was deepened and informed by our recent experiments studying the level structure of deeply-bound Cs_2 ground-state molecules.⁶ To address this issue, we now optically pump our trapped atoms to spin-stretched states, and plan to use appropriate laser polarizations and transitions to remain in a stretched state throughout the PA and STIRAP processes. Identification of the correct transitions requires knowledge of the hyperfine structure in each electronic level of the process, and we will use the first STIRAP laser to measure this structure in sufficient detail. A similar technique has now been demonstrated for producing ultracold trapped KRb molecules by the JILA group,⁷ validating our basic approach.

Once we have demonstrated the STIRAP transfer to the ground state, we plan to develop a variety of techniques for manipulating and studying this sample. Among the first questions will be the collisional stability of the ground-state molecules. Of particular concern in our approach is loss due to collisions with residual, vibrationally excited molecules. We plan to selectively reintroduce Cs atoms to the trap to address this problem: based on our measurements of “maximal” (i.e., unitarity-limited) inelastic cross-sections for the vibrationally excited molecules, it appears viable to use a high-density Cs cloud as a “scrubber” to eliminate the troublesome species. We note that $\text{RbCs} + \text{Cs}$ collisions (with both species in their absolute lowest hyperfine sublevel) have no two-body inelastic channel energetically available,⁸ so that Cs should not be able to cause loss of the desired ground-state molecules. We also plan to study inelastic loss of RbCs in excited hyperfine sublevels due to collisions with Rb, to see if the surprisingly large loss rates observed by the JILA group in $\text{KRb} + \text{Rb}$ collisions of this type⁹ are also present here.

A novel feature of our current system is the REMPI detection system, which should make it possible to state-selectively detect the products of ultracold chemical reactions in our sample. Based on the recent results from JILA,⁹ we anticipate that $\text{RbCs} + \text{Rb}$ samples will rapidly react to form $\text{Cs} + \text{Rb}_2$; we plan to map out the resulting internal state distribution of the outgoing products. In pure samples of ground state RbCs , chemical reactions are energetically forbidden; however, the reaction barrier can be overcome by vibrationally exciting the molecules.

We also are developing methods for imaging detection of the ground-state RbCs molecules. This is far more difficult than for atoms, because of the lack of cycling optical transitions. However, the experience of the community studying quantum-degenerate atomic gases makes it plain that imaging detection is a tool so powerful it must be maintained. We are now constructing an auxiliary system incorporating an imaging ion detection setup (microchannel plate + phosphor screen + fiber optic image conduit + CCD camera),¹⁰ which will be tested first on atoms in a MOT. Pulsed electric fields will be used to rapidly expand the ions and then accelerate them towards the detector, hence minimizing the effect of Coulomb self-expansion of the ion cloud. Simulations of the system have been performed and indicate that excellent spatial

resolution and detection efficiency should be possible. Once this method is established, we can effectively study the variety of interesting two-body and many-body physics associated with polar molecules. These include phenomena such as extraordinarily large ($\sim 10^{-8} \text{ \AA}^2$) elastic collision rates with nontrivial dependence on the strength of a polarizing electric field and the attendant possibility of evaporative cooling,^{11,12} many-body states such as liquid-crystal-like chains¹³ or dipolar crystals;¹⁴ etc.

Finally, we have recently investigated in more detail the behavior of polar molecules held in optical traps, in the presence of DC electric fields E to polarize the molecules. We find that the DC field modifies the optical tensor polarizability and at certain values of E different pairs of rotational states experience the same trap potential. Similarly, for a particular “magic angle” between the light polarization and E , the tensor shifts vanish and all rotational sublevels experience the same trap potential.

References

- ¹A.J. Kerman *et al.*, Phys. Rev. Lett. **92**, 033004 (2004).
- ²T. Bergeman *et al.*, Eur. Phys. J. D **31**, 179 (2004).
- ³J.M. Sage, S. Sainis, T. Bergeman, and D. DeMille, Phys. Rev. Lett. **94**, 203001 (2005).
- ⁴A.J. Kerman *et al.*, Phys. Rev. Lett **92**, 153001 (2004).
- ⁵Eric R. Hudson, Nathan B. Gilfoy, S. Kotochigova, Jeremy M. Sage, and D. DeMille. Inelastic collisions of ultracold heteronuclear molecules in an optical trap. Phys. Rev. Lett. **100**, 203201 (2008). [DOE SUPPORTED]
- ⁶D. DeMille, S. Sainis, J. Sage, T. Bergeman, S. Kotochigova, and E. Tiesinga. Enhanced sensitivity to variation of m_e/m_p in molecular spectra. Phys. Rev. Lett. **100**, 043202 (2008). [DOE SUPPORTED]
- ⁷K.-K. Ni *et al.*, Science **322**, 231 (2008).
- ⁸C.E. Fellows *et al.*, J. Mol. Spectrosc. **197**, 19 (1999); J.Y. Seto *et al.*, J. Chem. Phys. **113**, 3067 (2000); C. Amiot and O. Dulieu, J. Chem. Phys. **117**, 5155 (2002).
- ⁹S. Ospelkaus *et al.*, Science **327**, 853 (2010).
- ¹⁰D.W. Chandler and P.L. Houston, J. Chem. Phys. **87**, 1445 (1987); A.J.R. Heck and D.W. Chandler, Annu. Rev. Phys. Chem. **46**, 335 (1995).
- ¹¹D. DeMille, D.R. Glenn, and J. Petricka, Eur. Phys. J. D **31**, 275 (2004).
- ¹²M. Kajita, Eur. Phys. J. D **20**, 55 (2002); C. Ticknor, Phys. Rev. A **76**, 052703 (2007).
- ¹³D.-W. Wang, M.D. Lukin, and E. Demler, Phys. Rev. Lett. **97**, 180413 (2006).
- ¹⁴H. P. Buechler *et al.*, Phys. Rev. Lett. **98**, 060404 (2007).

Attosecond and Ultra-Fast X-ray Science

L. F. DiMauro and P. Agostini
OSU Dept of Physics
191 W Woodruff Ave, Columbus, OH 43210
dimauro@mps.ohio-state.edu
agostini@mps.ohio-state.edu

Attosecond light pulses from gases offer a transition to a new time-scale and open new avenues of science while complementing and directly contributing to the efforts at the LCLS. The main objectives of this grant is the development of competency in generation and metrology of attosecond pulses using Mid-Infrared drivers and a strategy of employing these pulses for studying multi-electron dynamics in atomic systems. It focuses on applications in which attosecond pulses are produced and transported to a different region of space and applied to a different target, thus providing the great degree of spectroscopic flexibility. The proposal has also a thrust at the LCLS for studying the scaling of strong-field interactions into a new regime of x-ray science.

The **recent progress** includes the measurement of the wavelength scaling of High Harmonic Generation, a study of Below Threshold Harmonics in a Keldysh-Scaled System, the completion of the new OSU Attosecond beamline/end-station and the start of an experimental program at the LCLS XFEL at SLAC.

Wavelength Scaling in High Harmonic Generation with Long Wavelength Fundamental Fields. The wavelength scaling of high harmonic radiation provides an interesting and viable route for producing shorter attosecond bursts in the x-ray regime. Thus, our program has focused on experimental verification using a high-energy optical parametric amplifier (OPA). The OPA system generates 40 fs pulses with 0.7-1.1 mJ energy over the 1-2 μm range while 0.8 μm pulses are derived directly from a Ti:sapphire pump. The high harmonic measurements establish the real world quantities for evaluating the source viability. Our studies show that the high harmonic distributions extend to higher photon energy as the wavelength changes from 0.8 μm to 2 μm *at constant intensity* and scale approximately as λ^2 , λ is the fundamental wavelength, as predicted by the rescattering model. Currently, we can generate 200 eV pulses from argon that are viable for attosecond applications. The harmonic yield in argon using 2 μm pulses is lower than that produced by 0.8 μm over a spectral bandwidth (35-50 eV) common to both. However, the brightness of the 2 μm -pumped harmonic source is superior to the 0.8 μm source at energies ($50 \leq h\nu \leq 200$ eV) unreachable by the latter. In addition, as described below the 2 μm source results in inherently shorter attosecond pulses than its 0.8 μm counterpart.

The attochirp is defined as the derivative of the emission times as a function of harmonic energy. It is easy to see that for a given class of quantum paths the attochirp is almost constant (i.e. nearly perfect quadratic spectral phase). It also follows that the attochirp is proportional to the ratio of the fundamental laser cycle period to the harmonic cutoff energy. An effective way to reduce the attochirp is to exploit the wavelength scaling. Since the laser period is proportional to λ and the cutoff energy to λ^{-2} , their ratio, and thus the attochirp should scale as λ^{-1} . Various methods based on two-color photoionization have been developed for spectral phase measurements. We adopted an all-optical method in which high harmonics are generated using a two-color field composed of an intense fundamental field (ω) phase-locked to a weak 2ω field. The 2ω field is sufficiently weak as not to produce high harmonics. The harmonic spectrum

is then composed of even- and odd-order harmonics and the amplitude of the even-order harmonics depends on the relative phase of the two fields and oscillates with a $\pi/2\omega$ periodicity. The phase information is obtained by analyzing the relative phase shift in the oscillating amplitude between even harmonics of successive orders. The measurement of the spectral phase of the high harmonic comb was performed at three different fundamental wavelengths (0.8 μm , 1.3 μm and 2 μm) and on two different inert gas atoms (argon and xenon). This is the first experimental measurement of the wavelength dependence of the attochirp. The experiment clearly demonstrates the reduction with fundamental wavelength of the attochirp, reduced from a value of 41.5 as/eV at 0.8 μm to 21.5 as/eV at 2 μm . Independently of any subsequent compensation, the optimum pulse duration goes down from 250 as at 0.8 μm to 120 as at 2 μm . In summary, our measurements confirm that longer wavelength fundamental fields produce shorter attosecond bursts, as well as higher photon energy.

Bellow-Threshold Harmonics in a Keldysh-Scaled System. Keldysh formulation implies that the same value of γ (Keldysh parameter) will result in equivalent ionization dynamics. This principle in strong-field physics will allow experimental investigations of HHG and attosecond generation that would otherwise be impractical.

For example, a low binding energy (~ 4 eV) alkali atom interacting with a 4 μm field generates high harmonics similar to an inert gas atom ($I_p \sim 15$ eV) exposed to 0.8 μm laser. Using a Keldysh-scaled system we have performed a temporal characterization of below threshold harmonics (BTH) using Sum Frequency Generation Cross-Correlation Frequency Resolved Optical Gating (SFG XFROG), a technique sensitive to the relative delay between orders. Harmonics were generated in a Cesium vapor interacting with 100 fs, 4 μm pulses. Harmonic orders 5-15 (1.7-5 eV photon energy) were investigated using the XFROG method and thus the experiment probes across the 3.9 eV binding energy threshold of Cesium. The observations reveal a negative group delay dispersion, in stark contrast to the zero-dispersion expected for perturbative harmonics. This result will be briefly discussed and suggests that under the Keldysh-scaling picture BTH VUV harmonics from the 0.8 $\mu\text{m}/\text{Ar}$ system could be used for synthesizing trains of high energy ≤ 1 fs pulses or VUV frequency combs.

Initial experiments at the LCLS XFEL: X-ray nonlinear processes. In October 2009 the first LCLS experimental program began using the AMO end-station. Our group was involved in the first seven weeks of runtime, two of which were awarded to OSU as the lead institution.

Our initial study focused on the interaction with simple atomic targets (helium and neon). Total ion yield and photoelectron energy spectrum were recorded as a function of intensity for wavelengths between 0.8-2 keV. The helium measurement provided valuable information on the XFEL performance. For example, the ratio of $\text{He}^{2+}/\text{He}^+$ ionization on x-ray pulse energy revealed a maximum intensity of 5×10^{16} W/cm², approximately an order of magnitude less than expected. Different analysis also provided insight into 2nd harmonic content in the x-ray beam. The lower intensity was a major impediment for observing ATI in helium and indeed, the measurements produced no evidence of an ATI electron peak (2-photon, one-electron ionization) near 1.6 keV.

For neon, ion and electron measurements were performed to study the ionization of a K-shell electron by simultaneous absorption. It was found that the LCLS easily ionizes at least 8-electrons from neon, the first case of sequential atomic ionization from the inside out. Preliminary simulations indicate that at the intensities actually achieved during the experiment a 2-photon, 2-electron valence stripping of excited states of Ne^{7+} (energetically permitted) could

produce a non-linear behavior. When confirmed by the ongoing analysis the measurement provides the first signature of a two-photon process in the x-ray regime.

The OSU Attosecond Beamline/End-station and LCLS Instrumentation. The OSU attosecond beamline/end-station is capable of performing RABBITT measurements, among others. The apparatus is operational and preliminary measurements will be presented. It consists of three vacuum chambers: harmonic generation source, x-ray optics and electron energy spectrometer. The optical system is contained within the vacuum chambers and has automated opto-mechanical positioning with a measured interferometric stability of 60 *as* during normal operation. In the harmonic source chamber, high harmonics are generated in a high density gas channel interacting with an intense long wavelength laser pulse. A probe beam, e.g. for RABBITT, is derived by splitting a small fraction (~5 %) of the fundamental beam. A crucial design feature of the harmonic source chamber is a sufficient large platform to support a variety of optical geometries, different configurations of the gas target, beam manipulation and different wavelength (0.8-2 μm) operation. The high harmonic and probe beams propagate independently before being recombined in the differential pumped x-ray optics chamber. The chamber contains a toroidal mirror (500 eV bandpass) for focusing the harmonic beam and a spherical mirror for focusing the probe beam. Both the focused harmonic and probe beams spatially overlap approximately at 1.5 m pass the toroidal mirror. The beamline is designed to allow user-specific end-station configurations.

Our attosecond program and the AMO end-station at LCLS had a similar need for an electron spectrometer with high collection efficiency and good energy resolution (1/100). We designed and constructed a magnetic bottle spectrometer for OSU and LCLS. The spectrometer has high collection efficiency while maintaining a high energy resolution (0.7%). The magnetic bottle provides an important single-shot spectral analysis of the LCLS and has also served as the primary instrument in a number of experiments, e.g. side-band dressing.

Future plans are focused on applying attosecond light for studying electron dynamics. The long wavelength driver strategy has established itself as the enabling technology for the proposed research. We envision both applications of the existing source for fundamental tests of attosecond control and metrology, and developments towards atomic length and time scales, pushing high harmonic generation into kilovolt photon energies (x-rays) while defining new limits on attosecond pulse durations. Assuming that the project will be renewed the following experiments will be pursued:

- **Time-resolved strong-field coherent (e, 2e) physics.** We will investigate strong-field double ionization using attosecond pulses to inject electrons into the single ionization continuum at a specific phase of an intense laser field.
- **Attosecond shake-up.** We will use attosecond pulse trains to investigate electron shake-up (impulsive excitation) following inner-electron atomic ionization.
- **Controlling final state electron-electron correlation** using the CIEL detector developed by Huetz et al.
- **Attosecond Probing of BTH:** RABBITT or streaking measurements are limited by the ionization potential of the target atoms thus rendering studies of BTH impossible. A solution to this problem is to use a target atom with a lower ionization potential than the generating atom.
- **A more precise measurement and broader survey of the wavelength-dependence** of the attochirp will be performed employing the RABBITT method.
- **A search for nonlinearities** at x-ray frequencies and the understanding of the strong-field limit at high=frequencies.

- **Auger decay and x-ray pulse measurements** will be performed with the LCLS using a novel self-referencing Streaking technique.

Publications:

1. "Progress Report on the LCLS XFEL at SLAC", L. F. DiMauro *et al.*, J. Phys. **88**, 012058 (2007).
2. § "Scaling Strong-Field Interactions towards the Classical Limit", P. Colosimo *et al.*, Nat. Phys. **4**, 386-389 (2008).
3. Complete Momentum Analysis of Multi-Photon Photo-Double Ionization of Xenon by XUV and Infrared Photons", O. Guyetand *et al.*, J. Phys. B **41**, 065601 (2008).
4. § "Atoms in high intensity mid-infrared pulses", P. Agostini and L. F. DiMauro, Contem. Phys. **49**, 179-197 (2008).
5. "Attosecond Synchronization of High Harmonics from Mid-Infrared Drivers", G. Doumy *et al.*, Phys. Rev. Lett. **102**, 093002 (2009).
6. "The Frontiers of Attosecond Physics", G. Doumy *et al.*, in Proceedings of the International Conference on Atomic Physics [ICAP 2009] (World Scientific Press, Singapore, 2009), 333-343.
7. "XFROG phase measurement of threshold harmonics in a Keldysh scaled system", E. Power *et al.*, Nature Photonics, **4**, 352-356 (2010).
8. "Observation of High-order Harmonic Generation in a Bulk Crystal", S. Ghimire *et al.*, Nat. Phys., submitted.
9. "Driving-frequency scaling of quantum paths", T. Augustine, P. Salieres, F. Catoire, P. Agostini and L. F. DiMauro, Phys. Rev. A, submitted.
10. "Femtosecond electronic response of atoms to ultraintense x-rays", L. Young *et al.*, Nature **466**, 56-61 (2010).
11. "Ultra-intense x-ray induced ionization, dissociation and frustrated absorption in molecular nitrogen", M. Hoener *et al.*, PRL **104**, 253002 (2010).
12. "Auger electron angular distributions of double core hole states in the molecular reference frame", J. Cryan *et al.*, PRL (2010), accepted.

Imaging of Electronic Wave Functions During Chemical Reactions

L. F. DiMauro¹, P. Agostini¹ and T. A. Miller²

¹The Ohio State University, Department of Physics, Columbus, OH 43210

²The Ohio State University, Department of Chemistry, Columbus, OH 43210

dimauro@mps.ohio-state.edu, agostini@mps.ohio-state.edu, miller@chemistry.ohio-state.edu

This work is part of an ambitious experimental program designed to meet the challenge of “watching” and “clocking” the electron motion during chemical bond breaking. It builds upon a novel approach combining the technical advances in both coherent attosecond (10^{-18} s) bursts of XUV light and tomographic methods for the imaging of the molecular wave function. Exploiting the fundamental wavelength scaling principles of strong-field physics that occur in these processes allows for improved spatial and temporal accuracy in the methods [1, 2].

Over the past years we have developed the tools, skills and metrology necessary to conduct the proposed imaging experiments. **Progress** on this project to date includes:

Long Wavelength Driven Tomography.

A benchmark of the proposal was to first reproduce and understand the elements for constructing an image of the N_2 ground state using $0.8 \mu\text{m}$ excitation, as reported by the NRC group [3]. In the experiment 30-50 fs light pulses from a 1-3 kilohertz repetition rate laser system interact with a *cw*-gas jet expansion of N_2 . The supersonic expansion produces some rotational pre-cooling and allows for improved impulsive alignment of the N_2 molecules. The experiment is performed using two temporally delayed linearly polarized pulses: (1) a weak ($< 10^{13} \text{ W/cm}^2$), $0.8 \mu\text{m}$ *pump* pulse impulsively aligns the molecule and (2) a delayed intense laser ($> 10^{14} \text{ W/cm}^2$) *probe* pulse at either $0.8 \mu\text{m}$ or $1.3 \mu\text{m}$ drives ionization and harmonic generation. The relative delay, intensity and polarization of both pulses can be independently varied. The first half-revival of the N_2 rotational wave packet near 4-5 ps after the pump pulse shows the usual characteristics, an increase around 4.1 ps corresponding to harmonic generation from N_2 that are strongly aligned along the probe’s polarization axis while the minimum at 4.5 ps corresponds to the N_2 molecules being anti-aligned. The $0.8 \mu\text{m}$ probe experiments have conditions and results similar to those reported by Itatani *et al.* Following spectral and spatial filtering the high harmonic radiation is spectrally dispersed by a Hettrick monochromator and recorded on an x-ray CCD.

The Tomographic Reconstruction.

The procedure for the tomographic reconstruction using the $0.8 \mu\text{m}$ and $1.3 \mu\text{m}$ harmonic data is functional and the initial results for the nitrogen HOMO have been obtained. The steps of the reconstruction procedure include a 2D inverse Fourier transform obtained from the 2D Fourier transform of the dipole moment obtained by successive 1D transforms and application of the Fourier slice theorem. It is based on a number of assumptions that impose limitations to the accuracy of the reconstructed wave function. We have, at this point, not tried to improve on the method itself but essentially endeavored to learn how to apply it, in order to assess the

importance of these assumptions for the long wavelength case. Besides the Fourier manipulation, the method involves the measurement of a reference harmonic spectrum from a spherically symmetric system with a similar ionization potential, e.g. Ar and N₂, and the knowledge of a spectral phase shift of the harmonics. Some serious issues concerning the uniqueness of the orbital reconstruction have revealed themselves. One of our goals is to evaluate the improved spatial resolution resulting from the sampling of the wave function in **k**-space, e.g. shorter deBroglie wavelength, over the extended harmonic comb produced by longer wavelength drivers. The increased resolution we have found substantiate the efficacy of long wavelength drivers. However, discrepancies between our reconstructed wavefunction and the theoretical modeling exist. Clarification of these issues is an essential part of the proposed work and is presently in progress. Some other issues of the reconstruction procedure must still be clarified, particularly the role of a phase rotation and, probably more importantly that of the harmonic polarization which has been ignored so far due to the lack of data.

Harmonics from Liquid Phase Systems

Because of the great potential in condensed phase studies, we have initiated exploratory experiments to ascertain the feasibility of high harmonic generation in such media with the use of long wavelength drivers since high harmonic light falls into the liquid's transmission window. In our approach a 100 μm flowing sample together with a 100 fs, 3.7 μm fundamental pulse emit radiation along the forward direction. Liquid water, H₂O, and heavy water, D₂O, were chosen for the first experiments. This first measurement of condensed phase harmonics beyond the fifth clearly shows that even though H₂O and D₂O have identical electronic structure, their propensity to generate harmonics is different in amplitude and maximum photon energy. While the intensity dependence of the harmonic yield is consistent with perturbation theory (possibly because the effective intensity in the liquid was significantly lower than estimated in vacuum) the feasibility of a study of molecular structure with sub-cycle resolution is sufficiently intriguing to warrant continued investigations.

Harmonic Beamline/End-Station for Tomography

Our ability to perform the tomography will be greatly enhanced with this apparatus which provides a more flexible platform for implementing our long wavelength drivers and increase our sensitivity and bandwidth for spectral phase measurements. The beamline consists of a high harmonic generation (HHG) source chamber followed by an x-ray optics chamber, each of which contains optical breadboards that are mechanically referenced to commercial optical tables. The vacuum chambers are supported by an independent structure and mechanically decoupled from the optical breadboards through soft-bellow seals. The HHG source chamber allows for different configurations of the gas target, focusing geometry, beam separation and manipulation. The differentially pumped, x-ray optics chamber contains x-ray filtering, dispersion compensation, automated delay line, recombining and focusing optics. A 0.75 m focal length, 4° grazing incidence, toroid mirror operating in a 2f-2f geometry located in the x-ray optics chamber defines the interaction region in the end-station. The end-station is a 2π magnetic bottle electron energy spectrometer. This system allows us to already further characterize 0.8 μm and

1.3 μm harmonics by measuring the relative phases of the harmonics generated from reference atoms Ar, Kr, and Xe as well as unaligned N_2 and CO_2 . Utilizing the space and flexibility designed into each chamber section, implementation of an improved, impulsive alignment scheme based on multiple pump pulses is underway in the HHG chamber while an x-ray ‘polarizer’ is in development for the x-ray optics chamber.

Future plans are aiming at the imaging using long wavelength drivers and towards time-resolved imaging.

Based on our recently acquired competency we plan:

- **Experiments on N_2 and CO_2 .** We will continue to push our studies on N_2 towards 2 μm . The problem of insufficient pre-cooled density which we have met will be solved with the Even-Lavie pulsed valve. The 2 μm reconstruction will provide an excellent benchmark against the shorter wavelength results for accessing the accuracy of the N_2 orbital image. Completion of these keystone investigations is a necessary step towards progressing to other molecular systems.
- **Experiments on Ground State NO.** The NO molecule is an open-shell species with a ground state $X^2\Pi$ rather than the $X^1\Sigma_g^+$ state of N_2 and lower ionization potential (9.26 eV). Moreover NO has a permanent dipole moment. Chemical reactions mostly occur via mechanisms involving open-shell species and it is with precisely such species that the time-dependence of the evolution of the electronic orbitals is of particular interest and most difficult to calculate.
- **Excited State of NO.** To ever succeed in imaging the formation/destruction of chemical bonds, the time evolution of this process must be “clocked” subsequent to initiation by laser excitation of a molecular excited state. To make progress towards this goal we consider the imaging of excited states of the NO molecule. While, in N_2 all accessible excited states lie in the vacuum-UV, in NO there are allowed transitions from the ground state to the $A^2\Sigma^+$ state at 228 nm and to the $B^2\Pi$ state at 218 nm. These wavelengths are short, but can be generated with a UV-OPA.
- **Imaging of a Dissociating State of ICN.** In NO, the electronic orbitals (and nuclear displacements) are “static” on the time-scale of the experiment. Even imaging a static electronic orbital (containing, of course, dynamic motion of the electrons) is a major achievement, particularly for an open-shell, possibly reactive electronic state. However potentially most exciting is the possibility of making a similar image as a chemical bond is made or broken.
- **Electron Diffraction from Unaligned Molecules in the Tunneling Regime** In the tomography method based on HHG, the information on the molecular wave function is carried by the recombination of the field-driven tunnel ionized electron wave packet with its parent core. Alternately, not the entire returning wave packet recombines but instead some are scattered and diffracted by the molecular structure giving rise to an electron momentum distribution that is a fingerprint of the HOMO wave function. We propose experiments based on this principle to complement the tomography

measurements based upon harmonic generation. A collaboration has been established with the theory group of Professor Chii-Dong Lin.

References Cited

1. P. Colosimo *et al.*, Nature Phys. **4**, 386-389 (2008).
2. G. Doumy *et al.*, Phys. Rev. Lett. **102**, 093002 (2009).
3. J. Itatani *et al.*, Nature **432**, 867 (2004).

Publications resulting from these grant.

1. "Scaling Strong-Field Interactions towards the Classical Limit", P. Colosimo *et al.*, Nat. Phys. **4**, 386-389 (2008).
2. "Atoms in High Intensity Mid-Infrared Pulses", P. Agostini and L. F. DiMauro, Contemp. Phys. **49**, 179-197 (2008).
3. "Attosecond Synchronization of High Harmonics from Mid-Infrared Drivers", G. Doumy *et al.*, Phys. Rev. Lett. **102**, 093002 (2009).
4. "The Frontiers of Attosecond Physics", G. Doumy *et al.*, in Proceedings of the International Conference on Atomic Physics [ICAP 2009] (World Scientific Press, Singapore, 2009), 333-343.
5. "High Order Harmonics from Mid-Infrared Drivers for Attosecond Physics", G. Doumy *et al.*, in the Proceedings of Atomic Processes in Plasmas [APiP 2009] (American Institute of Physics, New York, 2009), 1574-1580.
6. "Harmonic generation from the near-resonant excitation of liquid H₂O and D₂O from an intense mid-infrared laser", A. DiChiara, E. Sistrunk, T. A. Miller, P. Agostini and L. F. DiMauro, Opt. Lett., **17**, 113357 (2009).

High Intensity Femtosecond XUV Pulse Interactions with Atomic Clusters

Project DE-FG02-03ER15406

Progress Report to Dr. Jeff Krause

Principal Investigator:

Todd Ditmire

The Texas Center for High Intensity Laser Science

Department of Physics

University of Texas at Austin, MS C1600, Austin, TX 78712

Phone: 512-471-3296

e-mail: tditmire@physics.utexas.edu

Collaborators: J. W. Keto and K. Hoffman

Program Scope:

The nature of the interactions between high intensity, ultrafast, near infrared laser pulses and atomic clusters of a few hundred to a few thousand atoms has been well studied by many groups world wide. Such studies have found some unexpected results, including the striking finding that these interactions appear to be more energetic than interactions with either single atoms or solid density plasmas and that clusters explode with substantial energy when irradiated by an intense laser. Under this phase of BES funding we have extended investigation in this interesting avenue of high field interactions by undertaking a study of the interactions of intense extreme ultraviolet (XUV) pulses with atomic clusters, and most recently, interactions with intense x-ray pulses from the Linac Coherent Light Source (LCLS). The goal of our program is to extend experiments on the explosion of clusters irradiated at 800 nm to the short wavelength regime (1 to 50 nm). The clusters studied range from a few hundred to a few hundred thousand atoms per cluster (ie diameters of 1-30 nm). Our studies with XUV light are designed to illuminate the mechanisms for intense pulse interactions in the regime of high intensity but low ponderomotive energy by measurement of electron and ion spectra. This regime of interaction is very different from interactions of intense IR pulses with clusters where the laser ponderomotive potential is significantly greater than the binding potential of electrons in the cluster. With our XUV studies we are studying cluster explosions the low ponderomotive potential, high intensity short wavelength conditions found in the focus of the LCLS beam.

Most of our studies have been conducted with an XUV source created by converting a high-energy (1 J) femtosecond laser to the short wavelength region through high order harmonic generation. However, our most recent experiments have been conducted on the LCLS AMO beam line. In the harmonics experiments at UT, the harmonics are focused into a cluster jet and the ion and electrons ejected are analyzed by time-of-flight methods. We have been studying van der Waals noble gas clusters in both Xe and Ar. Experiments at higher photon energy at the LCLS examined not only Xe and Ar but CH₄ as well.

Progress During the Past Year

During the third year of this project, we concluded a campaign of experiments using our femtosecond laser-driven high harmonic (HHG) source beamline constructed in the first year of funding. This past year has represented a bridge year on a no cost extension. Work this year on the HHG beamline largely concentrated on data analysis and publication of the last campaign of results in anticipation of the upgrade of the HHG beamline planned for later this year (described below). Instead our major experimental activity this past year focused on the LCLS experiments we performed on clusters in November.

For our studies of femtosecond XUV interactions with clusters we constructed at the beginning of this project, a beamline based on high harmonic conversion of our femtosecond multi-TW Ti:sapphire laser (the THOR laser). Production of harmonic radiation was accomplished by loose focusing with a MgF f/60 lens the compressed output of the 20 TW, 40 fs THOR Ti:sapphire laser into a jet of argon at 200 psi. We separated the harmonics from the IR by imaging an annular beam mask in the infrared beam before the focusing lens onto an aperture after the focus, taking advantage of the fact that the XUV harmonics have substantially less divergence than the infrared beam. This allowed the removal of most of the infrared radiation. To reject scattered infrared light and to pass high harmonics with the energies between 15 eV and 73 eV an additional a 200 nm thin Al filter was used. To select a single XUV harmonic we then employed a specially designed Sc/Si short focal length multilayer mirror optimized for the 21st harmonic at 32.5 eV (38.1 nm) at close to normal incidence. The harmonics were refocused to a peak intensity of $\sim 10^{11}$ W/cm² assuming an XUV pulse duration of 20 fs. These harmonics were focused into the plume of a second, low density cluster jet. This cluster interaction region was located in a separated vacuum chamber. A Wiley McLaren time-of-flight (TOF) spectrometer was used to extract positive ions after photo-ionization of the clusters.

Our experiments centered on van der Waals bonded Xe and Ar clusters, though we have made significant progress on a solid material cluster generator which we anticipate employing on the upgraded HHG beamline described below. Our initial experiments in Xe clusters (reported in our 2008 report) showed evidence for production of Xe charge states up to Xe⁸⁺ and ion energy spectra characteristic of the explosion of a moderate temperature plasma with electron temperature of ~ 8 eV. From these data we concluded that a Xe nanoplasma was formed in large ($\sim 10,000$ atom) Xe clusters when irradiated by our 38 nm pulses, and that plasma continuum lowering created conditions in the nanoplasma that allowed single photon photo-ionization of Xe to at least 5+. We observed no evidence for a Coulomb explosion (which one might expect in a cluster which has been stripped of many of its electrons.) We then conducted a set of experiments during 2009 on large Ar clusters. Those Ar cluster data exhibited evidence for a combination of Coulomb explosion and hydrodynamic expansion. Toward the end of 2009 we collected data on the electron spectra of electrons emitted from the XUV irradiated clusters. Analysis of these data, with an example illustrated in figure 1, show that electrons emitted from the cluster exhibit a broad spectrum, with a shape characteristic of a cool, Maxwellian plasma, completely consistent with our previous conclusions about the formation of a photo-electron heated nanoplasma in these clusters. Both Ar and Xe clusters exhibit very similar electron spectra.

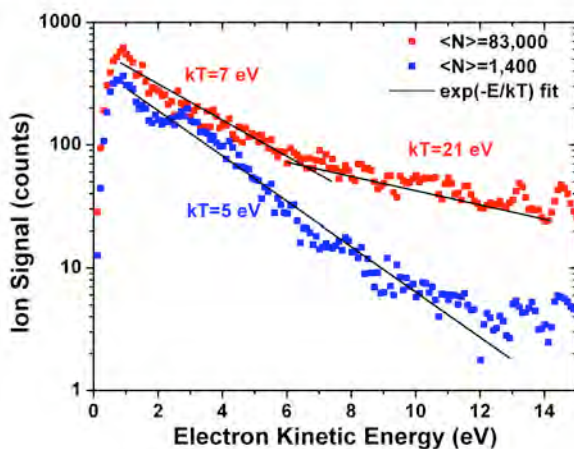


Figure 1: Electron energy spectra from Xe clusters irradiated by intense 38 nm femtosecond pulses. The sharp photo-electron feature from ionization of single atoms has been removed to show the smooth Maxwellian electron spectrum from the clusters.

The focus of our experimental activity during the past year was largely on our experiments on the LCLS. In these collaborative experiments we studied explosions of a wide range of clusters in the LCLS while it operated at both 800 eV and 1.7 keV photon energies. Our experiments were conducted in the AMO end station which was outfitted with our cryogenically cooled gas jet for large cluster production. Data were acquired using the ion and electro TOF spectrometers. Ions were characterized both with the ion TOF working in the a Wiley-McLaren configuration to yield charge states as well as in a field free configuration

to derive ion energy spectra. We are currently preparing a number of the results from this run for publication. One interesting result from these experiment is illustrated in figure 2.

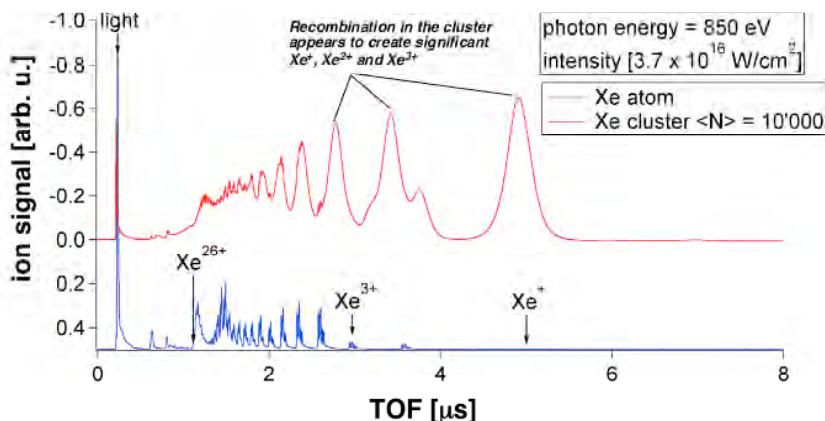


Figure 2: Ion TOF from the Xe atoms and Xe clusters irradiated by the LCLS. The 850 eV photon energy pulses of ~ 50 fs duration were focused to an intensity of $>10^{16}$ W/cm².

Here is shown ion TOF from both Xe atoms and Xe clusters irradiated by the LCLS operating with 850 eV photons focused to intensity of $>10^{16}$ W/cm². The single atoms show the production of charge states up to 26+, characteristic of saturated sequential single photon ionization up to the ionization potential accessible with 850 eV photons. There are virtually no 1+ and 2+ ions in this spectrum as expected because Auger decay further ionizes any single photon ionization. However, when large Xe clusters are irradiated under the same conditions, we observe copious 1+ and 2+ ion production. We attribute this to the formation of a nano-plasma in the Xe cluster and subsequent recombination in the cluster before it can explode.

The effects of recombination in the x-ray irradiation of methane clusters is even more striking. Figure 3 illustrates ion TOF data from CH₄ clusters irradiated by the LCLS at three different intensities. At the highest intensity, all methane derived fragments have disappeared, and the TOF spectrum is completely dominated by H⁺ ions, with virtually no corresponding C ions. We attribute this unexpected behavior to the dynamics of the cluster explosion when disparate ion masses are present. The hydrogen ions explode by Coulomb forces, leaving behind a slowly expanding carbon nano-plasma, which we believe then recombines by three-body recombination. Our data set from the LCLS is very rich, and we are writing up a number of papers describing our various findings from the experiments.

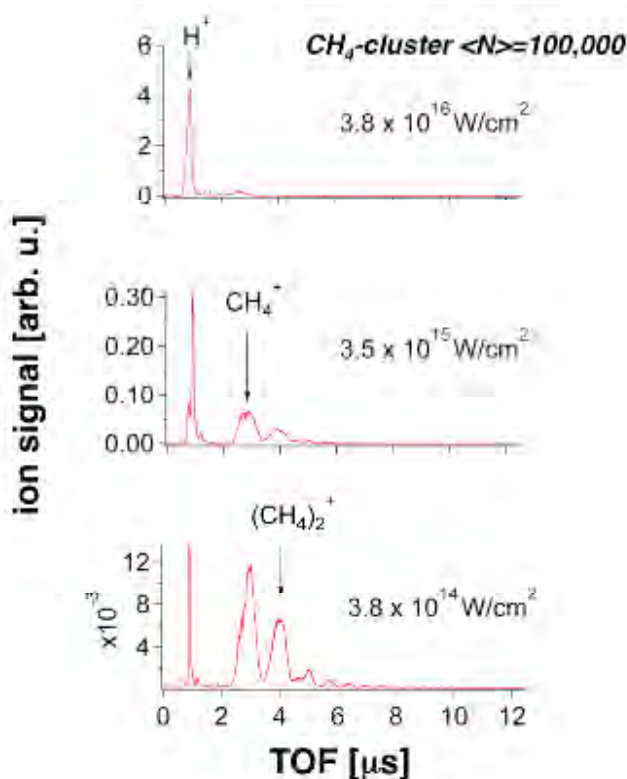


Figure 3: Time-of-flight spectrum of methane clusters irradiated by the LCLS with 1.7 keV photons at three different peak intensities.

Future Research Plans

Our future plans on the study of XUV irradiation of clusters involve moving to higher XUV intensities, with the particular aim of studying the effects of continuum lowering on the ionization dynamics of ions in the cluster nano-plasma. We are in the midst of upgrading the THOR laser to 1 PW (30 J/30 fs). In parallel to this laser upgrade we are completely redesigning the HHG beam line to permit a much longer focal length using a reflective focusing optic. This will allow us to use the entire 30 J to generate harmonics, essentially increasing the focused XUV intensity by over two orders of magnitude to nearly 10^{14} W/cm². With this improved source we would like to study the ionization of mixed clusters, such as tin oxide to explore the effects that a high Z ion has on the ionization potential of the low Z cluster ions (like oxygen). At the higher intensities we also may access a regime in which collisional heating of the cluster nano-plasma may become important.

Our future plans on the LCLS remain contingent on the availability of LCLS beam time. We have entered collaborations with a number of groups, and will be competing for LCLS beam time to explore the effects of photo-ionization heating in the clusters by tuning the LCLS photon energy above and below ionization edges in the cluster ions.

Refereed papers published on work supported by this grant during the past three years

- 1) K. Hoffmann, B. F. Murphy, B. Erk, N. Kandidai, J. Keto, and T. Ditmire, "Studies of Exploding Noble Gas Clusters Irradiated by Intense Femtosecond Pulses of Extreme Ultraviolet Light" *Phys. Rev. A*, submitted.
- 2) B. Erk, K. Hoffmann, N. Kandidai, A. Helal, J. Keto, and T. Ditmire "Transition from Coulomb Explosion to Hydrodynamic Expansion in Rare Gas Clusters" *Phys. Rev. A* submitted.
- 3) K. Hoffmann, B. Murphy, B. Erk, A. Helal, N. Kandidai, J. Keto, and T. Ditmire "High intensity femtosecond XUV pulse interactions with atomic clusters" *J. of High En. Den. Phys.*, **6**, 185 (2010).
- 4) A. P. Higginbotham, O. Semonin, S. Bruce, C. Chan, M. Maindi, T. D. Donnelly, M. Maurer, W. Bang, I. Churina, J. Osterholz, I. Kim, A. C. Bernstein, and T. Ditmire, "Generation of Mie size microdroplet aerosols with applications in laser-driven fusion experiments", *Rev. Sci. Instr.* **80**, 063503 (2009).
- 5) B. F. Murphy, K. Hoffmann, A. Belilopetski, J. Keto, and T. Ditmire, "Explosion of Xenon Clusters Driven by Intense Femtosecond Pulses of Extreme Ultraviolet Light" *Phys. Rev. Lett.* **101**, 203401 (2008).
- 6) S. Kneip, B. I. Cho, D. R. Symes, H. A. Sumeruk, G. Dyer, I. V. Churina, A. V. Belolipetski, A.S. Henig, T. D. Donnelly, and T. Ditmire "K-shell Spectroscopy of Plasmas Created by Intense Laser Irradiation of Micron-scale Cone and Sphere Targets" *J. High Energy Density Physics.* **4**, 41 (2008).
- 7) D. R. Symes, M. Hohenberger, A. Henig, and T. Ditmire, "Anisotropic Explosions of Hydrogen Clusters under Intense Femtosecond Laser Irradiation" *Phys. Rev. Lett.* **98**, 123401 (2007).
- 8) B. Shim, G. Hays, R. Zgadzaj, T. Ditmire, and M. C. Downer, "Enhanced harmonic generation from expanding clusters" *Phys. Rev. Lett.* **98**, 123902 (2007).
- 9) H. A. Sumeruk, S. Kneip, D. R. Symes, I. V. Churina, A. V. Belolipetski, T. D. Donnelly, and T. Ditmire, "Control of Strong-Laser-Field Coupling to Electrons in Solid Targets with Wavelength-Scale Spheres" *Phys. Rev. Lett.* **98**, 045001 (2007).
- 10) H. A. Sumeruk, S. Kneip, D. R. Symes, I. V. Churina, A. V. Belolipetski, G. Dyer, J. Landry, G. Bansal, A. Bernstein, T. D. Donnelly, A. Karmakar, A. Pukhov and T. Ditmire "Hot Electron and X-ray Production from Intense Laser Irradiation of Wavelength-scale Polystyrene Spheres" *Phys. Plas.* **14**, 062704 (2007).
- 11) D. R. Symes, J. Osterhoff, R. Fäustlin, M. Maurer, A. C. Bernstein, A. S. Moore, E. T. Gumbrell, A. D. Edens, R. A. Smith, and T. Ditmire "Production of periodically modulated laser driven blast waves in a clustering gas", *J. of High Energy Density Phys.* **3**, 353 (2007).

Ultracold Molecules: Physics in the Quantum Regime

John Doyle

Harvard University

17 Oxford Street

Cambridge MA 02138

doyle@physics.harvard.edu

1. Program Scope

Our research encompasses a unified approach to the trapping of diverse chemical species of both atoms and molecules. Our current goal is to study both CaH to NH and approach the ultracold regime. Our plan is to trap and cool NH and CaH molecules loaded directly from a molecular beam, and measure elastic and inelastic collisional cross sections. Cooling to the ultracold regime will be attempted. We note that as part of this work, we are continuing to develop an important trapping technique, buffer-gas loading.

2. Recent Progress

Milestones for this project include (x indicates complete):

- x-spectroscopic detection of ground-state NH molecules via LIF
- x-production of NH in a pulsed beam
- x-spectroscopic detection of ground-state NH molecules via absorption
- x-injection of NH beam into cryogenic buffer gas (including LIF and absorption detection)
- x-realization of 4 T deep trap run in vacuum
- x-injection of NH molecules into cryogenic trapping region
- x-loading of NH molecules into cryogenic buffer gas with 4 T deep trap
- x-trapping of NH
- x-measurement of spin-relaxation rate of NH with He
- x-removal of buffer gas after trapping of NH
- x-creation of a cold buffer gas cooled beam of CaH
- x-laser cooling of buffer gas beam of atoms
- x-measurement of elastic and inelastic atom-molecule (N-NH) cross sections
- o-evaporative cooling
- o-measurement of ultracold cross sections
- o-study cold chemical reactions
- o-prepare metastable NH for field studies
- o-introduce new molecules into system for further studies

NH and CaH, like many of the diatomic hydrides, have several advantages for molecular trapping including large rotational constant and relatively simple energy level structure. Some of the several key questions before us when this project began were: Could we produce enough NH using a pulsed beam? Is it possible to introduce a large number of NH molecules into a buffer gas? Would the light collection efficiency be enough for us to adequately detect fluorescence from NH? Could we get absorption spectroscopy to work so that absolute number measurements could be performed? Could we achieve initial loading of NH into the magnetic trap? Will the spin relaxation rates with helium be low enough for us to remove the buffer gas? We have now answered these questions, all to the positive. In addition, we have added several new features to the project including co-trapping of N with NH, laser cooling of buffer gas cooled beams (initially with atoms), and the addition of CaH to our program.

Recently, we have made preliminary measurements of both NH-N and N-N collision rates. These measurements are important not only for a fundamental understanding of cold molecular collisions, but also are critical in defining a path to ultracold molecule production using evaporative/sympathetic cooling. These results will be presented. There are still key questions as we move forward. What will be the nature of an ultracold dense sample of heteronuclear molecules? Specifically, what about the hydrides, with their large rotational constants? Can metastable molecular states be used to switch between atom-like objects and molecular-like objects? These questions are still partially open and answering them are some of the stated long-term goals of this work.

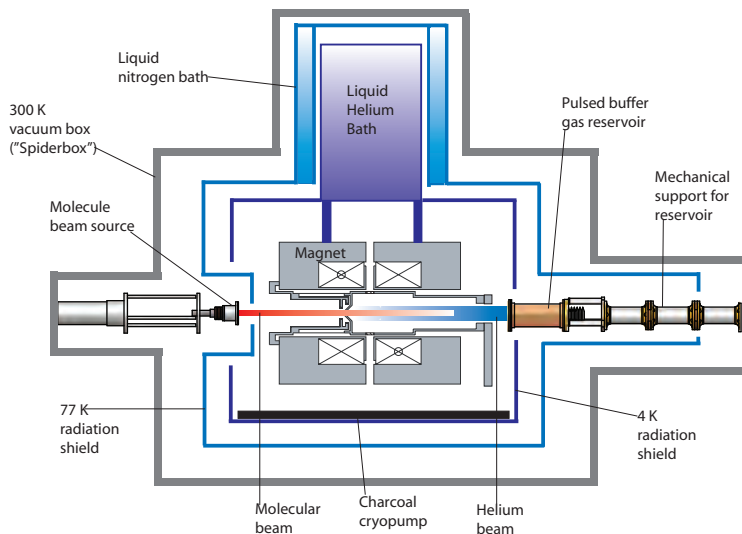


Figure 1: Schematic of current molecule trapping apparatus. The NH molecules and N atoms travel into the trapping region from the molecular beam source, where they are thermalized with the buffer gas and trapped. Simultaneous detection of NH and N is done spectroscopically.

Summary of Status of Project

The heart of the apparatus is a beam machine that we use to produce pulsed NH – alone or in combination with atomic N – in a beam (see figure 1). (Figure 3 shows a photo of the internals of the apparatus.) We have used two types of sources successfully, an “RF Plasma Source (CW)” and a “Glow Discharge Source (Pulsed)”. The plasma source is a commercial source used typically in MBE machines. The design of the pulsed source is based on the production of OH via DC discharge as executed by Nesbitt.

This beam is directed toward our trapping magnet, inside of which is a cryogenic buffer-gas cell. This cell can be cooled to as low as 500 mK by a He³ refrigerator. An entrance orifice of a few mm in diameter to allow the beam of NH to enter the cell. In a new addition to our apparatus, at the opposite end is a much larger orifice that allows for a new cold pulsed beam of helium to enter. The idea is that the helium pulse arrives simultaneously with the NH/N pulse, thermalizes the N/NH (leading to trapping), and then quickly exits. Thus, buffer-gas cooling and trapping of the NH and/or N takes place.

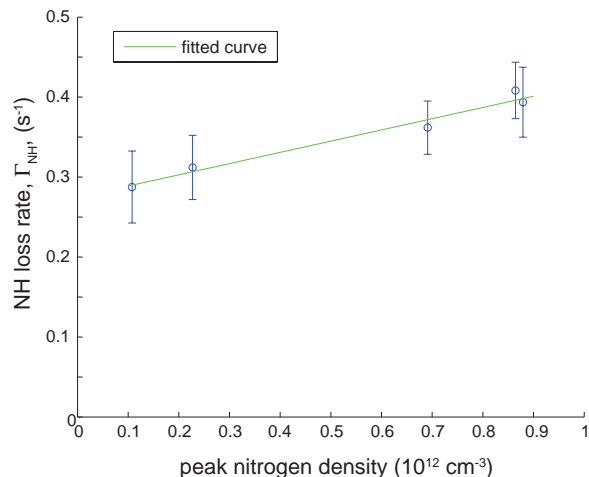


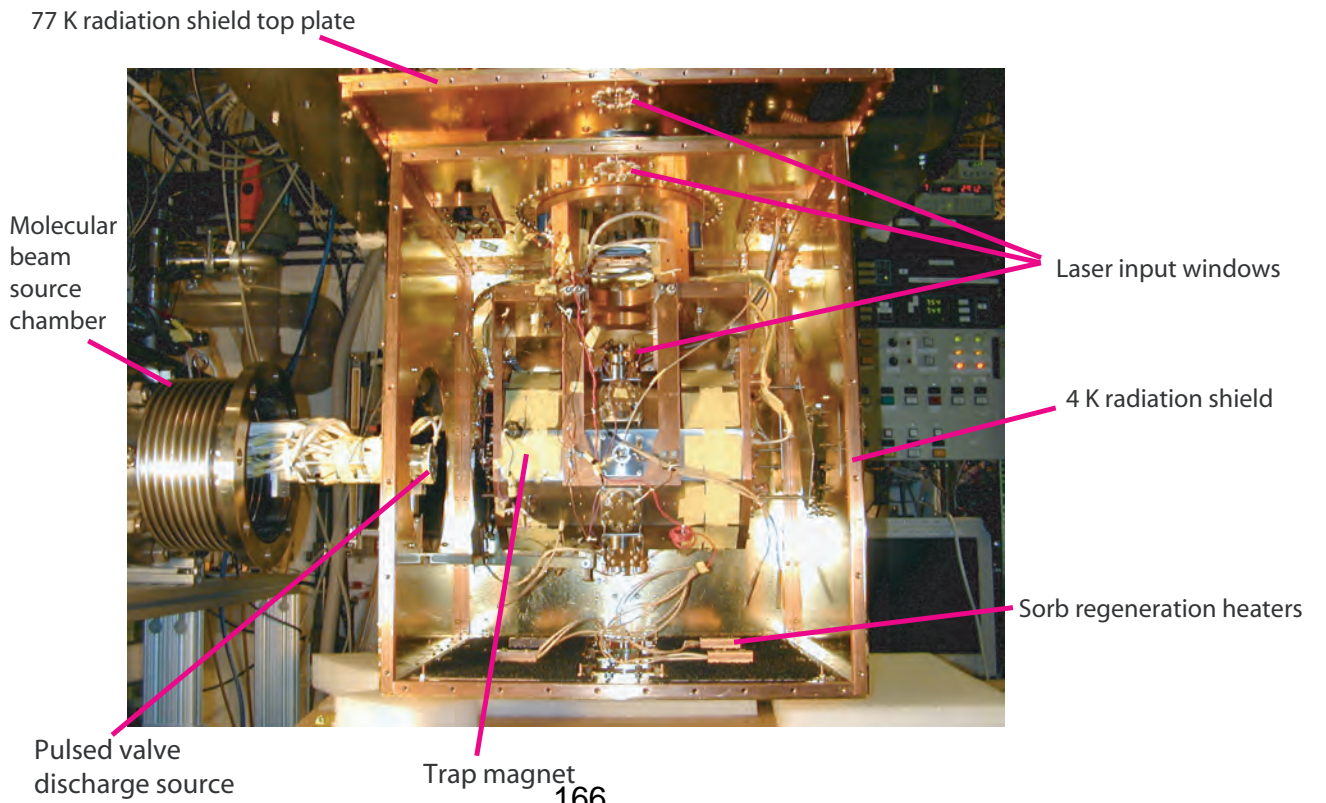
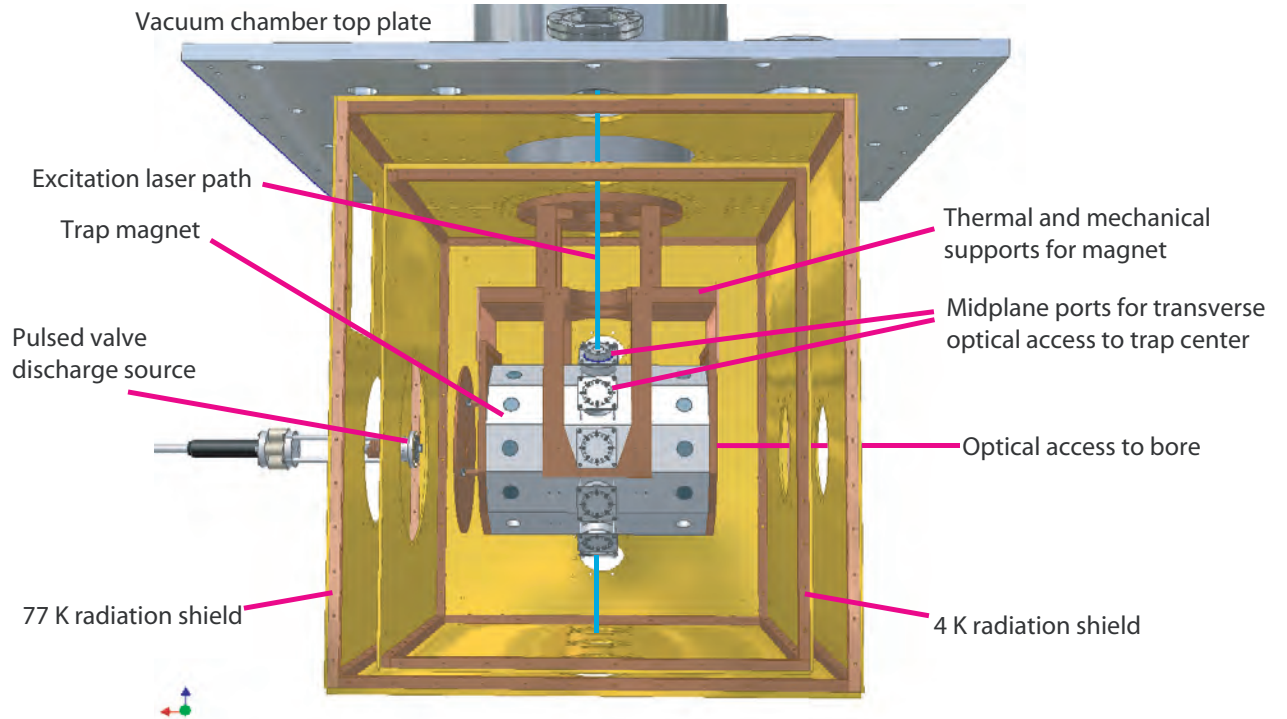
Figure 2: NH lifetime as a function of co-trapped Nitrogen atom density in our magnetic trap. This represents a first measurement of N-NH inelastic cold collision properties.

The basic experimental procedure is as follows. The source beam is directed toward the trap for times from about 10-100 ms. This long pulse beam travels about 10 cm to the face of the cell where some portion enter through the orifice and into the cell. The NH and/or N are then cooled by the buffer gas to their ground state by the helium resident in the cell. In our latest experiments we have been using fluorescence and absorption spectroscopy to detect trapped NH pulsed TALIF to simultaneously detect trapped atomic N. We have been able to observe trapped NH molecules and N for many seconds. Figure 2 shows condensed data of NH trapped lifetimes versus co-trapped N density. As will be described in my talk, this indicates a measurement of N-NH inelastic processes. We have submitted one combined theory/experiment paper on trapped N-N collisions and another, on N-NH collisions, is in preparation. Publications from earlier in this grant period include studies of NH-He collisions, *Magnetic Trapping and Zeeman Relaxation of NH*, W.C. Campbell, E. Tsikata, H. Lu, L.D. van Buuren, and J.M. Doyle, *Physical Review Letters*, **98**, 213001 (2007) and *Mechanism of Collisional Spin Relaxation in $^3\Sigma$ Molecules*, W.C. Campbell, T.V. Tscherbul, Hsin-I Lu, E. Tsikata, R.V. Krems, and J.M. Doyle, *Physical Review Letters* **102** 013003 (2009).

3. Future Plans

We continue on our program of trapping of NH with N and have embarked on a new approach to trap CaH, using combinations of optical and buffer-gas methods. With both species the technical challenge is to create high enough density to see collisions with a low background pressure.

Figure 3:



Atomic Electrons in Strong Radiation Fields

J. H. Eberly
Department of Physics and Astronomy
University of Rochester, Rochester, NY 14627
eberly@pas.rochester.edu

July 31, 2010

Scope: Electron Correlation under Strong Laser Fields

We are interested to understand how very intense laser light couples to atoms and molecules. Theoretical study faces substantial challenges in this domain. These arise from the combination of high intensity, fully phase-coherent character and short-time nature of the laser pulses in use, where the laser's electric-field force roughly matches the Coulomb forces among electrons and the nucleus. An important additional challenge arises when there is a need to account for more than one dynamically active electron, as there generally is in situations of highest experimental interest.

Our work builds on earlier results obtained from numerical experiments [1]. These were studies of two, three and four active atomic electrons in strong time-dependent and phase-coherent fields, using very large ensembles of classical multi-electron trajectories. The technique is capable of unique theoretical exploration. For example, it has achieved what we believe is the only direct comparison between theory [2] and experimental momentum distribution data [3] obtained in multiphoton triple ionization.

More recently, a surprising and very clear distinction has been found [4] between non-sequential double ionization (NSDI) and sequential double ionization (SDI) under elliptical polarization, as shown in the ion momentum distributions in Fig. 1. The distinct patterns in the polarization plane show that SDI and NSDI are separated cleanly by their different responses along the major and

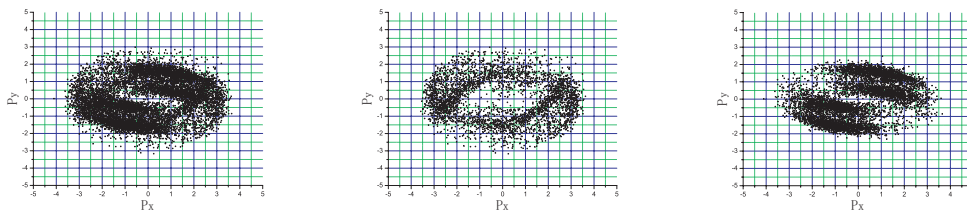


Figure 1: Under elliptical polarization, the ion momentum distribution of DI (left) can be cleanly divided into the momentum distribution of NSDI (center) and the momentum distribution of SDI (right). The ellipticity used here is 0.5, and $I = 0.6 \text{ PW/cm}^2$. From Xu Wang and J.H. Eberly, *Phys. Rev. Lett.* **103**, 103007 (2009).

minor axes of polarization. The theoretical data was obtained at an intensity high enough to include both SDI and NSDI.

Recent Progress #1: Elliptical Polarization and Multiphoton Double Ionization

Almost all near-optical-frequency double ionization experiments have been carried out with linearly polarized light. The familiar three-step recollision picture [5, 6], so successful for high harmonic generation, suggests dramatically lower ion yield under elliptical or circular polarization, because the return trajectory is carried away from the atomic core. This was tentatively affirmed experimentally [7], but double ionization has nevertheless been repeatedly reported even with circular or near-circular polarization, e.g., in studies of atomic magnesium [8] and of several molecules [9].

Our classical numerical experiments on multiple ionization are ideally suited to explore the effects of elliptically polarized fields because the topic is well beyond the reach of essentially all high-field quantum mechanical calculations. This includes solutions of the time dependent Schrödinger equation as well as applications of the so-called strong field approximation (SFA) [10, 11]. The lack of cylindrical symmetry is what puts the case of elliptical polarization beyond the capacity of those methods. We have now completed analytical derivations confirming numerical results for NSDI for a full range of ellipticities. Our results significantly extend findings reported from the Becker group in MBI-Berlin [12]. They are also complemented by results from the Uzer group at Georgia Tech, in which classical phase space analyses are used to tackle the special case of circular polarization [13].

We have recently reported new results on ionization timing, shown in Fig. 2, which have led to the first scaling formula for NSDI probability under elliptical polarization [14]. Further numerical experiments have led to the strong speculation that essentially all successful NSDI trajectories are in fact elliptical or nearly so [15]. The missing element in previous calculations was a suitable understanding of the important dynamical role that is played by the distribution of transverse veloc-

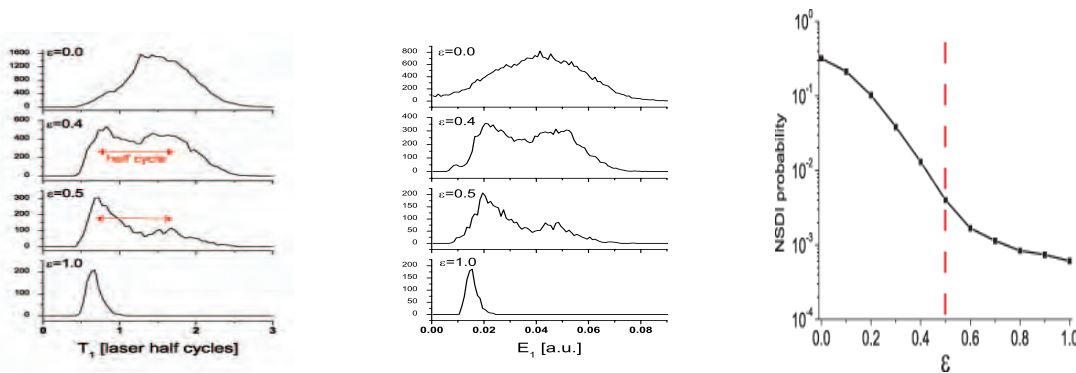


Figure 2: Numerical experiments provide the distribution of field strengths (left) at the time of first ionization, and the distribution of first ionization times (center), for successful NSDI events, for several different ellipticities from linear to circular. Note that the high ellipticity values act to strongly “pin” the effective field strengths in a narrow range. The right figure shows the distribution of successful NSDI events as a function of ellipticity, with substantially slower falloff for high values of ϵ than the standard recollision picture suggests. From Xu Wang and J.H. Eberly, *Phys. Rev. Lett.* **105**, in press (2010)

ities available to the first-ionized electron. Typical examples of successful NSDI trajectories under elliptical polarization are shown in Fig. 3.

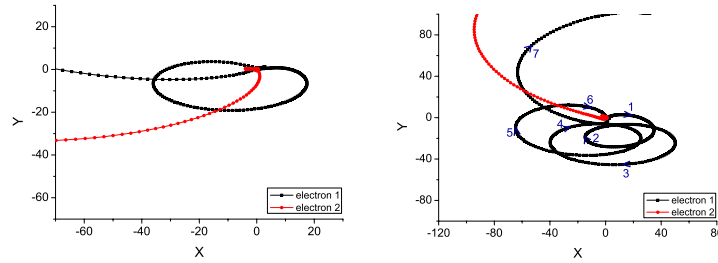


Figure 3: Two typical recollision trajectories for ellipticity 0.5. Left: the recolliding electron’s trajectory is an almost perfect ellipse. It returns to the origin in one laser cycle and kicks out the second electron. Right: the elliptical trajectory of the recolliding electron is not quite perfect and is encouraged by the ion’s Coulomb force to execute several cycles before coming close enough to eject the second electron. The arrows and numbers are used to show the temporal motion of the first electron. From Xu Wang and J.H. Eberly, arXiv:1006.5298.

Recent Progress #2: Theoretical Overview for RMP

A second project is the completion of an overview of the domain of high field ionization physics, focusing on theoretical understanding of multi-electron processes. It is well known that there is no orderly theory in the high field domain, in the sense that there is no well-defined procedure of the canonical S-matrix type, because there is no single small parameter serving as an analog to the fine structure constant. Instead, there are three or four theoretical approaches with differing heuristic bases in use. An invitation to provide a Colloquium style article for *Rev. Mod. Phys.* that would assess this situation has led to a cooperative effort with contributions so far from participants from Argonne, Berlin, Rochester and Wuhan [16]. The intention is to compare theoretical results to experimental findings with the goal of determining the ranges of validity and utility of the different approaches in current use.

Future Plans

The extension of the classical approach to 2d and 3d has opened the domain of elliptical polarization to study, and that topic will be pursued. In the past two months discussion about related experimental work has begun with groups in Garching and Barcelona.

We have previously promised more speculative work involving measures of the degree of quantum state entanglement between electrons, i.e., non-local entanglement rather than the local entanglement of atomic orbitals. This project remains very interesting but increasing success with understanding of the effects of elliptical polarization mentioned above has taken attention away from it. We expect that a fraction of our effort going forward will be devoted to an examination of questions related to this, in cooperation with the Fedorov group in the General Physics Institute in Moscow. We continue to value our cooperation on multi-electron strong-field effects with the group of Prof. S.L. Haan at Calvin College [17].

Publications supported by DOE Grant DE-FG02-05ER15713 are marked with * in the listing below.**

References

- [1] Phay J. Ho, R. Panfili, S. L. Haan and J. H. Eberly, *Phys. Rev. Lett.* **94**, 093002 (2005). See also Phay J. Ho, *Phys. Rev. A* **74**, 045401 (2005), ***Phay J. Ho and J.H. Eberly, *Phys. Rev. Lett.* **95**, 193002 (2005), ***Phay J. Ho and J.H. Eberly, *Phys. Rev. Lett.* **97**, 083001 (2006), and ***S.L. Haan, L. Breen, A. Karim, and J. H. Eberly, *Phys. Rev. Lett.* **97**, 103008 (2006) [also selected for Virtual Journal of Ultrafast Science].
- [2] ***P.J. Ho, Ph.D. Dissertation, University of Rochester (2007), and ***Phay J. Ho and J. H. Eberly, *Optics Expr.* **15**, 1845-1850 (2007).
- [3] K. Zrost, A. Rudenko, Th. Ergler, B. Feuerstein, V. L. B. de Jesus, C. D. Schröter, R. Moshhammer and J. Ullrich, *J. Phys. B* **39**, S371 (2006).
- [4] ***X. Wang and J.H. Eberly, *Phys. Rev. Lett.* **103**, 103007 (2009).
- [5] K.C. Kulander, K.J. Schafer and J.L. Krause, in *Super-Intense Laser-Atom Physics*, edited by B. Piraux, A. L'Huillier and K. Rzazewski (Plenum, New York, 1993), and K.J. Schafer, B. Yang, L.F. DiMauro and K.C. Kulander, *Phys. Rev. Lett.* **70**, 1599 (1993).
- [6] P. B. Corkum, *Phys. Rev. Lett.* **71**, 1994 (1993).
- [7] P. Dietrich, et al., *Phys. Rev. A* **50**, 3585(R), (1994).
- [8] G. D. Gillen et al., *Phys. Rev. A* **64**, 043413 (2001).
- [9] C. Guo and G. N. Gibson, *Phys. Rev. A* **63**, 040701(R)(2001); C. Guo et al., *Phys. Rev. A* **58**, R4271 (1998).
- [10] See the review in W. Becker and H. Rottke, *Contemporary Physics* **49**, 199 (2008).
- [11] For very early high-field calculations for single ionization under elliptical polarization, see A.M. Perelomov, V.S. Popov, and M.V. Terent'ev, *Zh. Eksp. Teor. Fiz.* **50**, 1393 (1965) [Sov. Phys. JETP **23**, 924 (1965)].
- [12] N. I. Shvetsov-Shilovski et al., *Phys. Rev. A* **77**, 063405 (2008).
- [13] F. Mauger, C. Chandre, and T. Uzer, *Phys. Rev. Lett.* **105** (in press 2010 and arXiv:1002.2903).
- [14] ***Xu Wang and J.H. Eberly, *Phys. Rev. Lett.* **105** (in press 2010 and arXiv:1006.5721).
- [15] ***Xu Wang and J.H. Eberly, arXiv:1006.5298.
- [16] ***Phay J. Ho, Xiaojun Liu, W. Becker, and J.H. Eberly, *Rev. Mod. Phys.* in preparation.
- [17] ***S.L. Haan, L. Breen, A. Karim and J.H. Eberly, *Optics Expr.* **15**, 767 (2007).

Reaction Imaging and the Molecular Coulomb Continuum

Department of Energy 2010-2011

James M Feagin

Department of Physics

California State University–Fullerton

Fullerton CA 92834

jfeagin@fullerton.edu

This report describes our ongoing work to extract basic understanding and quantum control of few-body microscopic systems based on our long-time experience with more conventional studies of correlated electrons and ions. Although the work is theoretical, our interest in these topics has been strongly motivated by the recent surge in and success of experiments involving few-body atomic and molecular fragmentation and the imaging of all the fragments. We accordingly continue two parallel efforts with (i) emphasis on *reaction imaging* while (ii) pursuing longtime work on *collective Coulomb excitations*. As in the past, we continue to place strong priority on research relevant to experiment. It might be noted that fresh insight into few-body science at molecular (nano) levels will be a critical component of ongoing national and international efforts to establish sustainable energy and environmental resources. The varied research paths to be taken will require the development of basic science on broad fronts with increasingly flexible views to crossover technologies.

Two-Center Interferometry

For the past few years, we have been working to develop a robust, albeit approximate, framework for describing two-center interferometry readily adaptable to either photon or charged-particle scattering.^{1,2} We have thus formulated an impulse-approximation description that allows one to track the relatively sluggish external center-of-mass motion of the target atoms and ions and thereby ensure momentum conservation explicitly while describing the excitation of the target's internal states. These projects continue to link to our more conventional longtime work in the AMO field of collective Coulomb excitations,^{3,4} although we have been particularly interested recently in characterizing the resulting entanglements among the recoiling reaction fragments and the scattered particle.

Electron-Pair Excitations

One of the surprises of early observations of photo double ionization of molecular hydrogen was the close similarity with the corresponding electron-pair angular distributions well established in helium, especially for relatively low-energy electron pairs.⁵ The helium (free-atom) double ionization angular distributions, viz. the triple differential cross sections TDCS, have a remarkably simple form for equal energy ejected electrons, namely,

$$\text{TDCS} \sim |\hat{\epsilon} \cdot \mathbf{k}_1 + \hat{\epsilon} \cdot \mathbf{k}_2|^2 = |\hat{\epsilon} \cdot \mathbf{k}_+|^2, \quad (1)$$

¹ J. M. Feagin, Phys. Rev. A **69**, 062103 (2004), Phys. Rev. A **73**, 022108 (2006)

² R. S. Utter and J. M. Feagin, Phys. Rev. A **75**, 062105 (2007). *This work was highlighted in the June 2007 issue of the Virtual Journal of Quantum Information, vjquantuminfo.org. Utter was a CSUF masters degree student.*

³ A. Knapp et al., J. Phys. B: At. Mol. Opt. Phys. **35**, L521 (2002). (*Feagin is a coauthor.*)

⁴ Th. Weber et al., Phys. Rev. Lett. **92**, 163001 (2004) and references therein. (*Feagin is a coauthor.*)

⁵ T. J. Reddish and J. M. Feagin, J. Phys. B: At. Mol. Opt. Phys. **32**, 2473 (1999); J. M. Feagin, J. Phys. B: At. Mol. Opt. Phys. **31**, L729 (1998).

with $\hat{\epsilon}$ the photon polarization. Here, $\hbar \mathbf{k}_+ = \hbar \mathbf{k}_1 + \hbar \mathbf{k}_2$ is the momentum of the photoejected electron-pair center of mass. The simplicity of this result derives from the underlying $^1S^e \rightarrow ^1P^o$ dipole excitation. In molecular dipole excitation, the geometry of the molecule naturally resolves the photon polarization into components parallel (Σ) and perpendicular (Π) to the relative momentum direction $\mathbf{K}_- \equiv (\mathbf{K}_1 - \mathbf{K}_2)/2$ of the Coulomb-exploding ion pair, so that

$$\hat{\epsilon} \rightarrow \epsilon_{\Pi} + \epsilon_{\Sigma} = \sin \theta_N \hat{\epsilon}_{\Pi} + \cos \theta_N \hat{\mathbf{K}}_- \quad (2)$$

with $\cos \theta_N \equiv \hat{\epsilon} \cdot \hat{\mathbf{K}}_-$. Thus, with the helium-like amplitude $\hat{\epsilon} \cdot \mathbf{k}_+$ from Eq. (1), one obtains an approximate *molecular* double ionization distribution or fully differential cross section FDCS for equal-energy ejected electrons according to

$$\text{FDCS} = |a_{\Pi} \sin \theta_N \hat{\epsilon}_{\Pi} \cdot \mathbf{k}_+ + a_{\Sigma} \cos \theta_N \hat{\mathbf{K}}_- \cdot \mathbf{k}_+|^2, \quad (3)$$

where the a_{Λ} are undetermined dipole amplitudes internal to the molecule but independent of the momenta of the ionization fragments. This expression helps to explain the observed close similarity of low-energy helium and molecular hydrogen angular distributions. It is readily extended to unequal energy sharing and thus gives remarkably good fits to a variety of data, especially for coplanar geometries with respect to the ion- and electron-pair momenta and photon polarization.

Gisselbrecht et al. recently identified, however, equal-energy-sharing electron-pair configurations in the molecular fragmentation for which the helium-like description categorically fails.⁶ Their observations were a follow-on to somewhat earlier experiments at the ALS by Th. Weber, R. Dörner, A. Belkacem, and coworkers.⁷ These anomalous angular distributions are noncoplanar and occur when one electron is observed perpendicular to the plane of the other and the polarization direction with the ion-pair direction \mathbf{K}_- either parallel or perpendicular to the polarization. Gisselbrecht et al. termed these and related configurations *frozen-correlation*, since the electron-pair angular separation $\hat{\mathbf{k}}_1 \cdot \hat{\mathbf{k}}_2$ is held fixed in all three cases.

Parallel to these experimental achievements, the community has seen decisive advancement in the *ab initio* computation of Coulomb few-body fragmentation, in particular from two groups, T. Rescigno, W. McCurdy, and coworkers at LBNL⁸ using a time-*independent* close-coupling approach, and J. Colgan, M. Pindzola and F. Robicheaux at Los Alamos and Auburn⁹ using a time-*dependent* close-coupling approach. Their abundant ‘virtual data’ are in excellent agreement in both magnitude and angular distribution with a wide variety of experimentally measured cross sections. Their results for the ‘frozen-correlation’ distributions observed by Huetz and Reddish agree well with experiment. Their achievements have set milestones in the computational study of the Coulomb continuum.

Analysis of the close-coupling results, albeit as expansions in individual electron angular momenta, show evidence for contributions to the fragmentation from higher electron-pair angular momenta. We have thus began a collaboration with J. Colgan, A. Huetz, and T. Reddish to generalize the helium-like molecular description to higher *total* angular momentum of the electron-pair. In the molecular ground state, the electron-pair total angular momentum $\mathbf{L} = \mathbf{l}_1 + \mathbf{l}_2$ is not a good quantum number, so the helium-like dipole selection rule $^1S^e \rightarrow ^1P^o$ generalizes to $^1S^e, ^1P^e, ^1D^e, \dots \rightarrow ^1P^o, ^1D^o, ^1F^o, \dots$ (the exchange and parity dipole selection rules remain the same). Based on our longtime experience with electron-pair excitations in helium and H^- ,¹⁰ it turns out to be advantageous—perhaps surprisingly so—to define states of

⁶ M. Gisselbrecht et al., Phys. Rev. Lett. **96**, 153001 (2006).

⁷ Th. Weber et al., Nature (London) **431**, 437 (2004).

⁸ W. Vanroose, F. Martin, T. N. Rescigno, and C. W. McCurdy, Phys. Rev. A **70**, 050703 (R) (2004); Science **310**, 1787 (2005).

⁹ J. Colgan, M. S. Pindzola and F. Robicheaux, J. Phys. B: At. Mol. Opt. Phys. **37**, L377 (2004); Phys. Rev. Lett. **98**, 153001 (2007).

¹⁰ M. Walter, J. S. Briggs and J. M. Feagin, J. Phys. B: At. Mol. Opt. Phys. **33**, 2907 (2000).

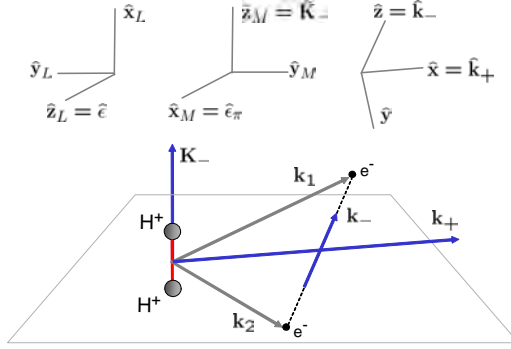


FIG. 1: Rotating $\mathbf{k}_1, \mathbf{k}_2$ plane of an ejected electron pair following the photo fragmentation of molecular hydrogen. Here, $\mathbf{k}_+ = \mathbf{k}_1 + \mathbf{k}_2$ and $\mathbf{k}_- = (\mathbf{k}_1 - \mathbf{k}_2)/2$ refer to the electron pair, and $\mathbf{K}_- = (\mathbf{K}_1 - \mathbf{K}_2)/2$ to the ion pair. The top three insets illustrate our three frames of reference used.

total L by quantizing rotations of the momentum plane of the electron pair based on a z axis along their relative momentum direction $\mathbf{k}_- = (\mathbf{k}_1 - \mathbf{k}_2)/2$, as depicted in Fig. 1. One thus introduces symmetric-top wavefunctions $\hat{D}_{Mm}^L(\hat{\mathbf{k}}_-)$ defined by projections $\hbar m = \mathbf{L} \cdot \hat{\mathbf{k}}_-$ and $\hbar M = \mathbf{L} \cdot \hat{\mathbf{z}}_M$, where $\hat{\mathbf{z}}_M$ is a *molecular-frame* z axis, which we take to be along the ion-pair relative momentum direction \mathbf{K}_- .

As depicted in Fig. 2, we have thus found that superpositions of just three molecule symmetrized electron-pair states, $^1P^o + ^1D^o + ^1F^o$, give a remarkably robust description of the molecular fragmentation distributions including the anomalous out-of-plane *frozen-correlation* configurations.¹¹ We also find that molecules require special axial-vector geometries in the momenta of the outgoing electron-pair, which are not seen in atoms, and in Fig. 3 we present evidence for them in the fragmentation cross section.

Our molecular fragmentation description might also be viewed as a judicious resummation of the expansions of the transition amplitudes used in the close-coupling approaches based on pairs of one-electron harmonics $Y_{l_1 m_1}(\hat{\mathbf{k}}_1) Y_{l_2 m_2}(\hat{\mathbf{k}}_2)$. The *frozen-correlation* configurations we have examined with fixed $\hat{\mathbf{k}}_1 \cdot \hat{\mathbf{k}}_2$, especially out of the $\hat{\mathbf{K}}_-, \hat{\mathbf{e}}$ plane, have proven to be a strong test of the convergence of these approaches. (Typically, ~ 100 channels are needed.) The usefulness

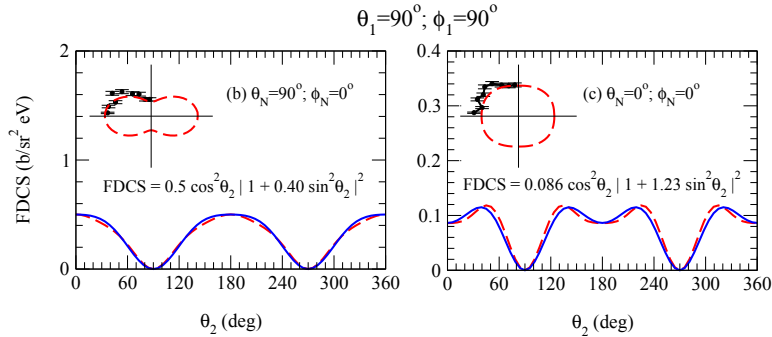


FIG. 2: Fits (solid curves) based on a three-state superposition $^1P_{\lambda=1} + ^1D_{\lambda=1} + ^1F_{\lambda=1}$ to the H_2 photo double ionization cross sections measured by Gisselbrecht et al. Here, the dashed curves show the TDCC results from J. Colgan.

¹¹ J. M. Feagin, J. Colgan, A. Huetz, and T. J. Reddish, Phys. Rev. Lett. **103**, 033002 (2009).

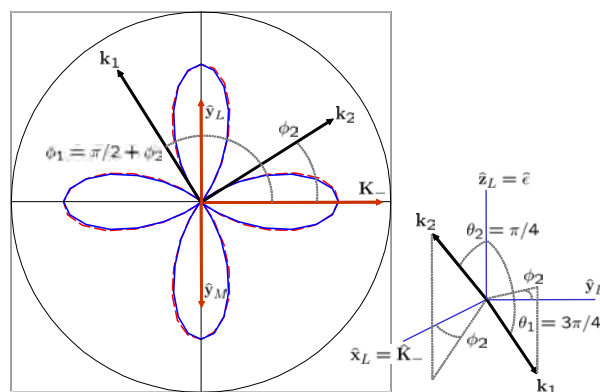


FIG. 3: An electron-pair angular distribution for fixed $\hat{\mathbf{k}}_1 \cdot \hat{\mathbf{k}}_2$ looking down a z_L axis along $\hat{\mathbf{e}}$ onto the $\hat{\mathbf{x}}_L = \hat{\mathbf{K}}_-, \hat{\mathbf{y}}_L$ plane as a function of the azimuthal orientation ϕ_2 of the pair. Here, \mathbf{k}_2 and \mathbf{k}_1 are oriented above and below, respectively, the $\hat{\mathbf{K}}_-, \hat{\mathbf{y}}_L$ plane (cf. 3D inset) with fixed polar angles $\theta_2 = \pi/4$ and $\theta_1 = \pi - \theta_2$ while varying ϕ_2 along with $\phi_1 = \phi_2 + \pi/2$. The solid four-lobe curve is the resulting $\cos^2 2\phi_2$ distribution predicted from the axial-vector contributions, arbitrarily scaled to a TDCC calculation shown with the dashed curve. The circle radius equals $0.03 \text{ b/sr}^2 \text{ eV}$.

of the electron-pair modes we define is in the compact description of the continuum spectrum they afford even for frozen-correlation configurations. The same modes should in principle describe *any* low-energy electron-pair continuum, once appropriately symmetrized. Different systems would only require different sets of internal-mixing coefficients. One might hope to thus establish a robust tool for analyzing a variety of experimental data including modeling of electron pairs ejected from more complex molecules, and even surfaces and solids, for which ab initio calculations may not exist for some time.¹²

Recent Publications

Electron-Pair Excitations and the Molecular Coulomb Continuum, J. M. Feagin, J. Colgan, A. Huetz, and T. J. Reddish, Phys. Rev. Lett. **103**, 033002 (2009).

Electron Pairs in the Molecular Coulomb Continuum, J. M. Feagin, Invited Talk to the International Symposium on $(e, 2e)$, Double Photoionization, and Related Topics, Lexington, KY, July (2009).

Trapped-Ion Realization of Einstein's Recoiling-Slit Experiment, R. S. Utter and J. M. Feagin, Phys. Rev. A **75**, 062105 (2007). (**Utter** was a CSUF masters degree student. This work was highlighted in the June 2007 issue of the Virtual Journal of Quantum Information, vjquantuminfo.org.)

Two-Center Interferometry and Decoherence Effects, J. M. Feagin, Phys. Rev. A **73**, 022108 (2006).

¹² Th. Weber, private communication.

Studies of Autoionizing States Relevant to Dielectronic Recombination

T.F. Gallagher
Department of Physics
University of Virginia
P.O. Box 400714
Charlottesville, VA 22904-4714
tfg@virginia.edu

Doubly excited autoionizing states of alkaline earth atoms are of interest since the reverse process, dielectronic recombination (DR), the recombination of ions and electrons via intermediate autoionizing states, provides an efficient recombination mechanism for high temperature electrons in both laboratory and astrophysical plasmas.¹⁻³ Recombination, due to any process, is important in fusion plasmas because the captured electrons lead to radiative power loss. The most important pathway for DR is through the autoionizing Rydberg states converging to the lowest lying excited states of the parent ion. As a result, DR rates are profoundly influenced by very small electric and magnetic fields, both of which are often present in a plasma.⁴ DR in two electron alkaline earth atoms presents physics similar to that found in other contexts, notably zero kinetic energy electron (ZEKE) spectroscopy⁵ and fluorescence yield spectroscopy.⁶

In storage ring experiments DR is observed to pass largely through energetically unresolved high ℓ states.⁷ Although these states are energetically unresolved, we have shown that it is possible to identify which ℓ states contribute to DR using the Stark effect. The basic idea is easily understood. In zero field the contribution of an $n\ell$ Rydberg state to the DR rate is proportional to $A_I(n\ell)/(A_I(n\ell)+A_R)$, where $A_I(n\ell)$ and A_R are the autoionization and radiative decay rates of the $n\ell$ state. For high ℓ states ($A_I(n\ell) \ll A_R$), and the contribution is negligibly small. The essential question is, "For what ℓ is the autoionization rate equal to the radiative rate?" To determine this ℓ we use the Stark effect. An electric field E converts the ℓ states to Stark states, and more states contribute to DR. The magnitude of the quantum defect for an isotropic core decreases with increasing ℓ , and for any value of E there is a value of ℓ , ℓ_E , such that $\ell \geq \ell_E$ states are converted to Stark states. When the E field becomes large enough that $A_I(n\ell_E) \geq A_R$ the DR rate will begin to rise. Since both the quantum defects and the autoionization rates are readily calculable,⁸ this technique is a powerful way of determining which of the energetically unresolved high ℓ states contribute to DR.

We have measured the autoionization yields of Ba $6p_jnk$ Stark states composed of high ℓ states as a function of the field. At low field the autoionization rate of the $6p_jnk$ state is essentially zero, and we measure the field at which the autoionization yield reaches 50% of its saturated high field value. At this field the autoionization rate equals the radiative rate, and from the known quantum defects of the ℓ states we are able to determine which ℓ state's addition to the manifold is responsible for the increased autoionization rate. For the Ba $6p_{1/2}n\ell$ states of $n \approx 28$ it is $\ell=7$.

A surprising aspect of this work is that the proposed method works for anisotropic cores as well as for isotropic cores. While the $\text{Ba}^+ 6p_{1/2}$ core is isotropic, with one quantum defect for each ℓ state, the $\text{Ba}^+ 6p_{3/2}$ core is not. It has a quadrupole moment, leading to quadrupole splittings of the $6p_{3/2}n\ell$ Rydberg states.⁹ The splittings are characterized by \bar{K} , the sum of the angular momentum of the ion core, \bar{j} , and the orbital angular momentum of the Rydberg electron, $\bar{\ell}$. For a $j = 3/2$ core there are four values of the quantum number K , and there is not one quantum defect for each ℓ state, but four. In spite of this apparent complication, the method works, due to a propensity rule for the electric dipole matrix elements. The electric dipole selection rules are $\Delta\ell = \pm 1$ and $\Delta K = 0, \pm 1$. However, the $\Delta K = \Delta\ell$ matrix elements are, by an order of magnitude, the largest, and as a result, the $6p_{3/2}nk$ Stark states behave as if they are four independent sets of states.

In a $6s_{1/2}nk$ Stark state the electron can be localized on the upfield or downfield side of the atom. If the field is in the z direction and the atom is photoexcited to the $6p_{1/2}nk$ state by a laser linearly polarized in the z direction, the electron ejected by autoionization should be preferentially ejected in the $+z$ or $-z$ direction. The Stark states are unusual: in photoionization or autoionization of an atomic state of well defined parity ejection in the $+z$ and $-z$ directions is equally likely. It is usually impossible to determine the angular distributions of electrons ejected from Stark states since relatively high fields are required to make the Stark states. However, since we can make Stark states in fields of 1 V/cm, using a microwave adiabatic rapid passage technique, we can make such measurements, and they are currently under way.

We previously observed multiphoton assisted recombination in the presence of a 38 GHz microwave field. Specifically, we were able to observe recombination even though the laser was tuned 20 cm^{-1} (600 GHz) above the $\text{Ba}^+ 6p_{1/2}$ limit.¹⁰ What was initially surprising about this result is that the ponderomotive energy in a 50V/cm 38GHz field is only 0.15 cm^{-1} , and using the simpleman's model, often used to describe above threshold ionization (ATI), we would expect to see microwave assisted recombination at energies up to three times the ponderomotive energy above the limit, 0.45 cm^{-1} in this case.^{11,12} The shortcoming of the simpleman's model is that it ignores the coulomb potential. Ignoring it is an excellent approximation in many cases, but not this one. We have developed an extension of the simpleman's model, taking into account the coulomb potential, which predicts the correct energy extent of the recombination above the limit. The extent is linear in the microwave field, as observed, and the model predicts a dependence on the phase of the microwave field at which the electrons are excited. We have phase locked a microwave oscillator to the pulse train of a mode locked Ti:sapphire laser and used this combination to excite atoms just above the ionization limit at a well controlled phase of the microwave field. We observe the predicted phase dependence of the recombination, with two maxima per microwave cycle. Our results are analogous to He ionization results obtained using an attosecond pulse train with a phase locked infrared pulse. The measurements differ in that we are removing energy from the electron with the low frequency radiation whereas they added energy with their low frequency radiation. In addition, we have a single high frequency pulse, while they have a train, and they attribute most of the effect they observe to the coherent process driven by the attosecond pulse train.

In the coming year we plan to finish the measurement of the angular distributions of electrons ejected from Stark states. We plan to begin high resolution measurements of the Ba $6p_{1/2}n\ell$ states of $\ell \geq 4$ in zero to weak electric fields. These fields are the ones most important for DR, and this range has never been explored. An interesting aspect of these measurements is that the $6p_{1/2}ng$ states have widths which overlap all the higher ℓ states. Finally, we plan to extend the measurements of phase locked recombination in several ways. One is to have more than one ps excitation pulse, using a Ramsey interference technique to start, to separate the effects of single and multiple excitation pulses. It is possible to excite the atoms in the presence of the microwave field with the exciting laser tuned below the limit. In this case it may be possible to observe phase dependent transfer to both higher and lower energy due to the microwave field.

References

1. A. Burgess, *Astrophys. J.* **139**, 776 (1964).
2. A.L. Merts, R.D. Cowan, and N.H. Magee, Jr., Los Alamos Report No. LA-62200-MS (1976).
3. S. B. Kraemer, G. J. Ferland, and J. R. Gabel, *Ap. J.* **604**, 556 (2004).
4. V. L. Jacobs, J. L. Davis, and P. C. Kepple, *Phys. Rev. Lett.* **37**, 1390 (1976).
5. E. W. Schlag, *ZEKE Spectroscopy* (Cambridge University Press, Cambridge, 1998).
6. C. Sathe, M. Strom, M. Agaker, J. Soderstrom, J. E. Rubenson, R. Richter, M. Alagia, S. Stranges, T. W. Gorczyca, and F. Robicheaux, *Phys. Rev. Lett.* **96**, 043002 (2006).
7. C. Brandau, T. Bartsch, A. Hoffnecht, H. Knopp, S. Schippers, W. Shi, A. Muller, N. Grun, W. Scheid, T. Steih, F. Bosch, B. Franzke, C. Kozhuharov, P. H. Mokler, F. Nolden, M. Steck, T. Stohler, and Z. Stachura, *Phys. Rev. Lett.* **89**, 053201 (2002).
8. R. R. Jones and T. F. Gallagher, *Phys. Rev. A* **38**, 2846 (1988).
9. L. Pruvost, P. Camus, J.-M. Lecompte, C. R. Mahon, and P. Pillet, *J. Phys. B* **24**, 4723 (1991).
10. E. S. Shuman, R. R. Jones, and T. F. Gallagher, *Phys. Rev. Lett.* **101**, 263001 (2008).
11. H. B. van Linden van den Heuvell and H. G. Muller, in *Multiphoton Processes*, edited by S. J. Smith and P. L. Knight (Cambridge University Press, Cambridge, 1988).
12. T. F. Gallagher, *Phys. Rev. Lett.* **61**, 2304 (1988).
13. P. Johnsson, J. Mauritsson, T. Reimetter, A. L'Huillier, and K. J. Schafer, *Phys. Rev. Lett.* **99**, 233001 (2007).

Publications 2008-2010

1. E. S. Shuman, R. R. Jones, and T. F. Gallagher, *Phys. Rev. Lett.* **101**, 263001 (2008).
2. J. Nunkaew, E. S. Shuman, and T. F. Gallagher, "Indirect spin-orbit K splittings in strontium," *Phys. Rev. A* **79**, 054501 (2009).
3. J. Nunkaew and T. F. Gallagher, "Dielectronic recombination and autoionization yields in weak static electric fields," *Phys. Rev. A* **81**, 054501 (2009).

Experiments in Ultracold Collisions and Ultracold Molecules

Phillip L. Gould
Department of Physics U-3046
University of Connecticut
2152 Hillside Road
Storrs, CT 06269-3046
<phillip.gould@uconn.edu>

Program Scope:

Ultracold atoms and molecules are important subjects of investigation within modern atomic, molecular and optical (AMO) physics. Potential applications are not limited to AMO physics, but also extend to other fields such as quantum information, condensed-matter physics, fundamental symmetries, and chemistry. Molecules are of particular interest because they have various internal degrees of freedom covering a wide range of energy scales. Also, heteronuclear molecules can have permanent dipole moments, leading to long-range and anisotropic interactions. Recent progress in producing and manipulating cold molecules has been impressive and a number of techniques are now available. These include buffer gas cooling, electrostatic slowing, photoassociation, Feshbach-resonance magnetoassociation, optical trapping, magnetic trapping, and electrostatic trapping. Applications of ultracold molecules include: quantum degenerate gases (bosons, fermions, and mixtures); simulations of condensed-matter systems; quantum computation; fundamental symmetries and fundamental constants; dipolar gases and novel quantum phases; ultracold chemistry; and ultracold collisions. The main goal of our experimental program is to use frequency-chirped laser light on the nanosecond time scale to coherently control the collision dynamics of ultracold atoms, including the process of photoassociative formation of ultracold molecules.

Our experiments utilize ultracold Rb atoms in a magneto-optical trap (MOT). Rb is the atom of choice for several reasons: 1) the convenient match of its resonance lines (780 nm and 795 nm) to commercially available diodes lasers; 2) the existence of two stable and abundant isotopes (^{85}Rb and ^{87}Rb); 3) ^{87}Rb is the widely used in BEC experiments; and 4) photoassociative formation of ultracold Rb_2 has been extensively studied. Our experiments utilize a phase-stable MOT loaded from a separate “source” MOT. Inelastic collisions, including photoassociation, are measured via trap loss, while ground-state molecules are directly detected by laser ionization.

Recent Progress:

We have made recent progress in several areas: simulating the influence of frequency chirp nonlinearity on the rate of ultracold trap-loss collisions; the use of resonance-enhanced multiphoton ionization (REMPI) for detecting ultracold molecules; characterization of ultracold molecules produced by MOT light; observation of ground-state molecules produced by chirped photoassociation light; characterization of the residual chirp produced by our electro-optical intensity modulator; and the production of arbitrary spectra with our electro-optical phase modulator.

The basic idea of using frequency-chirped light to excite colliding atoms is to vary the Condon radius R_C with time. R_C is the atomic separation at which the laser light is resonant with excitation of the ground-state atom pair to the attractive $1/R^3$ dipole-dipole molecular potential. Therefore, a given detuning of the laser light below the atomic resonance will preferentially excite the atom pair at a specific value of R . If the laser frequency is chirped on the appropriate time scale, the resonance condition can follow the motion of the atoms on this attractive potential.

An interesting question is how the collisional rate depends on the direction of the chirp. We have previously examined this issue for trap-loss collisions induced with a linear chirp. We found that for a certain range of center detunings of the chirp, the negative (blue-to-red) chirp results in a significantly smaller collision rate than the positive (red-to-blue) chirp. We attribute this difference to the fact that the attractive potential causes the excited atom pair to always accelerate *inward*, while the Condon radius R_C can move either *inward* (negative chirp) or *outward* (positive chirp), depending on the sign of the chirp. For the positive chirp, the atom pair can only be excited once because the atom separation and the Condon radius move in opposite directions following the initial excitation. For the negative chirp, however, the Condon radius and the trajectory of the excited atom pair both proceed inward and further interactions between the light and the atom pair can occur. This results in less excited-state collisional flux reaching short range, and therefore a reduced trap-loss collisional rate.

More recently, we have used nonlinear frequency chirps to examine the dependence of the trap-loss collision rate on the shape of the chirp. For comparison purposes, we fix the beginning and ending frequencies of the chirp, as well as the total time duration, but vary the shape of the chirp. Starting with a linear chirp, we superimpose a nonlinear variation with either positive curvature (concave-up) or negative curvature (concave-down). For negative chirps, we find a small but significant difference in collision rates for the concave-up versus concave-down shapes. In collaboration with the group of Ronnie Kosloff at Hebrew University, we have also developed quantum simulations of the collisions induced by nonlinear chirps. These predict the general trends that we observe in the experiment.

Having explored the effects of chirped light on trap-loss collisions, we are now applying these pulses to the formation of ultracold molecules by photoassociation. We can observe photoassociation resonances through the loss of trapped atoms, but we are more interested in the resulting ground-state Rb_2 molecules. We detect these directly with resonance-enhanced multiphoton ionization (REMPI) using a pulsed dye laser at ~ 600 nm. The resulting Rb_2^+ ions are distinguished from Rb^+ ions by time of flight. As a first step, we have looked at molecules produced by the light of the MOT and characterized their ionization spectrum. The formation rate of these MOT-produced molecules is much higher for ^{85}Rb than for ^{87}Rb . Since these constitute a significant background signal in our ultracold molecule experiments, we have switched to ^{87}Rb for our experiments. Very recently, we have used REMPI to observe ultracold molecules produced by pulses of chirped light. We have evidence that the chirped light also causes some destruction of these ground-state molecules, most likely through off-resonant excitation to states which dissociate into free atoms.

We continue to develop our system for producing fast (>1 GHz in 10 ns) and arbitrarily-shaped chirped pulses. The chirping is achieved with an electro-optic phase

modulator driven by an arbitrary waveform generator. The use of a fiber loop, in conjunction with injection locking of the diode laser after each pass, allows us to accumulate the desired time-dependent phase shift. The short pulses (<3 ns) are formed with an electro-optic intensity modulator also driven by the arbitrary waveform generator. This intensity modulator, based on a split-waveguide Mach-Zehnder interferometer, does cause some residual phase modulation which we have thoroughly characterized using heterodyne techniques. We have also shown that we can largely compensate this residual phase modulation using our phase modulator.

An interesting application of our fast phase modulation is to the production of arbitrary spectra. Since frequency is the time derivative of phase, a linear phase ramp gives a fixed frequency offset. By applying a sequence of voltage ramps to the phase modulator, we generate a series of sidebands whose offsets from the carrier are determined by the slopes of the corresponding ramps. Such multi-frequency light may prove useful in the efficient excitation of complex atomic or molecular systems.

Future Plans:

We will further refine our techniques for producing arbitrary chirps and pulses by incorporating faster electronics and using a tapered amplifier to yield higher intensities. We will also switch from using light near the $5p_{3/2}$ resonance (780 nm) to light near the $5p_{1/2}$ resonance (795 nm). This will simplify the photoassociation spectrum and avoid fine-structure predissociation of the excited molecules. We will continue to explore the effects of chirped light on the production (and destruction) of ground-state molecules. One goal is to optimize, via parameters of the chirped pulses, the production of ground-state molecules in various states. In general, we anticipate that our ability to control the temporal variation of both the laser frequency (by chirping) and amplitude (by pulsing) will open up new opportunities in the manipulation of ultracold molecule formation.

Recent Publications:

“Coherent Control of Ultracold Collisions with Chirped Light: Direction Matters”, M.J. Wright, J.A. Pechkis, J.L. Carini, S. Kallush, R. Kosloff, and P.L. Gould, *Phys. Rev. A* **75**, 051401(R), (2007).

“Generation of Arbitrary Frequency Chirps with a Fiber-Based Phase Modulator and Self-Injection-Locked Diode Laser”, C.E. Rogers III, M.J. Wright, J.L. Carini, J.A. Pechkis, and P.L. Gould, *J. Opt. Soc. Am. B* **24**, 1249 (2007).

“Cold Molecules Beat the Shakes”, P.L. Gould, *Science* **322**, 203 (2008) (invited “Perspective” article).

“Characterization and Compensation of the Residual Chirp in a Mach-Zehnder-Type Electro-Optical Intensity Modulator”, C.E. Rogers III, J.L. Carini, J.A. Pechkis, and P.L. Gould, *Opt. Express* **18**, 1166 (2010).

Physics of Correlated Systems

Chris H. Greene

Department of Physics and JILA, University of Colorado, Boulder, CO 80309
chris.greene@colorado.edu

Program Scope

The broad goal of this project is to develop and apply methods of modern theoretical atomic and molecular physics to study fundamental atomic and molecular phenomena having potential relevance to energy transfer, control, and production. This project in basic science concentrates on developing an understanding of correlated dynamics. Correlations arise whenever two or more degrees of freedom are tightly coupled. Phenomena of this type pose a severe challenge to our theoretical understanding because much theory in atomic, molecular, and chemical physics starts initially from an uncorrelated, independent-particle approximation. We have found that the identification of a key collective coordinate often sparks insights that can provide both deeper qualitative insight as well as an enhanced ability to develop a detailed theoretical description of reactive processes. This class of problems includes systems where photon interactions play a role, usually handled through a classical approximation for the electromagnetic field degrees of freedom. This research aims to be as topical as possible for cutting-edge experimental work across the field of atomic, molecular, and optical physics. It develops a number of different techniques, in some cases stressing new algorithms or theoretical techniques, often with a computational component. The work during the past year has primarily concentrated in two areas: (i) low energy collisions between an electron and a diatomic or triatomic molecule; (ii) ionization and harmonic generation from intense short-pulsed laser light interacting with an atom or molecule.

Recent Progress

The papers cited below [1-12] have been supported at least in part by this project. Some of the more recent developments are highlighted in the following summary.

(i) Low energy electron-molecule collisions

The dissociative recombination (DR) process and related electron-molecule collision phenomena have continued to receive theoretical attention, in part because there are only a limited number of existing theoretical methods capable of treating this prototypical chemical reaction. The DR process involves an exchange of energy from the electronic to the nuclear degrees of freedom. We have continued to study the dissociative recombination of triatomic molecules, continuing to expand and develop theoretical tools needed to predict the low-energy dissociative recombination rate coefficient for electrons that collide with the NO_2^+ , HCO^+ , LiH_2^+ , HeH^+ , and H_3^+ molecules. In order to make continued progress, we have found it necessary to extend our techniques to handle the direct surface-crossing pathways as well as the indirect Rydberg-mediated pathways. For NO_2^+ our preliminary results suggest that the direct pathways will probably be dominant, and the required scattering calculations have determined quantum defect matrices.

The most recent extensions that we have completed relate to the fundamental collision process between an electron and the simplest polyatomic molecule H_3^+ . One recent study has investigated bound state transitions in the neutral molecule formed after the incident electron is captured. This system has been proposed to lead to lasing transitions between $3d$ and $3p$ levels, and our results bear on recent measurements by the Berkeley group of Rich Saykally.[1] In another investigation, we utilized techniques that had been originally developed to treat dissociative recombination to compute rovibrationally-inelastic rate coefficients.[2] Another

process having fundamental importance is the three-body (ternary) recombination reaction involving an electron, a D_3^+ molecular ion, and a ground state He atom; this recombination process can become dominant in certain types of discharge or afterglow environments.[3]

In the past year we also published a theoretical prediction of a strongly reactive collision between a ground state Rb(5s) atom and the electronically-excited dimer $NH(^1\Delta)$ that can transfer the excitation from the molecule to the alkali atom. The results are reported in Ref.[4], and the main conclusion is that the cross sections for this quenching reaction are quite large, in fact approaching a substantial fraction of the unitarity limit at low collision energies.

(ii) Intense light pulse interactions with an atom, molecule, or cluster.

With D. Elliott's experimental group we have computed a class of single-photon and two-photon ionization processes in atomic barium. The calculated results for the separate one-photon and two-photon ionization spectra show encouraging agreement with experiment. Some coherent control aspects, which arise when both lasers simultaneously and coherently ionize the barium atom with a controllable phase difference, have begun to be considered. These interesting coherence phenomena are a main motivation of this study, as we aim to provide a quantitative theoretical description of phase-controlled directional electron ejection in the presence of two such coherent fields.

Even low-intensity XUV radiation that excites doubly-excited states of atoms as simple as the rare gases can prove tremendously challenging for theory. One example of this is a study of alignment and orientation of photofragments produced by photoionization of atomic argon, which has yielded insights into the nature of the angular momentum transferred by the one-photon ionization process.[11]

As part of Zach Walters' doctoral dissertation research that was wrapped up a year ago, we considered the theoretical description of molecular imaging through either high-harmonic generation or photoelectron angular distributions from aligned molecules. In that study, we made some headway in understanding the limitations of the frequently-employed but less-frequently justified plane-wave approximation; that approximation is in fact highly problematic for many of the imaging studies that have been carried out to date.[9]

Another topic of recent interest relates to the control of X-ray or XUV radiation transmission through a gas by applying infrared control fields. Interest in that area is partly being stimulated by the new X-ray free-electron lasers under construction around the world, notably in Stanford and Hamburg. Our collaborative study with the Leone group at Berkeley demonstrated how three-level physics relates closely to electromagnetically-induced transparency arises in the physics of enhanced XUV absorption, in addition to some regimes of diminished absorption caused by the infrared field coupling.[10]

Immediate Plans

One project currently underway but not yet completed is an exploration of laser-assisted collisions between an electron and a rare gas atom, where some puzzles remain from conflicting past literature on the subject.

Effort is still underway in the coherent control study of phase-controlled photoionization of barium, using interference between single-photon and two-photon ionization. We are still working on combining the two separate amplitudes, after which the results should be compared with experimental observations of the phase-dependent photoelectron angular distribution. This system shows promise to be the first nontrivial one in which first-principles theory can give a quantitative description of the experimental observations of this prototype control phenomenon.

The strong-field ionization of molecules and the theoretical description of high-harmonic generation will receive continuing attention, as a part of the whole discipline's thrust to increasingly describe the molecular physics at a plausible, realistic level. A doubly-adiabatic formulation of the helium transient absorption problem discussed in [10] is also under continuing exploration, to test the feasibility of an *ab initio* description of XUV absorption near laser-dressed autoionizing states.

Electron scattering from polyatomic molecules continues to be a long-term project, and eventually we plan to build on the progress we have made in recent years on the description of dissociative recombination in polyatomic molecules, including the role of the Jahn-Teller and Renner-Teller effects. A long-term project in collaboration with the experimental group of Andreas Wolf in Heidelberg is nearing completion, which will give the first detailed study of the dissociative recombination problem for H_3^+ at the level of individual resonances. This should be finished and submitted for publication in the coming months. We are also exploring some alternative approaches to R-matrix theory, for the calculation of electron-molecule scattering matrices, with the hope that methods that avoid using a confining box might better connect with advanced quantum chemistry codes that have been developed for electronic bound states.

Papers published since 2008 that were supported at least in part by this DOE project

-
- [1] Quantum-defect analysis of $3p$ and $3d$ H_3 Rydberg energy levels, Phys. Rev. A (in press, 2010), and online at arXiv:1006.3629.
 - [2] Calculation of rate constants for vibrational and rotational excitation of the H_3^+ ion by electron impact, Mon. Not. R. Astron. Soc. **405**, 1195-1202 (2010).
 - [3] Temperature dependence of binary and ternary recombination of D_3^+ ions with electrons, T. Kotrik, P. Donal, I. Korolov, R. Plasil, S. Roucka, J. Glosik, C. H. Greene, and V. Kokoouline, J. Chem. Phys. (in press, 2010).
 - [4] Theoretical study of the quenching of $\text{NH}(\Delta)$ molecules via collisions with Rb atoms, D. J. Haxton, S. A. Wrathmall, H. J. Lewandowski, and C. H. Greene, Phys. Rev. A **80**, 022708-1 to -10 (2009). (This study and some of the others in this list received partial support from NSF in addition to DOE.)
 - [5] Indirect dissociative recombination of $\text{LiH}_2^+ + e$, D. J. Haxton and C. H. Greene, Phys. Rev. A **78**, 052704-1 to -10 (2008).
 - [6] *ab initio* frame transformation calculations of direct and indirect dissociative recombination rates of $\text{HeH}^+ + e^-$, D. J. Haxton and C. H. Greene, Phys. Rev. A **79**, 022701-1 to -7 (2009).
 - [7] Diffraction in low-energy electron scattering from DNA: bridging gas-phase and solid-state theory, L. Caron, L. Sanche, S. Tonzani, and C. H. Greene, Phys. Rev. A **78**, 042710-1 to -13 (2008).
 - [8] Low-energy electron scattering from DNA including structural water and base-pair irregularities, L. Caron, L. Sanche, S. Tonzani, and C. H. Greene, Phys. Rev. A **80**, 012705-1 to -6 (2009).
 - [9] Limits of the plane wave approximation in the measurement of molecular properties, Z. B. Walters, S. Tonzani, and C. H. Greene, J. Phys. Chem. A **112**, 9439-9447 (2008).
 - [10] Femtosecond induced transparency and absorption in the extreme ultraviolet by coherent coupling of the He $2s2p$ ($^1P^o$) and $2p^2$ ($^1S^e$) double excitation states with 800 nm light, Zhi-Heng Loh, C. H. Greene, and S. R. Leone, Chem. Phys. **350**, 7-13 (2008).
 - [11] Use of partial-wave decomposition to identify resonant interference effects in the photoionization-excitation of argon, T. J. Gay, C. H. Greene, J. R. Machacek, K. W. McLaughlin, H. W. van der Hart, O. Yenen, and D. H. Jaecks, J. Phys. B **42**, 042008-1 to -17 (2009).
 - [12] Three-body breakup in dissociative electron attachment to the water molecule, D. Haxton, T. N. Rescigno, and C. W. McCurdy, Phys. Rev. A **78**, 040702(R)-1 to -4 (2008).

Using Strong Optical Fields to Manipulate and Probe Coherent Molecular Dynamics

Robert R. Jones, Physics Department, University of Virginia
382 McCormick Road, P.O. Box 400714, Charlottesville, VA 22904-4714
bjones@virginia.edu

I. Program Scope

This project focuses on the exploration and control of non-perturbative dynamics in small molecules driven by strong laser fields. Our goal is to exploit the current understanding of strong-field processes to implement novel ultrafast techniques for manipulating and probing coherent electronic and nuclear motion within molecules. Ultimately, through the application of these methods, we will work to obtain a more complete picture of the non-perturbative response of molecules to intense laser pulses.

Of particular interest to us are measurements requiring optical pulses and pulse sequences with well-defined optical phase, either the relative carrier phase between two pulses or the absolute phase of one optical field relative to the center of the intensity envelope of a second pulse. Such fields can assert a time-dependent, laboratory-fixed directionality in a system of interest. This directionality, particularly when used in combination with preferentially oriented molecular targets, can enable experiments in which electrons are driven in specific directions within molecules to probe and control molecular structure and dynamics.

II. Recent Progress

Our work during the past year has focused primarily on directional Coulomb explosion of molecules in asymmetric fields. First, we have extended our previous work employing phase-coherent 2-color, $1\omega+2\omega$, pulses to induce asymmetric multielectron dissociative ionization (MEDI) of diatomic and triatomic molecules. In particular, we have substituted a recoil ion momentum imaging spectrometer for a standard time-of-flight spectrometer which allows us to better separate various dissociation channels and to examine the effect of the relative phase on the full angular distribution of the dissociating fragments. We have also obtained absolute phase assignments for the asymmetries in several molecules. These can be used as 2-color phase standards for strong-field experiments in general. Second, in collaboration with several groups [Matthias Kling (MPQ and KSU), Gerhard Paulus (Friedrich-Schiller-Universität), Robert Moshhammer and Joachim Ullrich (MPI, Heidelberg), and Itzik Ben-Itzhak (KSU)] we have begun to explore asymmetric MEDI in diatomic molecules using few-cycle laser pulses with known CE-phase in a pump-probe configuration.

A. Controlled Directional Coulomb Explosion in an Asymmetric 2-Color Laser Field

In a previous funding period, we began a study of directional MEDI of diatomic and triatomic molecules. Specifically, we exposed N_2 , O_2 , CO , HBr , and CO_2 to strong, asymmetric 2-color laser fields, employing temporally overlapped 40 fs laser pulses with wavelengths of 400 nm and 800 nm and tunable relative carrier phase, ϕ . For the molecules studied, the yields of all atomic ion fragments with charges $q \geq 2$ originating from non-symmetric dissociation channels (i.e. non-identical fragments), show a pronounced, ϕ -dependent forward/backward asymmetry in the time-of-flight spectrum along the laser polarization axis. For a given ion species, we define an

asymmetry parameter, $\beta = (S_+ - S_-) / (S_+ + S_-)$ where S_+ and S_- are the number of ions detected with velocities toward and away from the detector, respectively. At combined laser intensities $I \sim 5 \times 10^{14} \text{ W/cm}^2$, asymmetries as large as $\beta \sim \pm 0.7$ are observed for $\text{N}_2^{2+} \rightarrow \text{N}^{2+} + \text{N}$ and $\text{O}_2^{2+} \rightarrow \text{O}^{2+} + \text{O}$, with comparable asymmetries in several CO channels, e.g. $\text{CO}^{4+} \rightarrow \text{C}^{2+} + \text{O}^{2+}$ or $\text{CO}^{3+} \rightarrow \text{C}^+ + \text{O}^{2+}$. Strong, though somewhat smaller asymmetries are found in other N_2 and O_2 channels as well as in HBr and CO_2 . By comparing the φ -dependence of the fragment asymmetries with that of the tunneling ionization yield for the parent molecule, we determine that for all fragments, the maximum β values are obtained at $\varphi_{\text{max}} = 0, \pi$ where the field has the greatest magnitude and greatest asymmetry. We observe no significant variation in φ_{max} with changes in the laser intensity. Moreover, for all fragment channels, the asymmetry curves for the ion species with the highest ionization potential share precisely the same phase-dependence.

Given the diversity in molecular structure and reactivity for the set of species studied and the variation in appearance intensity at which different multiply-charged fragments are produced, the uniformity in the observed φ -dependence is quite remarkable, and suggests a common, field-driven dynamical mechanism. This is contrasted by the recent report of 2-color asymmetric dissociation of deuterium, $\text{D}_2 \rightarrow \text{D} + \text{D}^+$, in which a strong variation in the φ -dependence of the directional asymmetry within the same species is observed for both different fragment energies and different laser intensities [1].

In an attempt to identify the mechanism for the directional Coulomb explosion, several auxiliary measurements have been performed. First, using circularly polarized pulses, we can suppress electron recollisions while maintaining a phase-dependent directional asymmetry in the 2-color field. In this case, we find comparable β values, indicating that field-driven electron rescattering does not play a dominant role in the dissociation processes. Second, using a 2-color pump field with reduced intensity ($I \sim 10^{14} \text{ W/cm}^2$) in conjunction with a more intense, time delayed 800 nm probe, we have confirmed that transient orientation of heteronuclear molecules or molecular ions in the two-color field is negligible in our experiments and, therefore, is not responsible for the asymmetries we observe. Third, we recently used a recoil ion momentum spectrometer to measure the angular distribution of the doubly-charged dissociation fragments from N_2 , O_2 , and CO. We find that the fragment angular distributions are highly localized in the forward and backward directions and show no significant 2-color phase-dependence other than the forward/backward asymmetry. Fourth, we have obtained an absolute phase calibration for the 2-color field, eliminating the uncertainty in the field directions for which fragments are preferentially ejected in the forward and backward directions, respectively. In an effort to make this calibration we first made consecutive measurements of asymmetric dissociation in N_2 and D_2 and compared our D_2 results to those of the KSU group [1]. We were able to reproduce their kinetic energy dependence of the phase at which maximum asymmetry was observed. However, our use of their absolute phase assignment resulted in an inconsistency with our modulo- π phase determination based on molecular tunneling ionization. Presumably this inconsistency is the result of the sensitivity of the D_2 measurements to laser intensity. However, comparison of our CO asymmetry measurements with unpublished results from the KSU group gives an absolute phase determination that is consistent with all of our results. According to this calibration, for all the species that we have measured, the ion with the highest ionization potential in a given fragment pair is preferentially formed on the downhill side of the combined Coulomb and optical potential.

In total, our measurements appear to be consistent with the notion that enhanced sequential ionization occurs as the molecule dissociates [2,3]. Charge-localization near one atomic ion, induced dynamically by the asymmetric field, makes further ionization much more likely from one ion center than from the other. Through enhanced ionization, higher charged states are most likely produced when the dissociating molecule has expanded to (for molecules with HOMOs of σ -symmetry) or beyond (non- σ HOMOs) a critical internuclear distance, R_c [3,4]. There the most weakly bound electrons can be localized on the uphill side of the combined molecular and optical potential, leaving less negative charge on the downhill side. Electrons located on the uphill side of the potential are most efficiently ionized *through the inner potential barrier* at phases, $\varphi_{\max} = 0, \pi$ where the field asymmetry is maximum. Following this final ionization, the atomic ions move apart rapidly under their mutual Coulomb repulsion. The ion angular distributions at the detector reflect their relative orientation at the instant of ionization. Thus, the direction of the maximum in the asymmetric field opposes the preferred emission direction for the most positive atomic ion species. This basic mechanism is insensitive to the details of the molecular structure. A manuscript describing this work is nearly ready for submission.

b) Pump-probe Studies of MEDI with Few-Cycle Pulses of known CE-Phase

If enhanced ionization is responsible for the directional MEDI observed with 2-color fields, a number of important questions remain unanswered. First, does the asymmetry arise solely from the final ionization step near R_c , or does the initial dissociation event that causes the molecule to expand also play a role? Second, is ionization at R_c optimal for directional fragment control, or does it simply give the largest contribution to the MEDI yield? To answer these questions one could use ultrashort pump and probe pulses to isolate the initial dissociation, expansion, and final ionization events. This would require laser pulses with durations much less than the expansion time to R_c (~ 20 fs for the molecules we have studied). Recognition of this short pulse limitation begs additional questions: Can a level of directional control similar to that realized with 2-color fields be obtained with asymmetric few-cycle laser pulses? If so, can directional Coulomb explosion be used as a robust single shot CE-phase detector?

To address these questions we, and the other members of a collaboration headed by Matthias Kling at MPQ, have performed preliminary pump-probe measurements of MEDI in N_2 and O_2 using sub-5fs pulses with known CE-phase. The experiments were performed in a standard COLTRIMS apparatus. A piezo-driven split mirror was used to create time-delayed pump and probe pulses from a single input beam and focus them to a single spot within the COLTRIMS spectrometer. The CE-phase of the few-cycle pulses was not locked, but instead, was measured on each laser shot using a stereo ATI optical phase detector [5].

The initial experiments focused on N^{2+} and O^{2+} fragments from N_2 and O_2 , respectively. Very preliminary results show signatures of enhanced ionization in both species, with depletion of some dissociation channels and enhancement of others occurring at pump-probe delays corresponding to internuclear separations near R_c . Surprisingly, compared to the long pulse 2-color measurements, we find little (if any) asymmetry in the directionality of the N^{2+} and O^{2+} dissociation fragments, for any kinetic energy release or pump-probe delay. This is not due to the lack of asymmetry in the few-cycle pump-probe pulses, as strong, directional recollision momentum transfer is observed in the non-sequential ionization of atomic targets in the same

apparatus. The apparent differences in the controllability of the system using a long 2-color pulse as opposed to two, shorter few cycle pulses is intriguing and our analysis is continuing.

III. Future Plans

Beyond our plan to continue the molecular pump-probe experiments at MPQ, we are currently upgrading our laboratory facilities for other experiments at UVa. First we are constructing a hollow-core fiber compressor which should allow us to produce few-cycle CE-phase stabilized pulses for molecular pump-probe experiments and the generation of attosecond pulses or pulse trains. We hope to utilize these attosecond pulses to photoionize molecules, near threshold, in the presence of a phase-locked laser field. We seek to characterize the effects of the ionic core on the electron energy spectrum to determine if such measurements might be useful for probing changes in molecular potentials with sub-femtosecond resolution. Second, we have acquired an Even-Lavie pulsed gas valve which should enable us to achieve sufficient rotational cooling (~1K) in our molecular beam apparatus to produce and study transiently oriented molecules at kHz repetition rates. To do this we will need to upgrade the Ti:Sapphire that is currently dedicated to the molecular beam experiments from a 15 Hz to 1 kHz repetition rate. We have obtained supplemental funding for the acquisition of a kHz pump laser to complete the laser upgrade.

IV. Publications from Last 3 Years of DOE Sponsored Research

- i) Brett A. Sickmiller and R.R. Jones, "Effects of Phase-Matching on High Harmonic Generation from Aligned N₂," *Physical Review A* **80**, 031802(R) (2009).
- ii) E. S. Shuman, R. R. Jones, and T. F. Gallagher, "Multiphoton Assisted Recombination," *Phys. Rev. Lett.* **101**, 263001 (2008).
- iii) D. Pinkham, T. Vogt, and R.R. Jones, "Extracting the Polarizability Anisotropy from the Transient Alignment of HBr," *J. Chem. Phys.* **129**, 064307 (2008).

References

1. D. Ray, F. He, S. De, W. Cao, H. Mashiko, P. Ranitovic, K.P. Singh, I. Znakovskaya, U. Thumm, G.G. Paulus, M.F. Kling, I.V. Litvinyuk, and C.L. Cocke., *Phys. Rev. Lett.* **103**, 223201 (2009).
2. T. Seideman, M.Yu. Ivanov, and P.B. Corkum, *Phys. Rev. Lett.* **75**, 2819 (1995); T. Zuo and A.D. Bandrauk, *PRA* **52**, R2511 (1995).
3. G. L. Kamta and A.D. Bandrauk, *Phys. Rev. A* **76**, 053409 (2007).
4. G. L. Kamta and A.D. Bandrauk, *Phys. Rev. A* **75**, 041401(R) (2007).
5. T. Wittman, B. Horvath, W. Helml, M.G. Schatzel, A.L. Cavalieri, and G.G. Paulus, *Nature Phys.* **5**, 357 (2009).

Progress Report and Continuation Request

Molecular Dynamics Probed by Coherent Electrons and X-Rays

DOE AMOP Grant # DE-FG02-99ER14982

P.I.: Henry C. Kapteyn, co-PI: Margaret M. Murnane
University of Colorado at Boulder, Boulder, CO 80309-0440
Phone: (303) 492-8198; E-mail: kapteyn@jila.colorado.edu

The goal of this work is to develop novel short wavelength probes of materials and of molecules. We have made exciting advances in several experiments that probe complex molecular and materials dynamics using ultrafast, coherent, x-rays and electrons emitted during the high harmonic generation process. Following are several highlights of recent work supported by this grant –

Probing coupled electron and nuclear dynamics in polyatomic molecules [31]

X-ray, electron, or laser beam scattering are common techniques used to probe crystalline or molecular structure and dynamics. To understand how complex reactions happen, the positions of atoms within a solid or a molecule must be monitored as the reaction occurs. Usually an external source of electrons or x-rays is used to monitor a fast process. In this work, we are employing two techniques. First, ultrafast soft x-rays generated by the ionization and recollision of electrons from the molecule itself can be used to

probe the internal structure and dynamics of a molecule. Second, the ionization of a molecule in a strong field can also be a powerful probe of molecular dynamics, raising new questions about the dynamics of a chemical bond.

In our most recent work, submitted for publication,[31] we probe the dissociation of a simple diatomic molecule by strong-field ionizing it during the dissociation. Through careful comparison with theory, we can probe the dynamics of the entire electron density (all orbitals) in the valence shell as it rearranges from molecular-like to atomic-like. The experimental data are also immediately surprising: strong molecular signatures exist for ~150 fs after excitation, and the localization of electrons onto the individual

atoms is abrupt. These data are in apparent contradiction to recent EUV photoemission experiments that indicated bond breaking after ~85 fs. In that work, the authors argue that the electronic structure of the bromine atom is established sooner, around 85 fs after dissociation. A plausible explanation for their faster dissociation timescale is that a linear spectroscopy technique was used, which primarily provides information on the binding energy. However, this remains unchanged once the potential energy curves corresponding to the dissociation channel become flat. Single photon XUV ionization is likely to be insensitive to parts of the wavefunction that interact weakly with the nuclei, while strong field ionization

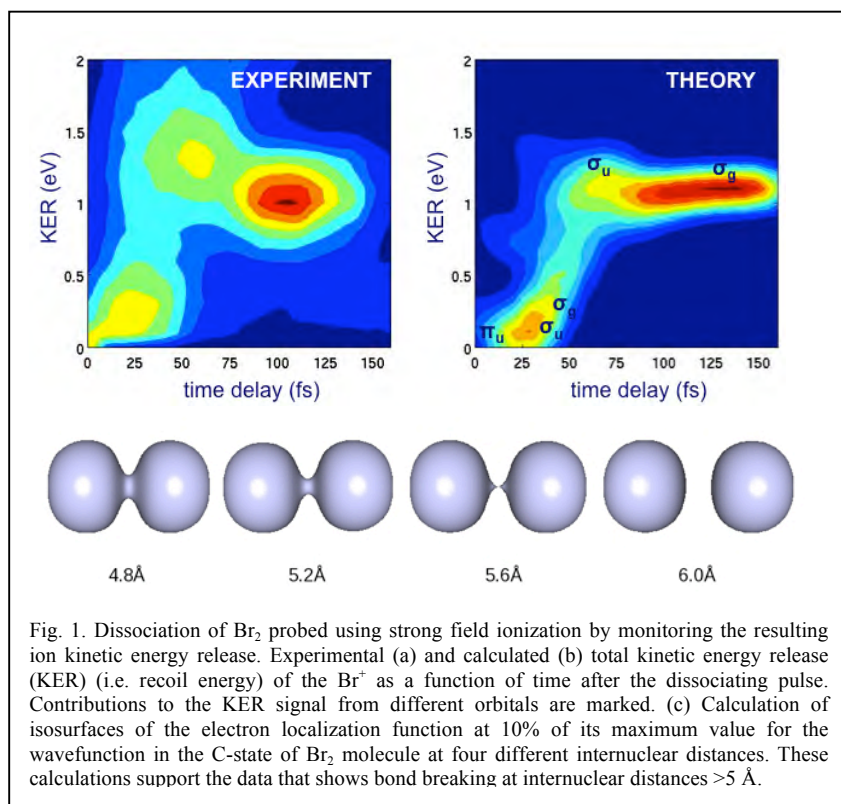


Fig. 1. Dissociation of Br_2 probed using strong field ionization by monitoring the resulting ion kinetic energy release. Experimental (a) and calculated (b) total kinetic energy release (KER) (i.e. recoil energy) of the Br^+ as a function of time after the dissociating pulse. Contributions to the KER signal from different orbitals are marked. (c) Calculation of isosurfaces of the electron localization function at 10% of its maximum value for the wavefunction in the C-state of Br_2 molecule at four different internuclear distances. These calculations support the data that shows bond breaking at internuclear distances $>5 \text{ \AA}$.

can readily field ionize this loosely-bound electron density. Thus, to identify the breaking point of a bond, an observation of electron dynamics beyond static features is needed (e.g. measurement of an angular distribution, as is done here). This work also goes beyond other recent work that followed the dynamics of a single electron orbital using high harmonic generation from dissociating Br₂.

In collaboration with the groups of Andreas Becker and Agnieszka Jaron-Becker, we have developed models that are in reasonable agreement with experiment. These calculations seem to indicate that the strong-field ionization rate is correlated with the Electron Localization Function (ELF), which is a measure of the degree of correlation between electrons in individual atoms.

Understanding high harmonic generation from molecules [3, 6, 12, 13, 14, 15, 17, 18, 19, 27]

Other work continues to explore the use of the high-order harmonic generation process to extract structural information on molecules. In work published in 2009,[19] we showed that elliptically polarized light could be generated by transiently aligned molecules illuminated with linearly polarized light. This work has drawn considerable interest from theorists, and more recently we have extended these measurements to a polarization analysis of high-order harmonic emission in simple molecules transiently aligned, and *driven* by elliptically polarized light. (see Fig. 2) Much of the behavior can be explained through a tunneling trajectory interpretation; however, currently we believe that some aspects may require

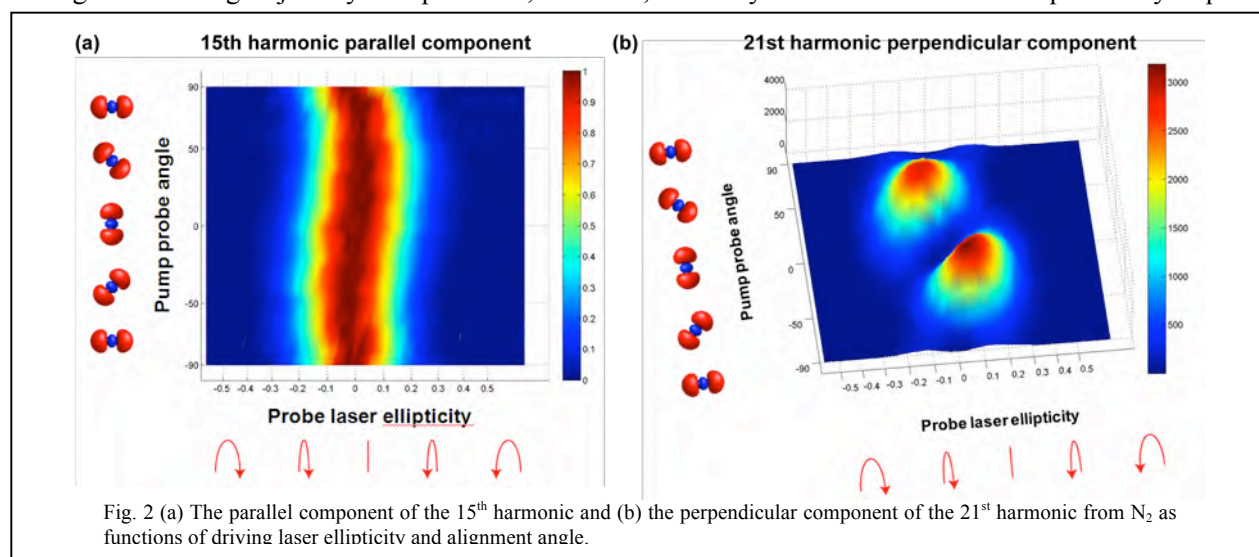


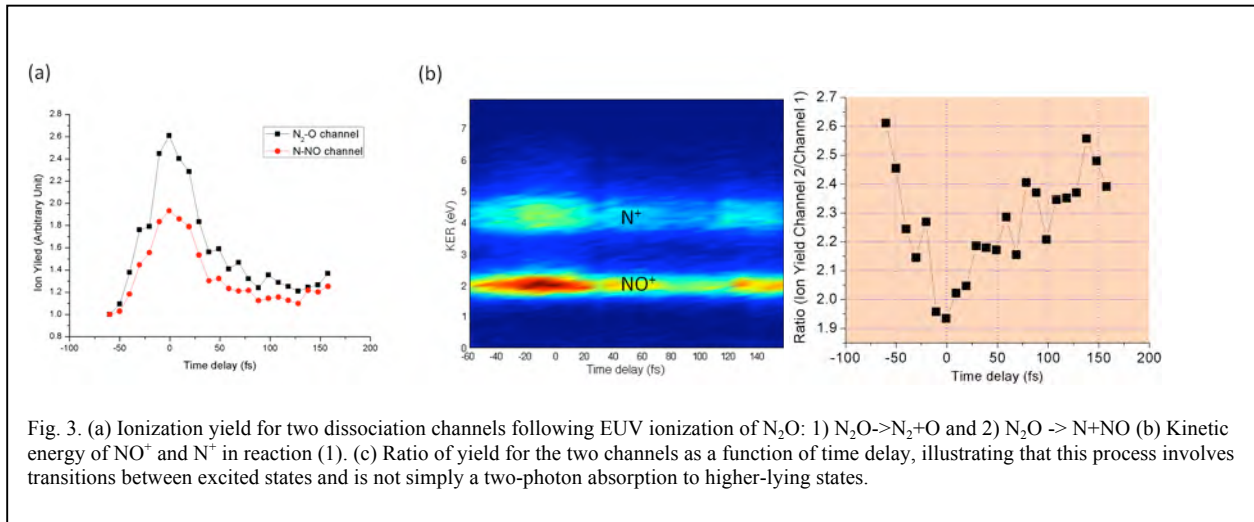
Fig. 2 (a) The parallel component of the 15th harmonic and (b) the perpendicular component of the 21st harmonic from N₂ as functions of driving laser ellipticity and alignment angle.

an interpretation that includes wavepacket dynamics in the ionized atom in the time between ionization and recombination. This work was presented at *Ultrafast Phenomena*, and is in prep for publication.

Radiation femtochemistry and coherent control of highly-excited molecules [10, 14, 15, 18]

In past experiments we made the first use of high-brightness, high repetition-rate high-order harmonic light in conjunction with a COLTRIMS momentum imaging apparatus to observe directly the chemical dynamics initiated by ionizing radiation i.e. *radiation femtochemistry*. This work immediately yielded new and unanticipated findings, exploring dissociation dynamics in highly excited states of N₂ and O₂ molecules.[10,18] These experiments are uniquely suited to the use of HHG light sources, and explore new science that cannot be accessed using other approaches. For example, we showed how EUV ionization of O₂ yields super-excited O⁺ through a very indirect, Feshbach-resonance process.[18] Bound states become unbound once the internuclear distance reaches 30 Å.

In our most recent work, we studied the possibility of *control* of the dissociation process in these highly excited dissociative states. Our prototype system for this is a triatomic, N₂O, and our goal is obtain selectivity in the breaking of the N-N bond vs. the N-O bond. In XUV-pump, IR probe experiments using COLTRIMS detectors, we can clearly see that we can manipulate this branching ratio (see fig 3). This work was presented at *Ultrafast Phenomena*, and is in preparation for publication.



Progress in other DOE-funded collaborations [1, 2, 4, 5, 7 - 9, 16, 20 -26, 28-9]

In work done in collaboration with Keith Nelson at MIT, used coherent EUV diffraction to observe, for the first time, “ballistic” dissipation of heat from a nanoscale heat source into a substrate. In work done in collaboration with Jorge Rocca at Colorado State University, we significantly extended the energy range of high harmonic generation from Ar ions to 550eV. We also demonstrated *full phase matching* in Ar, Ne and He at energies of 100eV, 200eV and 330eV for the first time. We have now demonstrated our understanding of phase matching of the HHG process in a very large range of parameter space, including phase-matched HHG to photon energies >0.5 keV. This understanding makes it clear that new phase matching schemes can be extended into the hard-x-ray region.

Unexpended Funds

We anticipate no unexpended funds at the end of this grant period.

Personnel supported by this grant

Xibin Zhou (until April 2010, now postdoc with Keith Nelson, MIT)

Robynne Lock

Chengyuan Ding

Publications as a result of DOE support since 2006

1. A. Paul, E. Gibson, X. Zhang, A. Lytle, T. Popmintchev, X. Zhou, M. Murnane, I. Christov, H. Kapteyn, “Phase matching techniques for coherent soft-x-ray generation”, *invited paper*, IEEE J. Quant. Electron. **42**, 14 (2006).
2. D. Gaudiosi, E. Gagnon, A. Lytle, J. Fiore, M. Murnane, H. Kapteyn, R. Jimenez, S. Backus, “Scalable multi-kHz Ti:sapphire amplifier based on down-chirped pulse amplification”, Opt. Express **14**, 9277 (2006).
3. N. Wagner, A. Wüest, I. Christov, T. Popmintchev, X. Zhou, M. Murnane, H. Kapteyn, “Monitoring Molecular Dynamics using Coherent Electrons from High-Harmonic Generation”, PNAS **103**, 13279 (2006).
4. D. Gaudiosi, B. Reagan, T. Popmintchev, M. Grisham, M. Berril, O. Cohen, B. Walker, M. Murnane, H. Kapteyn, J. Rocca, “HHG from ions in a capillary discharge”, Phys. Rev. Lett. **96**, 203001 (2006).
5. R. Tobey, M. Siemens, M. Murnane, H. Kapteyn, K. Nelson, “Ultrasensitive Transient Grating Measurement of Surface Acoustic Waves in Thin Metal Films with EUV Radiation”, Appl. Phys. Lett. **89**, 091108 (2006).
6. N. Wagner et al., “High-Order X-Ray Raman Scattering using Coherent Electrons from High Harmonic Generation”, “Optics in 2006”, Optics and Photonics News pp 43 (Dec. 2006). *Also featured on cover.*
7. D. Gaudiosi et al., “HHG from ions in a capillary discharge”, “Optics in 2006”, Optics & Photonics News, pp 44 (Dec. 2006).

8. Ra'anan I. Tobey, Mark E. Siemens, Oren Cohen, Margaret M. Murnane, and Henry C. Kapteyn "Ultrafast Extreme Ultraviolet Holography: Dynamic Monitoring of Surface Deformation", *Optics Letters* **32**, 286 (2007).
9. B.A. Reagan et al., "Enhanced High Harmonic Generation from Xe, Kr, and Ar in a Capillary Discharge", *Physical Review A* **76**, 013816 (2007).
10. Etienne Gagnon, Predrag Ranitovic, Ariel Paul, C. Lewis Cocke, Margaret M. Murnane, Henry C. Kapteyn, and Arvinder S. Sandhu, "Soft X-ray driven femtosecond molecular dynamics," *Science* **317**, 1374 (2007).
11. Henry C. Kapteyn, Oren Cohen, Ivan Christov, Margaret M. Murnane, "Harnessing Attosecond Science in the Quest for Coherent X-Rays," *Science* **317**, 775 (2007).
12. N. Wagner et al. "Extracting the Phase of High Harmonic Emission from a Molecule using Transient Alignment in Mixed Samples," *Phys. Rev. A* **76**, 061403(R) (2007).
13. Xibin Zhou, Robynne Lock, Wen Li, Nick Wagner, Margaret M. Murnane, Henry C. Kapteyn, "Molecular Recollision Interferometry in High Harmonic Generation," *Physical Review Letters* **100**, 073902 (2008).
14. E. Gagnon et al., "Time-resolved momentum imaging system for molecular dynamics studies using a tabletop ultrafast extreme-ultraviolet light source," *Rev. Sci. Instrum.* **79**, 063102 (2008).
15. I. Thomann, R. Lock, V. Sharma, E. Gagnon, S. Pratt, H. Kapteyn, M. Murnane, W. Li, "Direct Measurement of the Transition Dipole for Single-Photon Photoionization of N₂ & CO₂," *J. Phys. Chem. A* **112**, 9382 (2008).
16. T. Tenio Popmintchev, M.C. Chen, O. Cohen, M.E. Grisham, J.J. Rocca, M.M. Murnane, H.C. Kapteyn, "Phase-Matching of High Harmonics Driven by Mid-Infrared Light," *Optics Letters* **33**, 2128 (2008).
17. W. Li, X. Zhou, R. Lock, S. Patchkovskii, A. Stolow, H. Kapteyn, M. Murnane, "Time-resolved Probing of Dynamics in Polyatomic Molecules using High Harmonic Generation", *Science* **322**, 1207 (2008). (*on cover*)
18. A. S. Sandhu, E. Gagnon, R. Santra, V. Sharma, W. Li, P. Ho, P. Ranitovic, C. L. Cocke, M. M. Murnane, and H. C. Kapteyn, "Observing the Creation of Electronic Feshbach Resonances in Soft X-ray-Induced O₂ Dissociation," *Science* **322**, 1081 (2008).
19. X. Zhou, R. Lock, W. Li, N. Wagner, M. Murnane, H. Kapteyn, "Observation of Elliptically Polarized High Harmonic Emission from Molecules Driven by Linearly Polarized Light," *Phys. Rev. Lett.* **102**, 073902 (2009).
20. M. Siemens, Q. Li, M. Murnane, H. Kapteyn, R. Yang, E. Anderson, K. Nelson, "High-Frequency Acoustic Propagation in Nanostructures Characterized by Coherent EUV Beams", *Appl. Phys. Lett.* **94**, 093103 (2009).
21. T. Popmintchev, M. C. Chen, A. Bahabad, M. Gerrity, P. Sidorenko, O. Cohen, I. P. Christov, M. M. Murnane, and H. C. Kapteyn, "Phase matching of high harmonic generation in the soft and hard X-ray regions of the spectrum," *Proceedings Of The National Academy Of Sciences Of The United States Of America*, vol. 106, pp. 10516-10521, (2009).
22. M.C. Chen, M.R. Gerrity, S. Backus, T. Popmintchev, X. Zhou, P. Arpin, X. Zhang, H.C. Kapteyn, and M.M. Murnane, "Spatially coherent, phase matched, high-order harmonic EUV beams at 50 kHz," *Optics Express*, vol. 17, pp.17376-17383 (2009).
23. P. Arpin, T. Popmintchev, N. L. Wagner, A. L. Lytle, O. Cohen, H. C. Kapteyn, and M. M. Murnane, "Enhanced High Harmonic Generation from Multiply Ionized Argon above 500 eV through Laser Pulse Self-Compression," *Physical Review Letters*, vol. 103, pp. 143901/1-4 (2009).

The following publications were supported by DOE since November 14 2009

24. P. Ranitovic, Xiao-Min Tong, B. Gramkow, S. De, B. DePaola, K. P. Singh, W. Cao, M. Magrakvelidze, D. Ray, I. Bocharova, H. Mashiko, A. Sandhu, E. Gagnon, M. M. Murnane, H. C. Kapteyn, I. Litvinyuk and C.L. Cocke, "IR-Assisted Ionization of Helium by Attosecond XUV Radiation," *New Journal of Physics*, vol. 12, art 013008 (2010).
25. M. E. Siemens, Q. Li, R. G. Yang, K. A. Nelson, E. H. Anderson, M. M. Murnane, and H. C. Kapteyn, "Quasi-ballistic thermal transport from nanoscale interfaces observed using ultrafast coherent soft X-ray beams," *Nature Materials*, vol. 9, pp. 26-30 (2010).
26. C. La-O-Vorakiat, M. Siemens, M. M. Murnane, H. C. Kapteyn, S. Mathias, M. Aeschlimann, P. Grychtol, R. Adam, C. M. Schneider, J. M. Shaw, H. Nembach, and T. J. Silva, "Ultrafast Demagnetization Dynamics at the

- M Edges of Magnetic Elements Observed Using a Tabletop High-Harmonic Soft X-Ray Source," *Physical Review Letters*, vol. 103, pp. 257402/1-4 (2009).
27. R. M. Lock, X. B. Zhou, W. Li, M. M. Murnane, and H. C. Kapteyn, "Measuring the intensity and phase of high-order harmonic emission from aligned molecules," *Chemical Physics*, vol. 366, pp. 22-32 (2009).
 28. K. S. Raines, S. Salha, R. L. Sandberg, H. D. Jiang, J. A. Rodriguez, B. P. Fahimian, H. C. Kapteyn, J. C. Du, and J. W. Miao, "Three-dimensional structure determination from a single view," *Nature*, vol. 463, pp. 214-217 (2010).
 29. K. P. Singh, F. He, P. Ranitovic, W. Cao, S. De, D. Ray, S. Chen, U. Thumm, A. Becker, M. M. Murnane, H. C. Kapteyn, I. V. Litvinyuk, and C. L. Cocke, "Control of Electron Localization in Deuterium Molecular Ions using an Attosecond Pulse Train and a Many-Cycle Infrared Pulse," *Physical Review Letters*, vol. 104, art 023001 (2010).
 30. T. Popmintchev, M.M. Murnane and H.C. Kapteyn, " The Nonlinear Optics of Coherent X-Ray Generation: Photonics at the Timescale of the Electron ", invited paper in preparation, *Nature Photonics* (2010).
 31. Wen Li, Agnieszka A. Jaroń-Becker, Craig W. Hogle, Vandana Sharma, Xibin Zhou, Andreas Becker, Henry C. Kapteyn and Margaret M. Murnane, "Strong Field Ionization Probing of the Transition from a Molecule to Atoms," submitted (2009).

Detailed Investigations of Interactions between Ionizing Radiation and Neutral Gases

Allen Landers

landers@physics.auburn.edu

Department of Physics
Auburn University
Auburn, AL 36849

We are investigating phenomena associated with ionization of an atom or molecule by photon or charged particle with an emphasis on ionization-driven atomic and molecular dynamics, in particular electron correlation effects. We perform these measurements using variations on the well established COLTRIMS technique. The photoionization work takes place at the Advanced Light Source at LBNL as part of the ALS-COLTRIMS collaboration with the groups of Reinhard Dörner at Frankfurt and Ali Belkacem and Thorsten Weber at LBNL. Additional experiments on charged particle impact are conducted locally at Auburn University where we are studying the dissociative molecular dynamics following interactions with ions over a velocity range of 1 to 12 atomic units. Due to limited space, we present a sample of two recent (to be published) results.

1. Angular correlation of electrons emitted via the double Auger decay of K -shell ionized neon

The primary result from work we published in 2009 (pub. 5) indicated a breakdown in the 2-step picture of photoelectron emission followed by Auger decay for the small amount of phase space where the two are emitted in the same direction from the neon atom. To further investigate this phenomenon, we have now performed a similar measurement but restricted (*a posteriori*) the decay path to be a *double*-Auger to the Ne^{3+} state (Fig. 1 left). We used circularly polarized light from the ALS at LBNL to remove any lab-frame orientation of the photoelectron in the plane perpendicular to the photon propagation axis. This in turn allowed us to cleanly measure the momenta of *all three* continuum electrons (2 measured, 1 calculated by momentum conservation with the ion) for a kinematically complete measurement. By restricting the energy sum of two of the electrons, we were able to isolate the double-Auger channel (Fig. 1 right).

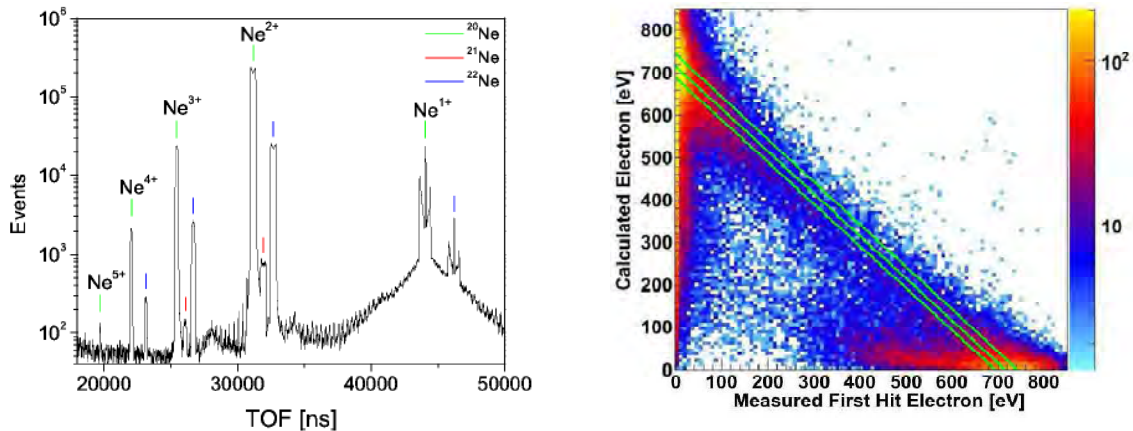


Figure 1 (Left): Neon ion time of flight spectrum following K -Shell photo-ionization just above threshold. The Ne^{3+} channel contributes about 6% to the total number of events and is only accessible through double-Auger. **(Right):** Energy correlation between the measured first hit and calculated electron. The diagonal line corresponds to the constant energy sum for the double Auger channel. The variation in resolution as a function of energy is apparent.

The isolated double-Auger channel resembles strongly the single-photon double-photoionization of helium. Figure 2 shows the energy sharing between the two double-Auger electrons. There is a much higher probability for asymmetric sharing than symmetric sharing. This is consistent with double photoionization result, where the “shake” and “knock-out” processes are often used to model the

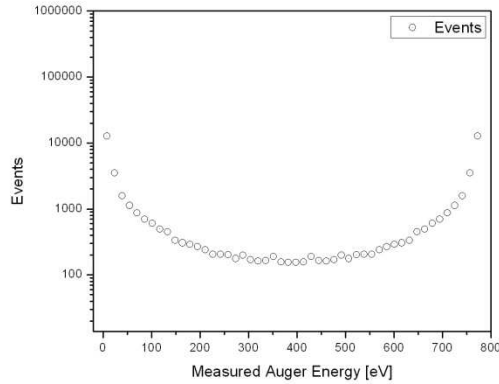


Figure 2: Energy sharing between the two double-Auger electrons. Note strong propensity for asymmetric energy sharing, which is similar to the well known single photon double ionization result.

asymmetric and symmetric energy sharing cases respectively. Figure 3 shows the angular correlation between the Augers for different energy sharing, where 0° is defined by the momentum vector of the fast electron. For extremely low energies where the photoelectron is indistinguishable from the low-energy Auger, we observe a distribution consistent with the single Auger case with the forbidden region. For symmetric and asymmetric cases that don’t overlap with the photoelectron energy, we observe roughly isotropic (“shake”) and $\sim 130^\circ$ peaked (“knockout”) distributions.

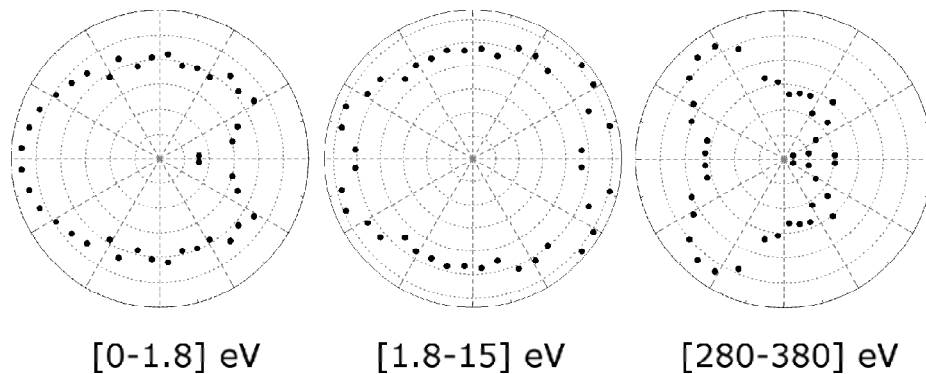


Figure 3: Distribution of the angle between double-Auger electrons as a function of the energy of one Auger. The left plot covers the same energy range as the photo-electron, so the low-energy Auger and photo-electron are indistinguishable. The middle plot covers an energy range just above the photoelectron energy where the two Auger electrons share energy asymmetrically. The right plot covers an energy range where the sharing is more symmetric.

We are currently analyzing this data further to explore the 3-electron coincidence to see if we can better understand the breakdown of the 2-step picture of Auger decay. For example: we can restrict the double-Auger to symmetric energy sharing where both Auger electrons have hundreds of eV energy. Is there a correlation between the Auger momentum sum for this case and the photoelectron momentum? This and other questions are being explored.

2. Formation and characterization of helium Rydberg atoms

One of the calibration techniques we use for COLTRIMS at the ALS is to singly photoionize helium gas slightly above threshold. During one such calibration run, we found an unexpected image on the helium ion detector shown in the left panel Figure 5. The expected features are the horizontal stripe and small spot just above it that correspond to photon interaction with background gas and ionization of the helium jet by harmonic contamination. The unexpected feature is the stripe that rises vertically from

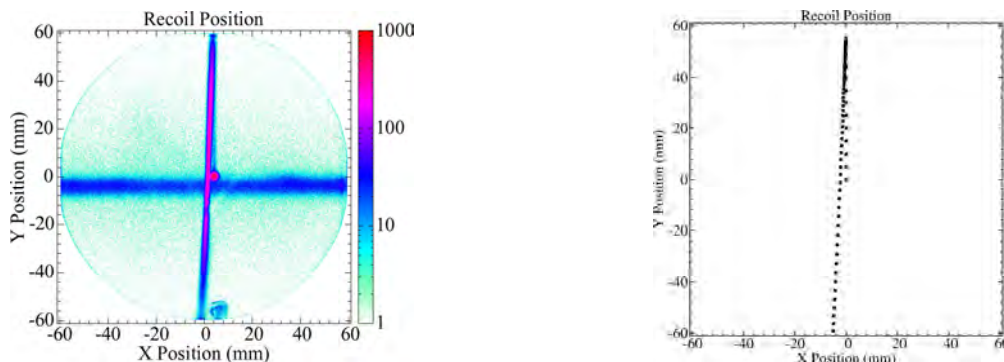


Figure 5 (Left): Helium ion detector showing vertical curved stripe produced from field-ionized Rydberg atoms. **(Right):** SIMION calculation reproducing the detector image.

the jet spot and then comes back down with a slight curve to the left. After further analysis and extensive simulation (see Fig. 5 right), we have concluded that we were producing helium Rydberg atoms.

The photon energy was tuned slightly below threshold and therefore excited the atoms in the jet to Rydberg states. These then traveled vertically at the jet velocity until they left the spectrometer. Because the spectrometer had a voltage bias relative to the grounded jet-catcher tube, they were field

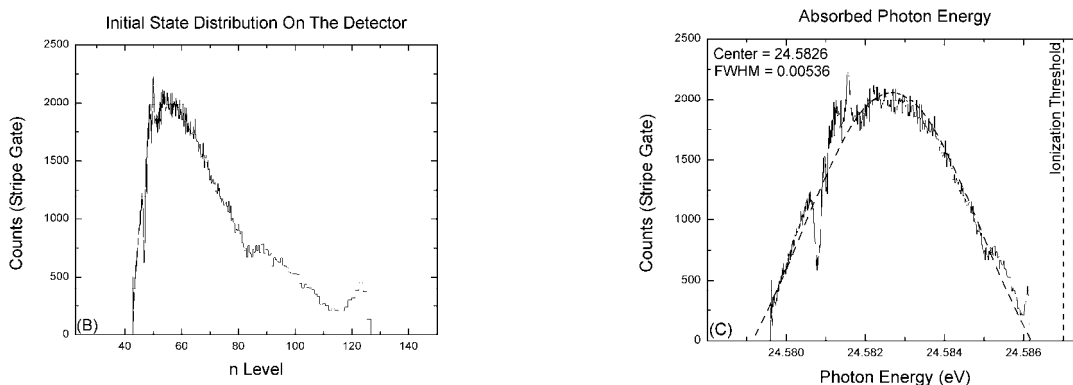


Figure 2 (Left): Distribution of principle quantum number of field-ionized helium Rydberg atoms. **(Right):** Energy distribution of absorbed photons derived from data in left panel. The structures on the left side of the peak are experimental artifacts that are well understood. The 5.36 meV width is consistent with the monochromator-defined resolution of the photon beam.

ionized just outside the spectrometer and then directed back into the spectrometer by the same voltage bias. Different n levels were ionized at different points along the path as the electric field increased, which lead to different ion trajectories and corresponding hit positions on the detector. After careful modeling of the spectrometer, we have been able to extract the populated n levels based on the hit positions on the detector. This distribution is shown in the left panel of Figure 6. Converting to binding energy and adding the helium ionization potential (Fig. 6 right) yields a distribution consistent with the expected photon distribution from the monochromator.

While no new science resulted directly from this measurement and analysis, it has nonetheless been useful. We are now designing of a new type of COLTRIMS experiment that will allow us to study

near threshold effects. By tuning the synchrotron energy to near (just above, just below, or straddling) the double ionization threshold, we can study in detail ionization-excitation by measuring *in coincidence* the photoelectron momentum and Rydberg state of the singly charged helium ion.

Supported Refereed Publications

1. **Angular Correlation of Electrons Emitted by Double Auger Decay of K-Shell Ionized Neon** M.P. Jones, M. Schöffler, T. Janke, K. Kreidi, J. Titze, R. Dörner, C. Stuck, A. Belkacem, Th. Weber, A.L. Landers, in preparation for *Phys. Rev. A* (2010).
2. **Auger decay of $1\sigma_g$ and $1\sigma_u$ hole states of N_2 molecule: II. Young type interference of Auger electrons and its dependence on internuclear distance** N. A. Cherepkov, S. K. Semenov, M. S. Schöffler, J. Titze, N. Petridis, T. Jahnke, K. Cole, L. Ph. H. Schmidt, A. Czasch, D. Akoury, O. Jagutzki, J. B. Williams, T. Osipov, S. Lee, M. H. Prior, A. Belkacem, A. L. Landers, H. Schmidt-Böcking, R. Dörner and Th. Weber, *Phys. Rev. A* (accepted 2010).
3. **Separation of Auger transitions into different repulsive states after K-shell photoionization of N_2 molecules** N. A. Cherepkov, S. K. Semenov, M. S. Schöffler, J. Titze, N. Petridis, T. Jahnke, K. Cole, L. Ph. H. Schmidt, A. Czasch, D. Akoury, O. Jagutzki, J. B. Williams, T. Osipov, S. Lee, M. H. Prior, A. Belkacem, A. L. Landers, H. Schmidt-Böcking, R. Dörner and Th. Weber, *Phys. Rev. A* **80**, 051404(R) (2009).
4. **Photo and Auger Electron Angular Distributions of Fixed-in-Space CO_2** F.P. Sturm, M. Schöffler, S. Lee, T. Osipov, N. Neumann, H.-K. Kim, S. Kirschner, B. Rudek, J.B. Williams, J.D. Daughhetee, C.L. Cocke, K. Ueda, A.L. Landers, Th. Weber, M.H. Prior, A. Belkacem, and R. Dörner, *Phys. Rev. A* **80**, 032506 (2009).
5. **Angular Correlation between Photo- and Auger electrons from K-Shell Ionization of Neon** A.L. Landers, F. Robicheaux, T. Jahnke, M. Schöffler, T. Osipov, J. Titze, S.Y. Lee, H. Adaniya, M. Hertlein, P. Ranitovic, I. Bocharova, D. Akoury, A. Bhandary, Th. Weber, M.H. Prior, C.L. Cocke, R. Dörner, and A. Belkacem, *Phys. Rev. Lett.* **102**, 223001 (2009).
6. **Fragmentation pathways for selected electronic states of the acetylene dication** T Osipov, T N Rescigno, T Weber, S Miyabe, T Jahnke, A S Alnaser, M P Hertlein, O Jagutzki, L Ph H Schmidt, M Schöffler, L Foucar, S Schössler, T Havermeier, M Odenweller, S Voss, B Feinberg, A L Landers, M H Prior, R Dörner, C L Cocke and A Belkacem, *J. Phys. B*, **41** 091001 (2008).
7. **Ultrafast Probing of Core Hole Localization in N_2** M. S. Schöffler, J. Titze, N. Petridis, T. Jahnke, K. Cole, L. Ph. H. Schmidt, A. Czasch, D. Akoury, O. Jagutzki, J. B. Williams, N. A. Cherepkov, S. K. Semenov, C. W. McCurdy, T. N. Rescigno, C. L. Cocke, T. Osipov, S. Lee, M. H. Prior, A. Belkacem, A. L. Landers, H. Schmidt-Böcking, Th. Weber, and R. Dörner, *Science*, **320**, 920 (2008).
8. **Interference in the collective electron momentum in double photoionization of H_2** Kreidi K, Akoury D, Jahnke T, Weber T, Staudte A, Schöffler M, Neumann N, Titze J, Schmidt LPH, Czasch A, Jagutzki O, Costa Fraga RA, Grisenti RE, Smolarski M, Ranitovic P, Cocke CL, Osipov T, Adaniya H, Thompson JC, Prior MH, Belkacem A, Landers AL, Schmidt-Böcking H, and Dörner R., *Phys. Rev. Lett.*, **100**, 133005 (2008).
9. **A two-electron double slit experiment: interference and entanglement in photo double ionization of H_2** D. Akoury, K. Kreidi, T. Jahnke, Th. Weber, A. Staudte, M. Schöffler, N. Neumann, J. Titze, L. Ph. H. Schmidt, A. Czasch, O. Jagutzki, R.A. Costa Fraga, R. Grisenti, R. Diez Muino, N. Cherepkov, S. Semenov, P. Ranitovic, C.L. Cocke, T. Osipov, H. Adaniya, M.H. Prior, A. Belkacem, A. Landers, H. Schmidt-Böcking, and R. Dörner, *Science*, **318**, 949 (2007).
10. **Single Photon-Induced Symmetry Breaking of H_2 Dissociation** F. Martín, J. Fernández, T. Havermeier, L. Foucar, Th. Weber, K. Kreidi, M. Schöffler, L. Schmidt, T. Jahnke, O. Jagutzki, A. Czasch, E. P. Benis, T. Osipov, A. L. Landers, A. Belkacem, M. H. Prior, H. Schmidt-Böcking, C. L. Cocke, R. Dörner, *Science* **315**, 629 (2007).

Program Title:

"Properties of actinide ions from measurements of Rydberg ion fine structure"

Principal Investigator:

Stephen R. Lundeen
Dept. of Physics
Colorado State University
Ft. Collins, CO 80523-1875
lundeen@lamar.colostate.edu

Program Scope:

This project will determine certain properties of chemically significant Uranium and Thorium ions through measurements of fine structure patterns in high-L Rydberg ions consisting of a single weakly bound electron attached to the actinide ion of interest. The measured properties, such as polarizabilities and permanent moments, control the long-range interactions of the ion with the Rydberg electron or other ligands. The ions selected for initial study in this project, U^{6+} , U^{5+} , U^{4+} , Th^{4+} , and Th^{3+} , all play significant roles in actinide chemistry, and are all sufficiently complex that *a-priori* calculations of their properties are suspect until tested. The measurements planned under this project should serve the dual purpose of providing data that is directly useful to actinide chemists and providing benchmark tests of relativistic atomic structure calculations. In addition to the work with U and Th ions, which takes place at the J.R. Macdonald Laboratory at Kansas State University, a parallel program of studies with stable singly-charged ions takes place at Colorado State University. These studies are aimed at clarifying theoretical questions connecting the Rydberg fine structure patterns to the properties of the free ion cores, thus directly supporting the actinide ion studies. In addition, they provide training for students who can later participate directly in the actinide work.

Recent Progress:

U^{6+} : We have worked hard to resolve RESIS signals in U^{5+} Rydberg ions, but so far without success. In a typical transition, 53-93, the resolved RESIS signals, if present, are less than 0.1% of the high-L signal. We think this disappointing result is due to a large fraction of metastable U^{6+} ions in the ECR beam. The lowest excited levels of the Rn-like U^{6+} ion represent the $6p^55f$ configuration about 13eV above the ground state, almost all members of which are metastable. After charge capture, these metastable U^{6+} ions form doubly-excited Rydberg U^{5+} ions that make our planned experiment very difficult in two ways.

1) Some of these metastable Rydberg ions spontaneously auto-ionize within our Rydberg detector at precisely the same location and electric potential where we intentionally Stark ionize the RESIS signal ions. This produces a large background that greatly increases the noise level in the measured RESIS signals.

2) The metastable Rydberg ions can also be excited by the CO_2 laser, and will contribute to the unresolved high-L signal. Due to the various high angular momentum values of the metastable levels, the metastable Rydberg ions do not produce a simple pattern in the RESIS excitation spectrum, but have the net effect of diluting the resolved signals from the ground state Rydberg ions.

For the present, we have given up on U and moved on to Th.

Th⁴⁺: Our work with Th Rydberg ions could not have been more different than our work with U. Almost immediately when we obtained a beam of Rn-like Th⁴⁺ and charge captured to form Rydberg Th³⁺ ions, we started to see resolved RESIS signals of approximately 1-2% of the size of the high-L signal, i.e. 10-20 times larger than the limit set in the U studies. It was also much easier to see these signals because the noise levels were much smaller. For example, the background rate in the detector was about a factor of ten larger than the high-L signal in U, but only a factor of two larger in Th. Taken together, the larger signals and the smaller background made the Th studies at least a factor of 100 less time consuming than the U studies, and I say at least because we still haven't definitively seen a resolved RESIS signal in U. Figure 2 below shows one of the Th³⁺ RESIS signals we obtained during this grant period. Along with another similar scan of a different RESIS transition, this formed the basis of our measurement of the dipole and quadrupole polarizabilities of Rn-like Th⁴⁺. A paper reporting this result has just been submitted for publication. The measured polarizabilities are

$$\alpha_d = 7.61(6) a.u., \quad \alpha_Q = 47(11) a.u.$$

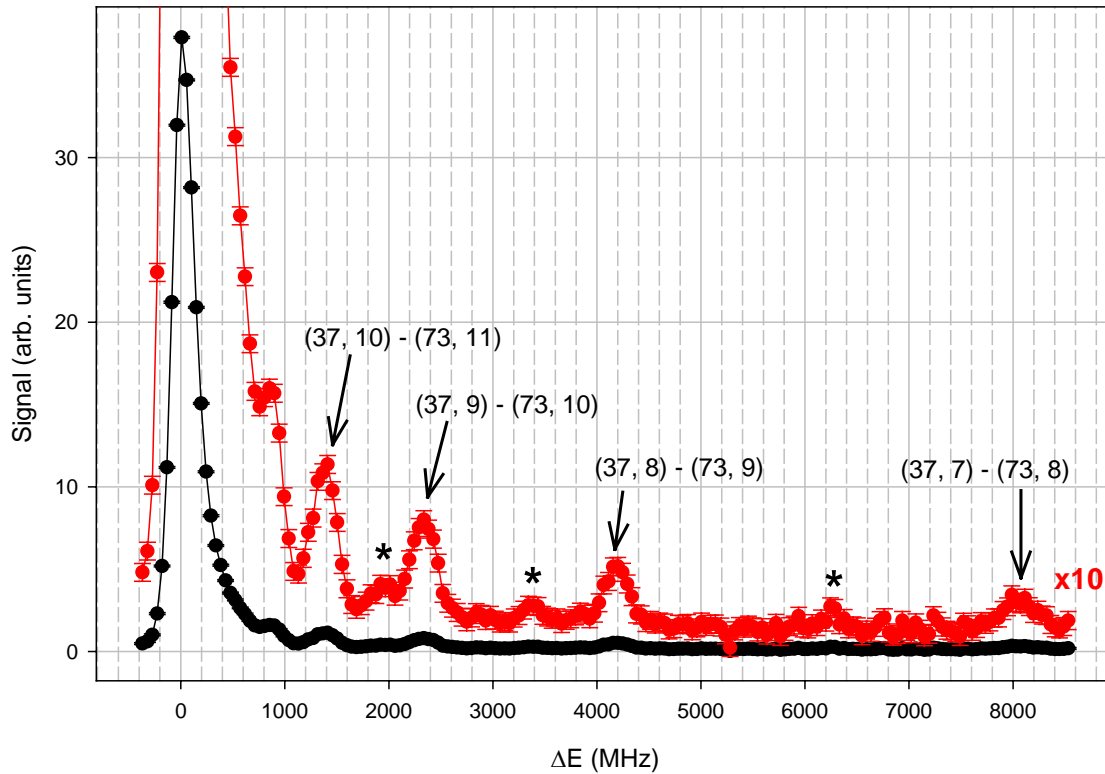


Figure 2: RESIS Excitation spectrum of the $n = 37 - 73$ transition in Th³⁺. The black points show the measured signal, and the red points are magnified by a factor of ten to display the resolved RESIS signals more clearly. The x-axis represents the energy difference from the hydrogenic energy of the 37 - 73 transition. The asterisks identify the weaker $\Delta L = -1$ transitions associated with each strong transition.

Th³⁺: We have also been able to measure resolved RESIS signals in Rydberg Th²⁺ ions whose core is the Fr-like Th³⁺ ion. Since the ground state of Th³⁺ is a ²F_{5/2} level, the fine structure pattern in these Rydberg ions is very complicated, comparable to the patterns we have been studying in Ni. We have just begun exploring these spectra, and Fig. 3 shows an early example, the n=29 to n'=72 RESIS excitation. As expected, the spectrum is complex, showing a great deal of structure, some well resolved, some unresolved. It is particularly interesting to see the splitting of the high-L peak due to the dominance of the quadrupole moment of Th³⁺ in the structure of the highest L levels. In addition to this spectrum, we have also observed similar structure in the n=27 to n'=60 and the n=28 to n'=66 transitions. From these we have obtained initial estimates of the quadrupole moment and scalar polarizability of the ²F_{5/2} ground state of Th³⁺.

$$Q = 0.61(2) \text{ a.u.} \quad \alpha_{d,0} = 15.7(6) \text{ a.u.}$$

Analysis of the Th²⁺ spectrum is complicated by the very low excitation energy of Th³⁺ excited states, especially the ²F_{7/2} (0.536 eV), ²D_{3/2} (1.139 eV), and ²D_{5/2} (1.795 eV) levels. This results in large non-adiabatic effects in the Rydberg fine structure. Our experience in analyzing similar effects in Ba Rydberg levels has been very helpful in this analysis.

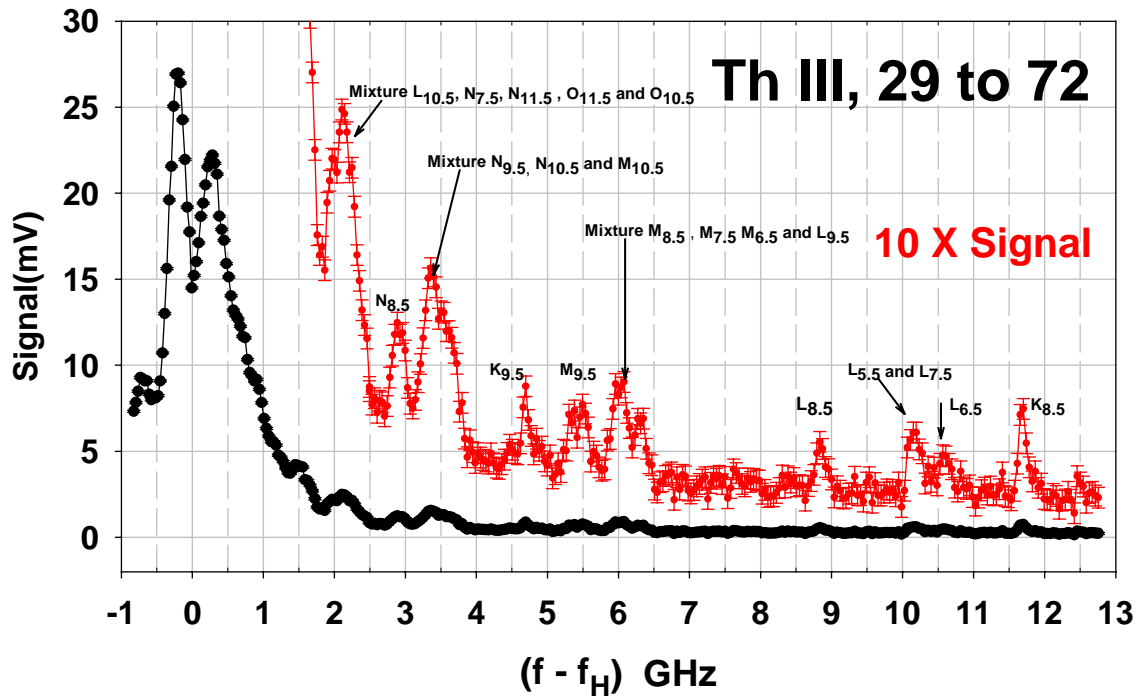


Fig. 3. RESIS spectrum of n=29 to n'=72 excitations in Th²⁺. The high-L peak is split by the quadrupole structure in the highest L levels. Partially resolved structure from lower L levels is also visible, including six fully resolved lines. Lines are identified by the n=29 level excited in the transition, using spectroscopic notation. The letters K, L, M, N, O stand for L = 7, 8, 9, 10, 11, and the subscript gives the value of the quantum number K=L+J_c.

One obvious remaining issue at KSU is clarification of the reason why the Th experiments have been so much easier than the U experiments. Both U^{6+} and Th^{4+} are Rn-like ions, and both should have many metastable levels, but the two RESIS studies are dramatically different. We have been thinking hard about this and consulting with others who may have insight, and one of our goals for the next year is to come up with a way forward for the U studies.

Ni: We have started measurements of the fine structure in high-L levels of Ni using microwave spectroscopy. So far we have measured 14 microwave transitions, but since the fine structure pattern is very complex, there is much more to do before this study is complete.

Immediate Future Plans:

- 1) Complete the analysis of optical RESIS spectra in Th III.
- 2) Complete the microwave spectroscopy of Ni Rydberg levels.
- 3) Begin microwave spectroscopy of Rydberg levels of Th IV and Th III.
- 4) Find a way to make the U VI optical studies work.

Recent Publications:

"Determination of dipole and quadrupole polarizabilities of Mg^+ by fine structure measurements in high-L, $n=17$ Rydberg states of Mg", E.L. Snow and S.R. Lundeen, Phys. Rev. A 77, 052501 (2008)

"Microwave spectroscopy of high-L $n=10$ Rydberg states of argon", M.E. Hanni, Julie A. Keele, and S.R. Lundeen, Phys. Rev. A 78, 062510 (2008)

"Dipole and quadrupole transition strengths in Ba^+ from measurements of K-splittings in high-L barium Rydberg levels", Shannon L. Woods, S.R. Lundeen, and Erica L. Snow, Phys. Rev. A 80, 042516 (2009)

"Optical spectroscopy of high-L Rydberg states of nickel", Julie A. Keele, Shannon L. Woods, M.E. Hanni, S.R. Lundeen, and W.G. Sturuss, Phys. Rev. A 81, 022506 (2010)

"Polarizabilities of Pb^{2+} and Pb^{4+} and Ionization Energies of Pb^+ and Pb^{3+} from spectroscopy of high-L Rydberg states of Pb^+ and Pb^{3+} ". M.E. Hanni, Julie A. Keele, S. R. Lundeen, C.W. Fehrenbach, and W.G. Sturuss, Phys. Rev. A 81, 042512 (2010)

"Dipole transition strengths in Ba^+ from Rydberg fine structure measurements in Ba and Ba^+ ", Shannon L. Woods, M.E. Hanni, S.R. Lundeen, and Erica L. Snow (To be published, Phys. Rev. A)

"Polarizabilities of Rn-like Th^{4+} from spectroscopy of high-L Rydberg levels of Th^{3+} ", M.E. Hanni, Julie A. Keele, S.R. Lundeen, and C.W. Fehrenbach (submitted to Phys. Rev. A)

Theory of threshold effects in low-energy atomic collisions

J. H. Macek

*Department of Physics and Astronomy,
University of Tennessee, Knoxville, Tennessee and
Oak Ridge National Laboratory, Oak Ridge, Tennessee
email:jmacek@utk.edu*

1 Program scope

Time-dependent wave functions for low-energy ion-atom collisions computed at the outset of our project have shown that vortices are present [1]. Further theory showed that the vortices can be observed as “holes” in electron momentum distributions and that these vortices play an important role in atomic dynamics at low energy. The present project focuses on the physical implication of vortices in time-dependent wave functions.

The main objective of our research is to understand the role that vortices may play in atomic physics, how they may be observed experimentally, and whether they can be exploited for applied purposes. The present report narrows the focus to identify the connection between angular momentum transfer and vortices. To be more precise, we examine the transfer of “orientation”, defined as the mean value of the vector angular momentum, in atomic processes.

We also continue our research into structure related to threshold phenomena. The projects listed in this abstract are sponsored by the Department of Energy, Division of Chemical Sciences, through a grant to the University of Tennessee. The research is carried out in cooperation with Oak Ridge National Laboratory under the ORNL-UT Distinguished Scientist program.

2 Recent progress

Previous work with the Regularized Lattice-Time-Dependent-Schrödinger equation (RLTDSE) method [1,2] has shown that time-dependent atomic wave functions $\psi(\mathbf{r}, t)$ may have vortices corresponding to rotation of the electron probability $|\psi(\mathbf{r}, t)|^2$ about centers \mathbf{r}_v . A surprising feature is that

\mathbf{r}_v need not correspond to a force center and the vortices can be located anywhere. This feature is unexpected, therefore our project has focused on whether vortices are of general importance for atomic physics. To that end we have addressed the following issues: (1) can vortices in atomic wave functions be observed?; (2) how general is the formation vortices in atomic processes?; (3) are there potential applications of vortex structure in time-dependent atomic wave functions?

To address the first question we have developed the “imaging theorem” namely the statement that measured momentum distributions $P(\mathbf{k})$ image *coordinate* space wave functions according to

$$P(\mathbf{k}) = \lim_{t \rightarrow \infty} \left[\left| t^3 \psi(\mathbf{r}, t) \right|^2 \right]_{\mathbf{r}=\mathbf{k}t} \quad (1)$$

where it is understood that $\mathbf{r} \neq \mathbf{r}_Q$ and \mathbf{r}_Q is any potential center. This equation allows structure in $P(\mathbf{k})$ to be traced to structure in $\psi(\mathbf{r}, t)$ at earlier times. Using the RLTDSE method and the imaging theorem we have shown that “holes” in highly accurate momentum distributions are due to free vortices [2]. It was also shown that the vortices are observable, in principle. We have further shown that an exact zero at any point other than at potential centers must be a vortex. Computation of the probability current \mathbf{w} shows that it circulates around the zero and is quantized according to $\oint \mathbf{w} \cdot d\mathbf{l} = 2\pi$.

The status Eq. (1) is somewhat ambiguous. To many researchers it is obvious, but to those accustomed to expressions for $P(\mathbf{k})$ in terms of the square of transition matrix elements $|T_{\mathbf{k}}|^2$ it is not immediately clear that the two interpretations are equivalent. We have shown [1,3] that the two interpretations are indeed equivalent. This means that structures in $P(\mathbf{k})$ where both the real and imaginary parts of $T_{\mathbf{k}}$ vanish relate to vortices in time-dependent wave functions.

Transition matrix elements for electron impact ionization where both the real and imaginary parts of $T_{\mathbf{k}}$ vanish were found in 1993 by Berakdar and Briggs for (e,2e) processes in atomic helium. Their theoretical work identified an exact zero near a measured minima. Using a 3C correlated final state, as in the previous calculations that found a minimum, we have computed the (e,2e) T-matrix element for helium targets [3]. The calculations show an exact zero, *i. e.* a vortex, as expected. It was proposed that this vortex had actually been observed experimentally.

The second question, namely, how general are vortices in atomic processes was addressed by examining the high energy limit of electron impact ioniza-

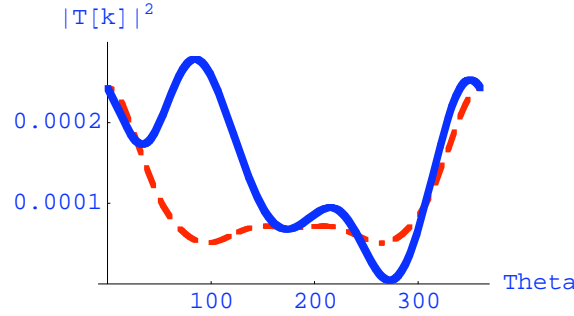


Figure 1: Plot of the square of the absolute value of the T-matrix¹ for ionization of carbon K-shell electron in atomic units versus the angle of ejection of a slow electron with $E_{\mathbf{k}} = 9.6eV$ relative to the momentum transfer axis when the incident electron with $E_i = 1801.2eV$ is scattered through an angle of 20° . The dashed curve (red online) is the plane wave Born approximation. The solid curve (blue online) is the Born T-matrix with an added vortex contribution extracted from the Coulomb Born theory.

tion when the ejected electron's energy is in the threshold region. The plane wave Born approximation is known to give the high energy limit of ionization for fixed *momentum loss* \mathbf{q} of the incident electron. For fixed *scattering angle* θ_f of the incident electron and $v \rightarrow \infty$, this is no longer true since the incident particle is primarily deflected by collisions with the atomic nucleus, not by collisions with the atomic electron. Owing to potential scattering from the nucleus, the incident electron must lose some angular momentum \mathbf{L} . Part of this angular momentum is transferred to the ejected electron. It follows that the mean value of the ejected electron's angular momentum (orientation) $\langle \ell \rangle$ is non-zero so that the $P(\mathbf{k})$ will have isolated exact zeros. We have found such structure for electron impact ionization of K-shell electrons in carbon computed in the Coulomb Born approximation. This approximation allows for collision of the incident electron with the atomic nucleus and therefore gives the high incident energy limit at fixed scattering angle.

Figure 1 shows a plot of $|T(\mathbf{k})|^2$ vs. the angle of ejection of the K-shell electron for 1801 keV electron impact on the K-shell of carbon in the Born approximation and in the Born approximation modified by adding an $m = 1$ contribution from the Coulomb Born amplitude. It is this modification that produces a vortex which appears in the figure as an exact zero near the point $\theta = 270^\circ$, where the angle θ is measured from the momentum transfer axis.

The eikonal Coulomb Born approximation has also been applied to ionization of atomic hydrogen by proton and antiproton impact. In both case we find that there are vortices in the electron momentum distribution. These vortices appear as holes in contour plots of $P(\mathbf{k})$.

Our main conclusion is that vortices commonly occur in atomic collisions. Since they strongly affect angular distributions they need to be understood theoretically. They are not, however, controllable in collisions, thus we are investigating vortices in short pulse ionization of atoms by linearly and circularly polarized light to see if controllable vortices are produced.

Other projects include structure that appears in elastic scattering [4], charge exchange reactions [4], low energy three-body interactions [5] and ionization by positron impact [6]. The threshold ionization cross section obeys the extended threshold law proposed earlier by us and verified by convergent close coupling model calculations. We find some unanticipated structure owing to hidden crossings of hyperspherical adiabatic potential energy curves.

3 References to DOE sponsored research that appeared in 2008-2010

1. Origin, evolution, and imaging of vortices in atomic processes, J.H. Macek J.S. Sternberg and S.Y. Ovchinnikov, T-G. Lee and D.R. Schultz, Phys. Rev. Lett, **102**, 143201(2009).
2. Evolution of quantum systems from microscopic to macroscopic scales, Sergey Y. Ovchinnikov, Joseph H. Macek, James S. Sternberg, Teck-Ghee Lee, and David R. Schultz, CAARI 2008 Proceedings AIP Conference Proceedings, **1099**, 164 (2009).
3. Theory of deep minima in (e,2e) measurements of triply differential cross sections, J. H. Macek, J. B. Sternberg, S. Yu. Ovchinnikov and J. S. Briggs, Phys. Rev. Lett. **104**, 033201 (2010).
4. Feshbach resonances in atomic structure and dynamics, J. H. Macek, Proceedings of the JointPhysics/Mathematics Workshop on Quantum Few-Body Systems, AIP Conf. Proc. **998**, 59 (2008).
5. Multiparticle interactions of zero-range potentials, J. H. Macek, Few-Body Syst, **45**,207 (2009).
6. Near-threshold positron impact ionization of hydrogen, S. J. Ward, Krista Jansen, J. Shertzer, and J. H. Macek, Nuc. Inst. Meth. B, **266**, 410 (2008).

Ionization of Free and Confined Atoms and Ions

Steven T. Manson, Principal Investigator

Department of Physics and Astronomy, Georgia State University, Atlanta, Georgia 30303
(smanson@gsu.edu)

Program Scope

The goals of this research program are: to provide a theoretical adjunct to, and collaboration with, the various atomic and molecular experimental programs that employ third generation light sources, particularly ALS and APS; to generally enhance our understanding of the photoabsorption process; and to study the properties (especially photoabsorption) of confined atoms and ions. To these ends, calculations are performed employing and enhancing cutting-edge methodologies to provide deeper insight into the physics of the experimental results; to provide guidance for future experimental investigations; and seek out new phenomenology, especially in the realm of confined systems. The general areas of programmatic focus are: manifestations of nondipole effects in photoionization; photodetachment of inner and outer shells of atoms and atomic ions (positive and negative); studies of atoms endohedrally confined in buckyballs, C_{60} , particularly dynamical properties. Flexibility is maintained to respond to opportunities that present themselves as well.

Highlights of Recent Progress

1. Confined Atoms

The study of confined atoms is in its early stages. There are a number of theoretical investigations of various atoms endohedrally confined in C_{60} [1,2], but experimental studies are sparse [3,4]. Thus, we are conducting a program of calculations at various levels of approximation, aimed at delineating the properties of such systems, especially photoionization, to guide the experimental community. Among our recent results, we have found that a huge transfer of oscillator strength from the C_{60} shell, in the neighborhood of the giant plasmon resonance, to the encapsulated atom for both $Ar@C_{60}$ [5] and $Mg@C_{60}$ [6]. Also, a new type of atom-fullerene hybridization in $Xe@C_{60}$ was discovered [7] which occur owing to the near-degeneracy of atomic and C_{60} states; these hybrid states exhibit rich photoionization structure, radically different from the cross sections of free atomic or fullerene states.

In addition, confinement resonances [8], oscillations that occur in the photoionization cross section of an endohedral atom owing to the interferences of the photoelectron wave function for direct emission with those scattered from the surrounding carbon shell have been found in a broad range of cases, and the photoionization of endohedral atoms within nested fullerenes, called buckyonions, has shown that, as a result of the multi-walled confining structures, the confinement resonances become considerably more complicated [9].

Recent experiment on the photoionization of $Xe@C_{60}$ in the region dominated by Xe 4d [4] has revealed evidence of these confinement resonances that agree with our best calculations [7] as far as amplitude is concerned but not with phase. We have shown that

the amplitudes of the confinement resonances are inversely related to the width of the confinement potential [10]. Further, we have found that consideration of the polarization of the C_{60} by an inner-shell atomic hole changes the phases of the confinement resonances [11].

While these various effects have been computationally demonstrated in particular cases, their importance is that they are, in fact, quite general and it is expected that they will arise in many confined atom systems.

2. Photoionization of Free Atoms and Ions

The study of photoionization of atoms and ions at high resolution leads to results of great complexity. One recent effort has focused upon the Be isoelectronic sequence. We have explored satellite processes (photoionization plus excitation) along the sequence and quantitatively characterized how these two-electron processes become less important with increasing Z [12], and we have looked how resonances converging to differing Be^+ thresholds overlap more and more with increasing Z [13]. We have also looked at the higher- Z transition metals and found that the $3p3d$ resonances which dominated the spectrum of Sc^{+2} , has partially moved below threshold for Ti^{+3} and are entirely in the discrete for higher Z , thereby changing the spectrum dramatically [14]. Experiment is available for Ti^{+3} and agreement is excellent.

We have also been developing a new methodology to treat photoionization termed Multiconfiguration Tamm-Dancoff (MCTD) which handles both coupling among the continuum channels in the same manner as the random phase approximation, and discrete state correlation is introduced *via* a multiconfiguration configuration-interaction expansion. MCTD should be useful because it can treat open-shell systems, satellite (two-electron) processes, and relativistic interactions. Preliminary results of this development on inner-shell photodetachment of Na^- [15] are quite encouraging.

3. Nondipole Effects in Atoms and Ions

Up until relatively recently, the conventional wisdom was that nondipole effects in photoionization were of importance only at photon energies of tens of keV or higher, despite indications to the contrary more than 35 years ago [16]. The last decade has seen an upsurge in experimental and theoretical results [17] showing that nondipole effects in photoelectron angular distributions could be important down to hundreds [18] and even tens [19] of eV. We have initiated a project to study nondipole photoelectron angular distributions over the entire periodic table to identify cases where nondipole effects are large and rapidly varying, particularly in the vicinity of Cooper minima, both dipole and quadrupole and a preliminary report on this study is published [20].

Future Plans

Our future plans are to continue on the paths set out above. In the area of confined atoms, we will perform many-body calculation on charged particle impact ionization of endohedral atoms and free fullerene molecules in an effort to elucidate any new insights inherent in the nondipole channels thus produced. In addition, we shall upgrade our theory to include relativistic interactions to be able to deal with heavy endohedrals with quantitative accuracy, nondipole effects, and charged particle

interactions. The study of the photodetachment of C^- shall move on to the photoabsorption in the vicinity of the K-shell edge of both the ground 4S and excited 2D states in order to understand how the slight excitation of the outer shell affects the inner-shell photoabsorption and to pave the way for experiment, in addition to further study of Na^- and K^- which shall also be studied using MCTD. Further, building upon our previous work, we shall attack the problem of inner-shell photoionization of the Sc atom. Additionally, the search for cases where nondipole effects are likely to be significant, as a guide for experiment, and quadrupole Cooper minima, will continue.

Publications Citing DOE Support Since November, 2007

- “Ionization in Fast Atom-Atom Collisions: the Influence and Scaling Behavior of Electron-Electron and Electron-Nuclear Interactions,” J. M. Sanders, R. D. DuBois, S. T. Manson, S. Datz, E.F. Deveney, H. F. Krause J. L. Shinpaugh and C. R. Vane, *Phys. Rev. A* **76**, 062710 (2007).
- “Spectacular Enhancement in Low Energy Photoemission of Ar Confined in C_{60} ,” M. E. Madjet, H. S. Chakraborty and S. T. Manson, *Phys. Rev. Letters* **99**, 243003 (2007)
- “Theoretical Studies of Photoabsorption by Atomic Systems,” S. T. Manson, W.-C. Chu, A. M. Sossah and H.-L. Zhou, *Advances in Atomic Molecular and Optical Sciences*, edited by E. Krishnakumar (Allied Publishers, New Delhi, India, 2008), pp. 89-98.
- “Photoionization of C_{60} : A Model Study,” M. E. Madjet, H. S. Chakraborty, J. M. Rost and S. T. Manson, *J. Phys. B* **41**, 105101 (2008).
- “Dynamical Effects of Confinement on Atomic Valence Photoionization in $Mg@C_{60}$,” M. E. Madjet, H. S. Chakraborty, J. M. Rost and S. T. Manson, *Phys. Rev. A* **78**, 013201 (2008).
- “Photoionization of atoms confined in giant single-walled and multiwalled fullerenes,” V. K. Dolmatov, P. Brewer and S. T. Manson, *Phys. Rev. A* **78**, 013415 (2008).
- “Relativistic-Random-Phase Approximation Calculations of Atomic Photoionization: What We Have Learned,” S. T. Manson, *Can. J. Phys.* **87**, 5 (2009).
- “Relaxation Effects in Photodetachment of Intermediate p shells of the Chlorine and Bromine Negative Ions,” V. Radojević, J. Jose, G. B. Pradhan, P. C. Deshmukh and S. T. Manson, *Can. J. Phys.* **87**, 49 (2009).
- “Correlation confinement resonances in photoionization of endohedral atoms: $Xe@C_{60}$,” V. K. Dolmatov and S. T. Manson, *J. Phys. B* **41**, 165001 (2008).
- “Fast charged-particle impact ionization of endohedral atoms,” A. S. Baltenkov, V. K. Dolmatov, S. T. Manson, and A. Z. Msezane, *Phys. Rev. A* **79**, 043201 (2009).
- “Photoionization of Doubly-Charged Scandium Ions,” A. M. Sossah, H.-L. Zhou, S. T. Manson, *Phys. Rev. A* **78**, 053405 (2008).
- “Spin-Orbit interaction Activated Interchannel Coupling in dipole and Quadrupole Photoionization,” S. Sunil Kumar, T. Banerjee, P. C. Deshmukh and S. T. Manson, *Phys. Rev. A* **79**, 043401 (2009).
- “Photoionization of novel hybrid states in endohedral fullerenes,” H. S. Chakraborty, M. E. Madjet, T. Rebger, J.-M. Rost and S. T. Manson, *Phys. Rev. A* **79**, 061201(R) (2009).
- “Photoionization of the Be Isoelectronic Sequence: Total Cross Sections,” W.-C. Chu, H.-L. Zhou, A. Hibbert and S. T. Manson, *J. Phys. B* **42**, 205003 (2009).
- “Photoionization of Mg and Ar isonuclear sequences,” G. B. Pradhan, J. Jose, P. C. Deshmukh, V. Radojevic, and S. T. Manson, *Phys. Rev. A* **80**, 053416 (2009).
- “Photoionization of endohedral atoms: Collective, reflective and collateral emissions,” H. S. Chakraborty, M. A. McCune, M. E. Madjet, D. E. Hopper and S. T. Manson, in *The Fourth International Symposium “Atomic Cluster Collisions: Structure And Dynamics From The Nuclear To The Biological Scale” (ISACC 2009)*, edited by A. V. Solov’yev and E. Surdutovich, AIP Conference Proceedings 1157, 111-118 (2009).

- “Quadrupole matrix element zeros and their effect on photoelectron angular distributions,” L. A. LaJohn, S. T. Manson and R. H. Pratt, *Nuc. Instr. Meth. A* **619**, 7 (2010).
- “Photoionization of Xe inside C₆₀: atom-fullerene hybridization, giant enhancement and interchannel oscillation transfer,” M. E. Madjet, D. Hopper, M. A. McCune, H. S. Chakraborty, J.-M. Rost and S. T. Manson, *Phys. Rev. A* **81**, 013202 (2010).
- “Effects of the fullerene (C₆₀) potential and position of the atom (A) on spectral characteristics of endohedral atoms A@C₆₀,” A. S. Baltenkov, U. Becker, S. T. Manson, and A. Z. Msezane, *J. Phys. B* **43**, 115102 (2010).
- “Satellite Lines in the Photoionization of Ions: The Be Isoelectronic Sequence,” W.-C. Chu, H.-L. Zhou, A. Hibbert and S. T. Manson, *Phys. Rev. A* **81**, 053412 (2010).
- “Photoionization of the Be-like O⁴⁺ ion: Total and partial cross sections for the ground 2s² and excited 2s2p ^{1,3}P states,” D.-S. Kim and S. T. Manson, *J. Phys. B* **43**, 155205 (2010).
- “Variation of photoelectron angular distributions along Ar and Ca isonuclear sequences,” G. B. Pradhan, J. Jose, P. C. Deshmukh, V. Radojević, and S. T. Manson, *Phys. Rev. A* **81**, 063401 (2010).
- “Overlapping Resonances in Atomic Ions,” W.-C. Chu, H.-L. Zhou, A. Hibbert and S. T. Manson, *Phys. Rev. A* **82**, 013417-1-4 (2010).
- “Inner Shell Photodetachment of Na⁻ Using the Multi-Configuration Tamm-Dancoff Approximation,” J. Jose, G. B. Pradhan, V. Radojević, S.T. Manson, and P. C. Deshmukh, in *The Physics of Ionized Gases* (2010) (in press).

References

- [1] V. K. Dolmatov, A. S. Baltenkov, J.-P. Connerade and S. T. Manson, *Radiation Phys. Chem.* **70**, 417 (2004).
- [2] V. K. Dolmatov, *Advances in Quantum Chemistry* **58**, 13 (2009).
- [3] A. Müller *et al*, *Phys. Rev. Letters* **101**, 133001 (2008).
- [4] R. Phaneuf *et al*, *Bull. Am. Phys. Soc.* **55**(5), 40 (2010) and private communication.
- [5] M. E. Madjet, H. S. Chakraborty and S. T. Manson, *Phys. Rev. Letters* **99**, 243003 (2007).
- [6] M. E. Madjet, H. S. Chakraborty, J. M. Rost and S. T. Manson, *Phys. Rev. A* **78**, 013201-1-4 (2008).
- [7] H. S. Chakraborty, M. E. Madjet, T. Renger, J.-M. Rost and S. T. Manson, *Phys. Rev. A* **79**, 061201(R) (2009).
- [8] V. K. Dolmatov and S. T. Manson, *J. Phys. B* **41**, 165001-1-4 (2008).
- [9] V. K. Dolmatov and S. T. Manson, *J. Phys. Rev. A* **78**, 013415 (2008).
- [10] A. S. Baltenkov, U. Becker, S. T. Manson, and A. Z. Msezane, *J. Phys. B* **43**, 115102 (2010).
- [11] V. K. Dolmatov and S. T. Manson, *Phys. Rev. A* (submitted).
- [12] W.-C. Chu, H.-L. Zhou, A. Hibbert and S. T. Manson, *Phys. Rev. A* **81**, 053412 (2010).
- [13] W.-C. Chu, H.-L. Zhou, A. Hibbert and S. T. Manson, *Phys. Rev. A* **82**, 013417 (2010).
- [14] A. M. Sossah, H.-L. Zhou, S. T. Manson, *Phys. Rev. A* (submitted).
- [15] J. Jose, G. B. Pradhan, V. Radojević, S.T. Manson, and P. C. Deshmukh, in *The Physics of Ionized Gases* (2010) (in press).
- [16] M. O. Krause, *Phys. Rev.* **177**, 151 (1969).
- [17] O. Hemmers, R. Guillemin and D. W. Lindle, *Radiation Phys. and Chem.* **70**, 123 (2004) and references therein.
- [18] O. Hemmers, R. Guillemin, E. P. Kanter, B. Kraessig, D. W. Lindle, S. H. Southworth, R. Wehlitz, J. Baker, A. Hudson, M. Lotrakul, D. Rolles, W. C. Stolte, I. C. Tran, A. Wolska, S. W. Yu, M. Ya. Amusia, K. T. Cheng, L. V. Chernysheva, W. R. Johnson and S. T. Manson, *Phys. Rev. Letters* **91**, 053002 (2003).
- [19] V. K. Dolmatov and S. T. Manson, *Phys. Rev. Letters* **83**, 939 (1999).
- [20] L. A. LaJohn, S. T. Manson and R. H. Pratt, *Nuc. Instr. Meth. A* **619**, 7 (2010).

ABSTRACT

ELECTRON-DRIVEN PROCESSES IN POLYATOMIC MOLECULES

Investigator: Vincent McKoy

A. A. Noyes Laboratory of Chemical Physics
California Institute of Technology
Pasadena, California 91125
email: mckoy@caltech.edu

PROJECT DESCRIPTION

The focus of this project is the development, extension, and application of accurate, scalable methods for computational studies of low-energy electron–molecule collisions, with emphasis on larger polyatomics relevant to electron-driven chemistry in biological and materials-processing systems. Because the required calculations are highly numerically intensive, efficient use of large-scale parallel computers is essential, and the computer codes developed for the project are designed to run both on tightly-coupled parallel supercomputers and on workstation clusters.

HIGHLIGHTS

Over the past year we have continued to pursue code development and applications related to electron interactions with biological molecules and have maintained productive collaborations with experimental groups. Principal developments include:

- An experimental/theoretical study of elastic electron collisions with ethyl vinyl ether, a prototype system for studying electron-driven dissociation of biomolecules
- Development of a parallelized replacement for the remaining sequential section of our electron-scattering codes

ACCOMPLISHMENTS

Low-energy electrons can initiate chemistry by exciting molecules to dissociative or reactive electronic states or by attaching to form metastable anions that then dissociate. We have recently studied a variety of such processes, with emphasis on larger polyatomics and in particular biomolecules, by carrying out fixed-nuclei calculations of the electron-molecule collision dynamics. Besides yielding cross sections that can be compared to experiment, such calculations give insight into the nature, energies, and lifetimes of resonant states that may play a role in promoting dissociative attachment or excitation. During 2010, we took steps to move beyond fixed-nuclei calculations and incorporate nuclear dynamics into our studies, with direct calculation of dissociation cross sections the ultimate goal.

Our main effort in this direction was developing a parallel replacement for the last remaining sequential section of our electron-molecule scattering codes. This section evaluates quantities that do not depend on the collision energy, including all matrix elements that involve only Gaussian orbitals. Such matrix elements are far less numerous than the mixed Gaussian/plane-wave matrix elements treated by the existing parallel code. However, as our interests have shifted to high-accuracy studies of low-symmetry polyatomic systems, and in particular as we begin to contemplate carrying out electron collision calculations at many different nuclear geometries in order to map out a dissociative potential surface, this remaining sequential code had become a bottleneck. Its parallel replacement not only evaluates the required matrix elements using fully parallel, scalable code but also incorporates extensions and generalizations that will allow us to employ more flexible and accurate descriptions of the molecular wave functions.

During 2010, we also initiated work on ethyl vinyl ether, $C_2H_5-O-C_2H_3$, by carrying out calculations of the fixed-nuclei elastic electron scattering cross section. Ethyl vinyl ether was chosen as a prototype for studying indirect dissociative attachment in biomolecules. The empty π^* orbital of the vinyl group gives rise to a low-energy resonance that can trap the projectile electron, and intramolecular electron transfer from

that π^* orbital to a C–O σ^* orbital can lead to either $\text{C}_2\text{H}_5\text{O}^- + \text{C}_2\text{H}_3$ or $\text{C}_2\text{H}_5 + \text{C}_2\text{H}_3\text{O}^-$ [1]. The relative importance of such “indirect” dissociative attachment versus direct attachment into the relevant σ^* orbital in a different prototype molecule, formic acid, has been the subject of recent debate [2–5], and detailed studies of ethyl vinyl ether should be illuminating. Our initial study of ethyl vinyl ether [6] was a collaborative effort with the experimental group of Murtadha Khakoo at Cal State Fullerton, whose measured differential elastic cross sections in general agree very well with our calculated results.

PLANS FOR COMING YEAR

We plan to continue our studies of ethyl vinyl ether by exploring the dissociative attachment dynamics. On the computational side, we will carry out calculations of the electron scattering cross section at multiple nuclear geometries in order to track the evolution of the π^* metastable anion as bonds rotate and stretch, leading to its mixing with one of the C–O σ^* orbitals and eventually to dissociation. Besides the qualitative insights gained from such calculations, we expect to be able to obtain estimates of the dissociative attachment cross section by using the resonance positions and widths as the real and imaginary parts of an anion potential surface within a model of the nuclear dynamics based on the formalism originally laid out by O’Malley [7]. Our calculations will be complemented, on the experimental side, by work in the Khakoo group to measure the dissociative attachment cross section, including its temperature dependence, using a recently installed negative-ion mass spectrometer. The temperature dependence gives information about the role of vibrational excitation in promoting dissociation and thus may provide insight about which vibrational modes are involved.

We also plan to undertake an extensive study of electron-impact electronic excitation of H_2O . Excitation of water, the most abundant and ubiquitous biomolecule of all, is of course extremely important in its own right, both for understanding energy deposition by slow electrons and for modeling the electron-driven chemistry, since some of the low-lying states dissociate impulsively to $\text{OH} + \text{H}$. However, we are also interested in electron-impact excitation of water as a prototype for inelastic electron collisions with alcohols and biomolecules in general. Our aim is to determine, through a systematic and thorough study, just what is needed to obtain accurate cross sections for excitation of several low-lying states of H_2O , with the idea that the lessons learned will carry over to larger systems. The Khakoo group will carry out corresponding cross section measurements to provide points of reference, while we will also collaborate and exchange ideas with computational groups in Brazil.

Code development will also continue. We are beginning to explore the use of graphics-processing units (GPUs) to provide an additional level of parallelism in our code and will focus on implementing key computational steps, including two-electron integral evaluation and matrix multiplication, on nVIDIA GPUs using the CUDA toolkit. Although adapting the integrals, in particular, to GPUs is likely to prove challenging, the enormous performance gains achievable make the effort highly worthwhile.

REFERENCES

- [1] C. Bulliard, M. Allan, and S. Grimme, *Int. J. Mass Spectrom.* **205**, 43 (2001).
- [2] T. N. Rescigno, C. S. Trevisan, and A. E. Orel, *Phys. Rev. Lett.* **96**, 213201 (2006).
- [3] G. A. Gallup, P. D. Burrow, and I. I. Fabrikant, *Phys. Rev. A* **79**, 042701 (2009).
- [4] T. N. Rescigno, C. S. Trevisan, and A. E. Orel, *Phys. Rev. A* **80**, 046701 (2009).
- [5] G. A. Gallup, P. D. Burrow, and I. I. Fabrikant, *Phys. Rev. A* **80**, 046702 (2009).
- [6] M. A. Khakoo, L. Hong, B. Kim, C. Winstead, and V. McKoy, *Phys. Rev. A* **81**, 022720 (2010).
- [7] T. F. O’Malley, *Phys. Rev.* **150**, 14 (1966).

PROJECT PUBLICATIONS AND PRESENTATIONS, 2008–2010

1. “Absolute Elastic Differential and Integral Cross Sections for Electron Scattering from the CF_2 Radical,” T. M. Maddern, L. R. Hargreaves, J. R. Francis-Staite, M. J. Brunger, S. J. Buckman, C. Winstead, and V. McKoy, *Phys. Rev. Lett.* **100**, 063202 (2008).

2. "Interactions of Slow Electrons with DNA," V. McKoy, Chemistry Department Seminar, University of Alabama, Tuscaloosa, Alabama, February 28, 2008.
3. "Low Energy Elastic Electron Scattering from Methanol and Ethanol," M. A. Khakoo, J. Blumer, K. Keane, C. Campbell, H. Silva, M. C. A. Lopes, C. Winstead, V. McKoy, R. F. da Costa, L. G. Ferreira, M. A. P. Lima, and M. H. F. Bettega, *Phys. Rev. A* **77**, 042705 (2008).
4. "Electron Scattering in Ethene: Excitation of the \tilde{a}^3B_{1u} State, Elastic Scattering and Vibrational Excitation," M. Allan, C. Winstead, and V. McKoy, *Phys. Rev. A* **77**, 042715 (2008).
5. "Elastic Electron Scattering from 3-Hydroxytetrahydrofuran: Experimental and Theoretical Studies," V. Vizcaino, J. Roberts, J. P. Sullivan, M. J. Brunger, S. J. Buckman, C. Winstead, and V. McKoy, *New J. Phys.* **10**, 053002 (2008).
6. "Interactions of Slow Electrons with DNA," V. McKoy, Physics Department Seminar, Federal University of Juiz de Fora, Juiz de Fora, Brazil, June 11, 2008.
7. "Interaction of Slow Electrons with Methyl Phosphate Esters," C. Winstead and V. McKoy, *Int. J. Mass Spectrom.* **277**, 279 (2008).
8. "Resonant Interactions of Slow Electrons with DNA Constituents," C. Winstead and V. McKoy, *Radiat. Phys. Chem.* **77**, 1258 (2008).
9. "Electron Collisions with Biomolecules," V. McKoy and C. Winstead, *J. Phys. Conf. Ser.* **115**, 012020 (2008).
10. "Electron-Impact Dissociation of Oxygen-Containing Molecules—A Critical Review," J. W. McConkey, C. P. Malone, P. V. Johnson, C. Winstead, V. McKoy, and I. Kanik, *Phys. Rep.* **466**, 1 (2008).
11. "Comment on 'Ring-breaking electron attachment to uracil: Following bond dissociations via evolving resonances' [*J. Chem. Phys.* **128**, 174302 (2008)]," C. Winstead and V. McKoy, *J. Chem. Phys.* **129**, 077101 (2008).
12. "Interactions of Slow Electrons with DNA Constituents," V. McKoy and C. Winstead, in *Advances in Atomic, Molecular and Optical Science* (Proceedings of the XVI National Conference on Atomic and Molecular Physics, Mumbai, January 8–11, 2007), E. Krishnakumar, editor (Allied Publishers, New Delhi, 2008), p. 146.
13. "Electron Scattering from H₂O: Elastic Scattering," M. A. Khakoo, H. Silva, J. Muse, M. C. A. Lopes, C. Winstead, and V. McKoy, *Phys. Rev. A* **78**, 052710 (2008).
14. "Elastic Scattering of Slow Electrons by *n*-Propanol and *n*-Butanol," M. A. Khakoo, J. Muse, H. Silva, M. C. A. Lopes, C. Winstead, V. McKoy, E. M. de Oliveira, R. F. da Costa, M. T. do N. Varella, M. H. F. Bettega, and M. A. P. Lima, *Phys. Rev. A* **78**, 062714 (2008).
15. "Differential and Integral Cross Sections for Elastic Electron Scattering from CF₂," J. R. Francis-Staite, T. M. Maddern, M. J. Brunger, S. J. Buckman, C. Winstead, V. McKoy, M. A. Bolorizadeh, and H. Cho, *Phys. Rev. A* **79**, 052705 (2009).
16. "Vibrational Excitation of Water by Electron Impact," M. A. Khakoo, C. Winstead, and V. McKoy, *Phys. Rev. A* **79**, 052711 (2009).
17. "Low-Energy Electron Collisions with Biomolecules," C. Winstead, Fortieth Annual Meeting the Division of Atomic, Molecular, and Optical Physics of the American Physical Society (DAMOP 2009), Charlottesville, Virginia, 20–23 May, 2009 (*invited talk*).

18. “Improved Nonlocal Resonance Model for Electron–HCl Collisions,” J. Fedor, P. Kolorenč, M. Čížek, J. Horáček, C. Winstead, and V. McKoy, XXVI International Conference on Photonic, Electronic, and Atomic Collisions, Kalamazoo, Michigan, 22–28 July, 2009.
19. “Elastic Electron Scattering by Ethyl Vinyl Ether,” M. A. Khakoo, L. Hong, B. Kim, C. Winstead, and V. McKoy, *Phys. Rev. A* **81**, 022720 (2010).
20. “Electron Scattering in HCl: An Improved Nonlocal Resonance Model,” J. Fedor, C. Winstead, V. McKoy, M. Čížek, K. Houfek, P. Kolorenč, and J. Horáček, *Phys. Rev. A* **81**, 042702 (2010).

ELECTRON/PHOTON INTERACTIONS WITH ATOMS/IONS

Alfred Z. Msezane (email: amsezane@cau.edu)

Clark Atlanta University, Department of Physics and CTSPS, Atlanta, Georgia 30314

PROGRAM SCOPE

The project's primary objective is to gain a fundamental understanding of the near-threshold electron attachment mechanism and determine accurate electron affinities (EAs). The elegant Mulholland formula, implemented within the complex angular momentum (CAM) representation of scattering, wherein resonances are rigorously defined as singularities of the S-matrix, is used for the investigations [1]. Regge trajectories allow us to probe electron attachment at its most fundamental level near threshold, thereby uncovering new manifestations and possibilities as well as determine the reliable electron affinities of tenuously bound and complicated atomic and molecular systems [2].

The development and application of the Random Phase Approximation with Exchange (RPAE) method to atoms (ions) with unfilled sub-shells continue. The theory has also been extended to open outer-shell and inner open-shell atoms (ions) and applied to photoionization, including of Ce^{3+} @ C_{60} [3]. Methods are developed for calculating the generalized oscillator strength, useful in probing the intricate nature of the valence- and open-shell as well as inner-shell electron transitions. Standard codes are used to generate sophisticated wave functions for investigating CI mixing and relativistic effects in atomic ions. The wave functions are also used to explore correlation effects in dipole and non-dipole studies.

SUMMARY OF RECENT ACCOMPLISHMENTS

A. Regge -Pole Analysis of Near - Threshold Scattering of Electrons by Complex Atoms: Extraction of Reliable Electron Affinities

The mechanisms of electron-electron correlations and core-polarization interaction are crucial for the existence and stability of most negative ions. In the calculations of the cross sections using the Regge-pole methodology the vital electron-electron correlation effects are accounted for through the Mulholland formula. This formula converts the infinite discrete sum into a background integral plus the contribution from a few poles to the process under consideration. The important core-polarization interaction is incorporated through the well-investigated Thomas-Fermi type model potential [4, 5]. The power of the method lies in that it extracts the binding energies (BEs) of tenuously bound and complex negative ions from the resonances in the near threshold elastic total cross sections (TCSs), requiring no *a priori* knowledge of the experimental or other theoretical data. The "Novel Mechanism for Nanoscale Catalysis" [6] is the most important accomplishment in this funding cycle of our research.

A.1 Low-energy electron elastic scattering from lanthanide atoms

The crucial importance of the lanthanide atoms in general and in the design and synthesis of novel functional compounds, in heavy fermion metals and heavy fermion compounds [7] have motivated our investigation of low energy electron scattering TCSs and differential cross sections (DCSs) for a fundamental understanding of electron attachment [8-10]. From the characteristic dramatically sharp resonance structures in the elastic TCSs and DCSs, reliable electron affinities were extracted and compared with available measurements and other theoretical calculations [11,12].

The large discrepancies in the comparison between our calculated EAs of the lanthanide atoms [8] and those of Ref. [11,12], motivated us to explore electron attachment to the lanthanide and Hf atoms resulting in the possible formation of stable excited lanthanide and Hf anions as Regge resonances in the near-threshold electron impact energy region, $E < 1.0$ eV. The extracted BEs for excited lanthanide anions were contrasted with those of the most recently calculated EAs (ground state BEs), concluding that the calculated BEs for many of the anions in [12] are not identifiable with the EAs as claimed. Formation

of bound excited anions has been identified for all the lanthanide atoms including Hf, except Eu and Gd. The imaginary part of the CAM, $\text{Im } L$ was used to distinguish between the shape resonances and the bound excited negative ions. The excited anions were found to be mostly tenuously bound (BEs < 0.1 eV). Shape resonances and Ramsauer-Townsend minima were also determined.

A.2 Electron elastic scattering cross sections for excited Au and Pt atoms

The ground state BEs (EAs) are essential for the fundamental understanding of chemical reactions, the quenching of Rydberg states and the creation of new molecules. Contrary to bulk, Au, Pt and Pd nanoparticles exhibit considerable catalytic activity. We note that manipulating the structure and the dynamics of metallic nanoparticles, attractive due to their optical, electronic and magnetic properties, including applications in catalysis, chemical sensing, biological markers and photonics, requires a fundamental understanding of the dynamic processes at the atomic level.

Electron elastic TCSs and DCSs in both impact energy E and scattering angle for the excited Au and Pt atoms have been explored in the energy range $0 \leq E \leq 4.0$ eV. The cross sections were found to be characterized by very sharp long-lived resonances whose positions were identified with the BEs of the excited anions formed during the collisions. The DCSs were evaluated using a partial wave expansion. The Ramsauer-Townsend minima, the shape resonances and the BEs of the excited Au^- and Pt^- anions were extracted from the cross sections, while the critical minima were determined from the DCSs [13].

When the near threshold electron TCSs for Au and Pt are contrasted with those of the lanthanide and Hf atoms, an amazing revealing picture emerges in the context of the behavior of Au and Pt in chemical reactions, particularly catalysis.

A.3 Multiple excited negative ions in low-energy electron elastic scattering

Significantly, the appearance of a large peak in the electron – atom scattering TCS at low energy manifests the presence of the ground state of the negative ion formed during the collision as a resonance. This facilitates considerably the identification of the BEs of negative ions in the electron elastic scattering TCSs in general, including excited anions. The results of Sections **A.1** and **A.2** have motivated us to explore further the possibility of identifying additional excited states beyond the first one. Toward this end, we predict the formation of two stable bound excited negative ionic states in low-energy electron scattering from Tm and Y atoms. In both cases one is tenuously bound while the second is weakly bound.

A.4 Novel mechanism for nanoscale catalysis

Recently, the direct synthesis of hydrogen peroxide from H_2 and O_2 using supported Au, Pd and Au-Pd nanoparticle catalysts was reported [14]. The experiment also found that the addition of Pd to the Au catalyst increased the rate of H_2O_2 synthesis significantly as well as the concentration of the H_2O_2 formed. How Pd promotes catalysis is a subject of considerable academic and industrial interest.

Very recently [6], the interplay between Regge resonances and Ramsauer-Townsend minima in the electron elastic TCSs for Au and Pd atoms along with their large EAs have been proposed as the fundamental atomic mechanism responsible for the observed exceptional catalytic properties of Au nanoparticles and to explain why the combination Au-Pd possesses even a higher catalytic activity than Au or Pd separately when catalyzing H_2O_2 , consistent with recent experiments. The investigation uses the recent CAM description of electron scattering from neutral atoms. The paper [6] provides a recipe for identifying new catalysts that could present advantages over Au, Pt and Pd, from the point of view of cost, for instance. We have now identified the atom Y as a possible candidate to enhance the catalytic property of Au/Pd even further. This could multiply the catalysis of H_2O_2 immensely.

A.5 Density Functional Theory Investigation of Small Pt Clusters

To obtain a sense of how the proposed fundamental mechanism [6] might be affected when small clusters are used rather than the atoms, we recently used Density functional theory to investigate the structural evolution of small minimum energy Pt_n ($n < 5$) clusters [15]. The clusters of $n = 2, 3, 4$ and 5 Pt atoms used were represented respectively by linear, equilateral triangle, tetrahedron, and triangular

bipyramid atoms. The geometric optimization was achieved using the DMol package under the generalized gradient approximation with the Perdew-Wang exchange-correlation functional. The adiabatic electron affinities and vertical electron affinities for the clusters were evaluated and compared with measurements and other theoretical calculation [16].

Our calculated EAs are closer to the measurements, particularly for n close to 2, demonstrating the importance of careful geometric optimization of the structures. The EA for Pt_4 is of concern, however, since it deviates significantly from the measured value. We believe that the reason is due to the importance of the spin-orbit interaction which has not been taken into account in our calculation.

B.1 Strongly Correlated Fermi-systems

The non-Fermi liquid (NFL) behavior in various strongly correlated Fermi-systems, such as high temperature superconductors, heavy-fermion metals, 2D electrons and ^3He , has been investigated [7], since it leads to the understanding of many-body effects and quantum phase transitions, responsible for the NFL behavior. The heavy-fermion f-electron alloys, such as CeRu_2Si_2 and $\text{CePd}_{1-x}\text{Rh}_x$ are important examples of strongly correlated Fermi-systems, with $\text{CeCu}_{6-x}\text{Au}_x$ being critical in demonstrating the atomic nature of antiferromagnetism [7]. These systems demonstrate the importance and need of accurate EAs for Ce, Cu, Ru, Si, Pd, Au, Rh and others, including the BEs for their excited states.

C.1 Photoionization of Ce^{3+} and $\text{Ce}^{3+} @\text{C}_{82}$ endohedral fullerene

The photoionization cross sections for Ce^{3+} and $\text{Ce}^{3+} @\text{C}_{82}$ in the energy region 100-150 eV have been studied using our open-shell RPAE method and a C_{82} model potential. The C_{82} was described by an attractive short range spherical well with potential $V(r)$, given by $V(r) = -V_0$ for $r_1 < r < r_0$, otherwise $V(r) = 0$. V_0 was obtained by solving the resultant transcendental equation using the DFT calculated EA value. The wave functions for the Ce^{3+} confined inside the C_{82} were calculated by solving the Schrodinger equation with both regular and irregular solutions and the continuous boundary conditions of the wave functions and their logarithmic derivatives at r_1 and r_0 . The RPAE equation was solved to obtain the partial cross sections with a total of 16 2D, 16 2G and 14 2F states. The photoionization of $\text{Ce}^{3+} @\text{C}_{82}$ shows both the resonance and suppression effects and demonstrates a stronger resonance peak at 106 eV.

Future Plans

The development and application of the Regge pole method to the interesting and challenging multichannel case continues, including the application to Feshbach resonances and cold collisions. We continue to develop the electron spectroscopy of tenuously bound and weakly bound systems for possible use in the detection of nanomaterials and extraction of EAs for complex atoms. This is accomplished through the calculated near threshold electron collision TCSs for various atoms as in [17]. The spin-orbit coupling in small Pt clusters, particularly in Pt_4 is being investigated. Accurate BEs for ground and excited Ce^- , Cu^- , Ru^- , Si^- , Pd^- , Rh^- , Pt^- anions and others continue to be extracted from resonances in near threshold electron elastic TCSs. These are critically needed in demonstrating the atomic nature of antiferromagnetism [7]. We continue to calculate the EAs of the 4d transition metals and the EA of C_{82} will be calculated as well. The value will be used to obtain the model potential of C_{82} so that the photoionization cross sections for $\text{A}@\text{C}_{82}$ can be obtained using our open-shell RPAE method.

References (1 – 17) and Project Publications 2008-2010

1. “Regge Oscillations in Electron-Atom Cross Sections”, D. Sokolovski, Z. Felfli, S.Yu. Ovchinnikov, J.H. Macek, and A.Z. Msezane, Phys. Rev. A **76**, 026707 (2007)
2. “Simple Method for Electron Affinity Determination: Results for Ca, Sr and Ce”, Z. Felfli, A.Z. Msezane, and D. Sokolovski, J. Phys. B **41**, 041001 (2008) (FAST TRACK)
3. “Photoionization of Ce^{3+} and $\text{Ce}^{3+} @\text{C}_{60}$ ”, Z. Chen and A. Z. Msezane, J. Phys. B **42**, 165206 (2009).
4. S. Belov *et al*, J. Phys. A **37**, 6943 (2004).
5. “On Regge-pole trajectories for a rational function approximation of Thomas-Fermi potentials”, S.

- Belov, K.-E. Thylwe, M. Marletta, A. Z. Msezane and S. Naboko, *J. Phys. A* **43**, 365301 (2010)
6. “Novel mechanism for nanoscale catalysis”, A.Z. Msezane, Z. Felfli and D. Sokolovski, *J. Phys. B*, (Under Revision, July 2010) (FAST TRACK)
 7. “Scaling Behavior of Heavy Fermion Metals”, V.R. Shaginyan, M.Ya. Amusia, A.Z. Msezane, and K.G. Popov, *Physics Report* **492**, 31-109 (2010)
 8. “Resonances in Low-Energy Electron Elastic Cross Sections for Lanthanide Atoms”, Z. Felfli, A.Z. Msezane and D. Sokolovski, *Phys. Rev. A* **79**, 012714 (2009)
 9. “Differential Cross Sections for Low-Energy Electron Elastic Scattering by Lanthanide Atoms: La, Ce, Pr, Nd, Eu, Gd, Dy and Tm”, Z. Felfli, A.Z. Msezane and D. Sokolovski, *Phys. Rev. A* **79**, 062709 (2009)
 10. “Complex angular momentum analysis of low-energy electron elastic scattering from lanthanide atoms”, Z. Felfli, A.Z. Msezane and D. Sokolovski, *Phys. Rev. A* **81**, 042707 (2010)
 11. S.M. O’Malley and D. R. Beck, *Phys. Rev. A* **78**, 012510 (2008).
 12. S.M. O’Malley and D. R. Beck, *Phys. Rev. A* **79**, 012511 (2009).
 13. “Low-energy electron elastic scattering cross sections for excited Au and Pt atoms”, Z. Felfli, A. R. Eure, A. Z. Msezane and D. Sokolovski, *NIMB* **268**, 1370 (2010)
 14. J. K. Edwards *et al*, *J. Chem. Soc., Faraday Discuss.* **138**, 225 (2008)
 15. Zhifan Chen and Alfred Z. Msezane, *Bull. Am. Phys. Soc.* **55**, 57 (2010).
 16. A. Nie *et al*, *Int. J. Quantum Chem.* **107**, 219 (2007)
 17. A. Z. Msezane, Z. Felfli and D. Sokolovski, arXiv: 0909.3067 (September 2009)
 18. “Near-Threshold Resonances in Electron Elastic Scattering Cross Sections for Au and Pt Atoms”, A. Z. Msezane, Z. Felfli and D. Sokolovski, *J. Phys. B* **41**, 105201 (2008)
 19. “Dramatic Resonances in Low- Energy Electron Scattering from Rb, Cs and Fr”, A.Z. Msezane, Z. Felfli, and D. Sokolovski, *Chem. Phys. Lett.* **456**, 96 (2008)
 20. “Near-Threshold Electron Attachment as Regge Resonances: Cross Sections for K, Rb and Cs Atoms”, A.Z. Msezane, Z. Felfli and D. Sokolovski, *J. Phys. Chem. A* **112**, 10, 199 (2008)
 21. “Strong resonances in low-energy electron elastic total and differential cross sections for Hf and Lu atoms”, Z. Felfli, A.Z. Msezane and D. Sokolovski, *Phys. Rev. A* **78**, 030703 (R) (2008)
 22. “Ionization of Sodium by the Impact of Alpha Particles”, S. Bhattacharya, K.B. Choudhury, N.C. Deb, C. Sinha, K. Roy and A.Z. Msezane, *Eur. Phys. J. D* **47**, 335 (2008)
 23. “Main Universal Features of the ³He Experimental Temperature–Density Phase Diagram”, V.R. Shaginyan, A.Z. Msezane, K.G. Popov and V.A. Stephanovich, *Phys. Rev. Lett.* **100**, 096406 (2008)
 24. “Low-Energy Electron Elastic Scattering from Complex Atoms: Nd, Eu and Tm”, Z. Felfli, A.Z. Msezane and D. Sokolovski, *Can. J. Phys.* **87**, 321 (2009)
 25. “Energy Scales and Magnetoresistance at a Quantum Critical Point”, V.R. Shaginyan, M. Ya. Amusia, A.Z. Msezane, K.G. Popov and V.A. Stephanovich, *Physics Letters A* **373**, 986 (2009)
 26. “[Ti II] lines observed in η Carinae Sr-filament and lifetimes of the metastable states of Ti⁺”, N. C. Deb, A. H. Hibbert, Z. Felfli and A. Z. Msezane, *J. Phys. B* **42**, 015701 (2009)
 27. “Fast charged-particle impact ionization of endohedral atoms: e + He@C₆₀”, A. S. Baltenkov, V. K. Dolmatov, S. T. Manson, and A. Z. Msezane, *Phys. Rev. A* **79**, 043201 (2009)
 28. “Large scale CIV3 calculations of fine-structure energy levels and radiative rates in Al-like Copper”, G. P. Gupta and A. Z. Msezane, *Can. J. Phys.* **87**, 895 (2009)
 29. “Photoionization of the I⁺ Ion”, Zhifan Chen and Alfred Z. Msezane, *J. Phys. B* **42**, 165203 (2009).
 30. “Magnetic-Field-induced Reentrance of Fermi-Liquid Behavior and Spin-Lattice Relaxation Rates in YbCu_{5-x}Au_x”, V.R. Shaginyan, A.Z. Msezane, K.G. Popov and V.A. Stephanovich, *Physics Letters A* **373**, 3783 (2009)
 31. “Fine-structure energy levels, oscillator strengths and lifetimes in Al-like Vanadium”, G. P. Gupta and A. Z. Msezane, *Phys. Scripta* **81**, 045302 (2010).
 32. “Effects of the fullerene (C₆₀) potential and position of the atom (A) on spectral characteristics of endohedral atoms A@C₆₀”, A. S. Baltenkov, U. Becker, S. T. Manson and A. Z. Msezane, *J. Phys. B* **43**, 115102 (2010).

Theory and Simulations of Nonlinear X-ray Spectroscopy of Molecules

Shaul Mukamel

University of California, Irvine, CA 92697

Progress Report 2010, August 1, 2010

DOE DE-FG02-04ER15571

Program Scope

This program focuses on developing a systematic theoretical and computational framework for the description of coherent resonant nonlinear ultrafast x-ray spectroscopies (all-x-ray as well as mixed optical/x-ray techniques). X-ray pulses provide a unique probe for interactions between the core-transitions and the electronic states that mediate these interactions. A hierarchy of possible spectroscopic techniques employing multiple x-ray pulses with controlled timing, phases, and intensities are considered, and models for their analysis and assessing their information content are developed. These experiments which can probe electronic and nuclear dynamics of molecules in the condensed phase with sub-femtosecond time and atomic spatial resolution, are made possible by the development of new bright soft and hard x-ray light sources. They provide novel windows into the valence electronic structure and chemical dynamics with much higher spatial and temporal resolution than possible in the visible regime. Coherent signals involving electron wavepackets created by attosecond pulses are described by extending concepts used for vibrational wavepackets in the femtosecond regime. Many-body coherence effects that go beyond the charge density and reveal multiple core excitations and dynamics are investigated. Resonant x-ray pump-probe and nonlinear wave mixing spectroscopy of core excitons provide attosecond snapshots of valence electronic excitations. By creating multiple core holes at selected atoms and controlled times it should become possible to study the dynamics and correlations of valence electrons as they respond to these perturbations. These measurements should provide critical tests for electronic structure theory and could be extended to highly correlated materials.

Recent Progress

Probing valence for electronic states with all x-ray stimulated Raman spectroscopy

A two-pulse coherent stimulated x-ray Raman spectroscopy (CXRS) technique has been proposed. The Raman interaction with the first x-ray pump tuned resonantly to a specific core-hole transition creates a valence electronic wavepacket, which is then detected by a delayed x-ray probe via a second Raman process. The dependence of the probe absorption on the delay provides information on the time evolution of the electronic states constituting the wavepacket. The valence wavepacket is initially centered at the atom whose core shell is resonant with the pump frequency. Similarly, the probe absorption reflects the unoccupied states in the vicinity of the core-shell, which are resonant with the probe frequency. By tuning the pump and the probe frequencies to different core transitions, one can control where the wavepacket is created and where it is probed and study the delocalization of the electronic states. CXRS has several advantages

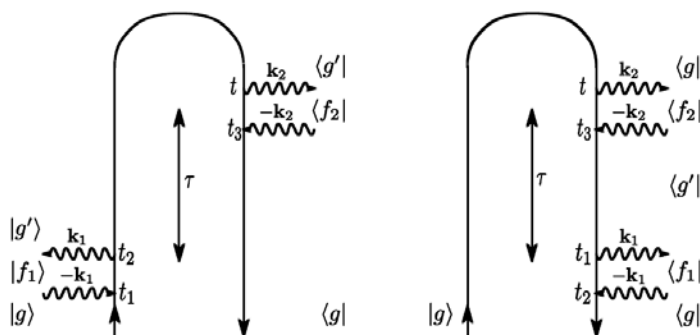


Figure 1: two closed-time-path loop diagrams that contribute to the stimulated Raman signal. $|g\rangle$ and $|g'\rangle$ are the ground state and valence-excited states with no core-hole, respectively. $|f_2\rangle$ and $|f_1\rangle$ are core-excited states for different localized core-holes, respectively.[P36]

compared to other four wave mixing signals. It only requires two pulses, and phase control is not necessary, making it feasible with the current LCLS source. It offers a much longer observation time window, not limited by the core-hole lifetime. Compared to spontaneous inelastic x-ray scattering (RIXS), the additional control offered by the pulses in CXRS allows to better compete with Auger processes. The valence wavepacket can be actively manipulated and probed in the time domain by other pulses which allow to monitor the excitation dynamics in the desired region of space and time. The signal can be expressed in a generalized Kramers-Heisenberg (transition amplitude) form which considerably helps the analysis. The technique offers a high temporal resolution and a bird-eye view of many valence electronic excitations covered by the broad (few eV) bandwidth. This is in contrast to resonant optical spectroscopy, which looks at one electronic state at a time and often has strict selection rules that limit the accessible states. Non-additive effects of functional groups in the stimulated Raman signal of conjugated molecules were predicted. The CXRS signal can be represented as a closed-time-path loop (Fig.1) that shows the evolution of the valence electronic wavepacket upon core electronic excitations. The signal is recast as the overlap between the doorway many-electron wave packet created by the

pump and the window wave packet generated by the probe: $S_{SR}(\tau; \omega_2, \omega_1) = 2 \text{Re}\langle W(\omega_2) | D(\tau; \omega_1) \rangle$. Closed expressions for the doorway and the window which depend explicitly on the pulse envelopes were derived. This representation provides an intuitive picture for the measurement by dividing it into three stages: wave packet creation, propagation, and detection. Applications to 5-quinolinol, a two-ring system in which the O and N atoms are located on the different rings is shown in Fig.2.

Manipulating Quantum Entanglement of Quasiparticles in Many-Electron Systems by Attosecond x-ray Pulses

Photoexcited electrons and holes in molecules or in semiconductors can be viewed as a bipartite entangled system. A bipartite quantum system in a pure state made of two distinguishable subsystems A and B is said to be entangled if the total wavefunction may not be factorized into a product of states in the two subspaces. Entanglement is the basis for numerous applications in quantum computing, secure communication, and information processing. A key element in all of these applications is the ability to separately excite and probe the individual subsystems. We have demonstrated that

the degree of entanglement of electrons and holes can be coherently controlled by x-ray sources. Thanks to their broad bandwidth, attosecond x-ray pulses can create valence electron-hole wavepackets by the stimulated Raman technique. The time dependent concurrence which is a measure of electron-hole entanglement can be manipulated by varying the pulse shapes which may be optimized by coherent control techniques to meet desired goals. For uncorrelated electrons the concurrence is time independent. The time dependent concurrence is therefore a sensitive and direct dynamical measure of electron correlations in the valence excited states.

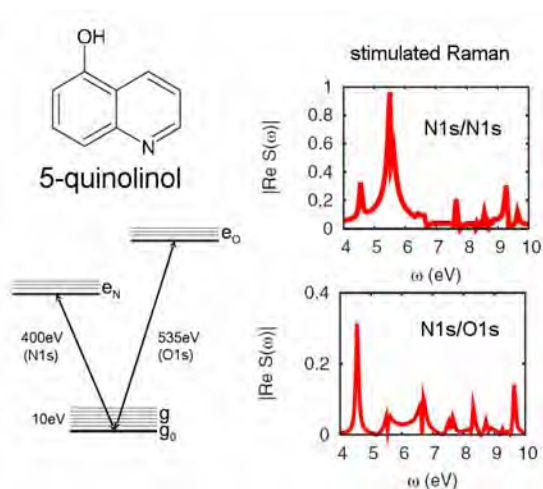


Figure 2: The coherent stimulated x-ray Raman signal of 5-quinolinol (upper left) can be described in terms of valence electronic states with differing core-occupations (lower left). Peaks in the one- (upper right) and two-color (lower right) frequency domain spectra represent valence excitations, weighted by their projections onto the nitrogen and oxygen.

Future Plans

Multidimensional Attosecond photoelectron spectroscopy

Photoelectron spectroscopy is a powerful tool for probing orbital energies in molecules and crystals. In time resolved photoelectron spectroscopy (TRPES) the system is prepared in a nonequilibrium state by a laser pulse, evolves for a delay time t and is eventually probed by detecting the electrons generated by a second, ionizing, pulse. The distribution of the electron kinetic energy (ε) reveals the underlying dynamics through its parametric dependence on the time delay. Multidimensional TRPES signals induced by a series of temporally-well separated pump pulses with variable delays, followed by a final ionizing detection pulse will be predicted and calculated. The technique will be further extended to attosecond electron dynamics. Here the pump ionizes the molecule to create one or several holes (core or valence type). The hole migration can then be probed by a second pulse and detected by either the generated photoelectrons or by directly looking at its absorption. Hole motion is very slow and negligible for deep core states and becomes faster for more shallow holes. Taking the quantum nature of x-ray fields into account could provide many additional control parameters and will enable new spectroscopic techniques. The field gets entangled with the matter and provides a window for viewing the matter. Photoelectron signals induced by entangled optical or x-ray photons will be predicted using Glauber's formalism. The signals are recast as products of matter and field multipoint correlation functions in the interaction picture. Parameters of the photon wavefunction provide a new class of control knobs for multidimensional spectroscopy. This theory may also be used to represent stochastic fluctuating classical x-ray fields rather than quantum fields. The manipulation of multidimensional x-ray response by coherent control pulse shaping algorithms will be explored. Spectra may be simplified and the resolution improved by optimizing the temporal profiles of the pulses.

Real Space Visualization of Particle-Hole Wave Packets using the Natural Orbital Representation

The attosecond snapshots of electron dynamics provided by resonant x-ray techniques call for developing real time/real space visualization schemes. It is not possible to display the many-electron wavefunctions that live in a high dimensional space.

In a work in progress we are developing techniques for visualizing many-electron wave packets in real space. This visualization should help in the interpretation of X-ray experiments. We adopt an approximate electronic structure theory in which the reduced doorway-window representation carries the same information as the full many-electron wave packets of the signal, by assuming that only single-particle excitations dominate the signal. We shall look for ways of visualizing information about electronic coherence that goes beyond the charge density. Valence excitations are effectively visualized in terms of few electron-hole pairs represented by natural orbitals. These describe the reduced single electron density matrix and carry information about electron delocalization and coherence.

Publications Resulting from the Project

- P1. "Multipoint Correlation Functions for Photon Statistics in Single Molecule Spectroscopy; Stochastic Dynamics in Liouville Space", F. Sanda and S. Mukamel, In "Theory, Modeling and Evaluation of Single Molecule Measurements", Editors E. Barkai, F. Brown, M. Orrit and H. Yang. World Sci. Pages 93-137 (2008).
- P2. "Partially-Time-Ordered Keldysh-Loop Expansion of Coherent Nonlinear Optical Susceptibilities", S. Mukamel, Phys. Rev. A, 77,023801 (2008).
- P3. "Two-dimensional Correlation Spectroscopy of Two-exciton Resonances in Semiconductor Quantum Wells", L. Yang and S. Mukamel, Phys. Rev. Lett., 100, 057402 (2008).
- P4. "Ultrafast Optical Spectroscopy of Spectral Fluctuations in a Dense Atomic Vapor, V.O. Lorenz, S. Mukamel, W. Zhuang and S.T. Cundiff, Phys. Rev. Lett. 100, 013603 (2008)
- P5. "Simulating Multidimensional Optical Wave Mixing Signals with Finite Pulse Envelopes", I. Schweigert and S. Mukamel, Phys. Rev. A. 77, 33802 (2008).
- P6. "Probing Interactions Between Core-Electron Transitions by Ultrafast Two-Dimensional X-Ray Coherent Correlation Spectroscopy", I.V. Schweigert and S. Mukamel, J.Chem.Phys. 128, 184307 (2008).
- P7. "Revealing Exciton-Exciton Couplings in Semiconductors by Multidimensional Four Wave Mixing Signals", L. Yang and S. Mukamel, Phys. Rev. B., 77, 075335 (2008).
- P8. Many-body Effects in 2-D Optical Spectra of Semiconductor Quantum-Dot Pairs; TPH Fund Beyond, R. Oszwaldowski, D. Abramavicius and S. Mukamel, J. Phys. Cond. Matt. 20, 045206 (2008).
- P9. "Probing Multiple Core-hole Interactions in the Nitrogen K-edge of DNA Basepairs by multidimensional Attosecond X-ray Spectroscopy; A Simulation Study", D. Healion, I. Schweigert and S. Mukamel, J. Phys. Chem. A,112, 11449-11461 (2008).
- P10. "Dissecting Quantum Pathways in Two-dimensional Correlation Spectroscopy of Semiconductors", L. Yang and S. Mukamel, J. of Physics Condensed Matter, 20, 395202 (2008).
- P11. "Coherent Multidimensional Optical Probes for Electron Correlations and Exciton Dynamics; from NMR to X-rays", S. Mukamel, D. Abramavicius, L. Yang, W. Zhuang, I.V. Schweigert and D. Voronine. Acct.Chem.Res. 42, 553-562 (2009).
- P12. "Coherent Multidimensional Optical Spectroscopy Excitons in Molecular Aggregates; Quasiparticle vs. Supermolecule Perspectives", D. Abramavicius, B. Palmieri, D. Voronine, F. Sanda and S. Mukamel, Chem. Rev. 109, 2350-2408 (2009).
- P13. "Double-quantum Coherence Attosecond X-ray Spectroscopy of Spatially-separated, spectrally-overlapping core-electron transitions," I.V. Schweigert and S. Mukamel. Phys. Rev. A. 78, 052509(2008).
- P14. "Isolating Excitonic Raman Coherence in Semiconductors Using 2D Correlation Spectroscopy", L. Yang, T. Zhang, A. Bristov, S. Cundiff and S. Mukamel, J.Chem. Phys. 129, 234711 (2008).
- P15. "Coherent Stimulated X-ray Raman Spectroscopy; Attosecond Extension of RIXS", U. Harbola and S. Mukamel, Phys. Rev. B. 79, 085108 (2009).
- P16. "Investigation of Electronic Coupling in Semiconductor Double Quantum Wells Using Coherent Optical Two-Dimensional Fourier Transform Spectroscopy", X. Li, T. Zhang, S. Mukamel, R. P. Mirin, S.T. Cundiff, Solid State Comm., 149, 361-366 (2009).
- P17. "Many-body Green's Function Approach to Attosecond Nonlinear X-ray Spectroscopy", U. Harbola and S. Mukamel, Phys. Rev. B. 79, 235129 (2009).
- P18. "Controlling Multidimensional off-resonant-Raman and infrared vibrational spectroscopy by finite pulse band shapes", S. Mukamel, J. Chem. Phys. 130, 054110 (2009).
- P19. "Probing Excitons and Bioexcitons in Coupled Quantum Dots by Coherent 2D Optical Spectroscopy", E. G. Kavousanaki, O. Roslyak and S. Mukamel, Phys. Rev. B. 79, 155324 (2009).
- P20. "Interplay of Slow Bath Fluctuations & Energy Transfer in 2D Spectroscopy of the FM O Light-Harvesting Complex Benchmarking of simulation protocols", B. Palmieri, D. Abramavicius and S. Mukamel, Phys. Chem. Chem. Phys. 12, 108-114 (2010).

- P21. "Two-Quantum Many-body Coherences in Two-Dimensional Fourier-Transform Spectra of Exciton Resonances in Semiconductor Quantum Wells", D. Karauskaj, A.D. Bristow, L. Yang, X. Dai, R.P. Mirin, S. Mukamel and S.T. Cundiff, Phys. Rev. Lett, 104, 117401 (2010).
- P22. "Stimulated Coherent Anti-Stokes Raman Spectroscopy (CARS) Resonances Originate from: Double-slit Interference of Two-photon Stokes Pathways" S.Rahav and S. Mukamel, PNAS 107, 4825-4829 (2010).
- P23. "Probing Many-Particle Correlations in Semiconductors Quantum Wells Using Double-Coherence Signals", L. Yang and S. Mukamel, Proc. of SPIE, 76001G (2010).
- P24. "Ultrafast Nonlinear Optical Signals Viewed from the Molecules Perspective; Kramers-Heisenberg Transition Amplitudes vs. Susceptibilities", S. Rahav and S. Mukamel, Advances in Atomic Molecular and Optical Physics, Vol. 59 (In Press, 2010).
- P25. "Manipulating Quantum Entanglement of Quasiparticles in Many Electron Systems by Attosecond X-ray Pulses", S. Mukamel and H. Wang, Phys. Rev. A. 81, 062334(2010).
- P26. "Population and Coherence Transfer Signals Induced by 3-Exciton Correlation in the Nonlinear Optical Response of Photosynthetic Complexes", L. Yang, D. Abramavicius and S. Mukamel, New J. Phys., In Press (2010).
- P27. "Simulation of Attosecond Coherent Resonant Raman X-ray Spectroscopy of the Nitrogen & Oxygen K-Edges in Glycine", H. Wang and S. Mukamel, Phys. Rev. A. (Submitted, 2009).
- P28. "Spontaneous and Stimulated Coherent and Incoherent Nonlinear wave-mixing and Hyper-Raleigh Scattering", O. Roslyak and S. Mukamel, Lectures of virtual university on lasers, Max Born Institute, Berlin, Germany, <http://mitr.p.lodz.pl/evu/> European Virtual University Lecture Notes (2010).
- P29. "Multidimensional Attosecond Photoelectron Spectroscopy with Shaped Pulses and Quantum Optical Fields", S. Rahav and S. Mukamel, Phys. Rev. A.81, 063810 (2010).

Nonlinear Photoacoustic Spectroscopies Probed by Ultrafast EUV Light

Keith A. Nelson
Department of Chemistry
Massachusetts Institute of Technology
Cambridge, MA 02139
Email: kanelson@mit.edu

Henry C. Kapteyn, Margaret M. Murnane
JILA
University of Colorado and National Institutes of Technology
Boulder, CO 80309
E-mail: kapteyn@jila.colorado.edu, murnane@jila.colorado.edu

Program Scope

This project is aimed at direct spectroscopic characterization of phenomena that occur on mesoscopic (nanometer) length scales and ultrafast time scales in condensed matter, including non-diffusive thermal transport and the high-wavevector acoustic phonon propagation that mediates it, complex structural relaxation and the density and shear dynamics that mediate it, and nanostructure thermoelastic responses. A primary effort in the project is directed toward nonlinear time-resolved spectroscopy with coherent soft x-ray, or extreme ultraviolet (EUV), wavelengths. Time-resolved transient grating (TG) measurements are conducted in order to directly define an experimental length scale as the interference fringe spacing Λ (or wavevector magnitude $q = 2\pi/\Lambda$) formed by two crossed excitation pulses or by a fabricated spatially periodic pattern that is irradiated by a single excitation pulse. The dynamics of material responses at the selected wavevector, including thermoelastically induced surface acoustic waves and thermal diffusion or non-diffusive thermal transport, are recorded through time-resolved measurement of coherent scattering, i.e. diffraction, of variably delayed probe pulses from the transient grating pattern. Progress in high harmonic generation has yielded femtosecond EUV pulses with sufficient energy and focusability for use in TG experiments. EUV probe pulses provide far greater sensitivity than optical pulses to surface acoustic and thermal responses, since the surface modulations change the EUV phase by far more than the optical phase and thereby yield far higher EUV diffraction efficiencies. Crossed EUV excitation pulses will produce interference fringe spacings of tens of nanometers, far smaller than is possible with crossed optical pulses, providing access to mesoscopic length scales, very high acoustic frequencies, and non-ballistic thermal transport.

In complementary measurements, the frequency rather than the wavevector of an acoustic response is specified by using a sequence of femtosecond excitation pulses at a specified repetition rate, with each pulse thermoelastically driving a single acoustic cycle. In this case the acoustic wave propagates through the sample rather than along the surface, and detection is carried out at the opposite sample surface, i.e. multiple-pulsed excitation is at the front and detection is at the back of the sample. This approach provides access to high-frequency bulk acoustic waves, while the EUV measurements are used to examine surface acoustic waves.

Recent Progress

EUV probing of nanoscale thermal transport and acoustic waves

In a collaboration between JILA, MIT and LBL, two major advances were made using ultrafast EUV beams to probe 1-dimensional nanostructured materials. First, optical measurements of surface acoustic waves were extended to frequencies of 50 GHz for the first time, to understand surface acoustic wave dispersion in nanostructures. These measurements are critical for accurate characterization of thin films and interfaces beneath very thin films. The results were published last year in *Applied Physics Letters*. Second, the transition from diffusive to quasiballistic thermal transport from nanostructured interfaces

was observed for the first time. This allowed us to understand how the Fourier Law of diffusive heat flow must be corrected in order to calculate heat flow in nanostructures. These findings are of great importance in understanding and manipulating nanoscale heat transport at interfaces, particularly for nano-electronics and energy recovery devices, where the rapidly shrinking scale of devices and nanocomposites fundamentally changes the way that heat is dissipated. These results were recently published in November 2009 in *Nature Materials*. In the experiments, an 800-nm pulse irradiated nanoscale nickel lines deposited on a transparent sapphire substrate, thereby depositing heat in a confined area and in a 1D spatially periodic pattern. The thermal expansion and acoustic response were observed by monitoring the diffraction of ultrafast coherent EUV beams at 45 eV, generated through high-order harmonic generation (HHG), from the nanostructure. This allowed us to observe heat propagation through the interface and into the substrate. The signal consisted of a sharp rise due to impulsive laser heating, a thermal decay due to interfacial thermal transport, and an oscillation due to surface acoustic wave (SAW) propagation. We extracted a corrective ballistic resistivity $r_{Ballistic}$, corresponding to the deviation between best fit to the data and bulk values. At the smallest line widths ($L = 65$ nm), the interface dimension was much smaller than the phonon mean free path in the sapphire substrate ($L < \Lambda_{Sa} \sim 120$ nm), and we measured an interfacial resistivity that was as much as three times higher than the bulk value.

We can enter the true nanoscale regime of ballistic energy flow by moving to patterned structures

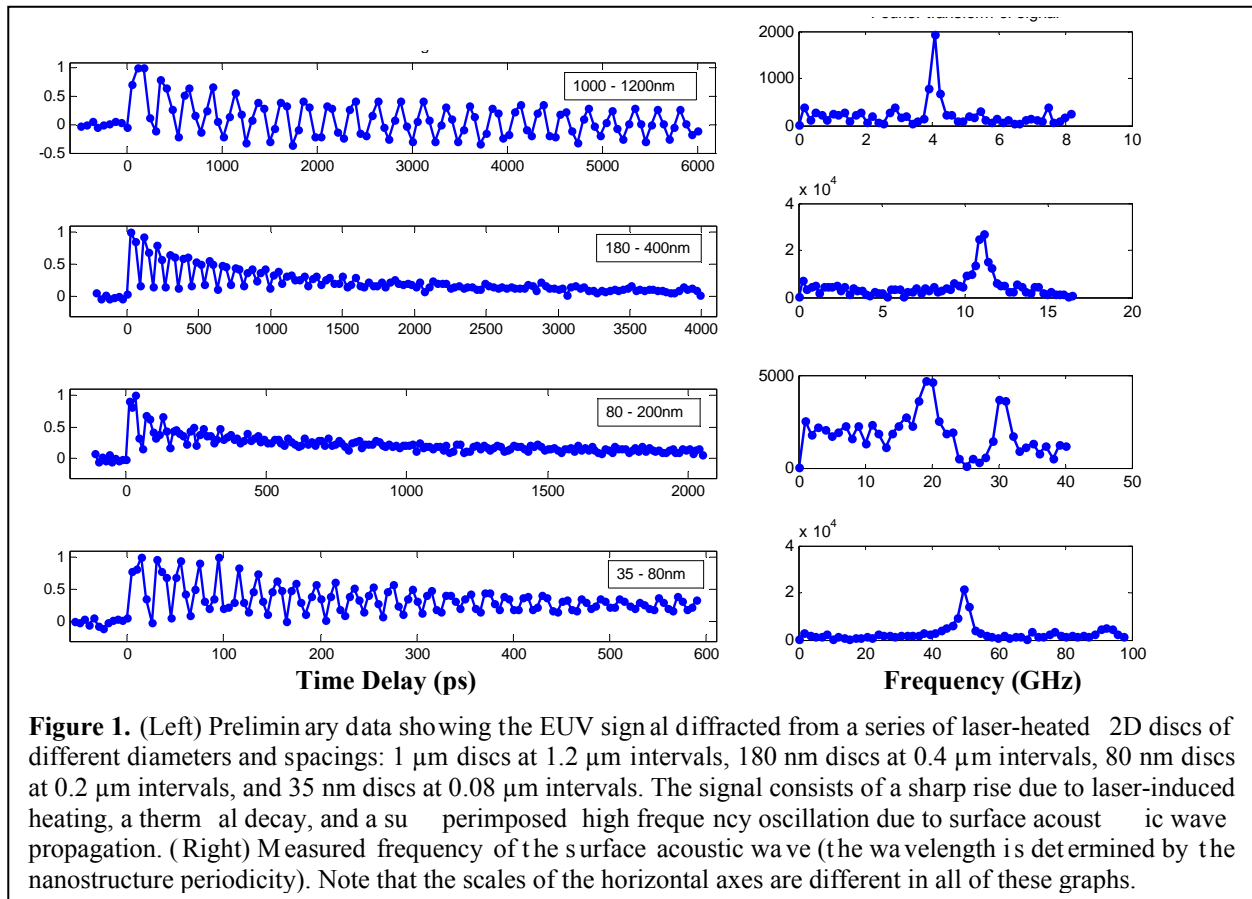


Figure 1. (Left) Preliminary data showing the EUV signal diffracted from a series of laser-heated 2D discs of different diameters and spacings: 1 μm discs at 1.2 μm intervals, 180 nm discs at 0.4 μm intervals, 80 nm discs at 0.2 μm intervals, and 35 nm discs at 0.08 μm intervals. The signal consists of a sharp rise due to laser-induced heating, a thermal decay, and a superimposed high frequency oscillation due to surface acoustic wave propagation. (Right) Measured frequency of the surface acoustic wave (the wavelength is determined by the nanostructure periodicity). Note that the scales of the horizontal axes are different in all of these graphs.

with even smaller periods and to two-dimensional arrays, where basic questions still need to be addressed and where theoretical and experimental tools are lacking. One concern was that the diffracted high harmonic signal from sub-50 nm, 2D nanostructures would be too weak to detect. Fortunately, we were able to obtain preliminary data showing acoustic oscillations and thermal decay from 2D arrays of multilayer magnetic discs with diameters down to ≈ 35 nm. The data in Fig. 1 demonstrate that the

diffracted EUV signal is strong and that we should be able to detect both the thermal decay and surface acoustic waves in nanostructures with dimensions down to 20 nm.

Optical generation and study of bulk GHz-frequency longitudinal and shear acoustic waves

We have developed novel methods for measurement of bulk acoustic waves at high frequencies, recently including shear as well as longitudinal waves. Acoustic waves at GHz frequencies play key roles in thermal transport. They also mediate structural relaxation in partially ordered and disordered materials including supercooled liquids. Last year we reported in *Physical Review Letters* the first measurements of GHz shear waves in glass-forming liquids, using femtosecond pulse sequences to excite the waves and single femtosecond pulses to monitor them after propagation through the sample. Figure 2a shows the experimental approach. We have measured longitudinal acoustic waves in supercooled liquids at frequencies up to up to 200 GHz, which corresponds to an acoustic wavelength of about 15 nm. Very recently we completed a comprehensive study of DC704, a van der Waals liquid, in which our GHz-frequency measurements were combined with transient grating measurements of acoustic waves at MHz frequencies and slower structural relaxation at times corresponding to kHz frequencies, and with piezomodulation measurements done by a collaborating group at Roskilde University (Denmark), covering lower frequencies all the way down to millihertz. The results, shown in Fig. 2b, produced an ultrabroadband compliance spectrum covering 13 decades, capturing the slowdown of structural relaxation in a temperature range of 140 K, essentially the complete transition from high-temperature, low-viscosity liquid to low-temperature glass. This is by many decades the most complete spectrum of its kind collected from any material. Our results supported a mode-coupling theoretical prediction of a quantitative connection between the fast dynamics at GHz frequencies and the much slower, highly T -dependent dynamics extending to much lower frequencies, expressed in terms of an arithmetic relation between power-law exponents describing the fast and slow dynamical responses and indicative of an underlying dynamic criticality in supercooled liquids.

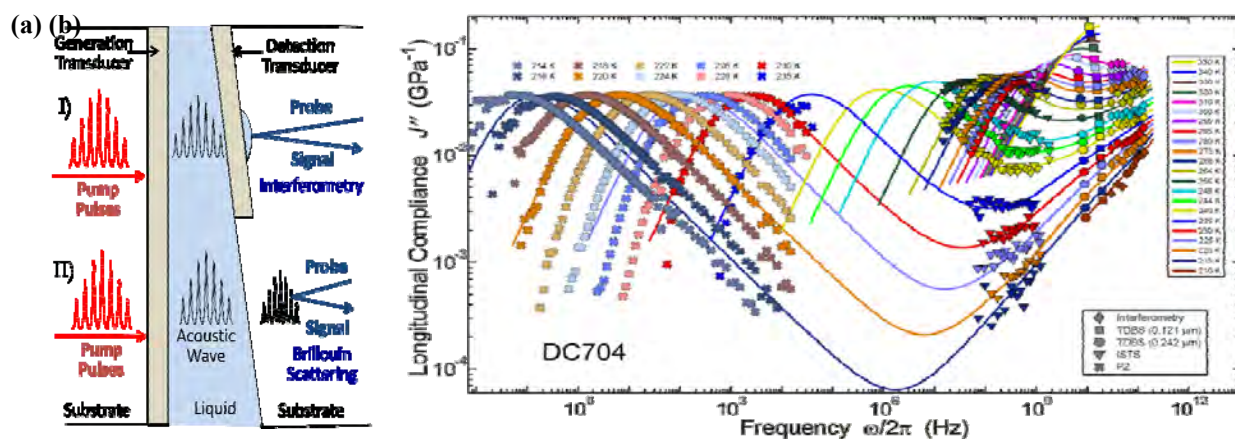


Figure 2. (a) Multiple-pulse generation of acoustic waves that are generated by fs optical irradiation of a ~ 20 nm metal transducer, propagated through a liquid sample, and detected either (I) interferometrically at a ~ 20 nm metal transducer on the other side or (II) through coherent time-domain Brillouin scattering (TDBS) in the liquid or the substrate. Measurements through different liquid thicknesses yield the acoustic speed and damping rate. (b) Loss compliance spectrum of DC 704 across 13 decades and 140 K determined as shown in (a) for GHz frequencies, through transient grating (ISTS) measurements for kHz-MHz frequencies, and through piezomodulation (PZ) measurements made by the group of J. Dyre in Roskilde University for mHz-kHz frequencies.

Future Plans

Our collaborator, Dr. Eric Anderson at LBL, is fabricating arrays of simple metal 2D Ni discs on uniform substrates. Using these samples that are the 2D analogs of the 1D samples we previously investigated, we should be able to extract the signatures of truly ballistic heat flow, and benchmark them with new codes that we are developing. Going further, recent advances in high harmonic generation produce EUV pulses

with sufficient energy for use as crossed excitation pulses in transient grating measurements, allowing us to examine nanoscale surface acoustic waves and non-diffusive heat transport without any patterned structure on the surface. This will simplify the analysis of our results and enable versatile measurement of ballistic transport in a wide range of materials. We also expect to extend the frequencies of bulk acoustic waves that we can generate to over 1 THz, capturing the full range of acoustic waves in many materials. This will enable us to determine directly the phonon mean free paths involved in thermal transport, thereby completing a microscopic description of the non-diffusive transport that we measure. It will also enable observation of the end of acoustic propagation in glasses and partially disordered materials. Finally, we are formulating detailed plans for conducting transient grating measurements of thermal and acoustic responses with hard x-ray pulses at the LCLS, thereby accessing the highest possible wavevectors in bulk materials and at surfaces.

Publications during Current Grant Period

1. M. E. Siemens, Q. Li, R. Yang, K. A. Nelson, E. Anderson, M. M. Murnane, and H. C. Kapteyn, "Measurement of quasi-ballistic heat transport across nanoscale interfaces using ultrafast coherent soft x-ray beams," *Nature Materials* **9**, 26 (2010).
2. M. E. Siemens, Q. Li, M. M. Murnane, H. C. Kapteyn, R. Yang, E. Anderson, and K. A. Nelson, "High-Frequency Surface Acoustic Wave Propagation in Nanostructures Characterized by Coherent Extreme Ultraviolet Beams," *Applied Physics Letters* **94**, 093103 (2009).
3. R. I. Tobey, M. E. Siemens, O. Cohen, M. M. Murnane, and H. C. Kapteyn, "Ultrafast Extreme Ultraviolet Holography: Dynamic Monitoring of Surface Deformation," *Optics Letters* **32**, 286 (2007).
4. "Nanoscale heat transport probed with ultrafast soft x-rays," M. Siemens, Q. Li, M. Murnane, H. Kapteyn, and K.A. Nelson, in *Ultrafast Phenomena XVI*, P. Corkum, S. De Silverstri, K.A. Nelson, E. Riedle, and R.W. Schoenlein, eds. (Springer-Verlag 2009), pp 149-151.
5. "Picosecond shear waves in nano-sized solids and liquids," T. Pezeril, C. Klieber, S. Andrieu, D. Chateigner, and K. A. Nelson, *Proc. SPIE* **7214**, 721408 (2009).
6. "Optical generation of gigahertz-frequency shear acoustic waves in liquid glycerol," T. Pezeril, C. Klieber, S. Andrieu, and K.A. Nelson, *Physical Review Letters* **102**, 107402 (2009).
7. "GHz longitudinal and transverse acoustic waves and structural relaxation dynamics in liquid glycerol," C. Klieber, T. Pezeril, S. Andrieu, and K.A. Nelson, in *Ultrafast Phenomena XVI*, P. Corkum, S. De Silverstri, K.A. Nelson, E. Riedle, and R.W. Schoenlein, eds. (Springer-Verlag 2009), pp. 499-501.

Free-Space Excitation of Propagating Surface Plasmon Polaritons

Lukas Novotny (novotny@optics.rochester.edu)

University of Rochester, The Institute of Optics, Rochester, NY, 14627.

1. Program Scope

In this project we study antenna-coupled light emission on the single molecule level. Here, 'single molecule' refers to any quantum emitter such as an ion, atom, quantum dot, or defect center. We tailor the properties of the optical antenna to control different photophysical parameters, such as the excited state lifetime, the saturation intensity, and the quantum yield [2, 3, 19]. A single molecule approach overcomes the problem of ensemble averaging and inhomogeneous broadening due to varying parameters and local environments. Furthermore, using a single molecule coupled to an optical antenna whose position and properties can be controllably adjusted we can establish a detailed and quantitative understanding.

2. Recent Progress

Recently we started to explore novel schemes for creating highly localized fields by use of nonlinear optical interactions. We discovered highly efficient four-wave mixing (4WM) in gold nanoparticle junctions [7] and used the nonlinear response as an excitation source for near-field fluorescence imaging [12]. While working on 4WM we also discovered the possibility of exciting nonradiative modes, such as surface plasmon polaritons (SPPs), with free propagating radiation [14]. This multiphoton excitation scheme is the subject of the current report.

As shown by the red curve in Figure 1, the dispersion relation of SPPs lies to the right of the light cone defined by $k = \omega/c$ (shaded area) and hence cannot be excited by a single free-propagating photon. Therefore, various alternative excitation schemes have been developed over the years, which either rely

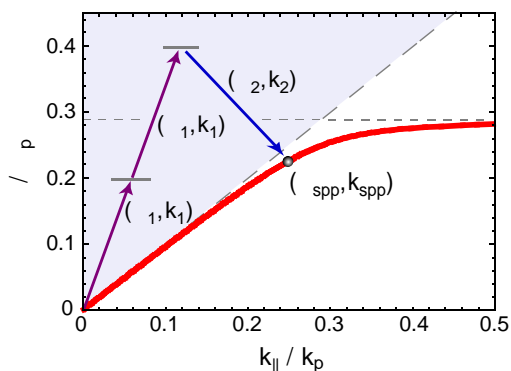


Figure 1: Principle of surface plasmon excitation by nonlinear four-wave mixing. The SPP dispersion curve $k_{\text{spp}}(\omega)$ (solid line) is located to the right of the light cone (shaded area) prohibiting the excitation by a single free-propagating photon. The vectorial summation of three incident photons, all contained within the light-cone, makes it possible to penetrate the light cone and to couple to the SPP dispersion curve. The axes are normalized by the plasma frequency ω_p and corresponding wavevector $k_p = \omega_p/c$. (b) Experimental configuration with overlaid scanning electron microscope image of the sample surface showing the gratings used for SPP outcoupling. (c) Experimental results showing the intensity of the outcoupled surface plasmons.

on coupling via evanescent waves, such as the Kretschmann-Raether configuration [20] and the Otto [21] configuration, or on gratings and defects [22] at the metal surface in order to bridge the momentum gap between the SPP and the incident radiation. However, these processes inevitably lead to increased losses (due to finite film thickness), leakage radiation or scattering, which reduces the SPP propagation length and increases background radiation. In contrast, our approach allows SPPs to be launched on any planar metal surface by nonlinear mixing of photons from two separate laser beams.

The multi-photon excitation scheme can be readily understood on the basis of energy and momentum conservation. The multi-photon process that we're exploiting is optical four-wave mixing (4WM). Two incident laser beams with frequencies ω_1 and ω_2 are used to produce radiation at frequency

$$\omega_{4wm} = 2\omega_1 - \omega_2. \quad (1)$$

Our experiments are schematically depicted in Fig. 2(a), which shows two incident beams at angles θ_1 and θ_2 with respect to the surface normal, and an outgoing beam at angle θ_{4wm} . Because of the translational invariance the in-plane momentum is conserved, which yields

$$\frac{\omega_{4wm}}{c} \sin \theta_{4wm} = \frac{\omega_2}{c} \sin \theta_2 - 2\frac{\omega_1}{c} \sin \theta_1. \quad (2)$$

To couple the 4WM field to surface plasmon modes we require that the left hand side of Eq. (2) matches the momentum of surface plasmon polaritons, i.e. The momentum condition for surface plasmon excitation becomes

$$\frac{\omega_{4wm}}{c} \sin \theta_{4wm} = \frac{\omega_{4wm}}{c} \sqrt{\frac{\epsilon_2(\omega_{4wm})}{\epsilon_2(\omega_{4wm}) + \epsilon_1}}. \quad (3)$$

which defines a resonance condition for the two incident angles θ_1 and θ_2 .

In our experiments we focus laser pulses from two laser beams on a gold surface (c.f. Figure 2b). By use of a delay line, the laser pulses are made to overlap in time. Because the excited SPPs are confined to the gold surface it is not possible to directly image their propagation. Therefore, as shown in Figure 2b, we have fabricated gratings into the gold surface to convert the SPPs into propagating radiation. The gratings consist of periodic grooves of depth 70 nm and width 150 nm, produced by electron beam lithography and reactive ion etching.

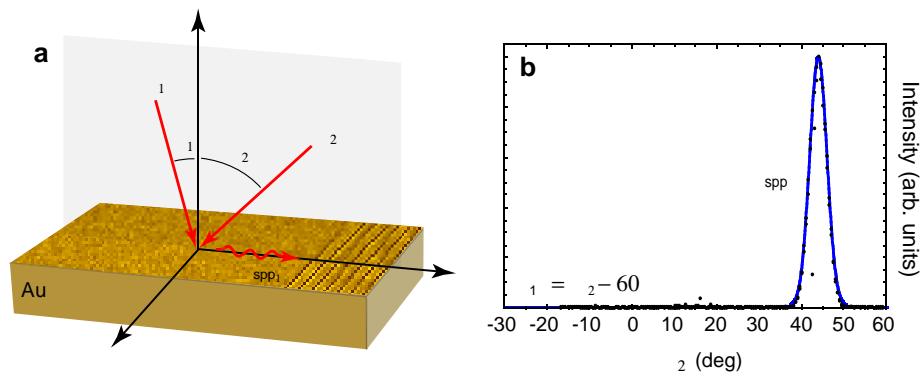


Figure 2: (a) Experimental configuration with overlaid scanning electron microscope image of the sample surface showing the gratings used for SPP outcoupling. (b) Experimental results showing the intensity of the outcoupled surface plasmons.

The multi-photon excitation scheme allows surface plasmons to be excited anywhere on a metal surface. The energy and momentum of the excited plasmons can be selected by proper choice of laser energies and excitation angles. The process makes use of vectorial photon momentum summation and doesn't rely on thin films, gratings, or scattering centers. In an extension of this work we are interested to excite SPPs with radially polarized annular beams [23] thereby providing the possibility of generating converging or diverging plasmon fields. Our work can also be extended to configurations using multiple SPP excitation spots, for example by use of zone plates or diffractive optics. Surface plasmons excited at different locations are then able to interfere with each other, which can be exploited for plasmon focusing, guiding and coherent control [24, 25]. It has to be emphasized that the method of vectorially adding different photon momenta can also be employed for the excitation of other planar modes, such as surface phonon polaritons, waveguide modes, surface exciton polaritons, and modes associated with two-dimensional electron gases (2DEG), such as magnetoplasmons and magnetorotons.

3. Future Plans

Our future experiments will build on the results and findings of the current project. In the next project period we are particularly interested in exploring the possibility of antenna-coupled electro-optical transduction. To date, optical antennas were mainly used to convert incident photons to outgoing photons. We now intend to study the local conversion between electrons and photons.

4. References (1-18 = DOE sponsored publications 2007-2010)

- [1] R. Kappeler, D. Erni, C. Xudong, and L. Novotny, "Field Computations of Optical Antennas," *J. Comp. Theor. Nanosc.* **4**, 686 (2007).
- [2] P. Bharadwaj, P. Anger, and L. Novotny, "Nanoplasmonic enhancement of single-molecule fluorescence," *Nanotechnology* **18**, 044017 (2007).
- [3] P. Bharadwaj and L. Novotny, "Spectral dependence of single molecule fluorescence enhancement," *Opt. Expr.* **15**, 14266–14274 (2007).
- [4] A. Bouhelier and L. Novotny, "Near-field optical excitation and detection of surface plasmons," in *Surface Plasmon Nanophotonics*, M. Brongersma, ed., (Kluwer Academic Press, 2007).
- [5] H. Gersen, L. Novotny, L. Kuipers, and N. F. van Hulst, "On the concept of imaging nanoscale vector fields," *Nature Photonics* **1**, 242 (2007).
- [6] L. Novotny, "The history of near-field optics," *Progress in Optics* **50**, 137–180 (2007).
- [7] M. Danckwerts and L. Novotny, "Optical Frequency Mixing at Coupled Gold Nanoparticles," *Phys. Rev. Lett.* **98**, 026104 (2007).
- [8] R. J. Moerland, T. H. Taminiau, L. Novotny, N. F. van Hulst, and L. Kuipers, "Reversible polarization control of single molecule emission," *Nano Lett.* **8**, 606–610 (2008).
- [9] L. Novotny, "Optical antennas tuned to pitch," *Nature* **455**, 879 (2008).

- [10] L. Novotny and C. Henkel, "Van der Waals versus optical interaction between metal nanoparticles," *Opt. Lett.* **33**, 1029–1031 (2008).
- [11] S. Palomba and L. Novotny, "Nonlinear excitation of surface plasmon polaritons by four-wave mixing," *Phys. Rev. Lett.* **101**, 056802 (2008).
- [12] S. Palomba, M. Danckwerts, and L. Novotny, "Nonlinear Plasmonics with Gold Nanoparticle Antennas," *J. Opt. A: Pure and Appl. Opt.* **11**, 114030 (2009).
- [13] P. Bharadwaj, B. Deutsch, and L. Novotny, "Optical antennas," *Adv. Opt. Phot.* **1**, 438 – 483 (2009).
- [14] J. Renger, R. Quidant, N. V. Hulst, S. Palomba, and L. Novotny, "Free-space excitation of propagating surface plasmon polaritons by nonlinear four-wave mixing," *Phys. Rev. Lett.* **103**, 266802 (2009).
- [15] L. Novotny, "Optical antennas: A new technology that can enhance light-matter interactions," *The Bridge* **39**, 14–20 (2009).
- [16] L. Novotny, "Strong coupling, energy splitting, and level crossings: A classical perspective," *Am. J. Phys.* accepted (2010).
- [17] L. Novotny and N. F. van Hulst, "Antennas for light," *Nature Phot.* in print (2010).
- [18] P. Bharadwaj and L. Novotny, "Plasmon enhanced photoemission from a single $Y_3N@C_{80}$ fullerene," *J. Phys. Chem. C* **114**, 7444–7447 (2010).
- [19] P. Anger, P. Bharadwaj, and L. Novotny, "Enhancement and quenching of single molecule fluorescence," *Phys. Rev. Lett.* **96**, 113002 (2006).
- [20] E. Kretschmann and H. Raether, "Radiative decay of non radiative surface plasmons excited by light," *Z. Naturforsch.* **23A**, 2135–2136 (1968).
- [21] A. Otto, "Excitation of nonradiative surface plasma waves in silver by the method of frustrated total reflection," *Z. Phys.* **216**, 398–410 (1968).
- [22] F. Lopez-Tejiera *et al.*, "Efficient unidirectional nanoslit couplers for surface plasmons," *Nature Phys.* **3**, 324–328 (2007).
- [23] L. Novotny, M. R. Beversluis, K. S. Youngworth, and T. G. Brown, "Longitudinal field modes probed by single molecules," *Phys. Rev. Lett.* **86**, 5251 (2001).
- [24] M. I. Stockman, S. V. Faleev, and D. J. Bergman, "Coherently controlled femtosecond energy localization on nanoscale," *Appl. Phys. B* **74**, S63–S67 (2002).
- [25] M. Aeschlimann, M. Bauer, D. Bayer, T. Brixner, F. G. de Abajo, W. Pfeiffer, M. Rohmer, C. Spindler, and F. Steeb, "Adaptive subwavelength control of nano-optical fields," *Nature* **446**, 301–304 (2007).

Electron-Driven Excitation and Dissociation of Molecules

A. E. Orel
Department of Applied Science
University of California, Davis
Davis, CA 95616
aeorel@ucdavis.edu

Program Scope

This program will study how energy is interchanged in electron-polyatomic collisions leading to excitation and dissociation of the molecule. Modern *ab initio* techniques, both for the electron scattering and the subsequent nuclear dynamics studies, are used to accurately treat these problems. This work addresses vibrational excitation, dissociative attachment, and dissociative recombination problems in which a full multi-dimensional treatment of the nuclear dynamics is essential and where non-adiabatic effects are expected to be important.

Recent Progress

We have carried out a number of calculations studying low-energy electron scattering from polyatomic systems leading to vibrational excitation and dissociative attachment, and studies of photoionization of diatomic and triatomic molecules. Much of this work has been done in collaboration with the AMO theory group at Lawrence Berkeley Laboratory headed by T. N. Rescigno and C. W. McCurdy. As a result of this collaboration one of my students has finished his thesis work with the AMO experimental group headed by A. Belkacen. He did experiments on dissociative attachment of water where we have carried out calculations.

Dissociative Attachment of Acetylene

We have performed nuclear dynamics calculations on C_2H_2 and C_2D_2 to study the isotope effect in DEA. Our previous calculations at 0K led to an isotopic ratio of the cross section for C_2H_2 compared to the cross section for C_2D_2 of ~ 28.9 , a factor of 2 higher than recent measurements [1]. Since this reaction proceeds by bending, and this mode is populated at room temperature at which the experiments were performed, the discrepancy was attributed to the contribution of higher vibrational modes. We included the four lowest bending vibrational states that had non-vanishing populations at the experiment temperature of $T = 333$ K. The resulting ratio is found to be 17.9 in closer agreement to the experimental value. The results of the calculation were described in a paper published in Physical Review A (Publication 4)

Dissociative Electron Attachment to HCN and HNC

Previously we have carried out studies on DEA of ClCN and BrCN [2]. We have extended these calculations to HCN and its isomer HNC. We have carried out electron scattering calculation using the complex Kohn variational method as a function of the three internal degrees of freedom to obtain the resonance energy surface and autoionization widths. We used this as input to a dynamics calculation using the MCTDH approach [3]. In contrast to acetylene, instead of bending, the H atom tunnels through the barrier to dissociation. The DEA cross section and branching ratios

were compared to available experiment and theory. The results of the calculation are described in a paper published in Physical Review A (Publication 5).

Formation of inner shell autoionizing CO⁺ states below the CO⁺⁺ threshold

Because of the long-range repulsive Coulomb interaction between singly charged ions, the vertical double ionization thresholds of small molecules generally lie above the dissociation limits corresponding to formation of singly charged fragments. This leads to the possibility of forming singly charged molecular ions by photoabsorption in the Franck-Condon region at energies below the lowest dication state, but above the dissociation limit for two singly charged fragment ions. These singly charged molecular ions can emit a second electron by autoionization, but only at larger internuclear separations where the ion falls into the electron+dication continuum. This process has been termed indirect double photoionization. Since these states are characterized by strong configuration mixing and numerous curve crossings, the inner valence regions of molecular ions continues to be a challenging subject both experimentally and theoretically. The AMO experimental group headed by A. Belkacem has carried a kinetically complete experiment on the production of CO⁺ autoionizing states following inner-valence photoionization of carbon monoxide below its double ionization threshold. Momentum imaging spectroscopy was used to measure the energies and body-frame angular distributions of both photo- and ejected electrons, as well as the kinetic energy release of the atomic ions. We have carried out *ab initio* theoretical calculations, calculating both the potential energy curves of the superexcited states and well as cross sections and molecular-frame photoelectron angular distributions in order to compare with experiment. This has provided insight into the nature of the molecular ion states produced and their subsequent dissociation into autoionizing atomic (O^{*}) fragments. The results of the calculation are described in a paper which was published in Physical Review A as a Rapid Communication (Publication 7).

Electron interactions with CF_x radicals

In collaboration with T.N. Rescigno, LBL, we have begun a study of the radical CF₂. We have performed fixed-nuclei scattering calculations using the Complex Kohn variational method and extracted the resonance parameters, for each geometry of interest, by analyzing the energy dependence of the eigenphase sums. These preliminary calculations have showed a single resonance at low energy that at the static exchange level is unbound at the equilibrium geometry of the ground state. However, at the relaxed SCF level of calculation, which correctly balances the anion and target correlation and has been used previously with great success to study similar resonances, the anion is bound at the equilibrium geometry. This is in contrast to the R-matrix calculations [4] that show the anion to be unbound at the equilibrium geometry. We are currently using this data as input to a dynamics calculation using the MCTDH approach [3]. A paper on this work will be submitted soon.

Dissociative Electron Attachment to HCCCN

Experiments on dissociative electron attachment (DEA) to HCCCN below 12 eV have led predominantly to formation of CCCN⁻, CN⁻, HCC⁻ and CC⁻ negative ions. It has been concluded that these fragments result mainly from the decay of p*-shape resonant state upon electron attachment that involves distortion of the symmetry of the linear neutral molecule. In order to study the dynamics of dissociation in these channels, we subdivided the molecule into three fragments (H), (CC) and (CN); therefore, four internal coordinates consisting in the distances between the center of masses of (H) and (CC) fragments, (CC) and (CN) fragments, the (H)-(CC) angle and the (CC)-

(CN) angle are included in the calculation. We have performed electron scattering calculations using Complex Kohn Variational method to determine the resonance energies and autoionization width for various geometries of the system and construct the complex potential energy surfaces relevant to the metastable HCCCN^- ion. The nuclear dynamics is treated using the Multiconfiguration Time-Dependent Hartree (MCTDH) formalism and the flux of the propagating wave packet is used to compute the DEA cross section relevant to 4 channels in question. There are some limited experimental studies available on this system. A paper on this work will be submitted soon to Physical Review A.

FUTURE PLANS

Dissociative Electron Attachment to HCN and HNC: Beyond Static Exchange

In our studies of the dissociative electron attachment to acetylene, the inclusion of polarization was important. We have begun calculations on dissociative electron attachment to HCN and HNC adding the effect of polarization. We will study both the total cross section and the isotope effect, but also whether the inclusion of polarization modifies the mechanism.

Formation of inner shell autoionizing OH^+ states below the H_2O^{++} threshold

Experiments on the production of OH^+ autoionizing states following inner-valence photoionization of water have been carried out by the group of Dörner in Frankfurt. These experiments are similar to those carried out at LBL on inner-valence photoionization of carbon monoxide. We have begun a series of *ab initio* theoretical calculations, calculating both the potential energy curves of the superexcited states and well as electron scattering calculations from OH^+ to determine which autoionizing states are involved. This has provided insight into the nature of the molecular ion states produced and their subsequent dissociation into autoionizing OH^* fragments.

Isomerization of HCCH: Snapshots of a chemical reaction

The Moshhammer group at Heidelberg has begun studies of the dissociative photoionization of HCCH. These are two photon experiments. The first photon ionizes HCCH (below the double ionization limit), and then at a later variable time a second photon ionizes the HCCH^+ . The experiment will focus on the $(\text{C}^+, \text{CH}_2^+)$ channel. We are performing calculations on the ion states and plan to carry out dynamics calculations to understand the isomerization that must occur to produce this channel. The goal is to produce snapshots of the path to products.

REFERENCES

1. O. May, J. Fedor, B. C. Ibanescu and M. Allan, Phys. Rev. A, **77**, 040701 (2008).
2. J. Royal and A. E. Orel, J. Chem. Phys, **125** 214307 (2006).
3. M. H.Beck, A. Jackle, G.A. Worth and H. -D. Meyer, Phys. Rep., 324 (2000).
4. I. Rozum, N. J. Mason and Jonathan Tennyson, *J. Phys. B*, **35**, 1583 (2002).

PUBLICATIONS

1. Electron-induced resonant dissociation and excitation of NeH^+ and NeD^+ , V.Ngassam, A. I. Florescu-Mitchell, and A. E. Orel, *Phys.Rev. A*, **77**, 042706 (2008)
2. Dissociative Electron Attachment of Acetylene, S. Chourou and A. E. Orel, *Phys.Rev. A*, **77**, 042709 (2008)
3. Theoretical study of asymmetric molecular-frame photoelectron angular distributions for C 1s photoejection from CO_2 , S. Miyabe, C. W. McCurdy, A. E. Orel, and T. N. Rescigno, *Phys. Rev. A* **79**, 053401 (2009)
4. Isotope Effect in the Electron Attachment of Acetylene, S. Chourou and A. E. Orel, *Phys. Rev. A* **80**, 034701 (2009)
5. Dissociative Electron Attachment of HCN and HNC, S. Chourou and A. E. Orel, *Phys. Rev. A* **80**, 032709 (2009)
6. Asymmetric molecular-frame photoelectron angular distributions for C 1s photoejection from CO_2 ; a theoretical study, S Miyabe, C W McCurdy, A E Orel and T N Rescigno, 2009 *J. Phys.: Conf. Ser.* **194** 012008 (2009)
7. Formation of inner-shell autoionizing CO^+ states below the CO_2^+ threshold, T. Osipov, Th. Weber, T. N. Rescigno, S. Y. Lee, A. E. Orel, M. Schöffler, F. P. Sturm, S. Schössler, U. Lenz, T. Havermeier, M. Kühnel, T. Jahnke, J. B. Williams, D. Ray, A. Landers, R. Dörner, and A. Belkacem, *Phys. Rev. A* **81**, 011401 (2010)
8. Electron-driven excitation and dissociation of molecules, S. Chourou A. Larson, and A.E. Orel, 2010 *J. Phys.: Conf. Ser.* **204** 012001 (2010)

“Low-Energy Electron Interactions with Liquid Interfaces and Biological Targets”

Thomas M. Orlando

School of Chemistry and Biochemistry and School of Physics,
Georgia Institute of Technology, Atlanta, GA 30332-0400

Thomas.Orlando@chemistry.gatech.edu, Phone: (404) 894-4012, FAX: (404) 894-7452

Project Scope: The program concentrates on the important issues dealing with electron initiated damage and energy exchange in the deep valence and shallow core regions of the collision targets. These types of excitations are extremely sensitive to many body interactions and changes in local potentials. The targets we will examine range in complexity from very controlled molecular thin films to realistic biological targets and complicated aqueous solution interfaces. Thus, our proposed investigations should be particularly fruitful in extracting important details regarding the roles of counter ions, interfacial energy exchange, and molecular structure in non-thermal damage of hydrated biological interfaces.

Recent Progress:

Project 1. Coulomb explosions at ice and hydrocarbon surfaces.

We have continued our studies of shallow valence hole mediated Coulomb explosions and water cluster ion production/ejection at ice surfaces. The cluster ion yields are very sensitive to local hydrogen bonding interactions and are very good probes of hole exchange. Specifically, when water is co-adsorbed with rare gases such as Xe, Ar and Ne, cluster ion production and escape is greatly enhanced. The yields, threshold energies and velocities indicate that cluster ion formation and removal involves hole mediated intermolecular Coulomb exchange. Initial hole production is in the rare-gas partner. Though the coupling is weak, the rare-gas:water complex can undergo Auger decay resulting in two-holes localized on small water clusters. This two-hole state Coulomb explodes releasing the water cluster ions. The distribution of experimentally observed masses is well described using simple Poisson statistics for cluster growth on the surface.

We have also begun studies of electron-stimulated process on water co-adsorbed with hydrocarbons and water adsorbed on graphite surfaces. Graphite has been chosen as a substrate since it is a weakly interacting surface that is used in our studies of electron beam induced damage of DNA. Though this is not the focus of our current program, it is also a material that is very relevant to plasma fusion and nuclear reactor technologies. Graphite and graphene screen holes on adsorbates very efficiently. This seems to turn off the Coulomb explosion mechanism that normally leads to water cluster ion production and desorption. Though water cluster ions do not desorb, we have found that in the sub-monolayer water coverage regime, direct carbon and oxidized cluster ion ejection occurs. Threshold data indicates that this is primarily via Auger decay of holes produced in the C 2S level.

Project 2. Coulomb explosions at ionic-aqueous interfaces.

We have extended our studies of intermolecular Coulomb explosions of water adsorbed on rare gases and hydrocarbons adsorbed on water to aqueous interfaces containing dissolved ions. Specifically, we have studied solutions containing either

NaCl, NaOH, HCl or MgCl₂ using the liquid beam apparatus at Pacific Northwest National Laboratory. Laser excitation at 193 nm produced and removed cations of the form H⁺(H₂O)_n and Na⁺(H₂O)_m from liquid jet surfaces containing either NaCl or NaOH. The protonated water cluster yield varied inversely with increasing salt concentration, while the solvated sodium ion cluster yield varied by anion type. We interpreted the production of these clusters in terms of a localized ionization/Coulomb expulsion model. However, the UV desorption of Na⁺(H₂O)_m is not accounted for by this model. Rather it required the ionization of solvation shell waters and a contact ion/Coulomb expulsion mechanism.

Since the contact ion expulsion mechanism requires Coulomb exchange primarily within the first solvation shell, stimulated desorption of cluster ions could provide a very good probe of interfacial ion concentrations and possible perturbations on the hydrogen bonding network. We have therefore extended these studies to solutions containing multiply charged cations (i.e. Mg²⁺, Ca²⁺, etc.) and anions (SO₄²⁻, PO₄²⁻, etc.) that disrupt the hydrogen bonding network of liquid water. These particular ions are also of interest since they are known to be present in biological targets such as DNA interfaces. Our initial results are very intriguing since they imply that the singly charged ions populate the interface. There is no indication of the presence of Mg²⁺ or Ca²⁺ at the interface.

Project 3. Low-energy electron induced damage of DNA constituents.

We have shown that water at the DNA interface is likely involved in the formation of both single and double strand breaks (SSBs and DSBs, respectively). The SSB threshold energy is very low (< 5 eV) and likely involves a shape resonance possibly initially localized on the π* base. The DSBs threshold is above 5 eV and likely involves compound core excited resonances involving water and the bases or phosphates. We believe that these compound core excited resonances can be important window states for the formation of DSBs. Specifically, autoionization of this core excited resonance leads to the formation of a low-energy emitted electron and an electronically excited target configuration. The low energy electron can excite the low-energy shape resonances (known to cause an SSB) at site within the mean scattering distance while the electronic excitation can decay to form another SSB at the initial collision point.

We are therefore directly examining this process using short oligomeric targets. We are also examining the resonances localized on the phosphate by measuring the neutral atomic oxygen yield from a thin film of aqueous Na₂PO₄ containing isotopically labeled water.

Future Work

- The program will continue to focus on the electron interactions with biologically relevant collision partners such as DNA oligomers as well as the building blocks of DNA and RNA. These include simple nucleobases, nucleotides, nucleosides, sugars and phosphates. In the near term we are investigating the direct interaction of water with adsorbed phosphates and phosphate containing adenosine monophosphate (AMP).

- Calculations have indicated efficient atomic oxygen removal during ionization of uracil imbedded in water. This may involve a similar Coulomb exchange process seen for simpler hydrocarbons. We will examine this directly using the same approach used for atomic oxygen detection from phosphates.
- Finally, the theoretical work will be extended by using more realistic scattering potentials and by examining other base pair sequences.

Presentations acknowledging support from this program during 2008-2010

1. T. M. Orlando, "Low-Energy Electron Interactions with Hydrated DNA and Complex Biological Interfaces", Department of Physics, University of Alabama, Al, Jan. 25, 2008.
2. T. M. Orlando, "Probing the interfacial ion composition of low-temperature ice and aqueous salt solution interfaces using Coulomb ejection of cluster ions", Liquid and Solid Aqueous Surfaces and Interfaces Workshop, Telluride, CO, Aug. 10-16, 2008.
3. T. M. Orlando, "Nonthermal Surface Processes: From the Real to the Sublime", Dept. of Chemistry, University of Alabama, Tuscaloosa, Al, Feb. 3, 2009.
4. T. M. Orlando, "Nonthermal Surface Processes: From the Real to the Sublime", Dept. of Chemistry, Louisiana State University, Baton Rouge, LA, Feb. 13, 2009.
5. T. M. Orlando, "Low-energy electron interactions with hydrated DNA", University of Notre Dame, Radiation Chemistry: A Visionary Meeting, July 2009
6. T. M. Orlando, "Low-energy electron interactions with hydrated DNA", Radiation Research Society Meeting, Oct. 9, 2009
7. T. M. Orlando, "The role of resonances and diffraction in the electron-beam induced damage of DNA and RNA thin-films", Dynamical Processes in Irradiated Materials, Donostia International Physics Center, San Sebastian, Spain July 26-28, 2010.
8. T. M. Orlando, "The role of resonances and diffraction in the electron-beam induced damage of DNA and RNA thin-films", Symposium on electron interactions with biomolecules, National American Chemical Society Meeting, Aug. 2010.

Publications acknowledging support from this program during 2008-2010

1. Y. Chen, H. Chen, A. Aleksandrov, and T. M. Orlando, "The Roles of Water, Acidity and Surface Morphology on Surface Assisted Laser Desorption", *J. Phys. Chem. C* **112**, 6953 (2008).
2. G. A. Grieves, N. Petrik, J. Herring-Captain, B. Olanrewaju, A. Aleksandrov, R. G. Tonkyn, S. A. Barlow, G. A. Kimmel, and T. M. Orlando, "Photoionization of Sodium Salt Solutions in a Liquid Jet", *J. Phys. Chem. C* **112**, 8359, (2008).
3. T. M. Orlando, D. Oh, Y. Chen and A. Aleksandrov, "Low-energy Electron Diffraction and Induced Damage in Hydrated DNA", *J. Chem. Phys.* **128**, 195102 (2008).
4. Y. Chen, A. Aleksandrov and T. M. Orlando, "Probing low-energy electron induced damage of DNA using single-photon ionization mass spectrometry", *Int. J. of Mass Spec. and Ion Physics.* **277**, 314 (2008).
5. D. Oh, M. T. Sieger, and **T. M. Orlando**, "The Theoretical Description and Experimental Demonstration of Diffraction in Electron-stimulated Desorption", *J. of Physics: Condensed Matter*, **22**, 084001 (2010). IOP - Special Recognition Paper
6. G. A. Grieves, J. L. McLain, and **T. M. Orlando**, "Low-energy Stimulated Reactions in Nanoscale Water Films and Water:DNA interfaces", *Chapter 18, Charge Particle Interactions with Matter: Recent Advances, Applications and Interfaces*, Book Chapter, Taylor, Francis Publishing Co. *in press*.
7. G. A. Grieves, C. D. Lane and T. M. Orlando, "Direct Observation of Intermolecular Coulomb Decay in a Complex Condensed Phase Targets", *Phys. Rev. Lett.* (*submitted*).

Structure from Fleeting Illumination of Faint Spinning Objects in Flight

Abbas Ourmazd and Peter Schwander

Dept. of Physics

University of Wisconsin Milwaukee

1900 E. Kenwood Blvd, Milwaukee, WI 53211

ourmazd@uwm.edu, pschwan@uwm.edu

Experiments are under way to determine the structure of molecules, viruses, and cells by intersecting them “in flight” with intense short pulses of radiation, and recording “snapshots” before the object is destroyed [1-3]. The group of this PI was the first to demonstrate an algorithm capable of determining the structure of single biomolecules at signal levels as low as $\sim 10^{-2}$ photons/detector-pixel, anticipated from single 500kD molecules [4][5]. In this approach, Bayesian inference is combined with Expectation-Maximization [6] to determine the orientation of the particle giving rise to each snapshot, whence the structure can be determined by iterative phasing [4,7]. Bayesian approaches are among the most general available.

Determining structure from such low-signal, random snapshots of a spinning particle is computationally expensive. It has been long known that the most general algorithms are the most inefficient, and the way to improve this involves introducing problem-specific constraints [8]. We have therefore developed a new generation of algorithms, which include the fundamental physics of image formation, and are thus substantially more efficient. These so-called manifold-mapping approaches combine techniques from graph theory, Riemannian geometry, and general relativity to determine snapshot orientations with higher computational efficiency [9]. Our progress in this area can be summarized as follows:

- a. Development of noise-robust graph-theoretic approaches for discovering manifolds at signals orders of magnitude below those previously demonstrated;
- b. Discovery of the fundamental symmetries underlying all image formation by scattering;
- c. The exploitation of (a) and (b) above to determine snapshot orientations at reduced computational cost.

Application to existing data from synchrotron and electron sources

We have applied these approaches to well-characterized datasets obtained with synchrotron and cryo-electron microscopic techniques. This is an important validation step, and may also extend the range of information extracted with existing techniques.

Fig. 1(a) shows an experimental diffraction snapshot of a superoxide dismutase-1 crystal. Manifold mapping was used to determine the orientation of the crystal for each of 1,800 experimental diffraction snapshots. Fig. 1(b) is a plot of the determined vs. correct orientations. No orientational information was provided to the algorithm. The root-mean-square error of 0.1° is to be compared with the goniometer step size of 0.05° , and crystal mosaicity of 0.8° . Similarly accurate alignment was obtained with experimental diffraction snapshots of a Au nanofoam sample at signals as low as 0.08 photons/pixel,

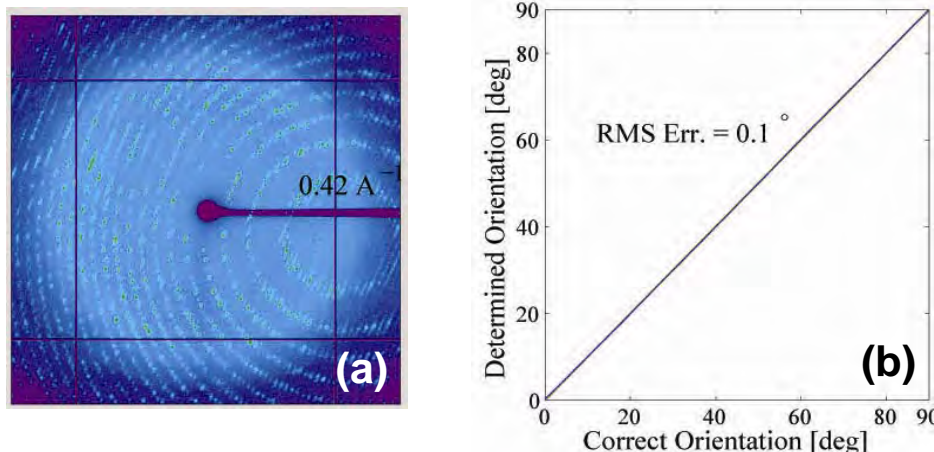


Fig. 1. (a) Experimental diffraction snapshot of superoxide dismutase-1 crystal. (b) Plot of correct orientations of 1,800 snapshots vs. those determined by manifold mapping. Compare the RMS error of 0.1° with the goniometer step of 0.05° and the crystal mosaicity of 0.8° . (Schwander and Ourmazd, unpublished.)

the lowest signal at which data were available. Successful orientation of experimental snapshots provides confidence that our approach is able to deal with experimental data.

Initial analysis of data obtained from the LCLS

We are performing a systematic analysis of the first set of single-particle data obtained from the LCLS. These concern diffraction snapshots obtained from microcrystals of photosystem-1, and lysozyme, and individual mimivirus particles, each intercepted by a single femtosecond pulse (Fig. 2).

Our analysis of data from microcrystals of photosystem-1 and lysozyme has shown that a large number of variables are at work in single-particle LCLS experiments. It is important to establish the nature of each of the variables so they can be rigorously treated in the analysis. The possible degrees of freedom (“variables”) include: the object orientation (Euler angles α, β, γ); pulse-to-pulse intensity variations; and the geometric overlap between the object and the photon pulse (determined by the relative position of the two (x, y, z)), i.e., a total of 7 parameters. When the object is a microcrystal, additional degrees of freedom include: shape variations; size variations; and polymorphism, (twins, and/or c-axis variations) (≥ 3 parameters). Other, as yet undiscovered factors may also be at work. The number of degrees of freedom and hence dimensionality of the data manifold can thus be expected to increase from ~ 3 in standard crystallography to ~ 10 . At present, the precise number and possible influence of these parameters are unknown. For microcrystallites, it is in principle possible to combine standard indexing methods with ad hoc corrections to orient the snapshots. However, the general reliability of the deduced intensity values will be difficult to assess. Indexing approaches cannot be applied to non-periodic objects, which do not produce Bragg peaks.

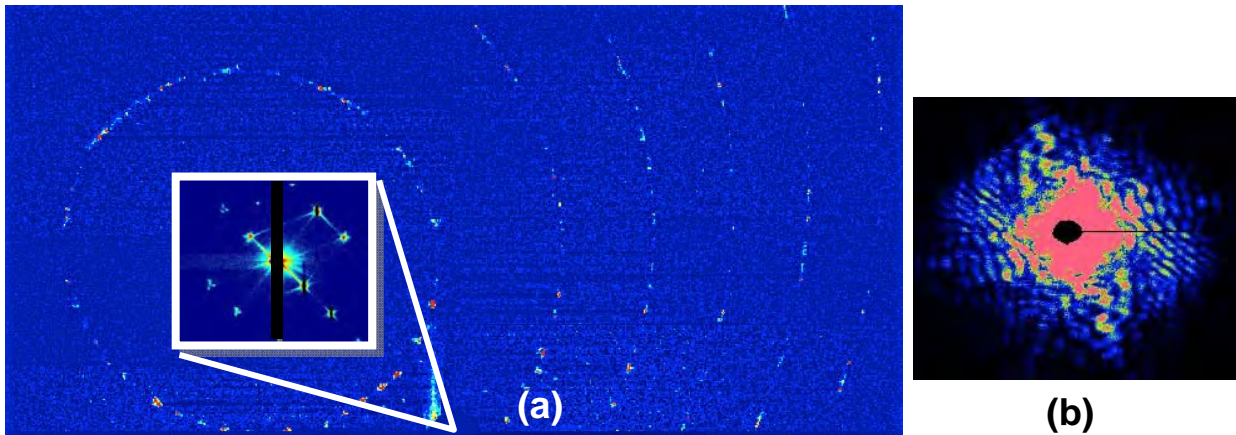


Fig. 1. (a) 80fs diffraction snapshot of a photosystem-1 microcrystallite in water (2mJ of 1.8keV X-rays). Inset shows the central region of diffraction pattern. (b) Snapshot of mimivirus. (Courtesy of H. Chapman et al.)

The algorithms we have developed offer a rigorous and principled means for quantitative extraction of structure from LCLS data. The large number of variables, however, significantly increases the computational cost of such analysis. Our current cycle time for analysis is several days, significantly hampering data analysis. We are working to further enhance the computational efficiency of our algorithms. Availability of additional computing resources would be of substantial help in alleviating this difficulty.

Future Work

We expect our work to lead to the availability of the analytical tools critically needed to extract structural information from LCLS data. In addition to our continued work in the international team which conducted the first LCLS scatter-and-destroy experiments, we have been requested by teams at UCLA, Lawrence Berkeley National Lab, University College (London), the Albert Einstein College of Medicine to participate in up to ten other planned experiments. The proposal from the Albert Einstein College of Medicine, for example, addresses the enzymatic details of multi-drug resistance in human tuberculosis, while the collaboration with University College addresses the structure of metal nanoclusters. Our approach will therefore be used in a number of key experiments to demonstrate the power of LCLS science, with direct impact on important BES research programs. The resulting algorithms will be widely disseminated in the user community.

List of Publications Resulting from Current One-year Period

1. Schwander, P., Fung, R., Phillips, G. N., Ourmazd, A., Mapping the conformations of biological assemblies, *New J. Phys.* **12**, 1-15 (2010).
2. Moths, B., Ourmazd, A., Bayesian algorithms for recovering structure from single-particle diffraction snapshots of unknown orientation: a comparison, submitted to *Acta Cryst. A.* (2010).

Cited References

1. Solem, J.C. and Baldwin, G.C. Microholography of Living Organisms. *Science* **218**, 229-235 (1982).
2. Neutze, R., Wouts, R., van der Spoel, D., Weckert, E. and Hajdu, J. Potential for biomolecular imaging with femtosecond X-ray pulses. *Nature* **406**, 752-757 (2000).
3. Gaffney, K.J. and Chapman, H.N. Imaging Atomic Structure and Dynamics with Ultrafast X-ray Scattering. *Science* **316**, 1444-1448 (2007).
4. Fung, R., Shneerson, V., Saldin, D.K. and Ourmazd, A. Structure from fleeting illumination of faint spinning objects in flight. *Nat Phys* **5**, 64-67 (2009).
5. An apparently different algorithm demonstrated later (Loh, N.-T.D. and Elser, V. Reconstruction algorithm for single-particle diffraction imaging experiments. *Phys. Rev. E* **80**, 026705 (2009)) has been shown to be a different implementation of the same approach (Moths and Ourmazd, submitted to *Acta Cryst A*.)
6. Dempster, A.P., Laird, N.M. and Rubin, D.B. Maximum likelihood from incomplete data via the EM Algorithm *Journal of the Royal Statistical Society. Series B (Methodological)* **39**, 1-38 (1977).
7. Fienup, J.R. Reconstruction of an object from the modulus of its Fourier transform. *Optics Letters* **3**, 27-29 (1978).
8. Le Cun, Y., Denker, J.S., Solla, S.A., Jackel, L.D. and Howard, R.E. Optimal brain damage *in* *Advances in neural information processing systems* 2. 598-605 (Morgan Kaufmann Publishers Inc., Denver; 1990).
9. Schwander, P., Fung, R., Phillips, G.N. and Ourmazd, A. Mapping the conformations of biological assemblies. *New J. Phys.* **12**, 1-15 (2010).

Energetic Photon and Electron Interactions with Positive Ions

Ronald A. Phaneuf,
Department of Physics /220
University of Nevada
Reno NV 89557-0058
phaneuf@physics.unr.edu

Program Scope

This experimental program investigates photon and electron initiated processes leading to ionization of positively charged atomic ions, as well as to ionization and dissociation of molecular ions. The objective is a more complete and quantitative understanding of ionization mechanisms and of the collective dynamic response of bound electrons in atomic and molecular ions to incident EUV photons and electrons. Monoenergetic beams of photons and electrons are merged or crossed with mass/charge analyzed ion beams to probe their internal electronic structure and their interaction dynamics. The primary focus is on processes in which the behavior of bound electrons is highly correlated. This is manifested by giant dipole resonances in the ionization of atomic ions and also of fullerene molecular ions, whose quasi-spherical cage structures characterize them as structural intermediates between individual molecules and solids. In addition to precision spectroscopic data for understanding their internal electronic structure, high-resolution measurements of absolute cross sections for photoionization and electron-impact ionization of ions provide critical benchmarks for testing theoretical approximations such as those used to generate photon opacity databases. Their accuracy is critical to modeling and diagnostics of astrophysical, fusion-energy and laboratory plasmas. Of particular relevance to DOE are those produced by the Z pulsed-power facility at Sandia National Laboratories which is currently the world's most efficient x-ray source, and the National Ignition Facility at Lawrence Livermore National Laboratory which is the world's most powerful laser. Both facilities are dedicated to high-energy-density science as well as to research aimed at harnessing thermonuclear fusion as an energy source.

Recent Progress

The major research thrust has been the application of an ion-photon-beam (IPB) research endstation to experimental studies of photoionization of singly and multiply charged positive ions using monochromatized synchrotron radiation at the Advanced Light Source (ALS). Measurements using the IPB endstation on beamline 10.0.1.2 define the state of the art in energy resolution and sensitivity for studies of photon-ion interactions in the 20 – 300 eV energy range. This program developed and retains responsibility for operation, maintenance and upgrades of this multi-user research endstation.

Due to their large number of atoms, nanometer size and hollow quasi-spherical cage structures, fullerene molecular ions are of intrinsic interest as structural intermediates between individual molecules and solids, and exhibit some of the properties of each. As is the case for conducting solids, their large numbers of valence electrons may be collectively excited in plasmon modes with broad energy signatures. Conversely, the

excitation of core electrons is spatially localized and of molecular character with narrower energy signatures characteristic of carbon-carbon bonding.

- An atom confined in a charged spherical shell is an intriguing quantum-mechanical system. Unusual phenomena associated with the interaction of EUV light with so-called endohedral fullerene molecules containing caged atoms have been predicted in several recent theoretical studies by M. Amusia, V. Dolmatov, S. Manson, A. Msezane and their collaborators, but remain untested by experiment. The broad 4d photoionization resonance in atomic Xe is predicted to be significantly distorted by the carbon cage in endohedral Xe@C₆₀, producing four maxima termed confinement resonances. The predicted pattern is a multi-path interference effect caused by reflection of Xe 4d photoelectron waves by the C₆₀ cage. Exchange of oscillator strength between plasmon modes of the fullerene cage and the trapped atom is also predicted. Measurements at ALS of photoionization of Ce@C₈₂⁺ in the 70 – 160 eV photon energy range show clear evidence of Ce 4d excitation, but neither interference structure nor exchange of oscillator strength. This is attributed to the fact that Ce forms ionic bonds and is not centered within the carbon cage. This work was completed with German collaborators from Giessen (A. Müller and S. Schippers) and Dresden (L. Dunsch) and published in Physical Review Letters [1]. Reference photoionization measurements on ions of the Ce isonuclear sequence in the same photon energy range constituted the Ph.D. dissertation of M. Habibi and were published in Physical Review A [4]. Follow-up experiments with Ce@C₈₂⁺ explored product photoion channels involving successive losses of two C atoms from the fullerene cage, which also exhibit significant Ce 4d oscillator strength. Product channels resulting in single and double ionization with loss of as many as 12 pairs of C atoms were found to have non-negligible cross sections with signatures of the Ce 4d resonance. The results of this collaborative study are being prepared for publication.
- A noble gas atom such as Xe is not expected to form ionic bonds and is predicted to be centered within a C₆₀ cage. A measurement of photoionization of Xe@C₆₀⁺ in the energy range of Xe 4d ionization is therefore critical to test theory. Such an experiment was not heretofore possible because of extremely low yields of synthesized noble-gas endohedral fullerenes. At ALS during a period of several months, a 200 eV beam of Xe ions from an ion sputter-gun bombarded the surface of a rotating metal cylinder onto which C₆₀ was being deposited in vacuum by evaporation. The accumulated powder on the cylinder (few tens of mg) was scraped from the surface and placed into a small oven for subsequent evaporation into a low-power Ar discharge in an ECR ion source. A very small fraction (~10⁻⁵) of the C₆₀ molecules in the accumulated samples containing a Xe atom was sufficient to produce a mass/charge analyzed beam of Xe@C₆₀⁺ ions with a current of 0.06 – 0.3 pA. Proof-of-principle measurements of photoionization of Xe@C₆₀⁺ made at ALS are presented in Figure 1. The data exhibit a clear signature of Xe 4d ionization in this photon energy range, and while there is structure suggestive of confinement resonances, the statistical precision of the data at this stage is insufficient to draw a definite conclusion.
- An *in situ* method was demonstrated at ALS for producing a beam of noble-gas endohedral fullerene ions. A 6-keV C₆₀⁺ ion beam directed through a differentially pumped gas cell containing Ne or Ar yielded mass-selected Ne@C₆₀⁺ and Ar@C₆₀⁺

ion beams with currents of approximately 0.05 pA. The ion beam intensities were adequate to demonstrate proof of principle of photoionization measurements by this method using the IPB endstation.

- Motivated by recent theoretical work of H. Chakraborty, an investigation of the n -dependence of photoionization cross sections of fullerene ions C_n^+ in the range $30 < n < 90$ was completed. The objective was to explore the effects of size, symmetry and shape of the fullerene cage on the strengths and widths of the collective plasmon modes. Subsequent measurements at ALS at higher mass resolution have indicated that the cross section for single ionization accompanied by release of a pair of carbon atoms or a carbon dimer is as large as or larger than that for pure ionization at some photon energies. The measurements did not fully separate these two product channels.

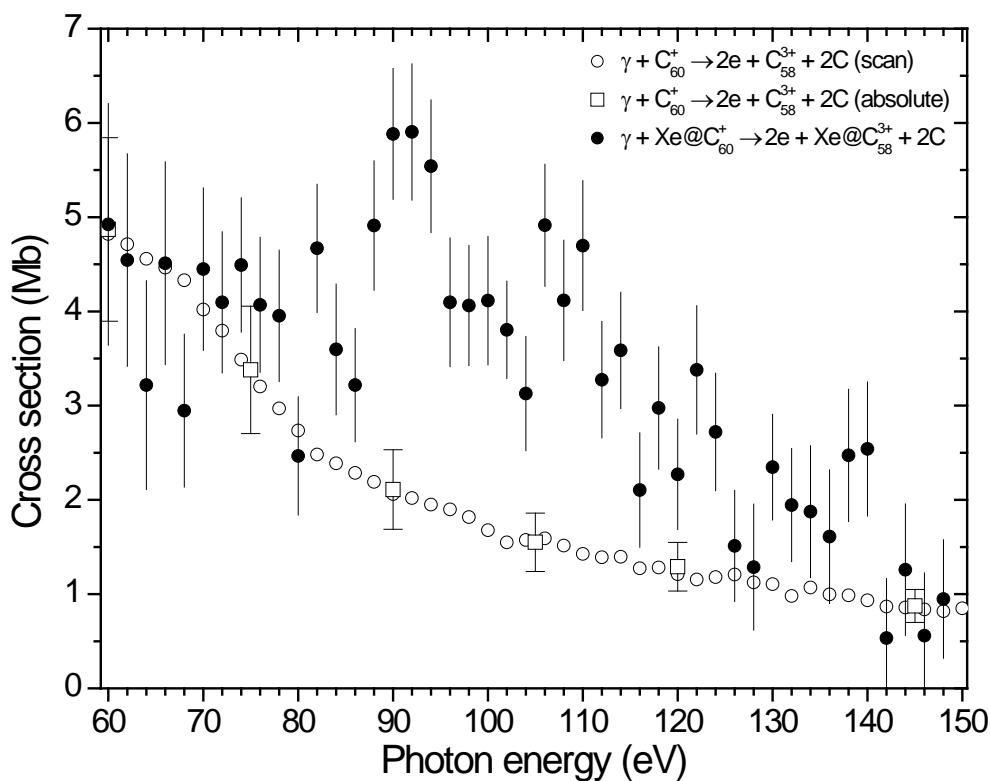


Figure 1. Measurements at ALS of double photoionization with loss of 2 C atoms of empty C_{60}^+ (open circles and squares) and of endohedral $Xe@C_{60}^+$ (solid circles) in the energy range of Xe 4d ionization.

Future Plans

A priority for future experiments at ALS will be to provide definitive experimental tests of theoretical predictions of novel phenomena resulting from the exposure of fullerenes and endohedral fullerenes to EUV light.

- Building upon the proof-of-principle results for photoionization of $Xe@C_{60}^+$, the near-term priority will be to improve upon the statistics of measurements for this and other product ion channels, such that the existence of confinement resonances can be

definitively confirmed or negated. The Xe 4d oscillator strength in the endohedral fullerene molecular ion will be accounted for by searching for additional product ion channels.

- The gas-cell method demonstrated for *in situ* preparation of Ne@C_{60}^+ and Ar@C_{60}^+ ion beams will be employed in photoionization measurements with these ions. The objective is to search for evidence of theoretically predicted effects in these ions, which include the exchange of oscillator strength between plasmon excitation of the fullerene cage and electronic excitation of the caged atom.
- Measurements of the n-dependence of photoionization cross sections of fullerene ions C_n^+ in the range $30 < n < 90$ will be repeated at higher mass resolution in the energy ranges of the plasmon oscillations (near 22 eV for the surface plasmon and 38 eV for the volume plasmon) to distinguish product channels involving pure ionization from those involving ionization plus loss of pairs of C atoms or C_2 dimers.

Publications of Research Fully or Partially Funded by DOE (2008-2010)

1. *Significant redistribution of Ce 4d oscillator strength observed in photoionization of endohedral Ce@C_{82}^+ ions*, A. Müller, S. Schippers, M. Habibi, D. Esteves, J.C. Wang, R.A. Phaneuf, A.L.D. Kilcoyne, A. Aguilar and L. Dunsch, *Phys. Rev. Lett.* **101**, 133001 (2008).
2. *Plasmons in Fullerene Molecules*, R.A. Phaneuf, chapter in “Handbook of Nanophysics,” K. Sattler ed. (submitted March, 2009; Taylor & Francis, in press).
3. *Photoionization of the cerium isonuclear sequence and cerium endohedral fullerene*, M. Habibi, Ph.D. Dissertation, University of Nevada, May, 2009.
4. *Photoionization cross sections for the isonuclear sequence of cerium ions*, M. Habibi, D.A. Esteves, R.A. Phaneuf, A.L.D. Kilcoyne, A. Aguilar and C. Cisneros, *Phys. Rev. A* **80**, 033407 (2009).
5. *K-shell photoionization of ground-state Li-like carbon ions [C^{3+}]: experiment, theory and comparison with time-reversed photorecombination*, A. Müller, S. Schippers, R.A. Phaneuf, S.W.J. Scully, A. Aguilar, I Alvarez, C. Cisneros, E.D. Emmons, M.F. Gharaibeh, G. Hinojosa, A.S. Schlachter and B.M. McLaughlin, *J. Phys. B: At. Mol. Opt. Phys.* **42**, 235602 (2009).
6. *Improved Neutron-Capture Element Abundances in Planetary Nebulae*, N.C. Sterling, H.L. Dinerstein, S. Hwang, S. Redfield, A. Aguilar, M.C. Witthoef, D. Esteves, A.L.D. Kilcoyne, M. Bautista, R. Phaneuf, R.C. Bilodeau, C.P. Balance, B. McLaughlin and P.H. Norrington, *Pub. Astron. Soc. Australia* **26**, 339 (2009).
7. *Photoionization of Se ions for the determination of elemental abundances in astrophysical nebulae*, D.A. Esteves, Ph.D. Dissertation, University of Nevada, May, 2010.
8. *Valence-shell photoionization of the chlorinelike Ca^{3+} ion*, G. Alna'Washi, M. Lu, M. Habibi, R.A. Phaneuf, A.L.D. Kilcoyne, A.S. Schlachter, C. Cisneros and B.M. McLaughlin, *Phys. Rev. A* **81**, 053416 (2010).

Resonant and Nonresonant Photoelectron-Vibrational Coupling

Erwin Poliakoff, Department of Chemistry, Louisiana State University, Baton Rouge, LA 70803, epoliak@lsu.edu

Robert R. Lucchese, Department of Chemistry, Texas A&M University, College Station, TX, 77843, lucchese@mail.chem.tamu.edu

Program Scope

Molecular photoionization provides an ideal testing ground for investigations that probe correlated motions of electronic and vibrational degrees of freedom. In order to investigate such phenomena, it is useful to probe molecular degrees of freedom explicitly, as such an approach can provide the most unambiguous insights into fundamental molecular scattering phenomena. In our research, we perform such state-resolved scattering studies by acquiring vibrationally resolved photoelectron spectra as a function of energy, using the capabilities of the high brightness Advanced Light Source at Lawrence Berkeley National Laboratory. On the theory side, we employ frozen-core Hartree-Fock single-center expansion calculations to provide a framework for interpreting the experimental results. The goal is to understand how photoelectrons traverse anisotropic molecular potentials and exchange energy with vibrations. This research benefits the Department of Energy because the results elucidate structure/spectra correlations that will be indispensable for probing complex and disordered systems of DOE interest such as clusters, catalysts, reactive intermediates, transient species, and related species.

Recent Progress

In the simplest view of molecular photoionization, one assumes that vibrational and photoelectron motion are decoupled, which leads to the Franck-Condon approximation. The Franck-Condon principle has two predictions that are relevant to molecular ionization: (1) vibrational branching ratios are independent of photon energy, and (2) single quantum excitations of nontotally symmetric modes are forbidden. Nonresonant and resonant processes can result in coupling molecular vibration and photoelectron motion, with the result that vibrational branching ratios become dependent on photon energy, and that forbidden vibrations can be excited. Recent examples of systems we have studied are covered briefly here.

Photoelectron spectroscopy of DNA/RNA bases

While most of our previous studies on relatively simple and symmetric systems, a major goal is to extend our work to complex, asymmetric systems, and a specific class of target systems that was selected was nucleic acid bases. We have made significant progress on this topic, as we illustrate here with the example of uracil, a pyrimidine base found in RNA.

While there have been intensive efforts focused on electron scattering studies,¹ there have been no highly resolved photoionization studies involving nucleobases. High-resolution, energy-dependent photoelectron studies can probe the nature of the initial resonant state by providing more detailed information, e.g., via mode-specific vibrational responses which are likely to arise. Our recent results in Fig. 1 demonstrate the feasibility of this strategy clearly.

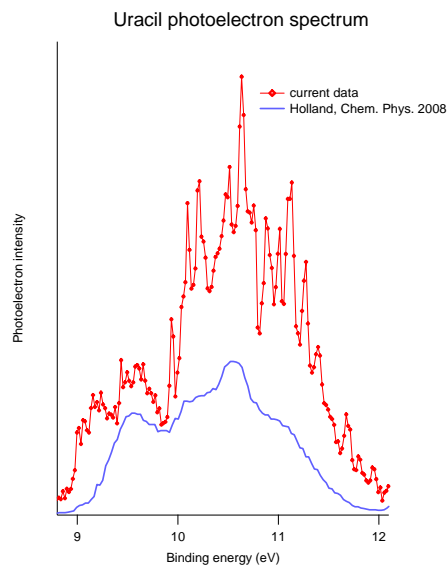


Figure 1. Photoelectron spectra of the first four electronic states of uracil, compared to a previous photoelectron study.² Both spectra were acquired at a photon energy of $h\nu = 40$ eV. The structure of uracil is shown below.

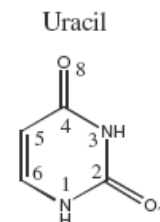


Figure 1 shows a photoelectron spectrum of uracil acquired during our May 2010 beam time at the ALS, and it is compared to the best previously obtained photoelectron spectrum.² Both spectra were acquired at a photon energy of 40 eV, and it is clear that vibrational resolution is achievable, and that we have achieved a major improvement over what was previously accessible. We are currently analyzing these data, including the energy dependence of the results.

Comparing CO and N₂: nonresonant vibrational photoelectron coupling

While it is well understood that resonances can result in coupling between vibrational and electronic degrees of freedom, it is usually assumed that the Franck-Condon approximation is valid in the absence of resonances. However, there are nonresonant mechanisms that can result from correlated vibrational-photoelectron motions. In order to develop a fundamental understanding of such effects, it is useful to focus on simple systems, and we have begun with the valence isoelectronic systems of N₂ and CO. In this study, we measure how deviations emerge from Franck-Condon predictions over a very broad energy range, and some key results are shown in Fig. 2. The two frames on the left apply to N₂ while the two on the right are for CO; the upper two frames are for the excited states while the lower frames are for the ground states. Several aspects of these results are noteworthy. First, it is amazing how broad the excursions in two of the curves are (upper left and lower right). To put this into context, consider that the sharp spike in the lower left frame is the well-known N₂ $3\sigma_g \rightarrow k\sigma_u$ shape resonance, usually considered to be a broad feature. Second, it is striking that these valence isoelectronic states have such radically different behavior; this can be seen by comparing each left hand frame to its corresponding right hand frame. Third, compare the ground state of N₂ to the excited state, i.e., the two frames on the left. The broad excursion observed in the N₂⁺($B^2\Sigma_u^+$) branching ratio is absent in the N₂⁺($X^2\Sigma_g^+$) state. The basis for the excursion in the $B^2\Sigma_u^+$ state data is established in dispersed fluorescence studies,³ but the data for the ground state raises entirely new questions. The N₂⁺($B^2\Sigma_u^+$) state excursion results from bond length-dependence of Cooper minima. It is not clear why the ground state data are so different; is it that there are no Cooper minima, or that there are Cooper minima, but that there is no R-dependence? Similarly, the CO data are the “opposite” of the N₂ data, in that the excited state data do *not* exhibit a broad range excursion, while the ground state data do.

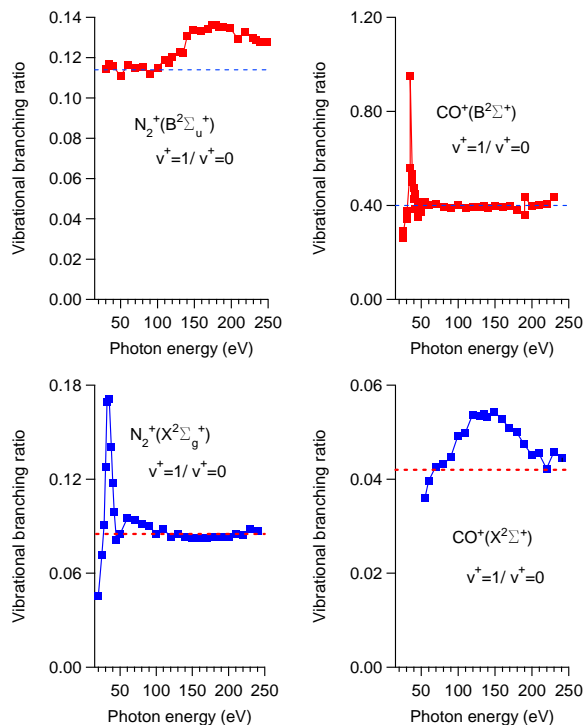


Figure 2. Comparison of the broad range behavior of vibrational branching ratio curves for N_2 and CO . The details are described in the text, but two points are noted here. First, both N_2 and CO show Franck-Condon breakdown over extended ranges that are normally assumed to be free of such behavior. This is the first time that photoelectron spectroscopy has revealed such behavior. Second, these valence isoelectronic systems show much different behavior in that the ground state of N_2^+ does *not* show a broad range excursion while the ground state of CO^+ does (bottom two frames). The situation is also reversed for the ionic excited states (top two frames).

We have completed calculations, and the agreement with experiment is very good. We are currently analyzing the calculations to reveal the sources of the observed differences.

Theoretical advances

A significant development of the computational part of this project is a new method for obtaining vibrational integrals for systems where we need to treat more than two coordinates at the same time. In the adiabatic approximation for photoionization, the vibration-state specific transition amplitudes $A_{v,v^+,k}(\omega)$ can be obtained as an integral over the normal coordinates q_i of the product of the initial $\chi_v(q_1, \dots, q_N)$ and ion-state $\chi_{v^+}(q_1, \dots, q_N)$ vibrational wave functions and the electronic transition matrix elements $T_k^{(-)}(\omega; q_1, \dots, q_N)$ computed within a fixed-nuclei framework

$$A_{v,v^+,k}(\omega) = \int_{-\infty}^{\infty} \cdots \int_{-\infty}^{\infty} [\chi_v(q_1, \dots, q_N)]^* T_k^{(-)}(\omega; q_1, \dots, q_N) \chi_{v^+}(q_1, \dots, q_N) dq_1 \cdots dq_N. \quad (1)$$

One can compute the fixed-nuclei matrix elements, $T_k^{(-)}(\omega; q_1, \dots, q_N)$, on a regular direct-product grid of points as we have done when we have simultaneously treated two vibrational modes.^{4,5} Interpolating these points to compute $A_{v,v^+,k}(\omega)$ then becomes straightforward. The computational effort with this approach scales as M^N where M is the number of points in each dimension and N is the number of dimensions. This approach is feasible for the three-dimensional system, although it will quickly become prohibitively expensive as more vibrational modes are treated. We have developed an interpolation method for which the required number of fixed-nuclei calculations does not grow as fast with N as the direct product approach does. Our approach is to compute the matrix elements along a series of lines in the N dimensional normal-mode space. The lines are chosen so that in a power series expansion with respect to the displacements, the low order derivatives can be accurately represented. This has made possible simultaneous treatments of multiple vibrational modes, even in the vicinity of resonances.

References

- ¹ S. Ptasinska and L. Sanche, *J. Chem. Phys.* **125** (2006).
- ² D. M. P. Holland, A. W. Potts, L. Karlsson, I. L. Zaytseva, A. B. Trofimov, and J. Schirmer, *Chem. Phys.* **353**, 47 (2008).
- ³ R. M. Rao, E. D. Poliakoff, K. Wang, and V. McKoy, *Phys. Rev. Lett.* **76**, 2666 (1996).
- ⁴ R. R. Lucchese, J. D. Bozek, A. Das, and E. D. Poliakoff, *J. Chem. Phys.* **131**, 044311:1 (2009).
- ⁵ R. R. Lucchese, J. Soderstrom, T. Tanaka, M. Hoshino, M. Kitajima, H. Tanaka, A. De Fanis, J. E. Rubensson, and K. Ueda, *Phys. Rev. A* **76**, 012506:1 (2007).

Publications 2007-2010

1. A. Das, J. S. Miller, E. D. Poliakoff, R. R. Lucchese, and J. D. Bozek, *J. Chem. Phys.*, **127**, 244309:1 (2007).
2. R. Montuoro, R. R. Lucchese, J. D. Bozek, A. Das, and E. D. Poliakoff, *J. Chem. Phys.*, **126**, 244309:1 (2007).
3. R. R. Lucchese, J. Soderstrom, T. Tanaka, M. Hoshino, M. Kitajima, H. Tanaka, A. De Fanis, J. E. Rubensson, and K. Ueda, *Phys. Rev. A* **76**, 012506 (2007).
4. N. Berrah, R. C. Bilodeau, J. D. Bozek, I. Dumitriu, D. Toffoli, and R. R. Lucchese, *Phys. Rev. A* **76**, 042709:1 (2007).
5. W. B. Li, J. C. Houver, A. Haouas, F. Catoire, C. Elkharrat, R. Guillemin, L. Journal, R. Montuoro, R. R. Lucchese, M. Simon, and D. Dowek, *J. Elec. Spectrosc. Relat. Phenom.* **156**, 30 (2007).
6. W. B. Li, R. Montuoro, J. C. Houver, L. Journal, A. Haouas, M. Simon, R. R. Lucchese, and D. Dowek, *Phys. Rev. A* **75**, 052718:1 (2007).
7. M. Hoshino, R. Montuoro, R. R. Lucchese, A. De Fanis, U. Hergenhahn, G. Prumper, T. Tanaka, H. Tanaka, and K. Ueda, *J. Phys. B-At. Molec. Optical Phys.* **41**, 085105:1 (2008).
8. G. Prumper, D. Rolles, H. Fukuzawa, X. J. Liu, Z. Pesic, I. Dumitriu, R. R. Lucchese, K. Ueda, and N. Berrah, *J. Phys. B-At. Molec. Optical Phys.* **41**, 215101 (2008).
9. A. Das, E. D. Poliakoff, R. R. Lucchese, and J. D. Bozek, *J. Chem. Phys.*, **130**, 044302:1 (2009).
10. A. T. Le, R. R. Lucchese, M. T. Lee, and C. D. Lin, *Phys. Rev. Lett.*, **102**, 203001:1 (2009).
11. A. T. Le, R. R. Lucchese, and C. D. Lin, *J. Phys. B-At. Molec. and Optical Physics* **42**, 211001:1 (2009).
12. A. T. Le, R. R. Lucchese, S. Tonzani, T. Morishita, and C. D. Lin, *Phys. Rev. A* **80**, 013401:1 (2009).
13. R. R. Lucchese, J. D. Bozek, A. Das, and E. D. Poliakoff, *J. Chem. Phys.*, **131**, 044311:1 (2009).
14. C. Jin, A. T. Le, S. F. Zhao, R. R. Lucchese, and C. D. Lin, *Phys. Rev. A* **81**, 033421 (2010).
15. R. R. Lucchese, R. Montuoro, K. Kotsis, M. Tashiro, M. Ehara, J. D. Bozek, A. Das, A. Landry, J. Rathbone, and E. D. Poliakoff, *Molecular Physics* **108**, 2055 (2010).
16. C. D. Lin, Anh-Thu Le, Zhangjin Chen, Toru Morishita, and Robert Lucchese, *J. Phys. B- At. Molec. and Optical Physics* **43**, 122001 (2010).

Control of Molecular Dynamics: Algorithms for Design and Implementation

Herschel Rabitz and Tak-San Ho, Princeton University
Frick Laboratory, Princeton, NJ 08540, hrabitz@princeton.edu, tsho@princeton.edu

A. Program Scope

This research is concerned with the conceptual and algorithmic developments addressing control over quantum dynamics phenomena. The research is theoretical and computational in nature, with a particular focus towards exploring basic principles of importance for laboratory studies, especially in conjunction with the use of optimal control theory and its realization in closed-loop learning experiments. This research program involves a set of interrelated components aiming at developing a deeper understanding of quantum control and providing new algorithms to extend the laboratory control capabilities.

B. Research Progress

In the past year several projects were pursued and the results are summarized below.

1. **Accelerated monotonic convergence of optimal control over quantum dynamics**[1] The control of quantum dynamics is often concerned with finding time-dependent optimal control fields that can take a system from an initial state to a final state to attain the desired value of an observable. This work presented a general method for formulating monotonically convergent algorithms to iteratively improve control fields. The formulation is based on a Two-point Boundary-value Quantum Control Paradigm (TBQCP) expressed as a nonlinear integral equation of the first kind arising from dynamical invariant tracking control. We showed that TBQCP is related to various existing techniques, including local control theory, the Krotov method, and optimal control theory. We also derived several accelerated monotonic convergence schemes for iteratively computing control fields based on TBQCP. Numerical simulations were compared with the Krotov method showing that the new TBQCP schemes are efficient and remain monotonically convergent over a wide range of the iteration step parameters and control pulse lengths, which is attributable to the trap-free character of the transition probability quantum dynamics control landscape.
2. **Environment-invariant measure of distance between evolutions of an open quantum system**[2] The problem of quantifying the evolution of an open quantum system is important in quantum control, especially for quantum information processing. Motivated by this problem, we developed a measure for evaluating the distance between unitary evolution operators of a composite quantum system that consists of a sub-system of interest (e.g., a quantum information processor) and the environment. The main characteristic of this

measure is the invariance with respect to the effect of the evolution operator on the environment, which follows from an equivalence relation that exists between unitary operators acting on the composite system, when the effect on only the sub-system of interest is considered. The invariance to the environment transformation makes it possible to quantitatively compare the evolution of an open quantum system and its closed counterpart. The distance measure also determines the fidelity bounds of a general quantum channel with respect to a unitary target transformation. This measure is also independent of the initial state of the system and straightforward to numerically calculate. As an example, the measure was used in numerical simulations to evaluate fidelities of optimally controlled quantum gate operations (for one- and two-qubit systems), in the presence of a decohering environment.

3. **Multi-polarization quantum control of rotational motion through dipole coupling [3]** In this work we analyzed the quantum controllability of rotational motion under the influence of an external laser field coupled through a permanent dipole moment. The analysis took into consideration up to three polarization fields, but we also discuss the consequences for working with fewer polarized fields.
4. **The landscape of quantum transitions driven by single-qubit unitary transformations with implications for entanglement [4]** This work considered the control landscape of quantum transitions in multi-qubit systems driven by unitary transformations with single-qubit interaction terms. The two-qubit case was fully analyzed to reveal the features of the landscape including the nature of the absolute maximum and minimum, the saddle points and the absence of traps. The results permit calculating the Schmidt state starting from an arbitrary two-qubit state following the local gradient flow. The analysis of multi-qubit systems is more challenging, but the generalized Schmidt states may also be located by following the local gradient flow. Finally, we showed the relation between the generalized Schmidt states and the entanglement measure based on the Bures distance.
5. **Gradient algorithm applied to laboratory quantum control [5]** The exploration of a quantum control landscape, which is the physical observable as a function of the control variables, is fundamental for understanding the ability to perform observable optimization in the laboratory. For high control variable dimensions, trajectory-based methods provide a means for performing such systematic explorations by exploiting the measured gradient of the observable with respect to the control variables. This study presented a practical, robust, easily implemented statistical method for obtaining the gradient on a general quantum control landscape in the presence of noise. To demonstrate the method's utility, we employed the experimentally measured gradient as input in steepest-ascent trajectories on the landscapes of three model quantum control problems: spectrally filtered and integrated second harmonic generation as well as excitation of atomic rubidium. We found that the gradient algorithm achieved efficiency gains of up to approximately three times that of the standard genetic algorithm

and, as such, is a promising tool for meeting quantum control optimization goals as well as landscape analyses. The landscape trajectories directed by the gradient should aid in the continued investigation and understanding of controlled quantum phenomena.

6. **Experimental quantum control landscapes: Inherent monotonicity and artificial structure**[6] Unconstrained searches over quantum control landscapes are theoretically predicted to generally exhibit trap-free monotonic behavior. This work made an explicit experimental demonstration of this intrinsic monotonicity for two controlled quantum systems: frequency unfiltered and filtered second-harmonic generation (SHG). For unfiltered SHG, the landscape was randomly sampled and interpolation of the data was found to be devoid of landscape traps up to the level of data noise. In the case of narrow-band-filtered SHG, trajectories were taken on the landscape to reveal a lack of traps. Although the filtered SHG landscape was trap free, it exhibited a rich local structure. We provided a perturbation analysis around the top of these landscapes to understand their topology. We found that, despite the inherent trap-free nature of the landscapes, practical constraints placed on the controls can lead to the appearance of artificial structure arising from the resultant forced sampling of the landscape. This circumstance and the likely lack of knowledge about the detailed local landscape structure in most quantum control applications suggests that the *a priori* identification of globally successful (un)constrained curvilinear control variables may be a challenging task.
7. **Accelerated optimization and automated discovery with covariance matrix adaptation for experimental quantum control**[7] Optimization of quantum systems by closed-loop adaptive pulse shaping offers a rich domain for the development and application of specialized evolutionary algorithms. In this work, we presented derandomized evolution strategies (DESs) as a robust class of optimizers for experimental quantum control. The combination of stochastic and quasi-local search embodied by these algorithms was especially amenable to the inherent topology of quantum control landscapes. Implementation of DES in the laboratory results in efficiency gains of up to ~ 9 times that of the standard genetic algorithm, and thus is a promising tool for optimization of unstable or fragile systems. The statistical learning upon which these algorithms were predicated also provided the means for obtaining a control problem's Hessian matrix with no additional experimental overhead. Finally, we introduced the forced optimal covariance adaptive learning method to enable retrieval of the Hessian matrix, which can reveal information about the landscape's local structure and dynamic mechanism. Exploitation of such algorithms in quantum control experiments should enhance their efficiency and provide additional fundamental insights.

C. Future Plans

The research in the coming year will mainly focus on the application of recently developed accelerated monotonically convergent algorithms [1] to the study of various

atomic and molecular dynamics control problems, including laser controlled photo-association processes of atoms in thermal gases and laser controlled collective excitation of Bose-Einstein condensates. We also plan to formulate monotonically convergent algorithms (1) beyond the linear dipole interaction, especially for the study of efficient molecular orientation/alignment control using short intense laser fields, and (2) in the context of the density matrix formalism for open quantum systems. Finally, we plan to closely examine the properties of quantum control landscapes subject to various constraints on the laboratory control field, which is a subject of prime importance in all optimal control experiments.

D. References

1. Accelerated monotonic convergence of optimal control over quantum dynamics, T.-S. Ho and H. Rabitz, *Phys. Rev E* (in press).
2. Environment-invariant measure of distance between evolutions of an open quantum system, M. D. Grace, J. Dominy, R. L. Kosut, C. Brif, and H. Rabitz, *New J. Phys.* 12, 015001 (2010).
3. Multi-polarization quantum control of rotational motion through dipole coupling, G. Turinici and H. Rabitz, *J. Phys. A: Math. Theor.* 43, 105303 (2010).
4. The landscape of quantum transitions driven by single-qubit unitary transformations with implications for entanglement, R. Cabrera and H. Rabitz, *J. Phys. A: Math. Theor.* 42, 275303 (2009).
5. Gradient algorithm applied to laboratory quantum control, J. Roslund and H. Rabitz, *Phys. Rev. A* 79, 053417 (2009).
6. Experimental quantum control landscapes: Inherent monotonicity and artificial structure, J. Roslund and H. Rabitz, *Phys. Rev. A* 80, 013408 (2009).
7. Accelerated optimization and automated discovery with covariance matrix adaptation for experimental quantum control, J. Roslund, O. M. Shir, T. Bck, and H. Rabitz, *Phys. Rev. A* 80, 043415 (2009).
8. Quantum optimal control of isomerization dynamics of a one-dimensional reaction-path model dominated by a competing dissociation channel, Yuzuru Kurosakia, Maxim Artamonov, Tak-San Ho, and Herschel Rabitz, *J. Chem. Phys.*, 131, 044306 (2009).
9. Landscape of unitary transformations in controlled quantum dynamics, T.-S. Ho, J. Dominy, and H. Rabitz, *Phys. Rev. A* 79, 013422 (2009).
10. Topology of the quantum control landscape for observables M. Hsieh, R. Wu, and H. Rabitz, *J. Chem. Phys.* 130, 104109 (2009).

Ultracold sodium and rubidium mixtures: collisions, interactions and heteronuclear molecule formation

Principal Investigator:

Dr. Chandra Raman
Assistant Professor
School of Physics
Georgia Institute of Technology Atlanta, GA 30332-0430
craman@gatech.edu

Program:

This program centers on quantum gases of ^{23}Na and ^{87}Rb , with the goal of quantifying the low temperature ground-state collisions and interactions between the species. Na-Rb remains a relatively unexplored system for which measurements of ultracold collisions are of fundamental importance.

Recent Progress:

Our main result in the current period is the demonstration of light-induced atomic desorption, or LIAD, for loading a sodium magneto-optical trap (MOT) [1]. This provides an alternative to Zeeman slowers for sodium. Moreover, we demonstrated that the MOT was compatible with vacuum-limited lifetimes in the several second range. Our MOT contained up to 3.7×10^7 atoms, a promising result for the creation of a vapor-cell-based atomic Bose-Einstein condensate of sodium.

The LIAD MOT allowed us to study the surface physics of photon stimulated desorption (PSD). PSD of neutral sodium from a silica (SiO_2) surface is a charge-transfer process for bound Na^+ ions. The photo-desorption rate was measured by monitoring the trap loading rate. Using this method, we observed a steep wavelength dependence of the desorption process above 2.6 eV photon energy that was consistent with a photo-electric threshold (see attached figure taken from Ref. [1]). Our result highlights the sensitivity of atom traps and their potential applications to surface science—we detected a significant sodium desorption in the range 2.6 to 3.4 eV, a region below the detection threshold of previous work[2]. Our measurements have significance for estimations of sodium vapor density in the lunar atmosphere.

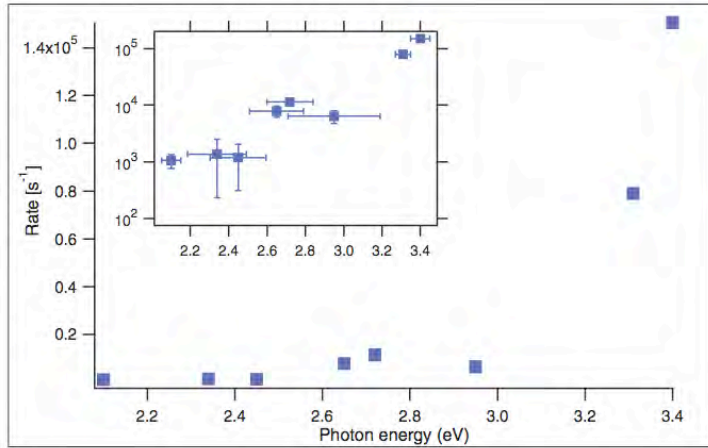


FIG. 5. (Color online) Photon energy dependence of desorption of sodium atoms from Pyrex glass. Plotted is the excess MOT loading rate due to LIAD for an average intensity of 2 mW/cm^2 . Each point is the average of three to four MOT loading curves. (Inset) The same data plotted on a logarithmic scale with the y error bars resulting from statistical data analysis. The energy error bars correspond to the typical half-width uncertainties directly provided by the manufacturer's specifications sheets.

Future Plans

Future work on photon stimulated desorption will focus on measurement of the velocity distributions of the desorbed atoms in order to quantify the charge transfer model. Future work on Na Rb experiments will concentrate on reducing the Na temperature by microwave evaporation and increasing the phase space density.

References

1. Telles, G., et al., *Light-induced atomic desorption for loading a sodium magneto-optical trap*. Physical Review A, 2010. **81**(3): p. 032710.
2. Yakshinskiy, B.V. and T.E. Madey, *Photon-stimulated desorption as a substantial source of sodium in the lunar atmosphere*. Nature, 1999. **400**(6745): p. 642-644.

“Coherent and Incoherent Transitions”

F. Robicieux

*Auburn University, Department of Physics, 206 Allison Lab, Auburn AL 36849
(robicfj@auburn.edu)*

Program Scope

This theory project focuses on the time evolution of systems subjected to either coherent or incoherent interactions. This study is divided into three categories: (1) coherent evolution of highly excited quantum states, (2) incoherent evolution of highly excited quantum states, and (3) the interplay between ultra-cold plasmas and Rydberg atoms. Some of the techniques we developed have been used to study collision processes in ions, atoms and molecules. In particular, we have studied the correlation between two (or more) continuum electrons.

Recent Progress 2009-2010

Laser cooling of OH: We proposed a method[13] for laser cooling OH molecules. The method was based on exciting $\Delta J = 2$ stimulated Raman transition in the ground electronic and vibronic state. Because the magnetic dipole moment substantially changes during a transition, relatively few photons are needed to cool the molecules from a few mK to roughly 100 μ K. A high Q cavity tuned to the rotational transition can enhance the decay rate and decrease the time needed for cooling.

Fluorescence as a probe of Ultracold plasmas: In a joint study with Bergeson's experimental group, we extended the method of Ref. [5] to study the nonequilibrium evolution of ultracold plasmas at early times.[14] We focused on the earliest times, when the plasma equilibrium is evolving and before the plasma expands. To correctly model the fluorescence, we solved the optical Bloch equation for each ion in the simulation. Both the simulation and experiment showed the initial increase in ion fluorescence, disorder-induced heating, and coherent oscillation of the rms ion velocity.

Studies inspired by anti-hydrogen research: In Ref. [15], a peculiar anti-proton loss mechanism was discovered to occur when the anti-protons were mixed with positrons. Through a series of calculations of various atomic and plasma processes, we discovered that the only mechanism that could explain the measurements was a resonance in the large scale motion of the anti-proton. In Ref. [16], we performed intensive calculations of atomic and plasma processes to simulate the formation of anti-hydrogen by three body recombination in a positron plasma. This included a realistic modeling of the large scale fields in the experiments. We found a peculiar scaling of the anti-hydrogen formation with the density of the plasma due to the competition with other loss processes. We also clarified the role of electric field ionization of the positron weakly bound to the anti-proton on the rates and on the properties of the atoms.

Electron impact double ionization/three electron continua: We performed two studies of electron impact double ionization: Mg[17] and Be[21]. These studies are computationally difficult because three continuum electrons must be accurately

treated in the calculation. We compared the time dependent close coupling method which uses a three dimensional radial grid of points and coupled angular momenta to the R-matrix with pseudostates method which uses a basis function technique. For Mg, we could compare with experiment and obtained good agreement. There are currently no experiments on double ionization of Be.

Relativistic effects for two electron continua: We performed two studies that went beyond non-relativistic and/or dipole transitions in two electron systems. In one study[18], we computed the double photoionization of He including the quadrupole term of the transition operator at a photon energy of 800 eV. This was undertaken at the request of A.L. Landers because experiments at the ALS were being proposed. We found that the energy differential cross section was insensitive to the quadrupole interaction but the triple differential cross section could show substantial effects. In Ref. [19], we gave the theoretical treatment for extending the time dependent close coupling theory to the Dirac equation. We performed test calculations for two electron systems where an electron ionized a H-like ion.

Proposal for using cold atoms to measure the neutrino mass: We proposed a β -decay experiment based on a sample of ultracold atomic tritium. The proposal required cold, trapped tritium and used a measure of the energy of the β and the recoil of the ion to determine the momentum of the neutrino. By using a gas of Rydberg atoms, the path of the β could be determined as a track of excitation. Simulations of the possible Rydberg transitions showed that the resulting track should be visible above background and should hardly perturb the energy and path of the β .

Transitions through a chaotic sea: Motivated by an experiment by T.F. Gallagher, we performed studies of microwave transitions when atoms were driven near, but not on, resonance.[10] The classical mechanism for the transition was an expansion of the chaotic sea to encompass the starting region of phase space; the surprise was that this mechanism could deliver the electron to a small range of n-states which is possible due to the stickiness of the edge the chaotic regions. We extended this study to the case of kicked Rydberg atom which we studied both classically and quantum mechanically.[22] We found that the kicked atom was not as efficient as the atom driven by microwaves; we also found that the spread in angular momentum was not nearly as large as for the microwave case. We attributed the main differences to the development of an island chain at the edge of the chaotic region which slowed the transition through the separatrix.

Attosecond double ionization of H₂: We investigated the energy and angle differential probabilities for 2-photon double ionization of H₂. [23] We used our time dependent close coupling program for molecules to compute how the chirp of the attosecond pulse affected the cross sections. We focused on two photon transitions. We found interesting effects from the chirp when the energy band width of the pulse becomes comparable to the difference in ionization thresholds of the neutral and positive ion that were similar to the effects we found in He. Different sign of the chirp can produce qualitatively different effects. For the case of a linearly polarized pulse parallel to the axis, a clear signature of the sequential double-electron above threshold ionization process can be seen in the spectra.

Finally, this program has several projects that are strongly numerical but only require knowledge of classical mechanics. This combination is ideal for starting undergraduates on publication quality research. Since 2004, thirteen undergraduates have participated in this program. Most of these students have completed projects published in peer reviewed journals. One of these students, Michael Wall, was one of 5 undergraduates invited to give a talk on their research at the undergraduate session of the DAMOP 2006 meeting. Three students hired Fall 2009 will return for continued studies in 2010. One or two new undergraduates will be hired into the group at the beginning of the Fall 2010 semester and I expect they will continue the successful tradition of undergraduate research.

Future Plans

Transitions through a chaotic sea: Our recent results[10,22] showing how to transport a system around a classical island has opened the door to studies of interesting systems. We plan to complete investigations into a molecular system (in particular, vibrational transitions). We will also study the situation where the frequency of oscillation does not monotonically increase (or decrease) with energy where simple chirping techniques fail.

Ultra-cold plasmas The recent collaboration with Bergeson's group[5,14] has raised some interesting questions about the early time evolution of ultracold plasmas. This involves the investigation of how low energy electrons scatter in the presence of ions. Extremely low temperatures, where naïve estimates give strongly coupled electrons, will be studied using collisional codes and molecular dynamics simulations. Experimental results from Bergeson and Killian's group indicate anomalous heating of the ions which we will investigate.

Anti-hydrogen motivated calculations The next generation experiments are aimed at trapping the anti-hydrogen atom. To address possible issues, we will investigate processes that arise from this goal. In particular, we plan to study the three body recombination rate when all of the particles have the same mass.

Coherent evolution Motivated by the collaboration with Landers,[12] we will devote substantial time to the interaction between two free electrons or the interaction between a free electron and a Rydberg atom. We plan to use this program to study both a scattering situation like Ref. [12] and the dynamics of two weakly bound electrons as experimentally studied by R.R. Jones. This was the most speculative aspect of the proposal and the last major component of the original proposal that hasn't been investigated.

DOE Supported Publications (7/2006-7/2009)

[1] M. S. Pindzola, F. Robicheaux, J. Colgan, and C. P. Balance, Phys. Rev. A **76**, 012714 (2007).

[2] M. S. Pindzola, F. Robicheaux, and J. Colgan, Phys. Rev. A **76**, 024704 (2007).

[3] J. Colgan, M. Foster, M. S. Pindzola, and F. Robicheaux, J. Phys. B **40**, 4391 (2007).

[4] J. Colgan, M. S. Pindzola, and F. Robicheaux, J. Phys. B **41**, 121002 (2008).

[5] S.D. Bergeson and F. Robicheaux, Phys. Rev. Lett. **101**, 073202 (2008).

[6] F. Robicheaux, J. Phys. B **41**, 192001 (2008).

- [7] M.S. Pindzola, F. Robicheaux, and J. Colgan, *J. Phys. B* **41**, 235202 (2008).
- [8] J. Colgan, M.S. Pindzola, F. Robicheaux, C. Kaiser, A.J. Murray, and D.H. Madison, *Phys. Rev. Lett.* **101**, 233201 (2008).
- [9] M.S. Pindzola, F. Robicheaux, and J. Colgan, *J. Phys. B* **41**, 235202 (2008).
- [10] T. Topcu and F. Robicheaux, *J. Phys. B* **42**, 044014 (2009).
- [11] T.-G. Lee, M.S. Pindzola, and F. Robicheaux, *Phys. Rev. A* **79**, 053420 (2009).
- [12] A.L. Landers, F. Robicheaux, T. Jahnke, M. Schoffler, T. Osipov, J. Titze, S.Y. Lee, H. Adaniya, M. Hertlein, P. Ranitovic, I. Bocharova, D. Akoury, A. Bhandary, Th. Weber, M.H. Prior, C.L. Cocke, R. Dorner, and A. Belkacem, *Phys. Rev. Lett.* **102**, 223001 (2009).
- [13] F. Robicheaux, *J. Phys. B* **42**, 195301 (2009).
- [14] A. Denning, S.D. Bergeson, and F. Robicheaux, *Phys. Rev. A* **80**, 033415 (2009).
- [15] G.B. Andresen et al. (ALPHA collaboration), *Phys. Plasmas* **16**, 100702 (2009).
- [16] S. Jonsell, D. P. van der Werf, M Charlton, and F. Robicheaux, *J. Phys. B* **42**, 215002 (2009).
- [17] M.S. Pindzola, J.A. Ludlow, F. Robicheaux, J. Colgan, and D.C. Griffin, *J. Phys. B* **42**, 215204 (2009).
- [18] J.A. Ludlow, J. Colgan, T.-G. Lee, M.S. Pindzola, and F. Robicheaux, *J. Phys. B* **42**, 225204 (2009).
- [19] M.S. Pindzola, J.A. Ludlow, F. Robicheaux, J. Colgan, and C.J. Fontes, *Phys. Rev. A* **80**, 052706 (2009).
- [20] M. Jerkins, J.R. Klein, J.H. Majors, F. Robicheaux, and M.G. Raizen, *New J. Phys.* **12**, 043022 (2010).
- [21] M.S. Pindzola, C.P. Balance, F. Robicheaux, and J. Colgan, *J. Phys. B* **43**, 105204 (2010).
- [22] T. Topcu and F. Robicheaux, *J. Phys. B* **43**, 115003 (2010).
- [23] T.-G. Lee, M.S. Pindzola, and F. Robicheaux, *J. Phys. B* **43**, 165601 (2010).

Table-Top Sources of Coherent Soft X-ray and X-Ray Light

Jorge J. Rocca,

Electrical and Computer Eng Department, and Department of Physics

Colorado State University, Fort Collins, CO 80523-1373

rocca@engr.colostate.edu

Henry C. Kapteyn

JILA/Physics Department, University of Colorado, Boulder, CO 80309-0440

kapteyn@jila.colorado.edu

Program description

This project explores schemes for the generation of intense coherent soft x-ray and x-ray radiation on a table-top. We have investigated the use of a pre-ionized medium created by a compact capillary discharge to guide high intensity laser light in order to - 1) extend the cutoff photon energy for high-order harmonic generation (HHG) using ions, and 2) implement new phase matching schemes in fully-ionized plasmas in order to generate bright, fully coherent, HHG beams. The use of a discharge-created plasma reduces ionization-induced defocusing of the driving laser as well as energy loss. In this work we extended high harmonic emission from Xe up to a photon energy of 160 eV, and observed HHG emission at energies up to 170 eV in Kr and 275 eV in Ar. We also employed a complementary technique of using longer wavelength driving light to extend full phase matching of high harmonic generation well beyond the phase-matching limit for 0.8 μm . Using a driving laser with 2 μm wavelength) we have demonstrated that we can generate a bright soft x-ray continuum that spans the entire water window region of the spectrum from <300 eV to >500 eV. The transform-limit for this spectrum corresponds to an 11 as pulse. These results opens the possibility of combine quasi-phase matching, infrared driving lasers, and plasma discharges to implement bright, ultrafast, fully coherent, x-ray beams.

In complementary work we have advanced the development of table-top soft x-ray lasers. We have demonstrated that injection-seeding with high harmonics of soft x-ray amplifiers created by laser heating of solid targets generates intense soft x-ray pulses with full spatial and temporal coherence, low divergence, short pulsewidth, and defined polarization. We have measured that the soft x-ray laser pulses generated by this technique are the shortest soft x-ray pulse duration demonstrated to date from a plasma amplifier, \sim 1ps. During the past year we have measured and modeled the temporal coherence characteristics of these new soft x-ray lasers. In related work we have extended the range of gain-saturated table-top soft x-ray lasers to 10.9 nm and have demonstrated the first diode-laser pumped soft x-ray laser. The latter result opens the path to new type of compact diode-pumped soft x-ray lasers with greatly increased repetition rate (eg. 100 Hz) and high average power on a small footprint.

New phase matching schemes for HHG at keV photon energies

In past work under this grant, we demonstrated that, by doing high-order harmonic generation within a capillary discharge plasma, we can avoid defocusing of the plasma that would otherwise limit the range of wavelengths accessible. We also showed that in a sufficiently low-pressure gas environment, defocusing can be confined by use of a glass capillary, likely augmented by nonlinear self-guiding of the beam. This makes it possible to observe high-order harmonics up to 500 eV photon energy originating from multiply-ionized Argon gas. Both these methods have promise when combined with quasi phase matching techniques than can correct for phase mismatch. We have previously demonstrated all-optical quasi phase matching of the high-order harmonic process, and are working to implement this in these highly-ionized media. To-date, work using a capillary discharge guiding has not been successful, likely because of the combined fluctuations in plasma conditions and the 10 Hz driver laser used in the experiment, limitations that are not fundamental. However, in the course of this work we realized that phase-matched generation of high-order harmonics can be extended to shorter wavelengths by using longer-wavelength driving lasers. In 2009 we published a comprehensive discussion of this concept in

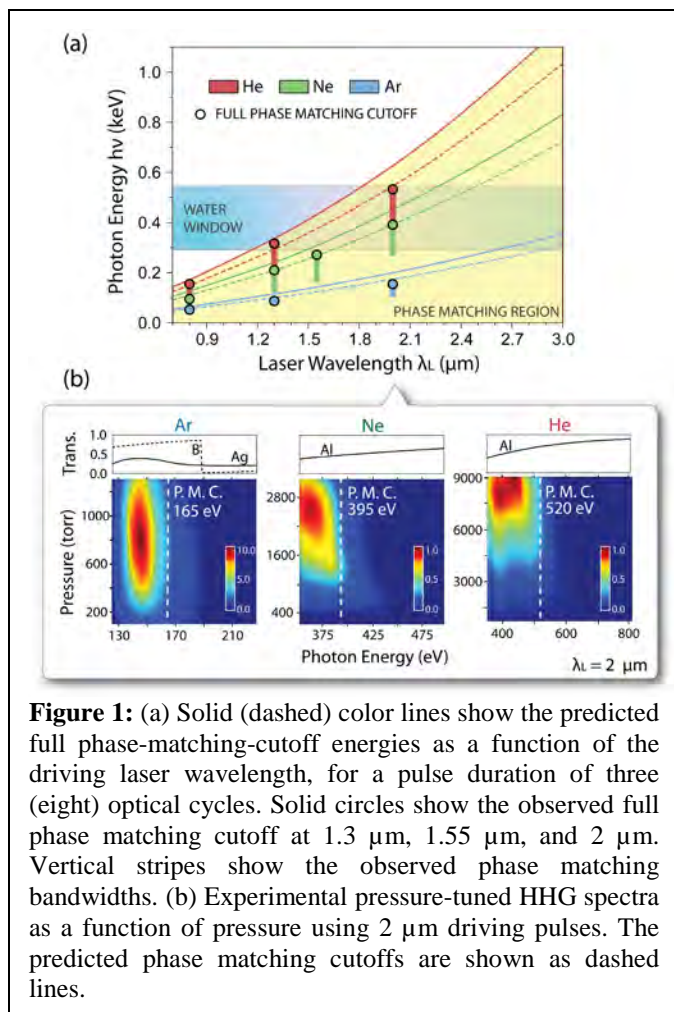


Figure 1: (a) Solid (dashed) color lines show the predicted full phase-matching-cutoff energies as a function of the driving laser wavelength, for a pulse duration of three (eight) optical cycles. Solid circles show the observed full phase matching cutoff at 1.3 μm , 1.55 μm , and 2 μm . Vertical stripes show the observed phase matching bandwidths. (b) Experimental pressure-tuned HHG spectra as a function of pressure using 2 μm driving pulses. The predicted phase matching cutoffs are shown as dashed lines.

ray beams.

Temporal Coherence of a Soft X-Ray Lasers Seeded with High Harmonics

Plasma-based soft x-ray lasers (SXL) are complementary to HHG due to their ability to generate pulses with significantly higher energy. Using injection-seeding soft x-ray plasma amplifiers created by laser heating of solid targets with HHG pulses we have created a fundamentally new regime for the generation of soft x-ray laser pulses with full phase coherence, low divergence and short pulse width. Our group demonstrated the saturated amplification of HH seed pulses in several transitions of Ne-like and Ni-like ions at wavelengths ranging from 32.6 nm to 13.2 nm. The seeding of this type of high density solid target plasma SXL amplifier with its characteristic broad laser line width can in principle support the generation of sub-ps SXL pulses. Two years ago using a streak-camera developed at Kansas State University we measured the pulse duration of Ne-like Ti laser operating

PNAS, and in the past year we have made considerable progress in further experimental validation of this concept. More recently, in a collaboration with the group of Andrius Baltuska at the Technical University of Vienna, we have demonstrated the first high-order harmonic generation in the x-ray region of the spectrum using 3.5 μm laser light, obtaining light to 400 eV photon energy using argon gas as the generation medium.

Phase-matched conversion in this weakly ionized regime is quite advantageous because the driving laser beam experiences minimal nonlinear distortion, resulting in an excellent spatial coherence. In work submitted for publication (Fig.2), we have done the first double-slit coherence measurements on the light from a water window harmonic source. Our totality of measurements on this source show that the optimum phase matching conditions scale very favorably to shorter wavelengths, and may even make multi-keV, sub-attosecond pulses hard x-ray region of the spectrum possible. In the future, we will combine quasi-phase matching, infrared driving lasers, and plasma discharges to implement bright, ultrafast, fully coherent, x-

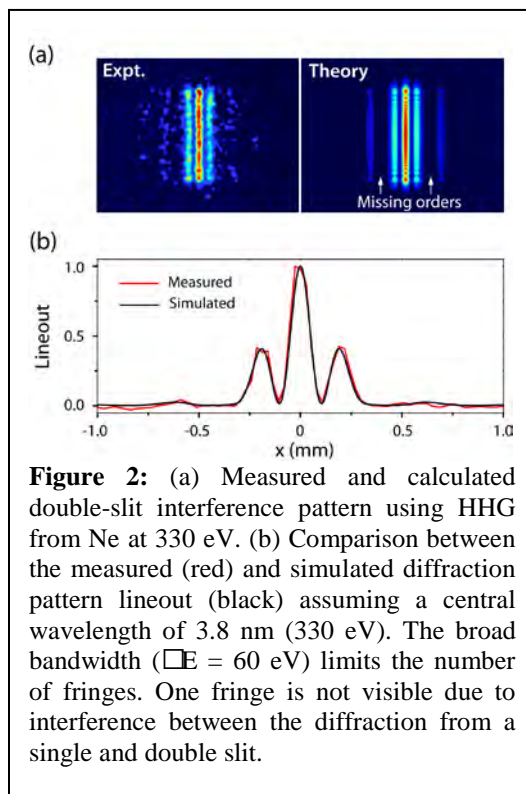
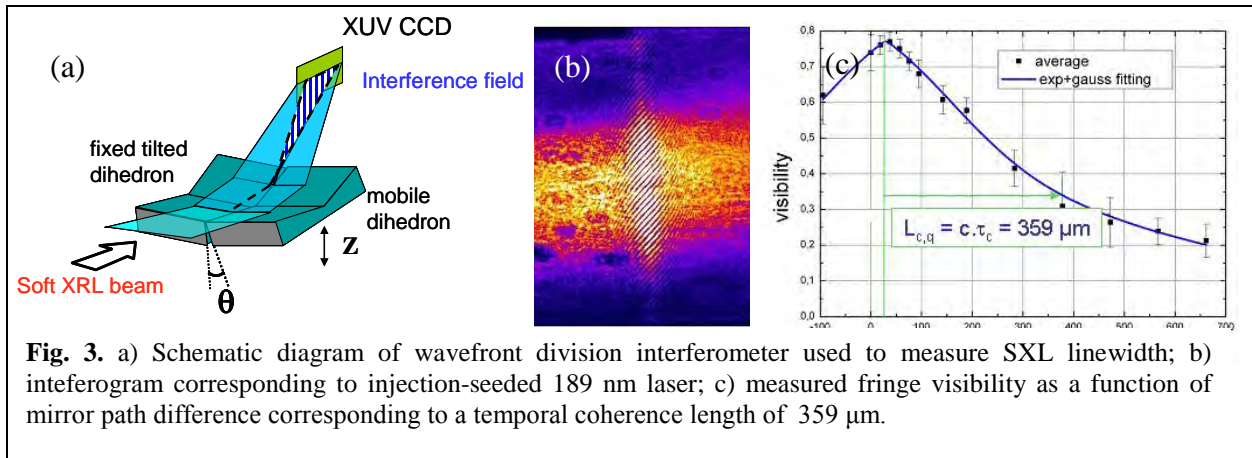


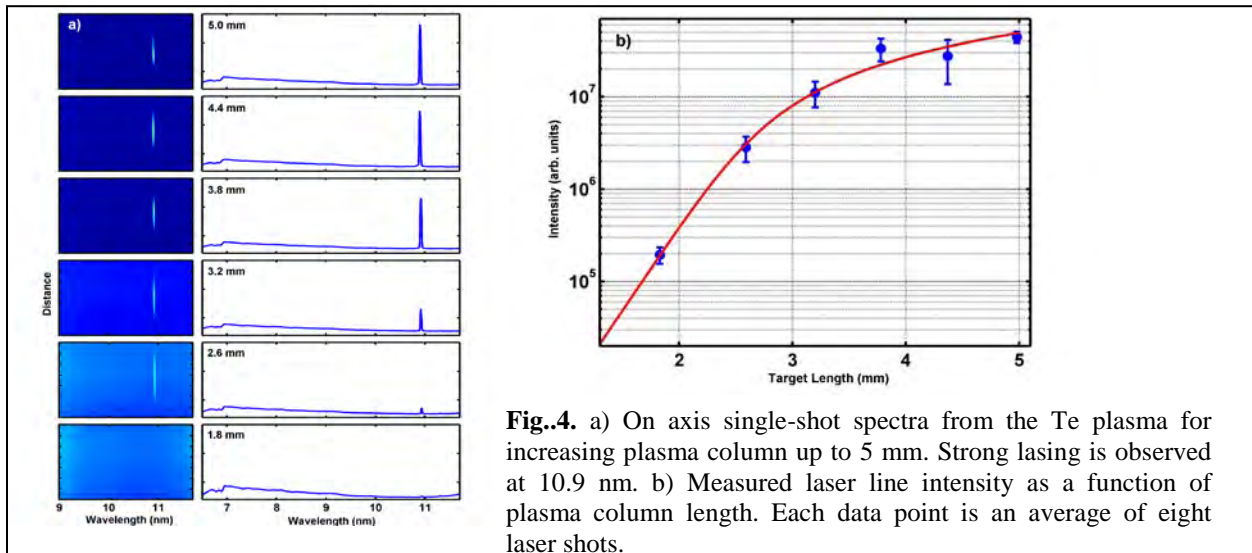
Figure 2: (a) Measured and calculated double-slit interference pattern using HHG from Ne at 330 eV. (b) Comparison between the measured (red) and simulated diffraction pattern lineout (black) assuming a central wavelength of 3.8 nm (330 eV). The broad bandwidth ($\Delta E = 60$ eV) limits the number of fringes. One fringe is not visible due to interference between the diffraction from a single and double slit.

at 32.6 nm to be ~ 1 ps [3], the shortest SXRL pulse duration obtained to date from a plasma amplifier. The results were compared with hydrodynamic/atomic physics simulations that predict that injection seeding of denser plasmas will lead to femtosecond SXLs. During the past year we have measured and modeled the temporal coherence of these new lasers. In collaboration with A. Klisnick et al. from the Univ. of Paris-Sud we measured the linewidth of an injection-seeded 18.9 nm laser using a bi-mirror interferometer (Fig.3). The results were compared to simulations that compute both the linewidth narrowing of the input seed pulse due to both line narrowing in the amplifier and saturation re-broadening [10]. We found that the coherence time of the SXL pulse is of the order of 1.8 ps in the ASE (unseeded) mode and slightly smaller when the amplifier is seeded with a high-order harmonic pulse. The latter corresponds to a near-transform limited soft x-ray pulse.



Extension of Gain-saturated Table-Top Lasers to $\lambda = 10.9$ nm

There is great interest in extending plasma-based table-top soft x-ray lasers to shorter wavelengths for applications. We have recently demonstrated of a gain-saturated table-top 10.9 nm in the $4d^1S_0 \rightarrow 4p^1P_1$ transition of nickel-like Te that operates at 1 Hz repetition rate. Gain-saturated lasing was generated by rapidly heating a solid Te slab target with pulses from a $\lambda = 800$ nm CPA Ti:sapphire laser system that produces with energies up to 8 J pulses before compression. Figure 4a shows a series of on-axis single-shot spectra for plasmas of different lengths between 1.8 and 5 mm. The total pump energy on target was fixed at 3.4 J. The soft x-ray 10.9 nm laser line intensity rapidly grows with target length to dominate the entire spectra, eventually reaching saturation (Fig.4b). A soft x-ray laser average power of



$\sim 1 \mu\text{W}$ was obtained pumping a 6 mm wide Te target with 4.2 J of total laser pump energy on target at a repetition rate of 1 Hz. The most intense laser pulses reached an energy of $\sim 2 \mu\text{J}$ [7]. The laser beam intensity is estimated to reach an intensity of $\sim 3.0 \times 10^{11} \text{ Wcm}^{-2}$, that exceeds the $0.6\text{-}1.4 \times 10^{10} \text{ W/cm}^2$ computed saturation intensity of this line for the plasma conditions of the experiment. This is the shortest wavelength gain-saturated table-top laser reported to date.

Demonstration of Soft X-ray Laser pumped by a an all-diode-pumped laser system

Direct diode pumping of the driver laser opens the possibility to develop a new generation of more compact, higher repetition rate soft x-ray lasers for applications. The much higher pumping efficiency that results from pumping small quantum defect materials with a narrow bandwidth laser-diode source of the optimum wavelength will allow for soft x-ray laser with greatly increased repetition rate and average power. In very recent work we demonstrated the first all-diode-pumped soft x-ray laser. Lasing was achieved at $\lambda = 18.9 \text{ nm}$ by transient electron-impact excitation of Ni-like Mo ions in a plasma created by ablating a solid Mo target (Fig.5). To pump this SXRL we developed a cryo-cooled Yb:YAG chirped-pulse-amplification laser system that generates 1 J pulses of 8.5 ps duration. To our knowledge this is the first diode-pumped laser chirped pulse amplification to reach 1 J energy in sub-10 ps pulses, which is necessary to efficiently pump soft x-ray lasers. This result opens the path to new type of compact diode-pumped soft x-ray lasers with greatly increased repetition rate (eg. 100 Hz) and high average power on a small footprint.

Journal Publications from DOE-BES supported work (2008-2010)

1. T. Popmintchev, M.-C. Chen, O. Cohen, M.E. Grisham, J.J. Rocca, M.M. Murnane, and H.C. Kapteyn, "Extended phase matching of high harmonics driven by mid-infrared light," *Optics Letters* **33**, 2128 (2008).
2. R.L. Sandberg, C. Song, P.W. Wachulak, D.A. Raymondson, A. Paul, B. Amirbekian, E. Lee, A.E. Sakdinawat, C. La-O-Vorakiat, M.C. Marconi, C.S. Menoni, M.M. Murnane, J.J. Rocca, H.C. Kapteyn, and J. Miao, "High Numerical Aperture Table Top Soft X Ray Diffraction Microscopy with 70 nm Resolution," *Proceedings of the National Academy of Science* **105**, 24 (2008).
3. Y. Wang, M. Berrill, F. Pedaci, M.M. Shakya, S. Gilbertson, Z. Chang, E. Granados, B.M. Luther, M.A. Larotonda, and J.J. Rocca, "Measurement of 1 Picosecond Soft X-Ray Laser Pulses from an Injection-Seeded Plasma Amplifier," *Physical Review A* **79**, 023810 (2009)
4. F. Furch, B. Reagan, B. Luther, A. Curtis, S. Meehan, and J.J. Rocca, "Demonstration of an all-diode-pumped soft x-ray laser," *Optics Letters* **34**, 3352 (2009).
5. T. Popmintchev, M.-C. Chen, A. Bahabad, M. Gerrity, P. Sidorenko, O. Cohen, I. P. Christov, M.M. Murnane, and H.C. Kapteyn, "Phase matching of high harmonic generation in the soft and hard X-ray regions of the spectrum," *Proceedings of the National Academy of Sciences*, p. 10.1073, 0903748106, (2009).
6. P. Arpin, T. Popmintchev, N. L. Wagner, A. L. Lytle, O. Cohen, H. C. Kapteyn, and M. M. Murnane, "Enhanced High Harmonic Generation from Multiply Ionized Argon above 500 eV through Laser Pulse Self-Compression," *Physical Review Letters*, vol. 103, pp. 143901/1-4 (2009).
7. D. Alessi, D.H. Martz, Y. Wang, M. Berrill, B.M. Luther, and J.J. Rocca, "1 Hz Operation of a Gain-Saturated 10.9 nm Table-Top Laser in Nickel-like Te," *Optics Letters*, **35**, 414 (2010).
8. M.C. Chen, M.R. Gerrity, S. Backus, T. Popmintchev, X. Zhou, P. Arpin, X. Zhang, H.C. Kapteyn, and M.M. Murnane, "Spatially coherent, phase matched, high-order harmonic EUV beams at 50 kHz," *Optics Express*, vol. 17, pp.17376-17383 (2009).
9. M.C. Chen, P. Arpin, T. Popmintchev, M. Gerrity, B. Zhang, M. Seaberg, M.M. Murnane and H.C. Kapteyn, "Bright, Coherent, Ultrafast Soft X-Ray Harmonics Spanning the Water Window from a Tabletop Source", submitted (2010).
10. M. Berrill, D. Alessi, Y. Wang, S.R. Domingue, D.H. Martz, B.M. Luther, Y. Liu and J.J. Rocca; "Improved beam characteristics of solid-state target soft x-ray laser amplifiers by injection seeding with high harmonics", *Optics Letters*, **35**, 2317, (2010)
11. T. Popmintchev, M.M. Murnane and H.C. Kapteyn, "The Nonlinear Optics of Coherent X-Ray Generation: Photonics at the Timescale of the Electron ", invited paper in preparation, *Nature Photonics* (2010).

Ultrafast holographic x-ray imaging and its application to picosecond ultrasonic wave dynamics in bulk materials

Christoph G. Rose-Petruck

* Department of Chemistry, Box H, Brown University, Providence, RI 02912
phone: (401) 863-1533, fax: (401) 863-2594, Christoph_Rose-Petruck@brown.edu

Program Scope

The focus of this work is to develop ultrafast, x-ray imaging methods suitable for use with laser plasma x-ray sources. The methods will image structural dynamics and motions in materials using phase shifts imparted on the x-ray waves as they propagate through the material. The planned work seeks to directly observe, for instance, shock waves propagating in the bulk of materials. This work was funded in the spring of 2008.

Several imaging modalities have been studied. The first method, called Propagation-based Differential Phase Contrast Imaging (PDPCI) measures the Laplacian of the real part of the index of refraction, n_r , of the material. No x-ray interferometers are used. The sensitivity to density variations is up to 1000 times larger than that of conventional x-ray absorption based imaging methods. The second method, called Spatial Harmonic Imaging (SHI), uses the x-radiation scattered off the sample for image formation. Both modalities do not require any x-ray optics between the sample and the x-ray source. As a consequence, they are suitable for ultrafast time-resolved imaging in a setup very similar to those used in conventional x-ray backlighting.

As an additional component of the program, an ultrafast x-ray absorption fine structure apparatus has been setup up at 7ID-C, APS, Argonne National laboratory. The ultrafast ligand substitution dynamics of $\text{Fe}(\text{CO})_5$ has been measured with 2-ps temporal resolution. A related partner-user proposal for 7ID has been submitted to the APS.

1 Recent Progress

During the last year progress has been made in three research topics funded by this DOE grant.

1.1 Propagation-based Differential Phase Contrast Imaging (PDPCI)

PDPCI measures under appropriate conditions the Laplacian of the real part of the refractive index, which is proportional to the material's electron density. Interfaces, where the 2nd spatial derivative of the density is large, are very visible. The underlying x-ray wave interference effect leads to an increase of the x-ray beam divergence similar to diffraction of visible light at the corners of a slit. PDPCI has been discussed in last year's abstract, has been the subject of 2 papers^{1,2}, and will not be discussed in any detail here. However, as I show below, the x-ray divergence that gives rise to the PDPC features in an image, can be enhanced by orders of magnitude by inserting a periodic absorption mask (grid) between the sample and the x-ray camera yielding a novel image method that is superbly sensitive to density variations in a sample and that simultaneously images the microscopic internal structure of the material. The sketch of a PDPCI setup is shown in the upper panel of Figure 1. The addition of a grid (lower panel) yields a SHI setup.

1.2 Spatial harmonic x-ray imaging: Small angle x-ray scattering off an object imaged in a single x-ray image with a full field of view

Spatial Harmonic Imaging uses the x-radiation scattered off the sample to form an image. A related method using single-crystal x-ray mirrors is known as diffraction-enhanced imaging. In SHI however, the deflection of x-rays from the primary beam direction is detected by placing an absorption grid between the sample and the camera as shown in the lower panel of Figure 1. The logarithm of the detected image intensity is proportional to the product of the absorbances of the sample and the grid. Fourier transformation of the image converts this product into a convolution. The grid, being a periodic structure, produces a series of peaks in the spatial frequency domain. Each peak is "surrounded" by the spatial

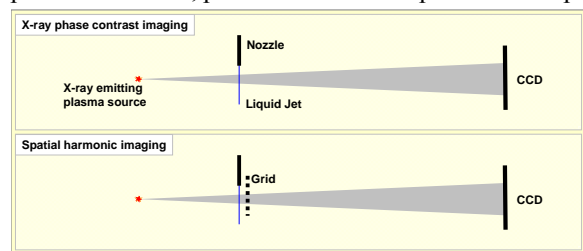


Figure 1: Layout of ultrafast imaging setups for PDPCI (top) and SHI (bottom). A liquid beam serves as a sample and the laser plasma source serves as an x-ray point source. The only significant difference between both arrangements is a metal grid with about 50- μm pitch in the SHI setup.

frequency spectrum of the sample. An example is shown in Figure 2. The test sample consists of three carbon fiber bundles that are oriented at approximately 60° to each other. A hexagonal grid is placed between the sample and the camera. After Fourier transformation the spatial frequency spectrum shows harmonic peaks surrounded by replicas of the spatial frequency spectrum of the sample itself. Owing to their refractive index discontinuities, much x-radiation is scattered at interfaces. Consequently, fibers scatter radiation primarily orthogonal to the fiber direction and the intensities around the harmonic peaks of a specific order are not equal. For instance peaks that are orthogonal to the scattering direction are not influenced by scattering while those in the scattering plane are.

The 0-order peak corresponds to the absorption image (without scatter) and can therefore be used for normalization. Selecting an area around a specific and the 0-order peaks and Fourier back-transforming these areas independently to real space results in the two images shown on the lower left of Figure 2. These two images are similar but not identical. In fact, their division yields the image on the lower right, which does not show one of the fiber bundles any more because the Fourier component that was picked for back-transformation was perpendicular to the x-ray scattering plane. This example demonstrates that in a single x-ray exposure the directionality of features in a sample can be imaged although the x-ray absorbances of the various sample components are identical. This feature of SHI can be used, for instance, for the imaging of turbulent flows in optically opaque media or inside of flow systems. Small fibers could be added to the medium. The fibers align in the laminar flow sections but will rotate in turbulent parts of the flow field. Since the directionality of all fibers can be measured by SHI, the entire flow field can be imaged in a single x-ray exposure.

Another example for the utility of SHI is the ability to image phase interfaces in media. Since SHI does not need any scanning of the x-ray detection system, but can image the entire sample during each exposure, laser-pump SHI-probe experiments of phase transitions are, in principle, possible. An example, measured in preparation for such experiment, is shown in Figure 3. One sample of water and one sample of ice/water slurry were placed into round vials and SHI-imaged simultaneously. The red line in Figure 3 depicts the absorbance along a line perpendicular to the symmetry axis of the vials. The left and the right peaks correspond to the slurry and the water, respectively. Water has a higher absorbance than the ice slurry because of its slightly higher electron density. After processing the image and extracting the scattering image, the signal profile is shown as a blue line. Clearly the contrast has increased from 4% to about 40%. Additionally, strong phase contrast peaks can be seen at the inside and outside edges of the vials. The enhancement of the phase contrast features is estimated to be about 2 orders of magnitude. Note that the phase contrast features in the absorption profile are barely visible as small discontinuities and inflections of the curves slope. The data are currently being prepared for publication.³

1.3 3-ps XANES of the ligand substitution dynamics of Fe(CO)₅ at the Advanced Photon Source, ANL

In collaboration with Dr. Bernhard Adams and Dr. Mathieu Chollet, Argonne National Laboratory, we have set up an UXAFS instrument at 7-ID-C. It consists of a high-speed x-ray chopper, liquid sample jet chamber with laser and x-ray beam diagnostic followed by an x-ray streak camera.

The experimental setup is sketched in Figure 4. The x-radiation is delivered from the undulator 7-ID and focused vertically by an x-ray lens in hutch B into the liquid sample jet in hutch C. About 10 meters downstream, a chopper reduces the synchrotron repetition rate to the laser repetition rate of 5 kHz. A second x-ray lens focuses the x-ray beam in horizontal direction into the liquid sample jet. Owing to the short focal length of the horizontal lens, the x-ray beam widens again on its way to the streak camera so that a large portion of the camera input slit is illuminated. The vertical beam remains compact, thereby delivering most of the x-ray photons onto the 10-μm camera input slit. The 400-nm pump laser beam is reflected off two dielectrically coated beryllium mirrors that transmit the x-radiation such that both beams are collinear within the sample chamber. The beams enter the sample chamber where they intersect a liquid sample jet. The chamber and the entire liquid handling system are kept under a protective dry nitrogen atmosphere. The chamber integrates the sample jet, two movable YAG screens – one before and one after the sample, and a timing diode. The YAG screens are imaged onto a camera and are used to collinearly align the x-ray and laser beams. The timing diode is used to adjust the laser x-ray pulse timing.

Time-resolved XANES spectra were measured at 7-ID. The results are currently being prepared for publication.⁴ The measurements proceeded by selecting a specific x-ray wavelength with the beam line's monochromator. Then, alternating streak images were measured with and without laser excitation of the sample. The process was then repeated at different x-

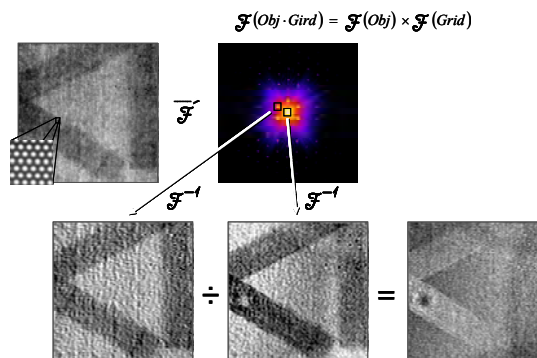


Figure 2: SHI processed image of three identical carbon fiber bundles. Sensible choice of a Fourier component for back transformation, results in the elimination of the vertical carbon fibers from the output image. Note the appearance of a dark round spot that is caused by a drop of (disordered) glue.

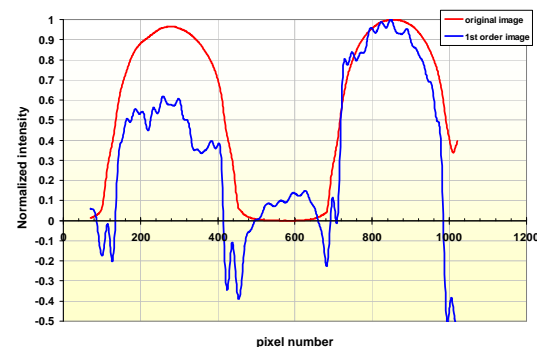


Figure 3: Red line: X-ray absorbance of ice slurry (left) and water (right). Blue line: 1-scattering signal for the same samples. Both curves are normalized for water.

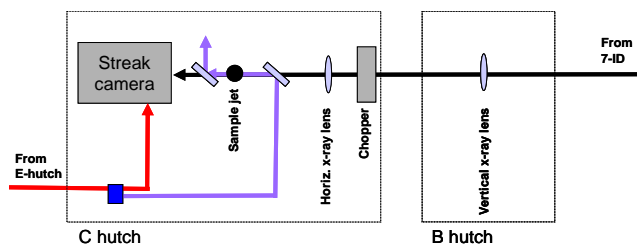


Figure 4: Simplified setup of the setup at the 7-ID. The distances between the vertical x-ray lens and the sample is about 15 meters.

Pentacoordinated transition metal carbonyls such as $M(\text{CO})_5$, $M = \text{Fe, Ru, and Os}$ are commonplace in organometallic syntheses, materials chemistry, and biological processes. While the theoretically most stable geometry for $\text{Fe}(\text{CO})_5$ is trigonal bipyramidal, we have shown previously that in aromatic solvents and alcohols IPC forms stable complexes with one of the solvent molecules distorting the IPC symmetry to C_{2v} . For instance, in ethanol the IPC-Ethanol complex has a Gibbs free energy of complexation of -4.7 kJ/mol , which implies that about 87% of all IPC molecules are complexed with a single ethanol molecule. We hypothesize that this complexation has significant implications for ligand substitution reactions in solution since the reactant molecules are interacting with each other prior to a reaction. For instance, UV-photo induced ligand substitution should not proceed via a dissociative process but instead might proceed through a concerted process. In this case, the leaving CO would be simultaneously replaced by an alcohol that was complexed to IPC prior to the photoexcitation. Based on photo-induced ligand dissociation studies in the gas and liquid phase, we estimate that the substitution should be complete on the 100-fs time scale. In contrast, the fraction of the molecules that are not complexed with $\text{Fe}(\text{CO})_5$ (13% in ethanol at room temperature) should proceed on the tens of picoseconds timescale.

The photo substitution reactions of IPC in methanol, n-butanol, n-hexanol, and t-butanol have been observed using UV-pump transient IR-absorption probe spectroscopy with a temporal resolution of several picoseconds. The authors found a substitution time constant of 42 ps for $\text{Fe}(\text{CO})_5$ in methanol and 94 ps in butanol. It is reasonable to expect that the time constant in ethanol is bracketed by these numbers. Thus, our experimental attempt to distinguish the concerted and the diffusive reaction paths is based on the measured time constants for product formation. While not specifically discussed in this proposal, our study is also of importance for understanding the influence of intersystem crossing because the $\text{Fe}(\text{CO})_5$ and the reaction product $\text{Fe}(\text{CO})_4\text{ethOH}$ have singlet ground states, while the possible intermediate $\text{Fe}(\text{CO})_4$ has a triplet ground state.

Figure 5 shows the measured XANES spectrum of $\text{Fe}(\text{CO})_5$ in ethanol. Also shown are theoretical XANES spectra calculated using FEFF 8.10 based on Density Functional Theory structures of $\text{Fe}(\text{CO})_5$ and $\text{Fe}(\text{CO})_4\text{ethOH}$. Four graphs are shown following the reaction mechanism that we believe to observe. First, ground state $\text{Fe}(\text{CO})_5$ (black) is excited resulting in hot $\text{Fe}(\text{CO})_5/\text{Fe}(\text{CO})_4$ (red). The intermediate $\text{Fe}(\text{CO})_4$ cools somewhat until it can combine with an incoming ethanol to vibrationally hot $\text{Fe}(\text{CO})_4\text{ethOH}$ (orange) which subsequently cools (blue). The measured and theoretical spectra agree on the position of peak C but deviate at peak A. This is due to the fact that XANES calculations close to the absorption edge suffer from uncertainties of the assumed ionization energy and the details of the atomic potentials used during the calculation of the photoelectron's multiple scattering paths.

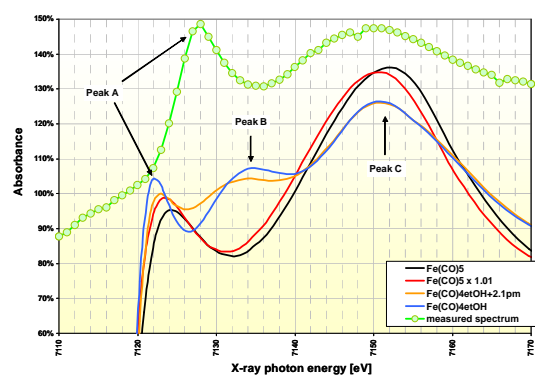


Figure 5: Experimental and theoretical XANES spectra of ground state $\text{Fe}(\text{CO})_5$ (black), hot $\text{Fe}(\text{CO})_5/\text{Fe}(\text{CO})_4$ (red), hot $\text{Fe}(\text{CO})_4\text{ethOH}$ (orange), and cooled $\text{Fe}(\text{CO})_4\text{ethOH}$ (blue). The measured spectrum is shown with data points on an arbitrary scale.

ray wavelengths. The data were analyzed by subtracting streaks from the photoexcited and unexcited sample at each x-ray energy. A solution of $\text{Fe}(\text{CO})_5$ in ethanol was prepared with 200-mM concentration. The preparation was carried out in a glove bag under nitrogen atmosphere. The solution was subsequently transported to the beam line and pumped under protective gas through the sample chamber. Our interest in this chemical system stems from our previous structural studies of the equilibrium structure of $\text{Fe}(\text{CO})_5$ in various solvents.

Furthermore, bound-bound x-ray transients are not considered, which explains the absence of any pre-edge features in the calculated spectra. Peak B is caused by the alcohol's OH-group that is bound to an iron center. It therefore only exists for the product molecule. Three time-resolved x-ray absorption measurements were done on the left, the top, and the right slope of peak A. Figure 6 shows two of the time-resolved difference (laser on – laser off) streaks in the spectral ranges from 7120 to 7124 eV (left of peak A) and from 7130 to 7132 eV (right of peak A). The streak measured at the top of the peak is constant within the experiment's precision.

We interpret the instantaneous increase of the x-ray absorbance between 7120 and 7124 eV as excitation of the solutes detected with an instrument-limited resolution of about 3.4 ps. Note that a decrease of the transmitted x-ray signal indicates a shift of the x-ray absorption edge to lower x-ray energies, which is consistent with the shift of the XAFS spectra to lower energies for increasing Fe-CO bond lengths. It is known from the literature that in solution

only $\text{Fe}(\text{CO})_4$ is formed. The dissociation of additional CO ligands is suppressed by vibrational cooling of $\text{Fe}(\text{CO})_4$ and geminate recombination. A time constant of 150 fs for geminate recombination of CO after 295-nm photo dissociation of $\text{M}(\text{CO})_6$ ($\text{M} = \text{Cr}, \text{Mo}, \text{W}$) in heptane and vibrational cooling time constant of about 20 ps have been reported in the literature. Coordinating solvents, such as ethanol, are likely to exhibit a faster cooling time. We measured a 9.1-ps time constant for the absorbance recovery of $\text{Fe}(\text{CO})_4$ as the molecule continues to vibrationally cool. Inspection of Figure 5 shows that the only species that produces an absorbance increase in 7130 and 7132 eV spectral range (which corresponds to the right side of the theoretical peak A) is $\text{Fe}(\text{CO})_4\text{EtOH}$. Thus, we interpret the transmission decrease shown in the lower panel of Figure 6 as the signature of the formation of the substituted product. The product formation becomes possible as the intermediates vibrationally cool, which is the reason why the cooling and product formation times are nearly identical. Eventually, the product cools leading to a recovery of the transmission signal which can be understood by comparing the theoretical XANES spectra for the hot product (orange curve) and the cold product (blue curve) in the right side of the (theoretical) peak A.

Note that the cooling of the reaction intermediate indicated by the x-ray transmission increase on the upper panel coincides with the product formation indicated by the x-ray transmission decrease on the lower panel. The cooling and the product formation time constants are very similar and both processes occur at the same time, which suggests that the product formation rate is primarily determined by the cooling rate of the reaction intermediate $\text{Fe}(\text{CO})_4$. This suggests that the ligand substitution rate is not limited by the diffusive encounter of $\text{Fe}(\text{CO})_4$ and ethanol. Furthermore, all time constants reported here have not been de-convoluted by the temporal resolution of 3.4 ps achieved in the experiment, which was independently measured by streaking 50-fs, 266-nm laser pulses. Thus, the measured dissociation time is rather instantaneous, which is in agreement with gas phase dissociation times of less than 100 fs. If vibrational heating could be avoided during the photolysis of $\text{Fe}(\text{CO})_5$, the ligand substitution would be completed within a picosecond or less. While more XAFS data are needed to make a definitive determination of the molecular dynamics, above results supports our hypothesis of a concerted ligand substitution process.

Future plans

Using SHI we have imaged the phase transition of clathrate hydrate slurries. These slurries are host-guest systems important for selective gas trapping but also exhibit interesting melting dynamics. We produced hydrates from tetrahydrofuran (THF) mixed with water and loaded with N_2 and CO_2 gas at about 3°C. Warming the slurry to 4°C melts the hydrate and releases the gas. The resulting contrast features upon phase transition are nearly identical to the ones shown in Figure 3. We recently began measurements that induce the melting and gas release dynamics in “clean” as well as carbon nanoparticle loaded THF/water systems using our laser-pump x-ray probe system.

The UXAFS experiment will be continued. Improvements to the beamline optics, laser beam transport system, and UXAFS instrument will be made.

Papers acknowledging this DOE grant

1. "X-ray Phase Contrast Imaging: Transmission Functions Separable in Cylindrical Coordinates," G. Cao, T. Hamilton, C. M. Laperle, C. Rose-Petrucci and G. J. Diebold, *J. Appl. Phys.* 105 (10), 102002 (2009).
2. "X-ray elastography: modification of x-ray phase contrast images using ultrasonic radiation pressure," T. Hamilton, S. Gehring, J. R. Wands, C. Rose-Petrucci and G. Diebold, *J. Appl. Phys.* 105 (10), 102001 (2009).
3. "Spatial Harmonic Imaging of microstructured materials," Y. Liu, B. Ahr, J. D. Gerald and C. Rose-Petrucci, *Appl. Phys. Lett.* in preparation (2010).
4. "2-ps x-ray absorption near edge measurements of the ligand substitution dynamics of $\text{Fe}(\text{CO})_5$," B. Ahr, M. Chollet, B. Adams, M. L. Christopher and C. Rose-Petrucci, *J. Chem. Phys.* to be submitted (2010).

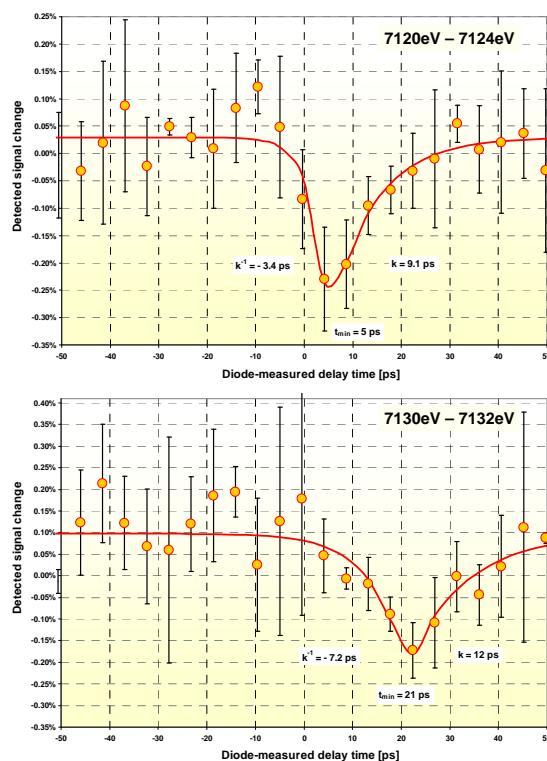


Figure 6: Difference x-ray absorption signal between 7120 and 7124 eV (upper panel) and between 7130 and 7132 eV (lower panel) of photo excited $\text{Fe}(\text{CO})_5$ in ethanol. The error bars indicate the 95% conf. intervals.

Tamar Seideman
 Department of Chemistry, Northwestern University
 2145 Sheridan Road, Evanston, IL 60208-3113
 t-seideman@northwestern.edu

New Directions in Intense-Laser Alignment

1. Program Scope

Alignment by moderately intense laser pulses developed, during the past 15 years, from a theoretical dream into an active field of research with a rapidly growing range of applications in optics, physics and spectroscopy.

The main goal of our DOE-sponsored research has been to extend the concept of nonadiabatic alignment from the domain of isolated, rigid diatomic molecules to complex systems, including large polyatomic molecules, solvated molecules, molecular assembly, and molecular junctions. This research has been essentially completed during the past year. In particular:

1. we developed and applied an optimal control approach to determine the best combination of laser fields that will induce a pre-specified field-free 3D alignment in an arbitrary polyatomic molecule,¹
2. we illustrated the possibility of controlling a surface reaction through alignment of the gas phase reactants,²
3. we extended alignment to induce sustained unidirectional torsion, hence a light-driven molecular rotor.³

These activities are detailed in Secs. 2.1–2.3. Future work on the application of the alignment concept to complex systems is discussed in Sec. 3.2.

In related research, inspired by experimental research of AMOS colleagues, we developed, during the past three years, a theoretical framework for the calculation of high harmonic generation (HHG) spectra from nonadiabatically aligned molecules.^{4–6} New results in this area are discussed in Sec. 2.4 and related planned research in collaboration with AMOS experimentalists is outlined in Sec. 3.1.

Likewise related, and equally fascinating, is the role of nonadiabatic alignment in laser filamentation. During the past year we have intensively investigated this problem, motivated in part by applications in environmental research and in part by the rapid surge of experimental activity. Our results in this area are summarized in Sec. 2.5 and several of our future plans are discussed in Sec. 3.3.

2. Recent Progress

2.1 On the Optimal Approach to Field-Free 3D Alignment of Polyatomic Molecules

As interest shifts to larger and more complex systems, it becomes essential to develop and test methods to establish field-free 3D alignment, that is, means of controlling all three rotational angles of a general polyatomic molecule. Several approaches to that end have been introduced over the past 5 years, and it has been the topic of controversy which method best achieves the goal.

We developed an optimal control approach and applied it to (a) resolve the controversy in the literature regarding the best method to induce field-free 3D alignment in polyatomic molecules; (b) determine the field parameters that would optimize a desired sense of 3D alignment in an arbitrary molecule; and (c) develop insight into the field-free 3D alignment problem in a molecule independent manner. We found that the general form of the optimal field comprises fully overlapping and essentially coincident in peak position orthogonally polarized pulses, with one pulse much longer

than the other. Interestingly, the optimal field displays little sensitivity to the molecular parameters. In addition, the optimal fields are robust, i.e., small variations in the optimal field configuration produce insignificant perturbations in the alignment observables.¹

We also showed that taking advantage of the structure of the total Hamiltonian in the symmetric top representation improves the efficiency of the TDSE solver, thus making the 3D alignment problem amenable to numerical quantum control methods. Our ability to solve the TDSE for an asymmetric top interacting with orthogonally polarized electric fields efficiently and nonperturbatively will have important implications and applications beyond the optimal control results. Finally, we introduced a new approach to visualizing 3D alignment with the advantage of being physically transparent and mathematically complete. The approach was applied to explore the mechanism through which molecules three-dimensionally align and thus rationalize the results of the optimization algorithm.

2.2 Intense Laser Alignment as a Route to Control of Surface Reactions

The development of means of producing aligned molecular layers on solid substrates may reward a variety of areas of science and technology. These include molecular electronics, controlled crystallography, structural determination of biological molecules, understanding of organic interfaces, and the development of advanced materials with preferred electric, magnetic, optical or mechanical properties. The reaction of aligned gas phase molecules with a substrate as a route to that end is of interest also from a chemical perspective. In Ref. 2, we explore the possibility of controlling the orientation of adsorbates, and their adsorption site, through alignment of a beam of gas phase molecules prior to the surface reaction. To that end we carry out classical trajectory simulations using ab-initio data for the specific example of the $I_2/Si(100)$ adsorption reaction. I_2 is found to adsorb with the molecular axis roughly parallel to the surface plane independently of the initial alignment. The orientation of the molecule in the surface plane and the adsorption site are controllable through alignment of the gas phase projectiles. Our results are explained in terms of the surface properties and the reaction dynamics, and the extent to which, and way in which, they may be generalized is discussed.²

2.3 Torsional Alignment and Unidirectional Rotation

The development of molecular machines has grown, during the past two decades, into an active and diverse subdiscipline of nanoscience. Here, the combination of laser orientation with torsional control⁷ introduces interesting opportunities. In a recent publication,³ we investigate the extent to which unidirectional intramolecular torsional motion can be created in an oriented bicyclic model system driven solely by laser light. We apply the machinery of quantum control via specifically tailored laser pulses to induce such motion, eliminating the need for the thermally constrained steps conventionally used in molecular motor systems. Our approach does not rely on specific details of the potential surfaces to create a preferred direction. Rather, we use matter-field interaction and the tools of coherent optimal control to create a wave packet with non-zero angular momentum among unbound torsional states on an excited electronic surface. Analysis of the results of the control algorithm provides general insight into when and how can optimal control theory find solutions that could not be generated through simple intuitive schemes. We find that, under constrained polarization, the control algorithm reduces to a simple intuitive coherent control strategy wherein a first IR pulse creates a non-stationary wave packet on the ground surface and a subsequent UV pulse transfers it to the excited state. Allowing for polarization shaping, however, we find new control routes that go beyond the intuitive scheme.

2.4 Origin and Implication of Ellipticity in HHG from Aligned Molecules

HHG from nonadiabatically aligned molecules has been the topic of rapidly growing experimental and theoretical interest since the 2004 illustration that harmonic signals from aligned molecules

can provide information regarding the electronic structure of the underlying molecule. This effort led to new insights regarding the interaction of molecules with intense fields, along with impressive progress of the experimental and numerical technologies to quantitatively describe these interactions. Nonetheless, several fascinating questions at the qualitative level remain open. In particular, recent experiments point to the interest in elliptically polarized harmonics for a variety of applications. The emission of elliptically polarized light from a linear molecule driven by a linearly polarized field is also a problem of significant fundamental interest, because it probes phase properties of the electronic subsystem while introducing new questions in angular momentum theory.⁴ This possibility, however, remained controversial for several years.

In Ref. 4, we derive and apply a theoretical framework to understand polarization experiments in high harmonic generation from aligned molecules. The theory explains analytically the observations published to date as well as several disparities among previous studies. It derives the conditions required for emission of elliptically polarized harmonics and points to the information content of ellipticity studies regarding the electronic scattering wavefunction. Reference 4 also develops a fully quantum mechanical numerical approach to compute the underlying electronic dynamics. Combined with the theory, this numerical method yields results in gratifying agreement with experimental data.

2.5 The Role of Nonadiabatic Alignment in Laser Filamentation

Filamentation of strong laser pulses results from a dynamic interplay between self-focusing and defocusing by the plasma produced by multiphoton/tunnel ionization of air molecules. Recent experiments provide enticing evidence for the potential of alignment to introduce a range of novel applications of laser filamentation. Thus, for instance, it was experimentally found that alignment can increase the length of the filament, modify the filament-generated supercontinuum, give rise to shock X-waves in the filament and tune their properties, and modulate inter-filament interactions.

In a recent publication⁸, we combine theoretical and experimental efforts to explore the time-dependence of the refractive index of a filament. The effects of the molecular revivals and the electronic Kerr effect on the refractive index are extracted, and applications are discussed. In a forthcoming publication we explore the interplay between rotational revivals and molecular trapping within a pump-probe study of filamentation physics in air. Numerical calculations are combined with experiments to examine the consequences of the combination of field-free alignment and molecular trapping on the filament dynamics.

3. Future Plans

In the course of the next 3 years, we will continue to focus intensively on attosecond science (Sec. 3.1), this topic being one of steadily growing interest to the AMOS program and a research field where there are opportunities for theoretical work to explore new physics. We will also continue and extend our work on the applications of alignment in complex materials (Sec. 3.2) and on opportunities for nonadiabatic alignment in the field of laser filamentation (Sec. 3.3).

3.1 High Harmonic Generation and Attosecond Science

Our short term goal in this area is to explore, in collaboration with the group of Murnane and Kapteyn, the problem of elliptical dichroism in HHG from aligned molecules. We hope to submit a joint publication within the next few months.

During the next 1–2 years, we will develop two new numerical methods for calculation of HHG signals that will extend the method of Ref. 4 in complementary ways. One approach will apply a fast spherical harmonics transform, recently developed by our group, to quantum mechanically compute harmonic signals from linear molecules in full 3D. The second will extend our formulation to nonlinear molecules in collaboration with AMOS theorists. Here we will combine 3D alignment¹ with a solution of the electronic dynamics that marries quantum, ab-initio recombination cross

sections with semiclassical propagation of the driven electron in the strong field. One of our long term goals will be to apply attosecond pulses to a condensed matter problem.

3.2 Alignment in Complex systems. Toward Applications in Material Science

Within the next 2-3 years, we will explore two new applications of intense laser alignment in material science. The first study, in collaboration with a Northwestern experimental group, will establish long-range orientational order in an assembly of semiconductor nanorods. The theoretical component will involve a molecular dynamics study using analytical polarizabilities and two-body interactions. The second study will apply torsional alignment⁷ to control transport via molecular heterojunctions. Here we will consider an array of substituted biphenyl molecules contacted to a semiconducting surface and a metal tip. We will account for the enhancement and spatial localization of the incident field by the tip using a three-dimensional finite-difference time-domain approach for the numerical solution of Maxwell's equations, and describe the current within the nonequilibrium Green Function framework.

3.3 Theory and Applications of Laser Filamentation

My immediate interest is in understanding, controlling, and hence utilizing the polarization separation and birefringence properties of filaments, which arise directly from the alignment evolution of the constituent N₂ and O₂ molecules. To that end we will compute the time-dependent refractive index via the method of Ref. 8 and employ it in solution of the nonlinear optics problem. In the long term, it would be of mathematical and technological interest to develop a self-consistent approach, wherein the alignment, the refractive index and the nonlinear pulse propagation are solved for iteratively. This work will be carried out in collaboration with Olga Kosareva (Moscow).

4. Publications from DOE sponsored research(past three years, in citation order)

1. M. Artamonov and T. Seideman, Phys. Rev. A, in press.
2. D. Shreenivas, A. Lee, N. Walter, D. Sampayo, S. Bennett and T. Seideman, J. Phys. Chem. A **114**, 5674 (2010).
3. G. Pérez-Hernández, A. Pelzer, L. Gonzalez and T. Seideman, Special Issue of New J.Phys. **12** 075007 (2010).
4. S. Ramakrishna, P. Sherratt, A. Dutoi and T. Seideman, Phys. Rev. A Rapid Communication **81**, 021802(R) (2010).
5. S. Ramakrishna and T. Seideman, Phys. Rev. A, **77**, 053411 (2008).
6. S. Ramakrishna and T. Seideman, Phys. Rev. Lett. **99** 113901 (2007).
7. S. Ramakrishna and T. Seideman, Phys. Rev. Lett. **99**, 103001 (2007).
8. C. Marceau, S. Ramakrishna, S. Génier, T.-J. Wang, Y. Chen, F. Théberge, M. Châteauneuf, J. Dubois, T. Seideman, and S. L. Chin, Optics Communications **283**, 2732 (2010).
9. S. S. Viftrup, V. Kumarappan, L. Holmegaard, H. Stapelfeldt, M. Artamonov and T. Seideman, Phys. Rev. A, **79**, 023404 (2009).
10. N. Elghobashi-Meinhardt, L. González, I. Barth, and T. Seideman, J. Chem. Phys. **130**, 024310 (2009).
11. M. G. Reuter, M. Sukharev, and T. Seideman, Phys. Rev. Lett. **101**, 208303 (2008).
12. I. Nevo, S. Kapishnikov, S. R. Cohen, K. Kjaer, T. Seideman, L. Leiserowitz, J. Chem. Phys. **140**, 144704 (2009).
13. I. Barth, L. Serrano-Andrés and T. Seideman, J. Chem. Phys. **129**, 164303 (2008).
14. A. Pelzer, S. Ramakrishna and T. Seideman, J. Chem. Phys. **129**, 134301 (2008).
15. M. Artamonov and T. Seideman, J. Chem. Phys. , **128** 154313 (2008).
16. S. S. Viftrup, V. Kumarappan, S. Trippel, H. Stapelfeldt, E. Hamilton and T. Seideman, Phys. Rev. Lett. **99**, 143602 (2007).
17. L. Holmegaard, V. Kumarappan, S. S. Viftrup, C. Z. Bisgaard, H. Stapelfeldt, E. Hamilton and T. Seideman, Phys. Rev. A **75** 051403 (2007).
18. A. Pelzer, S. Ramakrishna and T. Seideman, J. Chem. Phys. **126**, 034503 (2007).

New Scientific Opportunities through Inelastic X-ray Scattering at 3rd-and 4th-Generation Light Sources

Gerald T. Seidler, seidler@uw.edu,
Department of Physics
Box 351560
University of Washington
Seattle, WA 98195-1560

Program Scope

The goal of this program is to enable and exploit ultrafast measurement of resonant and nonresonant x-ray emission spectroscopies at both 3rd and 4th generation light sources. This especially includes studies of x-ray nonlinear and/or non equilibrium effects induced by the LCLS beam.

Recent Progress

The first year of this award has seen steady progress on the primary technology development needed for the targeted science, in addition to progress on a several secondary projects. Most importantly, our development of miniature x-ray spectrometers ('miniXS') suitable for use in time-resolved resonant and nonresonant x-ray emission spectroscopy (RXES and XES, respectively) has reached important milestones. Rather than use synchrotron beamtime solely for instrument development, each iterative step in this process has been coupled to a new scientific collaboration. Below, I'll briefly summarize the technical progress and then itemize the scientific outcomes.

Concerning technical progress, the lead achievement has been the successful embedding the optimal design algorithm for miniXS into the solidWorks 3D-CAD program, while at the same time standardizing a 'modular' design for the optic and also demonstrating 'rapid prototype machining' of the resulting optic. [1] Each of these is a major step toward the broader application of hard x-ray XES at the Advanced Photon Source and elsewhere.

These developments allow instant re-design and overnight re-fabrication of the x-ray optic for any chosen emission line from ~3 keV to ~12 keV. Collaboration with the APS Engineering Division [1] has led to a novel exploitation of this capability: appropriate files from the 3D-CAD program can be input into the APS's rapid prototype machining printer (3D plastic printer) to make the entire optic support at low cost and high convenience. See the photograph in Fig. 1. These instruments are immediately portable to other sectors (i.e., pump-probe beam lines such as ID-11) or other facilities (i.e., LCLS) for time-resolved studies. The Pilatus100k detector has sufficient time resolution to select individual bunches at the APS. We have also standardized the data processing software, including a highly user-friendly GUI so that miniXS can move into general user operations at the 20-ID microprobe endstation. This spectrometer system also plays a role in the spectroscopy portion of the CD-1 APS upgrade document.

As for scientific outcomes, RXES studies (not time-resolved) have been completed on Co- and Fe-rich catalyst systems [2, 3], on the famous metal-insulator system $V_2O_3:Cr$, [4] on lanthanide materials [5] of contemporary interest for questions about correlated electron physics, and on actinide compounds for the use of $M\beta$ RXES as a valuable

spectroscopic tool.[6] Each of these five studies is expected to yield at least one publication in the coming year, and several are anticipated to lead to follow-up studies.

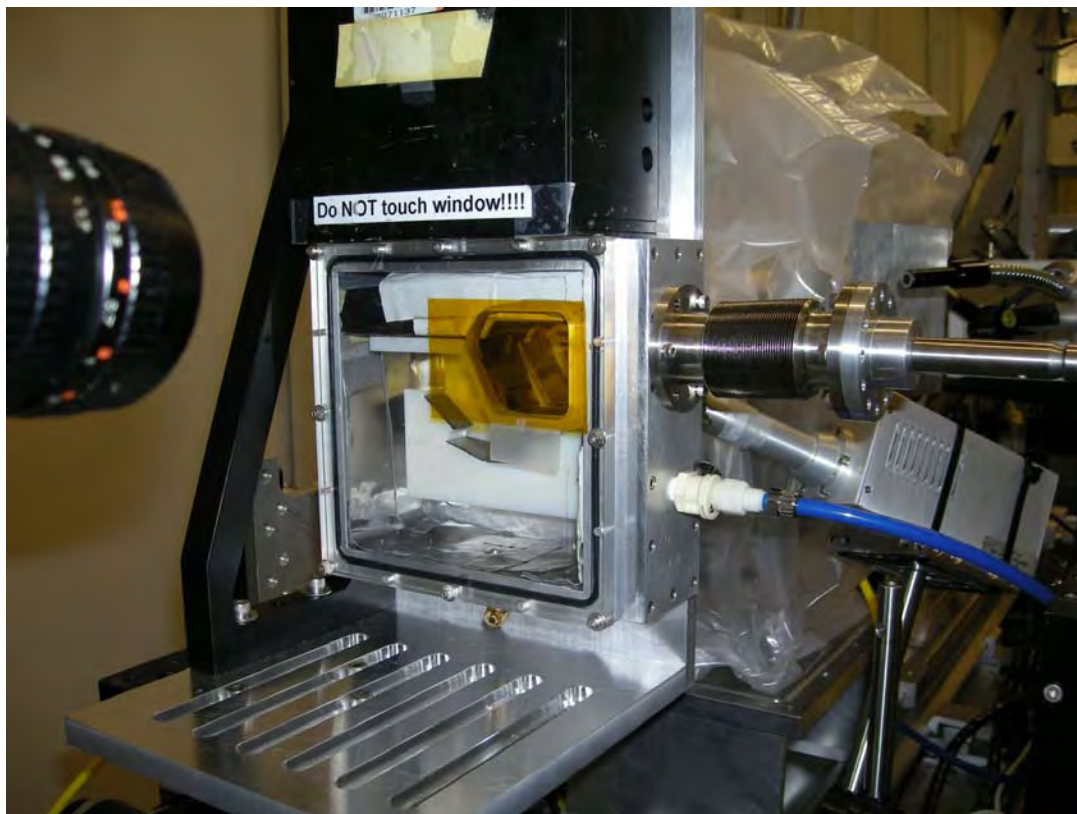


Figure 1: Photograph of the ‘modular miniXS’ during commissioning (April 2010) at the 20-ID XAS microprobe endstation of the Advanced Photon Source. For scale, the base platform (with the long slots) is ~8 inches wide. The white plastic part inside the square box is the holder for all optical components, and was constructed by rapid prototype machining in collaboration with the APS engineering division.[1] This part is exchanged for other, similar parts when changing the energy range of the spectrometer, with no other change in positioning of any spectrometer or beam line components. This instrument has the same collection efficiency as an array of 10 synchronized spherically bent crystal analyzers operating at 1-m working distance. An upgrade to triple the collection solid angle by moving to a larger camera and dispersive optics is expected to be part of the CDR-1 upgrade document for the APS.

Several secondary activities have received some support from this award through fractional PI or student time:

- A manuscript has been submitted and accepted to PRL which uses nonresonant inelastic x-ray scattering (NRIXS) to demonstrate that high energy electron scattering, when out of the dipole scattering limit, asymmetrically violated the first Born approximation even for bound-state excitations.[7] The main results from this paper are presented in figure 2. These results are closely related to ongoing work in reaction- microscope (e,2e) studies of

impact ionization, but the absence of an ionization event helps to clarify that post-collision interactions play at most a limited role in impact ionization experiments.

- A manuscript has been submitted and accepted to the Journal of the American Chemical Society; it describes the combination of soft- and hard x-ray techniques for the reliable, quantitative measurement of covalency in metal-oxides using O K-edge ligand pre-edge features.[8] This methodology opens the way to reliable, quantitative assessment of covalent bonding in actinide oxides and nitrides through ligand K-edge spectroscopy.
- Manuscripts were submitted and accepted by Applied Physics Letters [9] and by Physical Review B,[10] each addressing the nanophase SiO_x for possible photonics application. Both studies largely report the results of NRIXS studies using the LEARIX spectrometer at the Advanced Photon Source.
- A manuscript addressing the use of NRIXS to study semi-core levels in actinide materials was submitted and accepted by Physical Review B. This study lays groundwork for a new measurement of f-occupancy and ligand covalency.[11]
- A theory manuscript was submitted to Physical Review Letters; this manuscript from the Sawatsky group at UBC (with Seidler as co-author) proposes a broad re-assessment of semi-core level XAS spectra.[12] It is under consideration by the referees.
- A many-author manuscript surveying IXS capabilities at the Advanced Photon Source was submitted and accepted to Synchrotron Radiation News.[13]

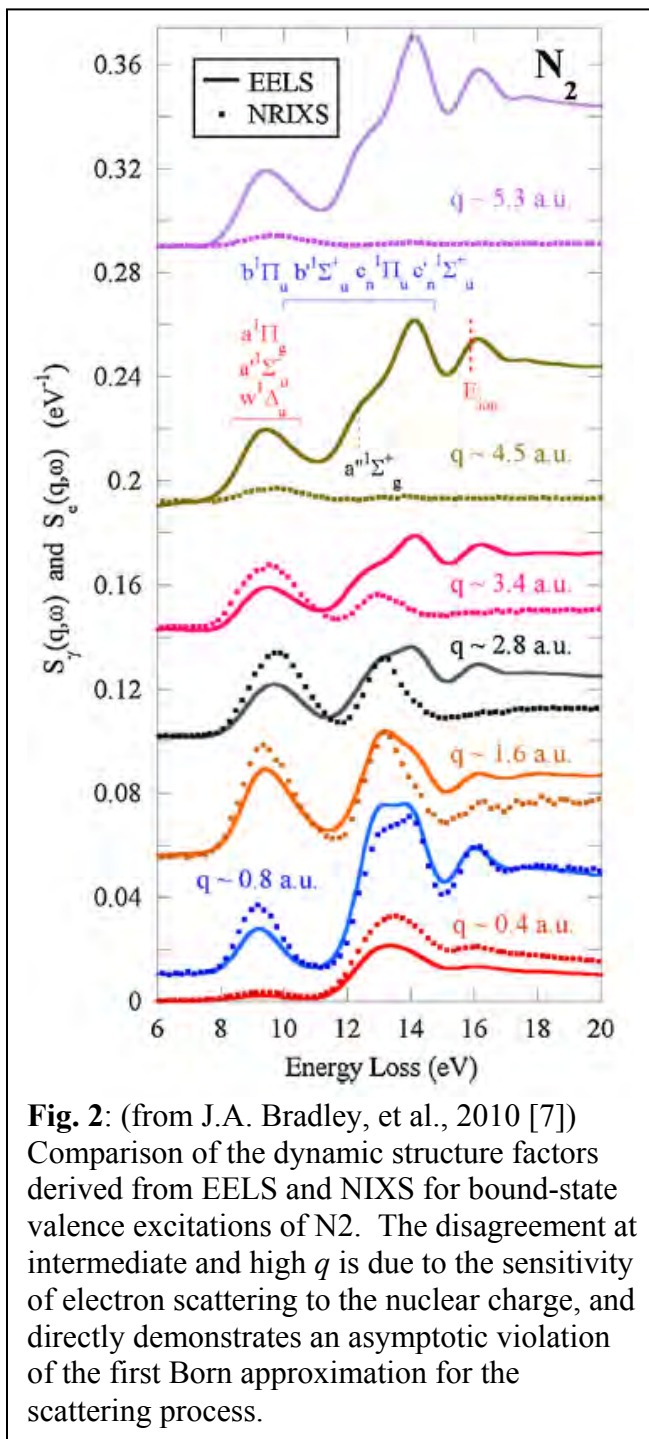


Fig. 2: (from J.A. Bradley, et al., 2010 [7]) Comparison of the dynamic structure factors derived from EELS and NIXS for bound-state valence excitations of N_2 . The disagreement at intermediate and high q is due to the sensitivity of electron scattering to the nuclear charge, and directly demonstrates an asymptotic violation of the first Born approximation for the scattering process.

Future Plans

We will continue to advance the technology and applications of the miniXS-style instruments. In addition to bringing many of the accomplishments from year 1 into publication, expected new highlights (most of which will involve one or more collaborating team) will include: implementing pump-probe XES studies of magnetic thin films and photosystem II at APS; improving stray scatter rejection and consequent ability to perform valence-level XES and so-called 'indirect RIXS' for TMO materials; implementing 2-D raster imaging of Co K β XES in commercial composite catalysts used for production of low-sulfur gasoline; *in situ* studies of TM K β XES during lithiation/delithiation cycles of electrochemical cells; constructing a cryostat-compatible miniXS instrument for Fe K β XES and investigation of possible x-ray induced spin-trapping effects in solid-state phases. In most cases, successful achievement of the above goals would be first-of-their-kind accomplishments. We will also continue to network with the many teams proposing photochemistry and plasma science projects at LCLS, with an eye toward joining strong collaborations which would benefit from the technology under development.

Comments and Bibliography

1. Quintana, J. and B. Rusthoven, Collaborators, ANL and APS.
2. Bare, S. and S. Kelly, Collaborators, UOP.
3. Myers, D. and J. Kropf, Collaborators, ANL and LANL.
4. Frenkel, A. and D. Pease, Collaborators, BNL and Univ. Mass.
5. Sham, T.K. and R.A. Gordon, Collaborators, Univ. Western Ont., and Simon Fraser Univ.
6. Clark, D.L., S.D. Conradson, and S.A. Kozimor, Collaborators, LANL.
7. Bradley, J.A., et al., *Comparative Study of the Valence Electronic Excitations of N₂ by Inelastic X-ray and Electron Scattering*. Physical Review Letters **105**, 053202 (2010)..
8. Bradley, J.A., et al., *NaReO₄, An Intensity Standard for O K-edge Covalency Studies Using XAS and NRIXS Spectroscopy*. Journal of the American Chemical Society, 2010. **accepted**.
9. Sternemann, H., et al., *Internal sub-oxide interfaces in bulk amorphous silicon mon oxide*. Applied Physics Letters, 2010. **96**: p. 081912.
10. Sakko, A., et al., *Suboxide interface in disproportionating α -SiO studied by x-ray Raman scattering*. Physical Review B **81**, 205317 (2010)..
11. Bradley, J.A., et al., *Probing Electronic Correlations in Actinide Materials Using Multipolar Transitions*. Physical Review B **81**, 193104 (2010). .
12. Sen Gupta, S., et al., *Coexistence of Bound and Virtual-bound States in Shallow-core to Valence Spectroscopies*. Physical Review Letters, 2010. **submitted**.
13. Gog, T., et al., *Momentum-resolved Resonant and Nonresonant Inelastic X-ray Scattering at the Advanced Photon Source*. Synchrotron Radiation News, 2009. **22**(6): p. 12.

DYNAMICS OF FEW-BODY ATOMIC PROCESSES

Anthony F. Starace

*The University of Nebraska
Department of Physics and Astronomy
208 Jorgensen Hall, 855 North 16th Street
Lincoln, NE 68588-0299*

Email: astarace1@unl.edu

PROGRAM SCOPE

The goals of this project are to understand and describe processes involving energy transfers from electromagnetic radiation to matter as well as the dynamics of interacting few-body, quantum systems. Investigations of current interest are in the general areas of strong field physics, attosecond physics, high energy density physics, and multiphoton and double photoionization processes. Nearly all projects under investigation involve large-scale numerical computations for the direct solution of the three-dimensional time-dependent or time-independent Schrödinger equation describing the interaction of atomic systems with electromagnetic radiation. Principal benefits and outcomes of this research are improved understanding of how to control atomic processes with electromagnetic radiation and how to transfer energy from electromagnetic radiation to matter. In some cases our studies are supportive of and/or have been stimulated by experimental work carried out by other investigators funded by the DOE AMO physics program.

RECENT PROGRESS

A. Plateau Structure in Resonant Laser-Assisted Electron-Atom Scattering

Nearly constant cross sections (as a function of the number of absorbed photons) have been predicted over a large range of scattered electron energies in laser-assisted electron-atom scattering (LAES) for both linear [N.L. Manakov et al., JETP Lett **76**, 258 (2002)] and circular [A.V. Flegel et al., Phys. Lett. A **334**, 197 (2005)] laser polarizations. Such “plateau” structures have been investigated for over two decades in other intense laser processes, e.g., above threshold ionization/detachment (ATI/ATD) and high-order harmonic generation. Interest in such plateaus centers on the possibility of transferring large amounts of energy from a laser field into either electron kinetic energy or high order harmonics without significant decreases in yields. However, for all processes the absolute values of the n -photon rates in the plateau region are orders of magnitude smaller than in the region of small n . Hence, mechanisms for increasing rates on the plateau are of great interest. For LAES, two such mechanisms exist: threshold-related phenomena at the closing of the stimulated multiphoton emission channel [4] and resonance scattering. These two mechanisms occur under different conditions: the former occur at incident

electron energies equal to multiples of the photon energy, while the latter occurs for those electron energies at which the electron is temporarily captured (following stimulated emission of μ laser photons) into a bound state of the potential $U(r)$ of the target atom and then detached by absorbing $n+\mu$ photons.

We have recently predicted significant resonant enhancements of plateau features in LAES for the case of electron scattering from neutral atoms supporting negative ions and show that the shape of the high-energy plateau in resonant LAES spectra coincides with that for ATD [6]. Since resonant phenomena disappear in a perturbative treatment of the potential $U(r)$, both the electron-atom and electron-laser interactions must be treated non-perturbatively. We thus employ time-dependent effective range (TDER) theory [4], which extends effective range theory for low-energy elastic electron scattering from a short-range potential $U(r)$ to the case of LAES. Resonance enhancements of the LAES plateau are significant for both electron scattering at fixed angle θ (relative to the incident electron momentum) and the angle-integrated electron spectrum. The magnitudes of resonance enhancements are found to significantly exceed those for threshold-related ones [4].

The remarkable similarity between plateau features in resonant LAES and ATD implies that information about ATD may be obtained from results for resonant LAES and vice versa. These results are useful for better understanding of resonant phenomena in intense laser-atom interactions, as well as for planning of experiments on laser-modified electron-atom scattering. (See reference [6] in the publication list below.)

B. Few-Cycle Attosecond Pulse Chirp Effects on Asymmetries in Ionized Electron Momentum Distributions

We have recently analyzed numerically the asymmetries of ionized electron momentum distributions produced by chirped few-cycle attosecond pulses having various fixed carrier-envelope-phases (CEPs). The central frequency of the pulse is chosen to be 25 eV, which is well above the ionization threshold, so that the contribution of excited states is negligible, the atomic structure is unimportant, and we can focus in the effects of the chirp. Our results are based on solutions of the time-dependent Schrödinger equation for the ground state of the hydrogen atom interacting with a chirped, few-cycle attosecond pulse. Our results allow one to make the following conclusions: First, for few-cycle attosecond pulses having even a small chirp, the asymmetry in the ionized electron momentum distribution can be changed significantly and is sensitive to the sign of the chirp. Second, this asymmetry is also quite sensitive to the CEP of the pulse, even for chirped pulses; the maximum asymmetry is very sensitive to both the chirp and the CEP, occurring for non-zero but small values of the chirp. Third, regarding the energy distributions along $\theta = 0$ and $\theta = \pi$ for chirped pulses, the asymmetry can vanish at particular electron energies that are very sensitive to the chirp. Finally, our results demonstrate clearly that asymmetries in the momentum distributions of electrons ionized by few-cycle, chirped attosecond pulses may provide a means for experimentalists to better characterize their pulses. (See reference [7] in the publication list below.)

C. Perturbation Theory Analysis of Attosecond Photoionization

We have recently presented a detailed analysis of ionization of an atom by a few-cycle attosecond xuv pulse using perturbation theory (PT), keeping terms in the transition amplitude up

to second order in the pulse electric field. Within the PT approach, we have presented an *ab initio* parametrization of the ionized electron angular distribution (AD) using rotational invariance and symmetry arguments. This parametrization gives analytically the dependence of the AD on the carrier envelope phase (CEP), the polarization of the pulse, and on the ionized electron momentum direction, \mathbf{p} . For the general case of an elliptically polarized pulse, we show that interference of the first- and second-order transition amplitudes causes a CEP-dependent asymmetry (with respect to $\mathbf{p} \rightarrow -\mathbf{p}$) and both elliptic and circular dichroism effects. All of these effects are maximal in the polarization plane and depend not only on the CEP but also on the phase of dynamical atomic parameters that enter our parametrization of the AD.

Within the single active electron model of an atom, for an initial *s* or *p* state we define all dynamical parameters in terms of radial matrix elements (analytic expressions for which are given for the Coulomb and zero-range potentials). For ionization of the H atom by linearly polarized pulses, our PT results are in excellent agreement with results of numerical solutions of the time-dependent Schrödinger equation of Peng *et al.* [3]. Also, our numerical results show that the asymmetries and dichroism effects at low electron energies have a *different physical origin* from those at high electron energies. Moreover, our results for Gaussian and cosine-squared pulse shapes are in good qualitative agreement. Finally, we show that our analytic formulas may prove useful for determining few-cycle extreme ultraviolet (xuv) pulse characteristics, such as the CEP and the polarization. (See reference [8] in the publication list below.)

D. Potential Barrier Features in Two-Photon Ionization Processes in Atoms

The development of novel, intense, and tunable X-ray sources opens a new regime in which nonlinear processes in the soft X-ray region can now be investigated. As was the case in single-photon ionization processes, in which many prominent features in photoionization cross sections and in photoelectron angular distributions were understood by means of a model potential approach (see, e.g., A.F. Starace, Theory of Atomic Photoionization, *Handbuch der Physik* **31**, ed. W. Mehlhorn (Springer-Verlag, Berlin, 1982), pp. 1-121), such an approach may be expected to provide similar understanding for multiphoton processes. We have obtained an extensive set of model potential results on the frequency dependence of two-photon ionization cross sections from inner subshells of rare gas and other closed-shell atoms. Our initial investigations have focused on potential barrier effects. We have used second order perturbation theory in the X-ray field and sum intermediate states using the well-known Dalgarno-Lewis method (A. Dalgarno and J.T. Lewis, *Proc. R. Soc. A* **233**, 70 (1955)). When one photon is above threshold, we employ a complex coordinate rotation method to calculate the two-photon amplitude (B. Gao and A.F. Starace, *Computers in Physics* **1**, 70 (1987)). We find that potential barrier effects occur not only in the final state of the ionized electron but also in its intermediate state(s). A manuscript on these results is currently in preparation. (See reference [9] in the publication list below.)

FUTURE PLANS

Our group is currently carrying out research on the following additional projects:

(1) We are analyzing *few-cycle XUV attosecond pulse carrier-envelope-phase effects on ionized electron momentum and energy distributions in the presence of a few-femtosecond IR laser pulse*; our nearly complete results have determined that IR laser-induced rescattering from the

atomic potential and the resulting interference between different electron ionization pathways is the origin of low-energy structures we have obtained numerically from time-dependent Schrödinger equation calculations [3].

(2) We are currently *modelling XUV attosecond pulse ionization plus excitation processes in He* using codes that enable us to solve the two-electron, time-dependent Schrödinger equation in its full dimensionality; our preliminary results show large CEP-sensitive effects.

(3) We are developing an *analytic theory for the effects of chirped, few-cycle attosecond pulses on ionized electron spectra* using perturbation theory; our preliminary results show good agreement with our numerical results obtained by solving the time-dependent Schrödinger equation [7].

PUBLICATIONS STEMMING FROM DOE-SPONSORED RESEARCH (2007 – 2010)

- [1] G. Lagmago Kamta, A.Y. Istomin, and A.F. Starace, “Thermal Entanglement of Two Interacting Qubits in a Static Magnetic Field,” *Eur. Phys. J. D* **44**, 389 (2007).
- [2] L.Y. Peng and A.F. Starace, “Attosecond Pulse Carrier-Envelope Phase Effects on Ionized Electron Momentum and Energy Distributions,” *Phys. Rev. A* **76**, 043401 (2007).
- [3] L.Y. Peng, E.A. Pronin, and A.F. Starace, “Attosecond Pulse Carrier-Envelope Phase Effects on Ionized Electron Momentum and Energy Distributions: Roles of Frequency, Intensity, and an Additional IR Pulse,” *New J. Phys.* **10**, 025030 (2008).
- [4] N.L. Manakov, A.F. Starace, A.V. Flegel, and M.V. Frolov, “Threshold Phenomena in Electron-Atom Scattering in a Laser Field,” *JETP Lett.* **87**, 92 (2008).
- [5] L.-Y. Peng, Q. Gong, and A.F. Starace, “Angularly Resolved Electron Spectra of H⁻ by Few-Cycle Laser Pulses,” *Phys. Rev. A* **77**, 065403 (2008).
- [6] A. V. Flegel, M. V. Frolov, N. L. Manakov, and Anthony F. Starace, “Plateau Structure in Resonant Laser-Assisted Electron-Atom Scattering,” *Phys. Rev. Lett.* **102**, 103201 (2009).
- [7] L.Y. Peng, F. Tan, Q. Gong, E.A. Pronin, and A.F. Starace, “Few-Cycle Attosecond Pulse Chirp Effects on Asymmetries in Ionized Electron Momentum Distributions,” *Phys. Rev. A* **80**, 013407 (2009).
- [8] E. A. Pronin, A. F. Starace, M. V. Frolov and N. L. Manakov, “Perturbation Theory Analysis of Attosecond Photoionization,” *Phys. Rev. A* **80**, 063403 (2009).
- [9] L.W. Pi and A.F. Starace, “Potential Barrier Features in Two-Photon Ionization Processes in Atoms,” *Bull. Am. Phys. Soc.* **55**(5), T1.34 (2010).

FEMTOSECOND AND ATTOSECOND LASER-PULSE ENERGY TRANSFORMATION AND CONCENTRATION IN NANOSTRUCTURED SYSTEMS

DOE Grant No. DE-FG02-01ER15213

Mark I. Stockman, PI

Department of Physics and Astronomy, Georgia State University, Atlanta, GA 30303

E-mail: mstockman@gsu.edu, URL: <http://www.phy-astr.gsu.edu/stockman>

Annual Report for the three-year Grant Period of 2008-2010 (Publications 2008-2010)

1 Program Scope

The program is aimed at theoretical investigations of a wide range of phenomena induced by ultrafast laser-light excitation of nanostructured or nanosize systems, in particular, metal/semiconductor/dielectric nanocomposites and nanoclusters. Among the primary phenomena are processes of energy transformation, generation, transfer, and localization on the nanoscale and coherent control of such phenomena.

2 Recent Progress and Publications

During the current report period, the following papers have been supported by this DOE grant. Published in 2010 are: Refs. [1-3], in 2009 are: Refs. [4-12], and in 2008: Refs. [13-25]. Most of these publications are in top-level refereed journals [1-4, 6, 8-9, 14-17, 20-23, 25]; there is also book chapters [12-13] and advance preprint publications in the ArXiv [5, 10, 18-19, 24, 26-27]. Below we highlight the recent publications that we consider the most significant.

2.1 Spaser as a Nanoscopic Generator and Ultrafast Amplifier of Nanolocalized Optical Fields [2, 11]

The Surface Plasmon Amplification by Stimulated Emission of radiation (SPASER) has been introduced by us in the DOE-supported work [28-31]. The SPASER is the “missing link” of nanoplasmonics: a quantum generator of nanolocalized optical fields. Recently, the SPASER has been experimentally observed in a series of publications [32-34].

The SPASER is now recognized as an invention protected by a US Patent [11] just issued by USPTO. We have shown recently that SPASER is ultrafast (bandwidth over 10 THz) and can work as a logical amplifier [2, 10]. Thus, it is capable of performing the same function as MOSFET within the same ~ 10 nm form factor but ~ 1000 times faster. We anticipate that the SPASER will become as ubiquitous and important an element in nanooptics as a transistor is in microelectronics.

2.2 Surface-Plasmon-Induced Drag-Effect Rectification (SPIDER) [5-6]

We have predicted a giant surface-plasmon-induced drag-effect rectification (SPIDER), a new effect that exists under conditions of the extreme nanoplasmonic confinement. In nanowires, this giant SPIDER generates rectified THz potential differences up to 10 V and extremely strong electric fields up to $\sim 10^5$ – 10^6 V/cm. The giant SPIDER is an ultrafast effect whose bandwidth for nanometric wires is ~ 20 THz. It opens up a new field of ultraintense THz nanooptics with wide potential applications in nanotechnology and nanoscience, including microelectronics, nanoplasmonics, and biomedicine.

2.3 Ultrafast Active Plasmonics [9]

Surface plasmon polaritons (SPPs), propagating bound oscillations of electrons and light at a metal surface, have great potential as information carriers for next-generation, highly integrated nanophotonic devices. A number of techniques for controlling the propagation of SPP signals have been demonstrated. However, with sub-microsecond or nanosecond response times at best, these techniques are too slow for future applications. We have reported that femtosecond optical frequency plasmon pulses can be modulated on the femtosecond timescale by direct ultrafast optical excitation of the metal, thereby offering unprecedented terahertz modulation bandwidth—a speed of many orders of magnitude faster than existing technologies. This work was done in collaboration with experimental group of Prof. N. Zheludev (University of Southampton, UK).

2.4 Nanoconcentration of Terahertz (THz) Radiation in Metal Plasmonic Waveguides [17-18]

We establish the principal limits for the nanoconcentration of the THz radiation in metal/dielectric waveguides and determine their optimum shapes required for this nanoconcentration [17-18]. We predict that the adiabatic compression of THz radiation from the initial spot size of order of vacuum wavelength (~ 10 - 100 micron) to the final size of ~ 100 - 250 nm can be achieved, while the THz radiation intensity is increased by a factor of ~ 10 to ~ 250 . This THz energy nanoconcentration will not only improve the spatial resolution and increase the signal/noise ratio for the THz imaging

and spectroscopy, but in combination with the recently developed sources of powerful THz pulses will allow the observation of nonlinear THz effects and a variety of nonlinear spectroscopies (such as two-dimensional spectroscopy), which are highly informative. This will find a wide spectrum of applications in science, engineering, biomedical research, environmental monitoring, and defense.

2.5 Efficient Nanolens in Full Electrodynamics [25, 35]

As an efficient nanolens, we have proposed a self-similar linear chain of several metal nanospheres with progressively decreasing sizes and separations [36]. The proposed system can be used for nano-optical detection, Raman characterization, nonlinear spectroscopy, nano-manipulation of single molecules or nanoparticles, and other applications. The second harmonic local fields form a very sharp nanofocus between the smallest spheres where these fields are enhanced by more than two orders of magnitude. This effect can be used for diagnostics and nanosensors. We have also obtained the first results on the Surface Enhanced Raman Scattering (SERS) in the nanosphere nanolens [35] where we show the SERS enhancement factor differs significantly from the commonly used fourth power of the local field enhancement. Recently, we have performed full electrodynamic modeling of the nanolenses [25]. We have confirmed the high predicted level of enhancement and found new electrodynamic resonances where the nanosphere aggregate works both as a plasmonic nanoantenna and as electrodynamic metal antenna.

2.6 Plasmonic Renormalization of Coulomb Interactions [23-24]

A significant field of activity has study of the effects of the proximity to plasmonic systems on Coulomb interactions in electrons in molecules and semiconductors, i.e., plasmonic resonant renormalization of the Coulomb interactions. We have developed a general theory of the plasmonic enhancement of the many-body phenomena resulting in a closed expression for the surface plasmon-dressed Coulomb interaction [23-24]. We have illustrated this theory by computing the dressed interaction explicitly for an important example of metal–dielectric nanoshells which exhibits a rich resonant behavior in magnitude and phase. This interaction is used to describe the nanoplasmonic-enhanced Förster resonant energy transfer (FRET) between nanocrystal quantum dots near a metal/dielectric nanoshell. The effects of the nanoplasmonic renormalization of the Coulomb interaction are of great importance for electron-interaction effects such as electron scattering, Auger relaxation and ionization, chemical reactions, and many-electron kinetics. Ref. [23] has been chosen by the Editors of the *New J. Phys.* for the collection *The NJP Best of 2008*.

2.7 Coherent Control on the Nanoscale [3, 20, 26]

Our research has significantly focused on problem of controlling localization of the energy of ultrafast (femtosecond) optical excitation on the nanoscale. We have proposed and theoretically developed a distinct approach to solving this fundamental problem [37-43]. This approach, based on the using the relative phase of the light pulse as a functional degree of freedom, allows one to control the spatio-temporal distribution of the excitation energy on the nanometer-femtosecond scale. One of the most fundamental problems in nanoplasmonics and nano-optics generally is the spatio-temporal coherent control of nanoscale localization of optical energy. However, a key element was missing: an efficient and robust method to determine a shape of the controlling femtosecond pulse that would compel the femtosecond evolution of the nanoscale optical fields in a plasmonic system to result in the spatio-temporal concentration of the optical energy at a given nano-site within a required femtosecond interval of time.

We have solved this problem by using the idea of the time-reversal [20, 26]. We have shown that by exciting a system at a given spot, recording the produced wave in one direction in the far zone, time reversing it and sending the produced plane wave back to the system leads to the required spatio-temporal energy localization. This method can be used both theoretically and experimentally to determine the required polarization, phase and amplitude modulation of the controlling pulses. Recently our idea of the time-reversal coherent control has been successfully tested in the microwave region experimentally [44]. Another significant development has been an ultrafast coherent control of the third-harmonic generation from a nanophotonic-plasmonic system [3]. This has been carried out in collaboration with University of Stuttgart and Max Planck Institute for Solid State Physics (Stuttgart, Germany).

2.8 Optimized Concentration of Optical Energy in Tapered Nanoplasmonic Waveguide [22]

In collaboration with D. Gramotnev (Queensland University of Technology, Brisbane, Australia), we have established the optimum shape of a tapered-rod plasmonic waveguide for the optimized nanolocalization of optical energy [22]. This, mostly computational, work allows one to eliminate the condition of adiabaticity. The maximum optical energy delivered to the tip of the structure is achieved when the rate of tapering slightly exceeds that imposed by the adiabatic condition.

2.9 Attosecond Nanoplasmonics [8, 12]

In collaboration with M. Kling, U. Kleineberg, and F. Krausz et al. from Max Planck Institute for Quantum Optics (Garching, Germany) and Ludwig Maximilian University (Munich, Germany), we have theoretically developed a novel concept called Attosecond Nanoplasmonic Field Microscope [45]. There has been a recent progress in this direction [8].

2.10 Surface Enhanced Raman Scattering (SERS) [21, 46]

We have revisited theory of one of the most important phenomena in nanoplasmonics, Surface Enhanced Raman Scattering [21, 46]. This theory shows that the predicted levels of enhancement in the red spectral region are still several orders of magnitude less than the enhancement factors $\sim 10^{13} - 10^{14}$ observed experimentally. The difference may be due to the effects not taken into account by the theory: self-similar enhancement [36] or chemical enhancement [47]. Recently, an important development of SERS has been achieved with our participation: an enhancing effect of nanolenses (see Sec. 2.8) have been observed [21]. This opens up a way to produce a reproducible, robust, and efficient substrate for SERS with very low background.

References

1. A. Rusina, M. Durach, and M. Stockman, *Theory of Spoof Plasmons in Real Metals*, Appl. Phys. A **100**, 375-1-4 (2010).
2. M. I. Stockman, *The Spaser as a Nanoscale Quantum Generator and Ultrafast Amplifier*, Journal of Optics **12**, 024004-1-13 (2010).
3. T. Utikal, M. I. Stockman, A. P. Heberle, M. Lippitz, and H. Giessen, *All-Optical Control of the Ultrafast Dynamics of a Hybrid Plasmonic System*, Phys. Rev. Lett. **104**, 113903-1-4 (2010).
4. A. Boardman, M. Brongersma, M. Stockman, and M. Wegener, *Plasmonics and Metamaterials: Introduction*, J. Opt. Soc. Am. B **26**, PM1-PM1 (2009).
5. M. Durach, A. Rusina, and M. I. Stockman, *Giant Surface Plasmon Induced Drag Effect (Spider) in Metal Nanowires*, arXiv:0907.1621, 1-5 (2009).
6. M. Durach, A. Rusina, and M. I. Stockman, *Giant Surface-Plasmon-Induced Drag Effect in Metal Nanowires*, Phys. Rev. Lett. **103**, 186801-1-4 (2009).
7. A. S. Kirakosyan, M. I. Stockman, and T. V. Shahbazyan, *Surface Plasmon Lifetimes in Metal Nanoshells*, ArXiv:0908.0647 (2009).
8. J. Q. Lin, N. Weber, A. Wirth, S. H. Chew, M. Escher, M. Merkel, M. F. Kling, M. I. Stockman, F. Krausz, and U. Kleineberg, *Time of Flight-Photoemission Electron Microscope for Ultrahigh Spatiotemporal Probing of Nanoplasmonic Optical Fields*, J. Phys.: Condens. Mat. **21**, 314005-1-7 (2009).
9. K. F. MacDonald, Z. L. Samson, M. I. Stockman, and N. I. Zheludev, *Ultrafast Active Plasmonics*, Nat. Phot. **3**, 55-58 (2009).
10. M. I. Stockman, *Spaser as Nanoscale Quantum Generator and Ultrafast Amplifier*, arXiv:0908.3559 (2009).
11. M. I. Stockman and D. J. Bergman, *Surface Plasmon Amplification by Stimulated Emission of Radiation (Spaser)*, USA Patent No. 7,569,188 (August 4, 2009).
12. M. I. Stockman, M. F. Kling, U. Kleineberg, and F. Krausz, *Attosecond Nanoplasmonic Field Microscope*, in *Ultrafast Phenomena XVI (Proceedings of the 16th International Conference, Palazzo Dei Congressi Stresa, Italy, June 9-13, 2008)*, edited by P. Corkum, S. D. Silvestri, K. A. Nelson, E. Riedle and R. W. Schoenlein (Springer, Heidelberg, London, New York, 2009), p. 696-698.
13. M. I. Stockman, *Adiabatic Concentration and Coherent Control in Nanoplasmonic Waveguides in Plasmonic Nanoguides and Circuits*, edited by S. I. Bozhevolny (World Scientific Publishing, Singapore, 2008), p. 353-404.
14. M. I. Stockman, *Attosecond Physics - an Easier Route to High Harmony*, Nature **453**, 731-733 (2008).
15. M. I. Stockman, *Spasers Explained*, Nat. Phot. **2**, 327-329 (2008).
16. M. I. Stockman, *Ultrafast Nanoplasmonics under Coherent Control*, New J. Phys. **10** 025031-1-20 (2008).
17. A. Rusina, M. Durach, K. A. Nelson, and M. I. Stockman, *Nanoconcentration of Terahertz Radiation in Plasmonic Waveguides*, Opt. Expr. **16**, 18576-18589 (2008).
18. A. Rusina, M. Durach, K. A. Nelson, and M. I. Stockman, *Nanoconcentration of Terahertz Radiation in Plasmonic Waveguides*, arXiv:0808.1324 (2008).
19. K. F. MacDonald, Z. L. Samson, M. I. Stockman, and N. I. Zheludev, *Ultrafast Active Plasmonics: Transmission and Control of Femtosecond Plasmon Signals*, arXiv:0807.2542 (2008).
20. X. Li and M. I. Stockman, *Highly Efficient Spatiotemporal Coherent Control in Nanoplasmonics on a Nanometer-Femtosecond Scale by Time Reversal*, Phys. Rev. B **77**, 195109-1-10 (2008).
21. J. Kneipp, X. Li, M. Sherwood, U. Panne, H. Kneipp, M. I. Stockman, and K. Kneipp, *Gold Nanolenses Generated by Laser Ablation-Efficient Enhancing Structure for Surface Enhanced Raman Scattering Analytics and Sensing*, Anal. Chem. **80**, 4247-4251 (2008).
22. D. K. Gramotnev, M. W. Vogel, and M. I. Stockman, *Optimized Nonadiabatic Nanofocusing of Plasmons by Tapered Metal Rods*, J. Appl. Phys. **104**, 034311-1-8 (2008).
23. M. Durach, A. Rusina, V. I. Klimov, and M. I. Stockman, *Nanoplasmonic Renormalization and Enhancement of Coulomb Interactions*, New J. Phys. **10**, 105011-1-14 (2008).
24. M. Durach, A. Rusina, V. Klimov, and M. I. Stockman, *Nanoplasmonic Renormalization and Enhancement of Coulomb Interactions*, arXiv:0802.0229 (2008).

25. J. Dai, F. Cajko, I. Tsukerman, and M. I. Stockman, *Electrodynamic Effects in Plasmonic Nanolenses*, Phys. Rev. B **77**, 115419-1-5 (2008).
26. X. Li and M. I. Stockman, *Time-Reversal Coherent Control in Nanoplasmonics*, arXiv:0705.0553 (2007).
27. M. Durach, A. Rusina, K. Nelson, and M. I. Stockman, *Toward Full Spatio-Temporal Control on the Nanoscale*, arXiv:0705.0725 (2007).
28. D. J. Bergman and M. I. Stockman, *Surface Plasmon Amplification by Stimulated Emission of Radiation: Quantum Generation of Coherent Surface Plasmons in Nanosystems*, Phys. Rev. Lett. **90**, 027402-1-4 (2003).
29. M. I. Stockman and D. J. Bergman, in Proceedings of SPIE: Complex Mediums IV: Beyond Linear Isotropic Dielectrics, edited by M. W. McCall and G. Dewar, *Surface Plasmon Amplification through Stimulated Emission of Radiation (Spaser)* (SPIE, San Diego, California, 2003), Vol. 5221, p. 93-102.
30. D. J. Bergman and M. I. Stockman, *Can We Make a Nanoscopic Laser?*, Laser Phys. **14**, 409-411 (2004).
31. K. Li, X. Li, M. I. Stockman, and D. J. Bergman, *Surface Plasmon Amplification by Stimulated Emission in Nanolenses*, Phys. Rev. B **71**, 115409-1-4 (2005).
32. M. T. Hill, M. Marell, E. S. P. Leong, B. Smalbrugge, Y. Zhu, M. Sun, P. J. van Veldhoven, E. J. Geluk, F. Karouta, Y.-S. Oei, R. Nötzel, C.-Z. Ning, and M. K. Smit, *Lasing in Metal-Insulator-Metal Sub-Wavelength Plasmonic Waveguides*, Opt. Express **17**, 11107-11112 (2009).
33. R. F. Oulton, V. J. Sorger, T. Zentgraf, R.-M. Ma, C. Gladden, L. Dai, G. Bartal, and X. Zhang, *Plasmon Lasers at Deep Subwavelength Scale*, Nature **461**, 629-632 (2009).
34. M. A. Noginov, G. Zhu, A. M. Belgrave, R. Bakker, V. M. Shalaev, E. E. Narimanov, S. Stout, E. Herz, T. Suteewong, and U. Wiesner, *Demonstration of a Spaser-Based Nanolaser*, Nature **460**, 1110-1112 (2009).
35. K. Li, M. I. Stockman, and D. J. Bergman, *Li, Stockman, and Bergman Reply to Comment On "Self-Similar Chain of Metal Nanospheres as an Efficient Nanolens"*, Phys. Rev. Lett. **97**, 079702 (2006).
36. K. Li, M. I. Stockman, and D. J. Bergman, *Self-Similar Chain of Metal Nanospheres as an Efficient Nanolens*, Phys. Rev. Lett. **91**, 227402-1-4 (2003).
37. M. I. Stockman, S. V. Faleev, and D. J. Bergman, *Coherent Control of Femtosecond Energy Localization in Nanosystems*, Phys. Rev. Lett. **88**, 67402-1-4 (2002).
38. M. I. Stockman, S. V. Faleev, and D. J. Bergman, *Coherently Controlled Femtosecond Energy Localization on Nanoscale*, Appl. Phys. B **74**, S63-S67 (2002).
39. M. I. Stockman, S. V. Faleev, and D. J. Bergman, *Coherently-Controlled Femtosecond Energy Localization on Nanoscale*, Appl. Phys. B **74**, 63-67 (2002).
40. M. I. Stockman, D. J. Bergman, and T. Kobayashi, in Proceedings of SPIE: Plasmonics: Metallic Nanostructures and Their Optical Properties, edited by N. J. Halas, *Coherent Control of Ultrafast Nanoscale Localization of Optical Excitation Energy* (SPIE, San Diego, California, 2003), Vol. 5221, p. 182-196.
41. M. I. Stockman, S. V. Faleev, and D. J. Bergman, in Ultrafast Phenomena XIII, *Coherently-Controlled Femtosecond Energy Localization on Nanoscale* (Springer, Berlin, Heidelberg, New York, 2003).
42. M. I. Stockman, D. J. Bergman, and T. Kobayashi, *Coherent Control of Nanoscale Localization of Ultrafast Optical Excitation in Nanosystems*, Phys. Rev. B **69**, 054202-10 (2004).
43. M. I. Stockman and P. Hewageegana, *Nanocalibrated Nonlinear Electron Photoemission under Coherent Control*, Nano Lett. **5**, 2325-2329 (2005).
44. F. Lemoult, G. Lerosey, J. de Rosny, and M. Fink, *Resonant Metalenses for Breaking the Diffraction Barrier*, Phys. Rev. Lett. **104**, 203901-1-4 (2010).
45. M. I. Stockman, M. F. Kling, U. Kleineberg, and F. Krausz, *Attosecond Nanoplasmonic Field Microscope*, Nat. Phot. **1**, 539-544 (2007).
46. M. I. Stockman, in Springer Series Topics in Applied Physics, edited by K. Kneipp, M. Moskovits and H. Kneipp, *Surface Enhanced Raman Scattering – Physics and Applications* (Springer-Verlag, Heidelberg New York Tokyo, 2006), p. 47-66.
47. J. Jiang, K. Bosnick, M. Maillard, and L. Brus, *Single Molecule Raman Spectroscopy at the Junctions of Large Ag Nanocrystals*, J. Phys. Chem. B **107**, 9964-9972 (2003).

Laser-Produced Coherent X-Ray Sources

Donald Umstadter, Physics and Astronomy Department, B58 Behlen Laboratory, University of Nebraska, Lincoln, NE 68588-0111, dpu@unlserve.unl.edu

Program Scope

In this project, we experimentally and theoretically explore the physics of novel x-ray sources, based on the interactions of ultra-high-intensity laser light with matter. Laser-accelerated electron beams are used to produce x-rays in the energy range 1-100 keV using techniques such as Thomson scattering off a second laser pulse, or betatron oscillations in a laser-produced ion channel. Such photon sources can provide information on the structure of matter with atomic-scale resolution, on both the spatial and temporal scale lengths—simultaneously. Moreover, because the electron beam is accelerated by the ultra-high gradient of a laser-driven wakefield, the combined length of both the accelerator and wiggler regions is only a few millimeters. The x-ray source design parameters are sub-angstrom wavelength, femtosecond pulse duration, and university-laboratory-scale footprint. The required components, laser system (delivering peak power >100 TW at a repetition rate of 10 Hz) and electron accelerator (delivering beams with energy up to 800 MeV and divergence of 2 mrad) have been developed and characterized.

This project involves the physics at the forefront of relativistic plasma physics and beams, as well as relativistic nonlinear optics. Applications include the study of ultrafast chemical, biological and physical processes, such as inner-shell electronic or phase transitions. Industrial applications include non-destructive evaluation, large-standoff-distance imaging of cracks, remote sensing and the detection of shielded nuclear materials.

Recent Results

Radiographic Imaging of Embedded Voids

High-intensity, short pulse lasers have been shown to produce bright, monoenergetic electron beams by the process of laser wakefield acceleration. We generate such electron beams (with energy >100 MeV) by the interaction of 50-TW, 30-fs laser pulses with a supersonic helium jet. These laser-driven electron beams have high energy, low divergence, and small source size, making them ideal for high-resolution and long-standoff radiographic studies of cracks or voids that are embedded in dense materials.ⁱ A highlight of our research over the past year was the demonstration of radiographic imaging with sub-millimeter resolution.

Pulses from the University of Nebraska, Lincoln, Diocles Ti:sapphire laser system were focused to an intensity of 1.7×10^{19} W/cm² [corresponding to a normalized laser vector potential ($a_0=eA/mc^2$) of 2.8] in order to drive a relativistic plasma wave. The quasi-mono-energetic electron beams that are routinely obtained are tunable over an energy range of 50-400 MeV, depending on the choice of acceleration distance (i.e., the nozzle diameter), plasma density, and laser intensity. For the purpose of radiography, 1.3 J of laser energy was focused over a 3 mm diameter gas jet, of the Laval type, with initial plasma density of 1×10^{19} cm⁻³. Radiographic images were obtained by interposing various objects between the electron beam source and a phosphor plate.

2.5-cm long voids were embedded within a 5-cm thick stainless steel block, and placed 2-m from the supersonic jet. Three side-by-side voids were imaged, each of different width: 250- μ m, 500- μ m, and 750- μ m. Ten electron beam shots, each with electron energy 150 ± 20 MeV and an angular divergence of

4.7 ± 0.5 mrad, were used to acquire the radiograph shown in Figure 1, which is recorded by an image plate placed behind the steel block.

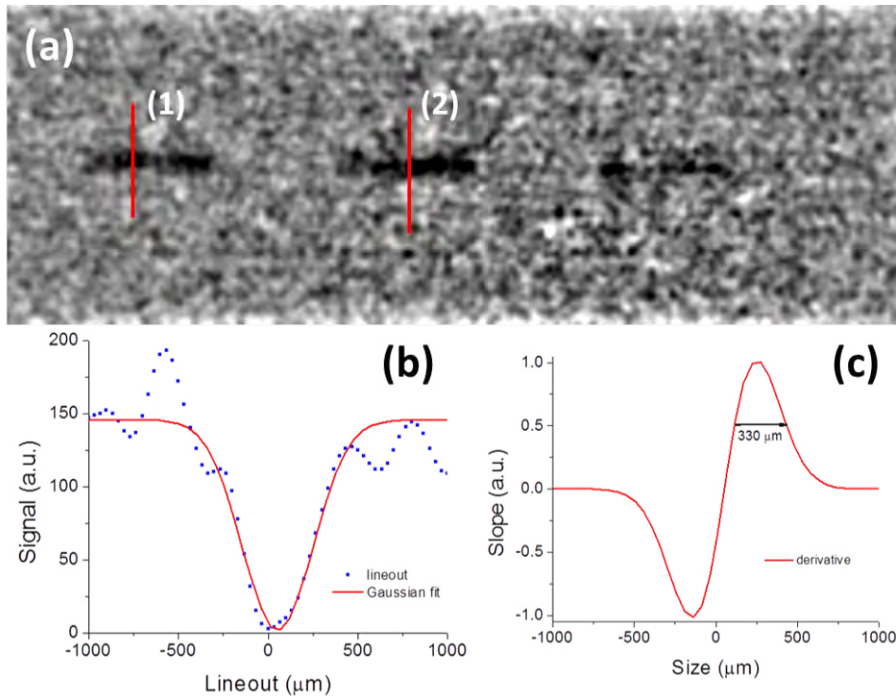


Figure 1: Electron radiographic images of voids embedded in steel (from left to right: 750- μm , 500- μm , and 250- μm). (a) Fourier enhanced image (red line indicates lineout location). (b) Lineout of crack (circles) and Gaussian fit (line). (c) Derivative of fitted profile indicates a source size of 330 μm .

Figure 1(a) is the Fourier-filtered image of the embedded voids. Figure 1(b) show a lineout of the imaged 750- μm gap (left-most gap in Figure 1(a)), as well as a Gaussian fit to the data. To compute the maximum spatial resolution obtainable by this method, the derivative of the lineout across the 750- μm gap was computed, shown in Figure 1(c) The full width at half maximum (FWHM) of the derivative of the Gaussian fit yields a resolution of 330 μm . To the best of our knowledge, this is the highest resolution ever achieved for a radiographic image of an embedded void.

The signal-to-noise level can be improved by means of magnetic filtering of secondary electrons, or by increasing the number of shots used to obtain images. For instance, the number of shots used to acquire an image can be increased by two orders of magnitude, to 1,000, by means of an image acquisition time of just two minutes—at the 10-Hz repetition rate of our laser accelerator. This should correspond to a 33x improvement in the signal-to-noise level over that shown in Figure 1(a).

This research addresses a pressing need for reliable nondestructive techniques to identify the presence of defects in dense structures, ranging from turbine blades to nuclear reactor vessels. The sub-millimeter resolution demonstrated here should allow DOE to better understand the process by which microstructures grow as critical materials age.

Upgrade of Laser System to the Petawatt Peak Power Level

The peak power of the Diocles laser system is being upgraded by an order of magnitude, to the petawatt (PW) level. An additional Ti:sapphire amplifier was added to the system—pumped by four Nd:Glass lasers, each producing 25 J of power—in order to amplify the 800-nm pulses to an energy of 50 J per

pulse. The amplified pulse is compressed to 30 fs with output energy of 30 J in a new compressor chamber. The system is capable of operating at 0.1-Hz repetition rate. A schematic diagram of the upgraded system is shown in Figure 2. A photograph of the installed high-energy pump lasers and vacuum compressor chamber is shown in Figure 3.

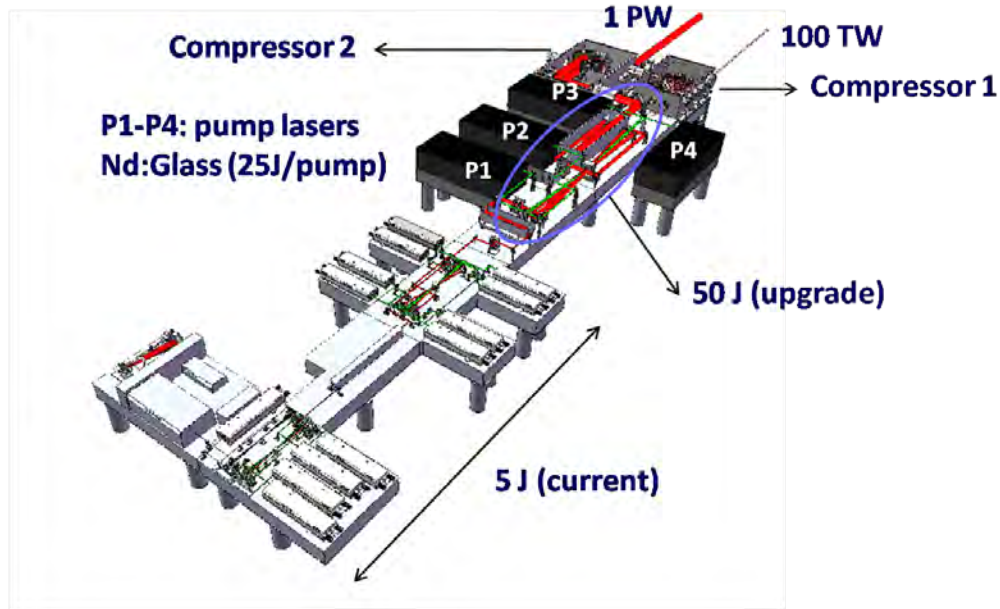


Figure 2: Schematic of the upgraded UNL laser system, capable of operating at the petawatt peak power level. The four new pump lasers (P1-P4) are shown in black. The new Ti:sapphire amplifier stage (with 115-mm diameter aperture) is circled in blue. The new vacuum compressor chamber (Compressor 2) is shown in the background, left.



Figure 3: Photograph of three of the four newly installed high-energy pump lasers (P2-P4) (foreground), and vacuum compressor chambers (Compressors 1-2) (background).

Future Plans: Petawatt Physics

At the focus of the upgraded laser, light can reach the highest intensities ever achieved in the laboratory, up to 10^{23} W/cm². At this intensity level, matter can thus be exposed to extreme field strengths: 870 TV/m. This is sufficient to ionize gallium to the hydrogen-like stage by means of over the barrier field ionization.ⁱⁱ In this ultra-high intensity regime, an electron can gain energy in the electromagnetic field—in the form of quiver energy—up to 217 times its rest mass energy. At such intensities, it is expected that not only will the electrons of ionized media relativistically quiver in the laser fields, but protons will also begin to quiver significantly. The propagation of light at these high intensities has never been studied experimentally.

Besides continuing our research on the development of ultrashort x-ray and electron probes, we also intend to study the novel high-field physics that is accessible in the highly relativistic regime enabled by this improved laser capability.

DOE-Sponsored Publications (published within last three years)

1. D. Umstadter, S. Banerjee, V. Ramanathan, N. Powers, N. Cunningham, and N. Chandler-Smith, "Development of a Source of Quasi-Monochromatic MeV Energy Photons," CP1099, *Application of Accelerators in Research and Industry: 20th International Conference*, edited by F. D. McDaniel and B. L. Doyle (AIP, 2009), p. 606.
2. S. M. Sepke and D. P. Umstadter, "Analytical solutions for the electromagnetic fields of flattened and annular Gaussian laser modes. I. Small F-number laser focusing," *JOSA B* **23**, 2157-2165 (2007).
3. D. Umstadter, S.Y. Chen, A. Maksimchuk, K. Flippo, V.Y. Bychenkov, Y. Sentoku, and K. Mima, "Short pulses of energetic electrons and ions produced by high-intensity lasers for laser fusion," *Current Trends in International Fusion Research: Proceedings NRC Research Press*, National Research Council of Canada, Ottawa, ON K1A 0R6, Canada (2007), p. 389.

ⁱ V. Ramanathan, S. Banerjee, N. Powers, N. Cunningham, N. A. Chandler-Smith, K. Zhao, K. Brown, and D. Umstadter, "Sub-millimeter-resolution radiography of shielded structures with laser-accelerated electron beams," *PRSTAB*, submitted (2010).

ⁱⁱ M. Protopapas, C. H. Keitel, et al., "Atomic physics with super-high intensity lasers," *Reports on Progress in Physics* **60**, 389-486 (1997).

Combining High Level *Ab Initio* Calculations with Laser Control of Molecular Dynamics

Thomas Weinacht
Department of Physics and Astronomy
Stony Brook University
Stony Brook, NY
tweinacht@sunysb.edu

and

Spiridoula Matsika
Department of Chemistry
Temple University
Philadelphia, PA
smatsika@temple.edu

1 Program Scope

We use intense, shaped, ultrafast laser pulses to control molecular dynamics and high level *ab initio* calculations to interpret and guide the control. We are applying the techniques and understanding we have developed to dissociative ionization pump-probe spectroscopy and pulse shape spectroscopy.

2 Recent Progress

There are a few key findings from our recent work. One of the most important points is that in probing molecular relaxation on an excited neutral surface via strong field dissociative ionization, different molecular fragments carry information about different relaxation channels. The link between fragments and relaxation channels comes from a combination of electronic structure calculations and organic chemistry fragmentation analysis. The basic idea is that different molecular geometries lead to the production of different molecular fragments when the molecule is exposed to an intense infrared laser pulse. This is driven by both changes in the ionic spectrum of the molecule accompanying changes in geometry as well as changes to the electronic/molecular orbitals in the excited neutral state of the molecule where the dynamics are taking place. Another important point is that the molecular relaxation dynamics are sensitive to pulse shape. This sensitivity to pulse shape is promising for both open and closed loop control experiments, and also closely related to a third important finding, which is that shaped laser pulses in the deep UV can be used to perform multidimensional spectroscopy (such as 2D Fourier transform spectroscopy).

In our pump-probe experiments, we studied two systems whose excited state dynamics are governed by conical intersections (CIs). These systems represent two general cases. In cyclohexadiene (CHD), the dynamics and decay to the ground state is governed by a single conical intersection causing a branching into different channels, while in cytosine the wave packet can branch into two different conical intersections which lead to radiationless decay to a single channel in the ground state.

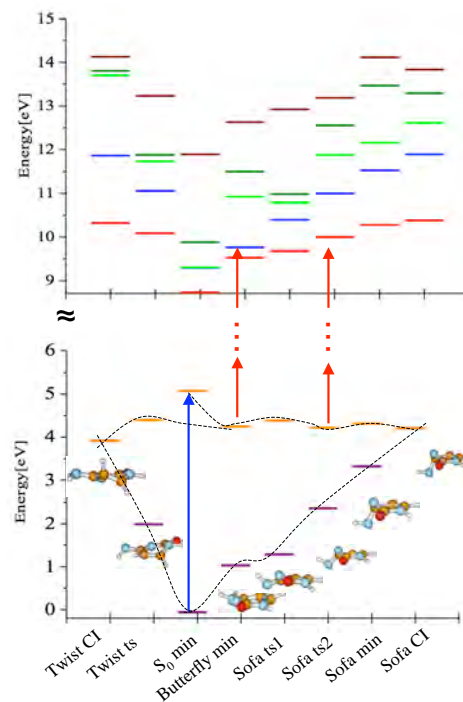


Figure 1: Bottom panel: PES in cytosine showing the two radiationless relaxation pathways after UV absorption. Top panel: Energy level diagram of the ionic states of cytosine that can be accessed after the IR probe.

Calculations identify more than one CI through which cytosine can relax after absorption of UV light from the S1 state of the neutral to S_0^{1-7} . One of them involves a twisting of the C-C double bond, similar to the conical intersection found in ethylene, and it is called the 'twist' CI⁶. The second pathway (or collection of pathways) involves an $n_N\pi^*/S_0$ CI which has been called the 'sofa' CI because the molecular conformation resembles a sofa, with one nitrogen being displaced from the plane.

Figure 1 shows the important points along the S1 potential energy surface (PES) associated with the relaxation. Initial absorption leads to the FC region which is about 0.8 eV above the S1 minimum, here dubbed the 'butterfly' minimum. This minimum is separated from each of the CIs by at least one barrier. There is only one barrier separating the minimum from the twist CI but there are two barriers towards the sofa CI, with the other minimum close to the sofa CI labeled as the sofa minimum. The energies and barriers associated with both twist and sofa CIs are similar and it is not easy to determine their relative importance in the radiationless decay based on energetics alone. We found that we were able to distinguish the dynamics along the S1 pathways by analyzing the observed fragmentation after the intense IR probe pulse.

The fragmentation of the molecule depends on the location of the wave packet on the S1 surface at the time when the probe pulse arrives. Considering vertical ionization (i.e. Condon approximation), we examined the properties of the low lying electronic states of the cation at geometries of interest on S1 - e.g. the minima associated with the barriers to the CIs. Figure 1 shows the ionic states in addition to the neutral ones along the S1 PES. Different fragments can be associated with locations on routes toward the different CIs. Using a combination of *ab initio* electronic structure calculations and fragmentation analysis, we identified fragments that label the geometry of the minima leading to twist and sofa CIs and used the measured dynamics of these fragments as a function of pump probe delay in order to map out the relaxation of excited cytosine through two separate CIs to the ground state.

The fragments that we have identified which label a pathway through a given minimum and not the other are the parent ion and fragment 95. The former is associated with the butterfly minimum leading to the twist CI, and the latter with the sofa minimum leading to the sofa CI. While there are two barriers and two minima along a minimum energy path between the FC region and the sofa CI, our measurements indicate that there is only one barrier which plays an important role in the relaxation of the molecule via the sofa CI since the 95 yield peaks very shortly after zero time delay, indicating that the wave packet reaches the sofa minimum rapidly without getting stuck in the butterfly minimum.

Figure 2 shows the UV-pump, near IR-probe data and fits for the parent ion and the 95 amu fragment. The data shows a sharp rise near timezero followed by a decay with increasing positive time delay. As is evident from the graph, the fits are in excellent agreement with the data. For generality, we fit the time dependent yield of each peak in the TOFMS to a sum of three exponentials multiplied by a step function and convolved with a gaussian to account for the finite pulse durations. Most peaks in the TOFMS could be modeled by a biexponential decay with a fast (< 300 fs) and slow (> 2 ps) decay.

For positive time delays, resonant excitation from S_0 to S1 via the pump pulse is followed by multi-photon ionization from S1 if the probe pulse arrives before the molecule has relaxed. For long positive time delays, the molecule is back in the ground state, from which it is much more difficult to ionize the molecule, since S_0 is much lower in energy than S1 and multi-photon ionization is quite sensitive to the ionization potential. For negative time delays, the ion yields are much smaller than for positive delays because the probe pulse finds the molecules in the ground state and is much less effective in ionizing them.

We interpret the fast exponential decay in terms of motion of the wave packet away from the FC region, in conjunction with the rapidly rising IP away from the FC region as shown in figure 2. The short exponential decay times are 150 fs and 50 fs for 95 and the parent ion respectively. We interpret the long time component of the decay in terms of the time it takes for the wave packet to get over the sofa and twist barriers for the wave packets leading to the 95 and parent ions respectively. The time constants for these from the fits are 4.1 ps and 2.4 ps for 95 and the parent ion respectively.

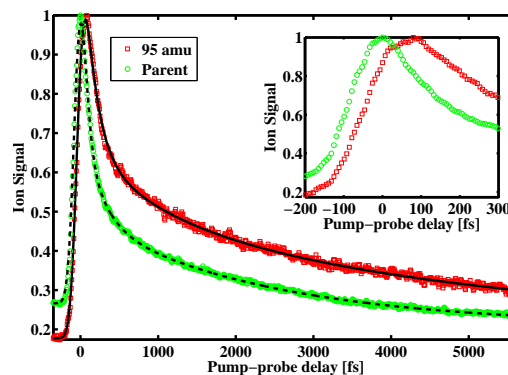


Figure 2: Pump-probe data and fits for the parent ion and the 95 amu fragment. The parent data is shown in green circles, while the 95 amu data is in red squares.

The other fragments in the TOFMS show a range of decay times, with the longer of the two timescales typically falling between 2 and 5 ps. Most fragments which can loosely be associated with the sofa CI (because of the stretching of bonds at the sofa min which must be broken for the appearance of these fragments) have long decay times between 3 and 5 ps, consistent with the 95 fragment. Similarly, most fragments which can be loosely associated with the twist CI have timescales between 2 and 3 ps. We interpret the range of decay times in terms of strong delocalization of the wave packet and varying fragment production at different geometries.

Figure 3 illustrates the relaxation dynamics of cytosine uncovered through our combination of theory and experiment. The molecule is excited at about 261 nm, from the S_0 minimum, onto the FC point on S_1 , where it begins to evolve towards nearby local minima on S_1 . The wave packet becomes delocalized and explores many pathways on the S_1 surface. Its de-excitation back to the ground state proceeds through two CIs that are traversed in parallel.

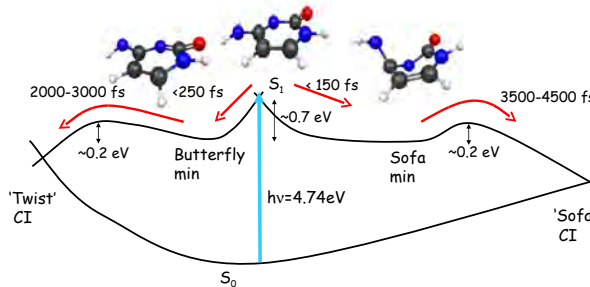


Figure 3: Cartoon of S_0 and S_1 PES showing important points and timescales extracted from experimental fittings.

Building upon our establishment of ultrafast pulse shaping in the deep UV, we have developed an apparatus for 2D Fourier transform spectroscopy in the deep UV using shaped laser pulses. One of the main difficulties limiting the development of 2D spectroscopy in the UV has been the difficulty of generating phase stable pulses at such short wavelengths. The use of a pulse shaper to generate pump pulse pairs allows for generating the pulse pair collinearly with both pulses sharing all optical components. This allows us to achieve a phase stability between pump pulses which is better than 0.017 Rad, corresponding to less than 2 attoseconds jitter in time delay between pulses! It also allows for control over the relative phase of the pulses independent of the time delay between pulses.

This can be used for rapid phase cycling and we are currently working on further developing our ability to shape the pump pulses for selectivity of features in the 2D spectrum.

3 Future Plans

Our plans for the near future consist of three interrelated thrusts with the common aim of probing and controlling molecular dynamics through CIs:

1. Extending our strong field dissociative ionization pump-probe measurements to other DNA/RNA bases. We have already performed calculations for adenine and uracil, which promise to show interesting differences from cytosine given the electronic structure of both the neutral and ions.
2. Extending our 2D Fourier transform spectroscopy measurements to other DNA/RNA bases and comparing these measurements in a condensed phase environment with our gas phase measurements. We are also interested in developing pulse shape spectroscopy based on the 2D Fourier transform spectroscopy work. The idea here is to develop pulse sequences which can select particular features or dynamics we are interested in studying.
3. Extending multiparameter, closed loop learning control to molecular relaxation through competing pathways and conical intersections. We have developed tools for discriminating between different relaxation pathways and there are multiple indications that the relaxation dynamics are sensitive to the initial wave packet launched on the excited state surface.

References

- [1] N. Ismail, L. Blancafort, M. Olivucci, B. Kohler, and M. A. Robb, *J. Am. Chem. Soc.* **124**, 6818 (2002).
- [2] M. Merchán and L. Serrano-Andrés, *J. Am. Chem. Soc.* **125**, 8108 (2003).
- [3] K. Tomić, T. Jörg, and C. M. Marian, *J. Phys. Chem. A* **109**, 8410 (2005).
- [4] M. Z. Zgierski, S. Patchkovskii, and E. C. Lim, *J. Chem. Phys.* **123**, 081101 (2005).
- [5] L. Blancafort, *Photochem. Photobiol.* **83**, 603 (2007).
- [6] K. A. Kistler and S. Matsika, *J. Phys. Chem. A* **111**, 2650 (2007).
- [7] H. R. Hudock and T. J. Martinez, *Chem.Phys.Chem.* **9**, 2486 (2008).

4 Publications of DOE Sponsored Research

- “Interpreting Ultrafast Molecular Fragmentation Dynamics with *ab initio* Calculations”, C. Trallero, B. J. Pearson, T. Weinacht, K. Gilliard and S. Matsika, *J. Chem. Phys.*, **128**, 124107, (2008)
- “Closed-Loop Learning Control of Isomerization using Shaped Ultrafast Laser Pulses in the Deep Ultraviolet”, M. Kotur, T. Weinacht, B. J. Pearson and S. Matsika *J. Chem. Phys.*, **130**, 134311, (2009)
- ”Two Dimensional Ultrafast Fourier Transform Spectroscopy in the Deep Ultraviolet C. Tseng, S. Matsika and T. C. Weinacht, *Optics Express* **17**, 18788 (2009)
- ”Distinguishing Between Relaxation Pathways by Combining Dissociative Ionization Pump Probe Spectroscopy and *ab initio* Calculations: A Case Study of Cytosine” M. Kotur, T. C. Weinacht, C. Zhou, K. Kistler and S. Matsika. *submitted to J. Am. Chem. Soc.*

Cold and ultracold polar molecules

Jun Ye

JILA, National Institute of Standards and Technology and University of Colorado

Boulder, Colorado 80309-0440

Ye@jila.colorado.edu

We have made a number of important advances in the study and control of cold and ultracold polar molecules over the last 12 months. In collaboration with D. Jin, we have prepared a rovibronic ground-state molecular quantum gas in a single hyperfine state and, in particular, the absolute lowest quantum state. This addresses the last internal degree of freedom remaining after the recent production of a near quantum degenerate gas of molecules in their rovibronic ground state, and provides a crucial step towards full control over molecular quantum gases. We have demonstrated a scheme that is general for bialkali polar molecules. It relies on electric-dipole, two-photon microwave transitions through rotationally excited states and makes use of electric nuclear quadrupole interactions to transfer molecular population between different hyperfine states.

We have also explored for the first time chemical reactions at ultralow temperatures. Simple quantum mechanical rules such as quantum statistics, single partial-wave scattering, and quantum threshold laws are found to provide a clear understanding of the molecular reactivity under a vanishing collision energy. Starting with an optically trapped near-quantum-degenerate gas of polar $^{40}\text{K}^{87}\text{Rb}$ molecules prepared in their absolute ground state, we have recovered experimental evidence for exothermic atom-exchange chemical reactions. When these fermionic molecules were prepared in a single quantum state at a temperature of a few hundred nanokelvin, we observed p-wave-dominated quantum threshold collisions arising from tunneling through an angular momentum barrier followed by a short-range chemical reaction with a probability near unity. When these molecules were prepared in two different internal states, the reaction rates were enhanced by a factor of 100 as a result of s-wave scattering, which does not have a centrifugal barrier.

In the next study, we have made experimental observations of dipolar collisions in the quantum regime. For modest values of an applied electric field, we observe a pronounced increase in the loss rate of fermionic molecules. We find that the loss rate has a steep power-law dependence on the induced electric dipole moment, and we show that this dependence can be understood in a relatively simple model based on quantum threshold laws for the scattering of fermionic polar molecules. In addition, we directly observe the spatial anisotropy of the dipolar interaction through measurements of the thermodynamics of the dipolar gas. These results demonstrate how the long-range dipolar

interaction can be used for electric-field control of chemical reaction rates in an ultracold gas of polar molecules.

To develop a robust tool to monitor the molecular gas dynamics, we have implemented a scheme for direct absorption imaging of an ultracold polar molecular gas near quantum degeneracy. Imaging molecules without closed optical cycling transitions is challenging. Our technique relies on photon-shot-noise-limited absorption imaging on a strong but open bound-bound molecular transition. We have made a systematic characterization of this imaging technique. Using this technique combined with time-of-flight expansion, we demonstrate the capability to determine momentum and spatial distributions for the molecular gas and also to image molecules in arbitrary external fields.

In the work on cold molecules, in collaboration with J. Doyle we have performed the first experimental study of cold collisions between two different species of neutral polar molecules. Combining for the first time the techniques of Stark deceleration, magnetic trapping, and cryogenic buffer gas cooling, we measure total trap loss cross sections between OH and ND₃ at a mean collision energy of 3.6 cm⁻¹ (5 K). The total cross section increases upon application of an external polarizing electric field. Cross sections computed from ab initio potential energy surfaces are in excellent agreement with the measured value at zero external electric field. The theory represents the first such analysis of a colliding ²Π and closed-shell polyatomic molecule. At sufficiently low collision energies we have thus reached beyond molecular orientation and steric effects and can now use electric fields to control intermolecular dynamics via long-range dipolar interactions. We can start to explore an intermediate regime between gas kinetics and quantum scattering.

Recent publications:

- [1] S. Ospelkaus, K.-K. Ni, G. Quéméner, B. Neyenhuis, D. Wang, M. H. G. de Miranda, J. L. Bohn, J. Ye, and D. S. Jin, "Controlling the hyperfine state of rovibronic ground-state polar molecules," *Phys. Rev. Lett.* **104**, 030402 (2010).
- [2] S. Ospelkaus, K.-K. Ni, D. Wang, M. H. G. de Miranda, B. Neyenhuis, G. Quéméner, P. S. Julienne, J. L. Bohn, D. S. Jin, and J. Ye, "Quantum-state controlled chemical reactions of ultracold KRb molecules," *Science* **327**, 853 – 857 (2010).
- [3] K.-K. Ni, S. Ospelkaus, D. Wang, G. Quéméner, B. Neyenhuis, M. H. G. de Miranda, J. L. Bohn, J. Ye, and D. S. Jin, "Dipolar collisions of polar molecules in the quantum regime," *Nature* **464**, 1324 – 1328 (2010).
- [4] D. Wang, B. Neyenhuis, M. H. G. de Miranda, K.-K. Ni, S. Ospelkaus, D. S. Jin, and J. Ye, "Direct absorption imaging of ultracold polar molecules," *Phys. Rev. A* **81**, 061404(R) (2010).
- [5] B. C. Sawyer, B. K. Stuhl, M. Yeo, T. Tschersbul, M. T. Hummon, Y. Xia, J. Klos, D. Patterson, J. M. Doyle, and J. Ye, "Cold heteromolecular dipolar collisions," submitted for publication (2010).

*Author Index
and
List of Participants*

Lucchese, R.	249
Lundeen, S.R.	201
Macek, J.H.	77, 87, 205
Manson, S.T.	209
Martínez, T. J.	95, 98
Matsika, S.	291
McCurdy, C.W.	59, 64, 69
McKoy, V.	213
Meyer, F.W.	77
Miller, T.A.	155
Msezane, A.Z.	217
Mukamel, S.	221
Murnane, M.M.	27, 29, 191, 447
Nelson, K.A.	225
Neumark, D.	69
Novotny, L.	229
Orel, A.E.	233
Orlando, T.M.	237
Ourmazd, A.	241
Pelton, M.	10
Phaneuf, R.A.	245
Poliakoff, E.	249
Rabitz, H.	253
Raman, C.	257
Reinhold, C.O.	77, 85, 86
Reis, D.	2, 3, 4, 95, 102
Rescigno, T.N.	59, 64
Robicheaux, F.	259
Rocca, J.J.	263
Rose-Petruck, C.G.	267
Santra, R.	2, 3, 4, 6, 7, 8, 11
Scherer, N.	10
Schoenlein, R.W.	69
Schultz, D.R.	77, 87
Schwander, P.	241
Seideman, T.	271
Seidler, G.T.	275
Southworth, S.H.	1, 2, 3, 5, 6, 8, 9, 11
Starace, A.F.	279
Stockman, M.I.	283
Stöhr, J.	95
Thumm, U.	25, 28, 29, 47
Trallero, C.A.	51
Umstadter, D.	287
Vane, C.R.	77, 80, 82
Weber, Tj. Ø.	59, 60, 69

Weinacht, T.	291
Ye, J.	9, 295
Young, L.	1, 2, 3, 4, 5, 6, 8, 9, 10, 11

Participants

Pierre Agostini
The Ohio State University
191 West Woodruff Avenue #4190
Columbus, OH 43210
Phone: 614-247-4734
E-Mail: agostini@mps.ohio-state.edu

Andreas Becker
JILA and Department of Physics
440 UCB, University of Colorado
Boulder, CO 80309-0440
Phone: 303-492-7825
E-Mail: andreas.becker@colorado.edu

Ali Belkacem
Lawrence Berkeley National Laboratory
MS: 2R0100
Berkeley, CA 94720
Phone: 510-486-7778
E-Mail: abelkacem@lbl.gov

Itzik Ben-Itzhak
Kansas State University
116 Cardwell Hall, Physics Dept.
Manhattan, KS 66506
Phone: 785-532-1636
E-Mail: ibi@phys.ksu.edu

Nora Berrah
Western Michigan University
Physics Department
Kalamazoo, MI 49008
Phone: 269-387-4955
E-Mail: nora.berrah@wmich.edu

Michael Bogan
PULSE Institute
2575 Sand Hill Road
Menlo Park, CA 94025
Phone: 650-926-2731
E-Mail: mbogan@slac.stanford.edu

John Bohn
JILA
UCB 440
Boulder, CO 80309
Phone: 303-492-5426
E-Mail: bohn@murphy.colorado.edu

Philip Bucksbaum
Stanford PULSE Institute
SLAC, 2575 Sand Hill Road
Menlo Park, CA 94015
Phone: 650-926-5337
E-Mail: phb@slac.stanford.edu

Michael Casassa
U.S. Department of Energy
19901 Germantown Road
Germantown, MD 20874
Phone: 301-903-0448
E-Mail: michael.casassa@science.doe.gov

Martin Centurion
University of Nebraska
Jorgensen Hall, 855 North 16th St.
Lincoln, NE 68588
Phone: 402-472-5810
E-Mail: mcenturion2@unl.edu

Zenghu Chang
University of Central Florida
4000 Central Florida Blvd., MAP310
Orlando, FL 32816
Phone: 407-823-4442
E-Mail: chang@phys.ksu.edu

Shih-I Chu
University of Kansas
Department of Chemistry
Lawrence, KS 66045
Phone: 785-864-4094
E-Mail: sichu@ku.edu

Participants

C. Lewis Cocke
Kansas State University
Cardwell Hall, Physics Dept., KSU
Manhattan, KS 66506
Phone: 785-532-1609
E-Mail: cocke@phys.ksu.edu

Steven Cundiff
JILA
440 UCB
Boulder, CO 80309-0440
Phone: 303-492-7858
E-Mail: cundiff@jila.colorado.edu

Marcos Dantus
Michigan State University
58 Chemistry Building
East Lansing, MI 48823
Phone: 517-355-9715 x314
E-Mail: dantus@msu.edu

Brett DePaola
Kansas State University
Cardwell Hall, Physics Dept., KSU
Manhattan, KS 66506
Phone: 785-532-6777
E-Mail: depaola@phys.ksu.edu

Todd Ditmire
University of Texas
1 University Station #C1600
Austin, TX 78712
Phone: 512-471-3296
E-Mail: tditmire@physics.utexas.edu

John Doyle
Harvard University
17 Oxford Street
Cambridge, MA 02138
Phone: 617-495-3201
E-Mail: doyle@physics.harvard.edu

Joseph Eberly
Univ. Rochester
600 Wilson Blvd.
Rochester, NY 14627
Phone: 585-275-4351
E-Mail: eberly@pas.rochester.edu

Robin Côté
University of Connecticut
2152 Hillside Road, U-3046
Storrs, CT 06269
Phone: 860-486-4912
E-Mail: rcote@phys.uconn.edu

Alexander Dalgarno
Harvard-Smithsonian Center for
Astrophysics
60 Garden Street
Cambridge, MA 02138
Phone: 617-495-4403
E-Mail: adalgarno@cfa.harvard.edu

David DeMille
Yale University
217 Prospect Street
New Haven, CT 06511
Phone: 203-432-3833
E-Mail: david.demille@yale.edu

Louis DiMauro
The Ohio State University
191 West Woodruff Ave #4178
Columbus, OH 43210
Phone: 614-688-5726
E-Mail: mkjackson@mps.ohio-state.edu

Gilles Doumy
Argonne National Laboratory
9700 S. Cass Ave.
Argonne, IL 60439
Phone: 630-252-2588
E-Mail: gdoumy@aps.anl.gov

Robert Dunford
Argonne National Lab
9700 S. Cass Ave.
Argonne, IL 60439
Phone: 630-252-4052
E-Mail: dunford@anl.gov

Brett Esry
Kansas State University
116 Cardwell Hall
Manhattan, KS 66506
Phone: 785-532-1620
E-Mail: esry@phys.ksu.edu

Participants

Jim Feagin
Cal State Univ Fullerton
800 N State College Ave
Fullerton, CA 92834
Phone: 657-278-3366
E-Mail: jfeagin@fullerton.edu

Kelly Gaffney
SLAC/Stanford
2575 Sand Hill Road
Menlo Park, CA 94025
Phone: 650-926-2382
E-Mail: kgaffney@slac.stanford.edu

Oliver Gessner
Lawrence Berkeley Lab
1 Cyclotron Road
Berkeley, CA 94720
Phone: 510-486-6929
E-Mail: ogessner@lbl.gov

Chris Greene
University of Colorado
JILA
Boulder, CO 80309-0440
Phone: 303-731-2824
E-Mail: chris.greene@colorado.edu

Robert Jones
University of Virginia
Dept. of Physics, 382 McCormick Rd.
Charlottesville, VA 22904-4714
Phone: 434-924-3088
E-Mail: bjones@virginia.edu

Henry Kapteyn
University of Colorado at Boulder/JILA
UCB 440
Boulder, CO 80309-0440
Phone: 303-492-6763
E-Mail: Henry.Kapteyn@colorado.edu

Bertold Kraessig
Argonne National Laboratory
9700 S. Cass Ave.
Argonne, IL 60439
Phone: 630-252-9230
E-Mail: kraessig@anl.gov

Gregory Fiechtner
DOE/Basic Energy Sciences
19901 Germantown Road, SC-22.11
Germantown, MD 20876
Phone: 301-903-5809
E-Mail: gregory.fiechtner@science.doe.gov

Thomas Gallagher
University of Virginia
Department of Physics
Charlottesville, VA 22904
Phone: 434-924-6817
E-Mail: TFG@VIRGINIA.EDU

Phillip Gould
University of Connecticut
Physics Dept. U-3046, 2152 Hillside Rd.
Storrs, CT 06269-3046
Phone: 860-486-2950
E-Mail: phillip.gould@uconn.edu

Markus Guehr
Stanford PULSE Institute
2575 Sand Hill Road
Menlo Park, CA 94025
Phone: 650-725-3306
E-Mail: mguehr@stanford.edu

Elliot Kanter
Argonne National Laboratory
XSD/401-B3170
Argonne, IL 60439
Phone: 908-617-1622
E-Mail: kanter@anl.gov

Victor Klimov
Los Alamos National Laboratory
MS-J567
Los Alamos, NM 87545
Phone: 505-665-8284
E-Mail: klimov@lanl.gov

Jeffrey Krause
Department of Energy
19901 Germantown Rd.
Germantown, MD 20874
Phone: 301-903-5827
E-Mail: Jeff.Krause@science.doe.gov

Participants

Vinod Kumarappan
Kansas State University
328 Cardwell Hall
Manhattan, KS 66506
Phone: 785-532-3415
E-Mail: vinod@phys.ksu.edu

Allen Landers
Auburn University
206 Allison Laboratory
Auburn, AL 36849
Phone: 334-844-4048
E-Mail: landers@physics.auburn.edu

Chii-Dong Lin
Kansas State University
2101 Hillview Dr.
Manhattan, KS 66502
Phone: 785-532-1617
E-Mail: cdlin@phys.ksu.edu

Robert Lucchese
Texas A&M University
Department of Chemistry
College Station, TX 77843-3255
Phone: 979-845-0187
E-Mail: lucchese@mail.chem.tamu.edu

Stephen Lundeen
Colorado State University
Dept. of Physics, CSU
Fort Collins, CO 80523-1875
Phone: 970-491-6647
E-Mail: lundeen@lamar.colostate.edu

Joseph Macek
University of Tennessee
Knoxville, TN 37996
Phone: 865-974-0770
E-Mail: jmacek@utk.edu

Steven T Manson
Georgia State University
Department of Physics and Astronomy
Atlanta, GA 30030
Phone: 404-824-0625
E-Mail: smanson@gsu.edu

Diane Marceau
Department of Energy
19901 Germantown Road
Germantown, MD 21702
Phone: 301-903-0235
E-Mail: diane.marceau@science.doe.gov

Todd Martinez
Stanford PULSE Institute
2575 Sand Hill Rd.
Menlo Park, CA 94025
Phone: 650-417-4612
E-Mail: toddjmartinez@gmail.com

Spiridoula Matsika
Temple University
1901 N. 13th Street
Philadelphia, PA 19122
Phone: 215-204-7703
E-Mail: smatsika@temple.edu

William McCurdy
Lawrence Berkeley National Laboratory
One Cyclotron Rd., MS 2-300
Berkeley, CA 94720
Phone: 510-486-4283
E-Mail: cwmccurdy@lbl.gov

Vincent McKoy
California Institute of Technology
1200 E. California Blvd.
Pasadena, CA 91125
Phone: 626-395-6545
E-Mail: mckoy@caltech.edu

Alfred Z. Msezane
Clark Atlanta University
223 James P. Brawley Drive, S.E.
Atlanta, GA 30314
Phone: 404-880-8663
E-Mail: AMsezane@cau.edu

Shaul Mukamel
University of California
1102 Nat. Sci. II
Irvine, CA 92697-2025
Phone: 949-824-7795
E-Mail: smukamel@uci.edu

Participants

Margaret Murnane
University of Colorado at Boulder/JILA
UCB 440
Boulder, CO 80309-0440
Phone: 303-492-6763
E-Mail: margaret.murnane@colorado.edu

Keith Nelson
MIT
MIT Room 6-235
Cambridge, MA 02139
Phone: 617-253-1423
E-Mail: kanelson@mit.edu

Daniel Neumark
Lawrence Berkeley National Laboratory
One Cyclotron Road
Berkeley, CA 94720
Phone: 510-642-3502
E-Mail: dneumark@berkeley.edu

Ann Orel
University of California, Davis
One Shields Ave.
Davis, CA 95616
Phone: 530-752-6025
E-Mail: aeorel@ucdavis.edu

Thomas Orlando
Georgia Institute of Technology
901 Atlantic Dr. NW
Atlanta, GA 30332
Phone: 404-385-6047
E-Mail: thomas.orlando@chemistry.gatech.edu

Abbas Ourmazd
University of Wisconsin
Physics, 1900 E. Kenwood Blvd.
Milwaukee, WI 53211
Phone: 414-229-2610
E-Mail: ourmazd@uwm.edu

Mark Pederson
Basic Energy Sciences
19901 Germantown Road, Room E-433
Germantown, MD 20874-1920
Phone: 301-903-9956
E-Mail: mark.pederson@science.doe.gov

Matthew Pelton
Argonne National Laboratory
9700 S. Cass Ave.
Argonne, IL 60439
Phone: 630-252-4598
E-Mail: pelton@anl.gov

Ronald Phaneuf
University of Nevada
Department of Physics /0220
Reno, NV 89557-0058
Phone: 775-784-6818
E-Mail: phaneuf@unr.edu

Erwin Poliakoff
Louisiana State University
Chemistry Department
Baton Rouge, LA 70803
Phone: 225-578-2933
E-Mail: epoliak@lsu.edu

Herschel Rabitz
Princeton University
Frick laboratory
Princeton, NJ 08544
Phone: 609-258-4180
E-Mail: jmcclelland@princeton.edu

Chandra Raman
Georgia Institute of Technology
School of Physics
Atlanta, GA 30332-0430
Phone: 404-894-9062
E-Mail: chandra.raman@physics.gatech.edu

David Reis
Stanford PULSE Institute
2575 Sand Hill Rd
Menlo Park, CA 94025
Phone: 650-926-4192
E-Mail: dreis@slac.stanford.edu

Thomas N. Rescigno
Lawrence Berkeley National Laboratory
One Cyclotron Road, BLDG 50F1650
Berkeley, CA 94720-8139
Phone: 510-486-8652
E-Mail: TNRescigno@lbl.gov

Participants

Francis Robicheaux
Auburn University
206 Allison Lab
Auburn, AL 36849
Phone: 334-844-4366
E-Mail: robicfj@auburn.edu

Jorge Rocca
Colorado State University
1320 Campus Delivery ERC B229
Fort Collins, CO 80523-1320
Phone: 970-491-8847
E-Mail: matilda@colostate.edu

Christoph Rose-Petruck
Brown University
324 Brook Str. Box H
Providence, RI 02912
Phone: 401-863-1533
E-Mail: crosepet@brown.edu

Norbert Scherer
University of Chicago
5735 S Ellis Ave.
Chicago, IL 60637
Phone: 773-702-7069
E-Mail: nfschere@uchicago.edu

Robert Schoenlein
Lawrence Berkeley National Laboratory
1 Cyclotron Rd. MS: 2-300
Berkeley, CA 94720
Phone: 510-486-6557
E-Mail: rwschoenlein@lbl.gov

David Schultz
Oak Ridge National Laboratory
Physics Division, Bldg. 6010, P.O. Box 2008
Oak Ridge, TN 37831-6372
Phone: 865-576-9461
E-Mail: schultzd@ornl.gov

Tamar Seideman
Northwestern University
2145 Sheridan Road
Evanston, IL 60208-3113
Phone: 847-467-4979
E-Mail: t-seideman@northwestern.edu

Gerald Seidler
University of Washington
Physics Dept, Box 351560
Seattle, WA 98195-1560
Phone: 206-427-8045
E-Mail: seidler@uw.edu

Steve Southworth
Argonne National Laboratory
401/B3164
Argonne, IL 60439
Phone: 630-252-3894
E-Mail: southworth@anl.gov

Anthony F. Starace
The University of Nebraska
208 Jorgensen Hall, 855 N 16th St.
Lincoln, NE 68588-0299
Phone: 402-472-2795
E-Mail: ASTARACE1@UNL.EDU

Carlos Trallero
Kansas State University
116 Cardwell Hall
Manhattan, KS 66506
Phone: 785-532-0846
E-Mail: carlos@phys.ksu.edu

Donald Umstadter
University of Nebraska-Lincoln
Behlen B58
Lincoln, NE 68588-0299
Phone: 402-472-8115
E-Mail: dpu@hfsserve.unl.edu

Thorsten Weber
Lawrence Berkeley National Lab
1 Cyclotron Road
Berkeley, CA 94607
Phone: 510-486-5588
E-Mail: TWeber@lbl.gov

Thomas Weinacht
Stony Brook University
Department of Physics
Stony Brook, NY 11974-3800
Phone: 631-632-8163
E-Mail: tweinacht@sunysb.edu

Participants

Jun Ye
University of Colorado at Boulder/JILA
440 UCB
Boulder, CO 80309-0440
Phone: 303-735-3171
E-Mail: Ye@jila.colorado.edu

Linda Young
Argonne National Laboratory
9700 S. Cass Ave.
Argonne, IL 60439
Phone: 630-252-8878
E-Mail: young@anl.gov